SMALL SCALE GREEN INFRASTRUCTURE. The environmental impacts within a context of tropical megacities, with a focus on Sao Paulo's public Schools

Matos Da Silva, Joao

This is a PhD thesis awarded by the University of Westminster.

https://doi.org/10.34737/wxq27

SMALL SCALE GREEN INFRASTRUCTURE

The environmental impacts within a context of tropical megacities, with a focus on Sao Paulo's public schools

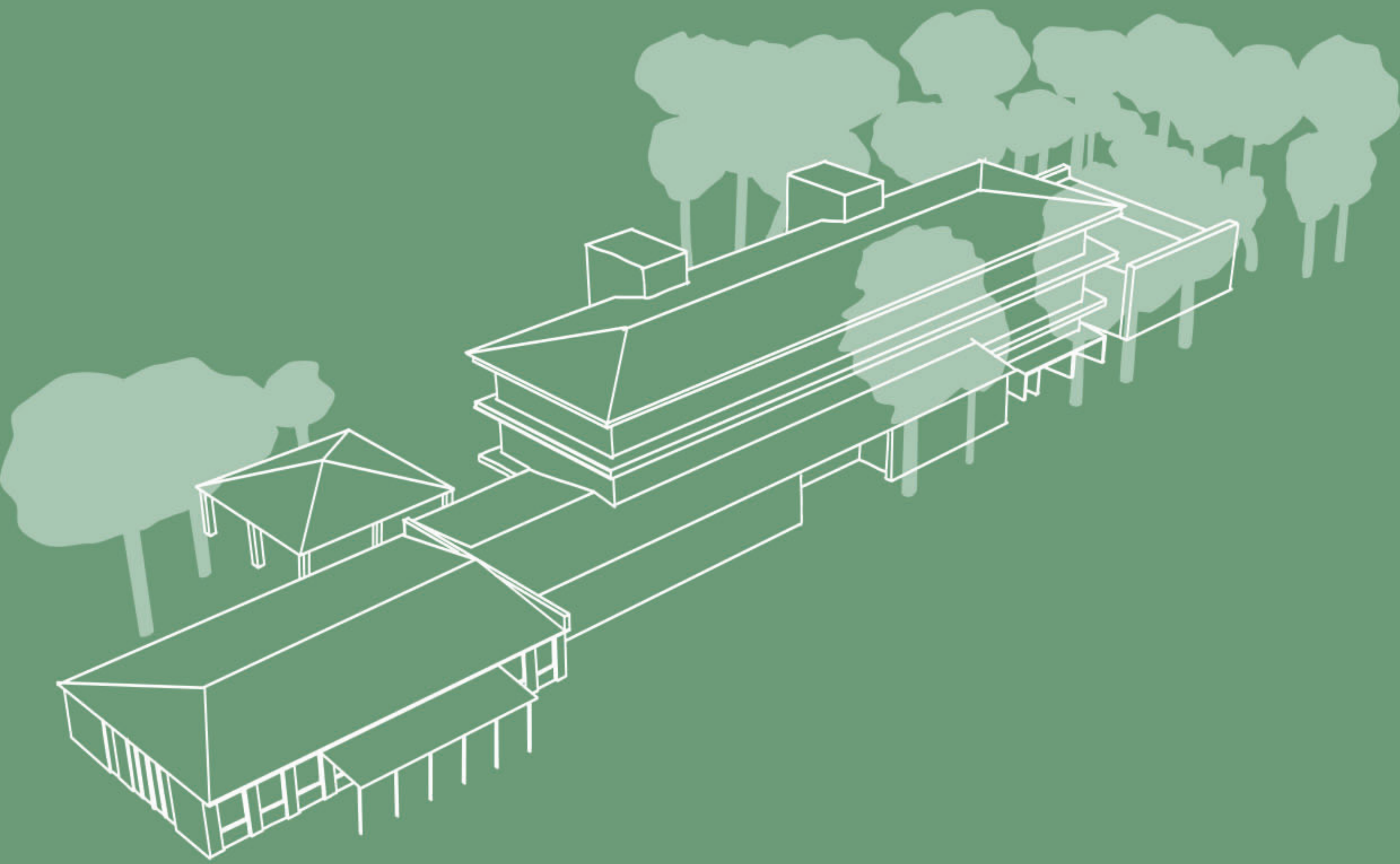

Joao Pedro Matos da Silva PhD 2024

SMALL SCALE GREEN INFRASTRUCTURE

The environmental impacts within a context of tropical megacities, with a focus on Sao Paulo's public schools

Joao Pedro Matos da Silva PhD- October 2024

Cover - Sketch of EMEF Amorim Lima (personal archive).

ABSTRACT

SMALL-SCALE GREEN INFRASTRUCTURE:

THE ENVIRONMENTAL IMPACTS WITHIN A CONTEXT OF TROPICAL MEGACITIES, WITH A FOCUS ON SAO PAULO'S PUBLIC SCHOOLS

JOAO PEDRO MATOS DA SILVA

Various typologies of greenery and green environments are part of people's everyday landscape almost everywhere in the world. Even if on different scales and degrees, most humans enjoy and seek some type of contact with greenery, and its importance has been the focus of research for many years. The beneficial impact of large bodies of vegetation, such as the Amazonian Forest, on the world's health and existence is globally discussed, and evidence has been gathered by the scientific community. In the environmental design field, green elements are a recurring topic, intrinsically associated with our work. Nevertheless, the knowledge of the favourable outcomes of having vegetation around people, often allowed for it to be introduced into urban environments without scrutiny or evaluation. The small-scale vegetation allocation within cities, in particular denser ones, should overall be praised. However, there isn't an expressive number of studies dedicated to investigating and calculating in depth its positive and perhaps negative repercussions, mainly regarding pollutant particles such as PM2.5 and PM10. Furthermore, in dense urban settlements, air pollution and other environmental risks represent one of the most significant risks to human health, with children and adolescents being heavily affected.

This doctoral research delves into a reasonably novel area of study, exploring the impacts of greenery as an infrastructure of a dense city on reduced-scale applications (Small-scale Green Infrastructure – SGIs). The study is set within a specific microclimatic and urban context, with a focus on tropical megacities using Sao Paulo as a prime example. With a specific focus on children's health, this research analyses the relationship between architectural elements and small-scale green infrastructure (SGI) within school environments. The aim is to define the most beneficial combination of the green and built elements mentioned before for their health and comfort. The methodology of this doctoral research is based on a multicriteria evaluation that encompasses three main subjects: health, comfort, and well-being. The study of these themes as performance indicators of the architecture and greenery relationship is crucial for providing support to decision-makers within the public school's context of Sao Paulo.

The outcomes of this research have direct implications for the design and management of public schools in Sao Paulo. The importance of air movement to enhance air quality and shading to enhance thermal comfort is emphasized. The cluster of trees is confirmed as the best SGI for human comfort while being the worst regarding pollutant particle concentration. However, it is also shown that the crowns of the trees are the main issue, highlighting the importance of having taller ones. The living walls are the best-performing vegetation element regarding air pollution, while also enhancing thermal comfort. Additionally, solid boundary walls protecting the site from pollutant sources are shown to be essential in reducing pollution in an area with various types of vegetation. The research also demonstrates how weather conditions can impact air quality. Finally, the guidelines for public schools in Sao Paulo are drafted, defining the best types of vegetation to be used within the open areas. The best morphological organization of those elements are also suggested as policies to be applied in the state.

AUTHOR DECLARATION

I declare that all the material in this thesis is my own work.

ACKNOWLEDGEMENTS

I want to start by expressing my gratitude to my supervisors, Rosa Schiano-Phan and Joana Goncalves, for all the support they have given me since my master's degree. I am grateful for your sensibility, for understanding my struggles and making me feel better during difficult circumstances. Thank you for sharing your extensive knowledge with me and doing everything possible to ensure the best outcome for my work. Also, thank you to Dr Krystallia Kamvasinou, Dr Nasser Golzari, and Dr Jorge Rodriguez Alvarez for assessing my work during different periods of its development and conclusion; your input and care for my work were of extreme value. To the Brazilian professionals, I had the pleasure of interacting with in this process, particularly Dr Alexandre Delijaicov and Helena Ayoub, your unique perspectives and insight were instrumental in making my work more relevant to the context of Sao Paulo public schools. It was an honour to have contributed a little bit to the knowledge produced in my country. Finally, I thank my colleagues and friends from Studio 4215 for their understanding and thoughtfulness during this turbulent period. I especially thank Shashank Jain, my boss and friend, for all the technical and emotional support during these five years, including giving me the necessary time to finish my research. I hope to be as kind and knowledgeable as you in my career and life.

To my family, blood or not, who have been by my side, every one of you has contributed enormously throughout this important stage of my life. I couldn't thank you enough for your support and presence. For my London family, with whom I have shared ups and downs, you make life worth living and have given me the strength to conquer difficult tasks like this. Thank you so much to Fabricio and Julia, who shared a home with me for many years and were always there, making me feel better during challenging times in this process and daily life. For the family back in Bahia and other places around the globe, you are my roots and strength; numerous times, your words kept me going. To Caio, thank you for all the talks these last five years and for being present in the saddest and happiest moments. To Carine, my partner in academia and "big sister", thank you for supporting me since even before we became friends and for not stopping at any second until today. London and life are better with you by my side. To my partner in life, Cameron, thank you for the late phone calls and conversations, for making me laugh, for your partnership, and for always offering me a hug and your presence whenever I need it. Finally, to my main supporter in life, my mom, "Dona Ja," I dedicate this achievement, as with all others, to you. I would not be here without your unstoppable and unwavering support and encouragement. Muito obrigado por tudo. Friends and family, I love you all deeply. Obrigado. Finally, I hope that when I read this in the future, I am reminded of how complicated this process was, so I will continue to recognise the importance of this achievement while remembering to be grateful, to keep believing and to keep moving.

TABLE OF CONTENTS

LIST OF FIGURES

1. INTRODUCTION

In dense urban settlements, air pollution represents one of the most significant risks to human health, and children's vulnerability to it can be even higher. For example, in 2016, WHO declared that more than one in every four deaths of children under five is directly or indirectly related to air pollution (World Health Organization, 2016). WHO also states that since 2022, globally, 442,000 children under five years old have died prematurely from air pollution exposure (World Health Organization, 2024). More specifically, concerning the school environments, the Landscape Institute (2013) indicated the importance of connecting children with nature (greenery) within the school grounds for cities' sustainable development. Moreover, the mentioned air quality deterioration and the start of an environmental movement caused, mainly in the past decade, pressure on companies to have better performance regarding sustainability (Netto et al., 2020 and Szabo and Webster, 2021). However, to address those concerns, many companies apply strategies that appeal to ecological consciousness without having environmental conduct, which is considered greenwashing. (Szabo and Webster, 2021). One aspect of greenwashing is the indiscriminate recommendation of vegetation use within urban environments without a proper understanding of the specific impacts that implementing those elements would cause.

This research is interested in producing design guidelines derived from the research on the effects of natural elements inserted in the context of schools in urban environments. The mentioned natural elements compose the small-scale green infrastructure (SGI), a concept that is explained in depth in Chapter 02. Naturally, the insertion or withdrawal of SGI components into the urban design will culminate in multidisciplinary repercussions. In other words, the impacts are always complex and multiple and require analysis that considers more than one criterion. Thus, this work explores two main aspects of human responses to the environment (comfort and physical health), which are studied through different performance indicators. Accordingly, this doctoral research is a multicriteria evaluation, so it could be feasible and still provide a meaningful contribution to knowledge. Considering more than one criterion at once is a slightly different approach to academic research, which traditionally looks at one problem at a time. However, Sanesi et al. (2006) mentioned that future studies should blend different methodologies and approaches, especially if the purpose is to support urban planners and other decision-makers in their works. Kiker et al. (2005) also defended using the Multicriteria Decision Approach (MCDA). They declared that environmental decision-making is often complicated and requires a combination of both quantitative and qualitative methodologies within scientific studies. Thus, a multifaceted analysis is contemplated in this work, allowing for identifying overlaps and synergy between the subjects. The mentioned approach enhances the understanding of the effects of SGI elements, which is necessary to establish the design guidelines.

1.1. KNOWLEDGE GAPS

Previous studies have explored the potential greenery components in urban environments to modify pollutant dispersion and removal (Abhijith et al., 2017; Al-dabbousand Kumar, 2014; Barwise and Kumar, 2019; Gromke, Jamarkattel and Ruck, 2016; Gromke and Ruck, 2007; Nowak et al., 2013). However, some studies also indicated that more research was needed on the subject. For example, Cameron et al. (2012) established that **more research is needed to determine which types of trees would benefit which building typologies and to understand other specific requirements for each scenario**. Salmond et al. (2016) affirmed that **the impact on climate and human health through the local scale study of trees on the street doesn't happen as in-depth as the study of urban scale effects of greenery.** Salmond et al. (2016) also state that **a local-scale approach can produce a much more precise result for the intervention studied**. Barwise and Kumar (2019) defined that **green infrastructures could be used to reduce pollutant concentrations; however, the typology and characteristics of the green barrier remain unclear.** Regarding the discussion about the morphology of the vegetation, Abhijith et al. (2017) studies have shown that trees led to air quality deterioration while hedges improved air quality. The same study observed the **need to express and standardise the vegetation density when the aim is to remove air pollutants.**

This doctoral research studies the Small Scale Green Infrastructure (SGI) within reduced and contained urban environments. It investigates the relationship between the architectural elements and SGI components within school environments. **The literature doesn't show such a study of the combined performances of individual architectural and natural elements.** Such a study is crucial to determine the thermal and air quality conditions on a human scale instead of an urban scale, which is commonly seen when Green Infrastructure impacts are examined. **Thus, this research fills this knowledge gap by focusing on the separate effects of trees, hedges, living walls and grass when placed close to cobogos, glazed windows, and vertical and horizontal shading elements**. The main aim was to define the combinations that best benefit children's health and comfort. Following the analysis of several pieces of research, Borna and Schiano-Phan (2020) expressed that **further work was needed to "determine the exact effectiveness of vegetation in urban spaces throughout the year (summer and winter scenarios). The air quality-vegetation relationship and studies on the variation of the results throughout a typical year lack in-depth information.** Thus, this work explores that gap through digital experiments conducted in São Paulo for a period that encompasses summer to winter. Moreover, Roy, Byrne, and Pickering (2013) stated that **from 33 analysed articles that investigated environmental impacts caused by urban trees, only 21.7% used a fieldwork-based methodology.** Thus, this research utilises field and analytical exercises to build its methodology and achieve real-life evidence-based outcomes.

1.2. RESEARCH OBJECTIVES

• Explore the impacts of small-scale green infrastructure (SGI) in school environments in tropical climates on users' comfort and physical health.

• Investigate the impact of different SGI components' typologies, arrangements, and amounts of vegetation in the context of their integration within schools` architecture.

• Develop design guidelines for the public school building typology using small green infrastructure (SGI) components that could be replicated in other urban contexts of the subtropical megacity of Sao Paulo.

• Propose generic design guidelines that can be suggested to schools within the state and other cities with similar climatic conditions and morphological characteristics.

1.3. RESEARCH QUESTIONS

• Can small green infrastructure within a school's environment in a tropical megacity improve users' comfort and health?

• What design guidelines and solutions can be proposed for schools in Sao Paulo to improve their environmental performance?

• Can design guidelines for one studied School be replicated in other contexts with similar climatic and morphological conditions within the same building typology?

1.4. STRUCTURE AND METHODOLOGY

1.4.1. INTRODUCTION

This doctoral research presents an overall approach reflecting applied research (with a pragmatic focus), followed by qualitative studies on social sciences and quantitative analysis. Quantitative studies are built from an evidence-based approach to design research (not from a statistical perspective). As section 1.1 (Knowledge gaps) mentions, this work bases its quantitative research on field and analytical work on two main foundations. Hence, within Sao Paulo, this research's city of interest, a school case is established as the environment for field exercises. The information, characteristics and reasoning for the case study selection are presented in Chapters 03 and 04. Following its selection and the permissions obtained, the school EMEF Amorim Lima is where field and analytical works are developed and are discussed in chapters 04 and 05 of this thesis. Furthermore, an analytical exercise is developed to guarantee the development of guidelines that can be applied to school buildings with similar climatic conditions. The mentioned study represents the main data outcome of this doctoral work and is called "The Environmental Performance Matrix" (Chapter 06). It examines the local impacts of the small green infrastructure when combined with architectural elements commonly found in Sao Paulo's public schools. As mentioned in the introduction, this thesis ends with forming design guidelines that can be applied to outdoor areas of Sao Paulos public schools. The guidelines are discussed in the Applicability Study section (Chapter 07), where the “best practices” concerning location and choice of SGI components are established.

1.4.2. SMALL SCALE GREEN INFRASTRUCTURE

The Literature review produced throughout this work is spread into the different chapters of this thesis. Yet, Chapter 02 is entirely based on existing literature examined to establish the meaning of this research’s main concepts and justify two of its study focuses, SGI components and Sao Paulo. This body of work explores the characteristics of the City of Sao Paulo, always as an allusion to similar cities. It also discusses the characteristics of global megacities, focusing on tropical ones. The air quality conditions, as well as other climatic and microclimatic aspects, are illustrated. The studied material shows the relevance of producing research on how to tackle these cities’ current environmental issues. Moreover, the chapter discusses the idea of nature within urban environments and then defines small-scale green infrastructure (SGI) and what composes it. The definition of the mentioned concept, which bears this research title, is built through literature and previous examples. The intention is that whenever the term is mentioned, readers can instantly connect it to the specific vegetation arrangement. Afterwards, the Literature explores the effectiveness of using SGI and its elements to tackle air pollution, the heat island effect, and physical health issues, demonstrating its importance in the current global context. The chapter also demonstrates pieces of evidence developed regarding the mentioned performance indicators.

1.4.3. PUBLIC SCHOOLS IN SAO PAULO

Chapter 03 is also heavily based on a literature review and is dedicated to justifying the focus of this research on Public Schools. Hence, it illustrates the threats children and young adolescents can suffer in dense urban environments and the relevance of the school environment to avoid that. The importance of SGI components in the mentioned space is also discussed. This section also focuses on the main issues that poor air quality can cause in the development of the younger population. Still, the reviewed literature also reflects on the impact of warmer thermal conditions on their behaviour and performance in school and daily activities. The chapter then moves into a review of the Sao Paulo state public school system and architecture. The organisation of the learning system in the state and the departments that design and administer the schools are briefly discussed. Additionally, it showcases and reviews the buildings’ possible environmental design performance based on their design patterns. The review also identifies the most common architectural components, which are further studied in the main analytical exercise (Chapter 06). The chapter is the theoretical foundation for choosing this research’s case study. .

1.4.4. CASE STUDY - FIELDWORK

Chapter 04 presents and discusses the characteristics of EMEF Amorim Lima and justifies its selection. EMEF stands for “Escola Municipal de Ensino Fundamental, “ meaning municipal high school. According to Sao Paulo’s state rules, the EMEFs are children and teenagers of people aged six to fifteen years. The city has numerous municipal schools; however, Amorim Lima was chosen mainly due to its location, size, and dense SGI occupying the outdoor area. Many EMEFs are located in less dense areas farther from the city centre and in massive sites with little urban surroundings. On the other hand, Amorim Lima is located close to densely populated areas with residential and commercial buildings surrounding the site. The school area is also connected to a hectic avenue with many people and vehicles daily. The chapter also defines the indoor and outdoor spots that are further studied. The spots are discussed individually, with each area's overall environmental performance perception. The fieldwork is conducted through spot measurements and is divided into two main exercises: microclimatic and air quality measurements. The microclimatic field study measures dry bulb temperature (DBT), humidity, mean radiant temperature (MRT) and wind speeds to indicate the thermal comfort within the site. The second batch of field measurements is of PM2.5 and PM10 concentrations. The health and comfort parameters mentioned showcase the school's "point in time" environmental performance. Finally, the exercises are conducted using methods observed in previous works which conducted field analysis, as discussed in more detail in the chapter.

1.4.5. CASE STUDY – ANALYTICAL WORK

Chapter 05 comprises the analytical exercises conducted for EMEF Amorim Lima. It also displays a literature review justifying the uses of each software selected for this work. The review exemplifies the software's use by other researchers who study the environmental performance of buildings and outdoor spaces. Moreover, previously used thermal comfort benchmarks and air quality indexes are also presented and discussed. The analytical exercises are divided into two main exercises: the building and the outdoors. The first study, concerning the main building and its façade design, is achieved through understanding solar geometry in the site and the annual solar radiation accumulated on the facades. The outdoor analysis is conducted through outdoor comfort software called ENVI-met, which provides thermal comfort perception, wind speeds, humidity, DBT, and surface temperature at the modelled site, considering the existing vegetation, focusing on summer and winter periods of the year. The software used to carry out this body of work is explained in detail, and literature demonstrating their previous uses is discussed in the chapter. As the ENVI-met is the essential digital tool for this thesis, literature has also been reviewed to illustrate how it works and its robustness. Finally, This body of work validates the field results while expanding the understanding of EMEF Amorim Limas' space throughout the year. The field and analytical works produce a holistic perspective of the schools' performance, focusing on the relationship between the small-scale green infrastructure and architectural elements

1.4.6. THE ENVIRONMENTAL PERFORMANCE MATRIX

After studying the city's public school architecture combined with the thorough analysis of EMEF Amorim Lima, façade treatments seen repeatedly as imperative elements of its architecture are selected to be studied in depth in Chapter 06. The chapter also discusses and identifies the SGI components of interest within the context of Sao Paulo's state and the public school to define the ones that are further studied. The mentioned selection of green and built elements is oriented by the outcomes of Chapters 04 and 05 (Case Study), but also from the knowledge acquired in Chapter 03, through the review of existent schools. Subsequently, the research structures a combination of each of the selected greenery and built elements, forming the environmental performance matrix. The location (orientation) of the architectural elements and SGI typologies are altered in the study, forming each scenario. The matrix informs the ten simplified scenarios that have lately been simulated and were built as a generic representation of school environments. The analytical exercises in this chapter are conducted using the ENVI-met software, which has its characteristics discussed in Chapter 05, where it's used for the first time in this thesis. This section focuses on the DBT, humidity, air movement speeds, and indoor DBT results, indicating thermal comfort perception within the site. However, the main performance indicator is Psychological Equivalent Temperatures (PET) in the outdoor area. Concerning air quality, the terrain's PM2.5 and PM10 concentrations are studied. This body of work also focuses on the weighted average calculation of the results within the terrain boundaries to simplify comparing the studied scenarios. The weighted average is explained in-depth in the chapter. Furthermore, after analysing the first batch of simulations, a second exercise is conducted to answer the main questions and hypotheses that have been raised. The final simulations are discussed, and the mentioned questions are answered, which closes this chapter.

1.4.8. APPLICABILITY STUDIES

The results from Chapter 06 inform this thesis's final chapter before its conclusion (Chapter 08). This section displays and discusses a set of guidelines constructed with the knowledge built in this doctoral research. The mentioned guidelines discuss "best practices" that could be followed when choosing SGI components to be used in schools' open areas to enhance air quality and thermal comfort. Generically, the advice is fit to be used in the city and state of Sao Paulo, in addition to any other city in similar microclimatic conditions. Yet, it is recommended that each case has its own evidence-based research when possible. Furthermore, this chapter has as one of its methods to validate the guidelines their presentation and discussion with an interest group composed of Brazilian architects directly connected to the design of public schools in the state. The architects are also contacted in the initial stage of this thesis and are essential for the choice of EMEF Amotim Lima as the case study. Their input brings this research closer to the reality of its study context, endorsing its value to be applied in the future. Another method is to demonstrate how SGI components that are already documented and indicated for use in the schools by the government in Sao Paulo could be best applied, creating a classification between the trees' species. The final method of this chapter is the applicability study. The exercise exemplifies how the presented guidelines could be implemented in existing schools in the state. The aim is to indicate to architects and policymakers how this research's main findings could change the open areas and even façade design when needed.

2. SMALL SCALE GREEN INFRASTRUCTURE

WITHIN SAO PAULO'S CONTEXT

2.1. INTRODUCTION

This chapter introduces the context of this research's application and explains the criteria for choosing Sao Paulo as a representative tropical megacity. The choice was based on recurrent and common environmental issues related to morphology, density, and microclimate. A definition of Small Green Infrastructure (SGI) is given, including the word's origin, and examples of SGI based on recurrent characteristics and use are provided. Finally, the crucial role that SGI has on air quality and outdoor thermal comfort is described.

2.2. MEGACITIES IN A TROPICAL CLIMATE

2.2.1. OVERVIEW

According to the UN, in 2012, there were already 23 cities worldwide with a population of 10 million or greater (UN 2012, as cited by Baklanov, Molina, and Glauss 2016). These cities, most of which are in poor and developing countries, are characterised by high levels of air pollution. According to Molina and Molina (2012, as cited by Baklanov, Molina, and Glauss 2016) and Folberth et al. (2015), megacities are urban agglomerations with a population that exceeds 10 million inhabitants. It is also established that despite covering less than 2% of the earth's surface, megacities are home to approximately 10% of the entire global population. In 2012, the UN estimated that in 2025, Asia would have gained another nine, Latin America two, and Africa, Europe, and Northern America one each" (UN 2012, as cited by Baklanov, Molina, and Glauss, 2016). This global significance of megacities underscores the relevance of understanding and addressing their environmental challenges. Furthermore, the phenomenon of migration from rural areas to highly developed urban areas has occurred globally, with a significant impact in emerging countries. Many factors motivate migration to urban centres, such as conflicts, land degradation, and the exhaustion of natural resources. However, it is the rapid population growth that is the largest factor contributing to cities' urbanisation, especially in developing countries (Montgomery, 2008). According to a 2022 UN report, Latin America has four of the world's largest megacities, two of which are in Brazil: Sao Paulo and Rio de Janeiro. The mentioned megacities have 17% of Latin America's urban population. Additionally, the report indicates that 51% of the population living in urban areas of Asia and the Pacific is equal to 54% of the world's urban population (UN-Habitat, 2022). The Indian megacities have approximately 20% of the world's megacities' population, with a projection to increase. In 2030, New Delhi is expected to become the largest one in the world (Molina et al., 2020). Additionally, Zheng et al. (2015) establish that particulate matter (PM) concentration levels in Asian and South American megacities drastically exceed those in North American and European ones. Moreover, literature has shown that some megacities, for example, London and Los Angeles, have implemented management plans and have more financial resources than those in poor developing countries to enhance air quality (Baklanov, Molina, and Glauss, 2016). This highlights the urgency of analysing megacities of the developing world, predominantly cities with tropical and subtropical climatic conditions.

2.2.2. ENVIRONMENTAL IMPACTS

As previously mentioned, Megacities are essential socio-economic hubs that strongly affect the world's environmental conditions. Indian cities are an example of the severe impacts of air pollution from biomass burning and increased demands for transportation, energy and other sources (Molina et al., 2020). Also, during the COVID-19 pandemic, a study of the Indian megacities registered a significant reduction in the cities' pollutant concentrations (Prakash et al., 2021). Molina et al. (2020) stated that air pollutants are transported between states and even across international borders, highlighting that megacities' local sources of emission cause issues beyond their bounds. Consequently, the emissions also severely impact Global climate change, affecting thermal comfort inside urban environments. Folberth et al. (2015) established the relationship between the activities conducted within megacities and the composition alteration of the atmosphere and the climate through gases and aerosol emissions. They also comment on the extreme level of emitted carbon dioxide from megacities under current circumstances and future conditions. The study states that if emissions from 2005 to 2015 are maintained (no decrease or increase) over the next 100 years, megacities will be responsible for 25% of the world's global warming since the pre-industrial era. Furthermore, concerning direct micro-climatic and climatic environmental impacts throughout the years, Luke Howard first documented temperature differences between urban and rural areas in London in the early 19th century (Parry and Chandler, 1966). Afterwards, several other studies have spotted a heat increase pattern caused by urban development when compared to rural areas. (Hua, Ma and Guo, 2008). With the increase of studies and consequent discussions related to heat pattern comparisons between urban and rural environments, the term "Urban heat island" (UHI) was soon created and became widespread worldwide. The UHI phenomenon, as we presently know it, was first proposed in 1958 by Manley (Manley G, 1958, as cited by Zhang, Wu, and Chen, 2010). It is then repeated and further studied in numerous pieces of research in diverse cities (Montavez, Rodriguez, and Jiménez, 2000; Lopes et al., 2013). Megacities are predominant environments that commonly display the UHI effects, underscoring the negative impacts it generates. For example, according to the World Urbanization Prospects (2003, as cited by Memon, Leung and Liu, 2009), "48% of the world population are living in urban areas which are directly exposed to urban heating problems, with no perspective of enhancement due to the constant growth of urban population". The issue repeats itself in the case of tropical/subtropical megacities. Hong Kong, for example, suffers from the extreme Urban Heat Island effect with an intensity ranging from 2°C to 4°C throughout the year (Siu and Hart, 2013). Finally, it is essential to state that UHI is considered, to some extent, a cause of health issues (Chan et al., 2018). Additionally, a study indicated that when there was a 1°C in dry bulb temperatures in a context already above 28°C, there was a 2% increase in heat-related human mortality (Lin et al., 2017). The studies above help illustrate the role of this typology of urban settlements in modifying essential atmospheric and thermal characteristics worldwide, directly impacting human comfort and health..

2.3. SAO PAULO

2.3.1. CONTEXT AND CHARACTERISTICS

IInterest in the city of Sao Paulo, the largest in Latin America, and consequently in the state is derived from the attraction towards Brazil. In 1985, Lombardo described the country as one of the most urbanised compared to other developing ones. They add that even smaller cities in Brazil suffer from urbanisation processes without proper care of land organisation. The country's context briefly mentioned naturally corresponds to the context of São Paulo. The city has also been through a strong urbanisation process, lacking proper planning. Its enrichment and the strong urban process started during the coffee cycle era, was extended to the entire country, and has expanded until now (Lima and Rueda, 2018). The territory of the São Paulo metropolitan area in the state of São Paulo (Brazil) is composed of 174 municipalities, five metropolitan regions, two urban agglomerations, and about 33,652,991 residents (Milz and Jacobi, 2019, as cited in Torres and Jacobi, 2020). The metropolitan area has 21 million inhabitants, constituting 11% of Brazil's population (UN, 2014; City Population, 2016; IBGE, 2016). Its population is one of the world's fastest-growing metropolitan ones, and it is the largest city within the entire Southern Hemisphere and considered one of the largest conurbations in the world (Schneider, Leite and Minkel, 2024). Today's estimated population is 22,806,704, projected at 24,490,136 in 2035 (World Population Review, 2024). It is constantly growing not only in inhabitants but also in the number of vehicles, with a fleet growth of 76% from 2001 to 2012; in 2014, it reached over 11 million cars (Andrade et al., 2017). Moreover, researchers and managers from different fields of knowledge are increasingly interested in the city (Milz and Jacobi, 2019, as cited in Torres and Jacobi, 2020). Sao Paulo's fast urban growth caused heterogeneity in its urban structure, which became one of its main characteristics, consequently causing a non-uniform distribution of greenery (Lima and Rueda, 2018). The growth has also created patterns similar to those of other Latin American cities, all characterised by extreme discrepancies in social, economic, and health status (Jacobi, 1997, as cited by McKay and Parker, 2018).

São Paulo is considered a subtropical city, with warm, humid summers and dry, cold winters. Temperatures can drop to 0°C in winter and rise to over 30°C in summer (INMET, 2016). The city is at latitude 23º24´S, with altitudes between 720m and 850m above sea level, and is 60 km away from the sea. Duarte and Goncalves (2006) indicate the complexity and heterogeneity of areas within Sao Paulo's urban climate. They also comment on how the city's metropolitan area has locations with urban heat island effects showing a 10 °C DBT difference compared to other areas within days of calmer air movement. Overall, Sao Paulo is a city with abundant rainfall, an average of 1,422mm per year, mainly from October to March. It is a frequent smog phenomenon, where humidity and air pollution combine to form a mist seen in the city's sky. The coldest month is in July, with a temperature average of 14°C. The hottest month is February, which has a 21°C average (Schneider and Leite, 2018). The projections for 2040 indicate that there will be a 5% to 10% increase in rainfall and a 0.5°C to 1°C increase in dry bulb temperatures (DBT), increasing environmental impacts and decreasing the city's capacity to recover from impacts (Di Giulio et al., 2018).

2.3.2. ENVIRONMENTAL ISSUES

As would be expected from a city of this magnitude, with the rapid growth previously described, Sao Paulo faces increasing environmental challenges, one of the most pressing being climate change (Lima and Rueda, 2018; Mckay and Parker, 2018). The trend in the past year is that air pollution levels in the city have usually been above national and international guidelines. Additionally, most of the environmental policies developed so far are focused on making vehicles cleaner, which is easily outweighed by the continuous increase in the vehicle fleet (Mckay and Parker, 2018). Already in 1996, the Environmental Company of the State of São Paulo (CETESB) established that traffic congestion was the most serious issue for the inhabitants, losing only to violence. CETESB discusses that from 1992 to 1995, the peak congestion grew from 36 km to 94 km, reaching 190km in 1996 (Jacobi 1997). According to the Technology and Environmental Sanitation Agency of Sao Paulo's state report, CETESB (2020), vehicles and industries are responsible for the deterioration of air quality in the metropolitan region of Sao Paulo. The report illustrates that Sao Paulo (metropolitan area) has 48% of the vehicle fleet while representing only 3.2% of the state's territory. In the central urban context of the city, there aren't functioning industries, so vehicles are the most significant cause of high pollutant levels. For example, there is no active industry in the Butanta neighbourhood, where this thesis Case Study is located. Therefore, vehicles are this area's most significant source of pollutants. Thus, the city has been facing specific issues related to air pollution for several years, which are related mainly to the number of vehicles but also other elements, such as the topography and a combination of climatic factors (Silva et al., 2013). Jacobi (1997) specifies that the regions' particular atmospheric conditions create an extreme thermal inversion phenomenon, disturbing air quality and consequently generating health issues, particularly lung diseases' increase. Moreover, Santana et al. (2020) identified the correlation between the increase in hospitalisation numbers between 2013 and 2016 and the PM10 and Pm2.5 concentration levels beyond the national and international standards. They also stated that the increase in the number of hospitalisations culminated in a total cost of 111 million USD. The study also revealed that ozone (O3), carbon monoxide (CO), sulfur dioxide (SO2), and nitrogen dioxide (NO2) are also connected with the number of hospitalisations due to respiratory diseases. Santana et al. (2020) also found that for all studied months, PM10 was always above 50 µg/m3; yet, in low rainfall months, it exceeded 100 µg/m3. It was also found to be higher than 20 µg/m3 every year, twice as high as WHO standards.

Naturally, São Paulo also suffers from thermal-related problems. Its UHI maximum intensity is 3°C higher than in Singapore, another megacity with tropical climatic conditions (Umezaki, 2020). Additionally, in the past 30 years, days where temperatures are higher than 32°C (considered extreme) are increasingly more common in the warmer periods (Lima and Rueda, 2018). Freitas et al. (2009, as cited by Silva Dias et al., 2013) stated that "when the sea breeze penetrates the metropolitan area of São Paulo, it may interact with the urban heat island, frequently triggering convective storms. The same event was noticed in other cities in the US (Bornstein and Lin, 2000)". In 1997, it was already observed that the city was suffering from increased flood risks due to the decrease in green areas. The mentioned phenomenon can cause severe environmental and economic impacts. (Jacobi, 1997). In addition to flooding and storms, heatwaves typically generate a drastic increase in the use of air conditioning. Furthermore, the rise in air conditioning use causes extreme energy consumption, which will trigger many issues, such as the rise in the CO^2 levels in the atmosphere (Andrade et al., 2017). Beyond the mentioned problems, studies have also illustrated that higher levels of the A. aegypti mosquito larva development, culminating in the Dengue disease, are connected to areas of the city with extreme temperatures (higher than 32°C), which, as previously mentioned, are created by the UHI effect (Araujo et al., 2015).

2.4. NATURE AMONGST URBAN ENVIRONMENTS

Before the concept of green infrastructures was adequately discussed and documented, the discussion about nature among cities and its relationship with city development took place for many years. Embodying the debate about the possible and needed alliance of natural and urban environments is at the heart of Architecture and Urban planning. For example, in 1898, Ebenezer Howard introduced the concept of "garden cities" as an alternative, which would use "mother earth as an essential source of life, happiness, wealth and power" (Howard, 2010). The "Garden Cities of Tomorrow", originally from 1898 but published with this name in 1902 (Howard, 2010), is the book that introduced the cited concept that can be considered the root of the idea of Green Infrastructure. The work also contains one of the first mentions of the connection between urban areas and ecosystem structures as a planning demand (Salata and Yiannakou, 2016). According to Hagan (2014), Ebenezer Howard's Garden City (cited above) is the great founding model of nature-in-the-city in the industrial age. Two other well-known counterpoints for the Garden City are "Le Corbusier's high-density version, the Ville Contemporaine, or City for Three Million (1922) and Frank Lloyd Wright's radically dispersed version, Broadacre City (1932)". In addition to the linear city of Magnitogorsk, a 1930 project by Leonidov (Hagan, 2014). Even Though some of the projects were never built, they are essential concepts and known references today for designing urban environments involving nature. Moreover, in the 1940s, there was already a cited concern about resource consumption and ecosystem damage. Additionally, before the 1970s, a few concepts were documented about "reintroducing nature into existing towns and cities" and "retrofitting with nature" (Douglas, 2019). Afterwards, the mentioned topic was more remarkably recalled in Ian McHarg's "Design with Nature" (1971) and the lesser-known Brian Hackett's "Landscape Planning: Introduction to Theory and Practice" (1971) (Kambites and Owen, 2006). Forwarding to 2019, one of the sustainable goals developed by the United Nations was to "make cities and human settlements inclusive, safe, resilient and sustainable". Lastly, as showcased, the knowledge surrounding the necessity of nature within the built environment with the potential of bringing positive impacts has been established for almost one hundred years.

2.5. SMALL-SCALE GREEN INFRASTRUCTURE

2.5.1. THE CONCEPT AND APPLICABILITY

Nowadays, the green infrastructure concept (GI) is widely known worldwide and among UK researchers (Matsler et al., 2021). For example, the Landscape Institute (2013) defined GI as "the network of natural and semi-natural features, green spaces, rivers and lakes that intersperse and connect villages, towns and cities". However, after reviewing the Literature concerning green infrastructure, It can be established that, despite the similarity between the definitions, there is a variation in the significance of the term for each research (Kambites and Owen, 2006; Jia et al., 2016; Salata and Yiannakou, 2016; Jerome, 2017; Shackleton et al., 2018; Benton-Short, Keeley and Rowland, 2017; Chatzimentor, Apostolopoulou and Mazaris, 2020; Abdulateef and Al-alwan, 2021; Fluhrer, Chapa and Hack, 2021; Matsler et al., 2021; Meerow, Natarajan and Krantz, 2021). The variety of definitions will be exposed and discussed next, identifying similarities to attempt a common description of the term.

Branas et al.'s 2002 study (cited by Nieuwenhuijsen, 2020) stated that GI is "an interconnected network of green space that conserves natural ecosystem values and functions and provides associated benefits to human populations." Additionally, most publications associate the term with urban planning strategies, demonstrating a large-scale characteristic (Kambites and Owen, 2006; Nieuwenhuijsen, 2020). Yet, other works also refer to GI as networks of green spaces that would improve the environment, provide ecosystem maintenance, clear air and water, and social outcomes, independent of their scale (Jia et al., 2016; Benton-short et al., 2019; Fluhrer, Chapa and Hack, 2021). For example, Kambites and Owen (2006) justified the use of churchyards, schoolyards, and trees planted along streets as examples of GI because studies showcased the users` benefits from those spaces. The UK government states that parks, green roofs, green walls, private gardens, playing fields, and different water bodies (for example, canals and ponds) could be part of the GI (Ministry of Housing, Communities & Local Government, 2019). Cameron et al. (2012) state that the green spaces (green infrastructure) network could be implemented in any urban environment of any morphology or size, and other researchers discuss the existence of minor elements that also compose a green infrastructure. Norton et al. (2015) established that urban trees could be considered part of a GI network. Shackleton et al. (2018) explored the concept of "safety nets", where GIs are not massive in size or ecological production, but as home gardens with trees. ". Additionally, as exemplified by Matsler et al. (2021), some publications have used the term GI only as a synonym for green walls (Hunter et al., 2014; Medl et al., 2017) or for "vegetation" (Lorbek & Martinsen, 2015) and most cited works about GI (H Hartig et al., 2014; Tzoulas et al., 2007) widely defined it as natural and green spaces (Matsler et al., 2021). Finally, Jerome (2017) examined the concept of community-scale or small-scale green infrastructure, defining it as a "network of groups and projects which aim to deliver locally relevant functions and benefits to respond effectively to changing social and environmental needs".

Based on the reviewed Literature, this doctoral research considers that the urban green spaces or even singular vegetation inserted within a city's context will usually benefit social and environmental purposes. Thus, the mentioned elements could be considered part of a town's green infrastructure. However, some urban environments can showcase natural features that are not directly connected to a broader network of green spaces but can still provide localised environmental benefits. Thus, based on the analysis of the Literature on the theme, this thesis uses the term small-scale green infrastructures (SGI) as a conjunction of single trees, schoolyards, green walls, roofs, and private gardens. In other words, hedges, living walls, grass, and trees are considered SGI components, which are the focus of this research and are studied in depth. Furthermore, as explained in Chapter 01, this work focuses on two aspects that can be impacted by SGI components: health and comfort, using air quality and microclimatic conditions as indicators. Therefore, the following Literature review sections display and review the main findings of previously studied green infrastructure and the aforementioned central aspects.

2.5.2. AIR QUALITY IMPACTS

A few papers have argued that implementing urban green infrastructure is a possible passive measure to reduce air pollution within the built environment (McNabola, 2010, as cited by Abhijith et al., 2017). For example, in the last two decades, some studies have investigated the role of green infrastructure components (green barriers, green walls and roofs, and trees), emphasising their ability to remove pollutants from roadsides and other urban environments (Brantley et al., 2014; Hagler et al., 2012; Joshi and Ghosh, 2014; Pugh et al., 2012; Tong et al., 2016). Additionally, Barwise and Kumar (2019) described how different greenery could be used as barriers to reduce traffic emissions into adjacent areas; however, their work does not detail the composition of the green barriers. Concerning the vegetation's typologies, Abhijith et al. (2017) studies showed that trees led to air quality deterioration while hedges improved air quality. They also observed the need to express and standardise the vegetation density when the aim is to remove air pollutants. The abovementioned works affirm that GI components can modify the environment's air quality in a specific urban configuration: vehicular roads with adjacent vegetation. They comment on the impact of vegetation characteristics on diffing the particulate removal potential, highlighting that it can enhance or decrease its capacity, and the mentioned process varies according to the pollution types. For example, gaseous pollutants mainly comprise sulfur dioxide and carbon monoxide, ozone and gaseous photochemical pollutants, nitrogen oxides, volatile and semi-volatile organic compounds, and ammonia (Seigneur, 2019). The mentioned pollutant types are usually removed by urban vegetation as a result of a process that happens on the leaf surfaces and in stomata absorption (Fantozzi et al., 2015). Nowak et al. (2013,2006, as cited by Abhijith et al., 2017) studied the removal of O3, NO2, SO2 and CO in addition to PM10 by measuring the downward pollutant movement, which is the process of removing pollutants from the atmosphere caused by deposition processes, as scavenging, sedimentation and precipitation (Watson, Bates and Kennedy, 1988). They specify that the pollution removal values for each pollutant vary among different studied cities, according to their urban morphologies and climatic conditions. They also affirm that the velocity of the pollutant deposition process is directly altered by the leaf length, the tree coverage (or size), and other diverse climatic and microclimatic variables. The study finds that in the city of Syracuse, the PM2.5 total amount removed by trees annually was 4.7 tonnes. On the other hand, in Atlanta, the annual removal was 64.5 tonnes (Nowak et al., 2013). The evidence produced in the last years, as the ones previously presented, has raised awareness about the positive impacts of vegetation within urban settlements and encouraged government proposals to increase the green infrastructure in the cities.

Overall, trees are by far the most discussed of the different vegetation typologies, also when talking about governmental encouragement. Several initiatives in cities advocate for "greener" cities through programs that protect the existing vegetation and reforestation and increase tree canopy cover's percentage. For example, the Melbourne initiative aims to achieve a 40% cover using tree canopies and the "Million Trees" initiative in New York City (Salmond et al. 2016). Moreover, some studies have already presented the impacts and indications of how to use it properly in the urban environment, mainly through the lens of enhancing air quality. A work by Roy, Byrne, and Pickering (2012) established that until the moment when the research was developed, 33 different journals published a total of 115 original research papers on urban trees, which were then identified and reviewed. The finding illustrates and validates the topic's relevance for environmental studies, as seen in this thesis project and other disciplines. Seven articles discussed social benefits, with five presenting evidence of it, followed by twenty-eight related to positive economic contributions, with twenty-seven showing proof. There were also eleven papers discussing health and visual, positive outcomes. However, only five pieces displayed evidence of the effectiveness of urban trees on noise reduction. According to the articles analysed in their study (Roy, Byrne, and Pickering, 2013), "only 21.7% used a field experiment method, and only 14.8% used surveys and questionnaires". Moreover, they affirm that some of the studies revealed that it is widespread that tree plantations can worsen the concentration of the pollutant, and its density is directly connected to this phenomenon. The greater the tree density, the more particles will be trapped in the environment. One example is the work by Gromke and Ruck (2007), which, through the development of different case studies, established that trees increase traffic-induce pollutant concentrations within street canyons in all cases when compared to the same canyons without them. They observed that the tree crown porosity was an essential variable in defining the amount of pollutant dispersion within the canyon. Even when the crown porosity was expressive, the impact on the concentrations was still identified. However, they also observed that the mentioned factor is only influential at a certain level; when it goes under a specific threshold of pore volume fraction, the changes in pollutant concentrations are not further seen. Furthermore, Buccolieri et al., 2009, also studied urban street canyons; however, it focused on air movement and defined which wind direction would be more successful in removing particles, coupled with using trees. Still, they started by analysing the canyon without trees and found that perpendicular winds in relation to the canyon result in a higher particle concentration. They then affirm that when there is a larger aspect ratio, the decrease in the pollutant is higher in inclined wind directions. The study concludes that the aerodynamic effects of trees depend on wind direction (Buccolieri et al., 2009). Gromke and Ruck (2009) then added that a two-parallel-aligned row of trees within a wider street canyon is preferable when planning urban environments. They define this configuration as one that urban planners should consider instead of a narrow street canyon with a single row of trees to enhance air quality. Yet, their research, combined with Buccolieri et al. (2009) findings, indicate that the ones responsible for urban planning should also consider the prevailing winds on the specific area of implementation whenever planting urban trees.

The studies discussed so far demonstrate the knowledge developed concerning urban trees at such a level that it is already possible to produce some guidelines regarding urban design. However, Salmond et al. (2015) also debate the fact that even though there is available research focused on the urban and regional scale impacts of vegetation on human health and overall climate, there is a lack of in-depth understanding of the effects of street trees on an immediate (local) scale. They discuss the necessity of an approach focusing on the local scale to produce more precise data that defines the true level of positive or negative impact of urban tree interventions. Naturally, the relationship between trees and urban environment air quality remains a study subject, and there are examples of studies with a local scale focus. For example, Borna and Schiano-Phan (2020) showed a high concentration of particulate matter (PM) around trees in London. They've found that the trees significantly reduce air movement and cause pollutant particles, which are more noticeable in the cases of PM10 and PM2.5 levels and less when compared to NO2, to settle around and under their canopies (crowns). They confirm that planting trees does not necessarily mean better air quality in an urban environment when analysing local scale impacts while emphasising the importance of properly defining the vegetation types, scales, distribution and locations. Borna and Schiano-Phan (2020) indicate the necessity of further research to determine the exact effectiveness of trees and other SGI components within urban configurations throughout the year, including summer and winter scenarios. The abovementioned outcomes and statements stimulate this thesis' study of green infrastructure components (including trees) on a smaller scale inside a "contained" environment, generating more variations and data on the typologies and amount of vegetation for diverse periods of the year.

This doctoral research also evaluated material that was produced related to using other typologies of vegetation (not including trees) in street canyons, such as hedges and other smaller SGI components. Al-dabbous and Kumar, 2014 found that a vegetation barrier composed of climbing plants on the borders of vehicular roads effectively reduced Respiratory Deposited Doses (RDD). The RDD are nanoparticles that, during crossroad winds, were reduced by 36% through the vegetation mitigation potential (Al-dabbous and Kumar, 2014). Another study by Wania et al. (2012) of street canyons considers diverse scenarios with both hedges and trees. They found that the hedges had a higher removal rate when compared to trees and indicated that the results are explained by the further distance that trees have from pollutant sources. The trapping effect is enhanced as hedges are closer to the particles than tree canopies. Additionally, Gromke, Jamarkattel and Ruck (2016) indicated that hedges in a row can positively affect traffic pollution dispersion at the street level and within a canyon formed by building facades. They also establish that hedges can extensively remove the exposure to pollution particles of pedestrians and other inhabitants closer to the strongest polluted areas of the street canyons. However, the researchers indicate that the findings can't be absolutely connected to PM concentrations. This is due to the particle deposition on the vegetation's leaf surfaces, causing a filtering capacity concerning gaseous pollutants. They conclude that further research is needed to understand roadside hedges' particulate matter dispersion effect.

The findings above exemplify the existence of guidelines on applying hedges in street canyons and how substantially effective they can be in this geometric configuration. However, urban environment morphology is also shown to be an essential factor in the GI components of space. For example, Abhijith et al. (2017) affirm that trees within a street canyon can decrease air quality if the configuration is not planned adequately, while in more open environments, trees and hedges combined can act as barriers to improve air quality behind them. Other studies explored the outcomes of the GIs and the urban configuration. According to Wania et al. (2012), where air quality was worse, and the aspect ratio was increased, the vegetation removal rates were also enhanced. Additionally, Gallagher et al. stated that different solid barriers within the urban environment can potentially change the pollution particles' patterns of dispersion and concentration and improve air quality behind them. Moreover, the research found that combining control measures that are not vegetation and small-scale green infrastructure components could improve the air quality in local environments (Abhijith et al., 2017).

2.5.3. IMPACTS ON MICROCLIMATIC CONDITIONS

Several publications present the relationship between SGI components and environment temperatures, leading to the perception of human comfort. Studies showcasing the relationship between urban canyons and vegetation regarding thermal outcomes were also found. Di Sabatino et al. (2015, as cited by Abhijith et al., 2017) establish that trees can alter the vertical thermal distribution within the canyons. At night, the bottom layer becomes warmer than the canyon top, diminishing the vertical exchange even more. Santamouris et al. (2007) and Sailor (2008) established that green roofs could reduce indoor temperatures. According to previous studies, it is possible due to the improved insulation via the substrate and evaporative cooling that living roofs can provide. In 2008, Tsoumarakis et al. researched the thermal performance of living walls in various weather conditions. They found that closer to the vegetation in the walls, the dry bulb temperature (DBT) was lower than in the non-vegetated portion. At certain periods of the studied days, the difference between vegetated and non-vegetated walls achieved 1.5°C of air temperature. They established the existence of a thermal insulation air layer between the plant leaves and the wall. Silva, Santos, and Tenedório (2017) also explored the role of trees in the urban environment and their capacity to reduce the heat island effect in Lisbon's Mediterranean climate. The research proved that trees could regulate environmental extremes, mainly during morning and afternoon periods, creating comfortable thermal conditions for users. Also, my master's thesis concluded that adding trees reduced the ground area's mean radiant temperature by 25% (Silva, 2019). Within the context of cities in Brazil, in 2017, a study developed by Santos et al. in Salvador displayed that the lower terrestrial surface temperature (TST) found in the town was in areas covered with vegetation, marking 26°C, whilst the built areas presented higher temperatures, reaching 41°C. Finally, concerning school environments, Baró et al. (2019) established that the tree coverage in the yards is directly related to urban cooling benefits.

The Urban Heat Island effect was further studied through the years, showcasing its impacts. For example, a study in New York and Atlanta in the US defined that Urban Heath Island (UHI) in large urban areas can increase rainfall and the number of occurrences of convective storms (Bornstein and Lin, 2000). The impact of vegetated areas inside the urban environment on mitigating the UHI effect is also observed in diverse research. A different study developed in New York found an average of 2°C difference in air temperature comparing the most and the least vegetated areas (Susca et al., 2011). In Beijing, Zhang, Wu, and Chen (2010) demonstrated that the temperatures would be higher if the vegetation cover were reduced, and vice versa. Additionally, a study in Addis Ababa explored the relationship between tree coverage and heat patterns, stating that different tree species can modify the final effects. It was also found that for each one per cent drop in the canopy cover, the dry bulb temperature (DBT) drops by 0.02°C (Feyisa, Dons and Meilby, 2014). In Hong Kong, it was established that a specific arrangement of urban trees could create profound reductions in the temperature during the daytime, indicating that tree planting combined with proper urban planning can be sufficient to mitigate daytime UHI (Tan, Lau and Ng, 2016). It was also found a 4°C difference between the dense urban city environment and the extensive planted area of Hong Kong (Wong and Yu, 2005). They also revealed that reducing the energy load on buildings using shading elements and an evaporative cooling strategy can reduce reliance and improve the efficiency of mechanical air conditioning units. Additionally, US-produced data suggested that strategic positioning of plants could reduce domestic buildings' energy consumption by 20–40% (Akbari et al., 1997, 2001; Huang et al., 1990, as cited by Simpson, 2002). Huan et al. (1990, as cited by Cameron et al. 2012) estimated that each tree could offer over 270 kWh of cooling per day only by considering its evapotranspiration impacts. They conclude that trees are a significant SGI component in providing cooling through shade. Additionally, the urban trees' size, maturity, adjacent buildings' morphology and even the reflectiveness of their facades will change their cooling effect (Simpson, 2002, as cited by Cameron et al., 2012 and Akbari, 2001). As with many other research studies on the impact of vegetation on thermal comfort, this one also indicates the necessity of more detailed research to understand which type of buildings would benefit from which type of trees.

2.5.4. HEALTH

This thesis only tackles health impacts through the air quality and thermal comfort indicators. Even though this research will not define vegetation outcomes to mental health conditions, it is essential to establish that green infrastructure components could positively affect them. For example, Hodson and Sander (2019) commented on research that has documented positive outcomes concerning academic, cognitive and behavioural benefits when adding greenery to school environments. They've found that students perform better at school when studying in classrooms that provide views of outdoor vegetation, when there are areas with an expressive amount of tree coverage near their houses, and when they are allowed to use vegetated environments within their schools. They also indicate that vegetation within their daily use and mainly playing environments can reduce attention deficit and hyperactivity disorder and enhance working memory and attentional capacity. Other studies investigate the connection between open spaces and reducing health issues related to air quality. For example, a piece was developed using three major cities in the UK, and the result was that "if 20% of the population which lived 2km of an 8-20ha green space used this area every day of the week for at least 30 minutes to any outdoor activity, the NHS would save more than 1.8 million pounds each year" (Bird, 2004, as cited by Tzoulas et al., 2007). Also, Akpinar, Barbosa-Leiker, and Brooks (2016) drew a connection between a more significant percentage of Green Infrastructure components and reduced mental and general health complaints. Cavaleiro Rufo (2020) indicated that children's respiratory health is associated with higher biodiversity, which is a probable consequence of GIs and SGIs. Moreover, Akpinar (2016) declares that high school greenery could effectively enhance student's health. Additionally, school greenery positively impacted social behaviour and stimulated physical activity in younger kids, according to Van Dijk-Wesselius et al., 2018). Finally, different studies have also indicated dietary behaviour and educational impacts (Huys et al., 2017; Iojă et al., 2014).

2.6. CONCLUSIONS

This chapter illustrates the conditions of the megacities, underscoring the environmental issues that they cause to their inhabitants worldwide. It demonstrates the constant and predicted growth of Megacities within tropical climates, indicating that new ones can also be created in the next years. The literature also suggests that compared to North American and European ones, there is a lack of financial resources to tackle environmental problems in the southern hemisphere. Additionally, the air quality and thermal issues within the mentioned environment are discussed in this chapter. The findings show the importance of discussing solutions to reduce negative environmental impacts created by megacities, mainly tropical ones, underscoring the relevance of this thesis's focus on the city of Sao Paulo. Furthermore, the city's characteristics are discussed in more depth to justify the interest in the city and state of Sao Paulo. The literature shows the city's current overall negative thermal and air quality environment and demonstrates the necessity of discussing possible improvements to reduce vehicular pollutant concentration while providing shade and evaporative cooling of vegetation in the city and state.

The chapter extensively discusses vegetation within urban environments, highlighting its positive and negative outcomes. It explores the existence of these elements in cities from the 1900s until today. The literature illustrates how nature within urban settlements has been constantly discussed while being defined as necessary and a requirement to be considered by urban designers and policymakers. The Green Infrastructure and Small-scale Green Infrastructure concepts are also discussed by reviewing diverse literature, which often defines them as greenery within urban areas that can positively impact the inhabitants. The specific concept of small-scale green infrastructure (SGI), which permeates this doctoral research, is also defined by using examples from the literature. It is established that a combination of any scale of vegetation typologies (trees, hedges, grass, and other plants) that are impacting its immediate environment, when in a smaller size when compared to a city scale, can be called SGI. In other words, this section clarifies how the SGIs can, for example, be school yards with any green typologies applied to them. In addition to establishing how single trees, hedges and even living walls can be considered components of an SGI.

The chapter then delves into an extensive review of the impacts of GIs and SGIs on air quality, thermal comfort, and children's health within an urban context. The literature establishes that trees and hedges have the potential to increase and decrease different typologies of pollutant concentrations, depending on several factors. The main underscored variables are climatic and microclimatic conditions, vegetation typologies, density, location and the morphology of the studied urban environment. The chapter indicates, through the literature review, the necessity of studying the relationship between vegetation and air quality, producing more detailed data. Further research can increase the understanding of locating and distributing SGI components within the urban environment. Finally, the literature clearly states that vegetation is essential in dense cities for human thermal comfort, the overall mitigation of heat stress, and the urban heat island (UHI) effect. In addition to increase mental health and well-being within the context of children and teenagers in their school environment.

3. PUBLIC SCHOOLS IN SAO PAULO.

CONTEXT AND ARCHITECTURAL REVIEW.

3.1. INTRODUCTION

This chapter is generally dedicated to the public schools in Sao Paulo state and city, their importance, and architectural components. The chapter starts by explaining why the schools are the focus of this research, first through the study of children's health. Hence, the impact of thermal and air quality circumstances on the health conditions of children and teenagers is explored. Subsequently, it is narrowed down to why public schools were chosen by explaining the existing teaching structure within the city of São Paulo. The competent public bodies responsible for the projects of new schools and the refurbishment of existing ones are also briefly explored. The mentioned public bodies produce guidelines for the state public school design, consequently creating architectural patterns for the schools in the state and city, which this chapter presents and reviews. The architectural review is conducted through school examples in the city and state, where the architecture is analysed with a focus on environmental performance indicators. The aforementioned actions identify the natural and built elements that can be seen mostly repeated, which is the focus of the chapter. This chapter's research information on the importance of schools and their built structure characteristics is extremely important in defining field and analytical work methods. It is also essential to define this thesis' case study and the final guidelines that are proposed by the closure of this research.

3.2. WHY SCHOOLS?

3.2.1. CHILDREN'S HEALTH AND WELLBEING

As mentioned in Chapter 02, the lack of air quality for the human population, mainly within urban centres, is a recognised widespread issue, causing a high cost to the global economy, reaching US$ 5 trillion in total welfare losses by 2013 (Ferreti et al., 2015). The outcomes aren't less concerning regarding children's health worldwide. For example, according to the World Health Organization (Air Pollution and Child Health Report, 2018), worldwide 93% of all children live in environments with air pollution levels above the WHO guidelines, with one of every four children with age under 5 dying directly or indirectly due to environmental related risks. Air pollution not only exacerbates chronic diseases such as asthma but is also related to "the development of major pediatric diseases, including adverse birth outcomes, abnormal lung and neurodevelopment, and pediatric cancer, as well as obesity and cardiovascular disease risk" (Brumberg and Karr, 2021). Irritation caused by air pollutant particles causes significantly higher obstruction in young children's airways than adults due to their narrow airways. Additionally, a study developed by Behrens et al. suggested that children who live in residential areas with higher traffic occurrence have a higher risk of developing asthma and allergic rhinitis. Another research study finds examples of chronic inflammation in the lower respiratory tract and other health issues in children due to Mexico City's air pollution (Calderón-Garcidueñas, 2008). Calderón-Garcidueñas (2011) discusses how the teenage and child years are crucial periods of brain development related to cognitive, behavioural, and emotional changes and how air pollution can disturb this development, creating cognitive deficits during childhood. Air pollutants can also interfere with "signalling pathways related to the sequence of chemical messages that guide Lung growth" (Salvi, 2007). Finally, the long-term exposure to PM2.5, PM10 and NO2 in a study in China was associated with metabolic syndrome (Zhang et al., 2021).

The World Health Organization (2018) also affirmed that health threats in early childhood could develop lifelong health consequences. A significant percentage of the population in urban environments can face severe health issues related to exposure to bad air quality in childhood in a few years. Therefore, it is possible to affirm that there is an urgency in protecting children and young adults, and the necessary protective measures can be on different intervention scales. Calderón-Garcidueñas (2004) displayed that "long-term exposure to severe air pollution can cause neuroinflammation and Alzheimers to adult megacities residents. In addition to being a risk against adults, pollution is a possible cause of a series of complications for children and teenagers. Furthermore, not only can the pollution impact children severely, but they can also have a higher intake of pollutant particles than adults. It happens due to the increased levels of activities, requiring much higher air intake. Consequently, increasing the amount of particle intake (Salvi, 2007). Finally, some findings even indicate which pollutants are harsher against health. For example, according to Salvi (2007), the pollutants most implicated in the increased prevalence of respiratory tract symptoms are NO2, ozone, and particulate matter (PM10 and PM2.5). Other studies indicate that in the United States, from 2011 to 2016, 20% to 30% of the children (aged 0 to 17) lived in areas with PM2.5 concentrations higher than the standards for that period (Brumberg and Karr, 2021). The data presented was used as part of the guidance on which pollutants should be further studied in this research.

Within the specific context of schools, a study by Kings College London (2019) indicated the existence of pollution within the grounds. However, the study, which was said to be the most extensive to minor children's exposure to air quality (250 children involved), showed that the path to the school had five times higher NO2 concentration on the surrounding paths. Also, the study detected lower PM2.5 and NO2 concentrations on minor roads connected to the schools. The highest concentrations were recorded along the main roads. Finally, it was suggested that parents who drive to school can also contribute to high levels of air pollution close to the school. The findings above showcase the necessity of thoroughly discussing and planning the designs of the learning environments and their urban surroundings. The research also concluded that small changes in user behaviours are essential to improve air quality (Kings College London, 2019). In the UK, there are other works in which the outcomes can guide teachers and parents in mitigating air pollution and the potentially caused issues. For instance, the National Education Union and the British Lung Foundation joined efforts to encourage possible solutions. The mentioned organisations suggested creating a street outside the school without traffic, sharing transport schemes for the children, and discouraging parents from parking close to the school, among other initiatives. Furthermore, there are ventilation, thermal comfort, and air quality guidelines to be followed by schools in the UK to ensure quality indoor standards for children (Education & Skills Funding Agency, 2014). London's reality of discussing and implementing protective measures regarding children and young adults differs from São Paulo's. Most cities in Brazil lack specific and urgent measures and definitions to mitigate the problem that air deterioration can cause to younger inhabitants.

Another aspect discussed in the last chapter and one of the main pillars of the entirety of this doctoral research is thermal comfort. In addition to air pollution, heat discomfort can also deteriorate children's health. Children's sensibility to extreme weather can be considered as expected information, but the seriousness of the issue is revealed in the number of hospitalisations in areas with sweltering conditions. Overall, the highest effects are observed in younger kids (Xu et al., 2014a; Kovats et al., 2004; Onozuka and Hashizume, 2011; Green et al., 2010, as cited by Iñiguez et al., 2016). For instance, Xu et al. (2012) declared that children are more sensitive to hot and cold temperatures than adults due to behavioural, metabolic and physiological characteristics. They also establish that regarding allergic and infectious diseases, extreme temperatures can cause higher morbidity rates in children and that the ones under one-year-old are at the highest risk of heat-related mortality. According to Xu et al. (2012), children under five years are even more vulnerable to intense heat; from five to fifteen, the psychological behaviour patterns are similar. The mentioned researchers also discuss the need to assess children's vulnerability to extreme temperatures in more detail as they are behaviourally and physiologically a heterogeneous group.

Regarding the context of Brazilian cities, children's and adolescents' hospitalisations due to pneumonia, mental health conditions, neoplasms, asthma and renal diseases can be associated with the relationship between heat health issues and inter-city socioeconomic disparities (Xu et al., 2020). The findings are based on data collected from daily hospitalisations in the four hottest months of the year over five years, considering 1,814 Brazilian cities, covering 78.4% of the country's population. The study also concluded that less-developed cities presented more heat-associated children and teenagers' hospitalisations. Xu et al. (2020) further illustrate the overall impact of the heat increase on the population by affirming that a 4% increase in hospitalisations of all causes is caused by a daily mean temperature increase of 5 ˚C during the warmer season. Additionally, the mentioned correlation is fortified when average household income, urbanisation and literacy rates and GDP per capita diminish. Furthermore, air pollution and thermal distress are not isolated factors in the context of detrimental impacts on the young population's health. Some researchers identified the negative impacts of the combination of air pollution and excessive heat on, for example, asthma clinical outcomes (Tran et al., 2023). Additionally, Grigorieva and Lukyanets (2021) pointed out the existence of a vast amount of documentation on the association between respiratory health and air quality. Also, according to Han et al. (2023, as cited in Tran et al., 2023), the negative impacts of pollutant particles (PM) on respiratory health in European children are intensified during heatwaves. Finally, global warming causes a higher number of heat waves, which are the moments when air pollution rises. The high-temperature polluted air acts in synergy, increasing the negative health effects on children more than those from the pollution of heat alone (Grigorieva and Lukyanets, 2021). The findings presented so far through the literature review demonstrate the urgency of protecting children and adolescents against pollution and thermal health threats by creating protective measures. Moreover, as previously highlighted, the built learning environment becomes the main location of interest for applying the mentioned protective measures.

3.2.2. RELATIONSHIP WITH THE SCHOOL ENVIRONMENT

As previously explained the focus became the study of air quality and thermal comfort impacts on children and young adults within the context of architecture. To allow for that, a built environment typology should be selected with two main characteristics: concentrates the biggest number of this population and applies to different urban contexts following a similar architectural program. Naturally, the built school environment became a focus of this doctoral work. The quality and importance of these spaces to younglings' mental and overall health will be discussed below.

Income, gender, and geographical location are some of the variables responsible for the increase or decrease in children's and adolescents' attendance at school. For example, there are areas where few children attend school, such as a small village in Kenya (Larson and Verma, 1999). Diversi, Filho, and Morelli (as cited by Larson and Verma, 199) noted that in poor communities in Brazil, some schools have their day organized in only one hour and a half to accommodate around 5 shifts of students daily. However, the teaching system`s-built environments, within most of the global society, correspond to spaces where humanity spends the majority of its developing years. In 1999 Larson and Verma stated that adolescents spent (within an average of seven days) 4 to 6 hours per day emersed in school activities in North America. The same study found an average of 4.5 to 6.5 hours in Europe and 6 to 8 hours in East Asia. The mentioned information is contextualized in a post-industrial schooled population (where schooling is the norm). According to the mentioned authors cited literature, across the US and in Europe the school day itself varies from 5 to 7 hours. While East Asia has 8-hour days with a half day on Saturdays. Larson and Verma (1999) discussed how the hours spent in school are translated into the capacity to produce goods and services. Finally, how the time education level impacts lifetime earnings. According to Twum-Antwi, Jefferies, and Ungar (2020): "The school setting serves as the hub where young people first learn to develop cooperative social relations as well as the skills necessary to successfully maintain relationships through their interactions with peers and adults other than their immediate family members". Well-being, mental health, and cognitive development are other components directly connected to the learning environment. Rakesh, Zalesky, and Whittle (2023), researched the role of the school space on the brain structure. The findings suggest that when improving the built environment a more positive youth functioning is accomplished.

The impacts of the absence of a built teaching environment for the children and adolescent's physical and mental health could be exemplified during the COVID-19 pandemic (Buchanan, Hargreaves, and Quick, 2022; Fegert et al., 2020; Lopez-Bueno et al., 2021; Magklara et al., 2022; Singh et al., 2020). According to Lee, 2020, "the nationwide closures of schools and colleges have negatively impacted over 91% of the world's student population" (as cited by Singh et al., 2020). Different short and long-lasting effects on the young population when absent from school can also be spotted within the COVID-19 pandemic context. Schuurman et al. (2021) suggested that the school cease could contribute to education inequality which could result in social inequality. Also, Rana and Daniel (2023), indicate how the online learning substitution could have opened space for the violation of children's rights in India. The quality of the learning environment is also an essential factor. According to Higgins et al. (2005) in a literature review report produced by the University of New Castle, "Physical elements in the school environment can be shown to have discernible effects on teachers and learners". The mentioned study states that poor air quality and thermal distress can cause detrimental effects on the users. Such as lack of concentration, poor mood, and other negative impacts to the overall well-being. Lighting and acoustics are also indicated to have an impact. Furthermore, Higgins et al. (2005), suggest that the mentioned effects could finally result in lower attendance.

The literature review presented until this point of the chapter justifies the focus of this thesis on the specific population group composed of children and adolescents. More importantly, the findings also illustrate the importance of the physical learning environments. In the condition of a Ph.D. thesis in architecture and environmental design, the educational buildings are a perfect case study, when considering the intention of protecting younglings' health and wellbeing.

3.3. WHY PUBLIC SCHOOLS?

This research focuses not only on schools in general but more specifically on schools in tropical climates within or adjacent to megacities (as explained in the previous chapter). Moreover, within the context of the city and state of Sao Paulo, this research didn't target the overall body of schools. Instead, the focus is set on public education and the text below will explore it in more detail to justify that choice.

3.3.1. BRIEF HISTORY

The formation of the public school in Brazil was preceded by three main phases (Saviani,2004, as cited by Oliveira, 2007): from the beginning of the colonization process of Brazil (around 1549) to approximately 1759, the Jesuits were responsible for education. Followed by the educational reforms that happened until 1827. From 1827 to 1890, there were several intents to organize the educational system, including the distribution of administrative responsibility to provinces. Finally, the educational system administered by the state of Sao Paulo started in 1890 with the start of the republican regime in Brazil, constituting the beginning of the public schools known today. In 1890, different scholarly groups started being established in Sao Paulo, which served as a model for other states in the country phases (Saviani,2004, as cited by Oliveira, 2010). The next substantial educational system reform since the republic proclamation happened in the decade of 1920 with the name of "Escola Nova" (New School). The reform focused on the states of Ceara, Bahia, the Federal District, and Sao Paulo (Oliveria, 2010). From 1930 onwards, a revolution in the country caused a change in the education system with a unified national plan, making education for children obligatory and free. The valorization of the educational system in the country resulted in the construction of the first buildings designed and planned specifically for schools in the country. Consequently, in 1936 and 1937, Sao Paulo built the school buildings representing the mentioned changes (Oliveira, 2010).

1948 in the state is represented by the formation of the "School Agreement" ("Convenio Escolar"). The "School Agreement" established a pact between the Sao Paulo state government and the city's mayor to build and administrate public schools. The mentioned year also marks the start of the works developed by EDIF. The Building Department of the city of Sao Paulo (EDIF) was responsible for developing several public school projects (Takiya, 2010). Consequently, the period from 1949 to 1954, while the school agreement was in place, was known as the turning point of the architectural concepts of public schools in Sao Paulo (Oliveira, 2010; Takiya, 2010) The architect Helio Duarte was a teacher at the Architecture University of Sao Paulo and the team leader of EDIF. He was the main responsible for defining the program and architectural concepts of the schools. Additionally, he and the EDIF team started to design with modernist architectural principles and aesthetics (Romero, 2023; Takiya, 2010). Furthermore, public schools designed and built by EDIF were the first cases to demonstrate an architectural pattern and guidelines to be followed within the city. Regarding the state of Sao Paulo, the Directorate of Public Buildings ("Diretoria de Obras Publicas" – DOP) was the agency responsible for the education system. In 1953, the "School Agreement between the state and municipality ended. Furthermore, in 1960, the government established the state school construction fund ("Fundo Estadual de Construcoes Escolares" – FECE) until 1976. Afterward, FCE was substituted by "CONESP", the School Construction Company of the state of São Paulo. Lastly, in 1987, the Education Development Foundation ("Fundacao para o Desenvolvimento da Educacao" – FDE) was created and develops projects and builds schools throughout the state until today (Oliveira, 2010, Fundacao para o desenvolvimento da educacao, 2023 and Spira, 2015). Forwarding to the years from 2001 to 2004, another important mark was the creation of the Unified Educational Centres ("Centros Educacionais Unificados" –

C.E.U.). which was developed by the Department of Education of Sao Paulo's municipality. The aim was to take cultural and leisure spaces into the peripheral areas of the greater city which will be lately discussed in more detail.

3.3.2. SCHOOLS' STRUCTURE IN SAO PAULO

There are several school typologies in the city and state of Sao Paulo, being mostly divided by age. However, typologies are created to attend to specific cases. For example, there is the Education and Indigenous Cultural Centre (CECI) to attend to Indigenous children. Additionally, there is the Integrated Education of Young Adults and Adults (CIEJA) for anyone older than 14 who did not have access to a formal education system. Another example is the Childhood Coexistence Centre (CCI) to attend the children of municipal public workers. The main typologies representing the city's formal educational system are the CEMEIs, EMEIs, EMEFs, and EMEFMs. The Municipal Childhood Education (CEMEI) is for children from 0 to 5 years old. The Municipal Childhood Education School (EMEI) is the "kindergarten" and is the first step of the basic education system, attending children for 4 to 5 years. The second step is the Municipal Elementary School (EMEF) with children aged 6 to 14. Some EMEFs have the disponibility of functioning as what could be compared to "high schools", encompassing ages from 15 to 17. The mentioned schools are called "Escola Municipal de Ensino fundamental e Medio" (EMEFM), attending the ages of 6 and 17 (Secretaria Municipal de Educacao de Sao Paulo, 2019). As previously mentioned, one other important typology is the CEU. One of the main objectives is to provide each community with libraries, sports centers, and cultural centers connected to the CEIs, EMEIs, and EMEFs (Padilha and Silva, 2004).

The school year calendar in Sao Paulo mostly reflects the Brazilian school year calendar. It usually starts on the first days of February and goes until the half of December, with 20 days of break in July. A regular year will have students using spaces in school buildings for 200 days, including mornings and afternoons (Fundacao para o desenvolvimento da educacao, 2023). Most schools have morning students and afternoon students. The classes in the EMEIs start at 7:30 am and go until 11:30 am for the morning period. The afternoon classes happen from 1:00 pm to 5:00 pm. The EMEFs are from 7:00 am to 12:00 am and 1:00 pm to 6:00 pm. On a list actualized in October 2020, 101 schools (including EMEFs and EMEIs) have whole-day classes. It means the students in the mentioned schools have classes from 07:00 am to 6:00 pm (Fundacao para o desenvolvimento da Educacao, 2022). As shown in the information above, the public educational system in the state of Sao Paulo is a massive structure built in a span of several years. The school buildings and all the other aspects of the learning environment have been and continue to be carefully tailored. Thus, the whole system state and city-wise needs to follow similar rules and directions. Consequently, the built environment becomes similar architecturally and repeats, many times, the same constructive elements. The previously mentioned characteristics will be discussed next, and their repetition is the main reason to focus on public schools in this doctoral work.

3.4. THE ARCHITECTURE

3.4.1. OVERALL COMMENTS

The interest in Modern Architecture for public schools as an architectural concept can be seen in the speech of Almeida Junior, the Director of Education of Sao Paulo's state (1936, as cited by Oliveira, 2010): "The opinion was frankly favorable to the modern architecture. The sober modernism, discretely sentimental, closer to the French balance than the baffling boldness of the Mexican compositions". In 1936, there were already some considerations about the environmental conditions within the orientations for school buildings. For example, the buildings' orientations, air movement inside the classrooms, and the daylight. Moreover, Francisco Prestes Maia (1936, as cited by Oliveira, 2010) developed a study about solar radiation and the climatic differences between cities on the coast, the capital, and other cities in the state's countryside. He was also interested in the buildings' occupation at different periods of the day and the uses that informed the characteristics of the building regarding the environment. It is possible to state that those considerations could sometimes be vague and not always properly implemented in the final buildings. However, the mentioned considerations are still extremely essential today and, in different ways, informed several school projects within the state. With today's knowledge and tools, buildings should undergo an assessment regarding environmental comfort to indicate improvements when needed.

According to Takiya (2010), the buildings designed during the period of the "School Agreement" had a modern character with a simple and cheap constructive (structure) system. The buildings were cheap because of the choice of simple and resistant elements. For example, concrete structure systems and internal floors are made of resistant and cheap ceramic. Additionally, windows with steel structure and single clear glazing were used. The false ceiling was usually under a concrete slab; when not, it was made with plywood as a thermal insulator. Finally, the roof systems would be of wood with fiber cement tiles. The mentioned principles of affordability and durability were followed in the development of the C.E.U.s in the 2000s. However, the CEUs are usually composed not only of conventional schools, as exemplified so far, but also buildings with cultural programs open to the surrounding community. Thus, it is a massive structure that usually occupies much bigger terrains and has more expressive built areas when compared with the EMEIs and EMEFs previously discussed. Nevertheless, the CEUs also presented the use of prefabricated elements made of concrete and steel for the structure (Takiya, 2010). The introduction of prefabricated elements probably induced the architects to standardize their structure systems and the overall organization of the buildings even more. Consequently, different buildings throughout the city would also present more uniform architectural solutions.

As previously mentioned, FDE is the state's Foundation for the Development of Education (Fundacao para Desenvolvimento e Educacao), and it has produced several catalogues/manuals, which are being used to this day. The mentioned material is dedicated to architects, builders, and administrators and must be followed in each school. There is a set of manuals called "technical catalogues" available online on their website (Fundacao para o Desenvolvimento da Educacao, n.d.). The production of guidelines naturally resulted in school buildings throughout the state and city with similar characteristics. The mentioned characteristics are relevant to this thesis as they indicate which architectural elements are repeated so they can be selected for further examination.

3.4.2. EXAMPLES

The examples illustrate the main orientations where the components are located. They also show the size of the terrains (open areas), the level of vegetation, and the context surrounding the schools. All the cited information implies the environmental performance of each case. Moreover, the examples of school buildings in the city and state will show the architectural similarities and differences between buildings. This section aims to showcase a clear architectural pattern by displaying components that are repeatedly used and the ways they are being applied. Furthermore, these buildings will be analyzed with a focus on environmental design, highlighting the already strong environmental strategies applied and what could be further improved.

SCHOOL PROF. MARCOS ALEXANDRE SODRE

Figure 3.4.01 - Top view of the of the School Prof. Marcos Alexandre Sodre, showing context (Google, 2024).

Figure 3.4.02 - Western facade of School Prof. Marcos Alexandre (© Pedro Kok, 2009).

The first example is the State School Prof. Marcos Alexandre Sodre, designed by FGMF architects, which was concluded in 2008. The school is in Varzea Paulista, in the Sao Paulo state, 57 km south of the city. It comprehends two main rectangular blocks, one with a multi-sport covered court and the other for all indoor school activities (figure 3.4.04). The building's structure is made of prefabricated elements in concrete with a ground floor plus two floors. Moreover, the classrooms face east and west, with the main circulation areas on the first and second floors in the middle (figure 3.4.04). Consequently, the main block has east and west facade openings (figure 3.4.04). The west façade is completely treated with perforated concrete elements, commonly called cobogos in Brazil (figure 3.4.02 and 3.4.03 (b)). The cobogos work as a second skin to the building, and beside it are small balconies accessed by the glazed openings of each classroom/indoor space, as seen on the floor plans. Overall, the perforated concrete elements are a visually interesting and environmentally effective solution. The second skin reduces direct solar radiation entering the indoor areas during the hottest hours (afternoons). The mentioned elements also help prevent classroom glare, mainly during the afternoon. Simultaneously, the cobogo wall will not obstruct air movement, increasing thermal comfort indoors. The main disadvantage of the mentioned element is that it will also block the direct sun radiation during colder periods. The blockage eliminates the possibility of passively heating the space through direct radiation. The East façade is also treated with a second skin. However, instead of cobogos, there are perforated aluminium roof tiles (figure 3.4.03 (a)). The elements help reduce the sun's radiation and daylight, even at a lower level than the cobogos (Fernandes, 2012). Shading that provides lower sun obstruction is adequate for a façade facing east (as applied in this school – figure 3.4.04) due to lower temperatures in the morning.

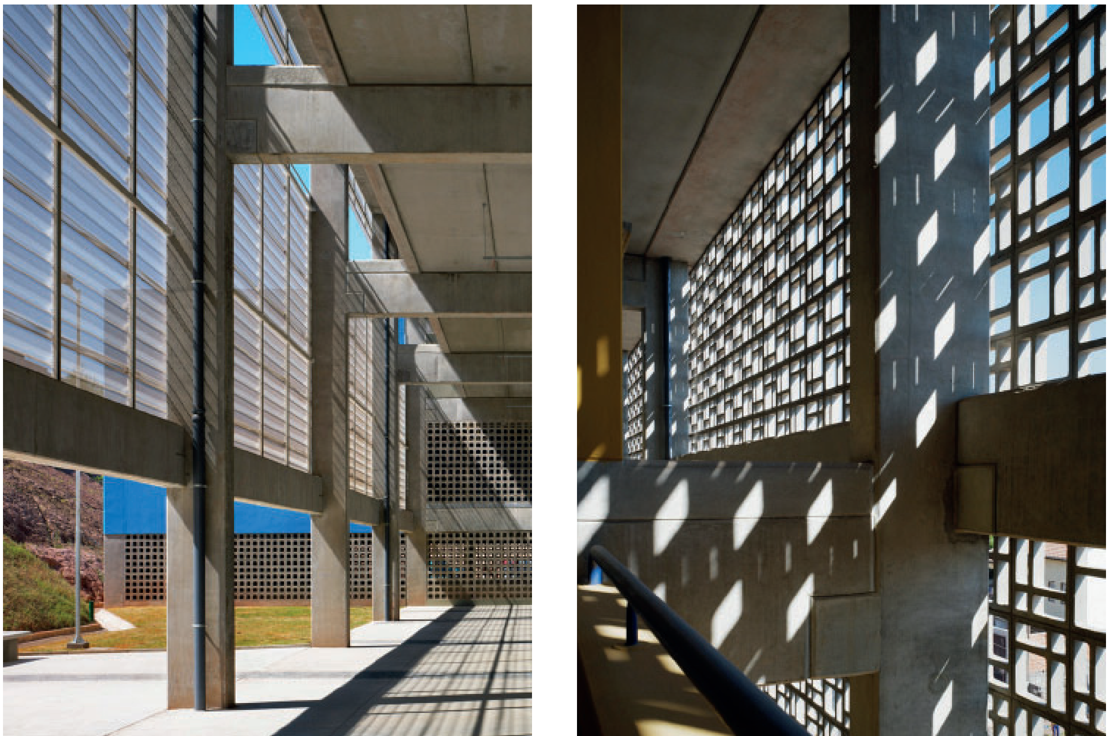

(a) *(b)*

Figure 3.4.03 (a) - Facade of School Prof. Marcos Alexandre with perforated aluminium roofs as facade treatment (© Pedro Kok, 2009). **(b)** - West facade of the school with concrete cobogos (© Pedro Kok, 2009).

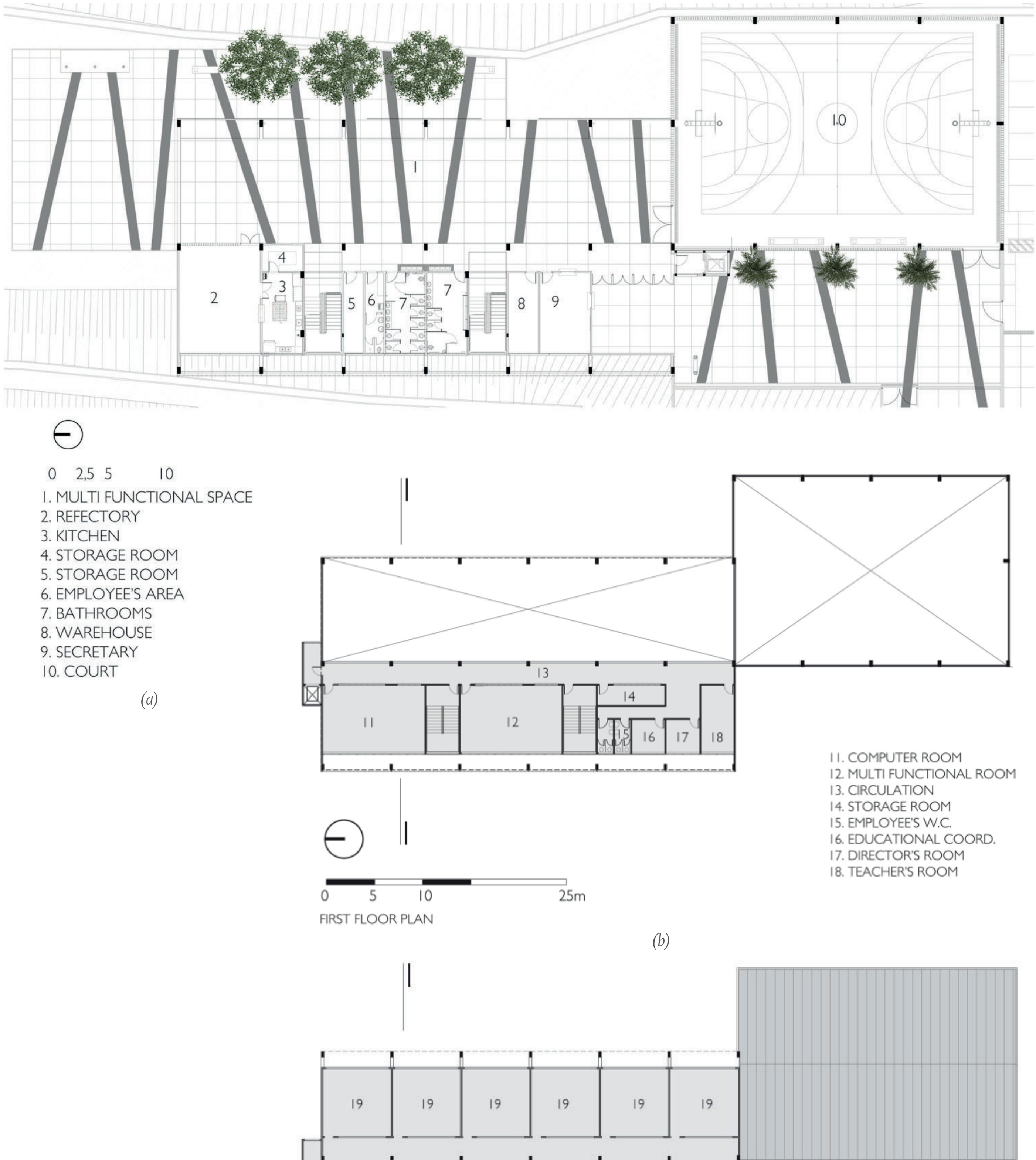

Figure 3.4.04 (a) - Floor plan of the Ground Floor of School Prof. Marcos Alexandre (FGMF Architects). **(b) -** Floor plan of the First Floor of School Prof. Marcos Alexandre (FGMF Architects). **(c) -** Floor plan of the Second Floor of School Prof. Marcos Alexandre (FGMF Architects).

SCHOOL PARQUE DOURADO V

Figure 3.4.05 - Top view of the of the School Parque Dourado V, showing context (Google, 2024).

Figure 3.4.06 - Facade of the Northewestern School Parque Dourado V (© Oliver de Luccia, 2007).

Figure 3.4.07 - Facade of the Southeastern School Parque Dourado V (© Carlos Kipinis, 2007).

The second example is the Parque Dourado V School, designed by Apiacas Architects and located in Ferraz de Vasconcelos. Unlike the previous school, this one is situated in a slightly denser urban context, with fewer surrounding vegetation areas (figure 3.4.05). The municipality is part of the greater metropolitan area of Sao Paulo. The school is 600 square meters bigger than the Varzea Paulista School and was built in 2007. However, the structure is also made of prefabricated concrete elements, with the addition of metallic structures in certain areas. The project is solved in one unique volume, including a multi-sport court (figure 3.4.08). Moreover, this school is also organised on three different levels, yet the circulation areas and access to the classrooms are mainly close to the facades (figure 3.4.08a). The mentioned areas create balconies that link all the rooms (figure 3.4.07). The Parque Dourado V building has two main facades with openings facing northwest and southeast. Once more, it is possible to observe a second skin made of cement cobogos placed on the most exposed façade (northwest as seen on figure 3.4.06). As explained in the first school example, the mentioned element is placed on the preferred façade, causing positive impacts for hotter periods and negative ones for colder days. The southeast façade, less exposed to direct sun, has no vertical shading element as a cobogo skin. However, the classroom façades are recessed and protected by balconies for circulation (figure 3.4.07). The open circulations function as horizontal shading and protect the indoor areas from direct radiation and possible glare (Fernandes, 2011a).

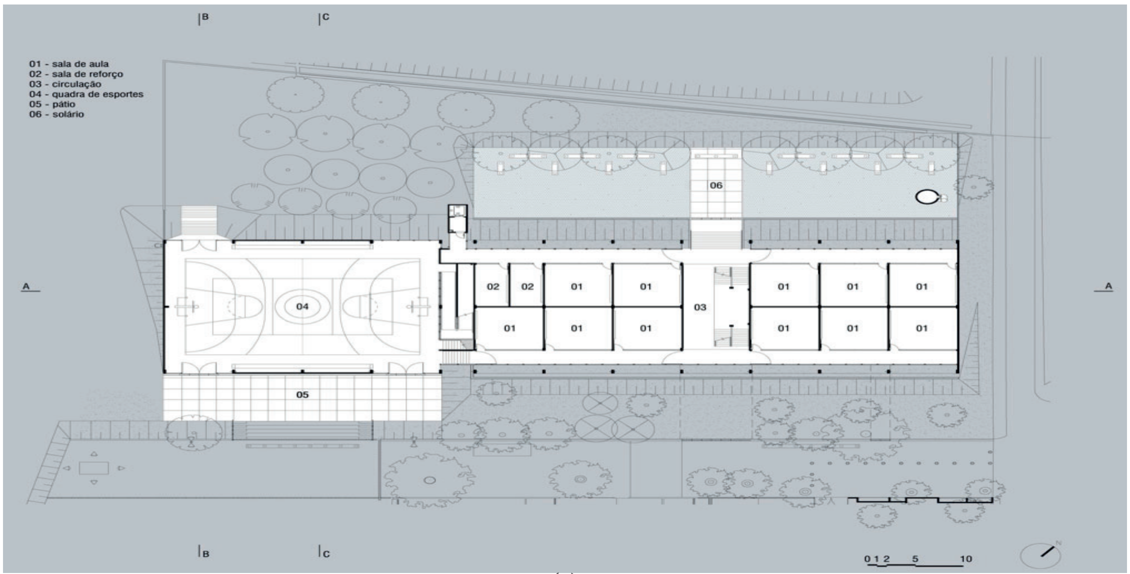

(a)

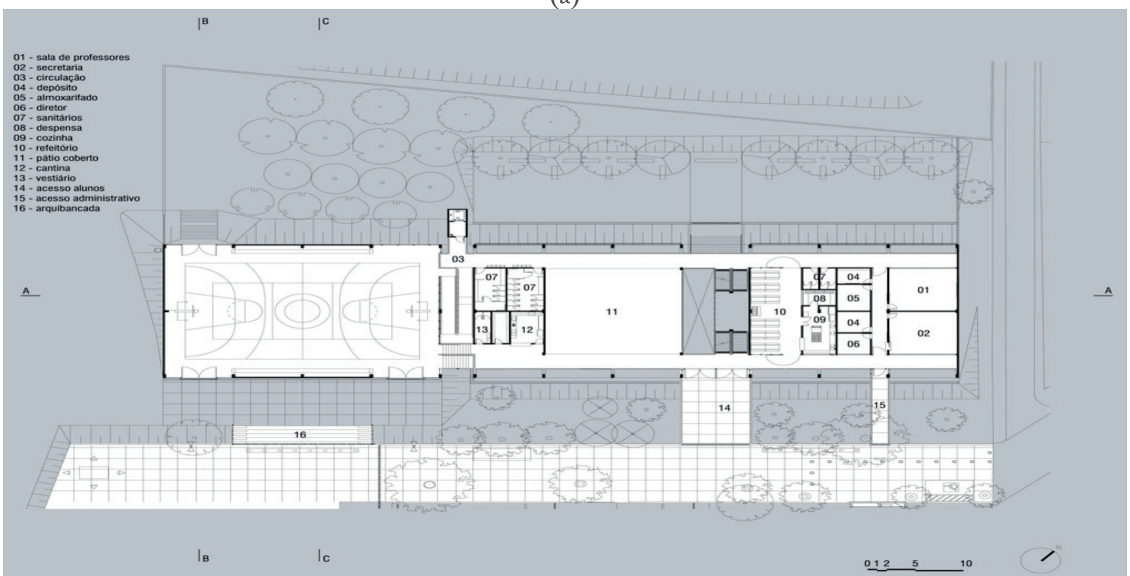

(b)

Figure 3.4.08 (a) - Floor plan of the Ground Floor of School Parque Dourado V (Apiacas Architects). **(b) -** Floor plan of the First Floor of School Parque Dourado V (Apiacas Architects).

STATE SCHOOL SELMA MARIA MARTINS CUNHA

Figure 3.4.09 - Top view of the of the State School Selma Maria Martins Cunha, showing context (Google, 2024).

Figure 3.4.10 - Southern and Eastern facades of State School Selma Maria Martins Cunha (© Carlos Kipinis, 2008).

Figure 3.4.11 - Nothern Facade of State School Selma Maria Martins Cunha (Google Maps, 2024).

The next example is a school building in the municipality of Votorantim, 105 Km east of Sao Paulo. The grupoSP architects designed the State School Selma Maria Martins Cunha, built in 2008. Similar to School Prof. Marcos Alexandre Sodre, this site is close to an expressive vegetated area (figure 3.4.09). The program is solved in two main blocks connected through covered ramps (figure 3.4.12). The same prefabricated structure elements previously spotted can be seen in this example: concrete beams, pillars, and metallic roofing elements (figures 3.4.10 and 3.4.11). Yet, this building presents a different solution as a façade design than the commonly spotted cobogos. The south/southwestern façades in this school building are treated with fixed wooden vertically placed fins, creating a second skin (figure 3.4.10). On the main block, the elements are placed before indoor circulation areas and classrooms' glazed windows on the first and second floors. Considering that the mentioned façade is not facing "true south" (figure 3.4.12), there are some hours in the afternoon that the façade will receive direct sun. Thus, it is possible that the wooden panels could be considered adequate to protect the interior areas. However, it could also be considered an "overkill", not allowing sun radiation to go through in colder periods. Finally, the multi-sports court block has all facades exposed and treated with the same fins and without solid facades, which could create thermal discomfort in colder periods. The north/northeast façade has no second skin; however, the structure and roof offset the building line. Additionally, concrete horizontal fins are placed, extending the solar protection (figure 3.4.11). Considering the sun angles facing the north/northeastern façade, the structures and extended roofs perform well to reduce direct solar irradiation on hotter days. However, some level of vertical elements may be added. The mentioned element also allows for direct sun incidence during colder periods due to lower sun angles. Succinctly, the design in this specific orientation successfully enhances the thermal comfort of indoor areas in different seasons.

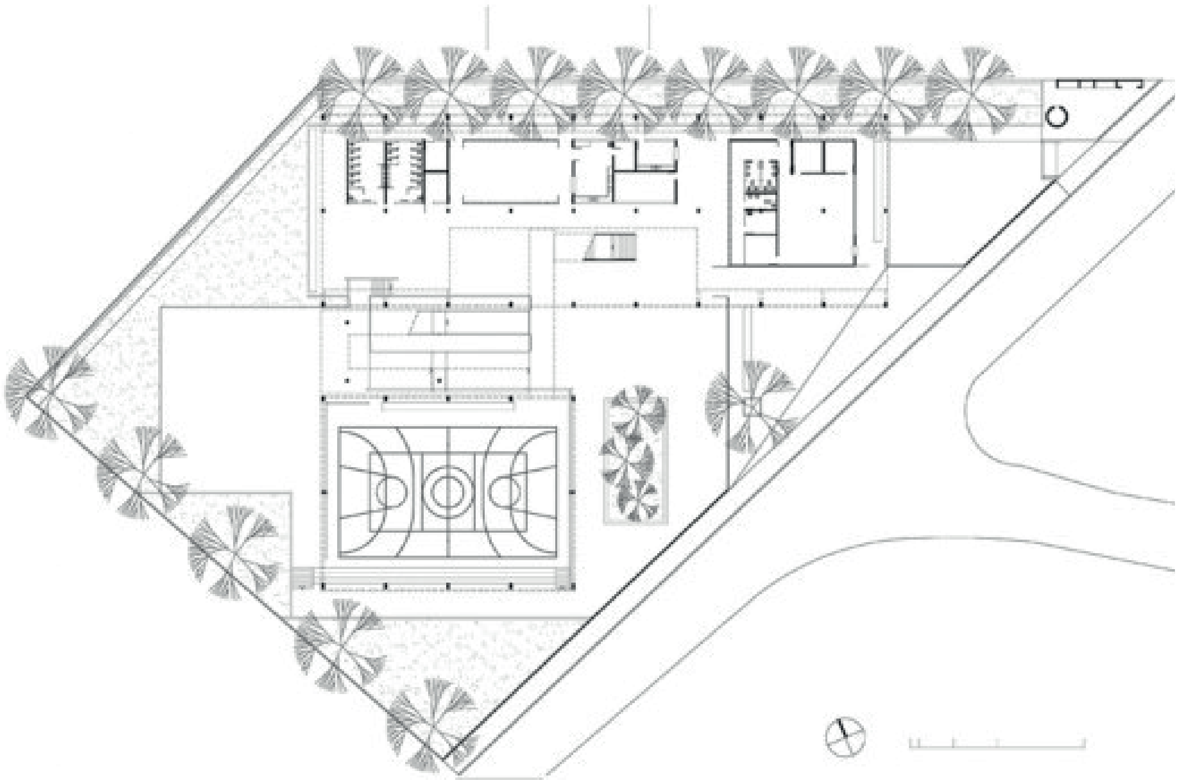

Figure 3.4.12 - Floor plan of the Ground Floor of State School Selma Maria Martins Cunha (grupoSP architects)

STATE SCHOOL PARQUE SAO BENTO

Figure 3.4.13 - Top view of the of the State School Parque Sao Bento, showing context (Google, 2024).

Figure 3.4.14 - West Courtyard of State School Parque Sao Bento (© Bebete Viégas, 2008).

Figure 3.4.15 - Facade facing courtyard without cobogos on the State School Parque Sao Bento (© Bebete Viégas, 2008).

The State School Antonio Carlos Lehman or Parque Sao Bento by bvy architects, built in 2008, comprises almost 4,000 square meters of built area. The school is for 6 to 10 years old and is in Campinas, which is one of the state's biggest cities, 99 Km northwest of Sao Paulo. It is surrounded by low-rise residential buildings and a massive open area with grass (figure 3.4.13). Unlike the projects exhibited until this point, this school program is organised in a building with an "H" shape with two main blocks and only two floors (figure 3.4.16). Nonetheless, the prefabricated structure, roofing elements, and concrete cobogos are spotted again in this school (figures 3.4.14 and 3.4.15). The building is one more example of the perforated panels in concrete possibly being applied in inadequate orientations (Fernandes, 2011c).

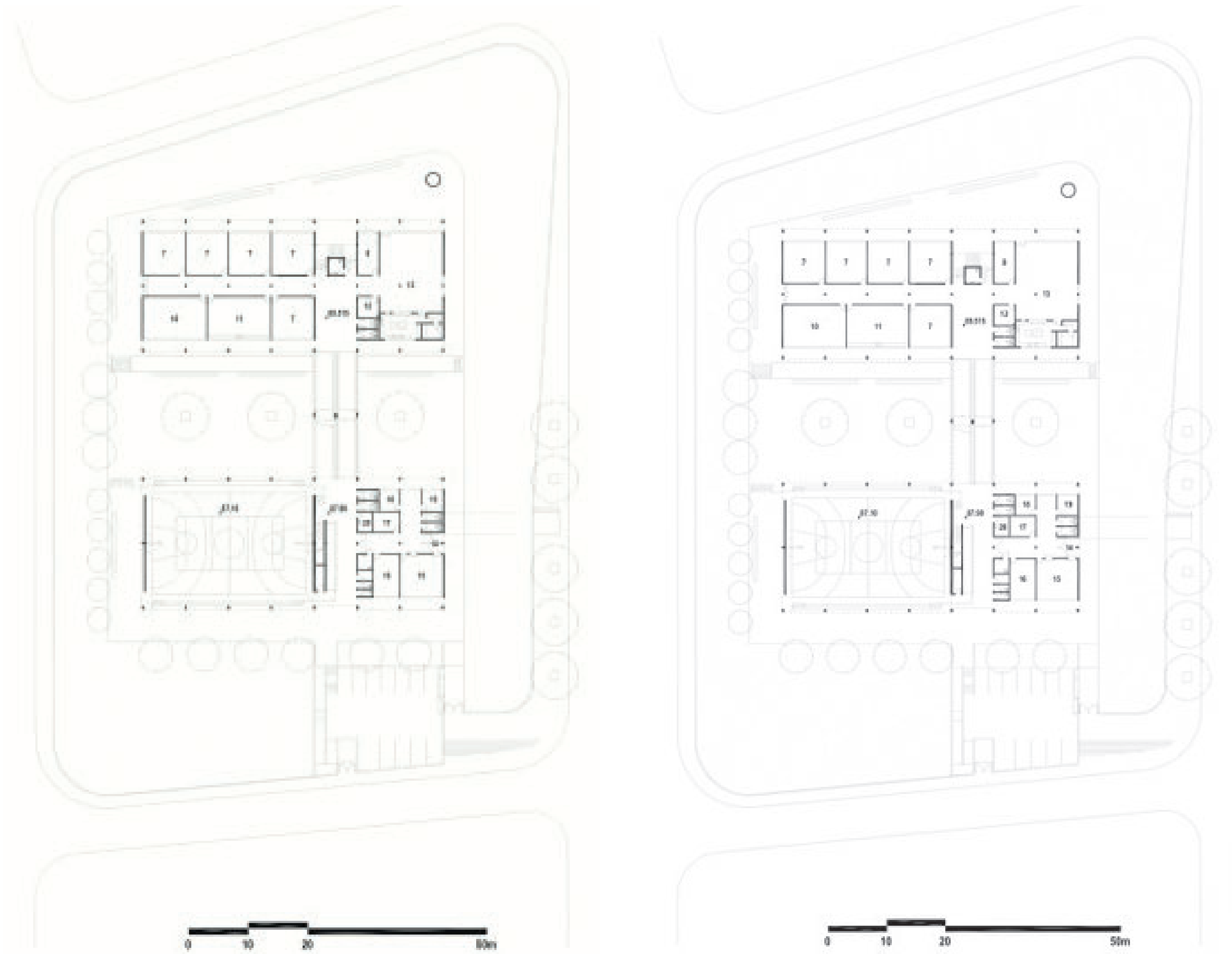

(a) (b)

Figure 3.4.16 (a) - Floor plan of the Ground Floor of State School Parque Sao Bento (bvy architects). **(b)** - Floor plan of the First Floor of State School Parque Sao Bento (bvy architects)

STATE SCHOOL JARDIM MARIA HELENA III

Figure 3.4.17 - Top view of the of the State School Jardim Maria Helena III, showing context (Google, 2024).

Figure 3.4.18 - Southeastern View of State School Jardim Maria Helena III (© Nelson Kon, 2006).

Figure 3.4.19 - Southeastern View of State School Jardim Maria Helena III (© Nelson Kon, 2006).

The State School Jardim Maria Helena III was designed by + K Architects, built in 2006, and located in the Municipality of Baruaeri, within a low-density urban settlement (figure 3.4.17). From all the examples in this chapter, this school is the only one in an area with a massive vegetated area (forest that can be seen on figure 3.4.18). The building is another example of using cobogos made of concrete on all the facades (figure 3.4.18 and 3.4.19). This project has the program solved in one unique block divided into two floors (figure 3.4.20). The school showcases two main facades, one facing east/southeast and the other west/northwest, with the exact design solutions. The Jardim Maria Helena is another example of the lack of green spaces surrounding the building and the same shading elements used indiscriminately (Fernandes, 2011b).

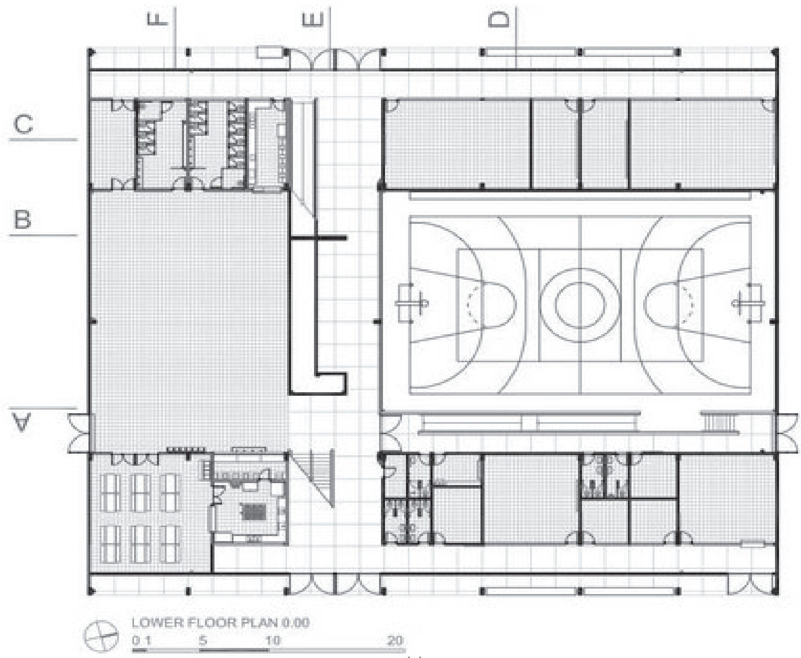

(a)

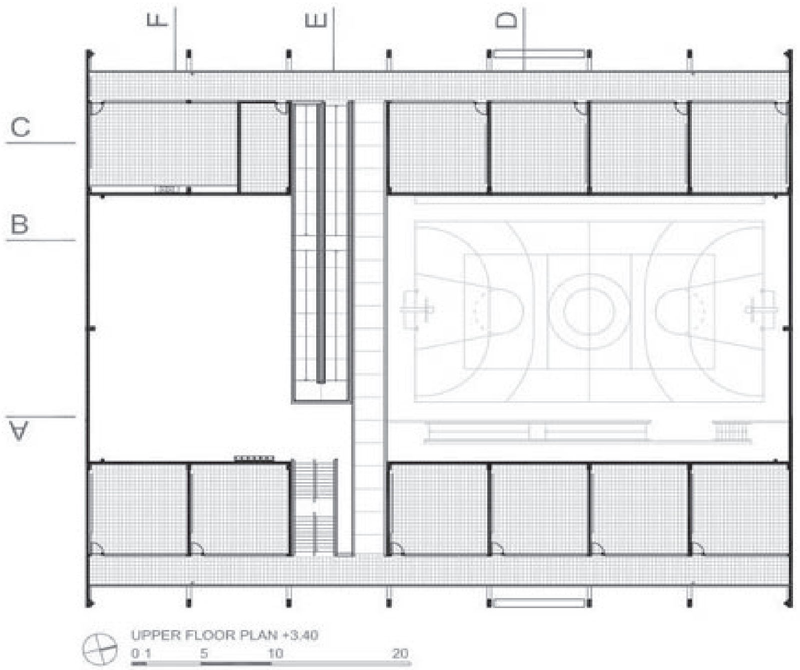

(b)

Figure 3.4.20 (a) - Floor plan of the Ground Floor of State School Jardim Maria Helena III (+K architects). **(b)** - Floor plan of the First Floor of State School Jardim Maria Helena III (+K architects)

STATE SCHOOL JARDIM UMUARAMA

Figure 3.4.21 - Top view of the of the State School Jardim Umuarama, showing context and with the site highlighted (Google, 2024).

Figure 3.4.22 - View of the Northwestern facade of State School Jardim Umuarama (© Nelson Kon, 2005).

Figure 3.4.23 - View of the Indoor area of State School Jardim Umuarama (© Nelson Kon, 2005).

This school building displays one more example of using perforated elements (cobogos), a prefabricated concrete structure, metal roofing elements, and metallic tiles (figures 3.4.22 and 3.4.23). However, this example displays cobogos in clay (3.4.22). The State School Fernando Gasparian was built in the city of Sao Paulo in 2005. The Estudio 6 architects' design resolved the program as a unique building with four levels (figure 3.4.25). This building has a main façade facing northwest (figure 3.4.23) and another oriented southeast (figure 3.4.25). Once again, both facades were designed the same way, with the perforated facade on the multi-sport court level and glazed windows in the classrooms on the other levels (Kon, 2018).

Figure 3.4.24 - View of the multi sports court of State School Jardim Umuarama (© Nelson Kon, 2005).

Figure 3.4.25 - View of the Southeastern facade of State School Jardim Umuarama (© Nelson Kon, 2005).

STATE SCHOOL SALVADOR ROMANO

Figure 3.4.26 - Top view of the of the State School Salvador Romano, showing context (Google, 2024).

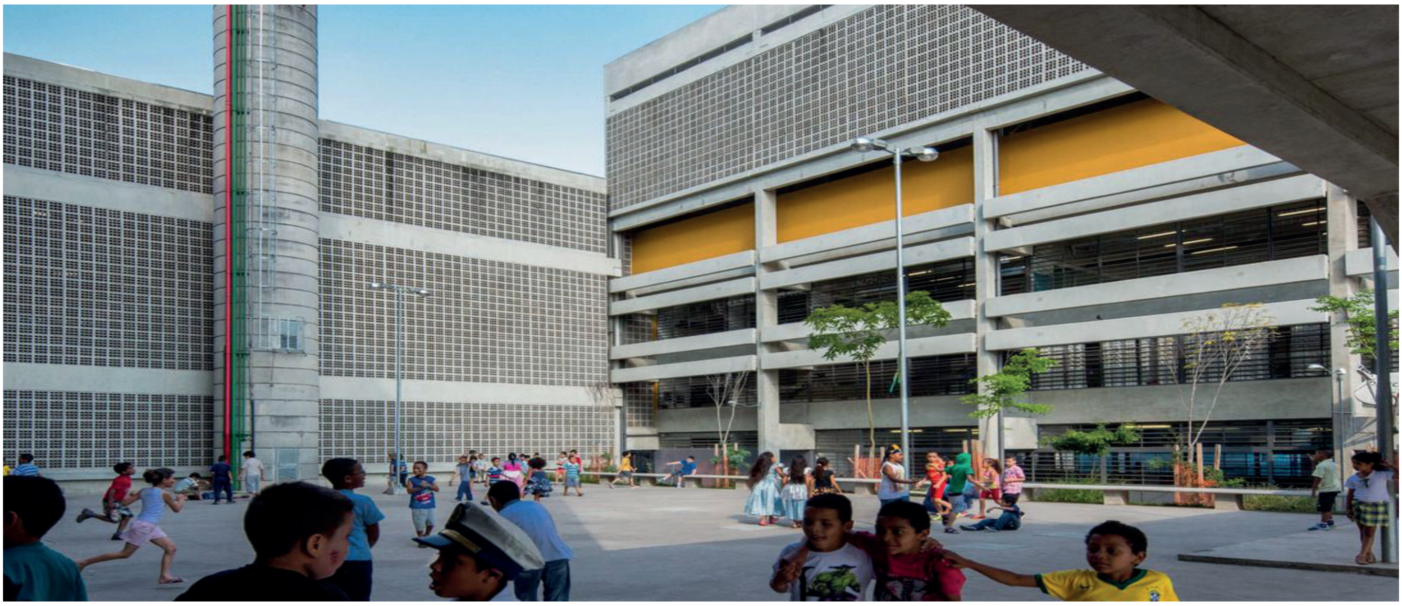

Figure 3.4.27 - View of the courtyard of State School Salvador Romano (© Pedro Napolitano Prata, 2008).

The State School Salvador Romano, also in the city, was designed by H+F architects and concluded in 2008. The building is one more example of using the components seen repeatedly so far with different program organisations and urban contexts (figure 3.4.26). However, that is the only school from this list of examples arranged into two shorter blocks, facing each other. In addition to the mentioned blocks, one smaller built mass is located on the east to connect all floors of the main blocks (figure 3.4.28). Also, there is a minimal mass on the west side of the terrain, connected to the bigger blocks, but only on the ground floor and first level (figure 3.4.28a). The mentioned elements form a main building in a “courtyard shape” with an open plaza. Finally, there are also two smaller buildings with ground floor and first pavement on the southern portion of the terrain (ArchDaily Brasil, 2020). Different from all the schools shown so far, the main building of this one has facades located on the edge of the terrain, directly connected with the sur-rounding pedestrian and vehicular roads. There isn’t a vegetated open area between the indoor spaces and the roads, functioning as “buffer” towards the conditions beyond the school`s land. Consequently, the classrooms and internal spaces are more exposed to the pollution from outside the terrain boundaries. However, is possible to indicate that the courtyard, where the students spend their free time, will be protected by the built blocks, and present a better air quality (figure 3.4.27). Additionally, the classrooms facing the private open area at least on the lower levels will receive air with lower pollution levels. While the classrooms facing the terrain boundaries will be directly connected with the pollutants. Finally, the courtyard could be a good place to add trees and other SGIs that could diminish the thermal discomfort and hotter periods without increasing pollutant concentration due to buildings protections against sources. The recessed facades and the extensive use of cobogos are appropriate to reduce thermal discomfort in indoor areas. However, the facades facing south could be designed without such massive shading system impacting the indoors with enhanced daylight. Likewise, the circulation block is in the eastern area of the terrain while if placed on the west would protect the patio from direct sun radiation during hours of more extreme temperatures (afternoons).

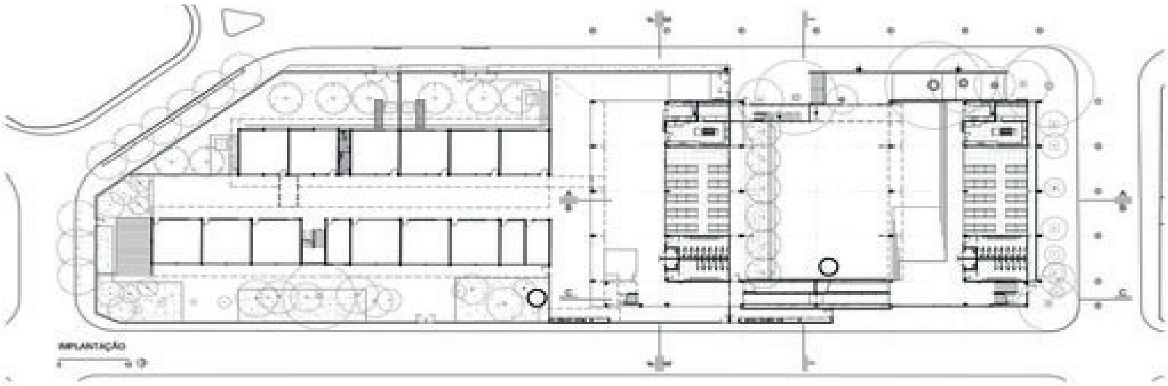

(a)

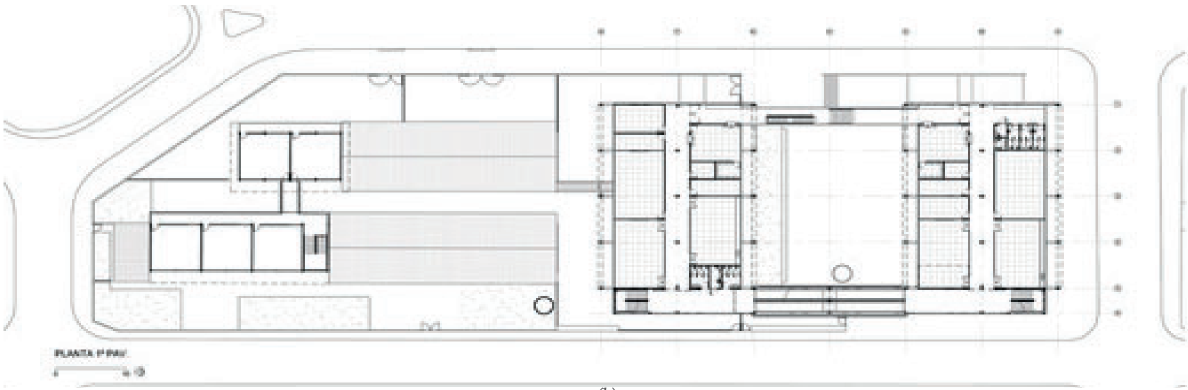

(b)

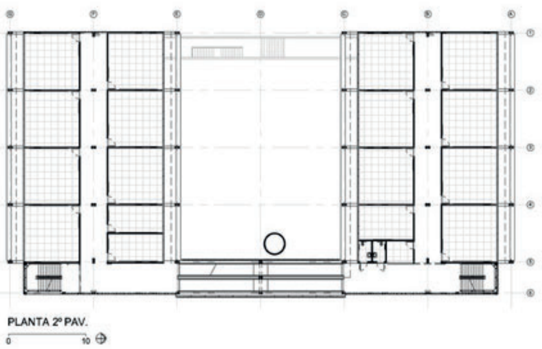

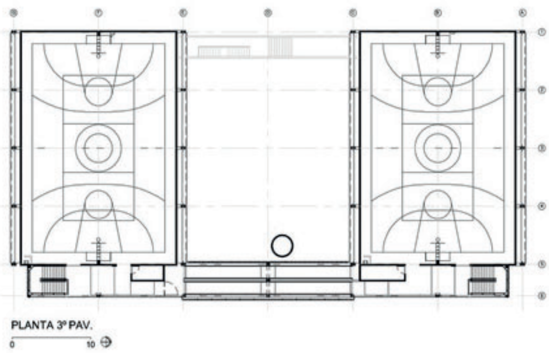

(c) *(d)*

Figure 3.4.28 (a) - Floor plan of the Ground Floor of State School Salvador Romano (H+F architects). **(b)** - Floor plan of the First Floor of State School Salvador Romano (H+F architects). **(c) -** Floor plan of the Second Floor of State School Salvador Romano (H+F architects). **(d) -** Floor plan of the Thrid Floor of State School Salvador Romano (H+F architects).

STATE SCHOOL TELEMACO MELGES

Figure 3.4.29 - Top view of the of the State School Telemaco Melges, showing context (Google, 2024).

Figure 3.4.30 - Nothern Facade of State School Telemaco Melges (© Nelson Kon, 2004).

Figure 3.4.31 - Southern Facade of State School Telemaco Melges (© Nelson Kon, 2004).

The State School Telemaco Melges is a project by UNA Architects in Campinas. The building was finished in 2004, and the program is resolved in one unique rectangular block with main façades facing south/southwest and north/northeast (Fracalossi, 2011 - see figure 3.4.32). This school is the first one from the examples that used translucid plastic elements on the facades. Moreover, once again, both facades are treated equally (figures 3.4.30 and 3.4.31). The mentioned façade treatment reduces glare and filtrates solar radiation. Each plastic element is positioned at an angle that allows airflow, yet it is fixed. Consequently, the air movement can be reduced, causing possible thermal discomfort. Lastly, the used material could not be the most efficient in reducing direct solar radiation, mainly in the north-northeast façade. Thus, some thermal discomfort could be expected during the hottest periods of the day.

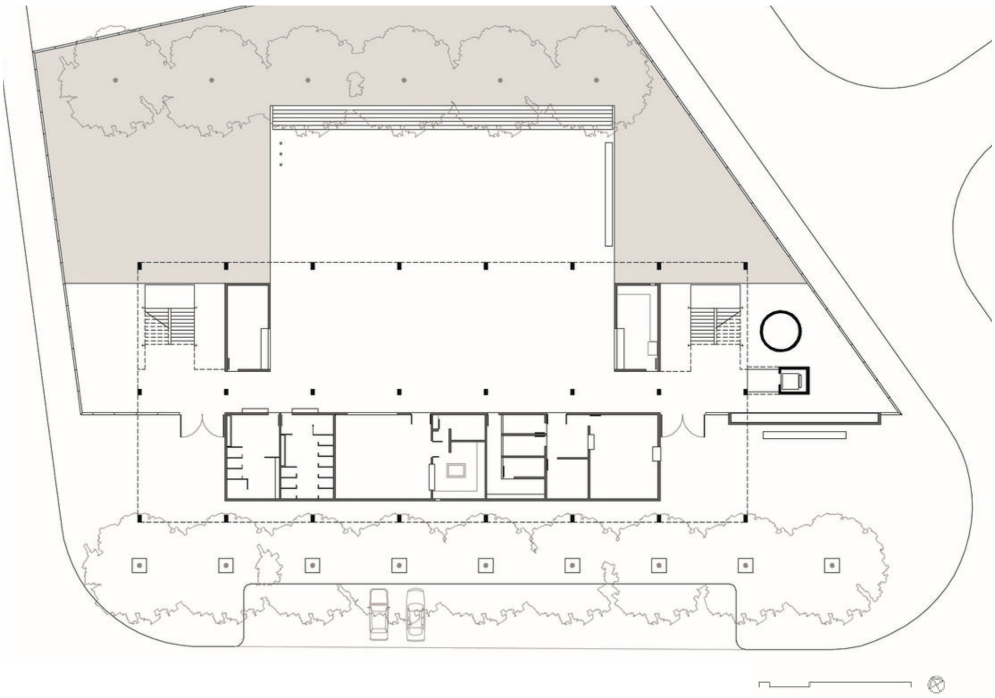

(a)

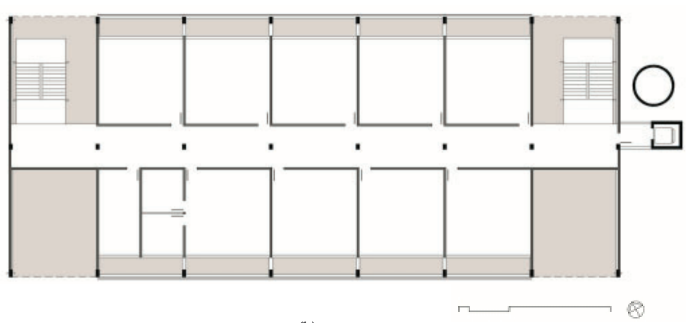

(b)

Figure 3.4.32 (a) - Floor plan of the Ground Floor of State School Telemaco Melges (UNA architects). **(b)** - Floor plan of the First Floor of State School Telemaco Melges (UNA architects).

STATE SCHOOL NOVA CUMBICA

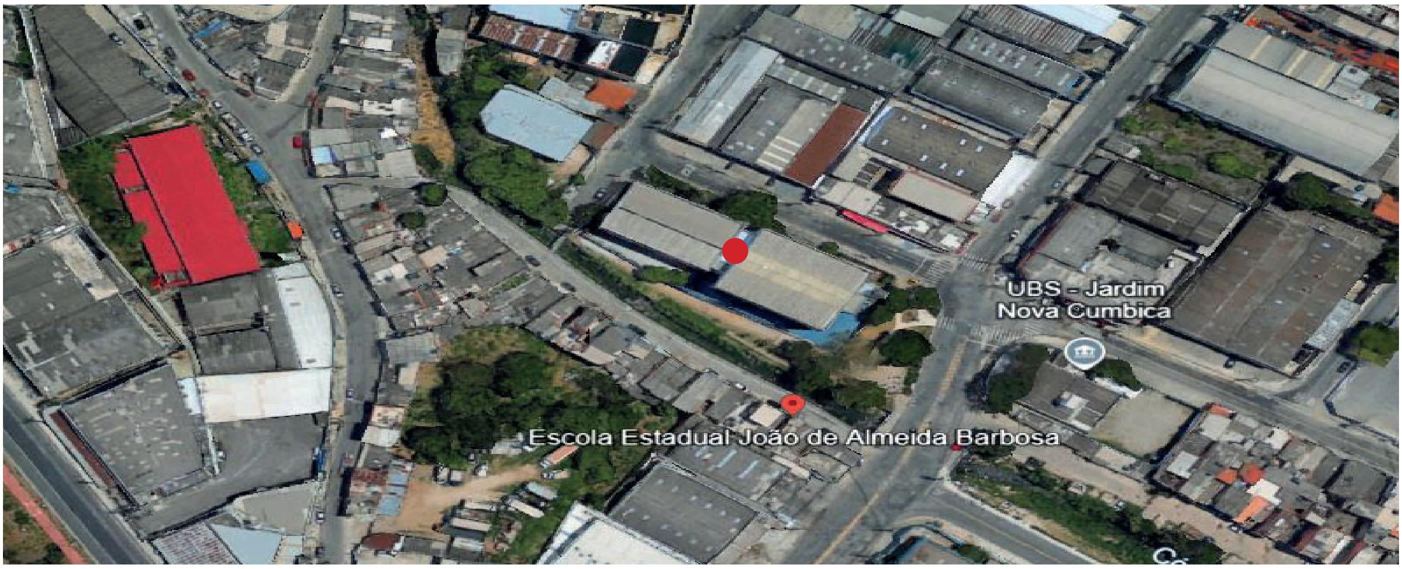

Figure 3.4.33 - Top view of the of the State School Nova Cumbica, showing context (Google, 2024).

Figure 3.4.34 - Southern Facade of State School Nova Cumbica (© Pedro Napolitano Prata, 2014).

Figure 3.4.35 - Circulation area of the State School Nova Cumbica, showing the facade treatment form the inside (© Pedro Napolitano Prata, 2014).

A more modern example of a second skin façade can be found in the State School Nova Cumbica by H+F Architects (figures 3.4.34 and 3.4.35). The building was constructed in 2014 in the municipality of Guarulhos, inside the metropolitan area of Sao Paulo. The façade design uses perforated metallic panels painted in different colors applied to the south/southwestern and north/northeastern facades (figure 3.4.34). The same criticisms and observations regarding the Telemaco Melges School are valid for this building (ArchDaily Brasil, 2015). Nevertheless, when compared with the translucent elements shown previously, perforated panels will probably have an overall improved performance. The latter is assumed due to the material's higher effectiveness in allowing for more air movement and protection against solar radiation.

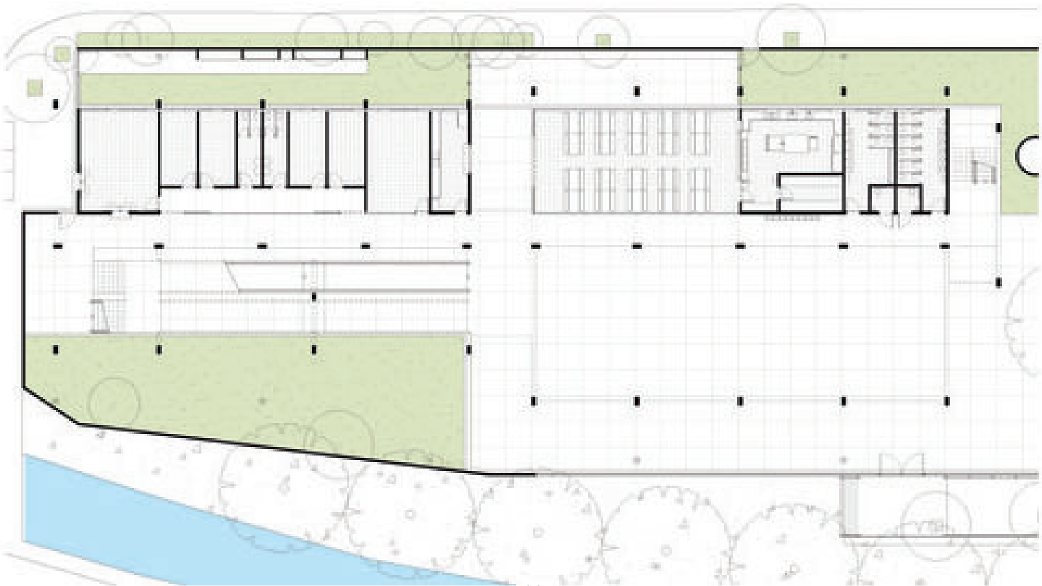

(a)

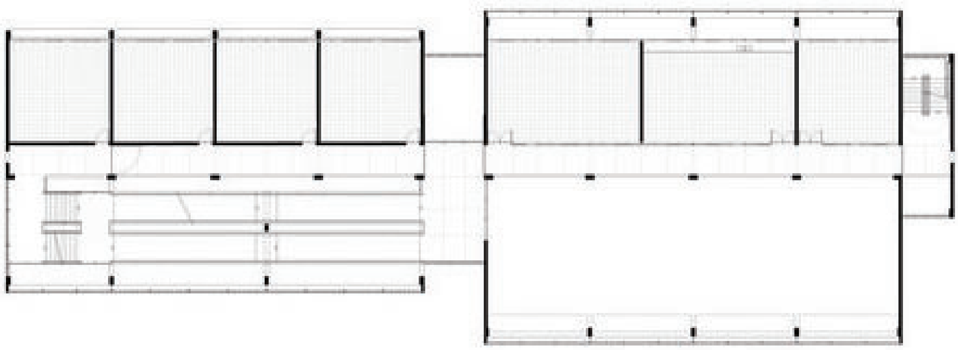

(b)

Figure 3.4.36 (a) - Floor plan of the Ground Floor of State School Nova Cumbica (H+F architects). **(b)** - Floor plan of the First Floor of State School Nova Cumbica (H+F architects).

EMEF MARIA APARECIDA MAGNANELLI FERNANDES

Figure 3.4.37 - Top view of the of the EMEF Maria Aparecida Magnanelli Fernandes, showing context (Google, 2024).

Figure 3.4.38 - Northeastern Facade of EMEF Maria Aparecida Magnanelli Fernandes, (© Fábio Arantes/Secom, 2017).

The EMEF Maria Aparecida Magnanelli Fernandes was inaugurated in 2012 in the city. The architects responsible were not found and neither further information about the school as school plans. Nonetheless, the discovered images demonstrate the use of metallic angulated panels in front of the windows as shading elements (figure 3.4.39). The northeastern facade of the building is recessed creating additional horizontal elements. Furthermore, vertical elements were created and placed evenly throughout the façade (figure 3.4.29). The combination of the mentioned components is probably successful in reducing the sun radiation that windows would be exposed to. However, is not possible to affirm the extent of the shading element's effectiveness.

CEU PARQUE DO CARMO

Figure 3.4.39 - Top view of the of the CEU Parque do Carmo, showing context (Google, 2024).

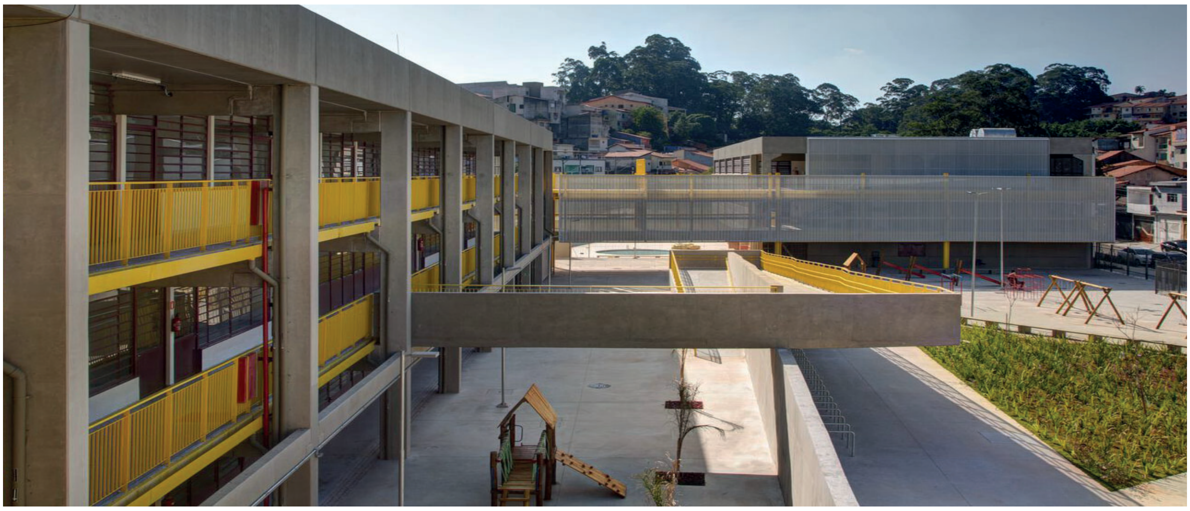

Figure 3.4.40 - View of the Southeastern Facade of the central block of CEU Parque do Carmo, (© Pregnolato & Kusuki fotografia, 2020).

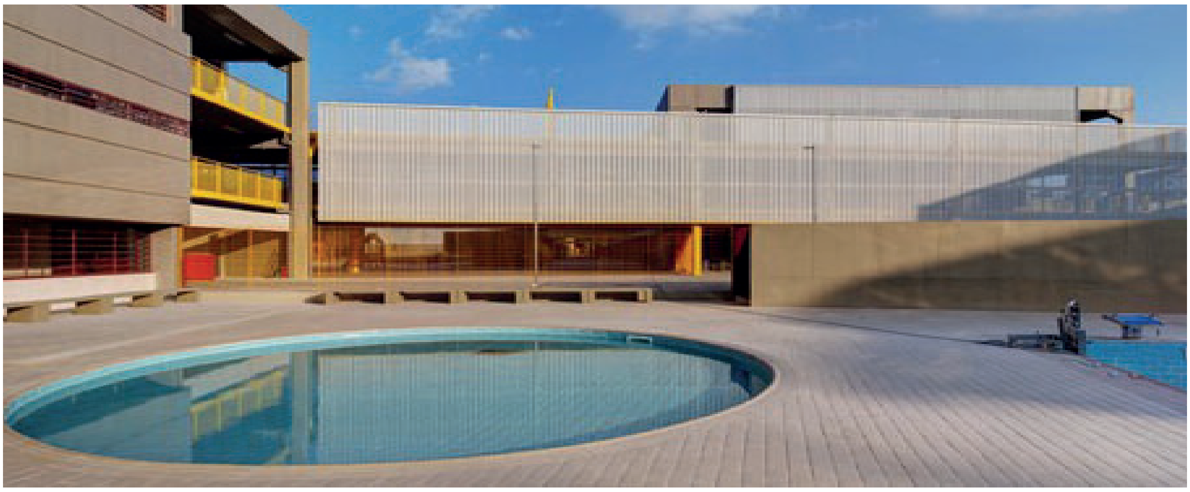

Figure 3.4.41 - View of the Nothern facade of the northern block of CEU Parque do Carmo, (© Pregnolato & Kusuki fotografia, 2020).

As a first example of CEUs (Unified Educational Centres), we have the Parque do Carmo by architects HASAA and SIAA, from 2020, with 12662m² of built area. This building complex is expressively larger than the schools displayed so far (ArchDaily, 2022 - see figure 3.4.42). The project is also the newest to be built with a 15-year gap from the State School Fernando Gasparian, also shown above. Yet, elements seen previously can also be identified in this building. For example, the combination of overall structure in prefabricated concrete elements with smaller components structured with metallic elements (figure 3.4.40). Once more there are recessed facades with connection paths to the classrooms on the outside of the building behaving as horizontal shading elements (figure 3.4.40 and 3.4.42). Moreover, the perforated aluminium tiles, like the used in the State School Prof. Marcos Alexandre Sodre, are applied here as secondary skin to provide shade (figure 3.4.41). The mentioned element is correctly used on the facades facing north, even though there needs to be a further test to define if the perforated panels are enough to reduce the sun radiation indoors. However, the areas of the buildings facing north and protected by the roof tiles are mainly for circulation between levels and an indoor swimming pool (figure 3.4.41 and 3.4.42). The described architectural program location is correctly selected as the long-stay classrooms were avoided, perhaps eliminating the need for a stronger façade shading system.

The perforated metallic panels are located with different dimensions on all building facades. The mentioned elements are placed even facing south and east orientations, which could indicate an overshadowing. The excesses of shading could result in uncomfortable indoor areas during colder periods of the year/day. Still, the façade of the building facing west has areas without the panels, which could be a poor environmental design choice. The statement is justified by the sun angle being more direct and the temperatures being higher when the sun is on the west.

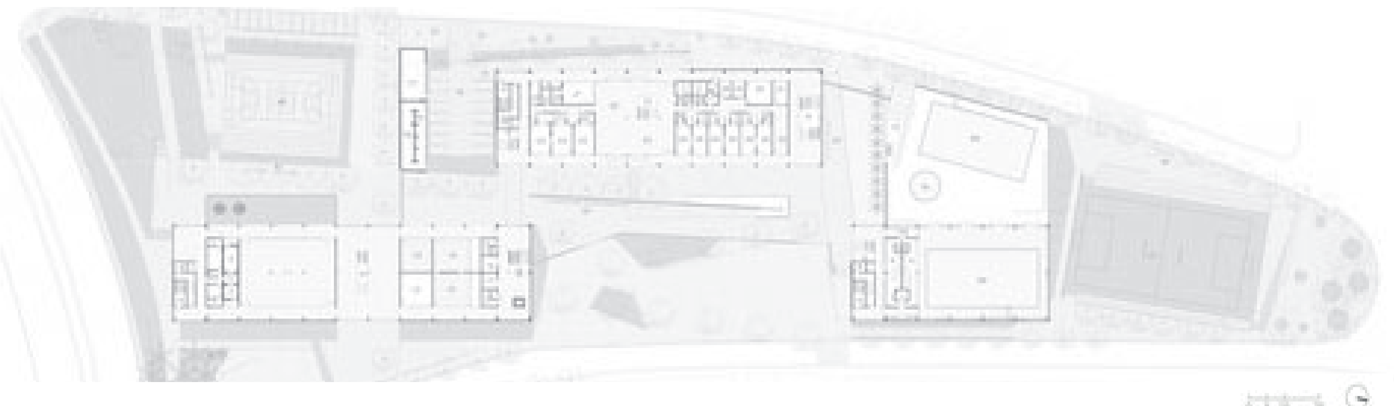

(a)

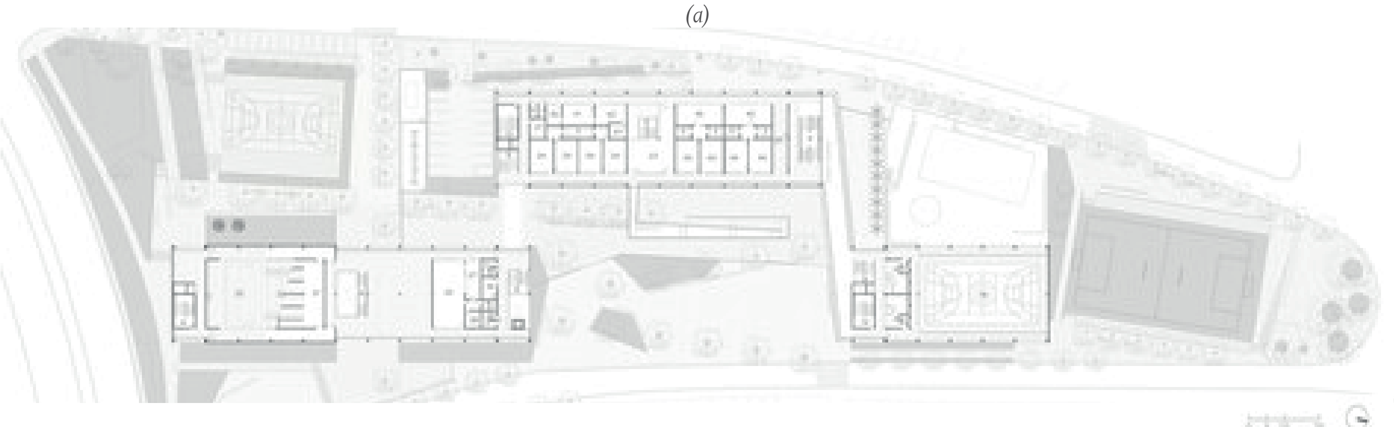

(b)

Figure 3.4.42 (a) - Floor plan of the Ground of CEU Parque do Carmo (SIA+HASAA architects). **(b)** - Floor plan of the First Floor of CEU Parque do Carmo (SIA+HASAA architects).

CEU PIMENTAS

Figure 3.4.43 - Top view of the of the CEU Pimentas, showing context (Google, 2024).

Figure 3.4.44 - Western view of the building (© Nelson Kon, 2010).

Figure 3.4.45 - Internal view of the main block of CEU Pimentas (© Nelson Kon, 2010).

The last building is the CEU Pimentas, in the city of Sao Paulo, by the Biselli+Katchborian architects. The educational center was built in 2010 and was chosen as an example to show a completely different design in comparison with all the buildings shown before. However, the school still showcases elements and building systems comparable to the other ones. For example, different from the CEU Parque do Carmo which has three different blocks spread on the terrain this one is composed of a unique mass. Yet, looking further the project is composed of smaller blocks with brick walls and pre-fabricated concrete structures sustaining a massive metallic roof (Fracalossi, 2012 - see figures 3.4.44 and 3.4.46). The mentioned structural and finishing materials are similar to the majority of buildings shown this far.

The main facades of the buildings face west-northwest and east-southeast, with the west-northwest ones being recessed and protected by metallic "brise soleil" style fixed panels (figure 3.4.44). As seen before the recess happens in the form of a circulation area separating the classroom from the outdoors. The use of the panels before the classrooms are another resemblance to the previous examples. Lastly, the classrooms are opened completely (with glazing) to the semi-outdoor area (covered with the roof, as seen on figure 3.4.45). The characteristics and strategies discussed before can be considered environmentally correct. Yet, it is possible that the shading structure is not sufficient and that the covered area is not delivering enough natural daylight to the classrooms.

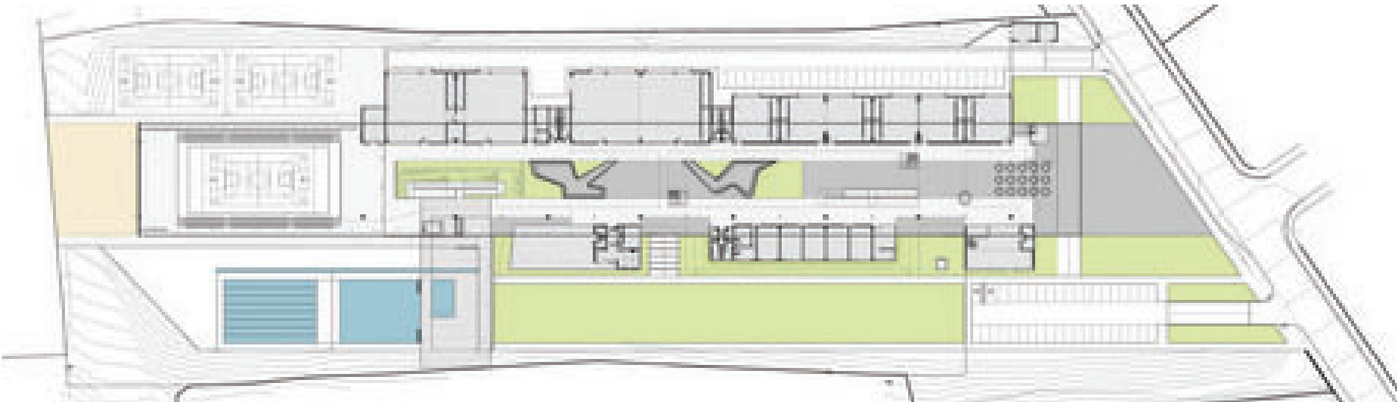

(a)

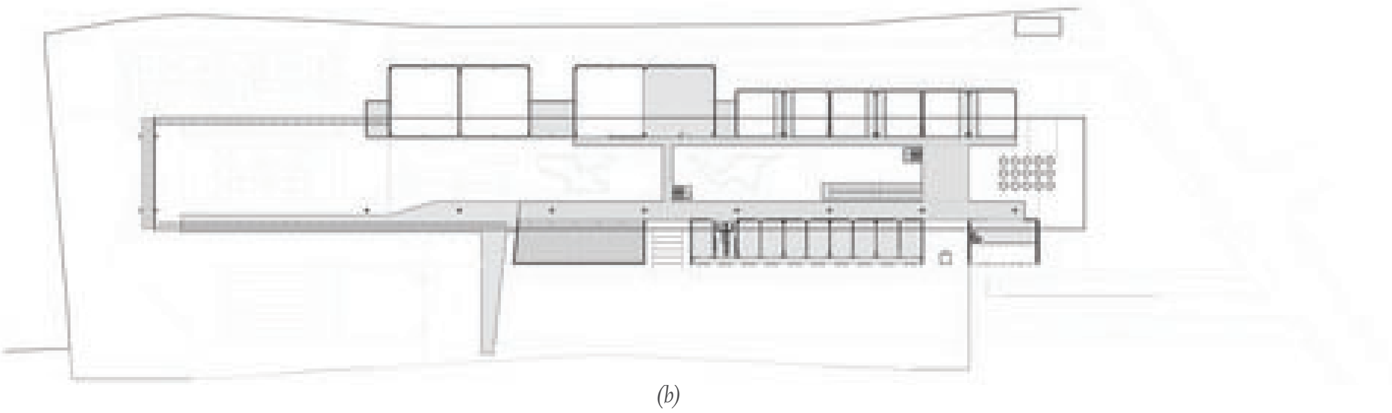

(b)

Figure 3.4.46 (a) - Floor plan of the Ground of CEU Pimentas (Biselli+Katchborian architects). **(b)** - Floor plan of the First Floor of CEU Pimentas (Biselli+Katchborian architects).

3.5. CONCLUSION

This chapter elucidated the essential character of school environments by highlighting the urgency of focusing on children's and teenagers' health issues caused by air pollution and thermal distress. Additionally, the importance of the overall school environment to the younglings' well-being was also established. Afterward, the chapter explains this doctoral research's specific interest in public schools. It was entrenched that the public school system in place within Sao Paulo's city and state presents strict guidelines to be followed and applied in each school. Finally, the chapter states how the presence of strong policies enhances the potential for the guidelines proposed by this thesis to be applied on a wider scale, perhaps, generating a city-scale impact, hence more significant.

Following the justification for the focus established in this thesis, the chapter moves to its main objective, which is discussing the architecture of public schools. The study of EMEIs and EMEFs examples showcased buildings with similar program organization, with similar built areas. However, the open areas surrounding the buildings varied substantially. The CEUs presented different programs with much more extensive built areas, keeping similar façade treatments and structural components. Moreover, most of the examples show reduced use of small-scale green infrastructure within school terrain. Some buildings are surrounded by paved, uncovered areas. Others have low grass in the outdoor areas. Moreover, most of the examples showcase a few numbers of trees scattered around the terrain. The described outdoor situations can indicate intense poor thermal conditions for the users during hotter periods. Moreover, another similar characteristic is the height of the classroom windows, with parapets height of 1m. The windows are usually composed of metallic frames and clear glass.

The use of prefabricated concrete beams and pillars and metallic roofing structures is also seen repeatedly in almost all examples. Some schools have the circulation between floors resolved in the middle between classrooms and other rooms facing out. While other examples show the circulation working as a "buffer zone" between the outdoors and the classrooms. The mentioned corridors naturally work as vertical overhangs against the direct sun. Finally, most buildings have perforated metallic panels as shading elements and only one example uses wood. A few schools use concrete vertical and horizontal overhangs as solar protection. Furthermore, most of the examples seemed to have their design process with a focus on shading and air movement. Yet, it is possible to indicate that some buildings could perform better regarding thermal comfort with shading addition and/or subtraction.

It is essential to emphasize that the architecture review made in this chapter focused on the best environmental design strategies. This assessment relies on analyzing the façade and roof treatments and their orientations. Thus, the comments do not consider other program necessities, which are general to every school and specific to each site. Additionally, the real effect of the shading elements or surrounding vegetation was not modeled. Consequently, the evaluation was done as a set of suggestions, with the use of environmental design principles, and not scientifically tested. Hence, the evaluation will naturally be less accurate, requiring a more in-depth analysis of the environmental performance of a school building within São Paulo's context.

The analysis made in this chapter was also fundamental for identifying one other building that represents them but on a smaller scale. The choice was made by spotting similar characteristics and programs while also considering the possibility of conducting fieldwork. Even though not all buildings presented exist within a context of urban density it was essential to choose an example which is. The mentioned is justified by this research's objective to study air quality with a focus on denser environments. Finally, to be analyzed and accessed in more detail, the EMEF Amorim Lima was selected as a case study. Unlike most of the previous examples, the Amorim Lima school is surrounded by small-scale infrastructure. Moreover, the building is older than most of the examples in this chapter. However, the elements of shading and glazing can be seen there once again. The specific characteristics of the building itself in addition to the outdoor and indoor areas aspects can be seen in the next chapter. Moreover, the field and analytical work conducted on the school will be presented in each of the following chapters.

4. CASE STUDY: FIELDWORK

THE CURRENT PERFORMANCE OF EMEF DESEMBARGADOR AMORIM LIMA

4.1. INTRODUCTION

This chapter describes the public school EMEF Desembargador Amorim Lima, a significant case study in small-scale green infrastructure. This school's characteristics and potential to serve as a model for other public schools in Sao Paulo make it a compelling subject of study. The chapter opens with an explanation of the crucial objectives of this case study fieldwork analysis, followed by the methods used for the task. Afterwards, the school's brief history, management, and overall characteristics are discussed. A section with a detailed analysis of the outdoor and indoor environments follows as the focus of the fieldwork. Finally, the chapter concludes with the results of the fieldwork measurements being displayed and discussed, setting important questions to be answered in the case study's analytical work chapter that follows.

4.2. OBJECTIVES

This chapter is dedicated to studying the current characteristics and overall environmental performance of EMEF Amorim Lima. Analysing this school's environment is the first step in identifying variables that could enhance or restrict human comfort, paving the way for healthier school environments. Moreover, the research on this school is intended to serve as a parallel indication of the environmental efficiency of similar public schools in Sao Paulo, with the potential to trigger widespread positive changes. By combining these objectives, the main aim is to provide a clear picture of EMEF Amorim Lima's current environmental performance.

This section also aims to indicate other environmental aspects, such as visual comfort, in addition to thermal comfort and air quality. Indoors, access to the right amount of light can drastically alter the perception of comfort. Also, concerning learning environments, light availability can be critical to students' performance (Nasrollahi and Shokri, 2016). Therefore, architectural design should prioritise creating indoor environments with reasonable daylight. The optimal amount would avoid glare issues and, most importantly, prevent the artificial light from being turned on during periods of the day when natural light is still available. In addition, using less artificial lighting can positively impact energy consumption (Nasrollahi and Shokri, 2016; Fasi and Budaiwi, 2015; Shishegar and Boubekri, 2017). As discussed, the amount and quality of daylight distribution in a school's indoor area can interfere with the student's learning capacity. This research focuses on the impacts of SGI on air quality and thermal comfort; however, due to their capacity to create shade when close to the windows, the components can reduce daylight in the environment. Thus, the context of an existing case study generates an opportunity to study indoor daylight levels through fieldwork, understanding the impact that vegetation can cause when close to the apertures.

Finally, this field research's main aim is to study the performance of an existing school case with abundant vegetation on its terrain, forming a small-scale green infrastructure. The aim is to determine what impacts this SGI has on the outdoor and indoor environments of Amorim Lima. As Chapters 01 and 03 explain, the performance has two main performance indicators: thermal comfort and air quality. Additionally, the primary variable considered in this exercise is vegetation and the effects of being close to it. This work section also wishes to shed light on other variables that can change the environment's conditions, identifying if and when vegetation is insufficient to overcome harsh and unfavourable weather and air quality conditions. Identifying why the studied environment performs in a certain way could pave the way to building guidelines on improving or creating high-performance urban school spaces and, consequently, cities, engaging the audience of policymakers. The intention is also that the outcomes presented at this stage will become a "tool" used to calibrate the inputs fed to the digital analysis in the next chapter (Case Study – Analytical Research). Additionally, the results are used to validate and critically review the analysis results, linking the different parts of the study.

4.3.METHOD

This chapter is dedicated to site-specific fieldwork in EMEF Desembargador Amorim Lima, a school in Sao Paulo. Section 4.4 discusses the school in more detail, including the reasoning behind its selection. The work developed at the school's site was developed in two specific periods with a total expansion of two years, while other activities were conducted in parallel. It was not continuous monitoring; all the data was collected through point-in-time measurements. The two years and the impossibility of continuous monitoring or further spot measurements are due to the site's location in Brazil. The limitation was even bigger, considering that most of the fieldwork happened during the COVID-19 lockdown. Thus, access to equipment and to the school itself was reduced. For the spot measurements, fifteen areas were selected, and their characteristics and why they were selected are discussed in section 4.5. Eight of them are outdoors, and seven are indoors. Inside the school, three spots were studied on the ground floor and four on the 1st and 2nd levels, two on each. The way the point-in-time measurements were conducted reflects the research by Oke (2006), which presents an extensively accepted method for fieldwork. They identified 1.5m as the lowest height acceptable for field measurements. Thus, as this thesis focuses on teenagers and children, that was the considered height for the entire field exercise.

The chosen parameters to identify the school's performance concerning thermal comfort were dry bulb temperature (DBT - °C), relative humidity (%), wind velocities (m/s) and surface temperatures. Theoretical knowledge of solar irradiation will also guide the assumptions of human comfort. Moreover, the visual comfort is represented by lux concentrations. Finally, the air quality conditions were measured through PM2.5 and PM10 levels. Five handheld monitoring instruments were used for the point-in-time measurements in the first exercise. The tools were one of each: anemometer, thermo-hygrometer, lux meter, and an infrared surface thermometer. The mentioned tools measured wind speed (m/s), dry-bulb temperature (°C), humidity (%), surface temperature(°C), and illuminance (lux), producing 720 measurements in total. The fieldwork conducted afterwards used only one measurement tool: the air quality monitoring device called Flow, which Plume Labs developed. It is a pocket-size instrument with a 360-degree air intake, which allows for quantifying the pollutant particles calculation and will further display the concentrations in a phone app (Plume Labs, 2018). In 2023, Plume Labs stopped producing and selling the flow device to focus on other technologies concerning air quality (Plume Labs, 2024). However, the device's capacity has been demonstrated in air quality monitoring studies by Tan and Smith (2020) and Watkins (2020). Additionally, Crnosija et al. (2022) reviewed it by testing 34 flow and other pollution measurement devices, exposing them to PM10 and PM2.5. The study defined that flow as a useful air quality monitoring tool to demonstrate individual (punctual) particulate matter exposure. For this doctoral research, the focus of the pollutants measured by the Flow device was the particulate matter PM2.5 (ug/m3) and PM10 (ug/m3).

There were two main periods studied: the first was during the month of March 2021, analysing thermal comfort and daylight availability. The second set of measurements took place in January 2022, focusing on air quality. For the first study course (March 2021), four different times of the day were explored: 08:00 am, 11:00 am, 04:00 pm and 06:00 pm. Moreover, three days were measured at 11:00 am (25/03/21, 26/03/21, and 04/04/21) and three others at 04:00 pm (27/03/21, 01/04/21, and 05/04/21). Two days were studied at 08:00 am (29/03/21 and 02/04/21) and two at 06:00 pm (30/03/21 and 31/03/21). The 11:00 am and 04:00 pm periods were explored for more days due to the harsher air temperature conditions expected during them. The 06 pm measurement, representing the period after sunset, was added to capture the environmental conditions without direct sun radiation. Early morning (08:00 am) and evening (06:00 pm) were selected as they would habitually display lower temperatures. The second studied course (January 2022), focusing on air pollution spot measurements, happened on four different days. Two days were studied at 12:00 am (20/01/22 and 22/01/22), one at 8:00 am (21/01/22), and the last at 04:00 pm (27/01/22). Thus, the mentioned times covered the typically busiest traffic hours of the day in the city. The measurements on Avenue Corifeu de Azevedo Marques were also made. To compare the interior areas of the school with the busiest vehicular road in the proximity. Finally, each measurement exercise started at the abovementioned times and finished roughly one hour later. The measurement order was the same, so each spot was analysed at the exact moment on different days (within the same period group).

As previously mentioned, the fieldwork was conducted during COVID-90. Hence, during most of the visits, the teaching staff did not use the school during this exercise. Mostly on the measurement days in 2021. Moreover, during the last four studied days in 2022, the school was also nearly empty due to summer vacation. Thus, all the indoor classroom spaces were closed, with internal and external windows and doors always shut. However, before starting the measurements, the windows of each classroom were opened. After opening the windows, the spot measurements for the outdoor areas were conducted. Afterwards, those in the indoor space were done. The situation was slightly different on the indoor patio and administrative entrance hall, where, as a minimum, staff were still working, and the doors were usually already open.

4.3.1. WEATHER DATA

As part of this chapter's method, the area surrounding EMEF Amorim Lima weather conditions and trends were analysed to compare them further with the measurements. Section 2.3.1 of Chapter 02 presents an overview of Sao Paulos climatic conditions. However, weather data recorded close to the school building was studied for specific comparisons with the studied days. The EMEF Amorim Lima is next to the University of Sao Paulo (USP) campus. Within the campus are two meteorological stations, WXT520 Weather Transmitters/VAISALA brand. The stations collect air humidity, dry bulb temperature, wind directions, and speed data. Both are fixed five meters above the ground and log meteorological measurements every fifteen minutes (Prata Shimoura and Ferreira, 2020). Therefore, the stations were selected as the data providers of weather conditions to be compared with the spot measurements.

During the first monitoring campaign (from 25 March to 5 April 2021), the ambient air temperature exceeded 30°C only once (30.7°C at 11:00 am on the 27th of March). Moreover, six analysed days have showcased air temperatures between 23.4°C to 27.9°C. During the six mentioned days, the highest and lowest temperatures recorded when com-

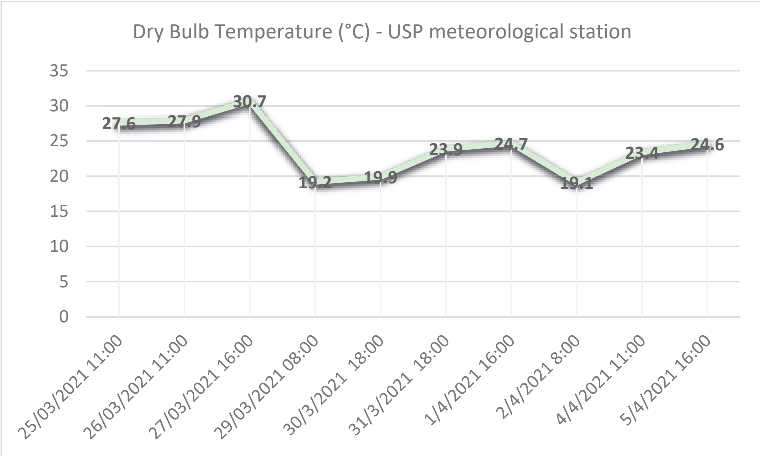

Figure 4.3.01 - Dry Bulb Temperature (°C) recording for the ten studied days by the meteorological stations located inside the University of Sao Paulo

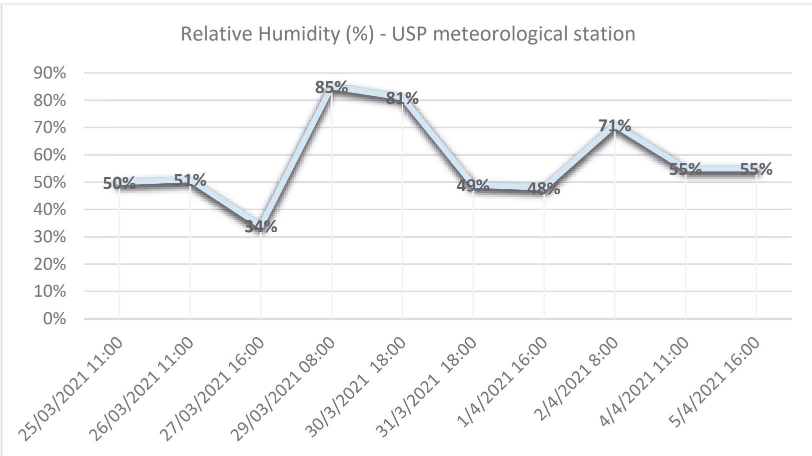

Figure 4.3.02 - Relative Humidity (%) recording for the ten studied days by the meteorological stations located inside the University of Sao Paulo

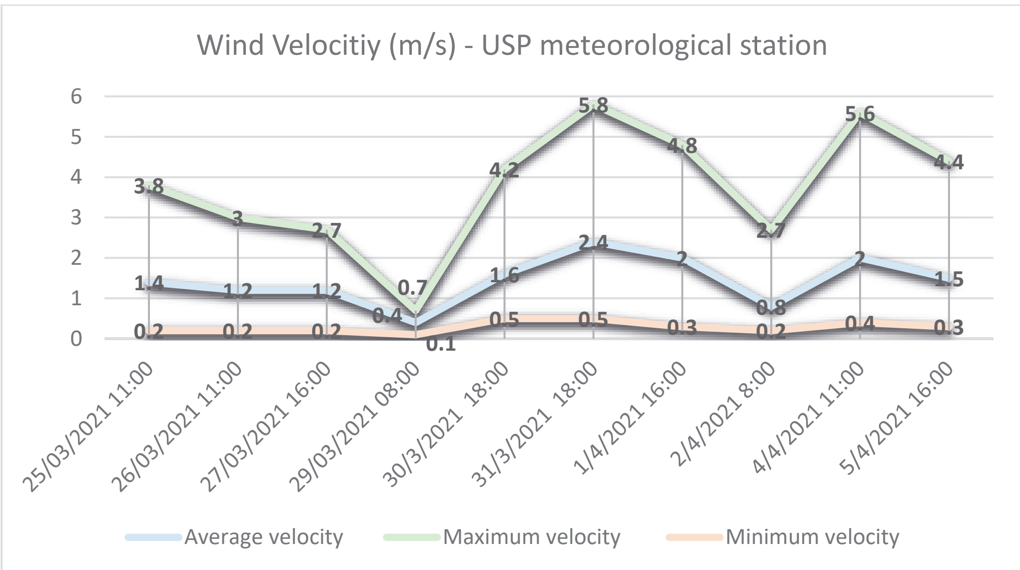

Figure 4.3.03 - Average, maximum and minimum wind velocities (m/s) recorded for the ten studied days by the meteorological stations located inside the University of Sao Paulo

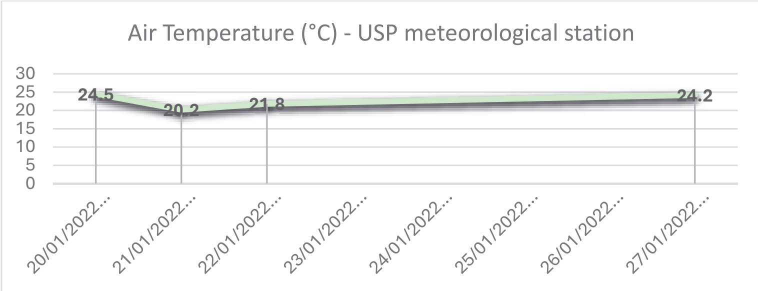

Figure 4.3.04 - Dry Bulb Temperature (°C) recording for the days of pollution study by the meteorological stations located inside the University of Sao Paulo

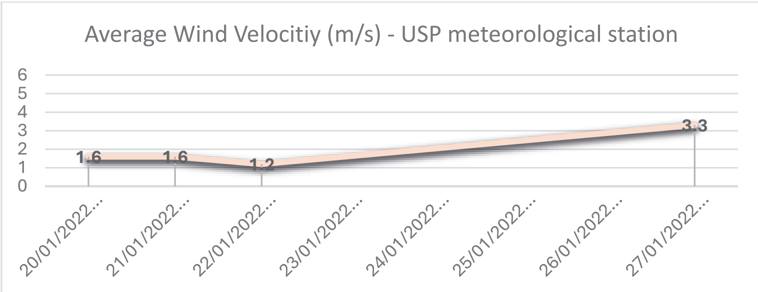

Figure 4.3.05 - Wind Speeds (m/s) recording for the days of pollution study by the meteorological stations located inside the University of Sao Paulo

paring all studied days were found in the morning (11:00 am). Temperatures under 20°C were recorded in the three remaining days, two at 08:00 am and one at 06:00 am. The one spotted at 06:00 pm was 19.9°C on the 30th of March. The morning recordings (08:00 am) were 19.2°C on the 29th of March and 19.1°C on the 2nd of April. Furthermore, the data collected by the weather station showed no rainfall during the analysis periods, and the relative humidity varied between 34% and 85%. The lowest humidity percentage happened simultaneously with the highest recorded air temperature (30.7°C). The highest humidity level occurred at the exact moment when the lowest temperature was spotted. The recorded data showed a variation in average wind velocities from 0.4m/s to 2.4m/s between the ten explored days. The maximum wind velocities recorded ranged from 0.7m/s to 5.8m/s. Both speeds were taken on the 29th and 31st of March. tions presented are essential for analysing the concentration of pollutants in each spot. To understand mainly how dry bulb temperature and wind velocity can impact the measured air quality.

As previously mentioned, the second batch of measurements focused on pollutant particle concentration and was conducted over four days in January 2022. During the four studied hours, on the 21st of January (2022), at 08 am, the lowest dry bulb temperature was registered at 20.2°C. The first studied hour was the warmest, with 24.5°C (midday, 20th of Jan), followed by the 27th of Jan at 04 pm, with 24.2°C. Finally, the 22nd of Jan, also at midday (the third studied hour), registered a dry bulb temperature of 21.8°C. Moreover, all studied days were sunny with no cloud obstruction. The average wind velocity recorded by the USP station during the study hours varied from 1.2m/s to 3.3m/s. The highest was on the 27th of Jan at 04 pm and the lowest on the 22nd at midday.

4.4. EMEF DESEMBARGADOR AMORIM LIMA

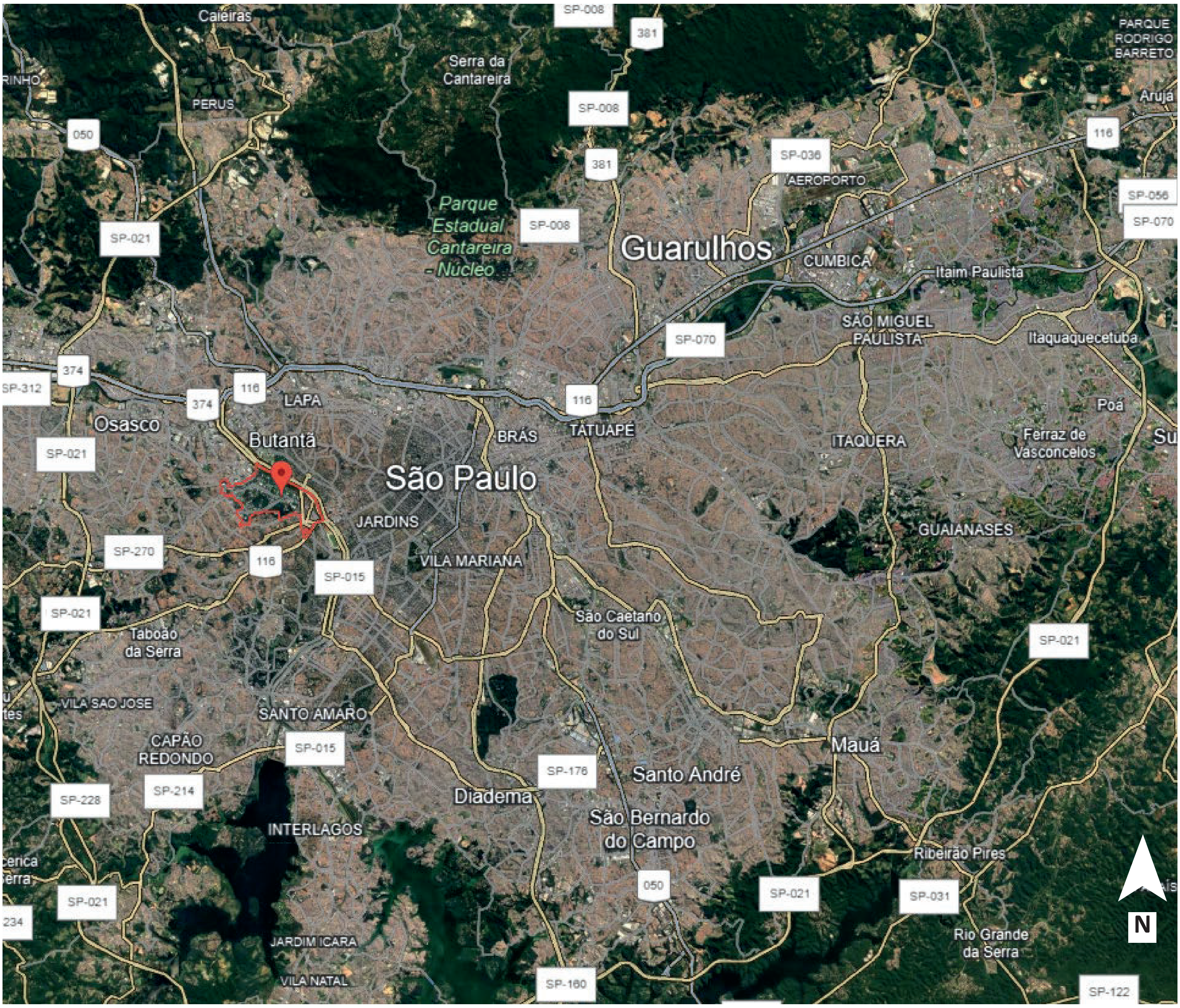

Figure 4.4.01 - Satellite image of the city of Sao Paulo and surroundings highlighting the Butanta neighborhood where EMEF Amroim Lima is located (Google, 2024).

As explained in the previous chapter, EMEFs are Municipal Elementary Schools, having children aged 6 to 14. It is the case of EMEF Desembargador Amorim Lima, which was created in 1956 and previously had other names and locations. In 1968, the school was set at its current address, and in 1999, it adopted its current name. The school is a reference to a “democratic school”, which allows for intense community participation and use of the built environment, inspired by the “Escola da Ponte” in Porto (Portugal). The implementation of the mentioned educational model started when the current director arrived at the school in 1996. (Aquino and Sayão, 2004) The mentioned director, Ana Elisa Siqueira, was substantial in allowing access to the development of studies in the school. She was also the main person responsible for understanding the organisation and activities of the environment. Furthermore, the school is in the Butanta district in the western area of the city, where the University of Sao Paulo’s (USP) main campus is situated. Moreover, the School maintains cooperation and research relationships with the University (EMEF Des. Amorim Lima, n.d.). The school’s terrain comprises the main building, one covered sports court, and an uncovered one. Most importantly, EMEF Amorim Lima has an open area in its southern/ southeastern portion called Cora Coralina Park. The Park and other vegetated areas have diverse trees, living walls, and hedges, while most of the land is composed of soil covered by

Figure 4.4.02 - Satellite image of the EMEF Amroim site and the surroundings in the Butanta neighborhood (Google, 2024).

grass. Wide roads with heavy vehicular traffic and low-rise and high-rise buildings characterise the adjacent context. As explained in the previous chapter, the environment mentioned can be considered a Small-Scale Green Infrastructure. Moreover, it is enclosed by brick walls, creating a boundary within the urban context.

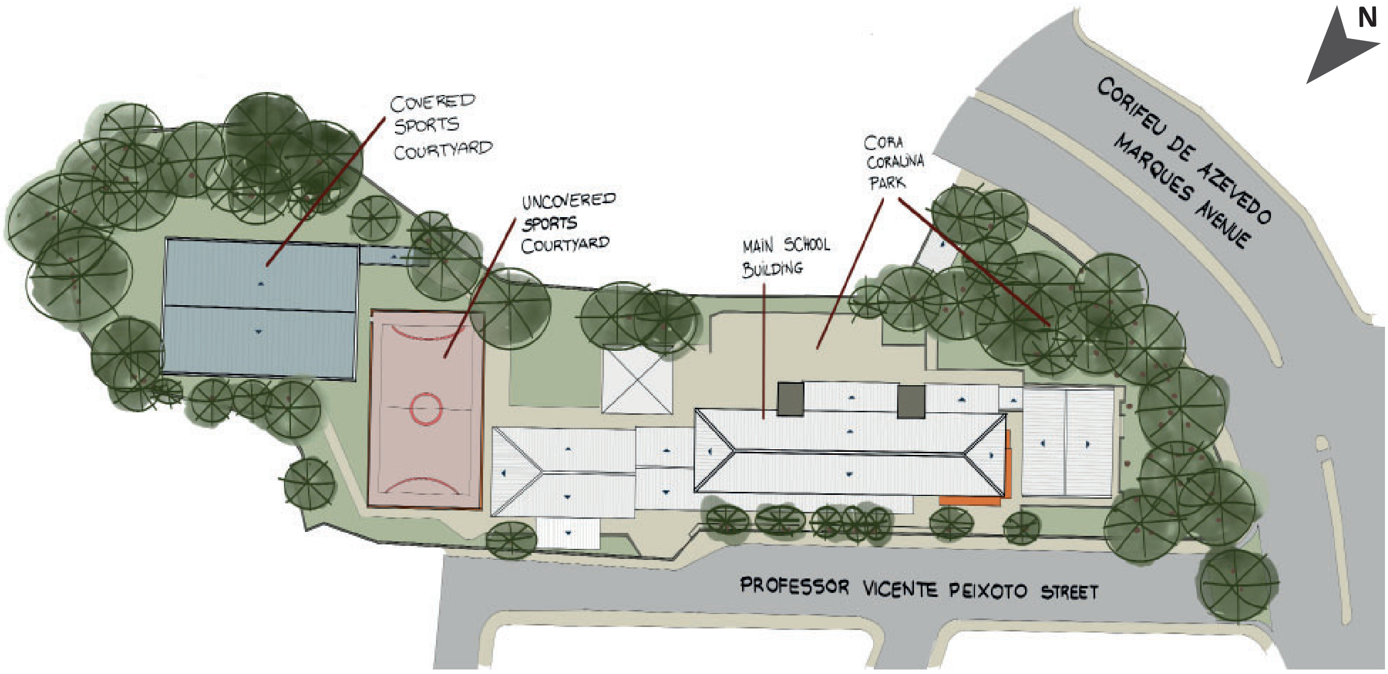

Figure 4.4.03 - Sketch of EMEFF Amorim Lima roof plan

The EMEF Amorim Lima terrain and building, analysed mainly from 2021 to 2022, is over 50 years old. Naturally, the built space has suffered various changes, but the overall structure remains unchanged. The schools chosen as examples of public schools in Sao Paulo and displayed in the previous chapter are substantially younger buildings, with dates ranging from 2004 to 2020. Consequently, the overall built system is more modern with the extensive presence of prefabricated elements, while Amorim Lima has a much simpler, built-on-site structure. However, the building displays components similar to those shown and extensively discussed in the previous chapter. For example, the glazed windows with metallic frames, seen in most of the mentioned schools, are spotted in this one. Moreover, the cobogo element, repeatedly demonstrated in the previously analysed schools, is also present, even if with a different design. Cobogos are elements vastly used in most areas of Brazil due to the country's climatic conditions, and their relationship with environmental design principles has been explained in more detail in the Architecture of Schools in Sao Paulo chapter. Furthermore, the building also showcases some sporadic cases of narrow steel frames without any glass. For the primary building block, consisting of the indoor patio and most classrooms, applying those materials follows a simple logic: northwest facades are glazed. The southeast openings mainly consist of cobogo panels (image below).

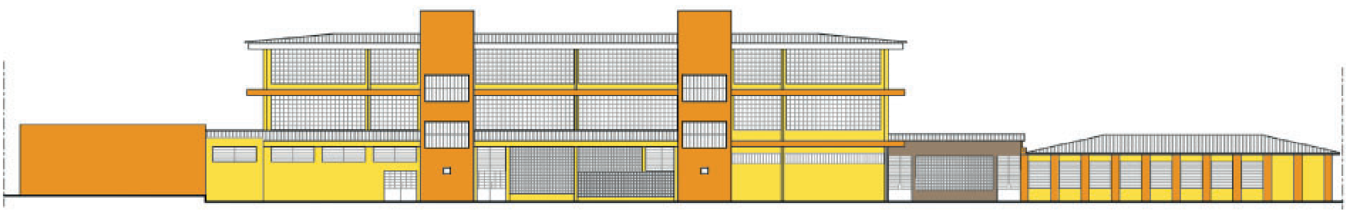

Figure 4.4.04 - Sketch of the southeastern facade of EMEF Amorim Lima

Figure 4.4.05 - Image of the Northwestern façade of EMEF Amorim Lima (personal archive)

Figure 4.4.06 - Image of the Cobogos on the south façade of the EMEF Amorim Lima (personal archive)

4.5. THE STUDIED AREAS

Specific spots for measurement were selected to analyse the school in more depth. A total of 15 spots were chosen, indoors and outdoors, with each indoor spot representing an entire room. The indoor area was studied in five classrooms, the administrative entrance hall, and the indoor patio. For the outdoor area, eight points were established, with two located closer to the adjacent vehicular road and the rest 'protected' by the surrounding houses and buildings. This study method provides a detailed understanding of the school's spatial dynamics and interaction with the surrounding environment. As the first stage of the analysis, each area of the school will be presented, and its characteristics discussed.

4.5.1. OUTDOORS

Concerning the outdoor areas of Amorim Lima, the aim was to study portions of the site with different morphological conditions. The method mainly expects to compare "protected" and "unprotected" outdoor spaces. The level of "protection" is related to the proximity to busy roads. For example, the southwestern area of the school grounds borders a busy highway (Corifeu Avenue), while the opposite side has walls with other buildings. The belief is that the abovementioned situation will cause two distinct environmental conditions. The changes will probably be microclimatic, but mainly on-air quality conditions.

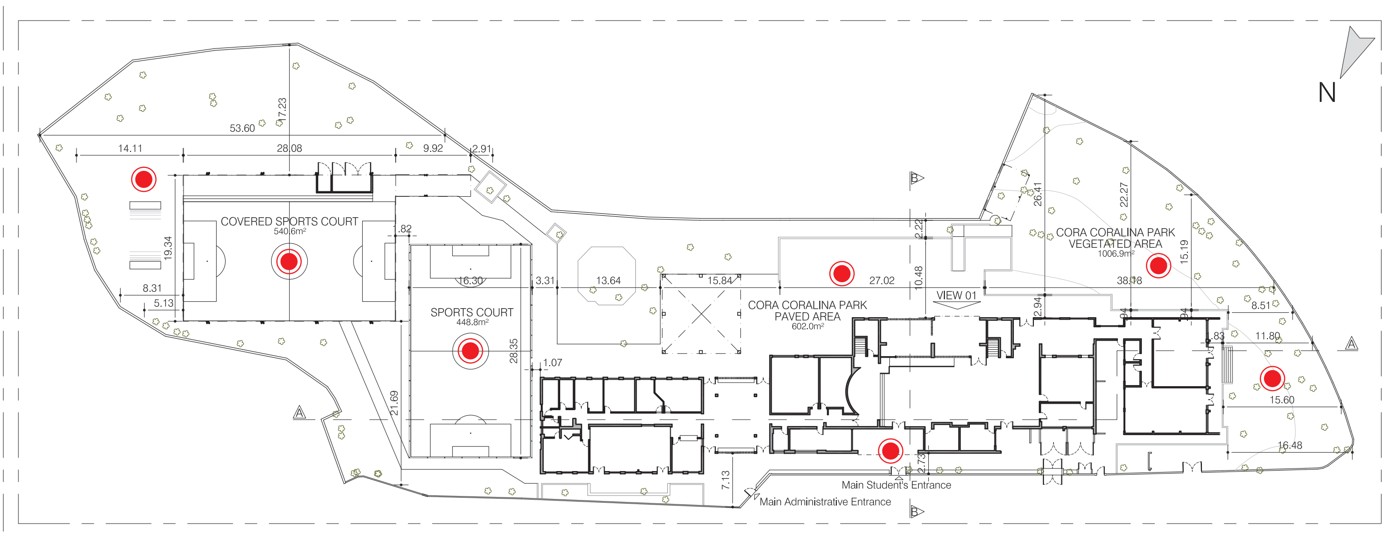

Figure 4.5.01 - The ground plan of the EMEF Amorim Lima with the indication of external studied points.

ENTRANCE (EP01)

The first outdoor study area is the entrance, which is the main student's entrance and could be considered a transitional space between the outdoor and the indoor. It is a small area between the boundary wall facing the access road (Professor Vicente Peixoto St) and the indoor patio door (the largest indoor area) The boundary wall in this zone is over two meters high, and just in front of it, the school building is over four meters high (see section on figure below). There

Figure 4.5.02 - Image, section BB, and location floor plan showing spot EP01 (personal archive).

are five trees in this area of two species: Ligustrum lucidum and Citrus sp.

The proximity between boundary walls and school buildings could generate a wind tunnel effect according to the wind orientation. This phenomenon could significantly impact the comfort and overall use of the school's outdoor spaces. The mentioned built features could also obstruct a different wind orientation, creating a protected area with less air movement. Beyond the corridor between the outdoor barrier and the school building, the entrance has a covered space. The covered space has a depth of roughly 3m and a ceiling height of 3.70. Independent of the wind directions, this area's geometry could restrict the indoor patio's wind velocities.

This study focused on the uncovered section, which received extra daylight and direct radiation. The location became essential to the study due to the exposure mentioned, combined with the wind and solar obstruction caused by the boundary wall. The blockage reduced the exposure to daylight and the direct sun, giving this space different characteristics from the unobstructed outdoor environments. The characteristics of this space create critical aspects, such as being enclosed, the extensive presence of hard pavement materials, and the presence of a few taller trees.

CORA CORALINA PARK

Cora Coralina Park is the open area that surrounds part of the building, forming the Small-scale green infrastructure of this school. It is located in the southwest and southeast areas of Amorim Lima. It consisted of a zone with greenery and an open, non-vegetated area. Moreover, the park was divided into three spots to be further analysed.

CORA SPOT 01 (EP02)

The first chosen spot represents the area directly connected with the annexe building, comprising the first-year classroom and the art room (figure 4.5.03). This park portion is established between the school building (northeast)

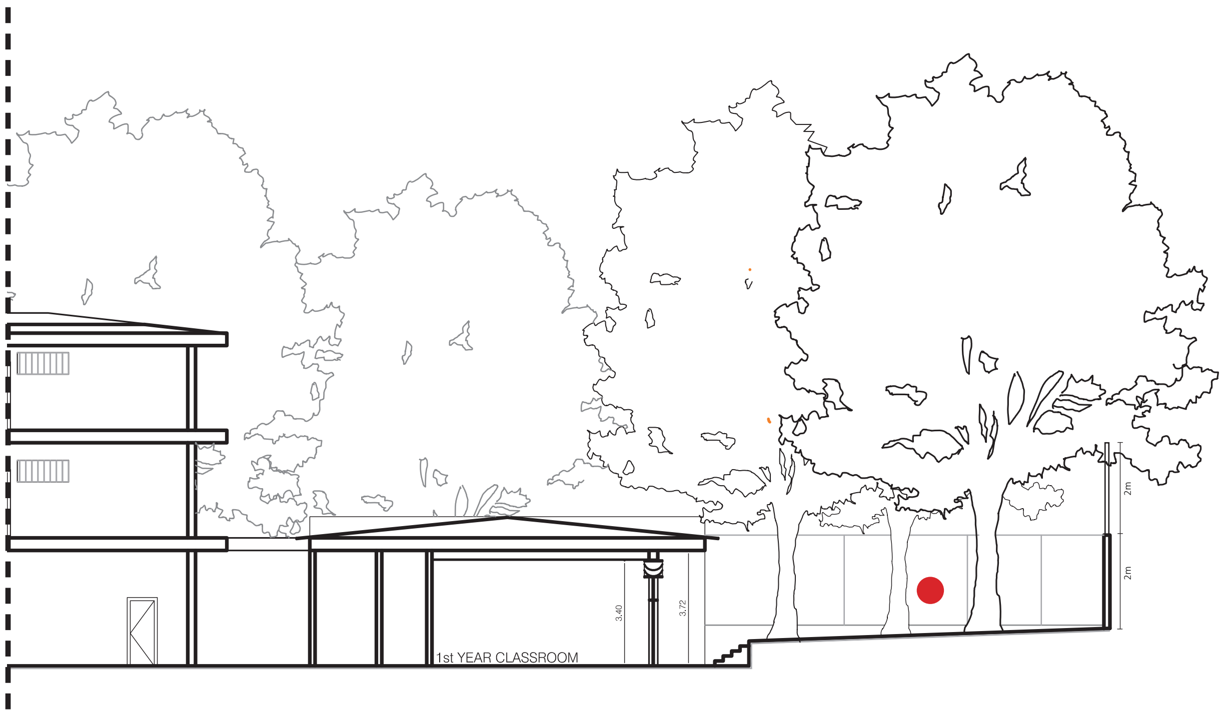

Figure 4.5.03 - Section AA showing Cora Coralina Park

and the busiest road (Corifeu de Azevedo Marques Avenue). Additionally, a boundary wall of approximately 2m height divides both areas. The materiality and levels of exposure shift drastically from Corifeu Avenue to Cora Coralina Park. The younger students heavily use this area, characterised by the heavy concentration of tall trees. Not all ground surfaces are grass; most are pure exposed soil with rugged topography (see pictures within figure 4.5.04). There are six tree species in this region: the Eugenia uniflora, Psidium guajava, Fraxinus americana, Ligustrum lucidum, Morus nigra and Persea americana.

Treetops cover this spot; however, the sun still penetrates the ground area due to their substantial heights and moderate density (figure 4.5.04). The sparsity of the treetops forms gaps where radiation and light can infiltrate the soil. As mentioned, trees are also expressively tall, creating extensive non-obstructed areas between them and the boundary wall. The northwestern wall within this area has trees near it. Additionally, a metallic structure sits on top of the wall covered by climbing vegetation, which could be considered a “green wall”. The mentioned brick and green wall achieves a final height of nearly four meters (see boundary wall in figure 4.5.03) and probably acts as a barrier to sun radiation and pollution. The characteristics of this space create critical aspects, such as having a medium to low sky view, the lack of hard pavement materials, an extensive area with exposed ground floor, and the presence of taller trees in the adjacent areas.

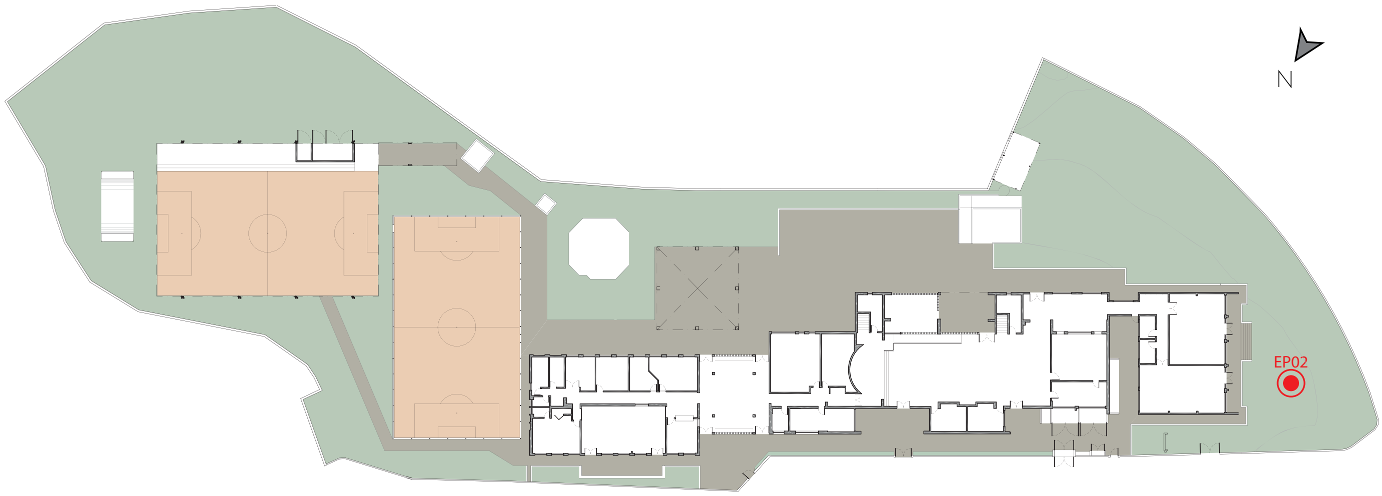

Figure 4.5.04 - Images, and location floor plan showing spot EP02 (personal archive).

CORA SPOT 02 (EP03)

Spot 02 of Cora Coralina Park is located southeast of the main building, directly connected to the first explored spot and the third spot. It has characteristics similar to spot 01, the main one being its proximity to Corifeu de Azevedo Marques Avenue. Another similarity is the high number of trees. A metallic structure on top of the boundary walls and some climbing plants are also spotted in this area. However, the sky view factor in the measured area is even lower than in the first spot, which I achieved by denser treetops, leaving the ground floor less exposed. Even though the permeability is lower in this zone, the trees are still tall, allowing for a connection with the avenue. The tree species in this portion of the park are: Ligustrum lucidum, Morus nigra, Mangifera indica, Lagerstroemia indica, Tipuana tipu, Psidium

Figure 4.5.05 - Images, and location floor plan showing spot EP03 (personal archive).

guajava, Fraxinus americana, Eriobotrya japonica, Lagerstroemia indica and Eugenia uniflora.

Spot 02 of Cora Coralina's Park is connected to Corifeu de Azevedo Marques Avenue in the southeastern part. However, on the north/northeast side of the boundary wall is a less busy street where the school's main entrance is located. Moreover, Spot 02 has most of its boundary area attached to the heavy vehicular avenue. The mentioned characteristics could indicate a higher exposure to pollutant particles on Spot 02 than 01. Conclusively, the main aspects of this space are the low sky view factor, the lack of hard pavement materials, an extensive area with exposed ground floor, and the presence of taller trees throughout the studied spot.

CORA SPOT 03 (EP04)

Spot 03 is a small plaza between the school building and the backs of several houses and other establishments with access to Corifeu de Azevedo Marques Avenue. All southeast openings in the main building are oriented to this area. This is the only spot in Cora Coralina Park without extensive vegetation, and its soil is covered with cement pavement. Moreover, other than the building itself, no built or natural elements provide shade into this area's pavement.

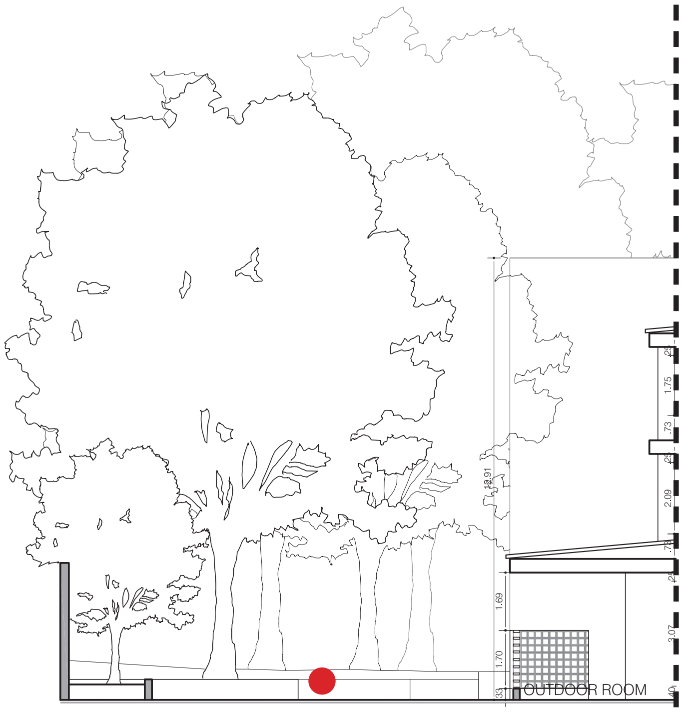

Figure 4.5.06 - Image, section BB, and location floor plan showing spot EP04 (personal archive).

As mentioned, in certain parts of the year, the building itself could block the sun, but when the sun angles are high (which will happen in the hotter periods), the area will be completely exposed to direct radiation. The level of exposure in this area and the materials used indicate high thermal discomfort on warmer days. The felt temperature may be much higher than in other school areas due to the heat absorbed and released by the materials. The direct incidence of the sun on human skin will also increase discomfort on hot days. On the other hand, the plaza may present high wind velocities due to the lack of obstructions, which could increase when the climatic conditions are not so extreme. Additionally, the buildings on the southeast will probably protect the plaza by blocking air pollution from the adjacent avenue. Conclusively, the main aspects of this space are the almost unobstructed sky, the bare inexistence of vegetation, an extensive area with hard paving materials, and the spots' considerable size.

OPEN CLASSROOM (EP05)

Another area studied was the open classroom, which is open but has a roof. It comprises two areas; cobogos delim-

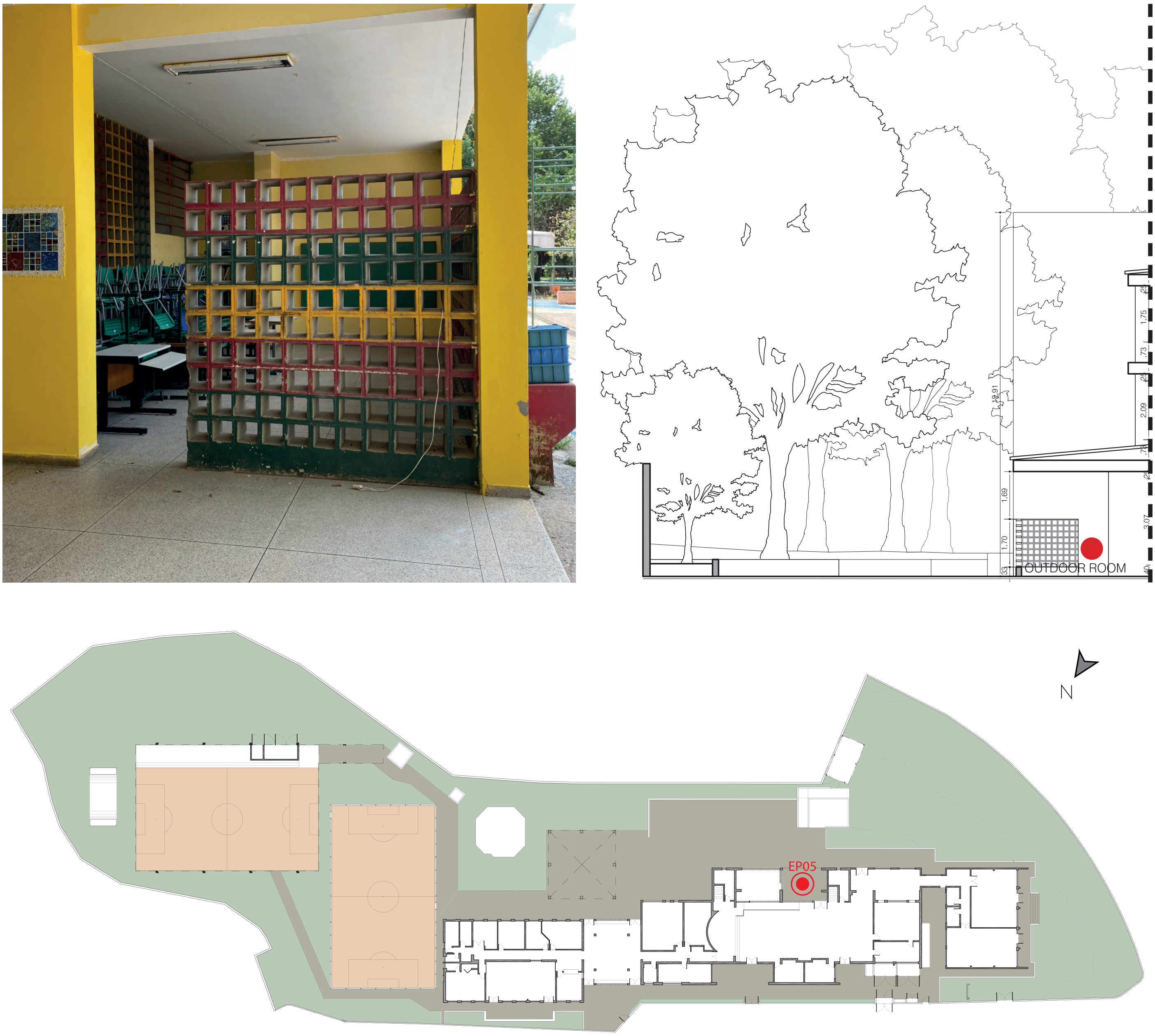

Figure 4.5.07 - Image, section BB, and location floor plan showing spot EP05 (personal archive).

itate one, which is approximately 2m in height. The other is open and connects the entrance to the indoor patio to Cora Coralina Park Spot 03. The second mentioned space is the focus of this measuring exercise. Additionally, the covered space is roughly 60 sqm and 5m deep and it is covered by a 10cm concrete slab and a roofing system consisting of steel structure and galvanised tiles. Furthermore, the motivation for selecting this area was its semi-outdoor and transitional aspects. The mentioned aspects happen due to the open space, however, protected horizontally and vertically by the building's structure. There is expected to be less solar incidence and less air movement than in other open areas. However, not being as low as the indoor spaces. Finally, The mentioned characteristics form a space with critical aspects, such as the horizontal cover protecting from the sky, the inexistence of vegetation, and the reduction of light, wind and direct solar radiation due to cobogos.

FOOTBALL COURT (EP06)

This football court is covered with cement and has an area of roughly 433 sqm. It has no roof and is surrounded by a metallic structure that does not obstruct light and air movement. Moreover, this structure is populated in some areas with climbing plants (mainly the southwestern wall). Due to its size and the surrounding context, which is composed mainly of lower buildings, this spot is more likely to overheat during warmer periods. Additionally, air movement is probably higher, reducing air pollution. The main aspects of this space are the unobstructed sky, the existence of veg-

Figure 4.5.08 - Images, and location floor plan showing spot EP06 (personal archive).

etation as living walls, an extensive area with hard paving materials, and the spots' considerable size.

COVERED FOOTBALL COURT (EP07)

The covered football court area comprises 590 sqm of cement-paved ground with an enormous roof structure. The roof system is over seven meters high and comprises a metallic frame covered by steel tiles on top and sides. These elements create steel "walls", which start around three meters from the ground. This court is located on the northeastern portion of the terrain, surrounded by the school terrain and low-rise buildings. It is considerably far from Cora Coralina Park and Corifeu de Azevedo Marques Avenue. The characteristics of this space, regarding air quality, are probably similar to the uncovered football court. However, the studies will probably indicate better thermal comfort performance in this space. The space's main features are the openness until approx. 3m on the sides, with an expressive tall ceiling and reduced daylight while possibly preserving higher wind movement.

Figure 4.5.09 - Internal and external images, and location floor plan of Spot 07 (personal archive).

GARDEN (EP08)

The garden spot is in the same area where the football courts are located and has similar characteristics. However, it is the only spot with vegetation in this northeastern portion of the terrain. It is covered in grass with some small trees and bushes, but the vegetation is low and sparse overall. The species of the mentioned vegetation are: Syagrus romanzoffiana, Mimosa caesalpiniifolia, Podocarpus sp., Malpighia glabra, Terminalia catappa, Thuja sp., Punica granatum, Astronium sp., Eugenia uniflora and Fraxinus americana. The existence of such different vegetated areas (Cora Coralina Park and Garden) with discrepant surrounding contexts within the same school environment forms a unique opportunity to develop a comparison study between areas. Conclusively, the main aspects of this area are the almost unobstructed sky, the existence of lower vegetation, and an extensive area with grass.

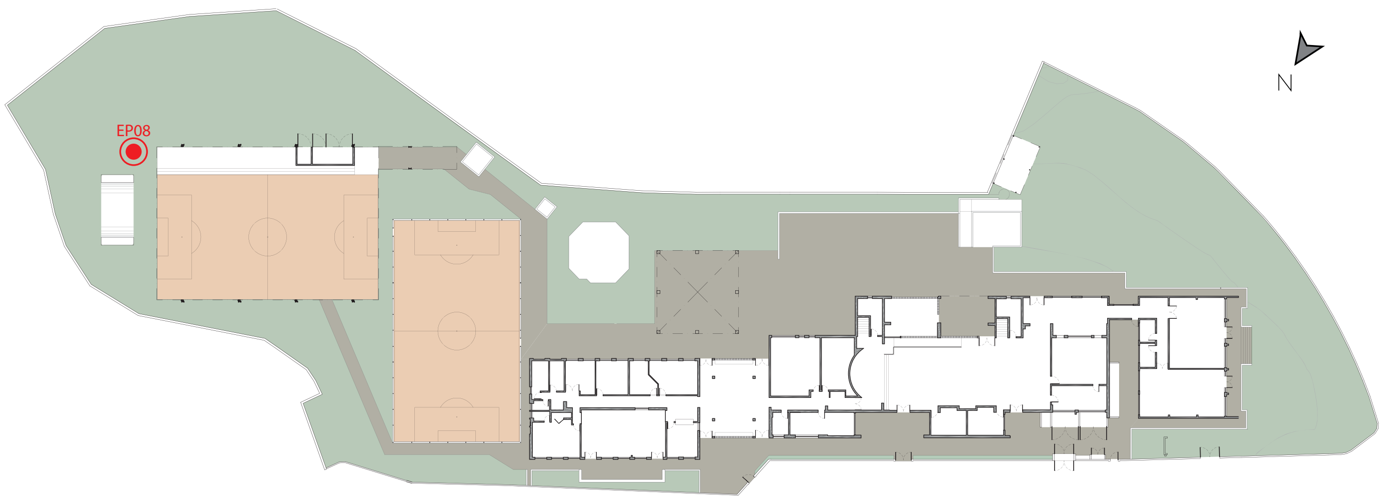

Figure 4.5.10 - Images, and location floor plan showing spot EP08 (personal archive).

4.5.2. INDOORS

The indoor areas of interest were spread over the building's floors (ground, 1st, and 2nd). One of the main reasons for selecting the rooms on the ground floor was their proximity to the outdoor Small-Scale Green Infrastructure (SGI). Another reason is the specific design characteristics of each room, such as facade design, size, and potential for cross ventilation. Consequently, the selected rooms on the ground floor were the indoor patio, the first-year classroom, and the administrative entrance hall.

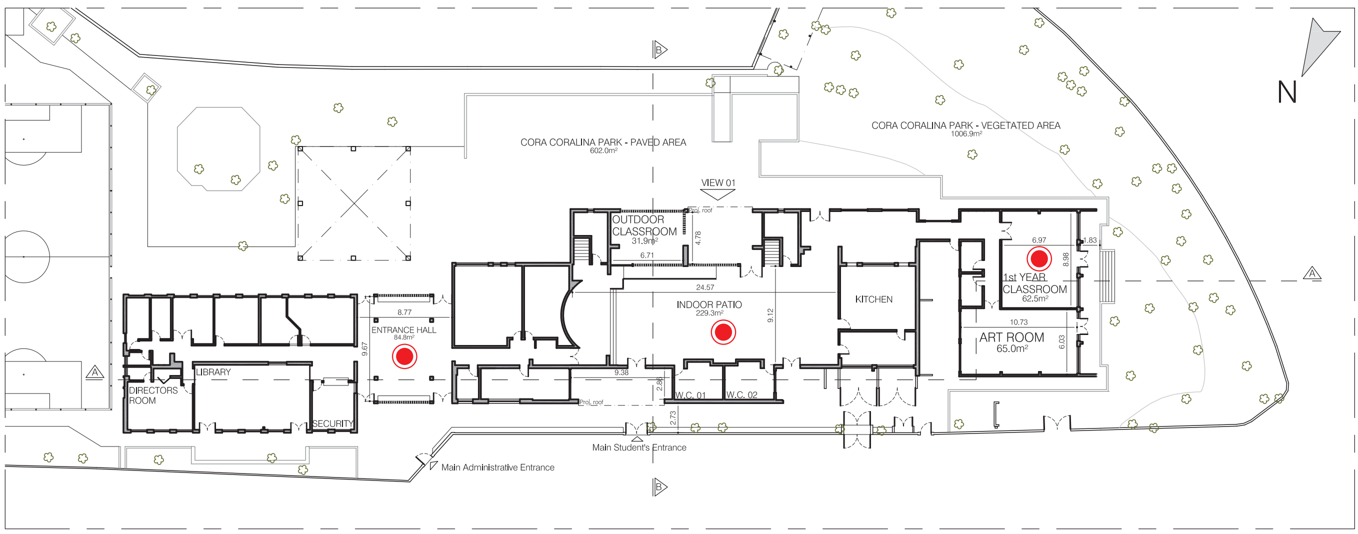

Figure 4.5.11 - The ground plan of the EMEF Amorim Lima with the indication of external studied points.

ADMINISTRATIVE ENTRANCE HALL (IP01)

The administrative entrance hall is the main entrance for staff and parents and is directly connected to the building's administrative section. This room is also connected to the indoor patio through a narrow corridor. The room has a 3.55m high ceiling and a 10cm concrete slab covered by a roof structure in carbon steel and galvanised tiles (as the entirety of the school's roof). The room has openings connected with the school's Northwest and Southeast outdoor areas. These facades have two glazed metallic frame doors and are almost entirely treated with cobogos. Combining the doors and cobogos, each wall that faces the outdoors possesses roughly 43% of its areas as unobstructed for air

Figure 4.5.12 - Images, and location floor plan showing spot IP01 (personal archive).

movement and an additional 21% for daylight (fixed glazed elements). The openings with cobogos on both sides are 2.60m in height by 4.80m in size, being .70m raised from the floor. Additionally, the four doors have a height of 2.30m and a total opening of 1.70m. The mentioned characteristics potentially display abundant daylight and cross-ventilation in the room. Thus, the entrance hall is a valuable spot for conducting environmental measurements. The characteristics of this space create critical aspects, such as the smaller square meterage, the continuous air movement through double-sized cobogos and the reasonably high ceiling.

INDOOR PATIO (IP02)

Concerning the overall school program, the indoor patio could be considered the "heart" of the building. It is the students' main entrance and the connection for all the other indoor areas, including the other floors. The room is directly connected to the school's kitchen and primary ground-floor bathrooms. Moreover, the indoor patio has around

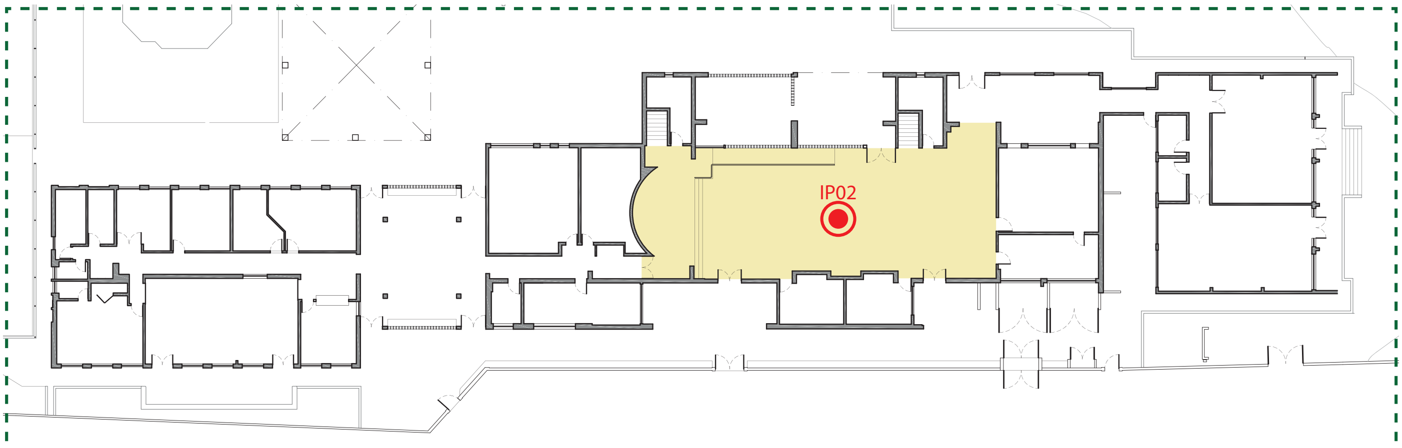

Figure 4.5.13 - Images, and location floor plan showing spot IP02 (personal archive).

220 sqm divided into two portions: the "stage" area with 30 sqm and the most extensive portion, the patio itself. The stage has a lower floor-to-ceiling distance of 3.50m, while the patio has a ceiling height of 4.0m.

The indoor patio's south/southeast has two main opening systems: the cobogos and double-leaf doors seen in the

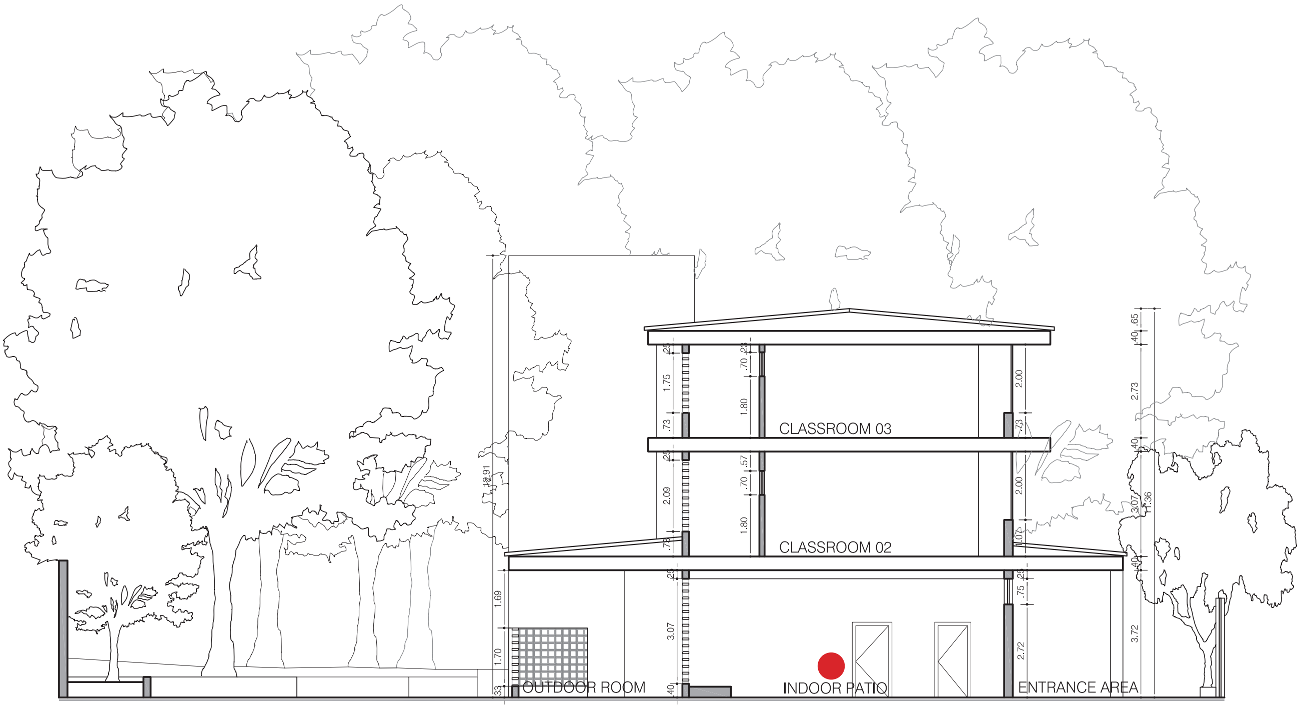

Figure 4.5.14 - Section BB showing IP02.

Figure 4.5.15 - Cobogo, doors, and windows in the indoor patio (personal archive)

administrative hall. The cobogo façade in this room is over four meters, placed approximately 50cm over the ground, ending at 3.70m in height. The door on this wall is the same as the one in the entrance hall but with a width of two meters. Additionally, the height and the proportions of opaque and open surfaces are the same. As stated before, the southeast wall is also composed of a fixed-glazed window with a steel frame and clear glass. The glass openings are approximately 1.0x.18m with a narrow frame, forming an element constantly open to daylight but with no inlet to the wind (as seen in the image above). The southeast facade faces the less vegetated area of Cora Coralina Park. It has a transitional covered semi-open space between them called the open classroom (discussed previously). Furthermore, the northwest wall is connected to the entrance environment of the school, which was also previously shown. The mentioned wall possesses four openings: two double-leaf doors and two windows. Both windows are roughly 2.70m from the ground, have similar sizes, and are made of the same steel as the doors; however, these windows do not have any glazing. The openings are approximately 25x25cm, forming an element of over four meters with a one-meter height. Considering the considerably narrow steel frame, the mentioned windows are open to daylight and ventilation. As a result of the architectural conditions of this room, for example, being between two semi-enclosed transitional spaces, having a significant floor area and ceiling height, the spaces could lack natural light and even enough ventilation to dissipate heat. During the visits, it was noticeable that the lights were always on, indicating the lack of natural light in the space. Nevertheless, the indoor patio does not seem to receive high direct solar radiation levels due to the transitional spaces previously mentioned, which indicates probable thermal discomfort for users during colder periods. Finally, the critical features are the highest square meterage from the other indoor spots, continuous air movement through the cobogos, the school's highest ceiling and a lower daylight level throughout the floorplan due to its extensive size.

FIRST-YEAR CLASSROOM (IP03)

The southwestern portion of the EMEF Amorim Lima comprises special needs toilets, an art classroom, and the first-year classroom, the last two directly connected to the densely vegetated area of Cora Coralina Park. The first-year

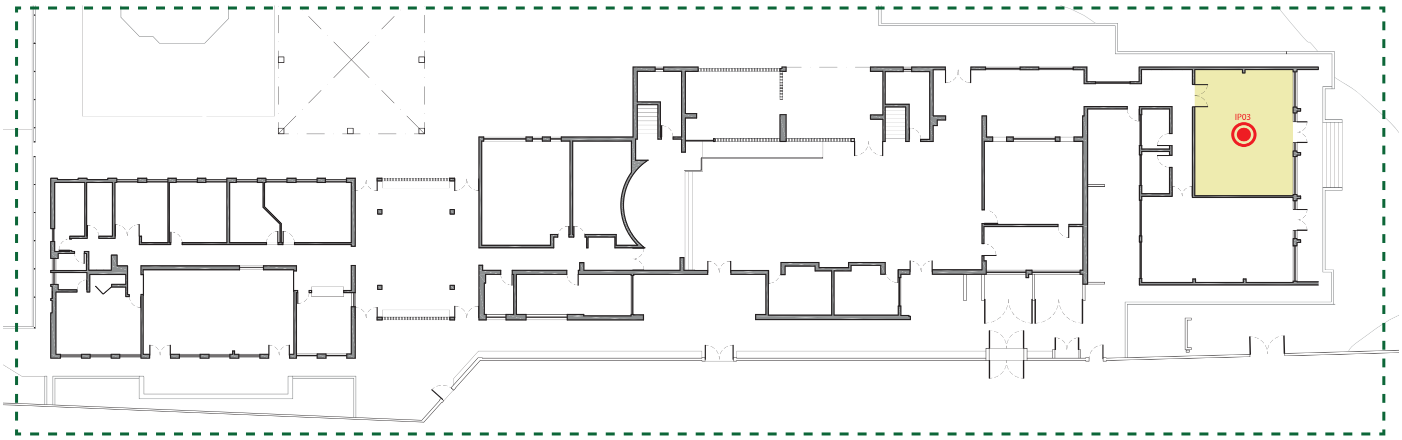

Figure 4.5.16 - Images, and location floor plan showing spot IP03 (personal archive).

classroom became of more interest as it was the only classroom with all openings facing the vegetated area. The classroom's false ceiling is composed of perforated plaster plaques, which are underneath the concrete slab. Above the slab is the same roofing structure explained before and used on the entire school. The southwest wall of the first-year classroom has three identical fixed windows of over 2m width by .60 height, being elevated 2.10m of the floor. Besides the windows, there is a double-leaf door element, entirely made of steel, apart from two minor components of 1.20 by 0.13m of clear glass. The small size of the glazed windows and high vegetation outside minimize daylight to reach the room. The vegetation combined with smaller inlets could also indicate lower wind velocities inside the room. The central aspects of this room are the lack of wider translucent openings that create lower daylight throughout the room and the connection to the vegetated area of Cora Coralina Park.

CLASSROOM 01 (IP04)

Three classrooms and the laboratory were selected on the following floors of the main building. The first one stud-

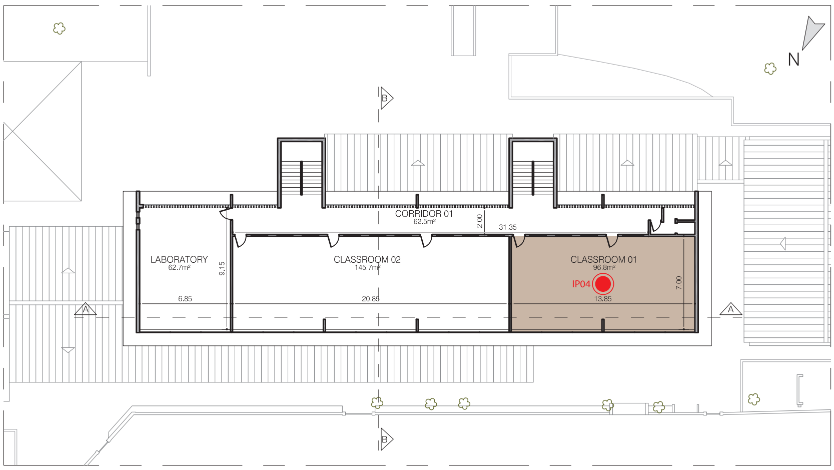

Figure 4.5.17 - Location 1st floor plan showing spot IP04 (personal archive).

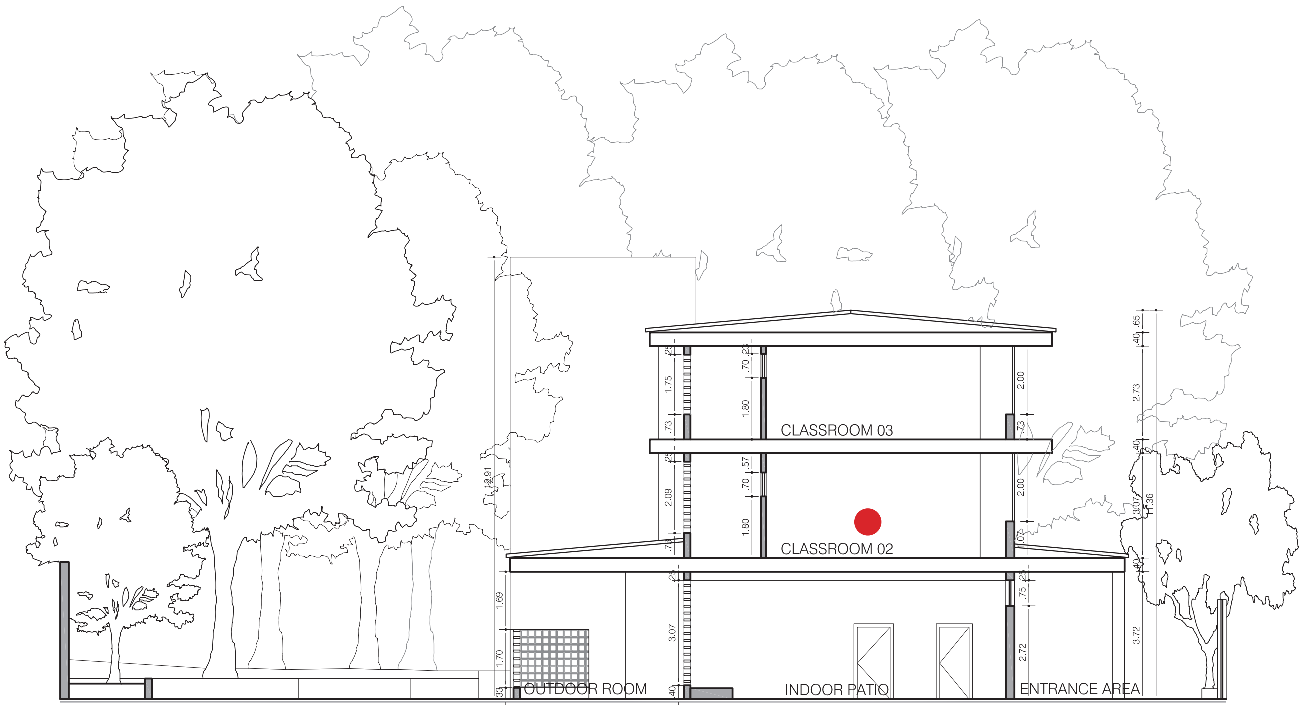

Figure 4.5.18 - Section BB showing clasroom 02, as a reference to IP04

ied (Classroom 01) is located on the first floor of the building and is around 96sqm, being a rectangle of 13.85x7.0m. One of the bigger faces of the room (13.85m) is northwest-oriented, facing the outdoors. Moreover, the parallel wall (southeast oriented) is the boundary to the circulation corridor. The northwest wall of this room carries a massive window composed of steel and various transparent glass sheets, with fixed and moveable pieces roughly representing 72% of the entire surface area. The window has approximately 57% of its area immovable and the remaining 43% openable, providing natural ventilation. Such a substantial open area in a room with a considerably small depth indicates the abundance of natural daylight. Furthermore, glare issues can happen due to the size and orientation of the openings (northwest). Additionally, thermal discomfort during hotter periods can be recurrent due to the mentioned orientation. However, the trees in front of the building massively obstruct the windows, changing the amount of daylight and radiation incidence.

The wall that separates the classroom and the corridor has two windows made of the same material as the external ones. The height is 56cm and 1.85m from the ground; however, the length of the first is 1.70m, and the other is 5.15m. Disregarding the steel structure of the windows, the element is translucent, having fixed and openable sheets of glass. Beyond the apertures described above, the circulation corridor is connected to the staircases, and the façade connecting to the outdoors is treated with a cobogo panel. The perforated façade here differs from the others seen so far and comprises numerous small openings (.05x20cm), a portion of them containing different types of glass. Finally, theoretically, crossed ventilation will happen in the 1st-floor classroom due to the cobogo panel in the corridor and the apertures in the southeastern wall whenever the northwestern windows are open. Conclusively, the main features are the extensive size of the openable translucent windows facing the primary solar exposure, with higher daylight distribution and glare at some periods of the day.

Figure 4.5.19 - Classroom and the corridor on the first floor of the school (personal archive)

LABORATORY (IP05)

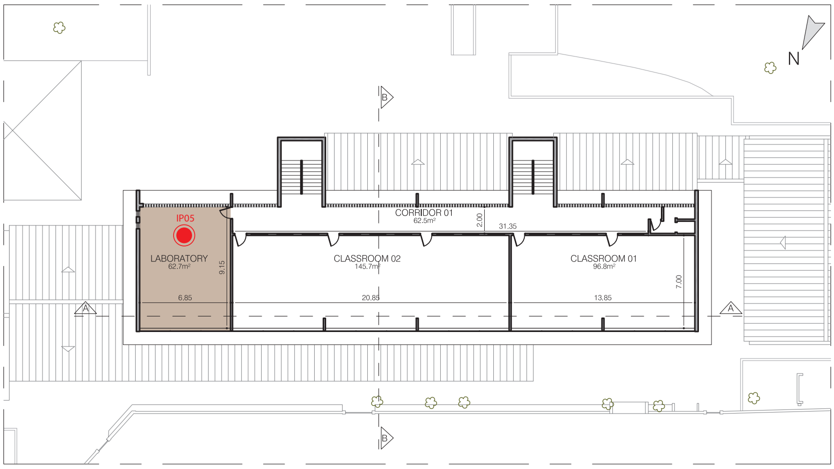

Figure 4.5.20 - Location 1st floor plan showing spot IP05 (personal archive).

The laboratory contrasts with the other classrooms as it does not have false plaster ceilings. Furthermore, it is the only room on the first floor with outdoor apertures on opposite walls (southeast and northwest). The perforated panel present in the corridor is extended to this room with the exact dimensions and characteristics. The northwest windows also have the same characteristics as the ones in the previously mentioned room. Moreover, the openable area is also 43% of the window. However, the walls with openings are half the length, and the laboratory is 9.15m deep. The features mentioned so far will change light distribution and air movement in the room compared to the ones displayed. Additionally, this room has two windows on the northeastern side, which will contribute to further light and morning direct sun radiation. The central aspect of this room is the double aspect with massive cobogo and glazed windows, which also cause higher daylight distribution and glare at some periods of the day.

Figure 4.5.21 - Laboratory on the first floor (personal archive)

CLASSROOM 03 (IP06)

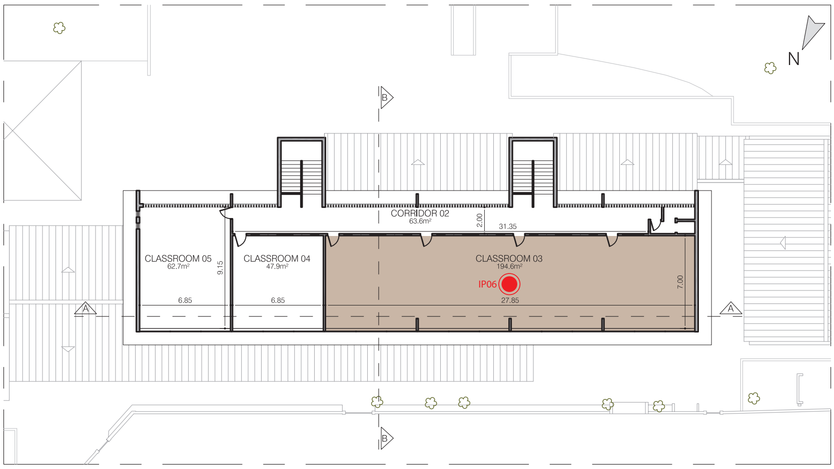

Figure 4.5.22 - Location 2nd floor plan showing spot IP06 (personal archive).

The overall structure of this room, regarding materials and apertures, is the same as the classroom on the 1st floor. Nevertheless, this one has two times the last area, with 194sqm. Additionally, the southeastern wall has four doors and four windows. The northwest wall of this room follows the exact structure of the space underneath it. Although the treetops still cause some obstructions, more portions of the apertures are exposed to direct sun. Even though this room is much bigger than classroom 01, the balance between apertures and floor area remains the same. The room has the same false plasterboard ceiling underneath the standard 10cm concrete slab. However, this is the last level of the building, with a conventional roof made of carbon steel and galvanized tiles above the slab. The characteristic previously mentioned could indicate a change in the heat distribution inside the room and, consequently, users' comfort. Finally, the main aspects are the highest square meterage of the room after the indoor patio, the massive size of the openable glazed windows facing the primary solar exposure, and higher daylight distribution and glare at some periods of the day.

Figure 4.5.23 - Classroom 02 on the second floor (personal archive)

CLASSROOM 05 (IP07)

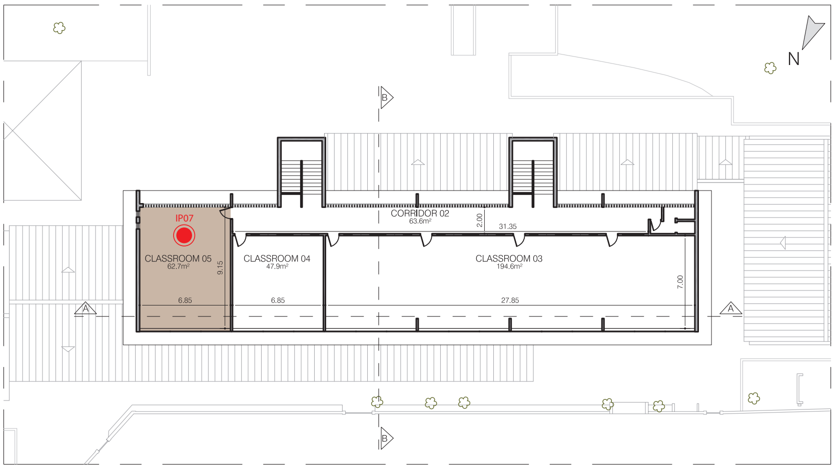

Figure 4.5.24 - Location 2nd floor plan showing spot IP06 (personal archive).

The available space and the openings are equivalent to the laboratory. The laboratory has additional fixed brick and stone tables that, perhaps, would change the air movement inside the room. Both rooms have no obstructions in front of the identical openings. This room represents a good opportunity for a comparative study with the laboratory as they are identical rooms with different height locations (1st floor and 2nd floor). The main aspects are also similar to the laboratory's; the main difference is a tree's presence, which could slightly diminish direct solar radiation and glare.

Figure 4.5.23 - Classroom 03 on the second floor, with focus on the cobogo in one of the facadades (personal archive)

4.6. RESULTS

4.6.1. THERMOHYGROMETRIC ENVIRONMENT

As previously mentioned, the first ten hours of the study were marked by significant climatic variations, including changes in temperature, wind speeds, and wind directions. These variations naturally led to temperature differences, with spot measurements showing a range of over 17°C between indoor and outdoor temperatures. The lowest temperature was recorded in the garden at night (19.1°C), while the highest temperature within the ten days was 37.3°C in Spot 3 of Cora Coralina Park, measured at 11:00 am.

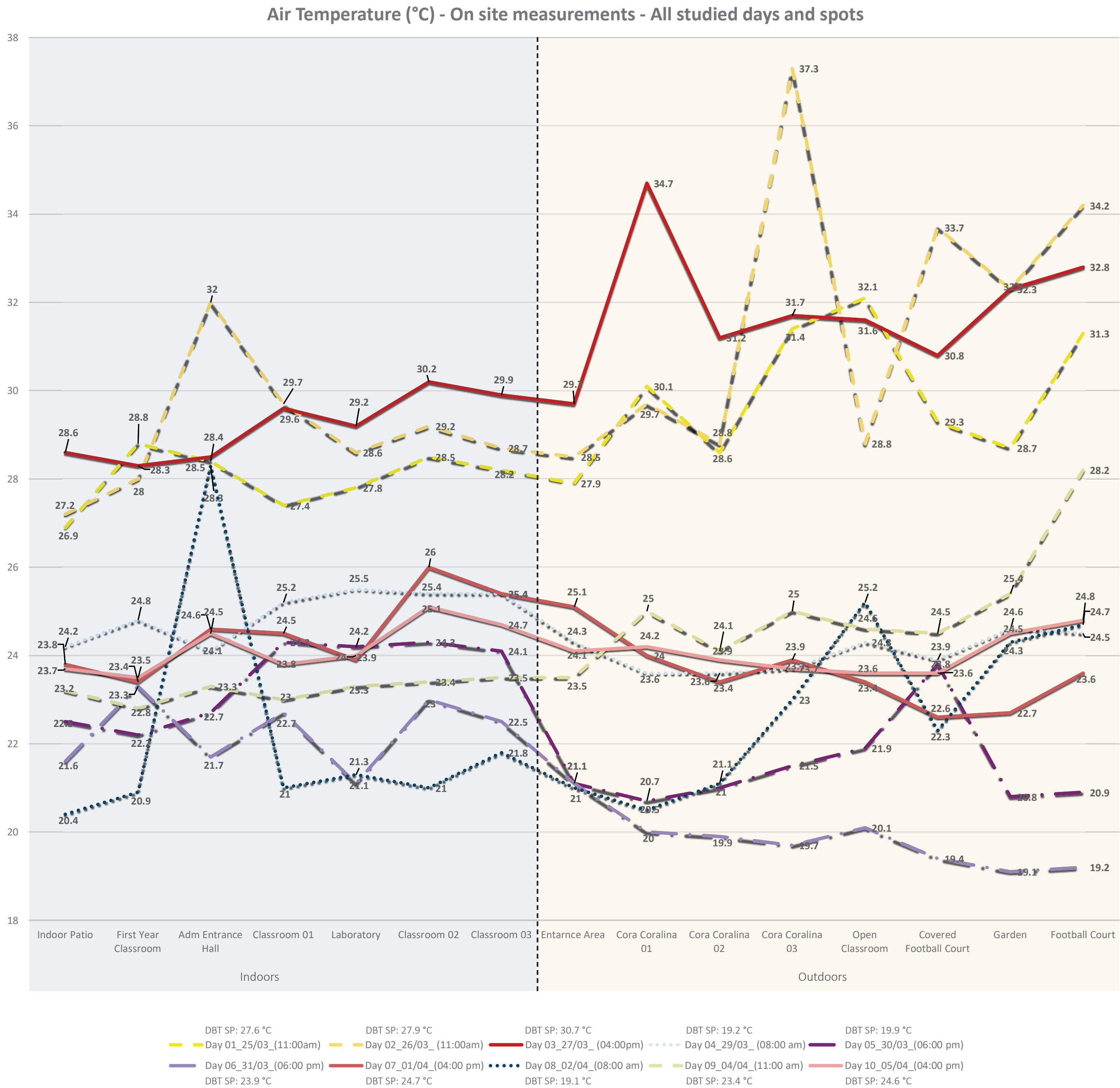

Figure 4.6.01 - Air temperatures (°C) recorded by spot measurements during the ten studied days in all analysed spots

OUTDOORS

On the first day of the study (29/03), the garden spot, despite being covered in grass and low vegetation that was not dense enough to block solar radiation, recorded the highest outdoor temperature. However, the presence of greenery was found to have a positive influence on the environmental conditions during the study period. This was evident on the 29th of March when areas with a high amount of vegetation (Cora Coralina Park, spots 01 and 02) presented the lowest temperatures (23.6°C). The dry-bulb air temperature in the vegetated area of Cora Coralina Park was lower than all the ones detected indoors. This finding showcases the effectiveness of shaded environments with air movement access and natural elements providing cooling against enclosed spaces covered by hard materials. Nonetheless, Cora Coralina Park's environmental quality is enhanced when the climatic conditions are not severe, as is the case at 08:00 a.m. (19.1°C dry bulb temperature). When mentioning the permeability of the outdoor sites, air movement is an important variable to consider, and analyzing the wind speed data can confirm that. On that day, when the air dry-bulb temperature was lower in the Cora Coralina Park spots 01 and 02, it was possible to spot air movement in those areas. Even though the detected wind speeds were low (0.9m/s at spot 01 and 0.4m/s at spot 02), the finding indicates the permeability of this space. It is expected to acquire higher air movement as a porous area, altering the surface and perceived temperatures (human comfort).

On the second studied day (02/04) at 08:00 am, Cora Coralina Park (spots 01 and 02) presented the lower air temperatures, with Spot 01 having the lowest within the outside ones (20.5°C). Once again, it was possible to register the air movements in both spots, respectively 1.3m/s and 1.2m/s. The highest air temperature outside was in the outdoor classroom, with 4.2°C more than the Park's spot 01 (25.2°C). Then, the transitional space had probably suffered from the direct sun in the early morning; the lack of vegetation and abundance of hard surfaces could have been responsible for the temperature increase. On both days (29/03 and 02/04), the uncovered football court presented high air temperatures, which is understandable due to the expressive amount of cement paving. However, the sizeable unobstructed area indicates increased air movement, which would, perhaps, prevent discomfort. Indeed, it registered a 1.8m/s wind movement at the court, the highest of the day.

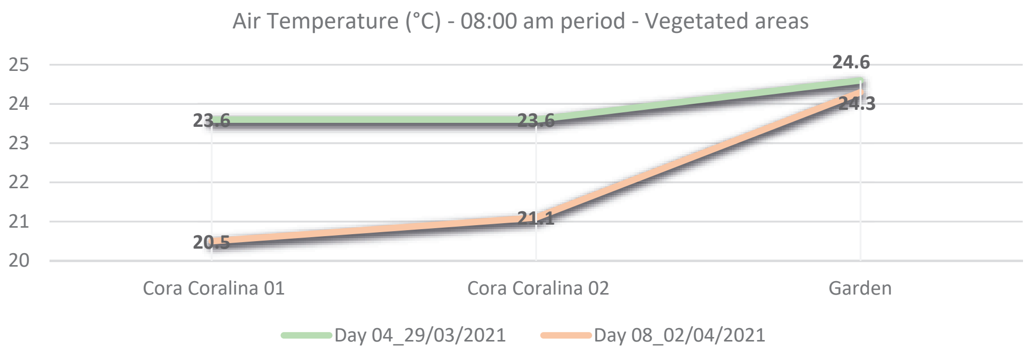

Figure 4.6.02 - Air temperatures (°C) recorded in outside areas with vegetation during the 08:00 am period.

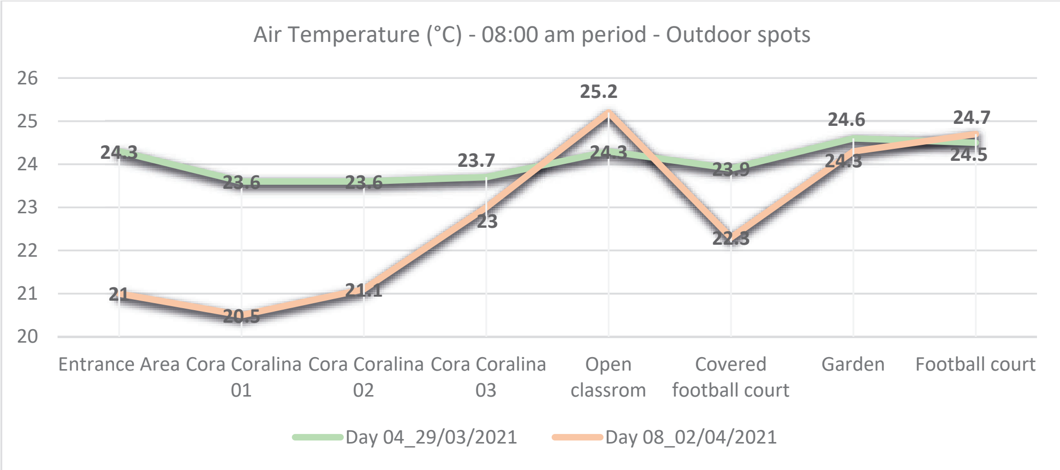

Figure 4.6.03 - Air temperatures (°C) recorded in outside areas with vegetation during the 08:00 am period.

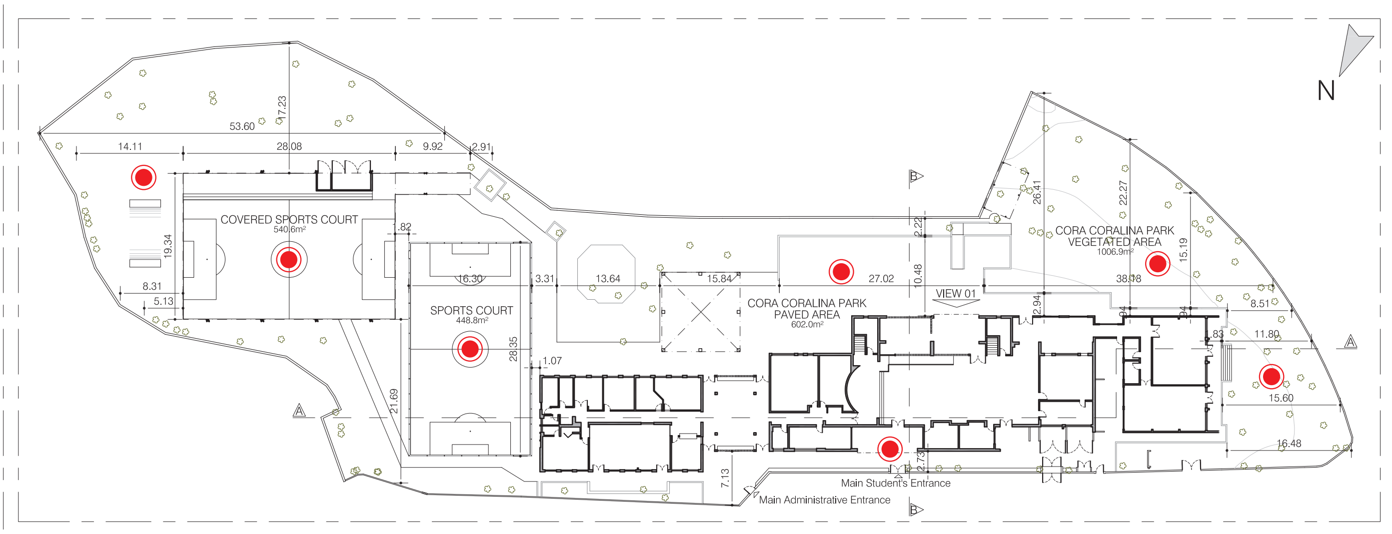

Figure 4.6.04 - The ground plan of the EMEF Amorim Lima with the indication of external studied points.

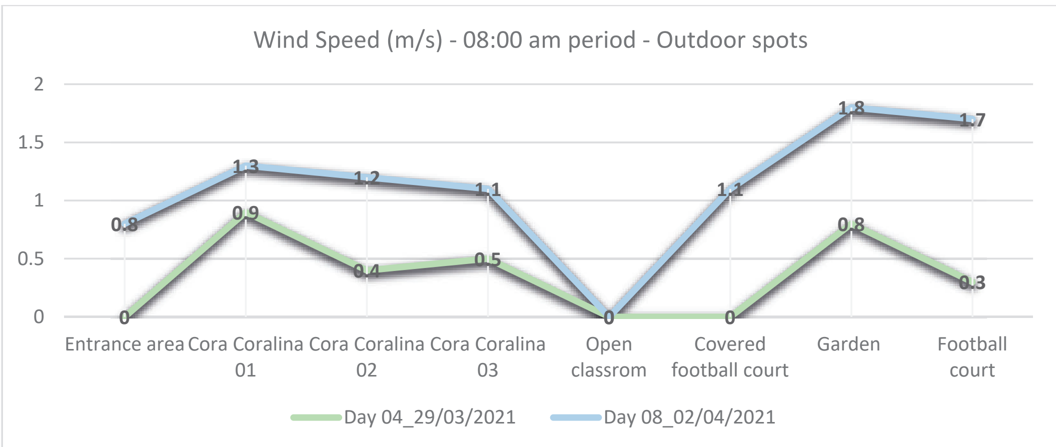

Figure 4.6.05 -Wind speeds (m/s) recorded on the outdoor spots during the 08:00 am period.

At 11:00 am, when studying the outdoor conditions, as the climatic conditions are usually harsher than at 08:00 am, it can be expected to find a more expressive variation between locations. The discussed fluctuations will happen because of the treatment levels and spaces' enclosure. Indeed, as expected, the variations were spotted. The first day (25/03) showcased a 4.2°C between the highest and lowest recorded air temperatures, while 4.7°C fluctuated on the third studied day (04/04). The second day (26/03) displayed the highest difference between the ten studied hours, including outdoor and indoor zones, 8.8°C. The minor hot outdoor conditions of the three days at 11:00 am were found in the entrance area. The more enclosed character of this transitional space was discussed previously in this work and was exemplified here through the measurement outcomes.

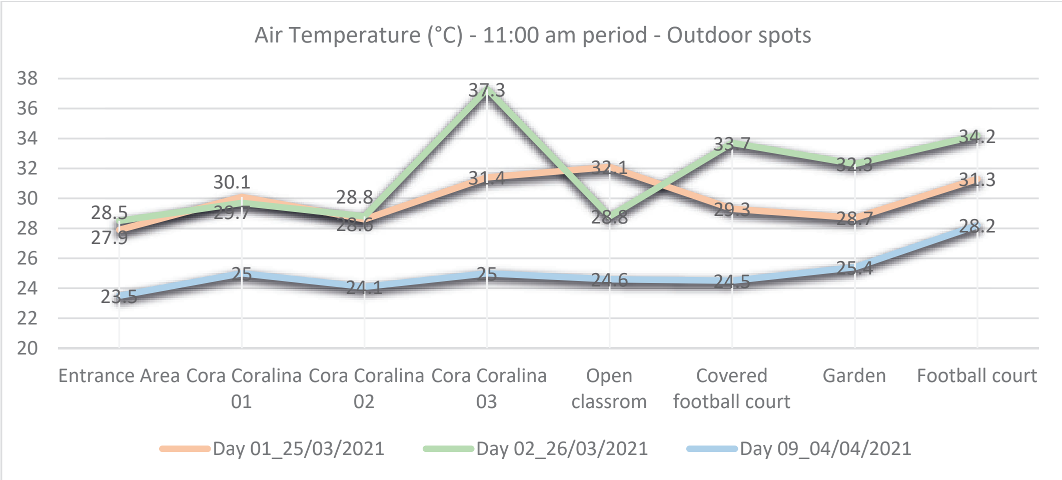

Figure 4.6.06 - Air temperatures (°C) recorded on the outdoor spots during the 11:00 am period.

On the 25th of March 2021, while the air temperature at Cora Coralina Park was 32.1°C, it was recorded at 27.9°C in the entrance zone. Moreover, on the 26th, the highest recorded temperature was 37.3°C on spot 3 of Cora Coralina Park; as for the entrance, 28.5°C was registered. The 04th of March showcased 35°C on Spot 3 and 23.5°C at the entrance area. The mentioned differences can be related to the building geometry and location of spaces regarding sun orientations. The entrance had direct sun incidence during the studied period (11:00 am). However, the Cora Coralina Park Spot 3 is much less protected than the entrance and receives direct sun from early morning. The first day's highest recorded outdoor temperature was in the open classroom, 31.2°C, while the Cora Coralina Park spot 03 presented 31.4°C. Both spaces are directly connected, but a ceiling protects the open classroom. A wind velocity of 1.2m/s was recorded in the park (spot 03). However, no air movement was recorded during the same period in the outdoor classroom. Finally, the wind speeds on Spot 3 could change human comfort conditions.

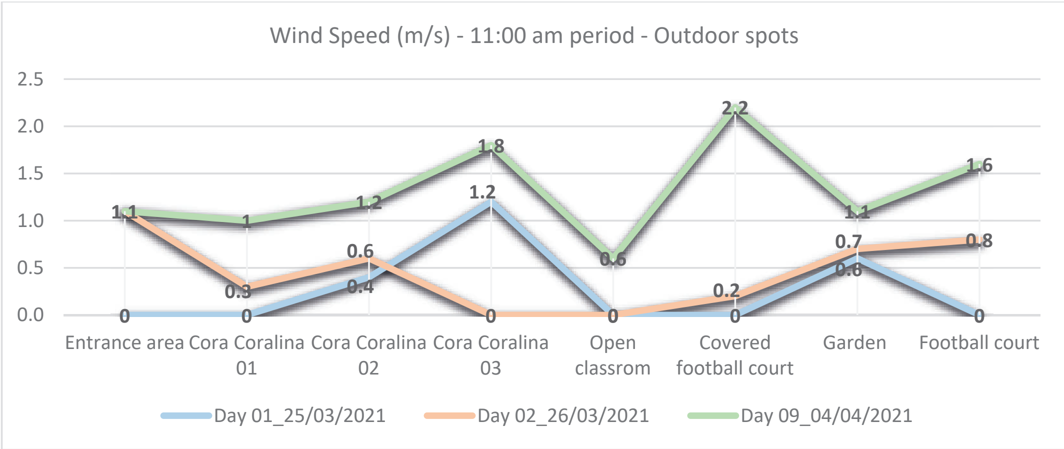

Figure 4.6.07 - Wind speed (m/s) recorded on the outdoor spots during the 11:00 am period.

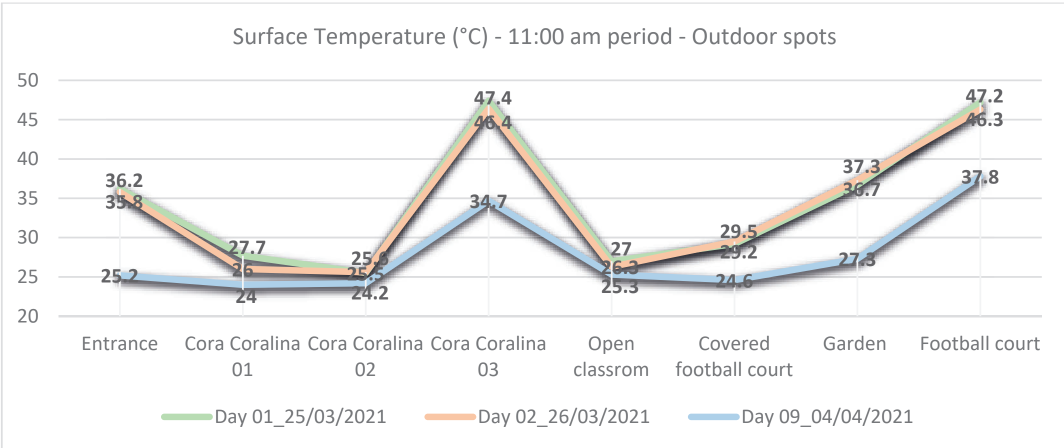

Figure 4.6.08 - Surface temperatures (°C) recorded on the outdoor spots during the 11:00 am period.

Even though there were higher wind levels in Spot 3, the surface temperature of the paved cement in Spot 3 (Cora Coralina) was 47.4°C, and the ground floor of the open room had a surface temperature of 27°C. The previous findings indicate that the mean radiant temperature of the outdoor classroom would probably be lower than the parking area, consequently enhancing the perception of human comfort. A similar situation will usually happen on the uncovered football court, which on the 4th of April (11:00 am) showed the highest air temperature of the day. The surface temperature of the paved cement in the court was also the highest recorded on the 04th of April, 37.8°C. The Cora Coralina Park spot 03 and the football court are highly exposed and will probably display high mean radiant temperatures. Additionally, the wind velocities in those spaces are usually higher due to fewer blockages. However, the collected data didn't show high wind speeds during most studied days, indicating enhanced thermal comfort perception in both spaces.

At the 04:00 pm study period, it was noticeable that each day had one different spot with warmer and cooler conditions. On the first day (27/03), while spot 01 of Cora Coralina Park reached 34.7°C, the entrance zone presented 29.7°C. As discussed previously, Cora Coralina Park Spot 01 has a space organisation that leaves gaps for permeability (sun and wind). The commented geometry allows, mainly at this period (04:00 pm), the direct sun incidence on the ground. Due to the entrance of solar radiation at this period of the day, the ground temperature at Spot 01 was 32.6°C. On the 27th of March at 04:00 pm, the weather station recorded an average velocity of 1.2m/s, with a maximum of 2.7m/s and a minimum of 0.2m/s. The wind speeds recorded in Cora Coralina 01 were 0.5m/s, while at Spot 03 of the park, the wind velocity was 2.4m/s. Even though Spot 01's small green infrastructure (trees and hedges) allows some sun to enter, the same elements could block the wind. The air temperature of Cora Coralina 3, which is highly exposed, was three degrees less than spot 01, which could indicate the importance of allowing air movement.

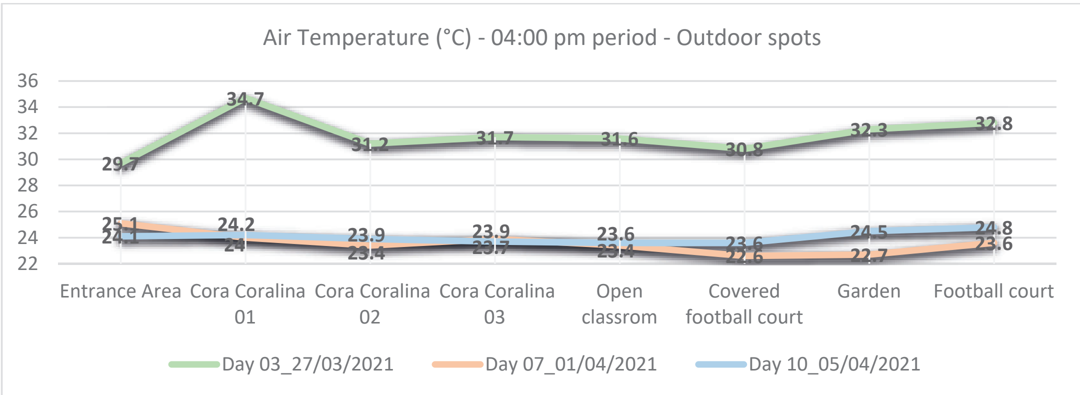

Figure 4.6.09 - Air temperatures (°C) recorded on the outdoor spots during the 04:00 pm period.

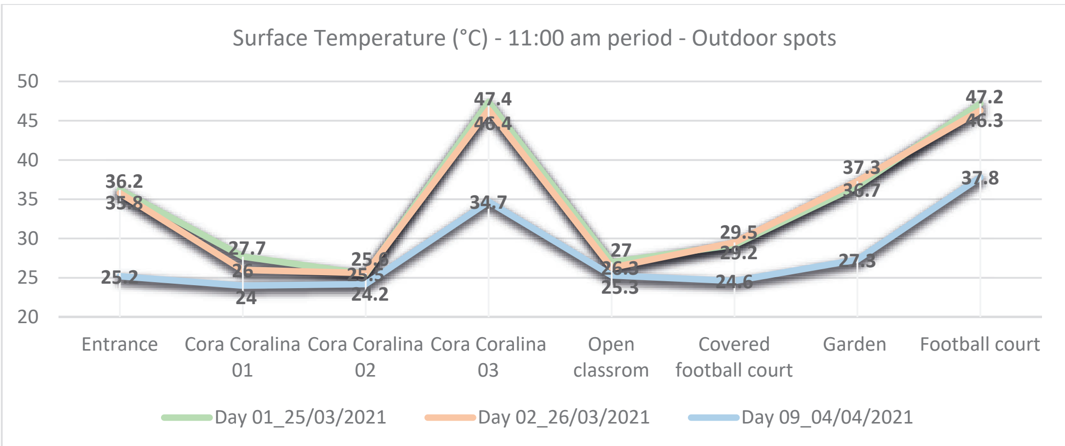

Figure 4.6.10 - Wind speeds (m/s) recorded on the outdoor spots during the 04:00 pm period.

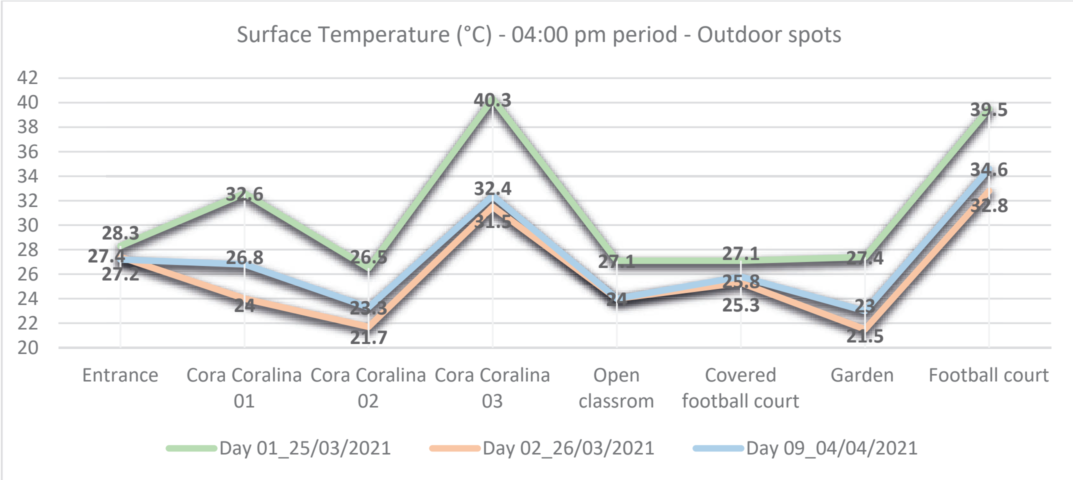

Figure 4.6.11 - Surface temperatures (°C) recorded on the outdoor spots during the 04:00 pm period.

As mentioned before, the entrance area presented the lowest temperature on the first day at 04:00 am (27/03); on the other hand, the spot had the highest recorded temperature on the second studied day (01/04). According to the weather stations, on the 27th of March, the main wind direction was from the south. On the 1st of April, the same station recorded the wind direction from the east. The proximity between the building and the boundary wall creates a corridor between the football uncovered court (NE) and Cora Coralina 01 (SW). Air movement orientation combined with the geometry of the mentioned area would allow for the creation of "wind tunnels." Therefore, there is a possibility that the air movement could play a part in the recorded air temperature differences between the 27th and 1st at 04:00 pm.

On the 1st of April at 04:00 pm, "cooler" conditions were spotted at the covered football court (22.6°C) and the garden (22.7°C). Both cited areas at this point were protected by the massive structure that covers the court. The roof element will block the northwestern and west sun (afternoon) from reaching the spots. The blockage resulted in lower surface temperatures on the garden and the covered football court, respectively 21.5°C and 25.3°C. Even though the cited football area is covered, it has shown a surface temperature of four degrees higher than the garden spot surface. The difference in surface temperatures happens due to the different ground treatments. Cement paving is the hottest surface (25.3°C), while grass and soil are the coolest (21.5°C). The surface temperatures in those protected areas contrast with those of the exposed zones. One example is the uncovered football courtyard with 32.8°C. The wind velocities recorded at the garden and covered court were around 1m/s and 2m/s that day. The discussed findings indicate a higher perceived thermal comfort in those areas than in the other outdoor ones. The enhanced comfort expected from the garden and football court shows, once more, the importance of protection from direct sun and the selected materials. During the last analysed day of the evening period (04:00 pm on the 5th of April), the covered courtyard had once more the lowest registered dry bulb temperature, accompanied this time of the open classroom, also with 23.6°C. It is important to remember that the open classroom is wholly protected from direct solar radiation at the mentioned time. The protection happens due to the portion of the school building on the northwest and the classroom's roof. The findings are one last example of the importance of sun protection during warmer periods of the year.

At the 06:00 pm period, on both analysed days, the air temperature in the city was 19.9°C and 23.9°C, respectively. Even though the city air temperatures were lower than the other eight studied days, variation between the zones could still be spotted. On the first day (30/03), a three-degree difference was noticed between the warmer and cooler outdoor spots. The second day (31/3) showcased a two-degree variation outside. On the 30th of March, the coolest conditions recorded were at Cora Coralina Park 01 (20.7°C).

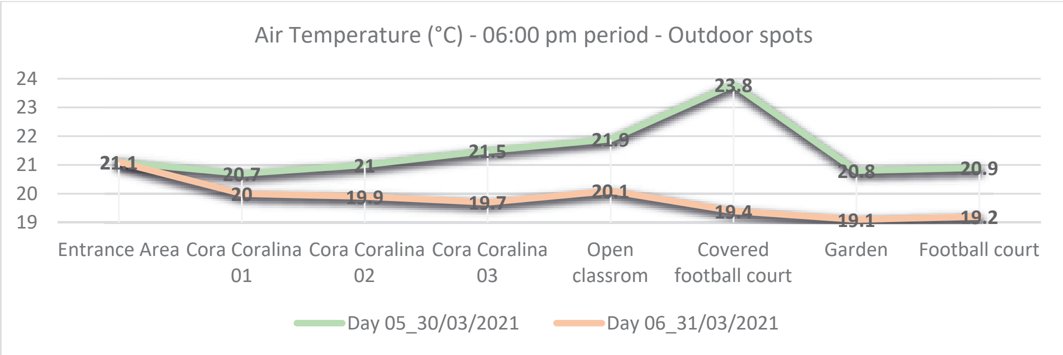

Figure 4.6.12 - Air temperatures (°C) recorded on the outdoor spots during the 06:00 pm period.

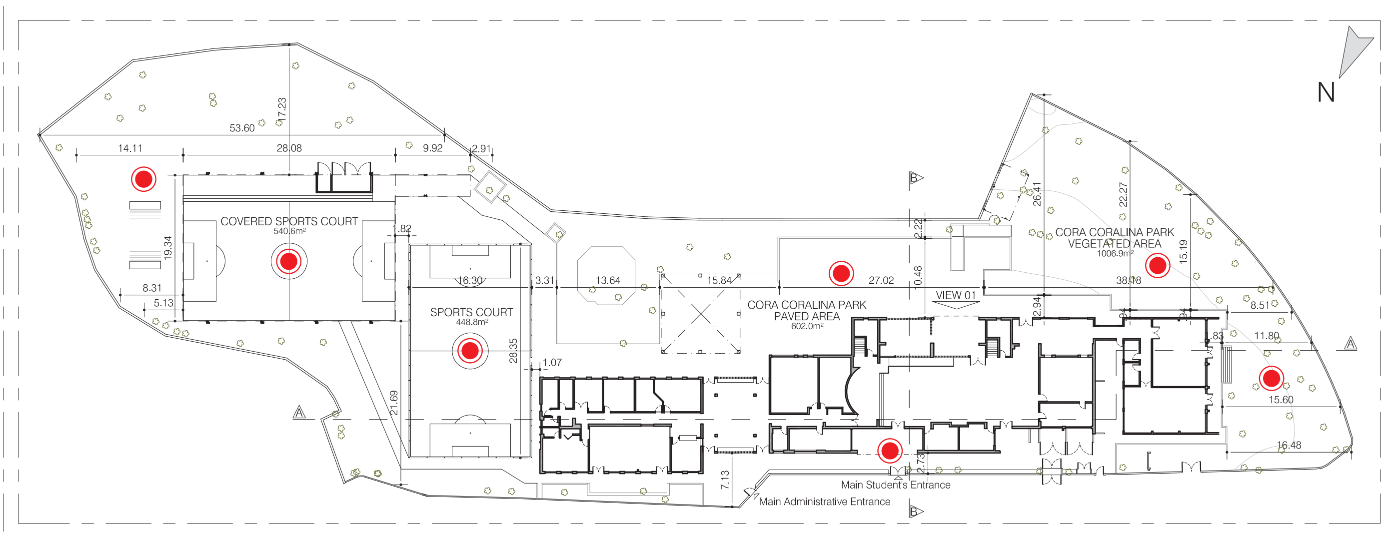

Figure 4.6.13 - The ground plan of the EMEF Amorim Lima with the indication of external studied points.

A similar outcome happened once at 08:00 am from all the explored days. The belief is that when the temperature drops, evaporative cooling will arise. The evaporative cooling will slightly modify the microclimatic thermal conditions until early morning. When studying the fieldwork outcomes regarding spots 01 and 02 of the park, it is possible to identify that the mentioned process will only happen when the temperatures are mild. The results until this point indicated that the cooling effect of the small green infrastructure would not be substantial in harsher climatic conditions.

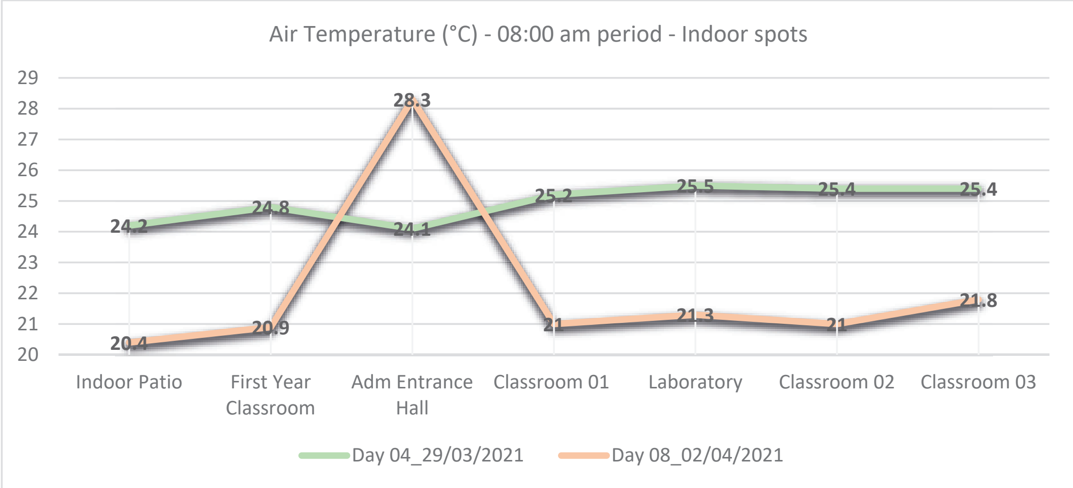

Figure 4.6.14 - Air temperatures (°C) recorded on indoor spots during the 08:00 am period.

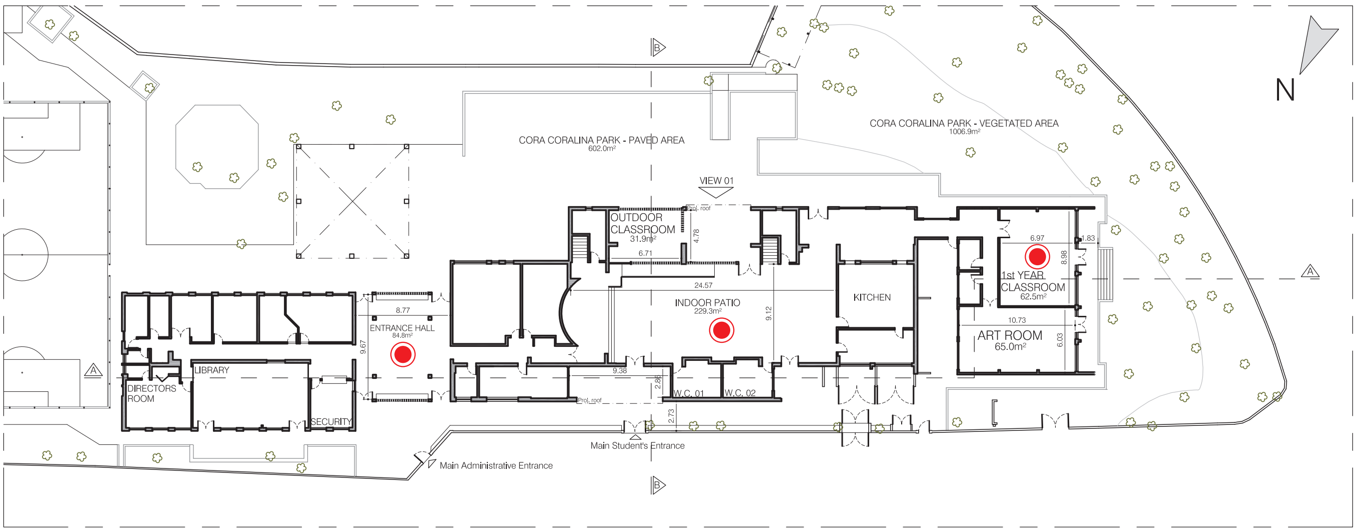

Figure 4.6.15 - The ground plan of the EMEF Amorim Lima with the indication of internal studied points.

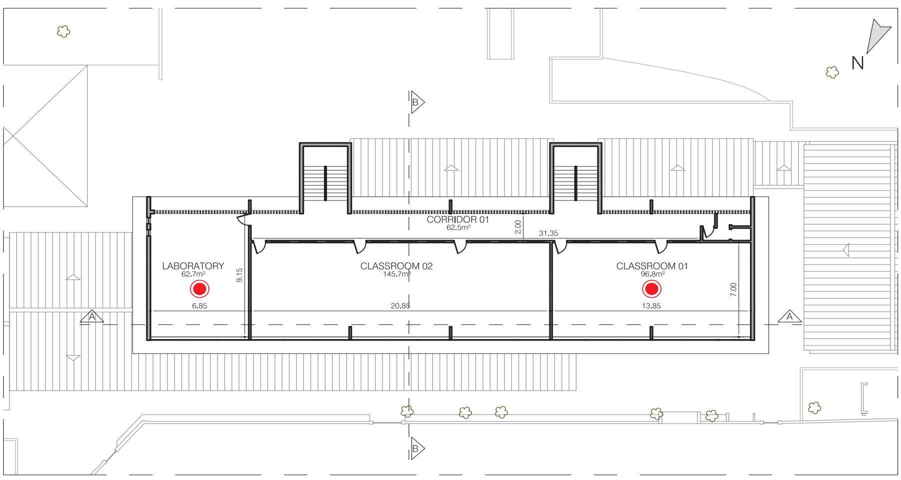

Figure 4.6.16 - The 1st floor plan of the EMEF Amorim Lima with the indication of internal studied points.

INDOORS

The first analyzed day within the 08:00 am group was 29/03. On this day, the highest indoor temperature was 25.5°C at the laboratory, and the lowest was 24.2°C on the indoor patio. On the second and last day of measurement, the 08:00 am group (02/04) recorded a temperature difference of almost 8°C between indoor spots. The administrative entrance hall was the zone with the highest dry bulb temperature (28.3°C). Additionally, the indoor patio presented the lowest (20.4°C). The temperatures on the first and second-floor spots were roughly one degree higher than the ground-floor areas, which also happened on the first day (29/03). It is possible that as the mentioned rooms stayed closed the whole day and night (indoor and outdoor openings), the heat absorbed during the entire day takes more time to be released, even when the temperature drops at nighttime. The massive, glazed area in the cited rooms and its northwestern orientation were probable reasons for the increased air temperature. The mentioned characteristic will probably be responsible for intensifying the heat storage in the room during the day.

Both days at 08:00 am (29/03 and 02/04) had their lowest indoor air temperature on the indoor patio, which, as explained before, is protected by transitional spaces: the entrance area and the outdoor classroom. The protection could be a reason for the lower temperatures; however, the room's size and the number of openings are more reasonable motives. The indoor patio has several open elements (cobogos and windows) that cannot be closed, allowing non-stop air movement and naturally reducing air temperatures indoors and outdoors at night. Air movement at lower temperatures would remove any heat stored during the day, and surfaces might not retain substantial heat due to the room's level of protection, as explained before.

The second explored group of days had the measurement made between 11:00 am and 12:00 am. For the cited period, three days were studied: 25/03, 26/03 and 04/04. Like the early morning (08:00 am), the indoor patio comprised the lowest dry bulb temperatures regarding indoor environments. The room had the coldest conditions within the outdoor and indoor environments during the first analysed days (25th and 26th of March). On the third and last day (the 4th of April), the temperature in the room wasn't as low as in the first-year classroom. The possible reasons for the room's performance were discussed for the early morning period and will remain valid for the other studied periods. The reasons will apply to different periods because the rooms endure direct solar radiation most of the day.

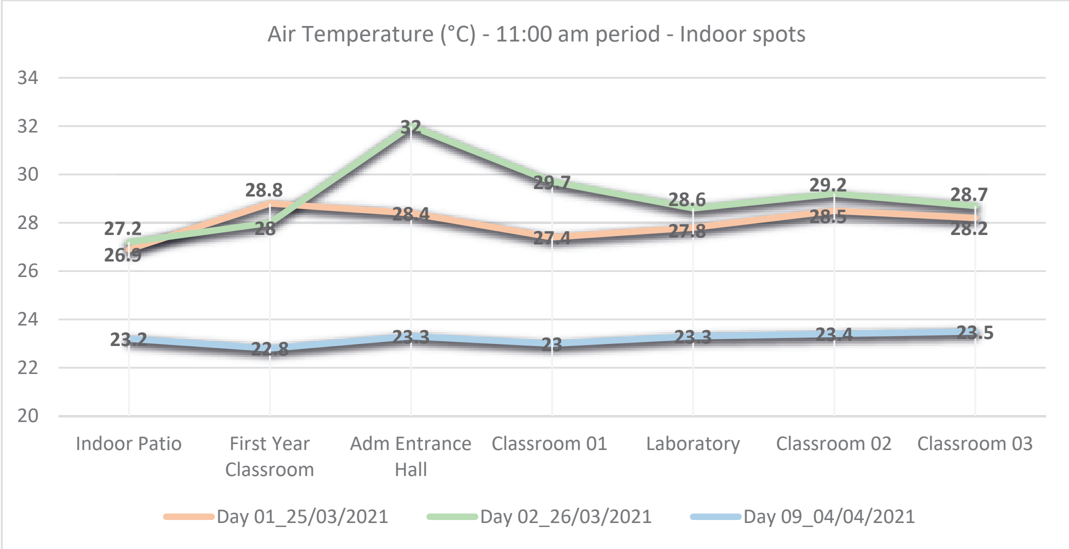

Figure 4.6.17 - Air temperatures (°C) recorded on indoor spots during the 11:00 am period.

Regarding the first-year classroom, it is located so that all the apertures are oriented southwest. The cited characteristic means that no direct sun enters through the room's openings until the last moments of the afternoon. The lack of sun and air exchange (due to the room being closed the whole time) could create a zone with colder temperatures than the outdoors. Indeed, the registered weather at this moment (11:00 am on the 4th of April) in the city was 23.4°C, while a dry bulb temperature of 22.8°C was recorded in the room. Another example of the impacts of the enclosed and protected geometry of the first-year classroom is that the variation between the outcomes was less than one degree in the first and second studied days (25/03 and 26/03) of this period (11:00 am). While the temperature registered in the city on the first day was 27.6°C, inside the first-year classroom, it was 28.8°C. On the second day, the city's condition was 29.5°C of dry bulb temperature whilst the room presented 28°C. In addition to space protection during the morning, temperature drops between the 25th and 26th of March could explain the findings above. Another observation was that 28.8°C was the highest dry bulb temperature spotted indoors on the 25th of March, a day that has not showcased high differences between internal spaces' air temperatures.

The third studied group of days was when the measurements were made from 04:00 pm to 05:00 pm. The sun is not at its peak at this portion of the day, and the temperatures are dropping. For this reason, it is a good time to try to register the cumulative impacts of the highest periods of solar exposure of the day. While the indoor measurements at 11:00 am presented the "coolest" air conditions in the indoor patio, at 4:00 pm, the first-year classroom had even lower temperatures. The previous finding could be explained by the enclosed characteristics of the 1st year room described above. The location of the cited room provides shelter against direct sun until the studied moment (04:00 pm). The patio presented, on all three days, conditions much closer to the first-year classroom. The temperature difference in both rooms was around five degrees on each studied day at 04:00 pm.

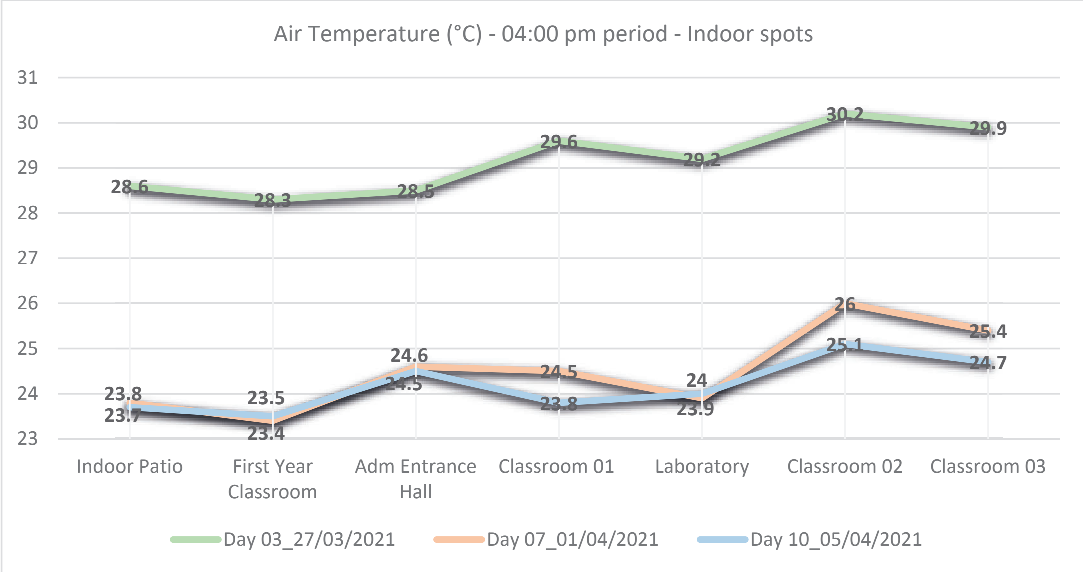

Figure 4.6.18 - Air temperatures (°C) recorded on indoor spots during the 04:00 pm period.

On all three days in the afternoon (04:00 am), the warmer spot inside the school was classroom 01 on the second floor. The room's characteristics were extensively commented on before, including the severe exposure to sun radiation. At four in the afternoon, the sun travelled from the east side of the building to the northwestern portion, facing the classroom façade. By this point, the air in classroom 01, which has had all windows and doors shut, was hotter than other indoor zones due to its exposure to solar radiation. It is possible to spot large areas where the sunlight directly reaches the classroom floor, made of wood. As a result of sun exposure, the wooden floor in two days had the highest surface temperature amongst the indoor zones, 31.3°C on the 1st of April and 30.8°C on the 5th. The 27th of March measurement of the classroom floor also presented a high surface temperature (29.3°C). As elaborated previously, high surface temperatures strongly indicate human discomfort. In other words, as was expected, the data suggest that this room is possibly an uncomfortable environment to stay in for long periods during afternoons on warmer days. One of the actions to prevent the situation from being aggravated is using the openable apertures on both sides of the room (northwest and southeast). With all windows and doors open. Classroom 02 recorded wind velocities higher than 1m/s, which could change the perception of comfort but would probably not be sufficient to provide a high-performance environment. Furthermore, all the first and second-floor rooms presented air and surface temperatures similar to Classroom 02. The orientation and location similarities of all rooms explain the previous finding.

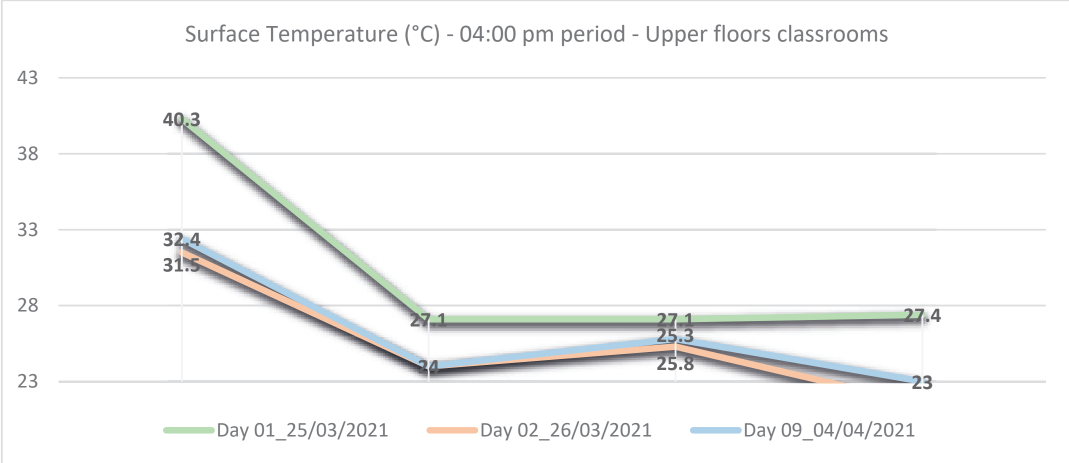

Figure 4.6.19 - Surface temperatures (°C) recorded on the classrooms of the upper floors during the 04:00 pm period.

The classroom on the first floor presented dry bulb and surface temperatures on all days at this period (04:00 pm), lower than classroom 2, which is just above it. On the first and second floors of the building, the registered dry bulb temperatures for the first and second days (25 and 26 March) at 11:00 am are lower than the outside measurements and the recorded in the city. On the first and third days (27/03 and 02/04), the air temperature was one degree, while the second day (01/04) showed a difference of over two degrees. Regarding the wooden floor surface temperatures,

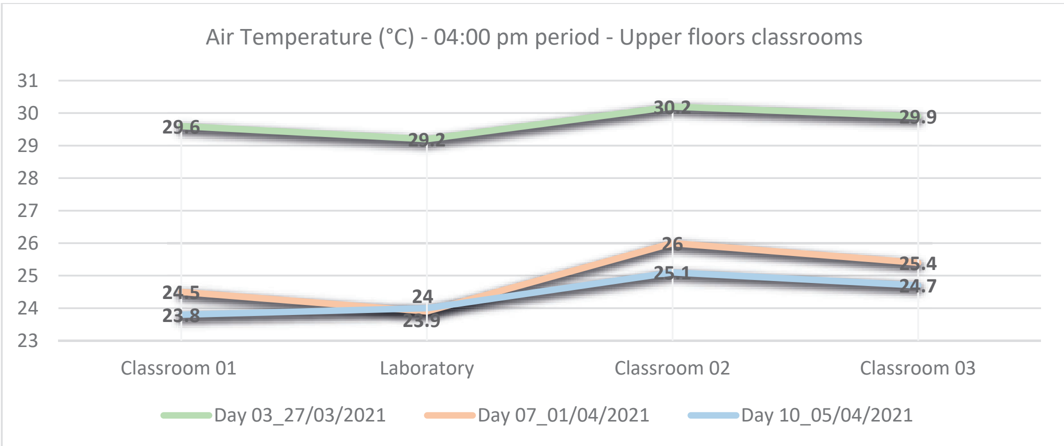

Figure 4.6.20 - Air temperatures (°C) recorded on the classrooms of the upper floors during the 04:00 pm period.

the classroom on top presented a higher temperature of one degree on the 27th of March, over five degrees on the 1st of April, and over six degrees on the 5th. As commented before, treetops protected larger areas of the first floor and the building's second level. Through the collected data, the level of protection was proven to change the degree of exposure and, consequently, human comfort inside the classrooms. However, it is vital to observe that classroom 01 will bear the same thermal discomfort issues despite an improvement between the discussed zones.

The final explored period of the day for this research section was 06:00 pm. There were two studied days: March 30 and 31. As explained in the methodology, this piece of the day was added for other reasons, such as checking the school conditions with lower air temperatures. Indeed, the weather station recorded the minor air temperature conditions from the ten studied days (regarding each studied period). Indoors, both days had a variation of two degrees between the lowest and highest recorded air temperature. All the dry bulb temperatures recorded inside the building for both days at 6:00 pm were higher than those recorded outside. On the 30th of March, the lowest temperature outside was 20.7°C, while the indoor area's lowest was 22.2°C. On the 31st, the recordings were 19.1°C out and 20.7°C inside. The mentioned outcomes suggest that the heat accumulated over the day slowly dissipates. Also, the open areas cool off more quickly with the temperature drop.

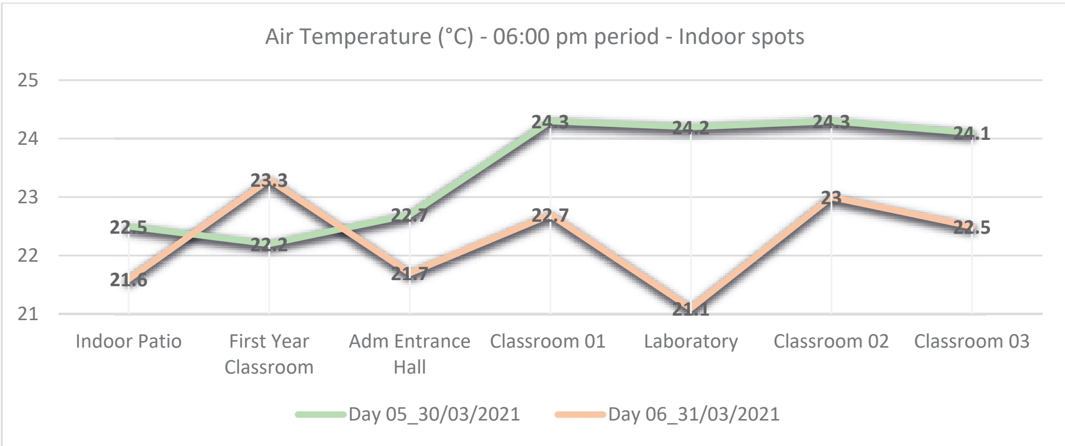

Figure 4.6.21 - Air temperatures (°C) recorded on the indoor spots during the 06:00 pm period.

The thermal variation inside the building was mainly between the ground floor and upper floors. On the first day (30th), the entire first and second floors explored rooms showing worse thermal conditions than the ground floor. The four studied rooms on the upper floors displayed dry bulb temperatures from 24.1°C to 24.3°C, roughly two degrees more than the ground-level zones. The northeastern portion (laboratory and classroom 03) has openings in the northwestern and southeastern walls facing outdoors. The southwestern rooms (classrooms 01 and 02) have apertures outside only one wall (northwest). As discussed before, it was expected that the laboratory and classroom 03 would have better conditions than the others. The expectation was built around the possibility of air movements occurring more frequently in the northeastern rooms due to crossed ventilation. However, it is crucial to remember that while one side of the mentioned rooms is permanently open, the other comprises moveable windows. As previously commented, the windows were always shut as students were not using the school. Without the windows opened, the crossed ventilation could not happen, meaning that the air movement inside the classrooms was probably meagre during the day. When the temperatures were recorded in the evening (06:00 pm), the classroom on the upper floors had been through similar environmental conditions, leading to almost matching results.

4.6.2. VISUAL ENVIRONMENT

The SLL Code for Lighting (Duff, James 2012) defines sufficient light in office spaces as providing around 500 lux in the working areas. The activities developed in a school building could be considered similar to an office. Consequently, the parameter will be used as a benchmark to identify the quality of the measured indoor spots in Amorim Lima. In the afternoon (04:00 pm), the explored rooms on the second floor were indoor spots with higher levels of natural light. Once more, the result is linked to the sun angles at this specific time. All the rooms on the upper levels will receive direct sun for most of the day, possibly creating glare issues. The highest amount of light recorded within the ten days indoors was 22,700lux inside classroom 02 on the second floor. Another example of the impact of sun orientation is that higher lux levels in the morning (08:00 and 11:00 am) occur inside the laboratory and classroom 3. Both cited rooms are in the northeastern portion of the building, receiving direct sun in all facades (southeast, northeast, and northwest) during the morning. However, it is essential to remember that the classroom on the first floor has treetops blocking a portion of the glazed area. It is possible that the obstruction could be why this room showed lower daylight levels compared to others on the upper floors.

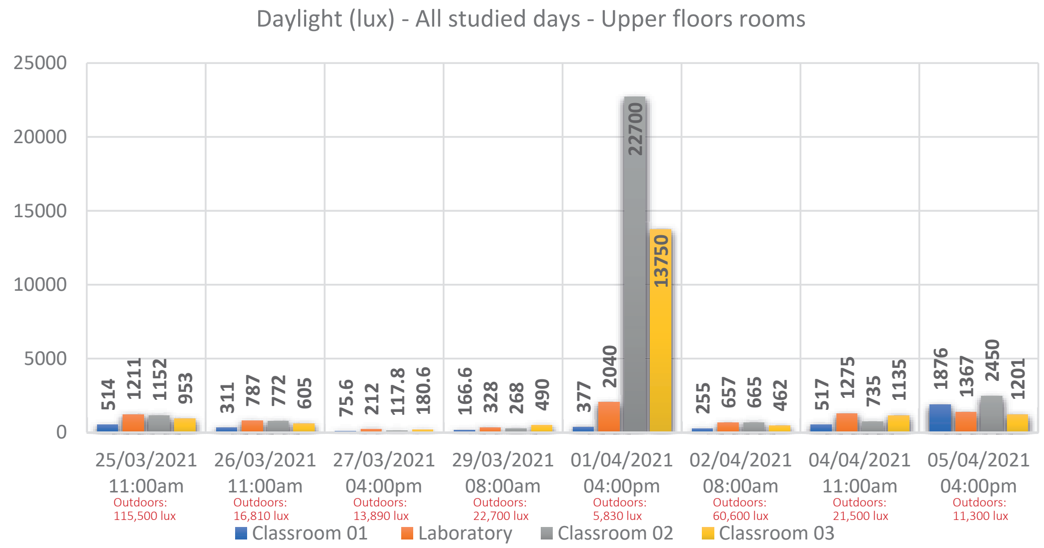

Figure 4.6.22 - Daylight levels (lux) recorded on the classrooms of the upper floors during the eight studied days.

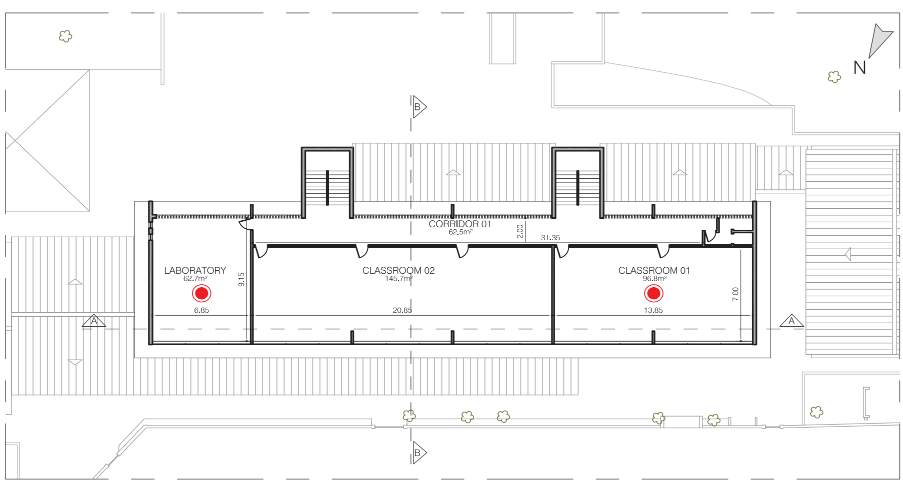

Figure 4.6.23 - The 1st floor plan of the EMEF Amorim Lima with the indication of internal studied points.

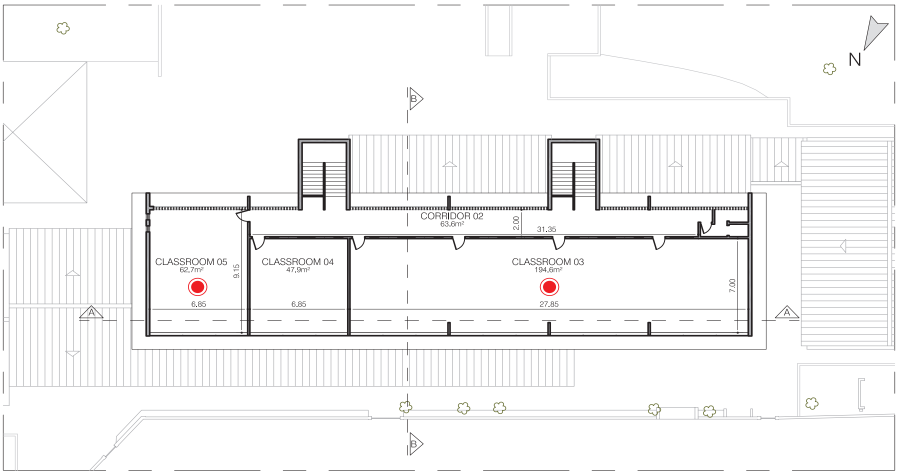

Figure 4.6.24 - The 2nd floor plan of the EMEF Amorim Lima with the indication of internal studied points.

As discussed, the quantity considered comfortable in office environments is 500 lux. Excluding the 08:00 am period, almost all upper floor rooms showcased higher amounts than 500 lux. The highest amount of light recorded indoors was 22,700lux inside classroom 02 on the second floor. The previous finding indicates glare issues in the classrooms for a more significant portion of the day, where the students and teachers will use the space. A schoolteacher spoke about the glaring issue during one of the visits. The teacher mentioned that a curtain was needed to enhance visual comfort during activities in the afternoon. Therefore, the spot measurements proved the issue accurately and confirmed the day was of greater concern regarding glare. The study has shown that all the analysed rooms on the second floor will have glare issues at 04:00 pm. Some days, glare issues possibly happen at the end of the morning and afternoon (11:00 am and 04:00 pm).

Nonetheless, it was not uncommon to spot zones on the upper floors with lux levels lower than the recommended for office spaces, even during the afternoon. At 08:00, only the laboratory and classroom 02 (both in the northwestern building zone) showcased a higher amount than 500 lux. The amount found in the mentioned rooms was 657lux (laboratory) and 665lux (classroom 02), and the northeastern room on the second floor showed 490lux. The other upper spots presented values between 166lux and 328lux. The lower amount in the previously discussed area of the school does not represent an express problem, considering that it has been proven to only happen during the early morning. It is possible that artificial light will necessarily be on for the first hours of the day.

Regarding the ground floor of Amorim Lima, natural light does increase at 04:00 pm, as usually happens in the rest of the indoor areas. However, it was impossible to spot daylight levels higher than 215Lux in the studied rooms (indoor patio and first-year classroom). The first-year classroom presented the lower light levels for the eight-day study, between 17.33lux and 92.2lux. It is essential to state that higher and lower daylight amounts were achieved during the 04:00 pm period on different days. The main suggestion that could explain the difference between findings for the same period would be the daily sky conditions. The discussed classroom is directly connected with a mass of vegetation in Cora Coralina Park spot 01. The blockage built by the small green infrastructure outside the room is probably the most significant element in reducing light inside.

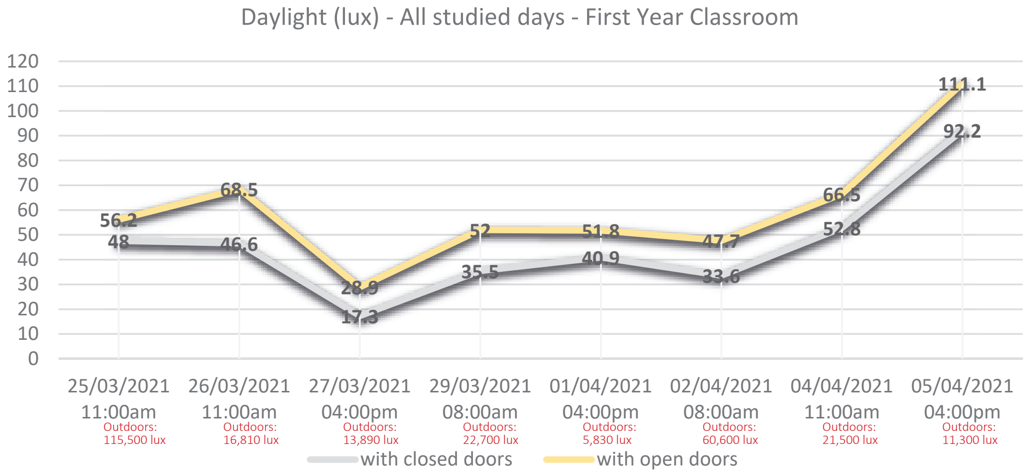

Figure 4.6.25 - Comparison between daylight levels (lux) recorded on the first year classroom with closed and open doors during the eight studied days

The recorded data shows that when the door is wide open, there is an increase of roughly 30% in the natural light levels inside the room. Moreover, on the lowest performance days of the first-year classroom, Cora Coralina 01 spot showed 4,410lux and 7,270lux. The results demonstrate that even with the expressive use of vegetation, light is abundant outside; however, the high levels are not spotted in the immediate indoor area (first-year classroom). The findings above indicate that the glazing apertures in this room could be enhanced to absorb more daylight. The indoor patio

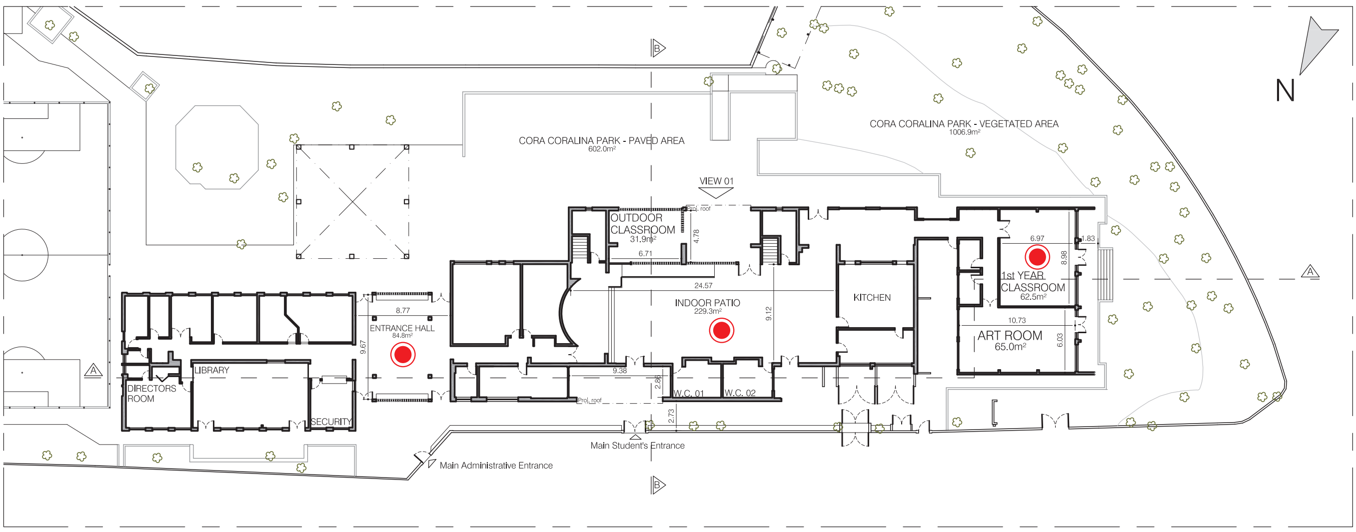

Figure 4.6.26 - The ground plan of the EMEF Amorim Lima with the indication of internal studied points.

demonstrates figures between 41.7lux and 100.9lux during the entirety of the study. Two main observations should be considered to analyse this room's outcomes. The first aspect is that all measurements were made in the centre of the room, keeping a similar distance from all the openings. The second and most important observation is that regular lectures and learning discussions also happen within the multiple activities hosted by this room. The use of this area indicates a need for a daylight level around what is required for office spaces (500 lux). It was described before that the patio has several significant openings in both facades. The conditions may be improved closer to the mentioned apertures. Nonetheless, the measurement in the middle indicates insufficient natural light coming in. The findings indicate an unsuccessful distribution of openings and, consequently, the light distribution internally.

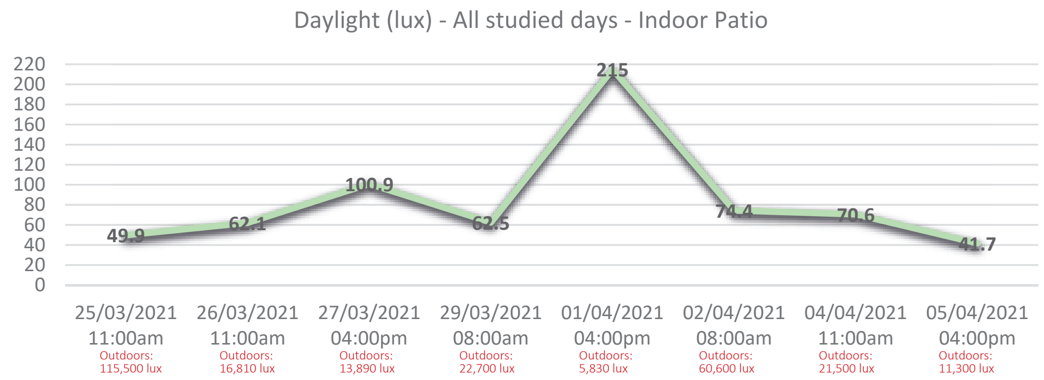

Figure 4.6.27 - Daylight levels (lux) recorded on the Indoor Patio during the eight studied days.

The administrative entrance hall variates between 121.9lux and 886lux within the eight studied days. The discussed room achieves 471lux, 886lux, and 806lux in the afternoon (04:00), which can be understood when considering the opening on both external facades. Nonetheless, the glazed doors and cobogo elements are insufficient to provide higher daylight levels in the morning (08:00 and 11:00 am), varying between 121.9lux and 252lux. Consequently, using cobogos on both facades could be considered excessive concerning daylight availability if this room was used as a classroom. However, natural light is considered satisfactory for this zone, which is used mainly for passage and brief encounters.

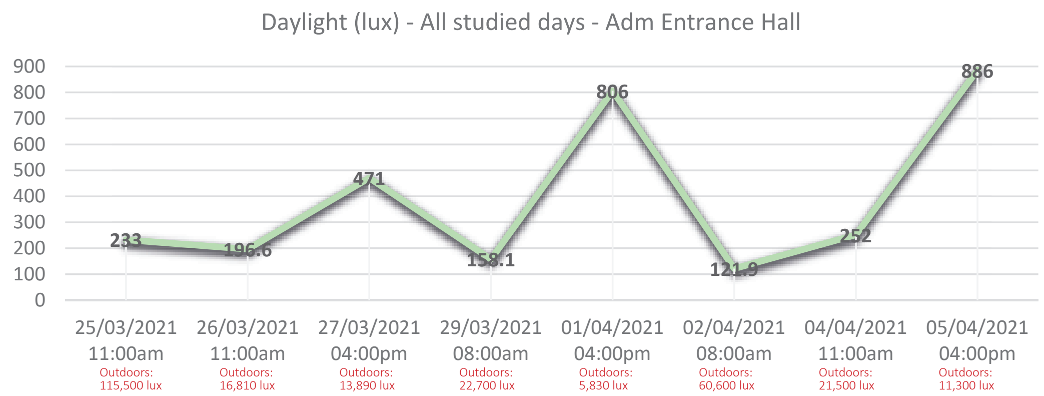

Figure 4.6.28 - Daylight levels (lux) recorded on the Adm Entrance Hall during the eight studied days.

4.6.3. AIR QUALITY

PM10

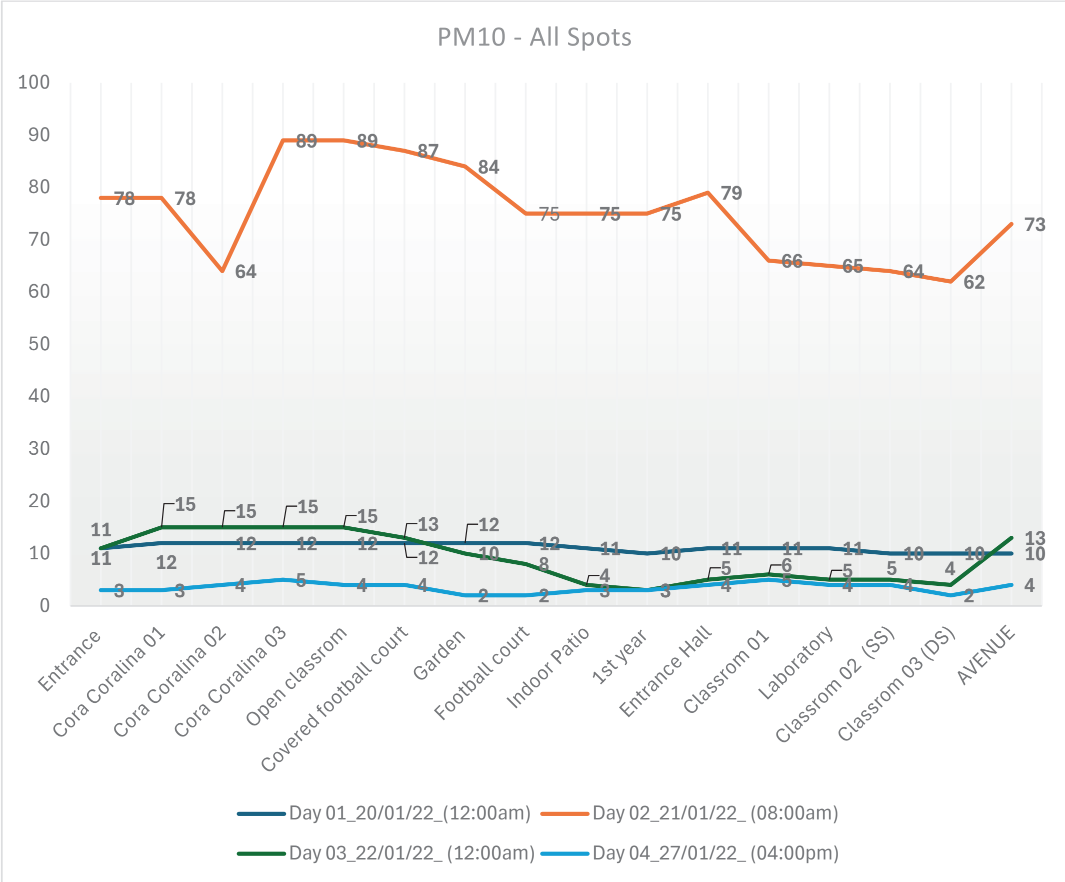

Figure 4.6.29 - PM10 (ug/m3) recorded by spot measurements during the four studied days in all analysed spots

During the four studied hours, the highest PM10 concentrations were spotted on the second one (21st of Jan), measured at 8 a.m. At this hour, the pollutant concentration on Avenue Corifeu de Azevedo Marques was 73 ug/m3. It

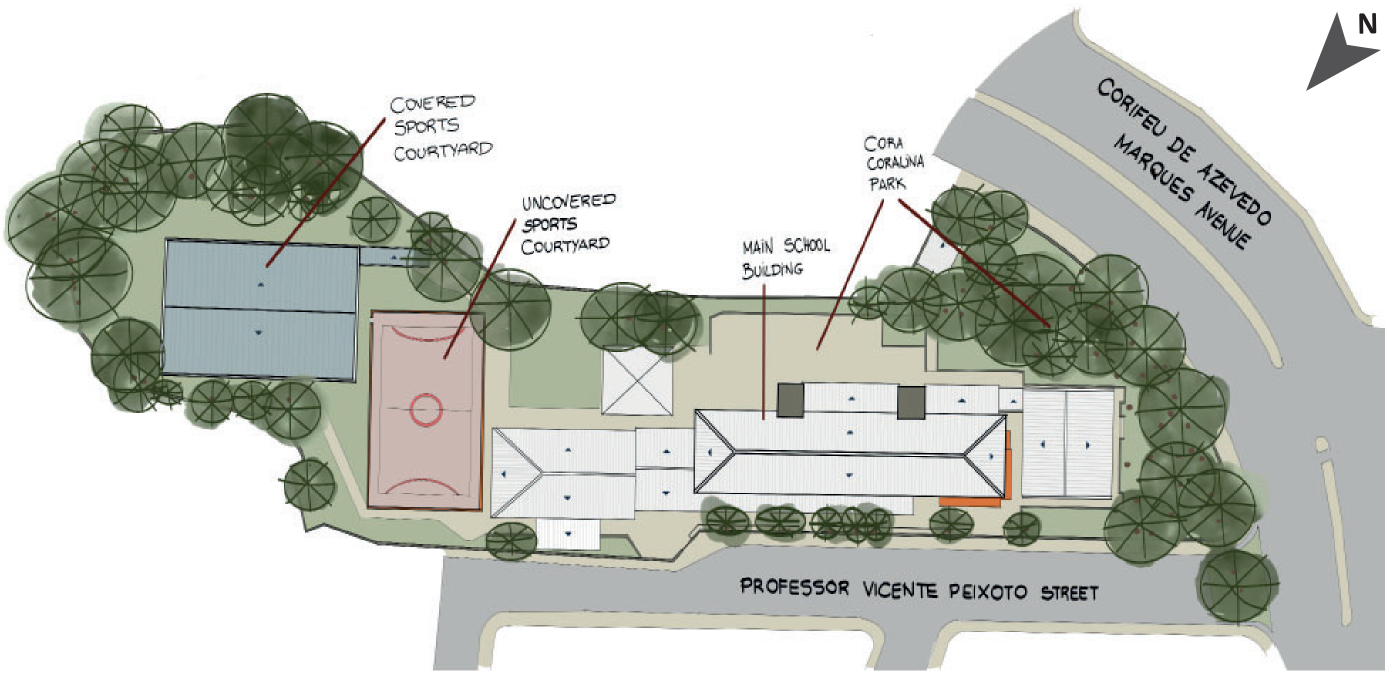

Figure 4.6.30 - Sketch of EMEFF Amorim Lima roof plan

indicates the amount of higher vehicular traffic close to the school. However, the results also show the negative impact of lower dry bulb temperatures, as the 08 a.m. studied hour presented a dry bulb temperature of 20.2°C (the lowest of all studied hours). On the worst day (21/01) of the studied spots, the worst performance was in Cora Coralina Park

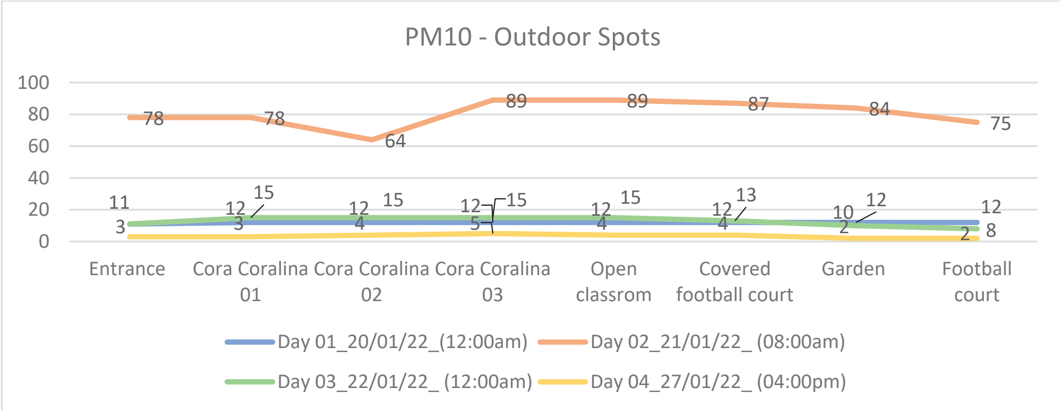

Figure 4.6.30 - PM10 (ug/m3) recorded by spot measurements during the four studied days on the outdoor spots.

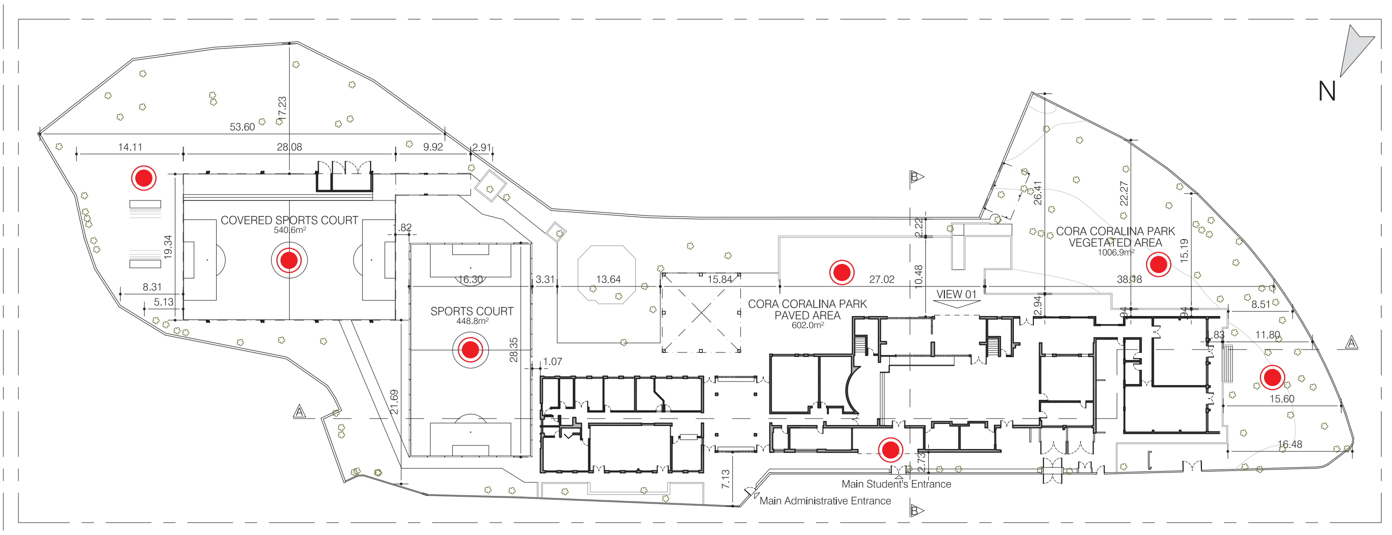

Figure 4.6.31 - The ground plan of the EMEF Amorim Lima with the indication of external studied points.

03, Open Classroom and Covered football court. All the mentioned spots presented higher concentration than the Avenue outside the site. This is contrary to the literature review in the previous chapters, which has indicated the overall negative impact of vegetation on the concentration of particulate pollution. However, the mentioned spots with higher concentration are areas with no application of vegetation and are open to air movement. Moreover, the mentioned spots are further away than the Avenue and surrounded by buildings. The outcome was unexpected; however, the 21st was the only day/hour when the wind mainly came from the southeast. The cited wind direction is against the main school building, which could be acting as a barrier. The protection against air movement would naturally diminish the velocities in the mentioned spots, decreasing the air quality.

The best-performing period was the 27th of January at 04 pm when the average wind velocity was 3.3 m/s. This is one more example of the positive impact of air movement on air quality. It was a hot (24.2°C) sunny moment with low traffic and a low pollution level on the Avenue (4ug/m3). Cora Coralina Spot 01 registered 3ug/m3 of Pm10 concentration, while spots 02 and 03 presented 4ug/m3 and 5ug/m3 respectively. Once more, the area without vegetation registered worse air quality. The main wind direction at that hour was from the northeast. It could indicate that the particles are transported from the northeastern avenue through the buildings into spot 03. The spots with lower PM10 concentrations were the garden and open football court (2ug/m3). Both areas have no expressive wind obstructions. A higher density of buildings between this portion of the site and the avenue could indicate further protection against particles.

Figure 4.6.32 - Satellite image of the EMEF Amroim site and the surroundings in the Butanta neighborhood (Google, 2024).

On both the 20th and 22nd studied days, higher pollution concentrations were registered in Cora Coralina Park at midday compared to the Avenue. All the park and the Open Classroom spots recorded the same level during both hours. On the first day (20th), the concentration was 15 ug/m/3, with a 10ug/m3 concentration in the Avenue Corifeu de Azevedo Marques. The third studied period (22nd) displayed 12ug/m3, with the avenue recording 13ug/m3. Both hours had prevailing winds from north and east, which are less polluted areas surrounding the school's terrain. The results presented so far illustrate how the proximity to pollutant sources and air movement will ensure similar pollution within the terrain. More importantly, it can be stated that the densely vegetated areas can act as a trapping barrier to particles. Allowing for the best performance of less vegetated areas protected by it. However, the mentioned trapping

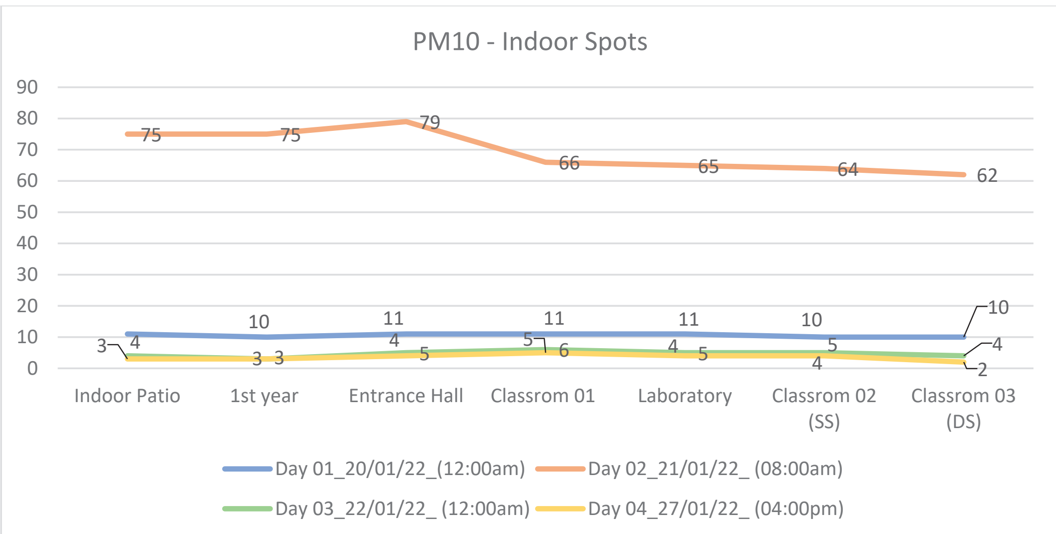

Figure 4.6.33 - PM10 (ug/m3) recorded by spot measurements during the four studied days on the indoor spots.

aspect does not ensure that the area with less dense vegetation will not be as polluted as the connected avenue.

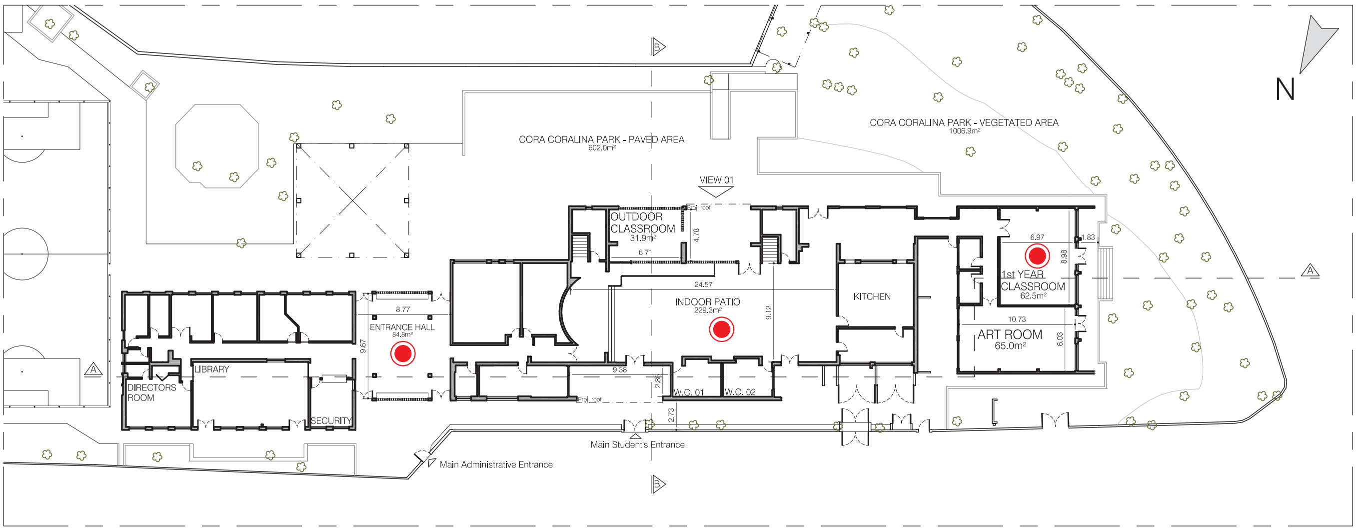

Figure 4.6.34 - The ground plan of the EMEF Amorim Lima with the indication of internal studied points.

During the studied hours, a few indoor spots registered higher PM10 concentrations than the outdoor spots and the avenue. On the most polluted day (21st Jan), the Indoor Patio, Entrance Hall, and 1st-year classroom had higher concentrations (75ug/m3, 79ug/m3, and 75ugm/3). than the Avenue Corifeu de Azevedo Marques (73ug/m3). The mentioned rooms are on the ground floor, directly connected to the exposed open areas. There is a reduction from adjacent outdoors to indoors; however, it is not substantial. For example, on the 21st, from the outdoor entrance spot to the indoor patio, the difference is only 3ug/m3 concentration. The outcomes illustrate how, at least on the ground

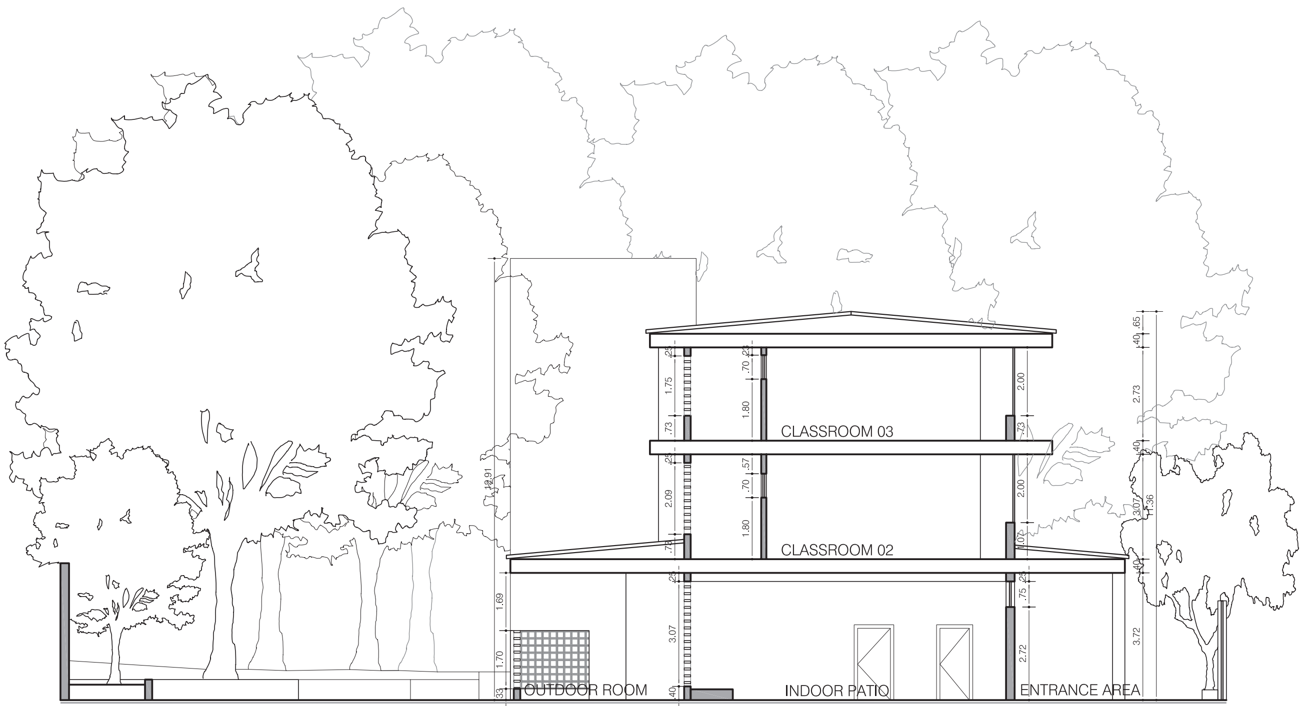

Figure 4.6.35 - Section BB

floor, the air pollution outside also represents the quality indoors. On the 22nd, the upper floors saw a 40% reduction in the pollutant concentration compared to the ground floor and outdoors. Moreover, there wasn't a substantial difference between the 1st and 2nd floors' studied spots. The 21st showcased a similar scenario of reduction on the upper floors. However, the difference was around 30% compared to the most polluted areas. Additionally, the difference was 20% compared to Cora Coralina Park spots and the avenue. Furthermore, the 20th and the 21st demonstrate constant PM10 concentrations throughout all spots. Nonetheless, the air quality is always slightly better in the second-floor rooms. The outcomes corroborate the expectation that the more distant (in height) from the sources, the less polluted the area will be.

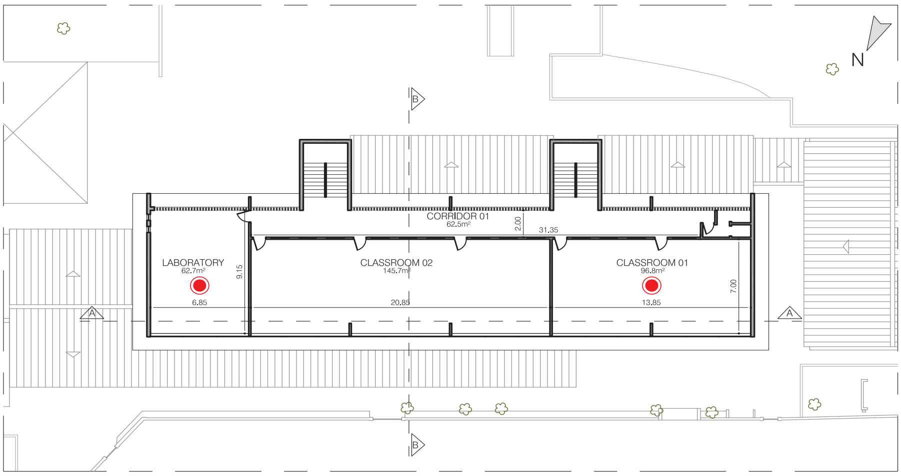

Figure 4.6.36 - The 1st floor plan of the EMEF Amorim Lima with the indication of internal studied points.

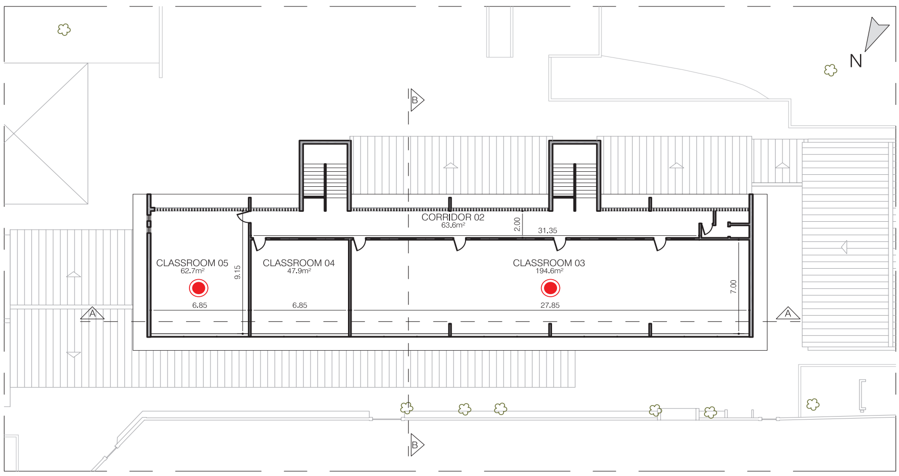

Figure 4.6.37 - The 2nd floor plan of the EMEF Amorim Lima with the indication of internal studied points.

PM2.5

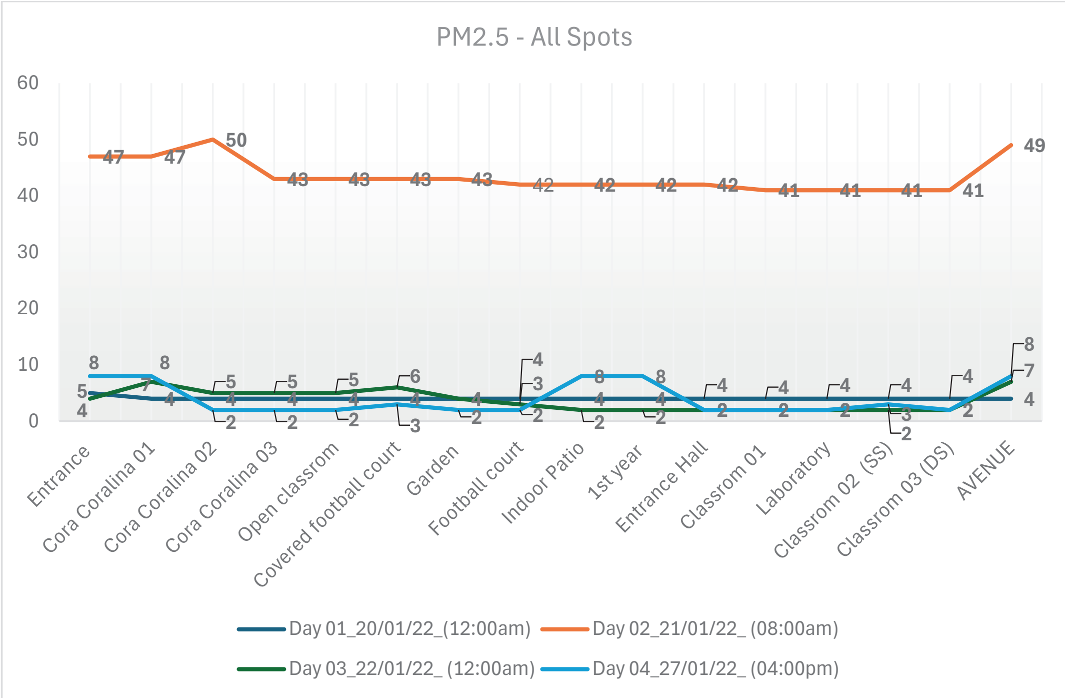

Figure 4.6.38 - PM2.5 (ug/m3) recorded by spot measurements during the four studied days in all analysed spots

The trends and patterns observed for the PM10 concentrations are comparable to those of the PM2.5 measured data. For example, as expected, the second day also had the highest pollutant concentration. The other three studied hours also presented lower concentrations within all spots. Yet, the concentration of particles on the worst day (21st of Jan) was lower than the PM10, with 49ug/m3 recorded on the avenue instead of 73ug/m3. The mentioned day presented a more constant result (41ug/m3 to 50ug/m3) compared with the PM10 concentrations (62ug/m3 to 89ug/m3). Moreover, on the 21st of Jan, the worst pollutant concentration was on Cora Coralina Park 02 with 50ug/m3, fol-

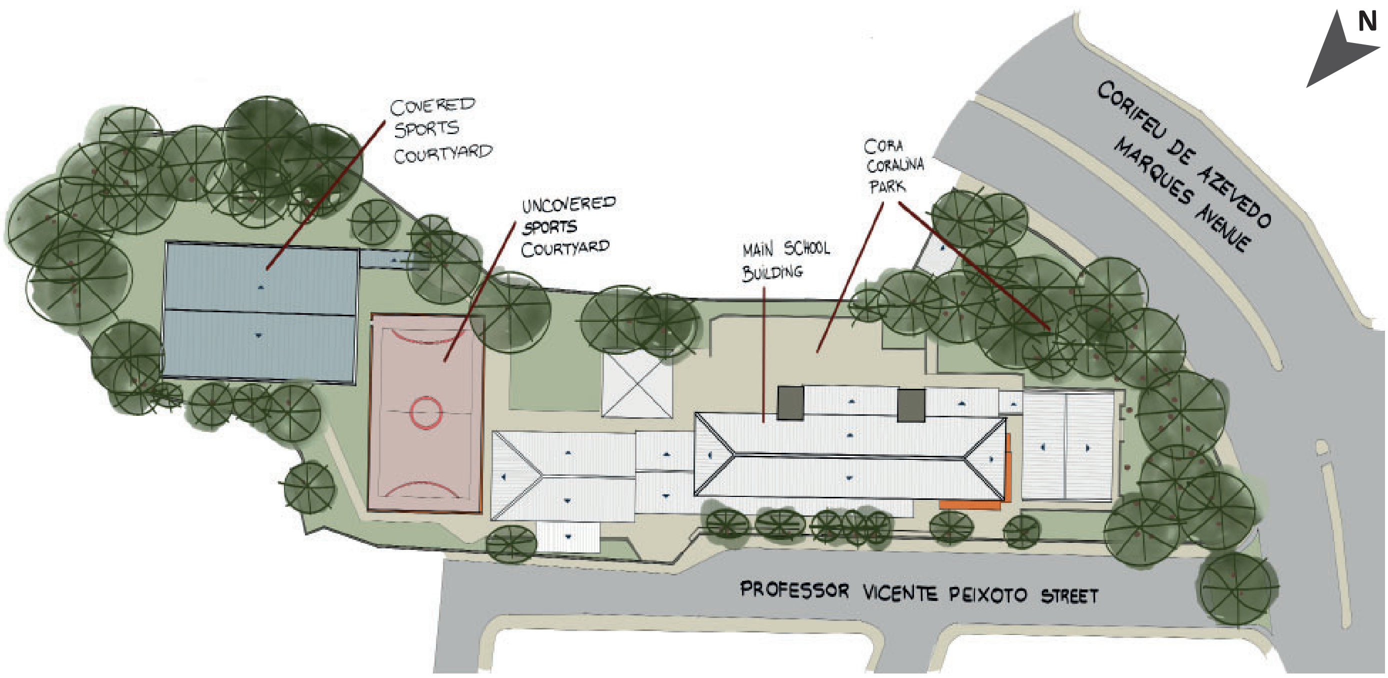

Figure 4.6.39 - Sketch of EMEFF Amorim Lima roof plan

lowed by the Entrance Area and Cora Coralina 01 with 47ug/m3. The PM2.5 values decrease as the spots get further away from the primary source (Avenue Corifeu de Azevedo Marques). The indoor spots on the ground floor have better air quality (42ug/m3), followed by those on the upper floors with 41ug/m3. The mentioned results are one more example of the trees' trapping capacity, creating small-screen green infrastructure within the school environment that is as polluted as the vehicular road.

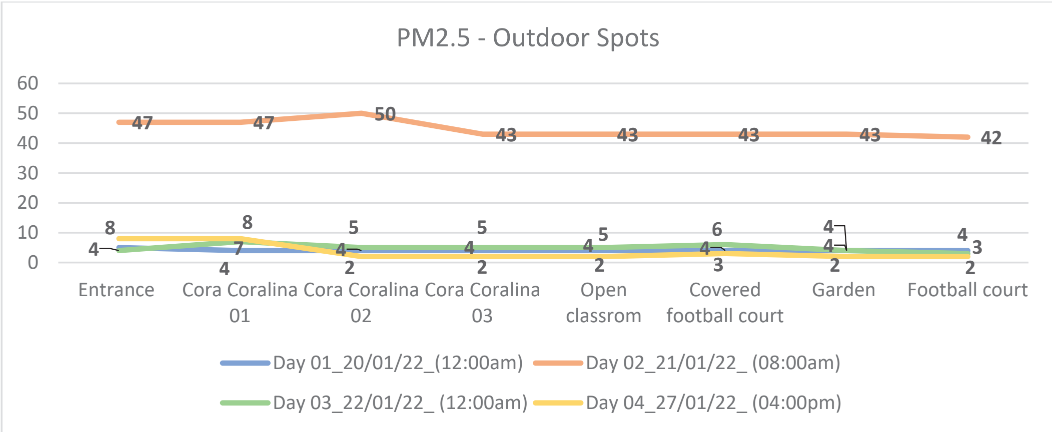

Figure 4.6.40 -PM2.5(ug/m3) recorded by spot measurements during the four studied days on the outdoor spots.

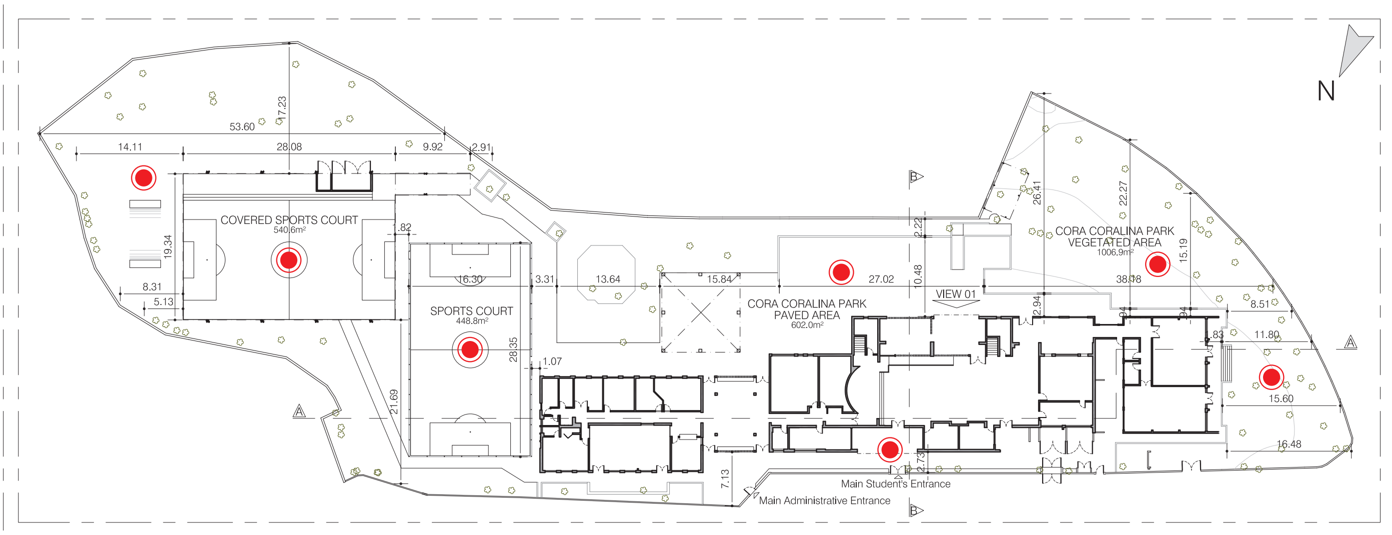

Figure 4.6.31 - The ground plan of the EMEF Amorim Lima with the indication of external studied points.

The fourth studied day (27th of January) showed the best PM2.5 performance in most outdoor spots (2ug/m3 to 3ug/m3). However, the entrance and Cora Coralina 01 registered the highest pollution levels within the best performance days (20th, 21st, and 27th). The concentration mentioned was 8ug/m3, the same as the outside avenue. The outcomes are expected as this studied hour has the highest wind velocity. Furthermore, the indoor patio and the 1st year classrooms presented 8ug/m3, the two spaces connected with the entrance and the Cora 01. The abovementioned illustrates again how the conditions in the outdoor areas can hint at the conditions in the adjacent indoor ones.

4.7. CONCLUSION

This chapter introduced the EMEF Amorim Lima, its areas of interest, and its main environmental characteristics. Additionally, the findings indicated the school's current environmental performance regarding thermal comfort, daylight, and air quality within a specific period. Concerning thermal comfort, the school area with denser vegetation (Cora Coralina Park) had the best outcomes, also considering indoors. However, the Smal Scale Green Infrastructure within the school terrain was observed to have a more substantial positive impact with lower dry bulb temperatures. The outcomes indicated that shading is more effective during harsher conditions than the cooling impact of trees. Furthermore, the findings also highlighted the importance of higher air movement to increase thermal comfort. Yet, it was illustrated that surface temperature was the most critical aspect in defining comfort. The finding indicates the relevance of reducing mean radiant temperatures through shading over enhanced wind speeds.

Fieldwork also proved the negative impact of locating unprotected glazed openings facing direct sun, mainly west and southern facades. The outcomes illustrated how the classrooms and other rooms with windows facing northwest indicated the poorest thermal comfort within the indoor studied areas. The measurements conducted inside the building also proved the importance of allowing for cross-ventilation when possible. Moreover, concerning the visual conditions, the study also indicated the poor performance of the mentioned rooms by proving the existence of glare in the late morning and afternoon periods. The study also demonstrated the negative impact of the densely vegetated Park by spotting directly connected indoor rooms with insufficient daylight throughout the day. Moreover, the mentioned finding also indicates the necessity of increasing glazed openings behind dense vegetation. Finally, the measurements showed that using cobogos on both room facades could cause a lack of daylight while not aggregating thermal benefits.

Regarding air pollution, represented by particulate matter (PM2.5 and PM10), the on-site measurements indicated that when dry bulb temperatures are lower, the air quality decreases. Additionally, hotter, sunnier days showcased lower pollution levels. Additionally, the positive impact of solid barriers (boundary walls or buildings) against pollutant sources was highlighted. The study also determined the necessity of higher wind speeds to "swipe" particles. Furthermore, most of the outcomes evidenced the negative impact of the small green infrastructure. Some results demonstrated pollutant levels as high as the vehicular avenue, mainly when considering PM2.5. However, research throughout the year must be conducted to test those outcomes further. Another significant result was that the air quality in the ground floor rooms was always similar to that of the immediate outdoor area. The finding indicates that further study of the outdoors can be enough to determine indoor air quality performance. Finally, the rooms on the upper floors performed better overall than the ground floor rooms.

As discussed, the fourteen days of fieldwork illustrated the current conditions of the school and surroundings during the specifically studied period. However, until this point of the study, there is no understanding of the school's performance during different seasons. The statement indicates the necessity of studying Amorim Lima further over the climatic changes of a year with a focus on the hottest and coldest periods. At this point, it is also necessary to study thermal comfort using more accurate tools to quantify it. To achieve the mentioned goals, analytical work was introduced and conducted. The analytical study's specific objectives, method, and results will be presented in the next chapter of this doctoral research.

5. CASE STUDY: ANALYTICAL WORK

EMEF AMORIM LIMA'S PERFORMANCE OVER A YEAR.

5.1. INTRODUCTION

This chapter is dedicated to the digital analysis of the public school EMEF Desembargador Amorim Lima, the central case study for this doctoral research. It was stated in the previous chapter that the conclusion achieved refers uniquely to a determined portion of a year. The fieldwork happens in January and March, both summer months. More precisely, the study focuses on only fourteen days. Each of the mentioned days was represented by a point-on-time measurement conducted during 08:00 am, 11:00 am, 04:00 pm and 06:00 pm. Thus, to complete the assessment of the school's performance, considering a typical year, the study initiated through fieldwork moves to an analytical exercise across different seasons, with a focus on summer and winter.

The chapter begins by clearly stating the objectives and the need for a comprehensive study beyond the previously conducted point-in-time measurements. The methods used are then detailed, highlighting the selection and justification of the computational programs. A comprehensive literature review of ENVI-met® is also presented, explaining its uses, key features, and operation. The main results of the various analytical exercises are presented and discussed, leading to a holistic understanding of the performance of EMEF Amorim Lima. This and the previous chapter provide a detailed environmental analysis of a public school's environment, whth focus on its architectural and green components within the context of Sao Paulo. This chapter is crucial to inform and guide the development of the main exercise of this doctoral research, presented in the next chapter.

5.2. OBJECTIVES

This work aims to build a comfort and health performance indicator for EMEF Desembargador Amorim Lima. The study is conducted in a typical microclimatic year in the school's specific region. If needed, the study aspires to start the conversation for significant improvements to the school`s current design. Moreover, the specific objectives of this chapter are:

- Demonstrate in more detail the impact of the built and vegetated environment by quantifying human thermal comfort and air quality.

- Indicate the indoor thermal performance of the school building throughout each season.

- Showcase a more in-depth understanding of the studied space's air pollution concentration and dispersion patterns. This helps to clarify the air quality relation with the site's existing greenery and architectural composition.

- Understand the impacts of green and architectural elements on thermal comfort and air quality within the EMEF Amorim Lima context.

Continuing the fieldwork, this section focuses on two leading indicators: air quality conditions and the site's thermal characteristics. The mentioned factors indicate human health, well-being, and comfort. The human comfort evaluation section has the aim to define which outdoor areas perform well throughout the year and highlight which areas perform better, specifically in each season. However, this chapter's primary distinction from the previous one is its intention to have a cumulative quantification of the parameters studied before instead of point-in-time measurements. Furthermore, the objective is to analyze the entire site's performance instead of individual spots. This study aims to quantify the perception of human thermal comfort instead of only quantifying microclimatic conditions as an indication of comfort, as was done in the Fieldwork chapter. Another intention of this chapter is to showcase how the building's orientation impacts the amount of radiation accumulated on the facades. Additionally, how different façade treatments can define the quantity of radiation transferred to the indoor areas. Hence, the simulations aim to prove if openings and materials are used in the appropriate locations in terms of environmental requirements. The studies conducted in the school's outdoor areas also aspire to be used as indicators of indoor performance, trough assumptions of those spaces' thermal and air quality conditions.

The analytical research mainly aims to substantiate the outcomes of the fieldwork process. For example, it aims to confirm the overall poor performance of the school's vegetated areas concerning pollutant particle concentrations. Another objective is to prove the importance of air movement and sunny, hotter days for air quality enhancement. The interest in also comparing the air conditions in areas of the school with and without vegetation. Observing which vegetated elements and architectural aspects of the site affect the dispersion and concentration of pollutants alters the air quality of the studied space. The cited observation of the individual elements' performance leads to the case study's final and most important objective: identifying which architectural and SGI components need further evaluation in different contexts. Also questions raised about the performance of the mentioned elements are essential to guide what needs to be answered in the following chapter.

5.3. METHODS

Two main methods evaluate the EMEF Amorim Lima's performance over a typical year. One focuses on building assessment, focusing on facades, while the other is dedicated to outdoor study. Consequently, the chapter is divided into two main groups of exercises: the Building Solar Geometry Study and the Outdoor Thermal Comfort and Air Quality Study. The chapter used different analytical methods to develop the research on the school's performance. The methods used in a few evaluation softwares are explained below. More than one software and several environmental performance indicators are necessary to understand the school's annual environmental characteristics fully. A complex and detailed awareness of EMEF Amorim Lima's performance throughout the year is a gap in knowledge concerning public schools in Sao Paulo.

5.3.1. SOLAR GEOMETRY STUDY

The first exercise group is related to the solar exposure of the school building and is developed through accumulative sun radiation simulations. The analysis is designed and completed through the Rhinoceros®, an architectural modelling program. Alongside the graphical algorithm editor of Rhinoceros®, called Grasshopper®, is used with the Ladybug® plug-in. The cited program is built to simulate the building's performance and help during the design process. It depends on external simulation engines, such as EnergyPlus®, OpenFoam®, and Radiance® (Bazafkan, Pont, and Mahdavi, 2019). The workflow that needs to be followed for the Ladybug® simulations is also available at Bazafkan, Pont, and Mahdavi (2019). The plug-in can also be applied to evaluate existing buildings. Chiesa and Li (2021), Fukuda and Hiroatsu (2016), Natanian and Aleksandrowicz (2018), Soflaei et al. (2020), and Touloupaki and Theodosiou (2017) are examples of studies that have used the discussed computational programs as research methods. Alammar, Jabi, and Lannon (2021), Peters and Peters (2018), and Vasigh and Shiri (2021) are examples of explicitly using solar radiation analysis as a study method. The solar irradiation simulation is conducted on the building's envelope. However, the envelope outcomes help suggest overheating risks within the schools' indoor environments. The mentioned method was used before by other studies focusing on buildings` thermal performances (Bakos and Schiano-Phan, 2021 and Peters and Peters, 2018).

The first step of the analysis is to develop a 3D model of the school with all the existing components that could obstruct solar irradiation. In addition to the school building, trees, boundary walls, and surrounding buildings were also modelled. Moreover, more complex components, such as trees, were constructed in simplified versions. To initiate the solar geometry evaluation of the specific site, a 3D solar diagram is simulated, as will be shown in the results section. The analysis clarifies the sun's path over a year, highlighting more and less exposed outdoor areas and facades. Afterwards, the sun irradiation analysis focuses on accumulative radiation over the year (kWh/m2). Consequently, the simulation shows the entire amount of solar radiation that falls on each façade of the primary school building. A weather file with Sao Paulo's climatic data is used to create the simulation. The data includes direct and indirect radiation, sunlight, wind speeds and directions, humidity, and other climatic information. Moreover, the information is derived from the weather database software Meteonorm® v.7.2. Finally, the simulated solar irradiance is demonstrated through coloured diagrams on the studied surfaces.

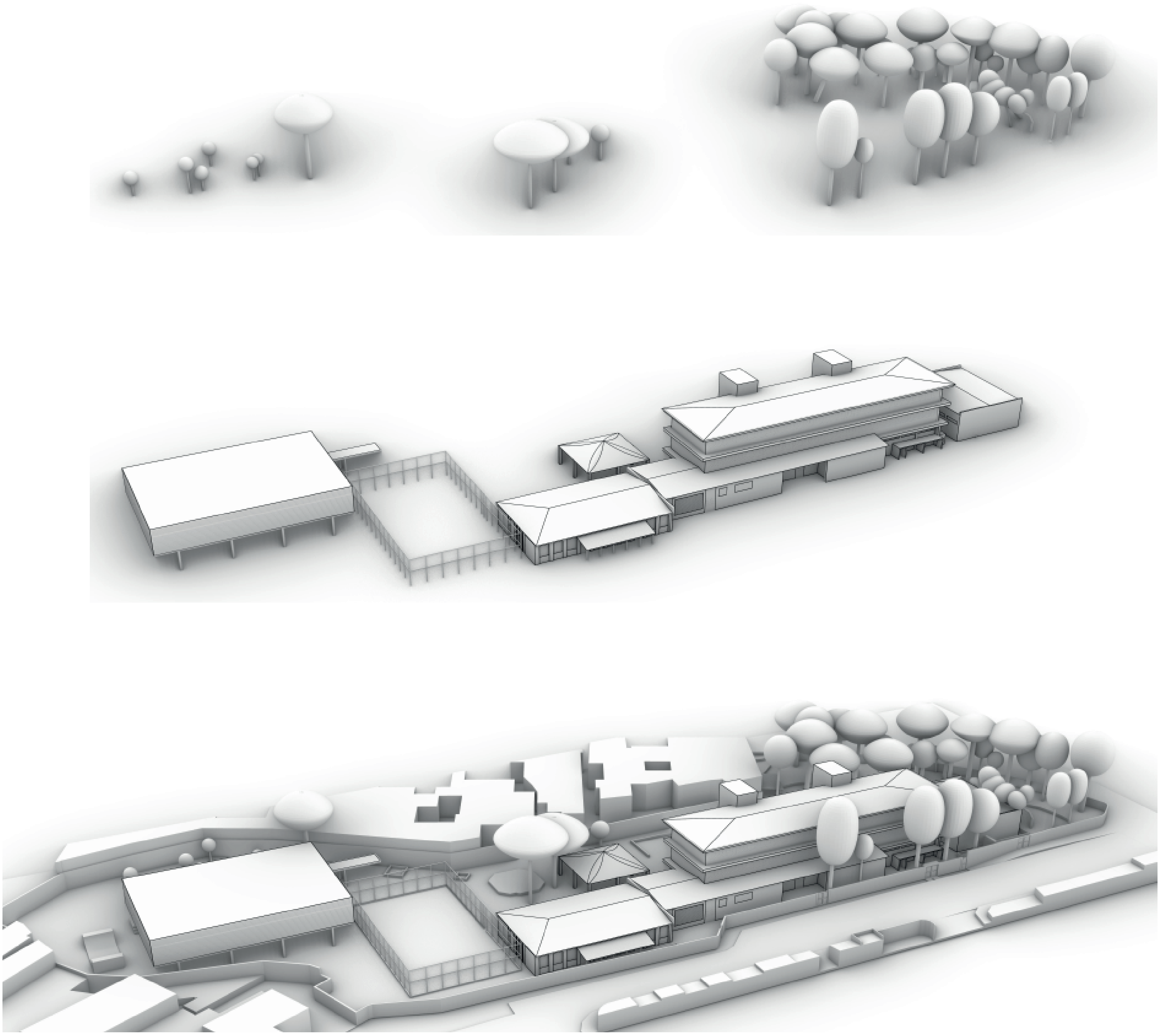

Figure 5.3.01 - Diagram of the Rhinoceros® model used for the sun irradiation simulation, separating the representative vegetation from the studied building.

5.3.2. THE ENVI-MET®

ENVI-met® is a microclimate simulator software crucial for developing this doctoral research. The program is the primary method for developing the second and later discussed group of exercises, in addition to the analytical study in the following chapter. Moreover, it is available on the company`s official website (ENVI-met, 2019) and is a 3D CFD (Computational Fluid Dynamics) (Borna and Schiano-Phan, 2020 and Shinzato, 2014). ENVI-met® can define the environmental conditions based on calculations of solar energy gains and pollutant particle dispersion, concentration, and chemical reactions (Bruse, 2004). In summary, the software was chosen due to its capability to calculate complex iterations between surfaces, vegetation, and atmosphere (Tsoka, Tsikaloudaki, and Theodosiou, 2018). As a result, it can provide an extensive range of environmental outcomes. The works referenced above, in addition to Jin et al. (2017), Ferreira (2019), Gusson and Duarte (2016), and Spangenberg et al. (2008), are a few examples of researchers that used ENVI-met® as a method to evaluate existing environmental conditions on different cities of the globe, including Sao Paulo.

TOOLS AND WORKFLOW

The software is comprised of several tools, including Spaces®, Albero®, Database Manager®, ENVI-guide®, ENVI-core®, BIO-met, and Leonardo®. Spaces® is a digital instrument for modeling and editing the built environment, possibly applying different façade and roof materials, and locating vegetation elements. The tool also applies pollution sources, soil types, and pavement materials while defining the study's location and north orientation. However, the Database Manager® tool constructs all the above elements while presenting a pre-defined database of materials that can be edited if needed. The tool allows for the pollutant concentration level, height, and dispersion patterns within 24 hours to be defined. Additionally, the database library allows users to choose the greenery elements considered "simple," such as hedges, grass, façade greenings, and even plantations like soy (image 03). The seasonal profile of the vegetation can also be defined. Moreover, the software allows for a more detailed design of the model's natural features through the Albero® tool. The tool is dedicated to trees but could also be used to construct complex hedges and living wall elements if needed. The tool defines vegetation LAD (leaf area density), height, and spatial organization of leaves and stems. Additionally, the instrument provides the opportunity to select the vegetation leaf's seasonal patterns, as the Database Manager® does. However, being a more complex tool, the patterns are defined over a year through a monthly calendar (figure 5.3.04).

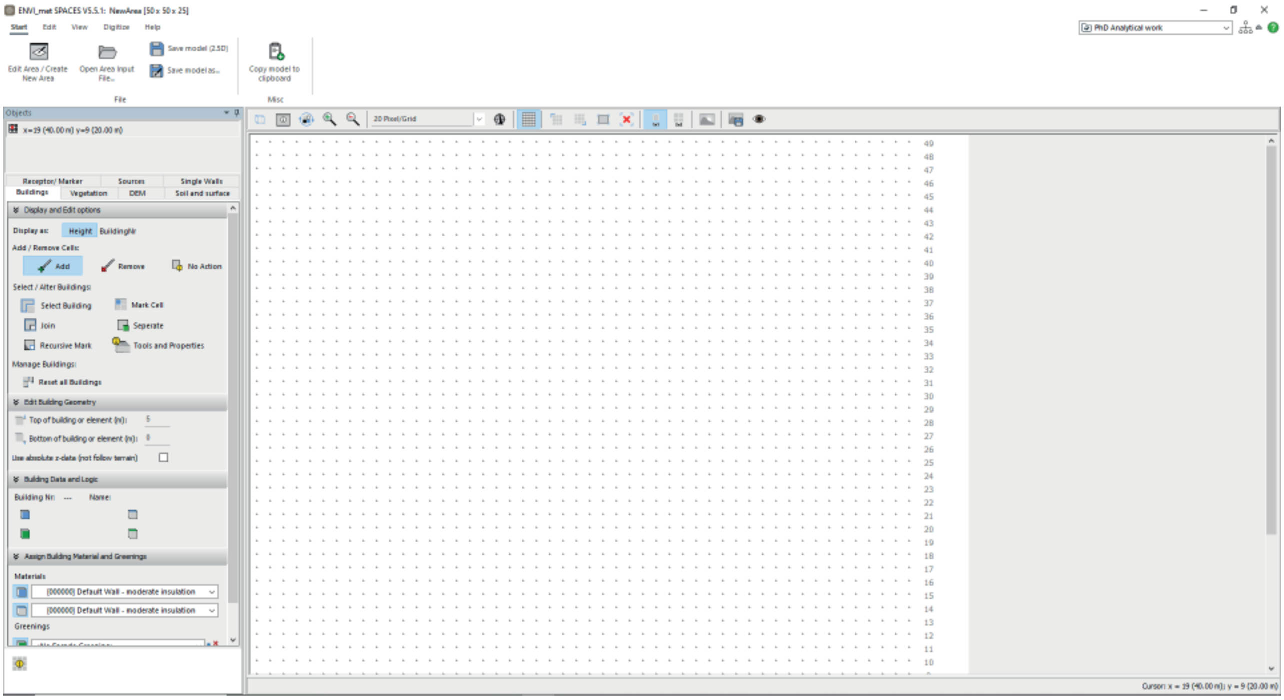

Figure 5.3.02 - Spaces® workspace.

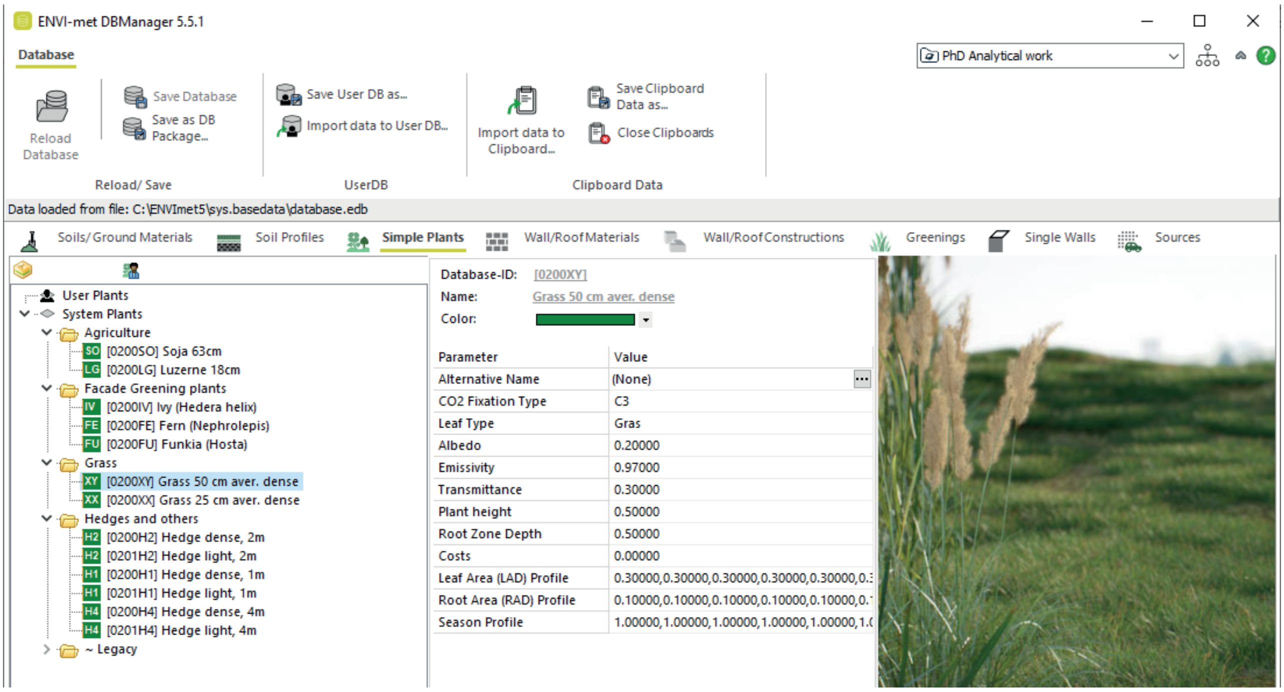

Figure 5.3.03 -The Database Manager® workspace showcases the simple plants' library and shows the characteristics of the 50cm Grass.

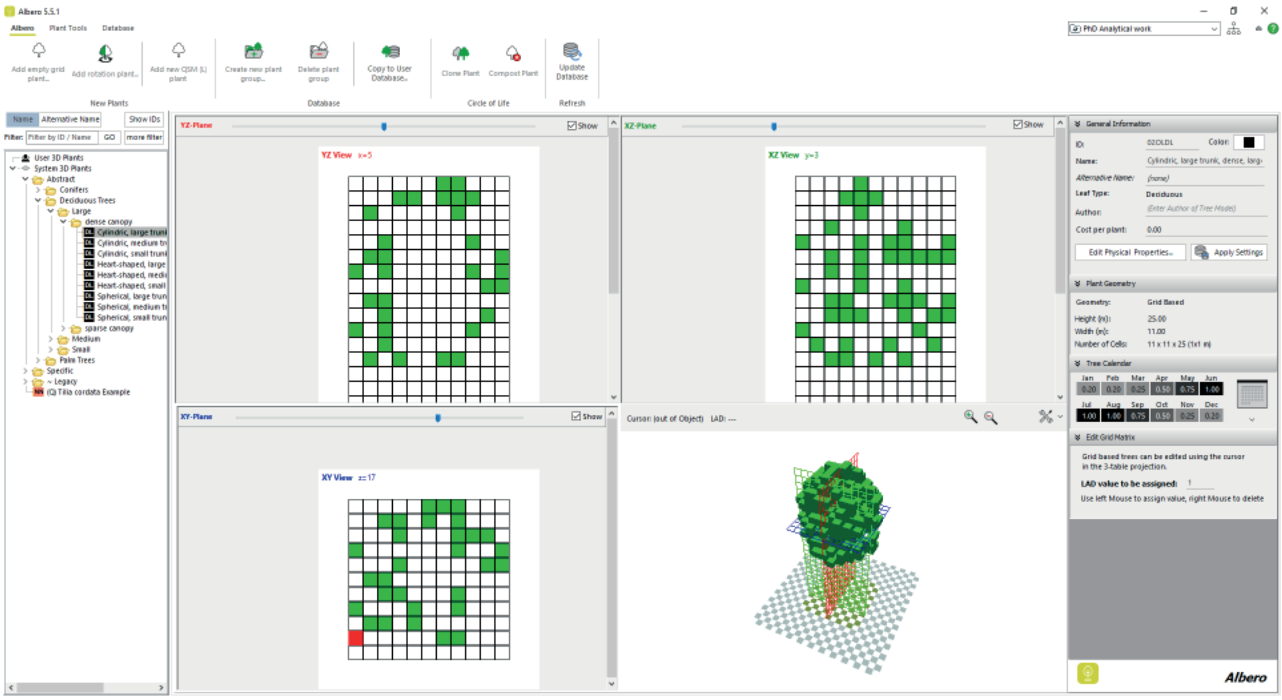

Figure 5.3.04 -Albero® workspace, showcasing an exemplary tree.

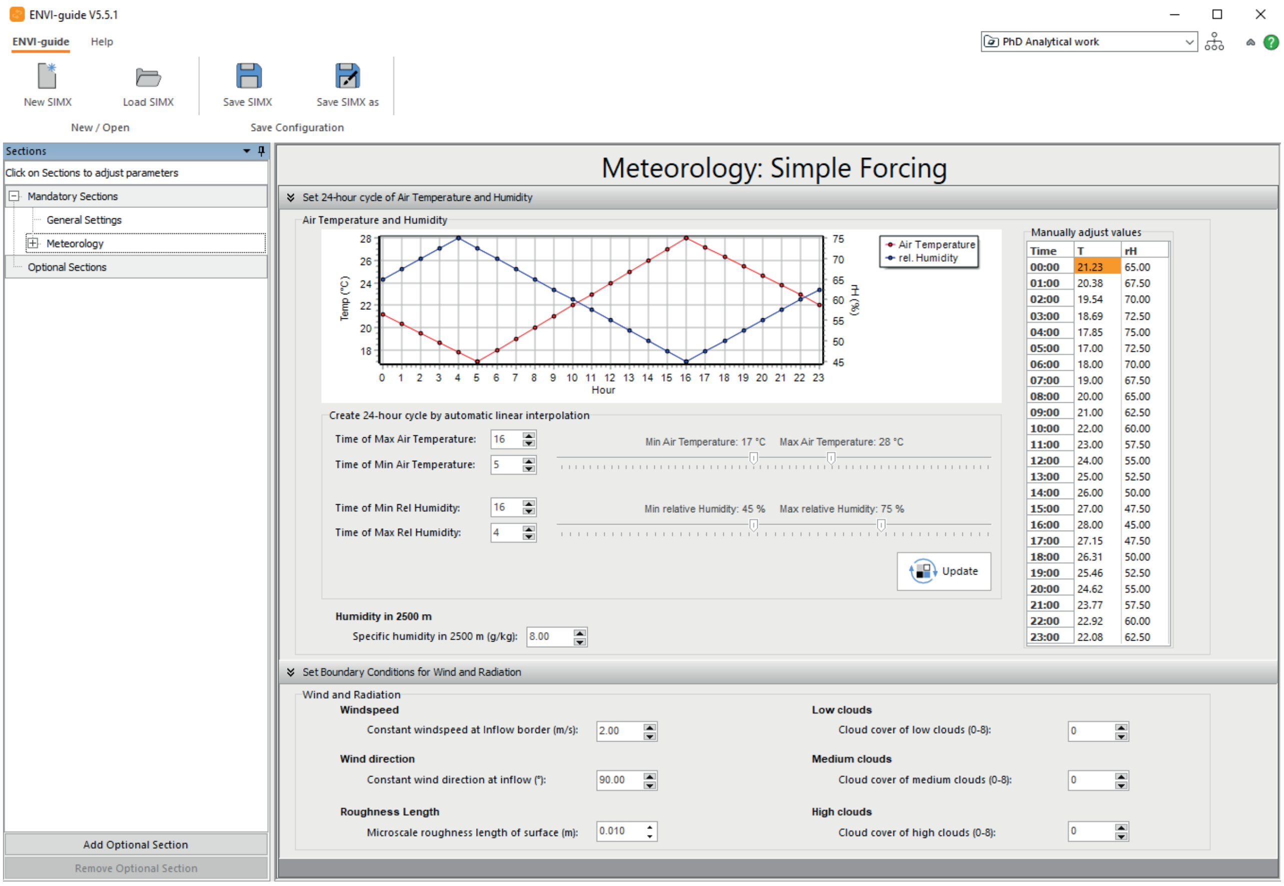

Figure 5.3.05 -ENVI-guide® workspace, showcasing the “Full-forcing” option.

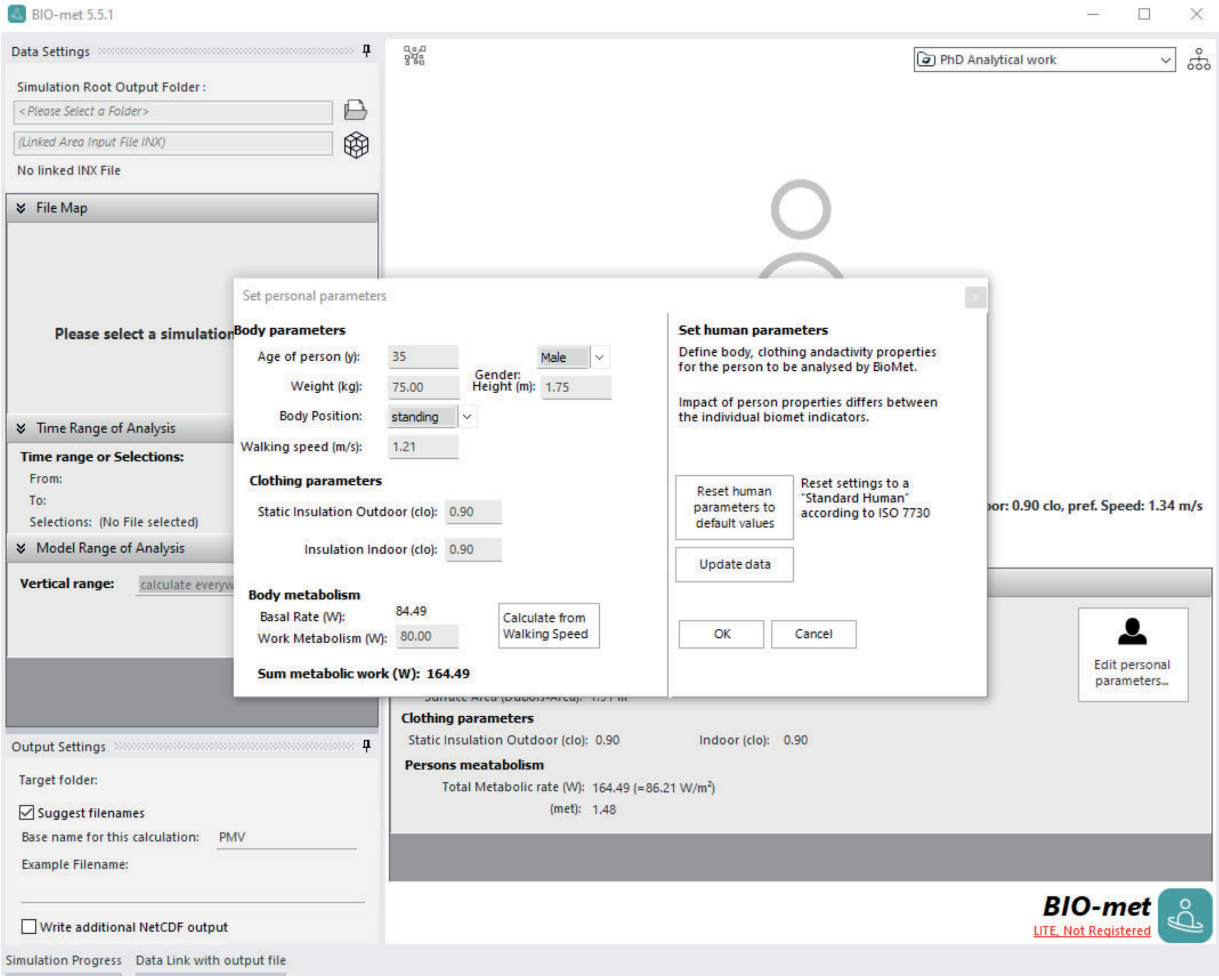

Figure 5.3.06 -BIO-met® workspace, showcasing the editing of human and clothing parameters.

Alongside the modeling tools previously exemplified, ENVI-met® also comprises a climatic conditions input tool called ENVI-guide®. The mentioned digital instrument allows for the definition of the simulation's times and dates. The tool permits the use of EPW with climatic data to be inputted. Still, it is also possible to manually establish the climatic conditions through "full-forcing", such as relative humidity, dry-bulb temperature, cloud coverage levels, wind speeds, and main wind directions. Additionally, the manual application of climatic conditions allows for the highest and lowest dry bulb temperatures and relative humidities to be placed at specific hours of the day (figure 5.3.05). Furthermore, in addition to the tools for climatic conditions, there are those used for running the simulations themselves, such as ENVI-core® and BIO-met®. The first runs the overall complex simulation, while the second is a complementary tool for specific analysis. For example, BIO-met® calculates the complex thermal comfort indexes as UTCI and PET. This digital instrument establishes the clothing levels, body parameters, and human metabolism characteristics. Age, gender, and even body position (if lying, sitting, standing, or moving) can also be edited in this tool for the calculations (figure 5.3.06). Finally, Leonardo® is the device within the software where the digital analysis results can be post-processed and visualized. The tool mentioned informs climatic and air quality conditions for each hour and each height of the spatial environment studied. The results are presented through color index 2D graphs, as shown in this doctoral research's results sections. Additionally, 3D images and animations of, for example, wind and pollution patterns can be generated. The information discussed above concerning ENVI-mets®'s different instruments is available on the software website (ENVI-met GmbH, 2024).

MAIN CALCULATIONS

The software functions through numerous equations dedicated to each simulation aspect, housing different disciplines, such as thermodynamics and plant physiology, fluid dynamics, and soil science (ENVI-met GmbH, 2024). Most formulas can be found in ENVI-mets®'s founder, Michael Bruse's PhD Thesis (Bruse, 1999). However, throughout the years, with model updates, which are now on the ENVI-met® version 5.6 (Bruse, 2023), the calculation suffered changes. For example, in 2004, the mean airflow equations were modified. Moreover, according to Bruse (2004a):

> "The three-dimensional turbulent airflow in the model is given by the non-hydrostatic incompressible Navier-Stokes equations:
>
> $$\frac{\partial u}{\partial t} + ui\frac{\partial u}{\partial xi} = -\frac{\partial p}{\partial x} + Km\left(\frac{\partial^2 u}{\partial xi^2}\right) + f(v - vg) - Su$$
>
> $$\frac{\partial v}{\partial t} + ui\frac{\partial v}{\partial xi} = -\frac{\partial p}{\partial y} + Km\left(\frac{\partial^2 v}{\partial xi^2}\right) + f(u - ug) - Sv$$
>
> $$\frac{\partial w}{\partial t} + ui\frac{\partial w}{\partial xi} = -\frac{\partial p}{\partial z} + Km\left(\frac{\partial^2 w}{\partial xi^2}\right) + g\frac{\theta(z)}{\theta ref^{(z)}} - Sv$$
>
> where f (=104 sec-1) is the Coriolis parameter, p is the local pressure perturbation and θ the potential temperature at level z. The reference temperature θref represents the larger-scale meteorological conditions and is calculated as an average temperature over all grid cells of height z, excluding those occupied by buildings."

Additionally, the software uses the following equations for humidity and temperature:

$$\frac{\partial \theta}{\partial t} + ui\frac{\partial \theta}{\partial xi} = Kh\left(\frac{\partial^2 \theta}{\partial xi^2}\right) + \frac{1}{c_p\rho}\frac{\partial R_{n,lw}}{\partial_z} + Qh$$

$$\frac{\partial q}{\partial t} + ui\frac{\partial \theta}{\partial xi} = Kq\left(\frac{\partial^2 q}{\partial xi^2}\right) + Qq$$

> where θ is the air temperature, q is the specific humidity and Qh and Qq are "used to link heat and vapor exchange at plants with the atmospheric model." Also, "∂Rn,lw/∂z is the vertical divergence of longwave radiation taking into account the cooling and heating effect of radiative fluxes" (Bruse, 2004a, p. 02).

The mean radiant temperature is another essential component analyzed in this doctoral research. According to Sinsel et al. (2022):

> Mean radiant temperature Tmrt [◦C] represents the radiative heat load a standing human body receives as a parametrized temperature-dimension index (Fanger, 1972; Kantor and Unger, 2011; VDI, 2008). From received radiative fluxes (Sstr), the emissivity of the human body – being equal to the absorption coefficient for longwave radiation according to Kirchhoff's law (εp = 0.97) –, and the Stefan-Boltzmann constant (σ = 5.67 • 10-8Wm-2K-4), a temperature can be calculated that represents a human body's heat load.

$$T_{mrt} = \sqrt[4]{S_{str}/(\varepsilon_p \bullet \sigma)} - 273.15$$

Furthermore, the calculation of mean radiant temperature in ENVI-met® was (Bruse, 1999 and Huttner, 2012, as cited by Sinsel et al., 2022):

$$T_{mrt} = \left[\frac{1}{\sigma} \bullet \left(L + \frac{a_k}{\varepsilon_p} \bullet \left(I^* \bullet f_{p_{envi}} + D\right)\right)\right] 1/4$$

Also, according to Sinsel et al. (2022):

> Incoming longwave (L) and diffuse solar as well as diffusely reflected global radiation (D) are based on both object/sky view factors, that are representing the upper hemisphere, and ground surface properties, that are representing the lower hemisphere, which are thus weighted by 50% each. The accordingly needed properties for calculating emitted longwave and reflected shortwave radiation, such as temperature, emissivity, and reflectivity, are averaged over the whole model domain. The projection factor (fpENVI) after Underwood and Ward (1966), which accounts for the surface being exposed to direct sunlight depending on the solar altitude angle (β), is defined in Eq. 5:

$$f_{pENVI} = 0.42 \bullet \cos(\beta) + 0.043 \bullet \sin(\beta)$$

However, after version 5.0 of ENVI-met® was implemented, the reflected shortwave radiation and longwave are now considered (Huttner, 2012 Simon et al., 2021, as cited by Sinsel et al., 2022). The mentioned alterations related to the new IVS radiation scheme form the equation:

$$Q_{Sec,Object,in}(i,j,k) = \sum_{a=1}^{VF} w(a) \cdot \tau_{Veg}(a) \cdot Q_{Sec,Object,out}$$

"To calculate these so-called secondary radiative fluxes (QSec) for a grid cell (i, j, k) in IVS, the individual contribution of objects (ω) is weighted by the angle (a) of a view facet (VF), altered by the vegetation transmission factor (τVeg), and then summed up" (Simon et al., as cited by Sinsel et al., 2022).

$$Q_{Sec,Object,in}(i,j,k) = \sum_{a=1}^{VF} w(a) \cdot \tau_{Veg}(a) \cdot Q_{Sec,Object,out}$$

Finally, as previously established, this chapter focuses on the "Universal Thermal Climatic Index" (UTCI), the newest human thermal comfort index (Win 2001, as cited by Huttner 2012). UTCI was first integrated in 2013 on version 4.0 of ENVI-met®. The index calculation within the software is limited to a wind speed range of 0.5m/s to 17m/s on a 10m height. The equation used by BIO-met® is:

$$Wind_{10m} = \frac{ln(10/z0)}{ln(zlevel/z0)} \cdot Wind_{zlevel}$$

where Windzlevel is the calculated local wind speed within the model domain at the pedestrian level (zlevel) (ENVI-met GmbH, 2021).

Concerning vegetation calculations and air quality, numerous equations and models intend to establish the equivalent behavior between modeled and actual vegetation. For example, in 2004, an update on the model for stomatal behaviors, including the effect of short-term and long-term variations, was published (Bruse,2004b). In more detail, the stomata are the vegetation pores that allow gas exchange, essential for the CO2 absorption and oxygen production cycle (Fricker and Willmer, 2012). Moreover, ENVI-met® uses the equation:

$$g_{s=}1.6\frac{A_n}{C_s - C_i}$$

"where An is the net photosynthesis rate, Cs and Ci are the CO2 concentrations at the leaf surface and inside the leaf, and the factor 1.6 results from the differing diffusivity of CO2 and H2O in the air" (Bruse, 2004b). However, as previously explained, particulate matter concentration and dispersion are the focus of this doctoral research regarding air quality. Regarding the mentioned topic, as previously mentioned, the particles can be inputted for each studied hour. According to Bruse (2007):

“To implement this, each source is defined by 24 values representing the emission rates q(h) for each hour h [0-23] of the day. The actual emission rate for an hour h and a minute m [0-59] is then linearly interpolated as:

$$q(h,m) = \frac{60-m}{60} \cdot q(h) + \frac{m}{60} \cdot q(h+1)$$

After hour h=23 the calculation restarts with h=0. The frequency of updating the emission rate can be selected by the user and should normally be around 10 min.

Concerning sedimentation and deposition of particles and the relation to leaf area density of the modeled vegetation, the “flux of particles towards the leaf surface (Xplant) can be written as:

$$X_{plant}(z) = LAD(x,y,z) \cdot f_{cap} \cdot v_d^p \cdot x(z)$$

LAD is the leaf area density (counted on one side), and fcap is the leaf filtering capacity, which varies according to the leaf’s cleanliness. For the calculations, the fcap is always considered 1, equivalent to a clean leaf. Additionally, x, y, and z are the cartesian coordinates within the model (Bruse, 2007). Moreover, the total pollutant balance as a result of deposition and sedimentation is demonstrated as the following equation:

$$\frac{\partial x(z)}{\partial t} = X^{\downarrow}(z) + X \downarrow (z) - X_{plant}(z)$$

∂ is a partial derivative, while “X is the local particulate matter concentration used in the pressure-independent SI-unit [mg(X)kg¡1(Air)]”. For the total amount of particle mass deposed on a leaf surface, the equation is:

$$\frac{m_{plant}}{\partial t} = X_{plant}(z) \cdot \frac{1}{LAD(x,y,z)} \cdot \rho$$

“with ρ being the density of air (=1.29 kgm¡3)”. It is essential to establish that ENVI-met® does not consider particle resuspension (Bruse, 2007). Finally, more specifically concerning the pollutant dispersion calculation, a standard advection-diffusion equation is applied (Bruse, 2007, as cited by Huttner, 2012):

$$\frac{\partial X}{\partial t} + u\frac{\partial X}{\partial \mathrm{x}} + v\frac{\partial X}{\partial \mathrm{y}} + w\frac{\partial X}{\partial \mathrm{z}} = \frac{\partial X}{\partial t}\left(K_X\frac{\partial X}{\partial \mathrm{x}}\right) + \frac{\partial}{\partial y}\left(K_X\frac{\partial X}{\partial \mathrm{y}}\right) + \frac{\partial}{\partial z}\left(K_X\frac{\partial X}{\partial \mathrm{z}}\right) + Q_X(x,y,z) + S_X(x,y,z)$$

“where X denotes the gaseous or particulate atmospheric component under investigation, and Q and S describe its source and sink terms (sedimentation or chemical transformation). The unit of X is [mgkg-1]” (Huttner, 2012). Finally, as previously mentioned, there are two forms of modeling vegetation in ENVI-met®. The implementation of a more complex method, an equation that calculated effects at leaf scale, was integrated (Bruse and Simon, 2015, as cited by Simon, 2016):

$$J_{trans}^{sum} = \iiint_{C(X,Y,Z)} LAD(x,y,z) \cdot \rho_a j_{f,trans}(x,y,z)dxdydz$$

Jsumtrans is the total sum of transpiration of the tree canopy in [g(H2O) s-1]. C (X, Y, Z) is the three-dimensional space of the tree crown. LAD is the Leaf Area Density inside the crown. if,trans is the local transpiration flux at the leaf scale and \rhoa is the air density (Simon, 2016).

5.3.3. OUTDOOR THERMAL COMFORT AND AIR QUALITY STUDIES

The second group of analytical exercises is chosen to achieve this chapter's outdoor thermal comfort and air quality study objectives. The method for this section of the EMEF Amorim Lima study also follows the logic of a typical year assessment. However, unlike the sun radiation simulation, specific days are studied rather than simulating a year's accumulative result. Considering the time frame for this exercise, the amount of data to be post-processed, and the time required for the simulation process, it would be unrealistic to simulate one full year. Moreover, it is essential to remember that this exercise focuses on evaluating the present conditions of the Amorim Lima School. Consequently, more in-depth examinations of the relationship between architectural elements and small-scale green infrastructure within other weather conditions are examined in more depth in the following chapter.

Sao Paulo can showcase significant average differences between seasons for a tropical city, mainly in summer and winter. However, the variations between seasons are not as expressive, considering that even during winter days, air temperatures could reach over 20°C. The data is collected from the climate analysis Excel table produced by Dr Juan Vallejo, and its information is collected from the weather data file SaoPaulo_2005-hour.epw. According to the mentioned source, the lowest mean average temperature of the year is in July: 16.65°C. The highest mean average air temperature is registered in February, being 22,9°C. July showcases a mean maximum dry bulb temperature of 21.42°C, while in February, it is 26.94°C. Additionally, the weather data file used to run the simulations was analysed to contextualise the results established in the next section. The evaluation was done with the online CBE Clima Tool (Betti et al., 2023), generating the climatic data summary for Sao Paulo city. The graphs plotted are the annual dry bulb temperature (figure 5.3.07) and the DBT for February (figure 5.3.08) and July (figure 5.3.09). Furthermore, two climatic profiles are manually built in ENVI-met based on the previously discussed conditions in addition to data from the Weather Spark website. One climatic profile references the mean air temperature and humidity conditions during summer, while the other references winter conditions. For example, the maximum air temperature applied on the representative summer day is 27°C at 04:00 pm, and the lowest is 19°C at 06:00 am. The winter day maximum input

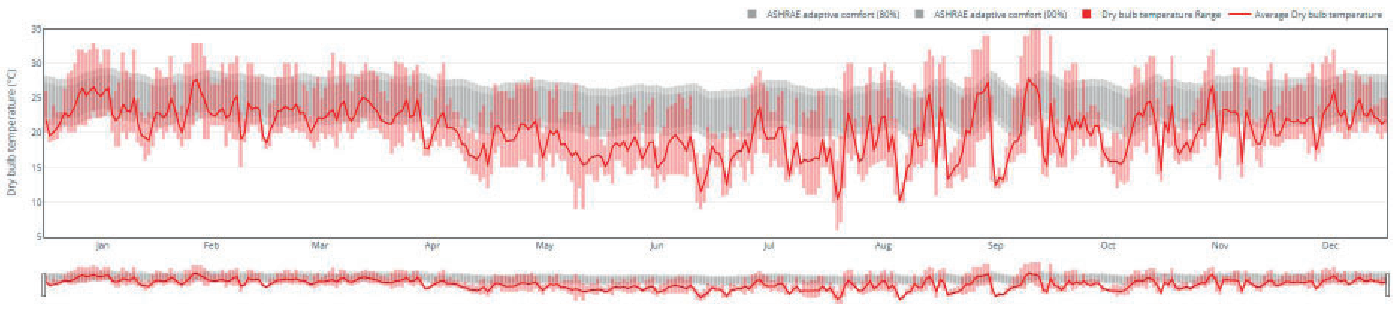

Figure 5.3.07 - Annual DBT for the city of Sao Paulo plot, from EPW file (CBE Clima Tool, 2023)

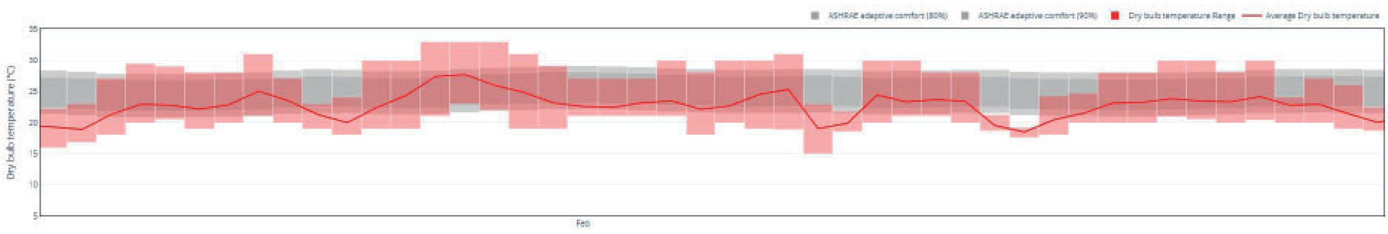

Figure 5.3.08 - February DBT for the city of Sao Paulo plot, from EPW file (CBE Clima Tool, 2023)

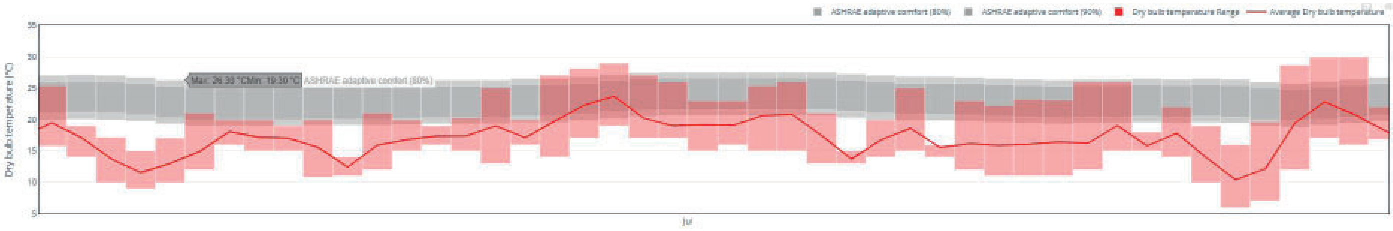

Figure 5.3.09 - Annual DBT for the city of Sao Paulo plot, from EPW file (CBE Clima Tool, 2023)

is 21°C at 03:00 pm, and the lowest is 13°C at 06:00 am. Regarding the wind characteristics of the site, the velocities and orientations do not change between the summer and winter days. Moreover, sky conditions remain the same between most of the studied days (sunny and unobstructed) to showcase the impacts of direct sun radiation. Even though simulations were developed for two days (summer and winter), four specific periods were analyzed more profoundly within the outcomes. The time was the same as the fieldwork was done: 08:00 am, 11:00 am, 04:00 pm and 06:00 pm. Additionally, it is essential to point out that the results were analyzed from 1.50m height above the ground, considering the average size between the school users (younger kids and adults). The studied height is also defined as following the method in the previous chapter (fieldwork) due to information from Oke (2006).

For this exercise, the school and building contexts are modeled in ENVI-met®, mimicking the studied area's current environmental and built characteristics. The grid used is of one meter (x,y, and z), which creates a domain of 270 x 400 grids. Moreover, the vegetation typologies (trees, hedges, and grass), diverse leaf area densities (LAD), and heights are also imitated as much as possible in the model. The building`s façade elements and materials are also represented in the model. The mentioned natural and built elements are carefully selected to represent the site's characteristics, being chosen on the ENVI-mets®`s database or built from scratch. For example, the perforated red brick covered by cement plaster is the main constructive element for the school building walls. Moreover, its characteristics are built into the database. Additionally, a material composed of metal and insulation is built to represent the galvanized roofs

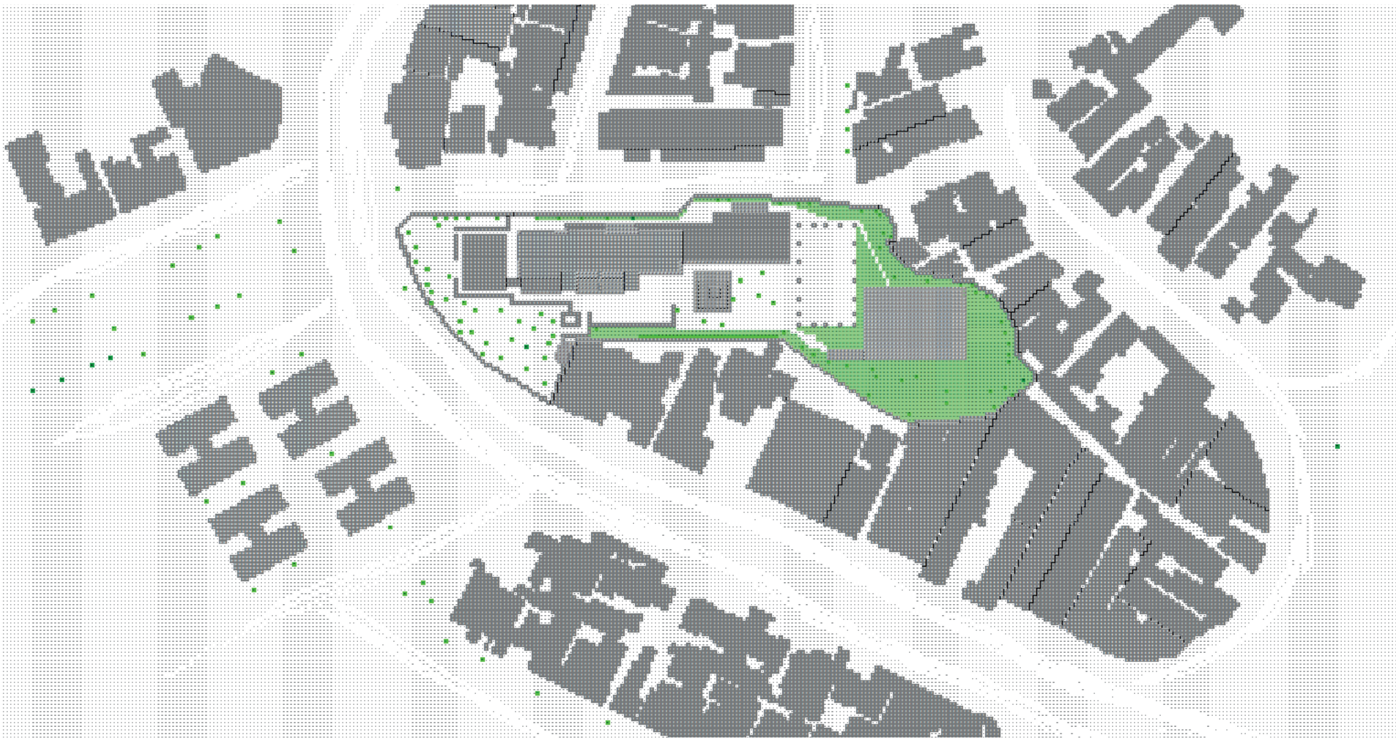

Figure 5.3.10 - ENVI-met® workspace, showing which surrounding buildings were considered. In addition to applied grass, trees and hedges.

that cover the school buildings. Concerning surrounding areas outside the site, the construction element is the same perforated red brick. It is a standard construction method in Sao Paulo; no specific details are considered. However, all surrounding greenery is added with all observed characteristics, as it could impact the particle distribution and concentration of the studied site.

As mentioned in the ENVI-met® characteristics section, the existing vegetation is emulated in the software using the Database Manger® and Albero® tools (built within ENVI-met®). The characteristics considered for developing the trees in this model are the approximate height, crown diameter, LAD (leaf area density), and typology. Albero® recognizes, by default, two different tree types, deciduous and coniferous, chosen as the base for constructing the Amorim Lima model trees. The software also presents two different LAD scenarios: High and low. Both configurations are used in the model depending on what is observed through the pictures and on-site. It is essential to state that in Sao Paulo, the trees do not suffer an extreme change in leaf area density throughout the year. Naturally, the characteristics discussed are considered when building the threes and their behavior patterns in the software. Furthermore, as previously discussed, the second section of the analytical study is dedicated to establishing perceived comfort in EMEF Amorim Lima. Therefore, the selected indicators for the analysis are mainly Radiant Temperatures (MRT) (°C) and the Universal Thermal Climate Index (UTCI). The UTCI is related to the body's perception of the thermal characteristics of the environment, and it depends on MRT values, wind speed, and humidity, expressed as relative humidity or water vapor pressure (Błażejczyk et al., 2013). According to Blazejczyk et al. (2012), the UTCI is better than other indices due to its ability to express slight differences in meteorological stimuli intensity. Furthermore, a study developed by Park, Tuller, and Jo (2014) defined the UTCI as having great potential to analyze possible human thermal effects of landscape and urban design. Moreover, Bröde et al. (2011) indicated that UTCI could be suitable for studying urban thermal comfort in sub-tropical regions.

In addition to thermal conditions, health through air quality is encompassed in this study section. As explained in the Small-Scale Green Infrastructure chapter, the different typologies can absorb gaseous pollutants through stomata and remove particles by deposition, affecting the air quality conditions directly (Janhäll, 2015; Van den Berg et al., 2015; Salmond et al., 2016; Livesley et al., 2016; Abhijith et al., 2017; Buccolieri et al., 2018 and Rui et al., 2019). For that reason, the dispersion of PM2.5 and PM10 (ug/m3) arising out of the primary sources into the school's outdoor and indoor spaces is simulated in the analytical exercise. Furthermore, as previously mentioned, ENVI-met® allows manually adding pollution sources within the workspace. Therefore, the pollutants input into the software are based on data collection from the Technology and Environmental Sanitation Agency of Sao Paulo`s state, CETESB, air quality report (CETESB, 2021). The daily air pollution bulletin also developed by CETESB (CETESB, 2019), the air quality web-site`s index map (Purelogic Labs India Pvt Ltd, 2020), and the real-time air quality index map produced by the World Air Quality Project (The World Air Quality Index Project, 2020) are also considered. Finally, to input pollutant particles into the software`s workspace, PM10, and PM2.5 sources are applied over the traffic lanes adjacent to the school. The considered height is 0.4m to mimic traffic-induced pollution, as seen in Rui et al. (2019).

Figure 5.3.11 - Pollution source spatial input into ENVI-met®

5.4. RESULTS

5.4.1. SOLAR GEOMETRY STUDIES

The sun path diagram establishes the studied site's spatial location concerning sun movement throughout the year. It illustrates how, in Sao Paulo (southern hemisphere), the sun rises to the east, moves to the north, and sets to the west. The earliest it rises is at 5:10 am and the latest at 06:55 pm, occurring during summertime. The latest sunrise and earlier sunset naturally happen in winter, 06:50 am and 05:25 pm. This indicates that sunlight and radiation are available most of the day throughout the entire year. Thus, most of the school day activities happen while there is natural light and radiation. The sun path diagram also illustrates that the sun can rise in the southeast and set in the southwest during some peak summer days.

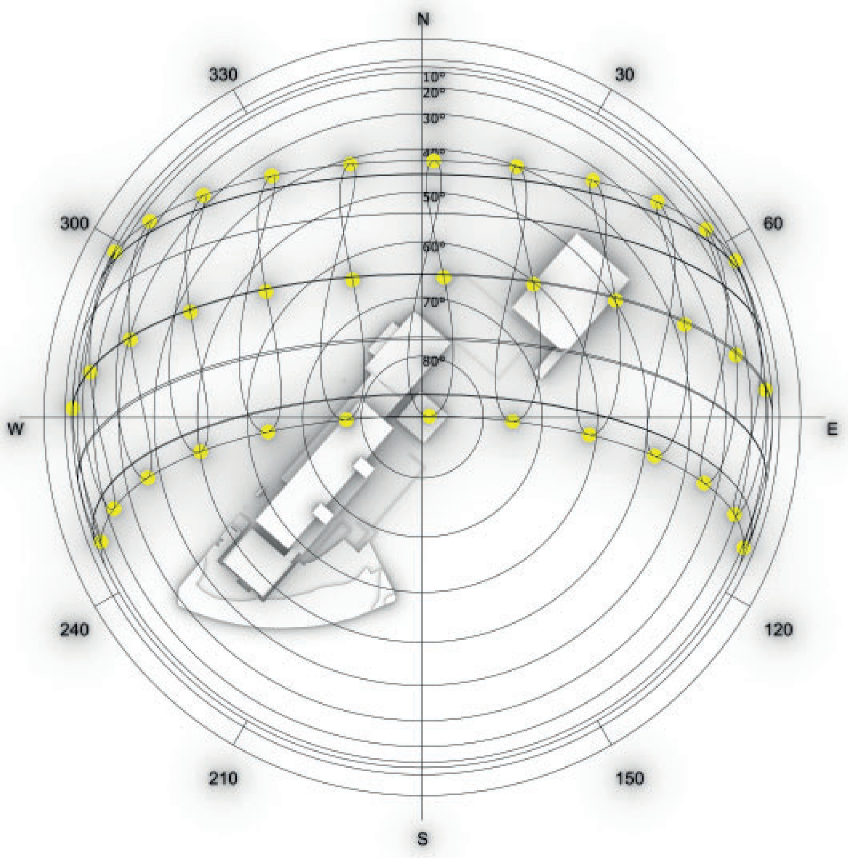

Figure 5.4.01 - Sunpath diagram of the Sao Paulo city, within the context of the EMEF Amorim Lima model.

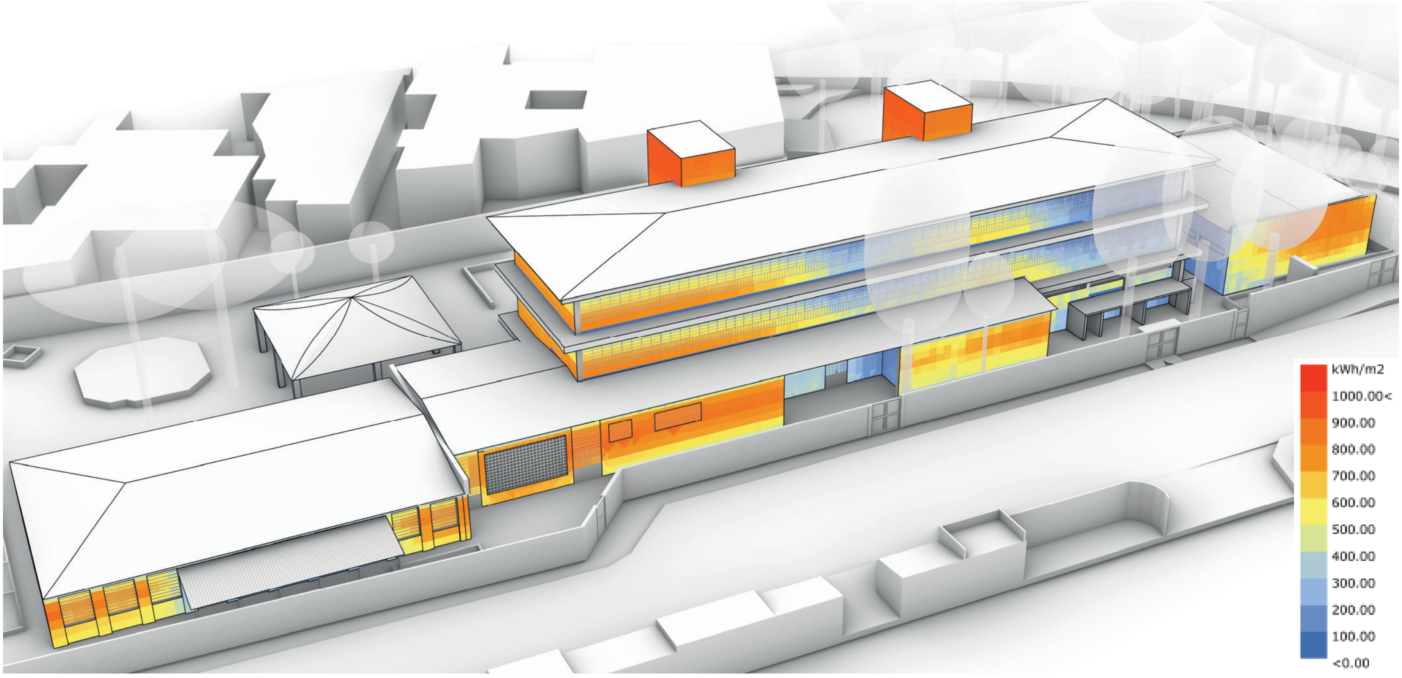

Figure 5.4.02 - North/northwest view of the solar radiation simulation diagram.

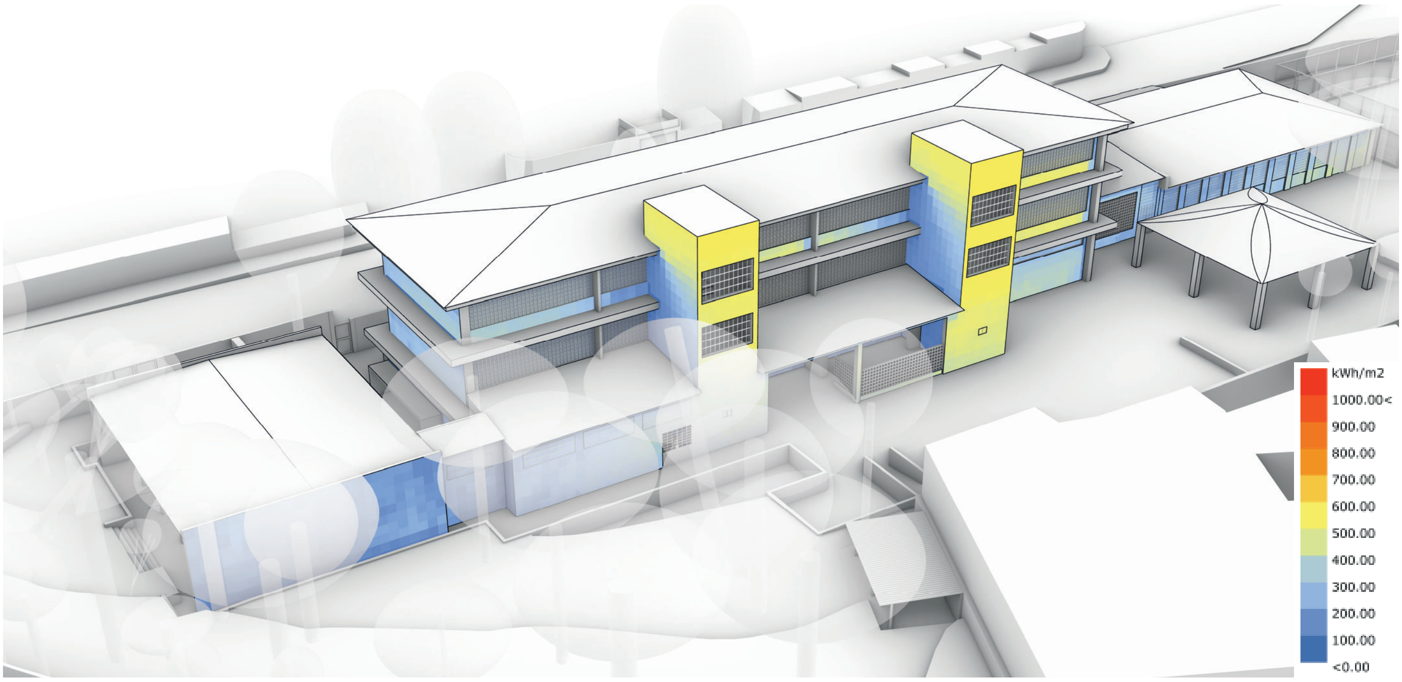

Figure 5.4.03 - South/southeast view of the solar radiation simulation diagram.

In the solar irradiation simulation, as expected from the sun path diagram analysis, the southern facades of the building showcased lower radiation levels in open areas than the north-oriented ones. Hence, on unobstructed portions, the highest amount of solar radiation accumulated in one year is 600 kWh/m2, while the northwestern facade collects over 1,000 kWh/m2 (40% more). The southeastern front area, closer to Cora Coralina Park, presents annual accumulative radiation levels between 100 to 200 kWh/m2, even on the first and second floors, due to the tree`s obstruction. It is essential to remember that the trees were built as solid elements in the model, which does not correspond to the reality of vegetation. The conventional tree porosity would probably allow higher solar radiation levels to accumulate on the facades behind it. The opposite side of the southeastern façade, connected to the non-vegetated area of Cora Coralina Park, has no obstruction to the east and northeast sun. Therefore, it showcases accumulative radiation levels 10 to 20% higher than the surfaces obstructed by trees.

All main building facades have 100cm overhangs on each floor. The southeastern and northwestern facades have additional vertical elements, 50cm deep, approximately every seven meters. Furthermore, the areas closer to the mentioned architectural features showcase accumulative radiation levels below 100KWh/m2, a reduction of 80% compared with northwestern surfaces. The cobogos on this façade have only 20cm x 0.5cm openings, creating massive panels. However, most of the southeastern façade, where the cobogo is applied, had up to 300kWh/m2 of solar irradiation incidence. The low solar radiation levels, open cobogos, and the constant possibility of air movement could indicate thermal discomfort indoors in colder periods. Moreover, a portion of the façade is exposed to the morning (east) sun, demonstrating radiation levels up to 600kWh/m2; the radiation level is still insignificant. Additionally, the morning sun happens on lower dry bulb temperature periods of the day. Consequently, the cobogo would not be necessary, even in this portion of the façade.

Figure 5.4.04 - View of the southeastern façade with solar radiation simulation diagram.

Overall, concerning the southeastern façade, results suggest a lack of heat gains through radiation, enhancing comfort indoors during warmer periods. However, the number of shading elements on the mentioned façade is unnecessary and can cause thermal discomfort in colder periods of the year. Additionally, the façade treatment is a missed opportunity to have unobstructed openings to maximize useful daylight indoors. The excess of shading indicates unnecessary levels of daylight entering the spaces. Zani et al. (2018) have indicated how the direct sun radiation falling into the human body can lead to unacceptable levels of thermal discomfort, consequently decaying human health and reducing productivity and learning proficiency. However, as mentioned, the entire southeast façade receives sun only during the morning when temperatures are usually lower, and the direct radiation probably doesn’t negatively impact human comfort. On the indoor patio, as noticed in the fieldwork, the daylight situation and lack of solar heat gains are worse than in first and second-floor classrooms. The conditions mentioned above are justified by the indoor patio`s openings being obstructed by the building geometry and the cobogo elements.

Figure 5.4.05 - Picture of the northwestern façade, showing existing trees.

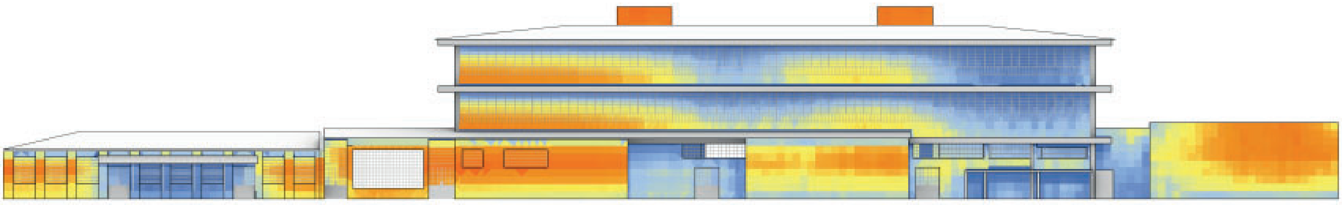

Figure 5.4.06 - View of the northwestern façade with solar radiation simulation diagram.

On the Northwestern façade, the unobstructed areas presented annual accumulative radiation levels over 900KWh/m2. The 100cm overhangs showcased on the southeastern facade are also part of the Northwestern one. It generates a 90% reduction in solar radiation in the façade's higher areas (closer to the elements). In addition, high trees with sizable crowns are planted close to the façade, causing declining radiation and light availability (image 07). However, most of the northwest-oriented front on the first and second floors shows annual accumulative radiation of over 800KWh/m2. Most of the Northwestern façade is composed of glazed windows. Additionally, it receives direct sun during the day's portion with higher air temperatures (end of morning and afternoon). Furthermore, the cited parts of the day correspond to the hours students and teachers use the classrooms. Therefore, the outcome indicates possible human thermal discomfort within the upper floor`s classrooms through solar and internal heat gains. However, those gains could be used to enhance human comfort during winter. The results corroborate the fieldwork findings regarding the existence of glare and thermal discomfort. Again, it is possible to see all the northwest-oriented apertures of the indoor patio (ground floor) protected by the building's geometry, with solar radiation levels 50% to 80% lower than what was spotted on the exposed walls. The cited outcomes are additional evidence of the lack of available light on the indoor patio, which also happens because of the expressive footprint area of the room.

The Northeastern wall of the three storage buildings is also profoundly exposed to the sun, presenting areas with over 800KWh/m2 of annually accumulated radiation. Still, the only existent openings on the cited facades are small and protected by the typical overhang, which reduces the accumulative radiation levels to only 150KWh/m2 on the glazed surfaces. Nevertheless, it is crucial to consider that radiation is being transferred indoors through the wall, adding to the heat gains of the classrooms. The Southwestern walls receive the last hours of direct sun, showcasing the lowest radiation levels. Thus, the unobstructed area's highest accumulative radiation amount was 600KWh/m2. The first-year classrooms on the ground floor are southwest-oriented, and Cora Coralina Park`s trees obstruct their façade, which has a 100 kWh/m2 radiation outcome. The mentioned characteristics, combined with the small, glazed apertures of the room, indicate the lack of sufficient daylight during the year. However, the classrooms may be the most comfortable during winter due to reduced internal heat loss.

5.4.2. THERMAL COMFORT

On the emulated summer day at 08:00 am, the dry-bulb air temperature input is 22°C on the EMEF Amorim Lima`s site. In winter (08:00 am), the air temperature is defined as 16°C. As expected, on both days at 08:00 am, the potential dry-bulb temperature within the studied domain is constant. Within the site's boundaries, the hour with 22°C had air temperatures of 20.5°C to 21.85°C. The cold day (16°C) was between 15.5°C to 16.5°C. Furthermore,

Figure 5.4.07 - Potential Air Temperature (°C) at 08:00 am in the studied area on the summer day.

Figure 5.4.08 - Potential Air Temperature (°C) at 08:00 am in the studied area on the winter day.

at 8 am, the mean radiant temperatures were higher in the site's vegetated areas (SGIs) than in the paved zones on both summer and winter days. On the summer day, vegetated zones had a mean radiant temperature of 15°C to 18°C. While non-vegetated ones showcased an MRT of 9°C to 10°C. In the winter studied period, the zones with greenery had a mean radiant temperature of 10°C to 13°C and the paved areas showed 6°C to 9 °C. The periods when dry bulb

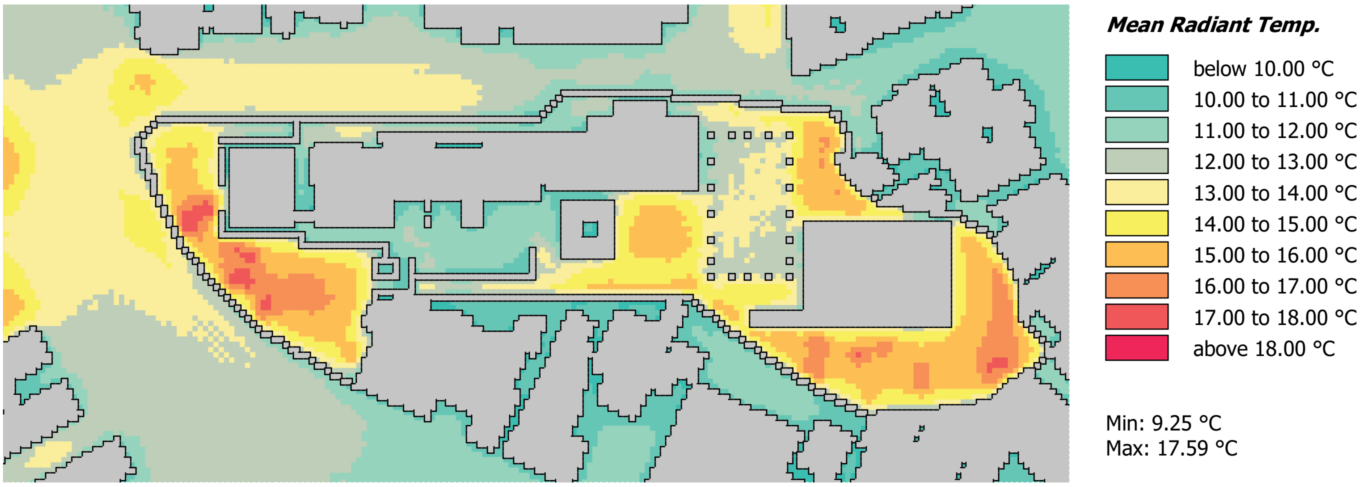

Figure 5.4.09 - Mean Radiant Temperature (°C) at 08:00 am in the studied area on the summer day.

temperatures are lower are summer and winter at 06 pm and 08 am, and winter at 11 am. In the mentioned periods the mean radiant temperatures demonstrated the same pattern of increasing in the vegetated areas. For example, at 11:00 in winter (17°C air temperature), areas without vegetation displayed mean radiant temperatures of 2°C to 5°C degrees lower. Hard pavement materials are effective in storing heat from direct sun radiation. However, the results suggest that the mentioned heat is also quickly released, while grass and soil surfaces can make it take longer. Consequently, the outcomes indicate that the vegetated areas have higher temperatures in colder periods of sunny days.

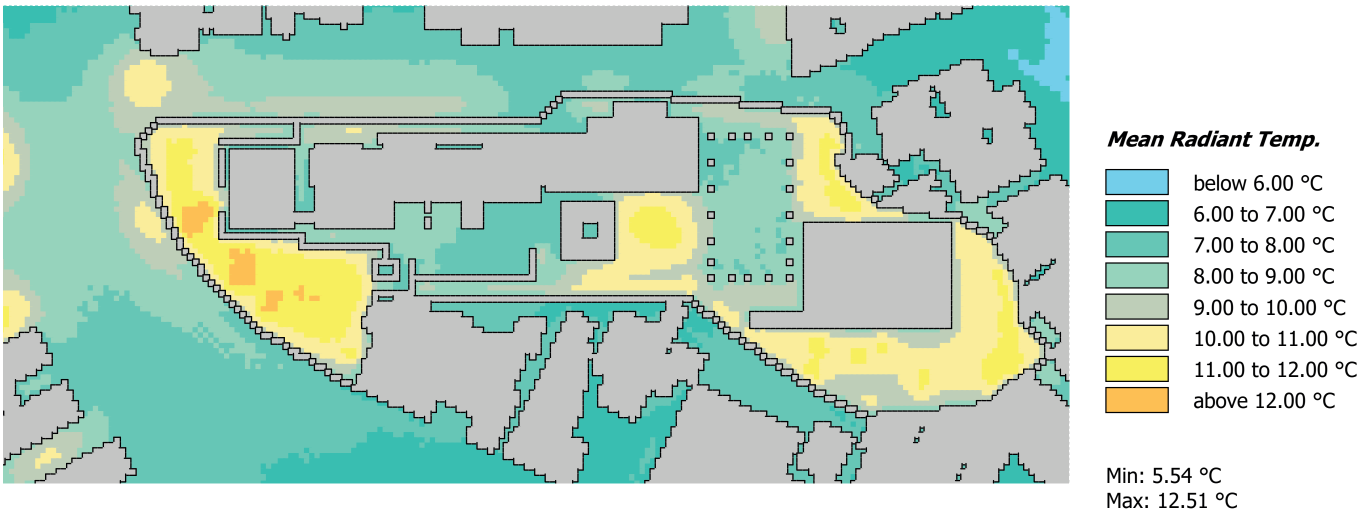

Figure 5.4.10 - Mean Radiant Temperature (°C) at 08:00 am in the studied area on the winter day.

The assumptions above are corroborated by the mean radiant temperature results at 04 pm in summer. At this hour, the vegetation in the area presented MRTs of 30°C to 42.5 °C. Still, the exposed hard pavement spaces showed 40°C to 50°C. This period shows an inversion compared to the previously mentioned colder studied hours. The outcome is explained when considering that at 04 pm the areas have been exposed to sun radiation most of the day. Consequently, the heat is being stored and transferred to the environment. It confirms the negative impact of unobstructed paved areas on sunny days.

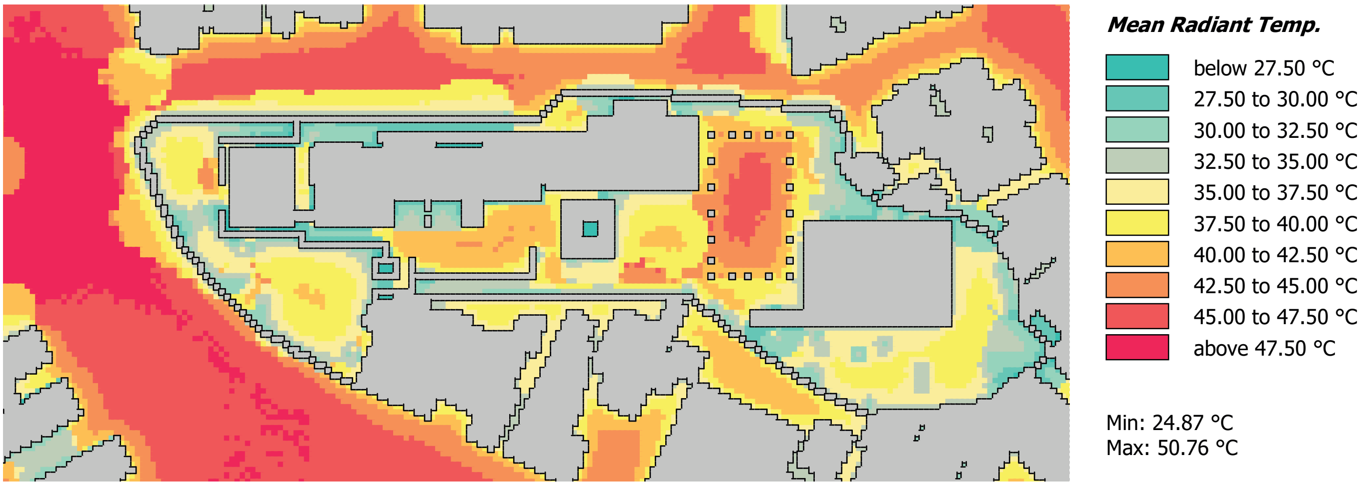

Figure 5.4.11 - Mean Radiant Temperature (°C) at 04:00 pm in the studied area on the summer day.

Concerning the universal thermal climate index (UTCI), it is essential to establish that 9°C to 26°C does not represent thermal stress (Błażejczyk et al., 2013). However, it is possible to affirm that in a tropical city such as Sao Paulo, users could feel slight cold stress when experiencing temperatures below 15°C. Furthermore, the outcomes at 08:00 am in summer show that the sensed temperature in Cora Coralina Park (area with tall trees) was 21°C to 22°C, and the lower greenery and grass area showcased between 20°C to 22°C. Lastly, the paved area perceived temperature was 19°C to 21°C. During winter, at 08:00 am and 11:00 am, the temperature sensation was 13°C to 15°C on the paved open spaces, which could be considered slight cold stress for users in Sao Paulo.

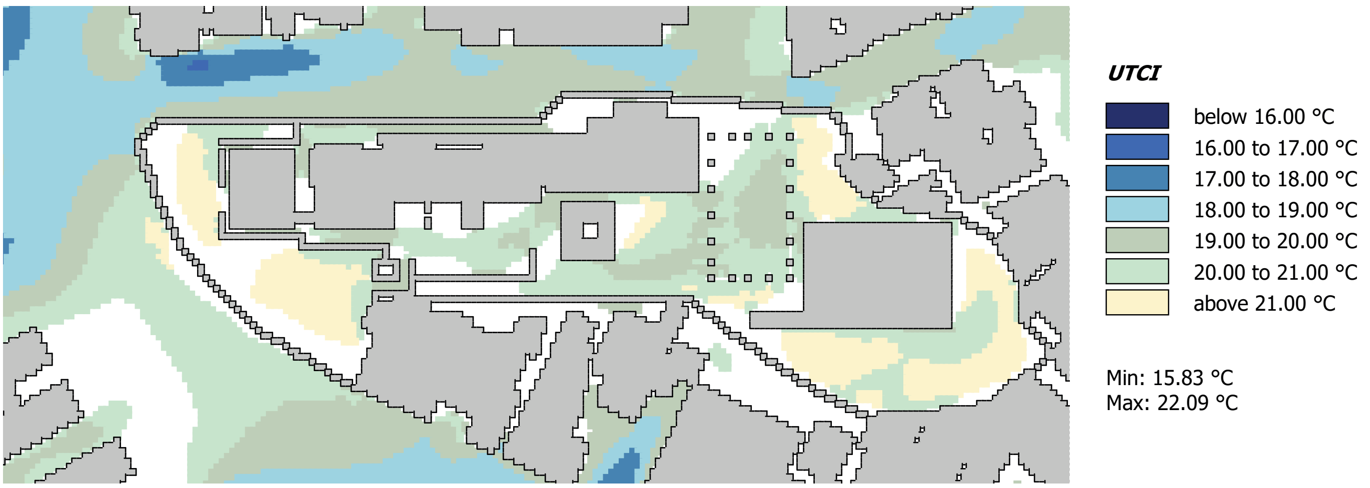

Figure 5.4.12 - UTCI (°C) at 08:00 am in the studied area on the summer day.

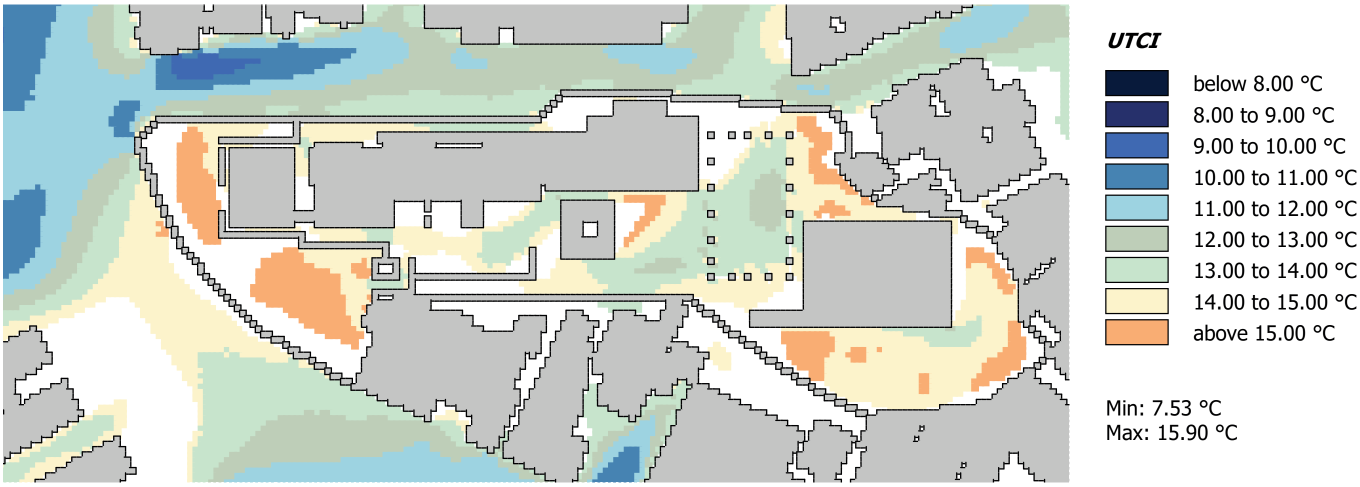

Figure 5.4.13 - UTCI (°C) at 08:00 am in the studied area on the winter day.

The results emphasize what was discussed before regarding the mean radiant temperatures surrounding paved and vegetated spaces: the non-vegetated areas absorb heat and release it faster during night periods. On the other hand, in areas with grass and trees, the heat takes more time to be released. Moreover, the Cora Coralina Park areas, which have tall trees, conserve even more heat due to the protection from the night sky (low sky view factor). The previously discussed process illustrates how areas with small green infrastructure are slightly more comfortable due to higher temperatures, as shown in the UTCI outcomes. At 11:00 am, the dry-bulb air temperature was 23°C on the summer day within the school's site. Besides, it is not possible to spot a significant mean radiant temperature difference between vegetated and non-vegetated zones. Some spots of Cora Coralina Park (with tall trees) presented an MRT of over 40°C, also showcased in paved areas. At the discussed point in time, grass and small vegetation areas showed 19°C to 20°C MRT. Even though the air temperature difference between 08:00 am and 11:00 am was only one degree, the

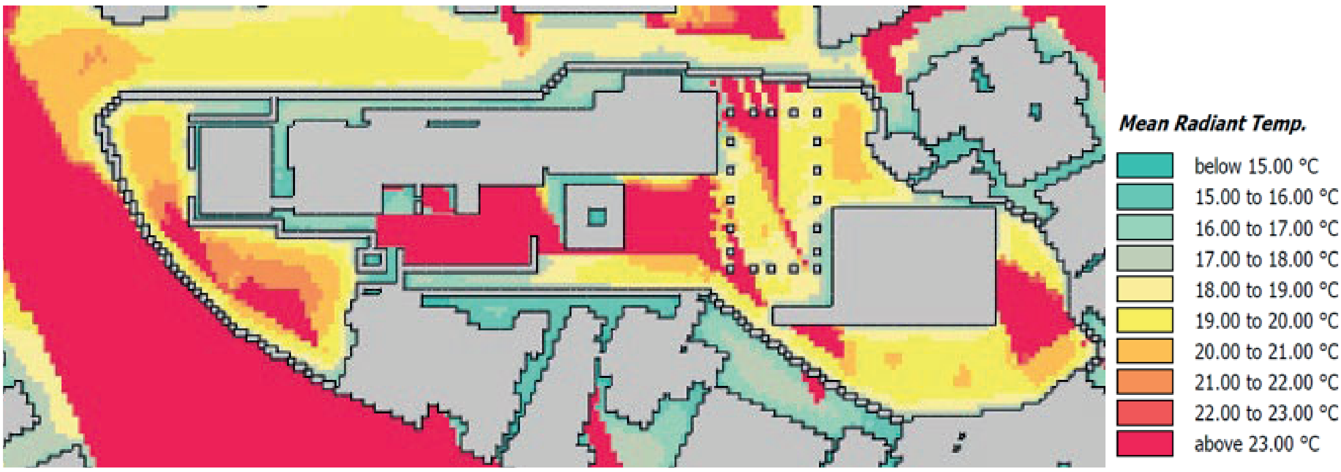

Figure 5.4.14 - Mean Radiant Temperature (°C) at 11:00 am in the studied area on the summer day.

mean radiant temperatures are expressively different. The mentioned result suggests that higher solar radiation levels in the later morning increase the surface temperatures and, consequently, the MRT. Additionally, the higher sun angles at 11:00 am are probably accessing more areas of the school site without the building context obstruction. At the time and day discussed, the only regions displaying MRTs below 17°C were the small areas between buildings or boundary walls. The previous outcome exemplifies how solid protection against direct sun radiation on some occasions is the best strategy for reducing higher temperatures.

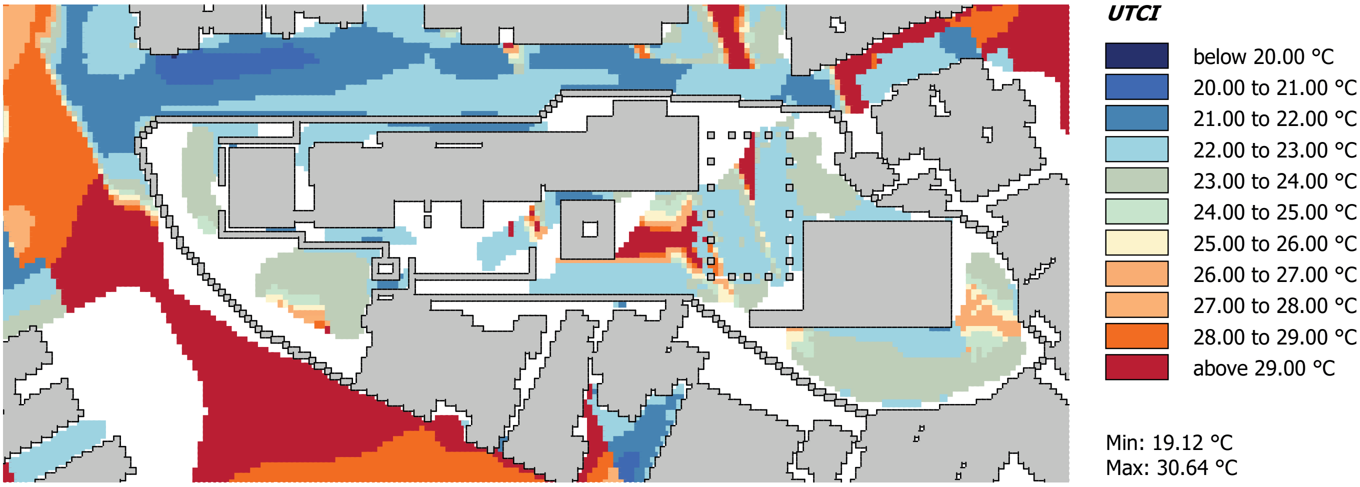

Figure 5.4.15 - UTCI (°C) at 11:00 am in the studied area on the summer day.

The UTCI outcomes for the same period (11:00 am, summer) showed lower perceived temperatures on smaller spaces between buildings or boundary walls. The mentioned temperatures were 20°C to 21°C, representing no thermal stress, which was the comfort indication for most of the site, mainly showcasing 22°C to 25°C. However, it is essential to point out that the hotter areas (31°C to 32°C) were the open, non-vegetated, paved spots. Furthermore, UTCI outcomes indicate that staying in all the school's recreational areas in the late morning is generally comfortable, even with the high MRT previously showcased. The air movement within the studied site is probably one of the responsible elements that enhanced thermal comfort displayed in ENVI-met®. During the afternoon period, there is a natural increase in the dry bulb temperatures. Taking the 04:00 pm period as an example, the air temperature shown in summer is 25°C. The winter day showcased 22°C, even though the morning temperatures varied between 16°C and 18°C. Thus, the outcome exemplifies how Sao Paulo can still showcase the same dry bulb conditions seen on summer days even on colder days. Accordingly, the mean radiant temperatures were also higher for the afternoon (04:00 pm). On the summer day, the increase is substantial, achieving an MRT of 50°C, which could be explained considering the amount of solar radiation received by the site surfaces until 04:00 pm. Nevertheless, it is still possible to spot the MRT differences between zones with vegetation (35°C to 40°C) and unprotected paved areas (42°C to 50°C). Furthermore,

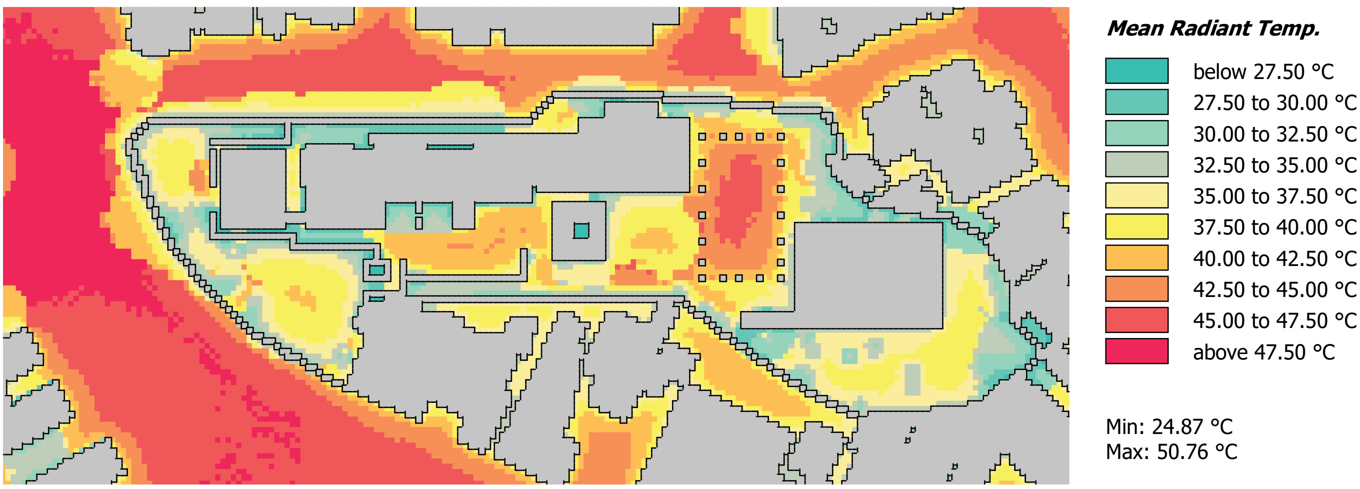

Figure 5.4.16 - Mean Radiant Temperature (°C) at 04:00 pm in the studied area on the summer day.

the mean radiant temperatures on Spot 3 of Cora Coralina Park are almost 8°C lower than those on the uncovered football court. At this point (04:00 p.m.), the school building itself is protecting Spot 3 from direct sun. The previous outcome could illustrate the importance of avoiding direct solar radiation for enhanced thermal comfort. The UTCI at

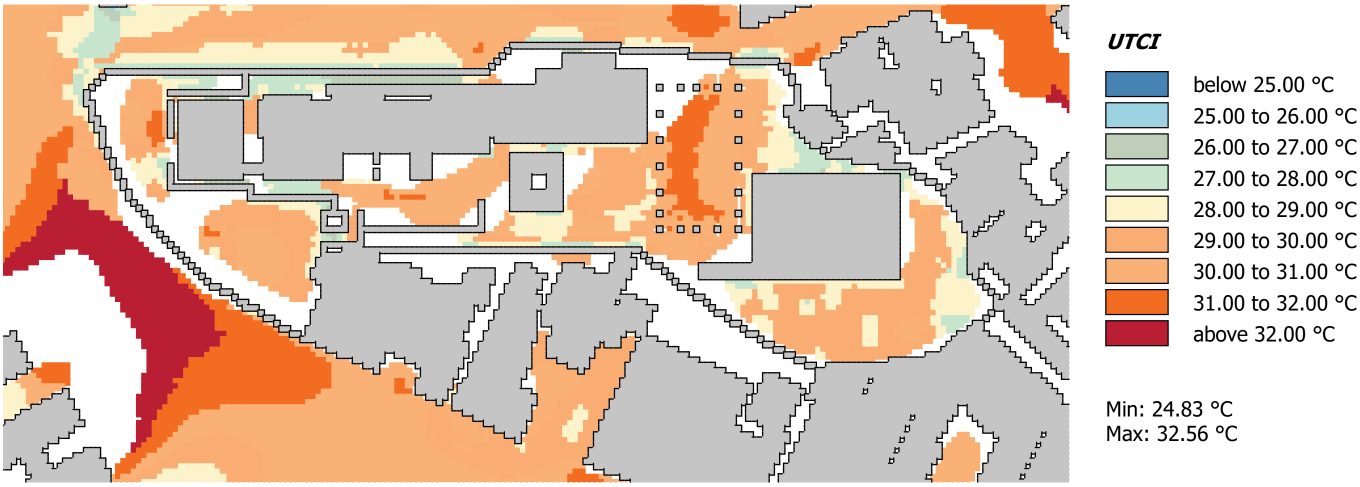

Figure 5.4.17 - UTCI (°C) at 04:00 pm in the studied area on the summer day.

04 pm in summer demonstrates that most parts of Amorim Lima`s site are under moderate heat stress, with perceived temperatures from 30°C to 32°C. Moreover, no significant thermal comfort distinction exists between the green and the non-vegetated areas. On the other hand, on the winter day (at 04:00 pm), the site's perceived temperatures range from 20°C to 32°C, and the typical lower temperatures on the green infrastructures can be spotted again. Thus, the finding above exemplifies how the vegetation has a greater potential to increase human comfort when the thermal conditions are not so extreme.

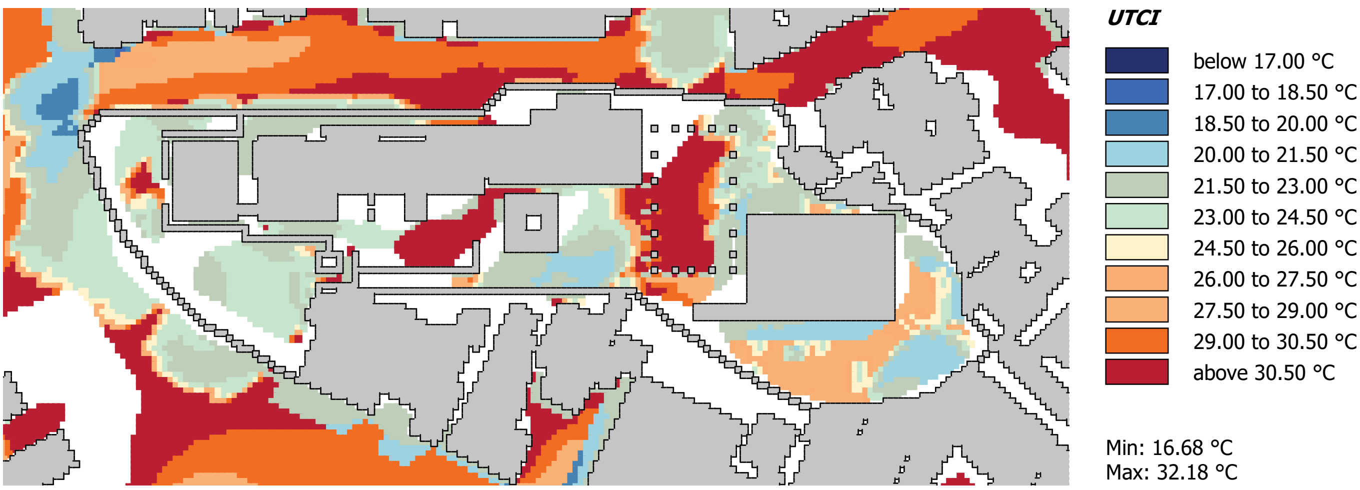

Figure 5.4.18 - UTCI (°C) at 04:00 pm in the studied area on the winter day.

By the end of the afternoon (at 06:00 pm) on the summer day, the dry bulb temperature is still 24°C, and the mean radiant temperatures registered by ENVI-met® were extremely high. Within the School`s site, MRTs from 30°C to 63°C were reported. Moreover, the graph clearly illustrates the impact of the building`s and tree`s shading. Spots under trees presented MRT below 30°C to 32°C; in areas with uncovered grass, there is a maximum of 51°C. On the paved unobstructed regions (football court), the MRT goes to over 60°C. The UTCI index outcomes corroborate the positive effects of greenery previously discussed. Cora Coralina Park vegetated areas users would experience moderate heat stress (29°C to 31°C), while in the areas with grass and lower vegetation, strong heat stress would be felt (32°C to 33°C). Hence, the software probably registers the trees' cooling performance and the shading aspect itself. Lastly, the unprotected paved spots showcase perceived temperatures from 34°C to 36°C. The results demonstrate how the constant exposure to solar radiation over the day has the potential to diminish thermal comfort at the last hours of the day.

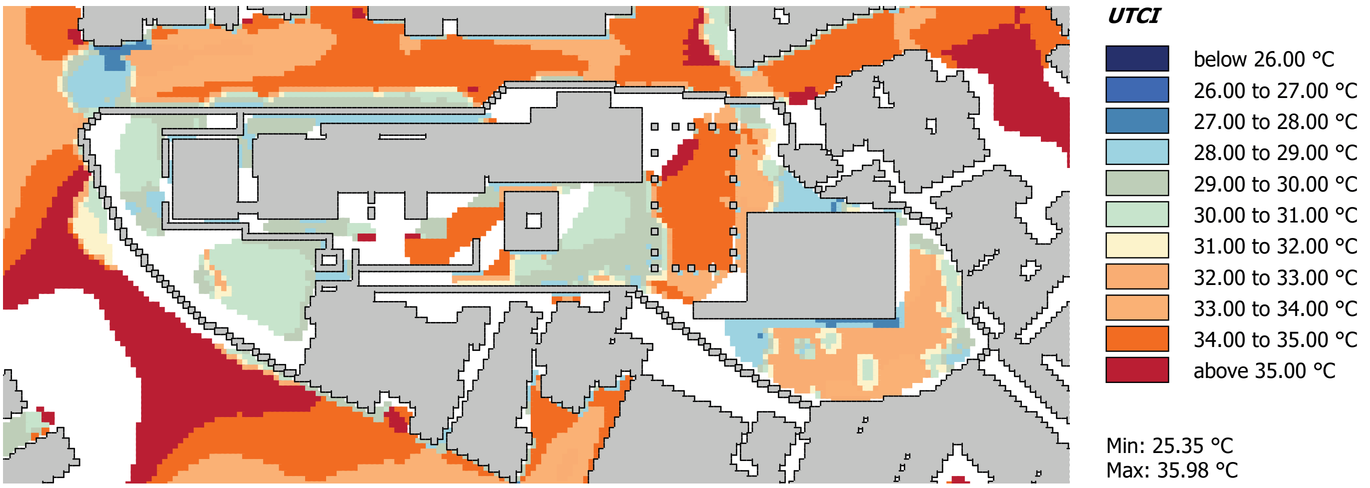

Figure 5.4.19 - UTCI (°C) at 06:00 pm in the studied area on the summer day.

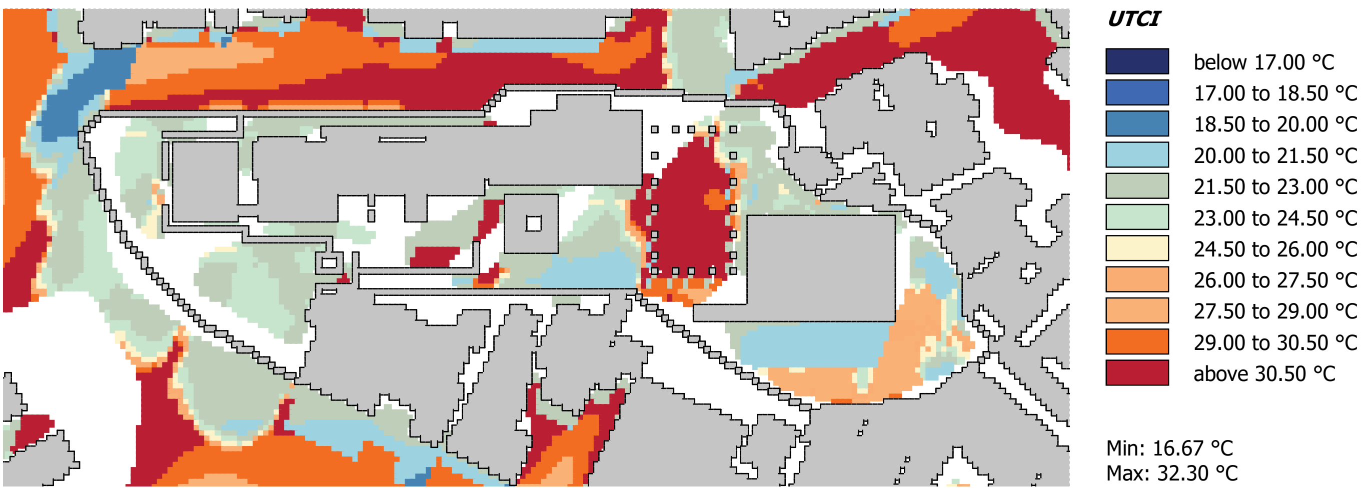

Figure 5.4.20 - UTCI (°C) at 06:00 pm in the studied area on the winter day.

5.4.3. AIR QUALITY

As previously mentioned, the pollutant inputs were regulated according to the traffic intensity at each period of each day. For this reason, the air quality study focus was not on comparing outcomes in each studied period, as done for thermal comfort. Instead, the focus of this section is on the comparison of between areas out and within the school's site. It is essential to remember that the analysis was also made at 1.50m from the ground. As explained in the method, the sources of PM2.5 and PM10 were the Avenue and streets surrounding the site. The Corifeu de Azevedo Avenue is the primary source of daily pollution due to the high number of vehicles. As expected, it is the area with the highest pollutant concentration among the outcomes. On the summer studied day, the level of PM2.5 and PM10

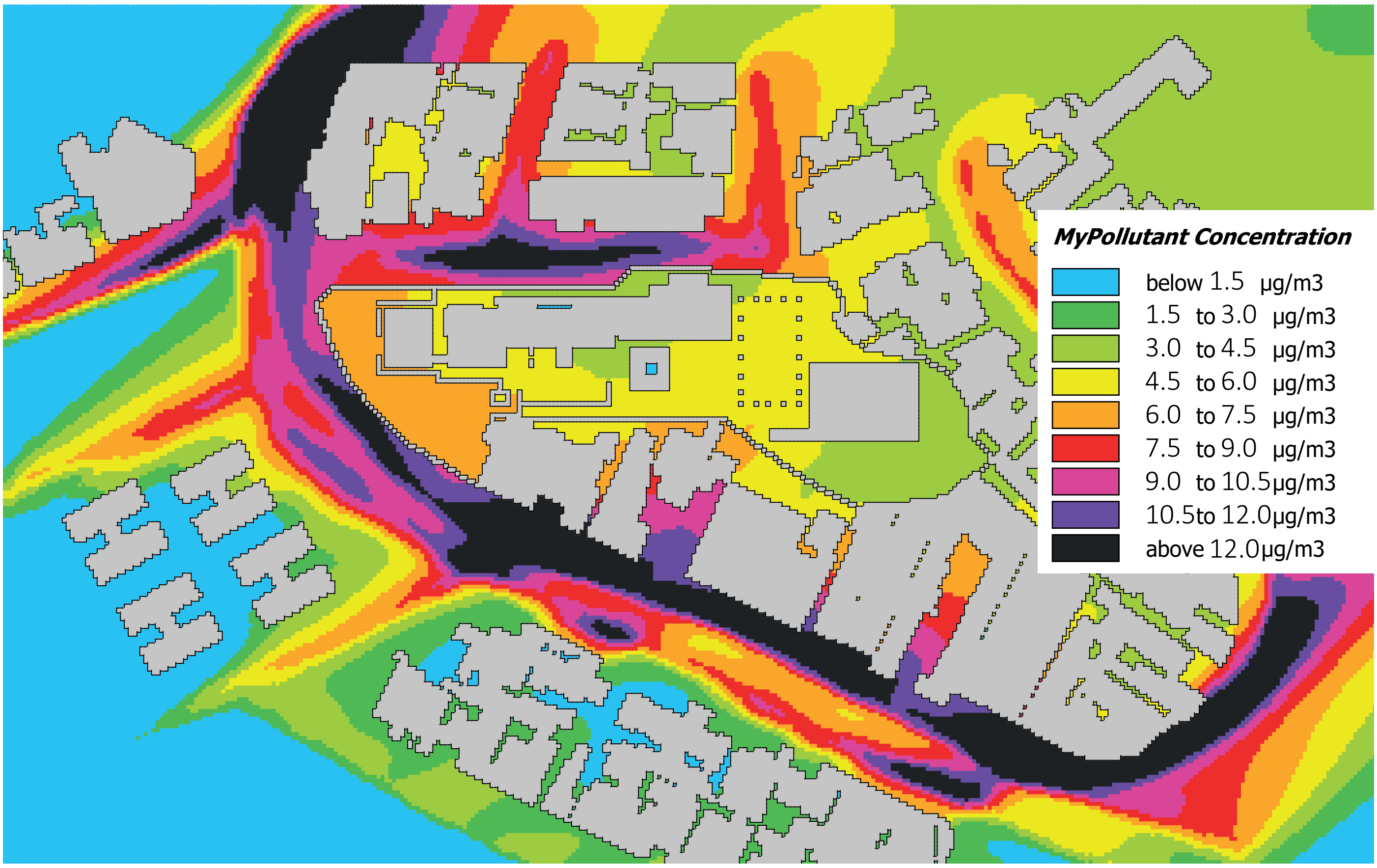

Figure 5.4.21 - PM2.5 and PM10 on the studied area at the summer day.

combined was approximately 12ug/m3 to 15ug/m3, while the pollution levels within Cora Coralina Park were 6ug/m3 to 7.5ug/m3. The Park shows a reduction of up to 30% from the main avenue, which indicates the positive impact of the solid boundary wall. Moreover, the rest of the site registered concentration levels of 4ug/m3 to 5ug/m3 compared with the densely vegetated area (Cora Coralina Park). Therefore, even though it is an adjacent area to the Park, the pollution levels are reduced by 20% compared to it and 40% compared to the avenue. It was also shown that the zone with grass and low vegetated elements presented the lowest pollutant concentration within the Amorim Lima`s site: around 3ug/m3. The vegetation in this area is not dense, enhancing air movement and has the highest level of protection from the sources. The previous outcomes exemplify the importance of solid barriers to reduce air pollution. The results also suggest the negative impact of dense vegetation on trapping pollutant particles.

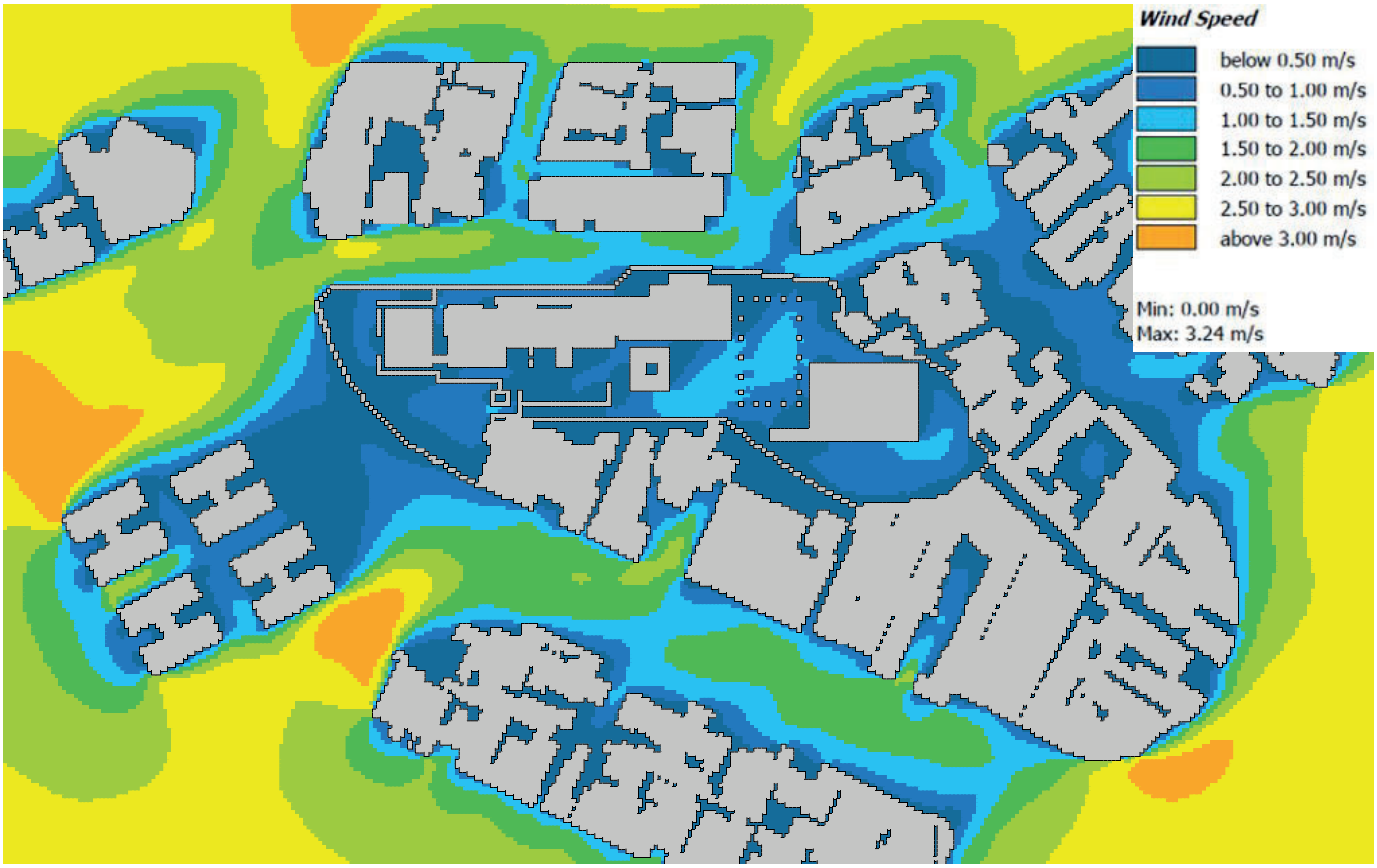

Figure 5.4.22 - Wind Speed in the studied area at 08:00 am on the summer day.

Overall, on all studied days, as exemplified by the 08 am summer period, the areas do not show an expressive difference in air velocities within the site's outdoors. Furthermore, when comparing the studied hours on the summer day the PM2.5 concentrations have similar patterns. In all the studied hours displayed, Cora Carlina Park's vegetated areas always had the worst air pollution. On the other hand, the other side of the terrain, close to the covered sports court, constantly performed best. The results corroborate what was found in the combined analysis of PM10 and PM2.5 par-

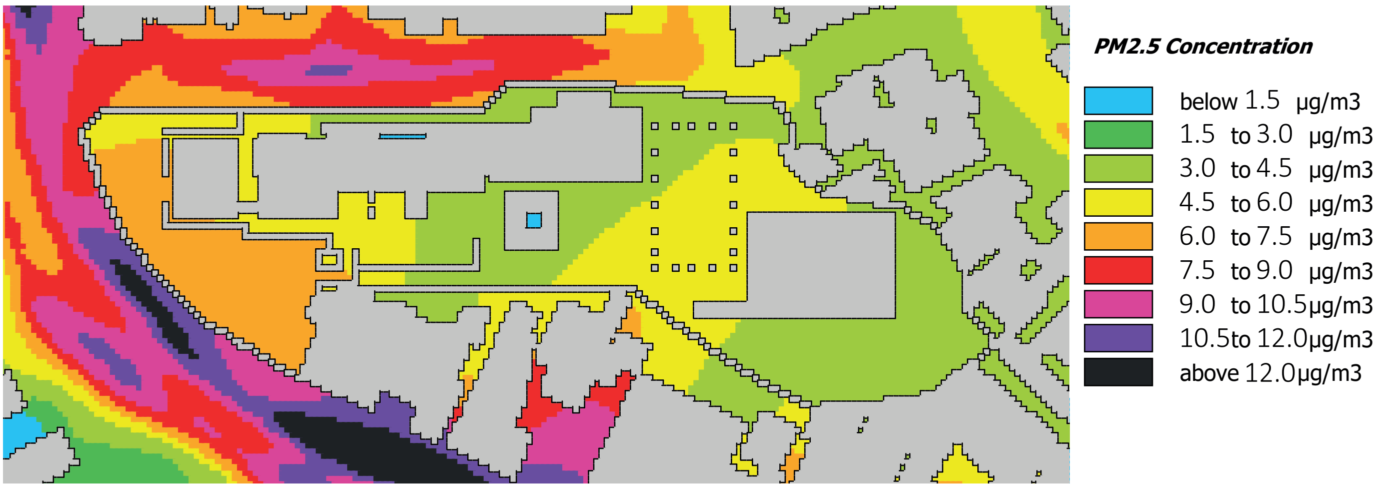

Figure 5.4.23 - PM2.5 concentration in the studied area at 08:00 am on the summer day.

ticles. It raises the question of whether the vegetated areas are more polluted because of the dense trees, the direct connection with the main pollution source, or both factors combined. Finally, the winter day was analysed, and it was observed that both days had similar concentration patterns. However, the coldest hours always had a higher pollutant concentration than the hottest hours.

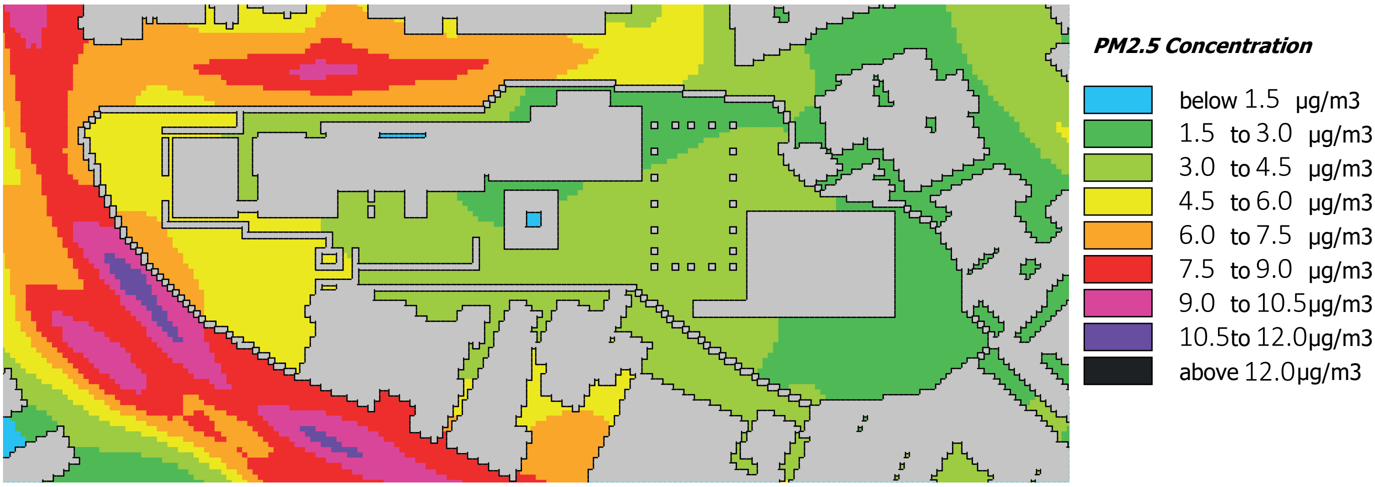

Figure 5.4.24 - PM2.5 concentration in the studied area at 11:00 am on the summer day.

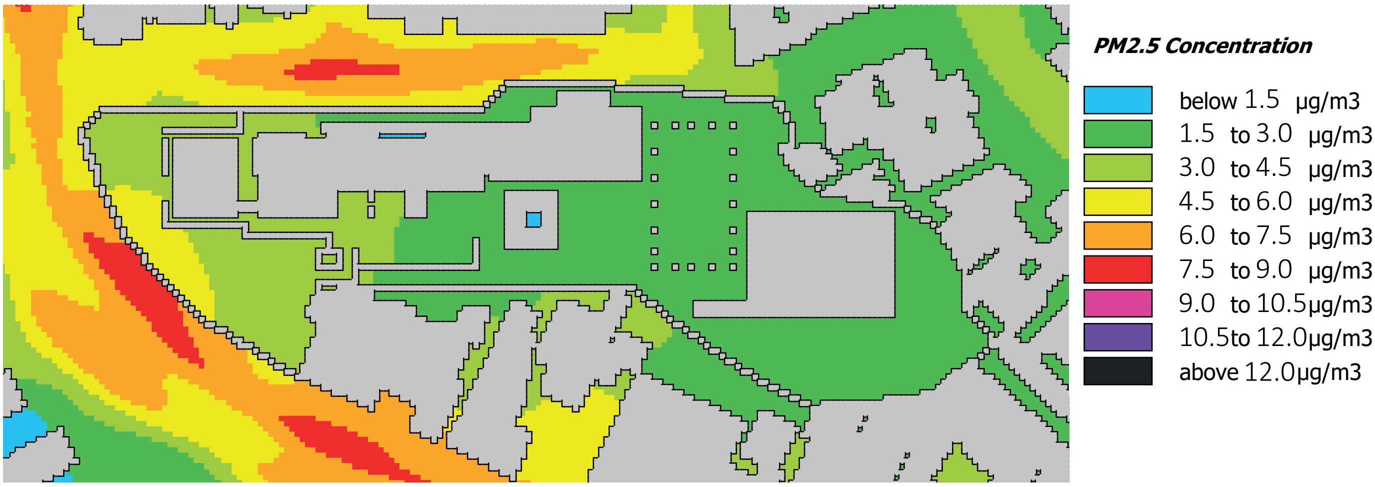

Figure 5.4.25 - PM2.5 concentration in the studied area at 04:00 pm on the summer day.

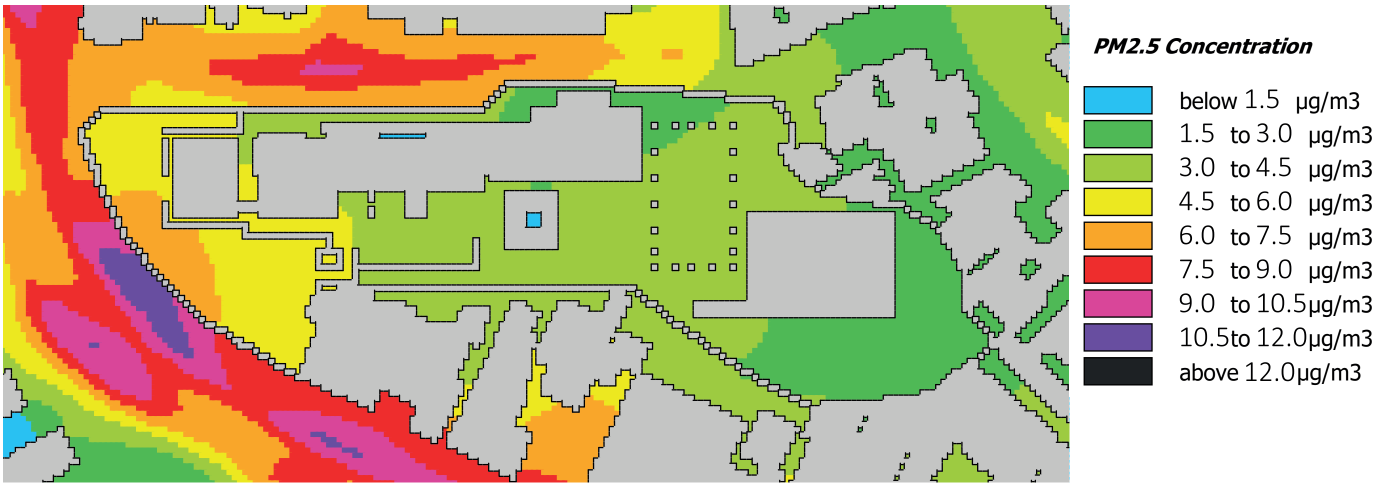

Figure 5.4.26 - PM2.5 concentration in the studied area at 06:00 pm on the summer day.

5.5. CONCLUSION

This chapter analysed the EMEF Amorim Lima throughout a typical year, focusing on the environmental conditions to which the site and building are exposed. It establishes the school's performance through thermal comfort (using the UTCI index), air quality (represented by PM2.5 and PM10—ug/m3), solar radiation exposure (the amount of kWh/m2 that falls on the school facades), and wind movement (in m/s within site boundaries and the surrounding areas). The chapter used different analytical methods to develop the research on the school's performance. Additionally, two evaluation software methods were used: Grasshopper® and ENVI-met®. Furthermore, the analytical results first demonstrate that the facades' treatments in the primary school building are not applied to the correct facades (positions). In more detail, the cobogos placed on the southeastern facade should be on the northwest façade, which receives 40% more sun radiation. Moreover, glazed windows should be on the southeastern facades to enhance daylight indoors. The outcomes also suggest that the mentioned façade could benefit from vertical shading elements to block the direct eastern sun. However, the specifications of shading devices for each façade need to be further investigated to be adequately defined. Conclusively, solar radiation studies and fieldwork outcomes indicate that most indoor areas would benefit from architectural modifications to enhance daylight distribution and possibly allow for a solar heat gain strategy in cold periods.

The studies conducted on ENVI-met® illustrate the entire site's lack of perceived thermal comfort during the hotter periods of the day. Results also show how the ability of vegetation to increase human comfort is reduced in the mentioned periods. The discussed phenomenon mainly occurs when direct sun radiation enters the terrain, as it happens at 04 pm during the studied hour. However, the cooling and shading effects of the site`s small-scale green infrastructure components are proven moments of the day and year when DBT is not expressively high and sun angles are higher. Regarding thermal comfort, the best performance of trees compared to grass and hedges is also proven throughout the studied summer day. The outcome discussed was repeated on the colder studied day, showing that the vegetated zones were warmer than the unprotected surroundings. Generally, it is possible to affirm through the outcomes that the areas with vegetation are more stable environments, suffering less thermal variations than paved areas within the same site. The mentioned outcome demonstrates that the mentioned thermal variations are deduced in the portions of the school terrain with sky coverage (mainly caused by trees). Thus, it can be concluded that with a higher sky view factor (amount of the sky seen from the human perspective), the thermal variations (colder and warmer feelings) also increase. Additionally, the outcomes established how paved areas without shading can harm thermal comfort, mostly in summer. Finally, the importance of higher wind velocities in increasing summer comfort is also highlighted.

Furthermore, the air quality studies illustrate how the densely vegetated area had constantly higher concentrations of PM2.5 and PM10 within the school's site—indicating the capability of dense vegetation to trap pollutant particles. The results also suggest the importance of the solid boundary between the green area and the main pollutant source (Avenue Corifeu de Azevedo) in reducing pollutant concentration. Additionally, increased air movement is proven to be another essential factor for air quality enhancement, which is usually reduced in dense green areas. Outcomes also suggest the negative impact of reduced dry bulb temperatures on air quality. This section raises the question of to what extent the higher levels of pollutant particles in the green area happen due to the proximity to pollution sources or the existence of dense vegetation. The ENVI-met® simulations prove that the unprotected spaces (no vegetation or other shading) perform poorly in terms of thermal comfort. In contrast, the mentioned zones are showcasing the lowest air pollution concentrations. Finally, the study conducted in this chapter gives an insight into the performance of different vegetation elements within the specific context of a school and its architectural characteristics. Thus, the outcomes represent an original contribution to studying small-scale infrastructure in a tropical background. Additionally, this chapter's findings demonstrate the need for further analysis of the small-scale green infrastructure components within different locations regarding pollutant sources. In addition, the study should be conducted in a "generic" environment where the positive and negative impacts of each green and built component can be more clearly defined. The suggested exercise is the theme of this thesis' next chapter.

6. ENVIRONMENTAL PERFORMANCE MATRIX

THE STUDY OF ARCHITECTURAL AND SGIs COMPONENTS

6.1. INTRODUCTION

According to the Cambridge Dictionary, the word “Matrix” in algebra refers to a rectangular arrangement of numbers or symbols used for solving specific math problems. In other situations, “Matrix” can mean a collection of related factors that influence how something progresses or changes. That’s why the term “Environmental Performance Matrix” is used in this chapter. It succinctly describes the study of how architectural and green elements (“related factors”) combine to interfere with the performance of air quality and thermal conditions in the environment (“the way things develop or change”). Furthermore, this chapter comprises the central analytical framework of this doctoral research, mainly achieved in the software ENVI-met® (see Chapter 05). The study developed at this point is derived from the information gathered throughout this research’s chapters. The architectural review conducted in the “Public Schools’ Chapter” was instrumental in developing the work presented here. Additionally, the chapter’s foundation is the Case Study Fieldwork and Analytical Work materials and their acquired knowledge.

The chapter comprises the objectives and methods undertaken to achieve them. The Environmental Performance Matrix is established, presenting the studied elements and analysed scenarios. Finally, with the outcomes analysis, the chapter presents a second version of the Environmental Matrix with the most important results. The final matrix in this section allows for essential conclusions on the definition of guidelines and policies drawn in the next chapter.

6.2. OBJECTIVES

MAIN OBJECTIVES:

- Evaluate the perceived thermal comfort and air quality impacts of the combination of architectural and small-scale green infrastructure (SGI) components.

- Display in more detail the impacts of different characteristics of the SGI components concerning outdoor thermal conditions and air quality.

- Define the best combination of SGI and architecture features to enhance environmental performance outdoors.

- Suggest indoor thermal comfort and air pollution performance using the combined SGI and architectural elements.

- Inform the best location of the SGI features within the context of outdoor areas of public schools in Sao Paulo.

The EMEF Amorim Lima study established the current conditions of the outdoor and indoor areas of the school. Additionally, it evaluated how certain architectural and natural elements are responsible for the (positive and negative) thermal and air quality outcomes. However, the study could not determine the isolated impact of each SGI component towards the mentioned environmental performance indicators. Thus, considering the broad vegetation typology under tropical regions, this chapter aims to evaluate the impacts of each main component of the small-scale green infrastructures. Previous research has also identified the main design components in the Sao Paulo and EMEF Amorim Lima public schools. Hence, this exercise also seeks to study each architectural element in different morphological conditions. Finally, this exercise aims to answer questions raised during the case study's field and analytical work stages. Consequently, the objective is to separate the effects of vegetation and architectural elements to better understand their individual impacts.

The chapter also seeks to define where the combined architectural and green elements are best assigned to school projects in Sao Paulo. In addition, it establishes a list of best to worst combinations of the mentioned elements to enhance thermal comfort and air quality. Other than focusing on combinations between architecture and nature, the study aims to identify which types of greenery are the best fit to reduce air pollutant concentration while enhancing thermal comfort. Conclusively, the chapter aims to produce findings that can contribute to formulating design guidelines that will be discussed in the next chapter. These guidelines are tailored for application in public schools throughout Sao Paulo state. However, shaped by the local meteorological and morphological conditions, they can also be applied in similar environments beyond the confines of Sao Paulo.

6.3. METHOD

The environmental performance matrix evaluates the combination of different elements through an analytical method. As mentioned in the objectives, the combination will be architectural features and components that form small-scale green infrastructure on site. The first step is to identify the mentioned elements to be further analysed, which is achieved through recapitulating findings from previous chapters into this one. The findings concern the architectural characteristics of the Sao Paulo public schools and identify the most repeated building elements, which are at the interface of indoor and outdoor. This is further validated by a review of components which are present in the state and city construction manuals. Subsequently, the same evaluation is conducted for the green features. Furthermore, the method will simplify the abovementioned features into components that can be modelled considering the software's limitations.

In this chapter, ENVI-met® is also used as the evaluation tool. The Analytical Work chapter of the case study demonstrates why ENVI-met® was chosen, including examples of similar studies using it and its main equations. However, besides the outdoor studies section of the research, the soft-ware is also used within this section to evaluate indoor areas. Therefore, the software's capacity to produce insights into a building's internal thermal conditions is also explored. Although assessing the internal situation is a new feature, it has already been employed in a few pieces of research. For ex-ample, Li et al. (2021) demonstrated the internal thermal comfort results concerning various green walls with the use of ENVI-met®. Facinelli and Johansson (2021) also used the software to investigate the effect of green roofs on indoor areas in southern Brazil. Moreover, the indoor impacts of green walls and ceilings were simulated by Evola et al. (2021). The results that ENVI-met® produces con-cerning indoors are calculating the potential dry-bulb temperature (DBT) average of an entire room. Consequently, this chapter utilises the available information to indicate possible thermal comfort per-ception, similar to the method used in Chapter 04 (EMEF Amorim Lima fieldwork). It is essential to remember that indoor conditions are not the focus of this research. However, what is recorded out-side can indicate the approximate condition of the indoor environment. For example, studies have shown the relationship between outdoor and indoor spaces concerning air quality (Baek, Kim and Perry, 1997; Challoner and Gill, 2014; Hassanvand et al., 2014; Lee and Chang, 2000; Monn et al., 1997; Pekey et al., 2010; Poupard et al., 2005; Ścibor et al., 2019). Challoner and Gill (2014) found that inside naturally ventilated shops in Dublin, the PM2.5 concentrations showed no significant reduction com-pared to the immediate outdoors. Another study carried out in 179 locations in Krakow establishes that the increase, even though the daily average of PM2.5 and PM10 concentrations are higher out-doors than indoors, is statistically correlated with both (Ścibor et al., 2019). The study then concluded that the increase of PM2.5 and PM10 levels outside represents an indoor increase. Hassanvand et al. (2014) estimated that 67% of PM2.5 and 45% of PM10 concentrations in an indoor space originated from the outdoors. The study also confirmed the correlation between the out and in concentrations.

This chapter uses Climate Studio® to define which facades and architectural elements should be used for the ENVI-met® studies. Afterwards, the "Environmental Performance Matrix" is created by defining the studied elements and scenarios. How the modelling of the scenarios was achieved in ENVI-met® is presented below, including used materials and other details. Furthermore, the inputs considered for the simulations are presented, followed by a discussion of the choice of thermal comfort performance indicators. Finally, the results are discussed by comparing the scenarios within each studied hour and the studied hours themselves. Additional simulations are then conducted to answer the questions raised in the results, forming final conclusions.

6.4. THE ELEMENTS

This section defines the small green infrastructure (SGI) and architectural components that are studied in this analytical exercise.

6.4.1. ARCHITECTURAL ELEMENTS

The public schools in Sao Paulo have a set of repeated elements and materials, which are seen in several built schools in the state. The aspects are also present in a set of government documents as guidelines to be followed for new constructions, as well as seen in the case study EMEF Amorim Lima.

Figure 6.4.01 - Example of Cobogo perforated screens at Parque Sao Bento School built in 2008 in the state of Sao Paulo (© Bebete Viégas, 2011).

Figure 6.4.02 - Example of the use of prefabricated concrete structure and the use of glazed windows with metallic frames in the Elementary School built in 2003 in the state of Sao Paulo (© Nelson Kon, 2011).

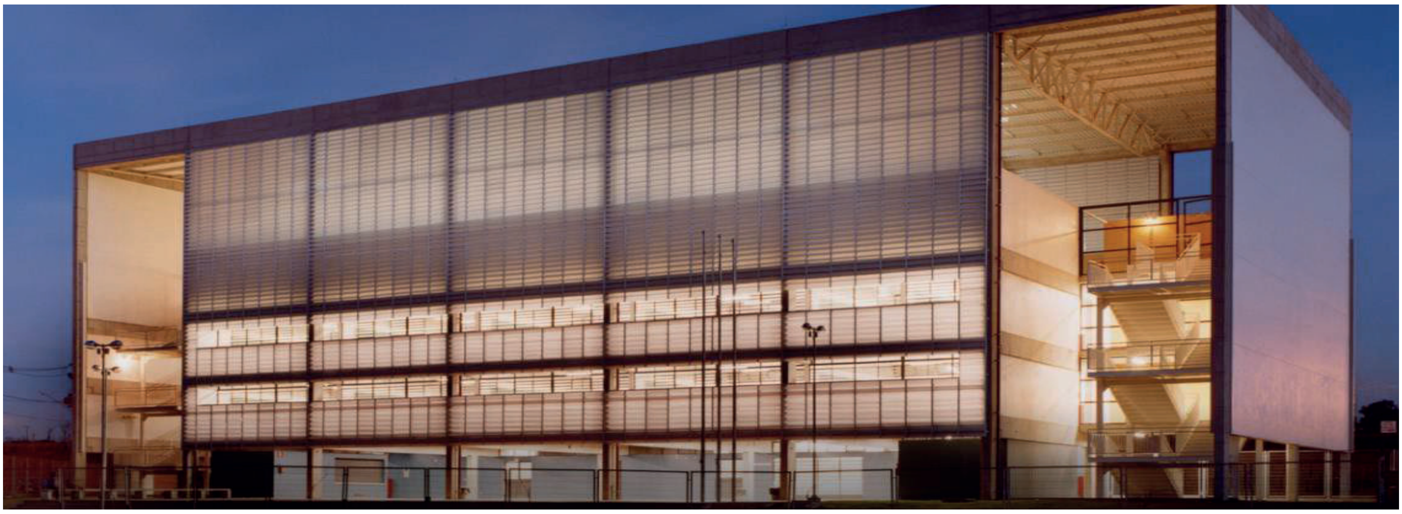

Figure 6.4.03 -A more uncommon example of façade treatment, using perforated panels in Telemaco Melges School built in 2004 in the state of Sao Paulo (© Nelson Kon, 2011).

Figure 6.4.04 - Another example of the use of concrete Cobogo panels and the pre-fabricated concrete structure in the Parque Dourado V School, built in 2007 in the state of Sao Paulo (© Oliver de Luccia, 2011)

The previous images are examples of schools in the state, illustrating the resemblance between architectural solutions. The chapter "The Public Schools" reviewed all the examples above. Moreover, when studying the buildings and technical manuals, four features are repeatedly seen: glazed windows, cobogos (perforated panels - figure 6.4.01), and horizontal and vertical fixed elements that could provide shading. The horizontal elements were commonly slab projections acting as circulation and access for other rooms (see figure 6.4.04). Moreover, the vertical built parts are usually structural and shading design solutions. The most seen façade element is the cobogo, which is commonly used in Brazil and other tropical regions. The reason for its widespread application is that it is a successful tool for allowing wind movement while reducing direct solar incidence. These characteristics are essential to provide comfortable indoor conditions in tropical climates. Therefore, most of the FDE and EDIF projects in the city and state use those elements, even on entire facades. However, as shown in the Case study's evaluation, cobogos must be installed in orientations exposed to the sun; otherwise, it will unnecessarily reduce daylight availability. Moreover, cobogos can have various designs (image 05); hence, the simulation will model and assess a simplified design.

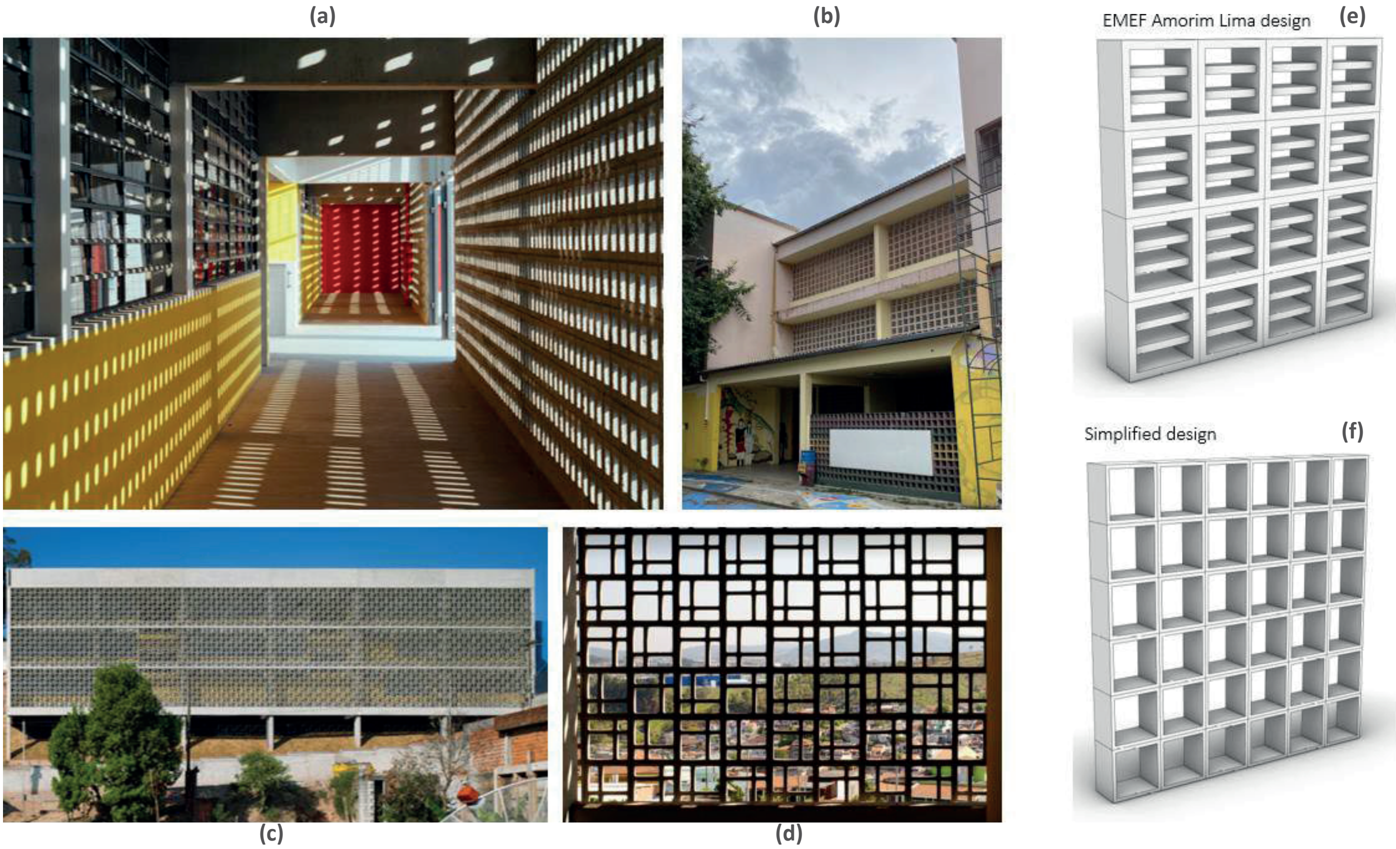

Figure 6.4.05 (a) - Example of cobogo in front of a corridor with classrooms behind, in school Parque Dourado V (© Oliver de Luccia, 2011). **(b)** - Example of cobogo in EMEF Amorim Lima (personal archive). **(c)** - Example of cobogo in Western facade of School Prof. Marcos Alexandre (© Pedro Kok, 2009). **(d)** - Construction detail of the cobogo panel in School Prof. Marcos Alexandre (© Pedro Kok, 2009). **(e)** - 3D model of EMEF Amorim Lima Cobogo. **(f)** - 3D model of the cobogo simplified design that will be further analyzed.

As expected, glazed windows are widely used in school environments. Consequently, it is another component studied in this work. The windows have similar designs within the schools used as examples above and the ones in the architecture review chapter. They generally comprise several minor openable pieces of clear glass with aluminium frames, commonly known as louvres. Additionally, the windows are usually placed from 1m of the ground to the beams. The Amorim Lima's evaluation shows that unobstructed glazed windows will have better environmental performance if installed in orientations with less direct sun radiation. Therefore, if the windows are placed on more exposed facades, they must be coupled with the other elements to cause shade, such as cobogos.

Figure 6.4.06 (a) - Example of school facade with perforated aluminium roofs as facade treatment in the School Prof. Marcos Alexandre (© Pedro Kok, 2009). **(b)** - School Parque Dourado V, showing one example of glazed windows with metallic frames placed in a recessed facade, protected by a corridor © Oliver de Luccia, 2011). **(c)** - Indoor image of a classroom in EMEF Amorim Lima, with another example of the glazed window and metallic frame (personal archive). **(d)** - 3D model of EMEF Amorim Lima Cobogo. **(e)** - 3D model of the cobogo simplified design that will be further analysed.

Furthermore, as previously mentioned, horizontal projections are constantly seen in the facades of the schools of interest. For example, EMEF Amorim Lima has simple concrete overhangs on all the facades and levels. It can be contemplated that the mentioned elements were implemented to protect the walls and apertures from rain and even from solar irradiation. Moreover, most EDIF and FDE school projects use vertical elements as classroom circulation areas, usually around 2m wide. Yet, even with no peripherical walking areas, the roofs are usually offset, creating a horizontal overhang on top of openings. Therefore, a simplified version of a horizontal overhang is studied in this chapter.

Figure 6.4.07 (a) - Example of recessed facades, treated with glazed windows, with walking corridors in front of them in Parque Dourado V (©Carlos Kipnis, 2011). **(b)** - Another example of a recessed facade with walking corridors in front of the Elementary school (©Nelson Kon, 2011). **(c)** - 3D model of the horizontal elements shown in the schools' examples. **(d)** - 3D model of the simplified design that will be further analysed.

Finally, the schools often showcase vertical elements that compose the building structure. They are mostly prefabricated columns of approximately 20 to 30cm. Sometimes, those elements are camouflaged into the building walls and are even elongated, becoming vertical fins. Some buildings also include those elements only as aesthetic compositions or even with the intention of solar protection. As a matter of fact, if designed correctly, those elements could successfully function as shades to protect glazed facades from direct sun radiation. Furthermore, they increase the surface area of exposed concrete on the facades, possibly generating thermal impacts outdoors. Like all the other architectural features, a simplified version of the vertical overhang is modelled to be analysed.

(a)

(c)

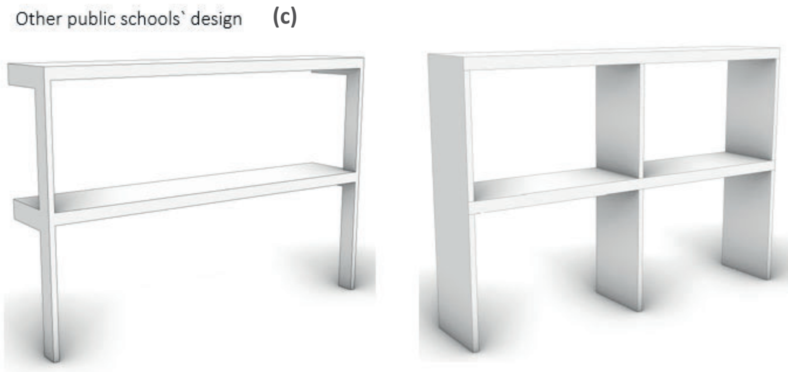

(b)

(d)

Figure 6.4.08 (a) - Example of recessed facades, treated with glazed windows, with walking corridors in front of them in EMEF Maria Aparecida Magnanelli Fernandes (©photoarantes,2012). **(b)** - Another example of a recessed facade with walking corridors in front of the Elementary school (©Nelson Kon, 2011). **(c)** - 3D models of the horizontal elements shown in the schools' examples. **(d)** - 3D model of the simplified design that will be further analysed.

6.4.2. SGI COMPONENTS

The city green areas of Sao Paulo and smaller towns of the state encompass numerous species of trees and other vegetation typologies. The EMEF Amorim Lima is one example of how diverse the small-scale infrastructure can be, even within a school's terrain. The case study showcases different tree species with various heights and leaf area densities (LADs). Additionally, various types of hedges, shrubs and climbing plants forming different living walls are spotted in the school's terrain. As mentioned in "The Public Schools in Sao Paulo" chapter, the Foundation for Education Devel-

(a) (b) (c)

(d) (e)

Figure 6.4.09 - Images of examples of typologies of green elements found in EMEF Amorim Lima (personal archive). **(a)** - Tall trees in the Cora Coralina Park. **(b)** - Trees in front of Amorim Lima's main facade. **(c)** - Hedges close to a facade with a Cobogo panel. **(d)** - Living wall is in front of the school's boundary wall. **(e)** – Living wall growing on the metallic mesh surrounding the uncovered sports court.

opment (FDE) of Sao Paulo has created several manuals for public schools. The cited documents concern the materials, furniture, architectural program guidelines, and all the necessary information for developing a project. Additionally, the FDE produced a catalogue of vegetated species that should be used within the school terrain including species at risk of extinction (FDE, 2015). The mentioned manual presents around seventy species of trees containing ornamental, fruitful and palms. Additionally, there are thirty types of hedges, three climbing plants, twenty-five forage plants and three grass species (FDE, 2015). Each vegetation element in the catalogue has its own page with technical information, dimensions and how it should be applied (as seen in figure 6.4.10). However, there is no information on the presented species' LAD (leaf-area density) or LAI (leaf-area index).

The EMEF Amorim Lima study and the FDE catalogue (2015) are examples of SGI components that can be spotted in the state's public schools. The mentioned information was substantial enough to define trees, hedges, grass, and

Ornamentais

Pau-brasil

ESPÉCIE EM EXTINÇÃO

FICHA TÉCNICA

NOME CIENTÍFICO	*Caesalpinia echinata*
FAMÍLIA	Fabaceae
CLIMA	Tropical / Subtropical
SOLO	Solo seco
CRESCIMENTO	Moderado
CLASSIFICAÇÃO	Secundária / Semidecídua
FLOR / FLORAÇÃO	Amarela / SET-DEZ
ALTURA / DIÂMETRO	10M / 10M

APLICAÇÃO

Pode ser utilizada no paisagismo urbano e a sua aplicação em escolas pode ter caráter pedagógico. Possui tronco avermelhado com espinhos, folhagem verde escura e flores de amarelo intenso oferecendo boa sombra. Deve ser evitada em áreas de intensa circulação de crianças, como áreas de recreação devido aos espinhos.

Código de listagem: 16.03.498

Simbologia

Ø10

Flor

MONTAGEM SOBRE FOTO DE NELSON KON

E.E. ODILON LEITE FERRAZ

Catálogo de Espécies Vegetais
Especificações da Edificação Escolar

Respeite o Meio Ambiente. Imprima somente o necessário

FDE FUNDAÇÃO PARA O DESENVOLVIMENTO DA EDUCAÇÃO

97

Figure 6.4.10 - Image of an extract from one of the pages of the FDE catalogue of vegetation species (FDE, 2015).

climbing plants (living walls) as the components of interest for this research. Consequently, the mentioned elements are studied in this chapter. Moreover, concerning the simulation of trees, a single height and crown size are defined to reduce the number of studied cases and other variables. Consequently, the average height of all the tree species in the FDE vegetation catalogue (2015) is calculated. Amongst the sixty-one fruitful and ornamental trees in the catalogue, the average height is 13.4m, and the average crown diameter is 8.6m. The catalogue does not define the trees' leaf area (LAD) (as mentioned on the previous page). A proper measurement tool must be used to assess each species' leaf area density. Thus, this doctoral research doesn't have the LAD information. Regarding hedges, the average height calculated with the characteristics found in the FDE catalogue (2015) is 2.3m with a 1.6m diameter. However, the three climbing plants in the catalogue don't have any height or diameter information. Finally, from the grass examples in the catalogue, the average calculated was 0.15m.

6.4.3. ELEMENTS COMBINED

In summary, the architectural and greenery elements considered for this analytical exercise can be found on the diagram and list below. The complex characteristics and other details of the SGI components modelling ENVI-met® are discussed in the modelling section of this chapter.

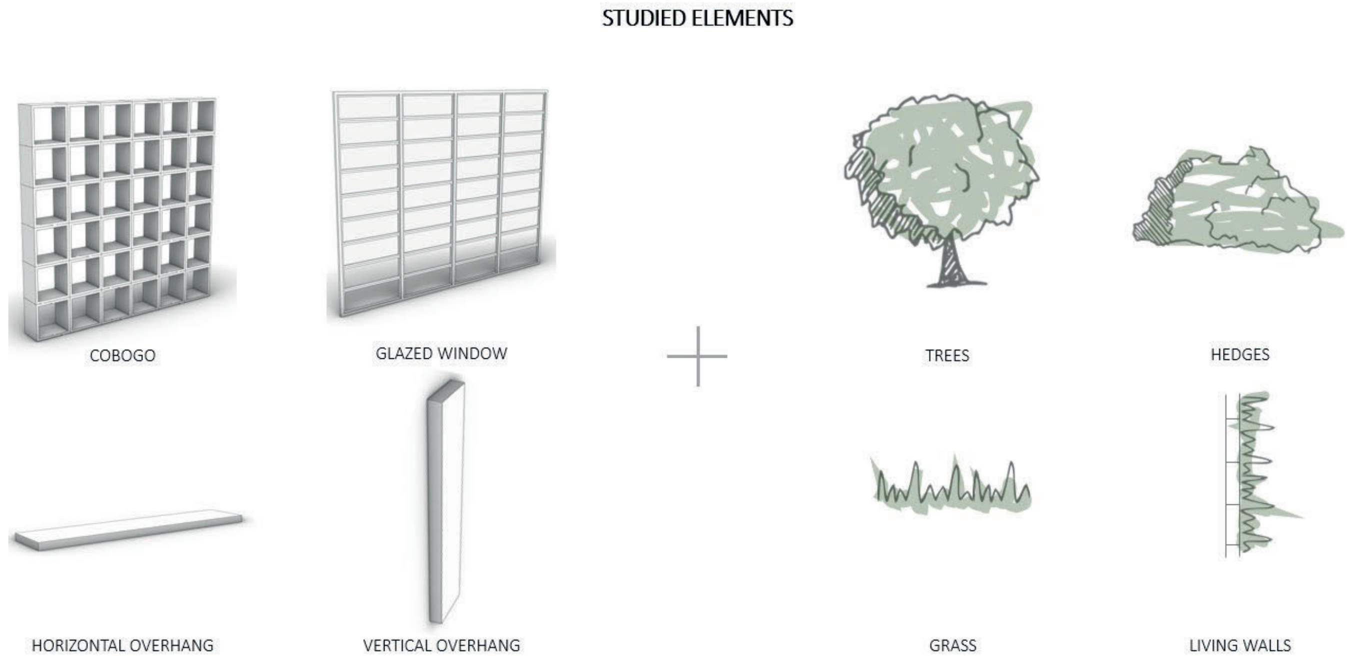

Figure 6.4.11 - Diagram demonstrating the architectural and natural features studied.

ARCHITECTURAL ELEMENTS:

1. Glazed windows;
2. Cobogos (perforated panels);
3. Horizontal overhangs;
4. Vertical overhangs.

SGI ELEMENTS:

1. Grass;
2. Hedges;
3. Living walls;
4. Trees.

6.4.4. THE STUDY OF ARCHITECTURAL ELEMENTS' LOCATIONS

As previously highlighted, the main example of architectural components found in Sao Paulo's public schools are, generally, the single-glazed windows. Additionally, the facades can have small concrete overhangs on top or overhangs working as circulation (horizontal shading). Finally, mostly the concrete cobogos. Thus, to build a generic model to be analysed in ENVI-met®, the previous architectural elements need to be considered. However, the correct location of the elements also needs to be defined through evidence-based design. The main method of this small exercise is understanding the annual amount of solar radiation that would fall on the glazed surfaces of the building modelled in ENVI-met®. A similar exercise is present in Chapter 5 (Case Study – Analytical Work) to demonstrate if the sun radiation levels could indicate internal overheating during hotter periods of the year. Furthermore, the radiation analysis uses the Climate Studio® (Solemma LLC, 2023) plug-in within the Rhinoceros® program. Climate Studio® has been used in several studies published in the past years (Falih et al., 2023; Ji and Sawyer, 2022; Surapaneni, 2021; Vazquez-Molinary and Beltran, 2022; Xiang and Matusiak, Weber, Mueller, and Reinhart, 2022; Zhao and Gou, 2023) with focus on façade solar radiation and indoor daylight.

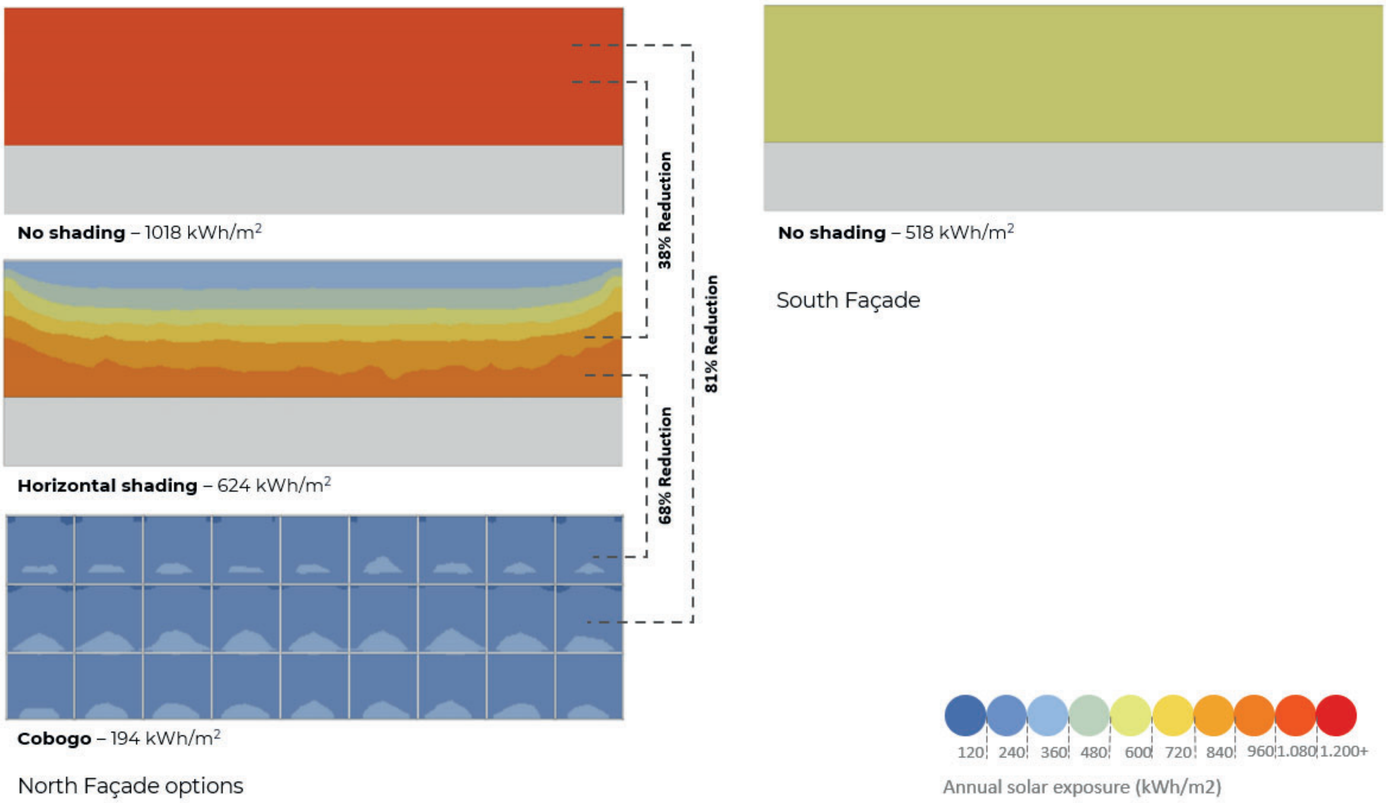

Figure 6.4.12 - Diagram with the North and South facades solar radiation with and without the use of shading elements.

A simple model is built with the same dimensions and conditions used in the ENVI-met® software, which are explained in the modelling section of this chapter (Sec. 6.6). Each façade is analysed individually, with different options of shade for each one. The south facade is the only one with no elements, as there is almost no direct sun during the year. The south-facing glazing showcases an annual average of 518 kWh/m2 and, in this analysis, serves as a guideline for the maximum acceptable solar irradiation average for the other facades to mirror. The north façade is exposed during most part of the day, showcasing a 1080 kWh/m2 irradiation annual average. The first step is to test the horizontal shading on the north façade, which shows a 38% reduction in the glazing's average annual radiation concentration (624 kWh/m2). Furthermore, the simplified cobogo element is added to the south façade where the glazed areas show an average annual irradiance of 194 kWh/m2. The outcome is an 81% reduction from the exposed façade. The results prove the cobogo is the best option for the northern facade among the studied elements.

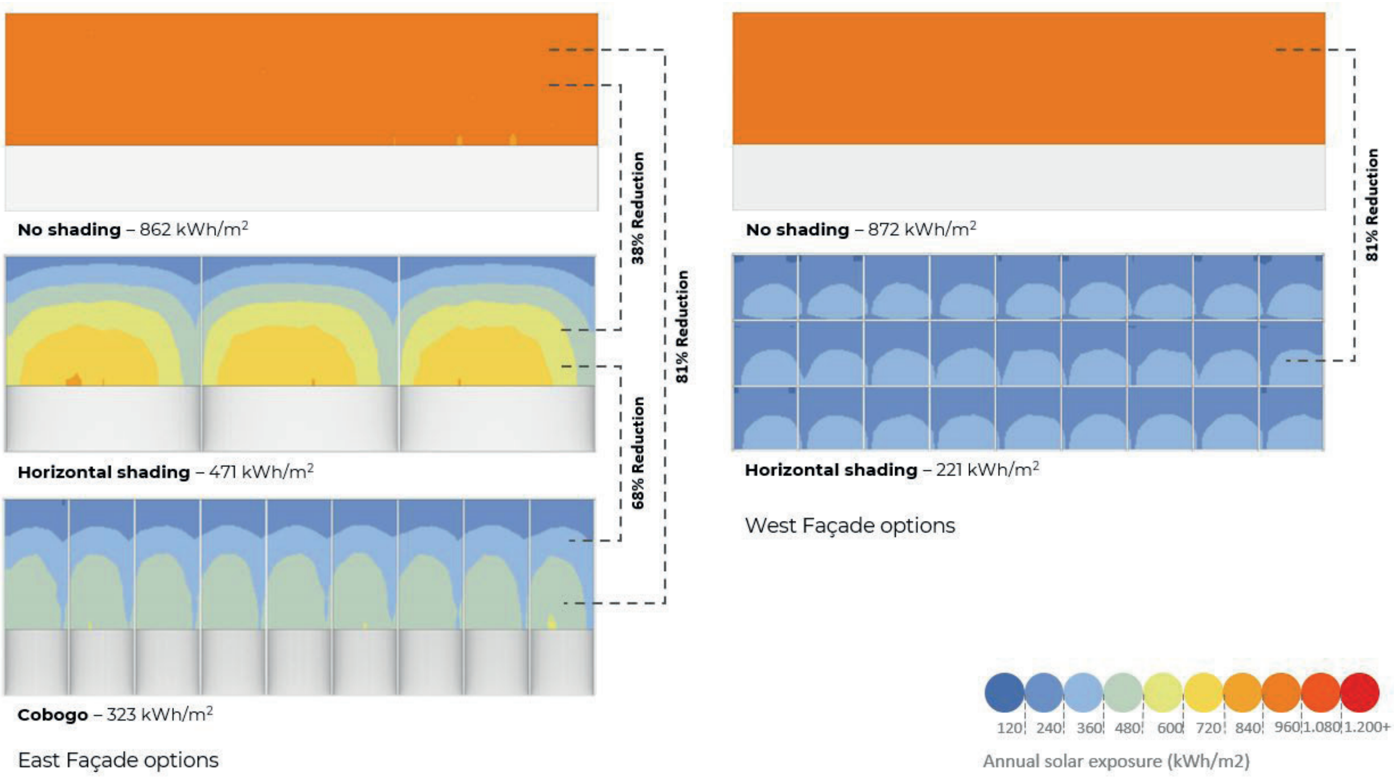

Figure 6.4.13 - Diagram with the East and West facades solar radiation with and without the use of shading elements.

The west side of the building receives direct sunlight in the afternoon, which can lead to overheating. To address this, the cobogo reduces the amount of sunlight entering the façade. The addition results in an 81% decrease in the average amount of sunlight hitting the glazed area, reducing it from 872 kWh/m2 to 221 kWh/m2. The east side of the building, which is most affected by morning sunlight, has an average of 862 kWh/m2. Vertical shading is added to block direct sun from the south. Initially, the shading elements are placed every 3 meters, reducing the sunlight by 38% to 471 kWh/m2. However, some areas still get too much sunlight (600 to 800 kWh/m2). Additional vertical shading elements are added for every meter to address the issue. The addition creates an 81% reduction compared to the exposed façade, bringing it down to 323 kWh/m2. These measures effectively reduce the direct sunlight hitting the glazing and heat entering the building, helping maintain a comfortable indoor temperature. Finally, based on the outcomes and previous research on schools in Sao Paulo, the cobogos are used in the ENVI-met® analysis for sun protection primarily on the more critical orientations. Thus, the sides that receive higher sun exposure, specifically the north and west facades. Windows without additional protection are reserved for the less exposed side, the south-facing facade. Furthermore, the east-facing facade has ten vertical shading elements, evenly spaced at one-meter intervals.

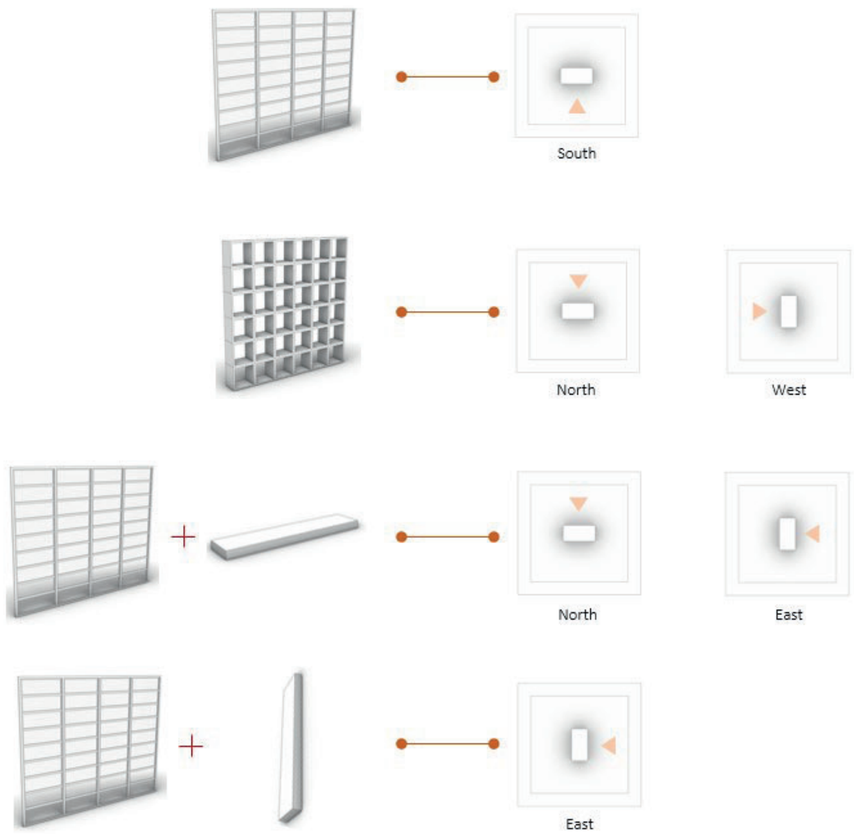

Figure 6.4.14 - A diagram showcasing each architectural feature's different orientations will be studied.

6.5. THE ENVIRONMENTAL PERFORMANCE MATRIX

As introduced at the beginning of this chapter, the “Matrix” represents a compilation of interconnected factors that collectively influence environmental developments or changes. So far, the architectural and SGI factors have been displayed. How these elements are combined and studied in this chapter composes the “Environmental Performance Matrix,” illustrated on the next page. This version of the matrix is dedicated to the scenarios studied in this analytical research. It comprises five different interactions, with two main sets of exercises, concluding a set of ten different simulations. The columns show the scenarios, while the rows show the architectural and SGI components and their location within the building and site modelled in ENVI-met®. The first set of exercises has windows facing north and south (NS). Additionally, the same five combinations are also analysed with windows facing east and west (EW). The architectural and SGI components remain the same in both NS and EW cases. However, for the cases with windows facing east-west, the vertical shading is added to the east façade (as previously discussed). Also, in the EW scenarios, the boundary walls in the terrains’ limits were not added. The decision is made to understand the impact of the boundary walls. Furthermore, the difference between the studied scenarios is the types of vegetation. The first case (NS01 and EW01) is the base case scenario, with no vegetation, and this scenario has only hard pavement. The second case has the addition of grass (NS02 and EW02). All the studied scenarios after the mentioned ones have grass. The third set of interactions has the addition of grass and living walls (NS03 and EW03). The fourth pair of scenarios combine built elements with grass and hedges (NS04 and EW04). Finally, the fifth scenario integrates grass and trees (NS05 and EW05).

ARCHITECTURE SCENARIOS:

1. NS – North façade with glazed window and cobogos + South façade with glazed window (with terrain's boundary walls).

2. EW – East façade with glazed window and horizontal shadings + West façade with glazed window and cobogos (without terrain's boundary walls).

GREENERY SCENARIOS

1. 01 – No vegetation

2. 02 – Grass

3. 03 – Grass + Living walls

4. 04 – Grass + Hedges

5. 05 – Grass + Trees

FINAL SCENARIOS (ENVIRONMENTAL MATRIX):

1. NS01 and EW01 - Architecture elements.

2. NS02 and EW02 - Architecture elements + grass.

3. NS03 and EW03 - Architecture elements + grass and living walls.

4. NS04 and EW04 - Architecture elements + grass and hedges.

5. NS05 and EW05 - Architecture elements + grass and trees.

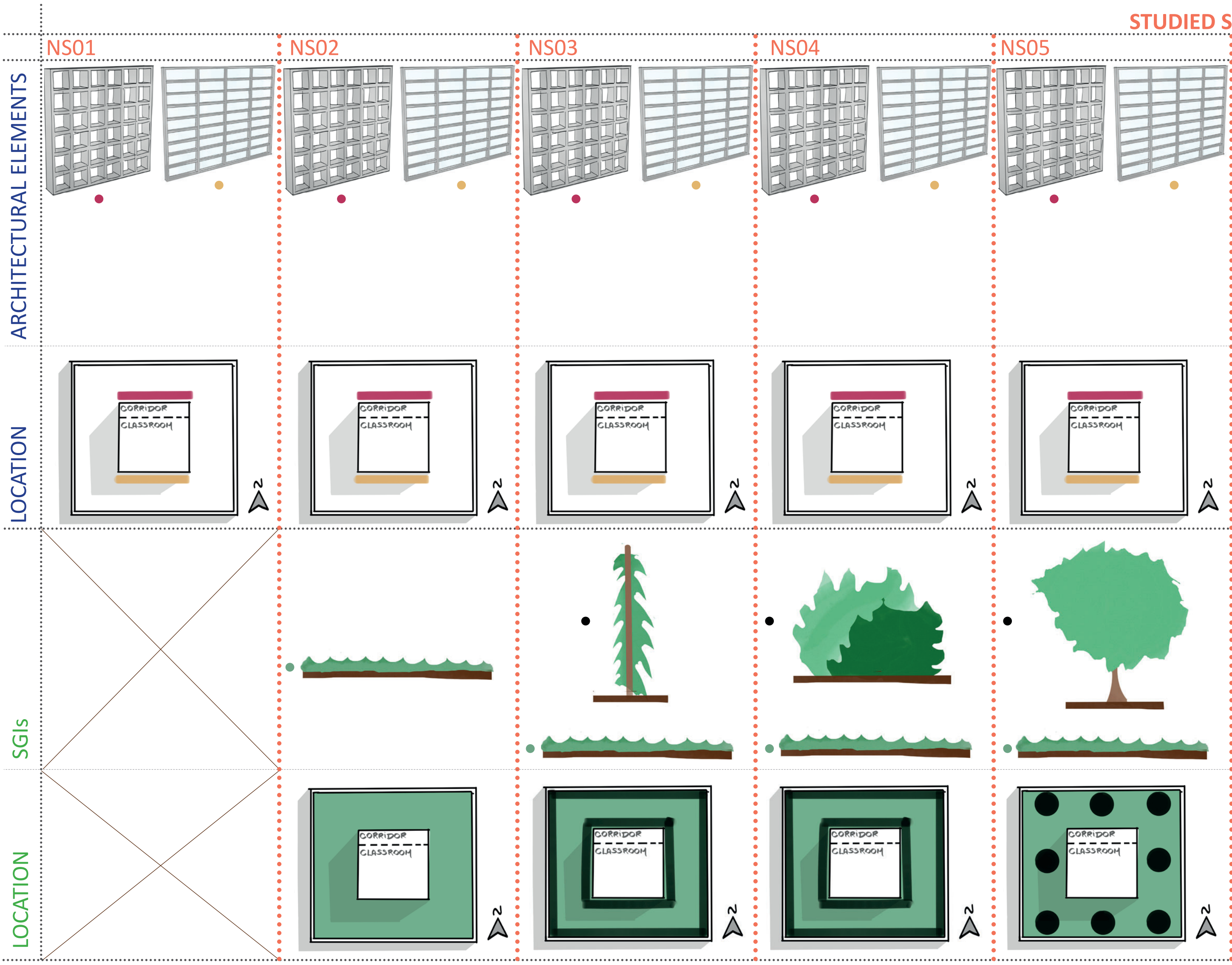

Figure 6.5.01 - Diagram of the Environmental Performance Matrix, showing all the scenarios to be simulated.

CENARIOS

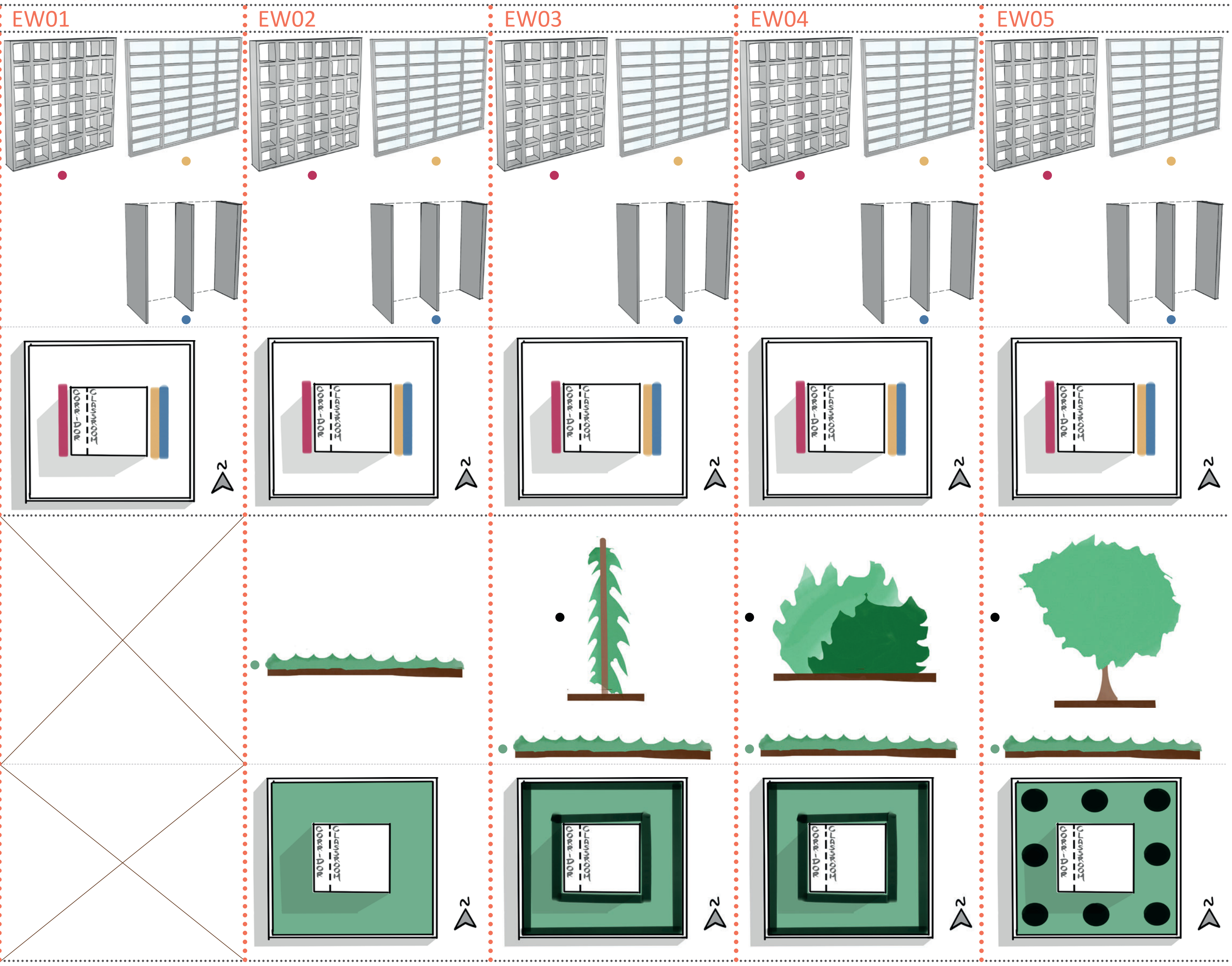

6.6. MODELING THE MATRIX

The scenarios on the Environmental Performance Matrix are all modelled in ENVI-met®. One single simplified model is designed for all simulated scenarios for comparison purposes. The choice of materials and dimensions are assumptions based on the knowledge from the "The Public Schools" and "Case Study" chapters. However, the model in Envi-met needs to be a simplified representation of the school environments in the state. For the mentioned reason, the model consists of a single-storey building with indoor space divided into one classroom and a corridor. Modelling only the ground floor has the benefit of focusing on the impacts of the elements on the ground level, where the vegetation is implemented. Also, the fieldwork in the Case Study chapter showcased the natural reduction of pollutant particles on the upper floors of the building, making the conditions on the ground floor the worst-case scenario to investigate. Finally, simplifying building models is an overall method to improve the clarity of results, reduce unnecessary complexity and reduce simulation time, which is one of this research's limitations.

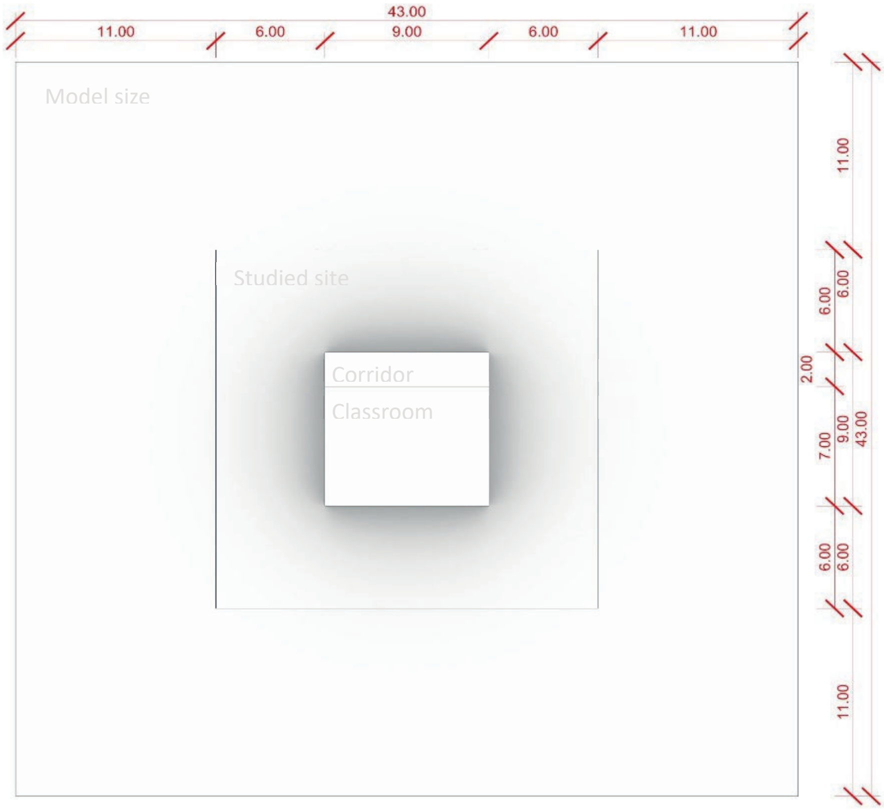

Figure 6.6.01 - Diagram of the designed model with dimension

The classroom size and building organisation are not arbitrary but are defined based on the information extracted from the FDE design and refurbishment manuals. These manuals illustrate different school project possibilities and are a cornerstone of this research. They establish the classroom area as 51.84 m2 (7.20m x 7.20m), with the window area occupying 1/10 of the floor area. Therefore, following these guidelines and the dimensions of the case study EMEF Amorim Lima, the ENVI-met model is built with a classroom of 7m x 8m, achieving an area of 56 m2 and a corridor of 2m x 8m with 16 m2. Both spaces are modelled with a 3m height from floor to ceiling, generating a final volume of 9m x 9m x 3m. The building is also modelled with a single-loaded design, where the side walls have no apertures. Finally, a 2m tall boundary is also created between the site and the surrounding area, as commonly seen in Sao Paulo's public schools. The dimensions of the outside space are defined based on examples of schools in the city and state of Sao Paulo. The indoor ground and the school's outdoor areas are calculated to establish the size of the open spaces in

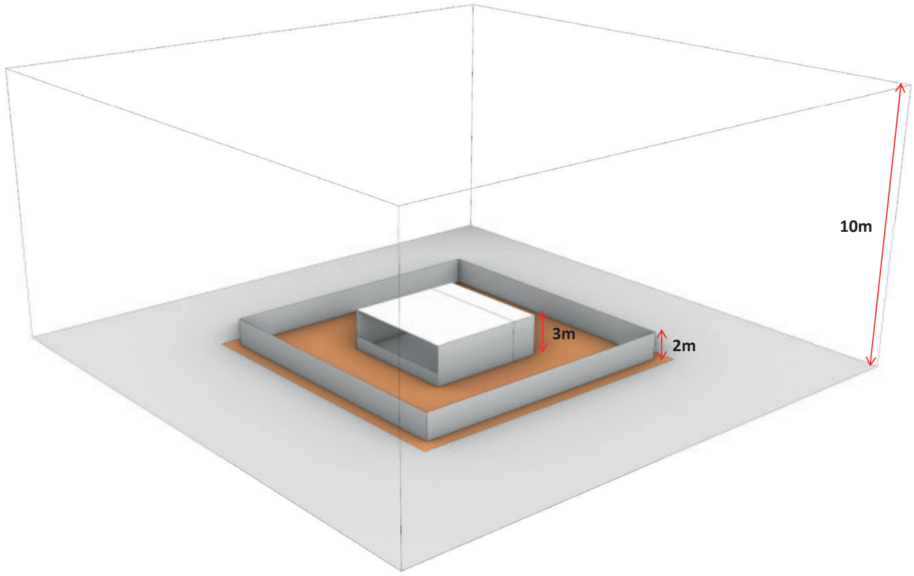

Figure 6.6.02 - 3D diagram of the designed model with heights.

percentages (figure 6.6.02). For example, Parque Sao Bento is an FDE school where, considering the entire terrain, 41% is occupied by the built-ground floor. Consequently, 59% of the terrain is a non-built area. Six schools were selected as examples, illustrating a variety of sizes to the outdoors. Within the FDE examples, there was a range of 13% to 86% of open areas compared to the terrain's entire area (figure 6.6.02). As mentioned on the previous page, the indoor area is modelled with a total of 72m2. Considering the minimum outdoor percentage (13% in School CHB Campinas), 72m2 is the remaining 87% of the terrain when applied to this exercise model. Thus, in the mentioned case, the entire terrain

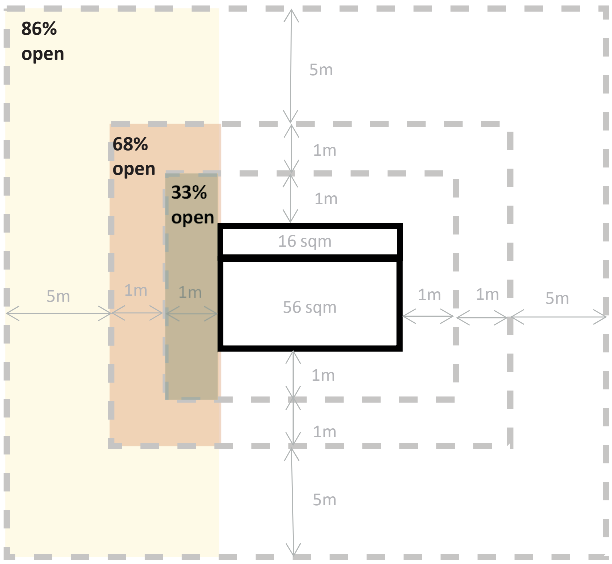

FDE SCHOOLS:

- Parque Sao Bento – 41% built / **59% open**
- CHB Campinas F1 – 87% built / **13% open**
- Telemaco Melges – 82% built / **18% open**
- Parque Dourado V – 67% built / **33% open**
- Jardim Maria Helena – 14% built / **86% open**
- Varzea Paulista – 42% built / **58% open**

Figure 6.6.02 - Diagram illustrating the possible zones and dimensions.

would have approximately 82m2 and the open area 10m2. It would mean a very small offset between the built area and the end of the terrain. The maximum outdoor percentage found was 86% in Jardim Maria Helena. In the mentioned case, 72m2 would be 14% of the terrain; the entire area would be around 514m2, and 86% would be 442m2. A larger area represents a better possibility for testing bigger SGI components, such as trees, which would create a more extensive shade. Also, the selected grid in ENVI-met is 1mx1m with 1m height, and the model is designed considering the possibility of dividing it by "zones". The first 1m grid represents the schools with open areas reaching 33%, while a 2m offset would indicate a 68% open area. A 7m offset reaches an open area of 448 m2, which was the final offset built into ENVI-met®. One meter of the 7m offset is used as the walking area surrounding the terrain (figure 6.6.02).

6.6.1. MATERIALS AND VEGETATION

The materiality of the building and site was selected within ENVI-met®'s database. However, the materials unavailable in the database were created for the simulation using the existing database as the foundation. Hence, the ground floors within the site are built as light grey cement pavement. Surrounding the boundary walls is a 1m grid set as light grey cement representing the walkways around schools. The asphalt material is applied just after the "walkways", representing the surrounding roads. The buildings and boundary walls are modelled as a combination of the most commonly used in Brazil, regular red bricks with cement plaster. The white colour is used for all built elements. The roof structure is also designed as a combination of a solid concrete slab and metallic roof tiles. The modelled element

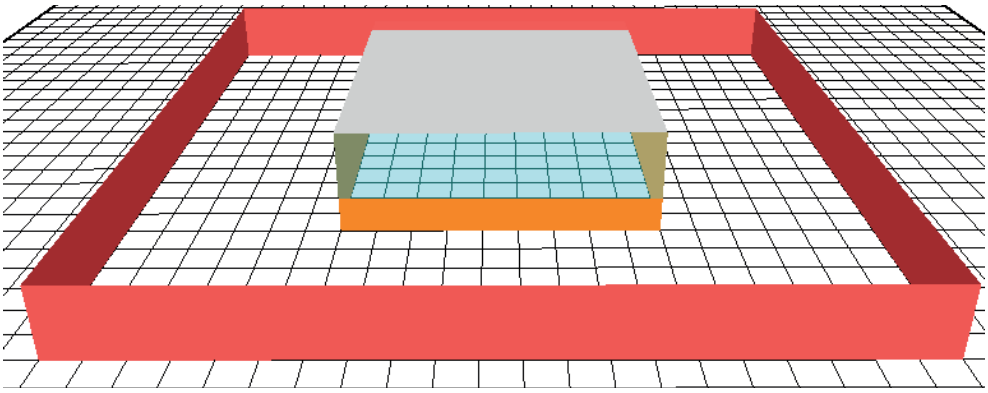

Figure 6.6.03 - ENVI-met modelling software showing the simplified version of the façade with simple, unobstructed glazing.

represents the galvanised roofs, which are widely used in the school buildings in Sao Paulo. Moreover, the window selected from the database consists of a sheet of single glass with no frame. The windows in the schools are usually framed with aluminium; however, to simplify the modelling, the elements are also simplified. Additionally, it has a 2m

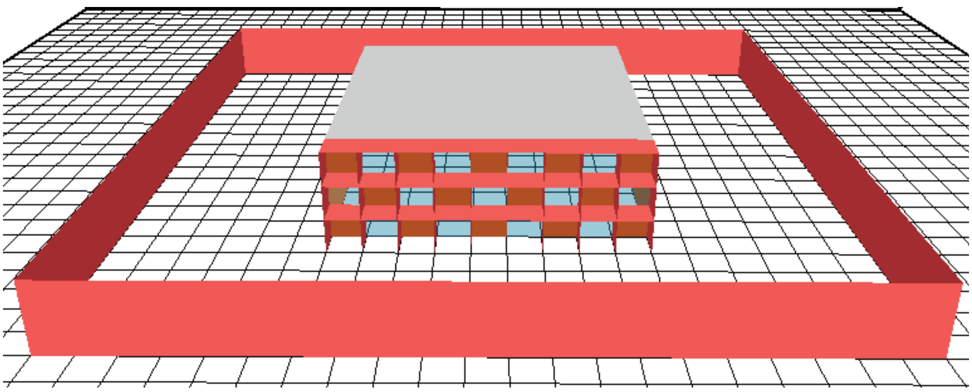

Figure 6.6.04 - ENVI-met modelling software showing the simplified version of the cobogo.

height starting at 1m off the ground (figure 6.6.03).

The cobogos are designed with the same material as the walls. However, considering the ENVI-met® modelling restrictions, the element is simplified. The cement cobogos spotted in different public schools usually have around 10cm openings with 10cm depth. However, for this analysis, the elements are approximated to 1m opening and 1m depth. Also, the cobogo has solid 1m2 panels and glazed 1m2 areas, as seen below. As section 6.4.4 of this chapter mentions,

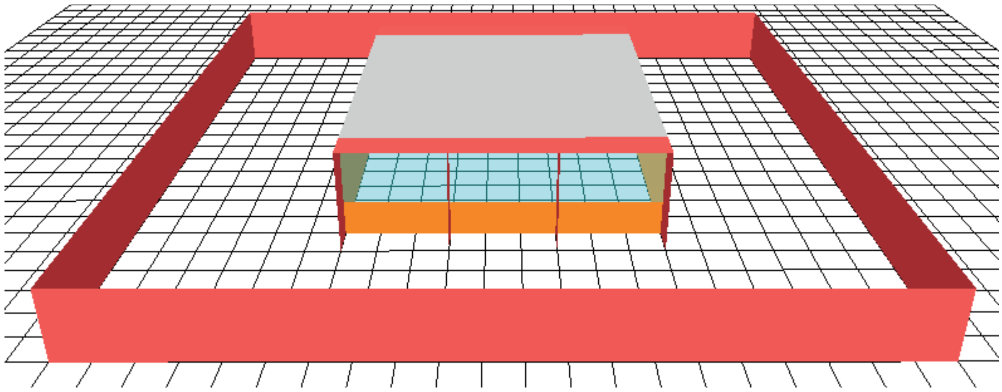

Figure 6.6.05 - ENVI-met modelling software showing the simplified version of the horizontal and vertical shadings.

horizontal and vertical shading is designed at 1m. Also, on the east façade, there is one horizontal overhang on the building's top and ten vertical shades. All elements are modelled using the same material for the walls: brick, cement plaster, and white paint (image 6.6.05).

The SGI components are also modelled in ENVI-met® using the existing database. The materials are stored and can be modified and constructed in the DBManager® inside the software. For example, the 25 cm-high grass was selected as a base for constructing a new one. The used grass has all the characteristics of the base one. However, the height was modified to 15cm to match the average from the FDE catalogue (2015) examples. Finally, grass is applied to the entire site area within boundary walls. As mentioned in section 6.4.2, hedges and living walls have the same characteristics and dimensions. The only difference is the height: hedges are 1m while living walls are 2m. The height choice reflects the average height of the boundary walls in Sao Paulo's public schools. Additionally, it is linked to the chosen 1m grid in ENVI-met®. The modelling choice intends to reduce variables and simplify case comparison. The database is

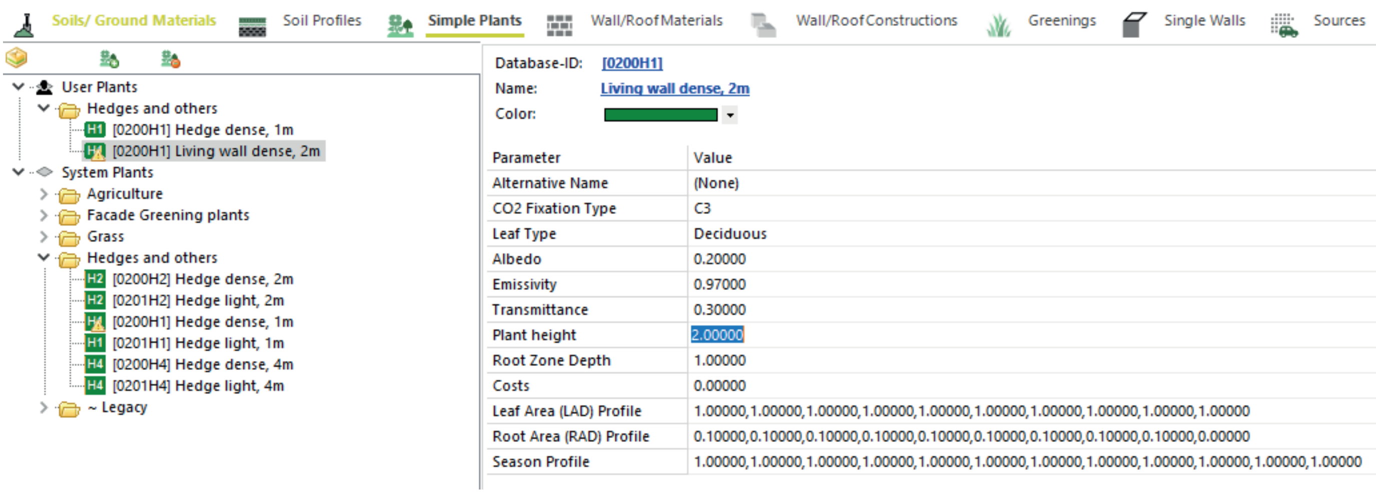

Figure 6.6.06 - Image of an extract of the ENVI-met®s DBManager® with the constructed living wall.

also used as a base to construct these elements. The component selected is a dense hedge in the DBManager® library with deciduous leaves, and the configurations were changed so that there is no loss of foliage during the year. All vegetation used in this analytical exercise has a high LAD due to the interest in exploring worst-case scenarios concerning pollutant particle trapping effects and representing the typical high-density tropical vegetation. The hedges and living walls are situated within the site next to its boundary walls and building's facades without windows. The building's walls with windows have hedges, or living walls placed one meter away from the openings (as seen in the image below). The location choice when there are apertures allows for grid space for the application of shading elements when needed. The trees are designed using complex vegetation-modelling software inside ENVI-met® called Albero®. Like the DBManager®, this tool has pre-defined trees. A 15-meter-high, spherical tree is used as the base to construct the 13-meter trees used in the simulations. The tree has the closest morphological characteristics to the FDE catalogue (2015) examples. Moreover, the crown size is adjusted to 9m, matching the average calculated from the catalogue. Also, the "tree calendar" is set not to have changes in foliage during the year. The trees are located to bring shade and populate the entire terrain. Thus, 08 trees are implemented around the site with similar dimensions, and are placed three meters from the building and three meters from the boundary walls (figure 6.6.09).

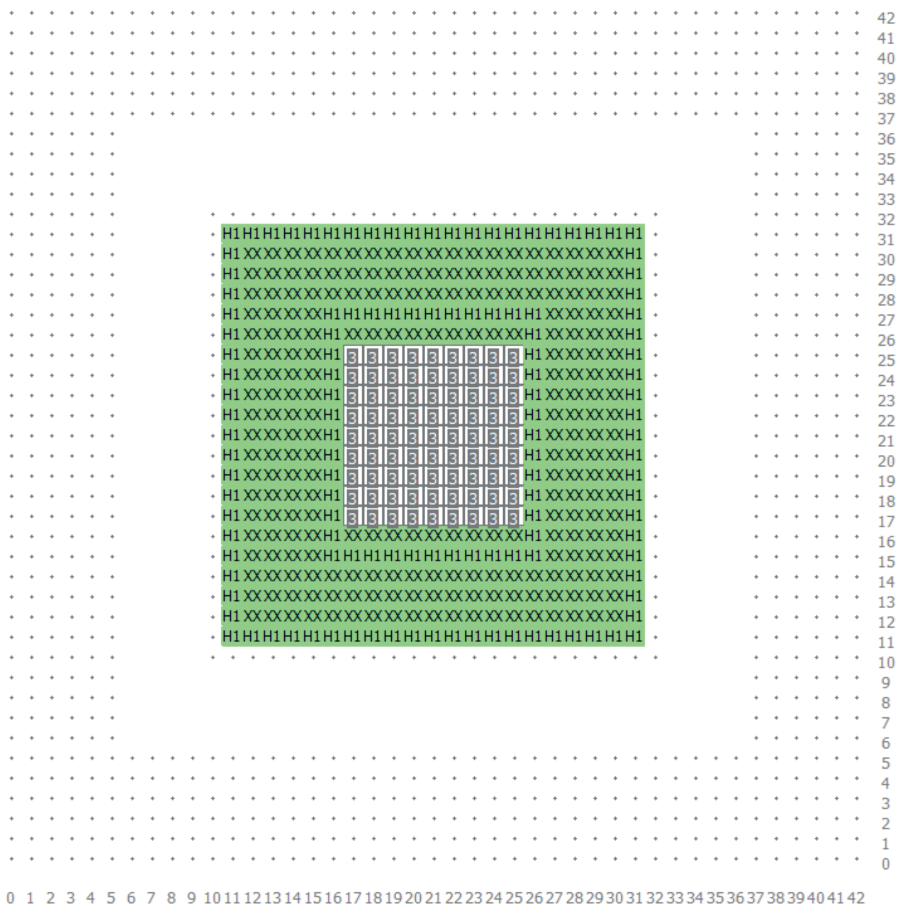

Figure 6.6.07 - Image of an extract of the ENVI-met®'s DBManager® with the constructed living wall.

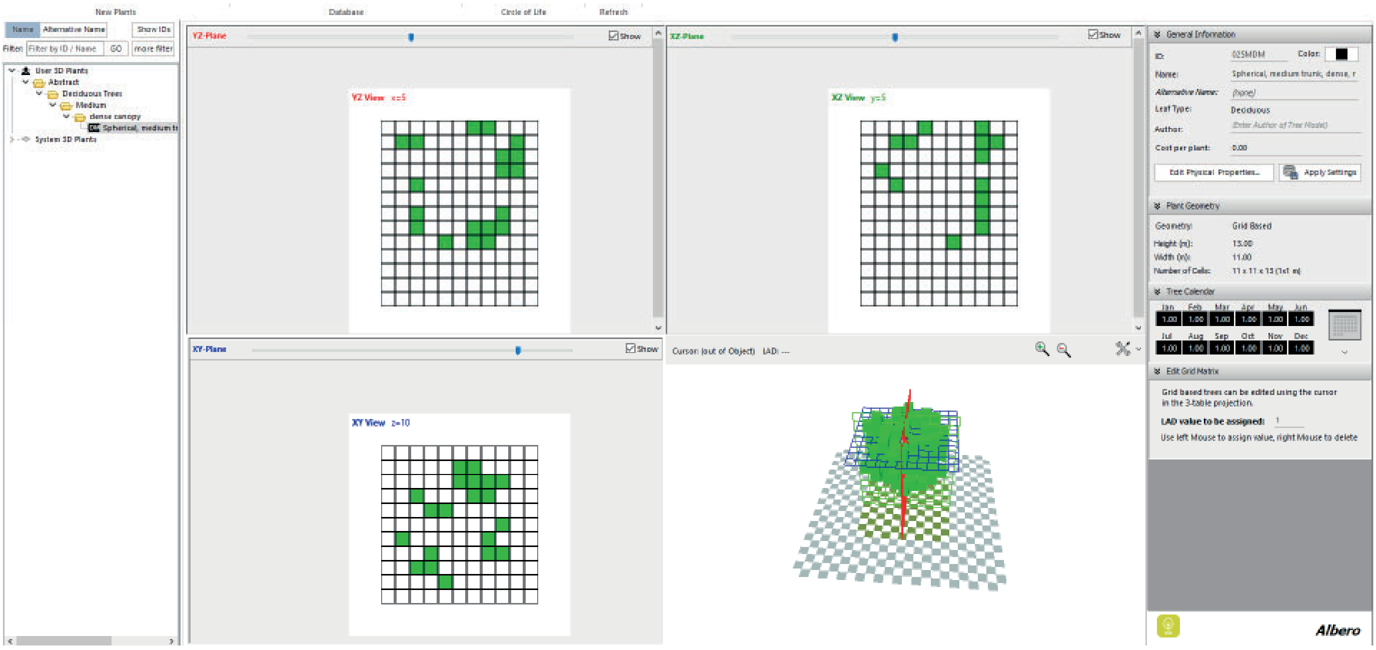

Figure 6.6.08 - Image of an extract of the ENVI-met®s Albero® with the constructed living wall.

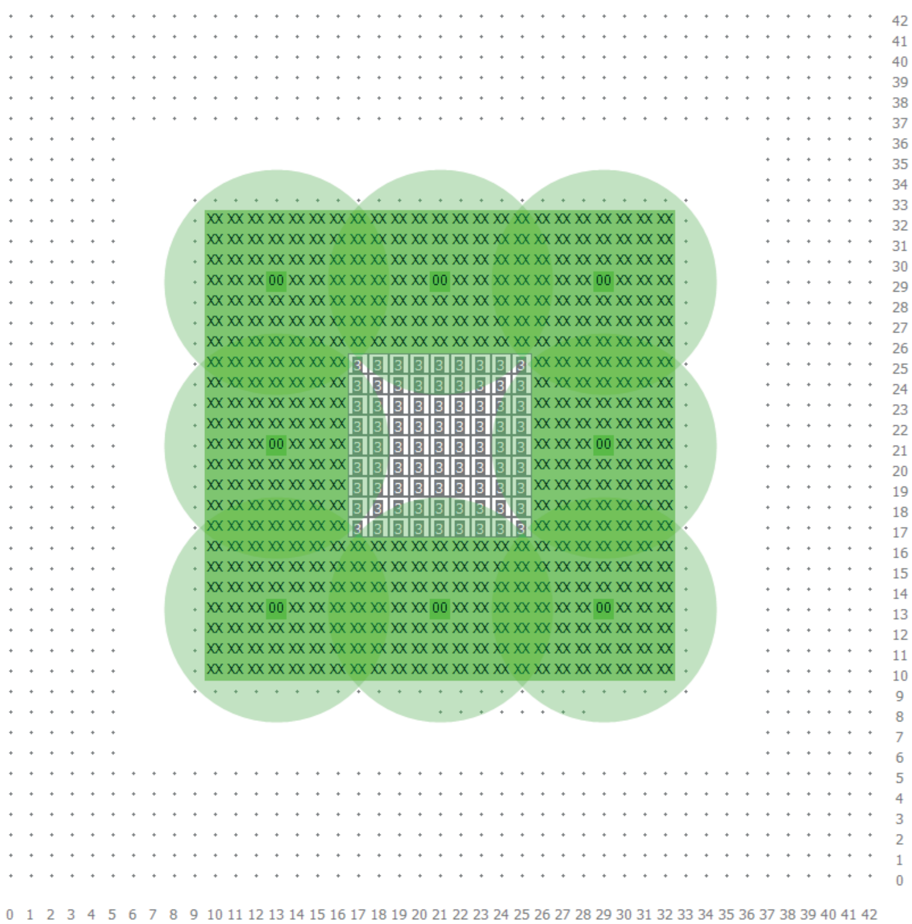

Figure 6.6.09 - Image of an extract of the ENVI-mets®'s SPACES® showing the location of the trees in one of the studied scenarios.

6.6.2. SCENARIOS

This section is dedicated to a sketch rendition of each studied scenario, focusing on vegetation elements. It is important to remember that the EW scenarios do not have boundary walls.

1. NS01 and EW01 - No vegetation applied, only light pavement.

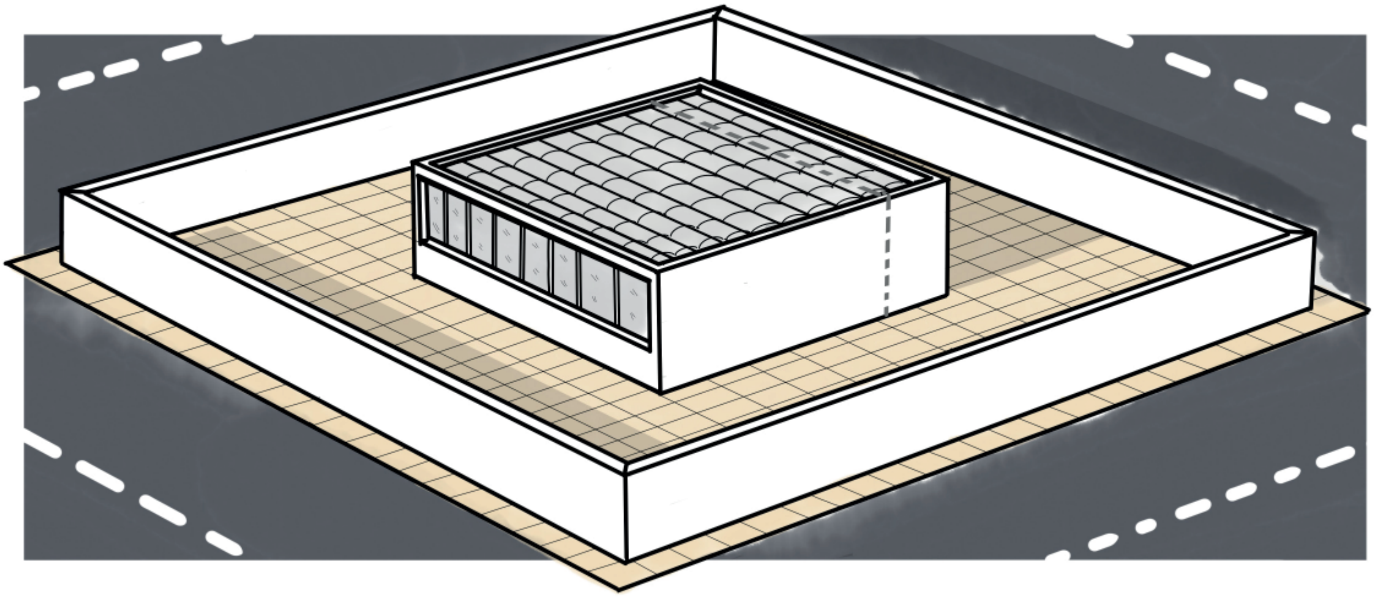

Figure 6.6.10 - Sketch of Scenario 01

2. NS02 and EW02 - Grass addition.

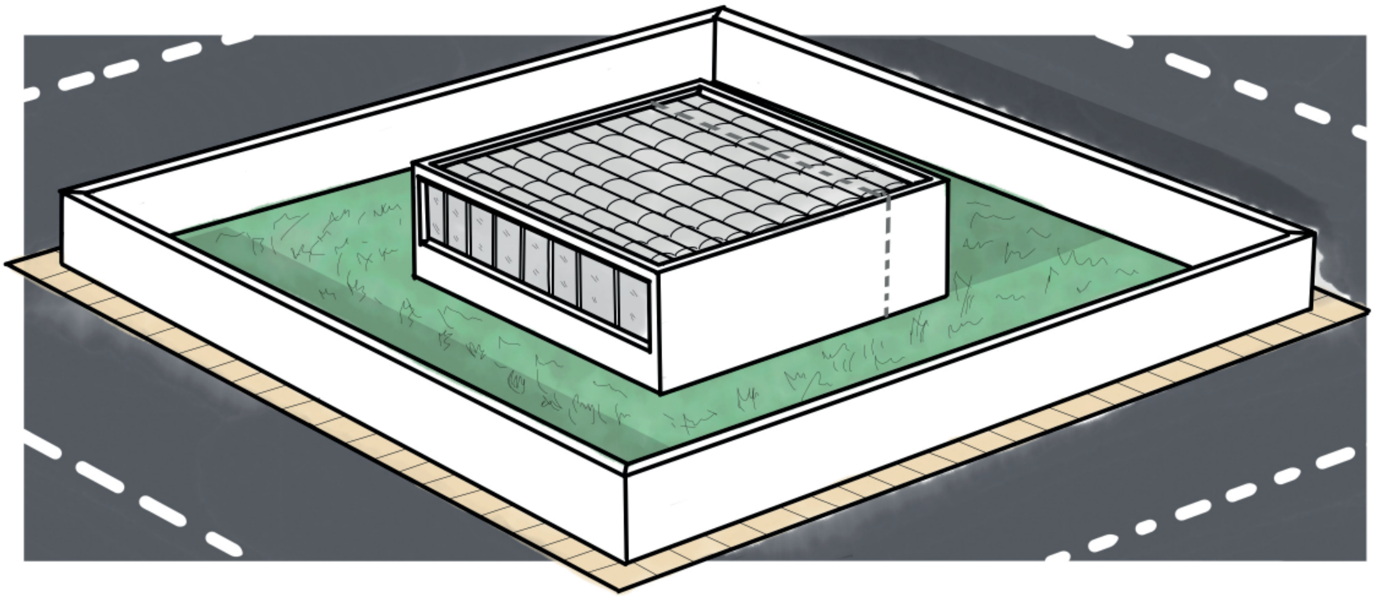

Figure 6.6.13 - Sketch of Scenario 02

3. NS03 and EW03 - Grass + Living walls.

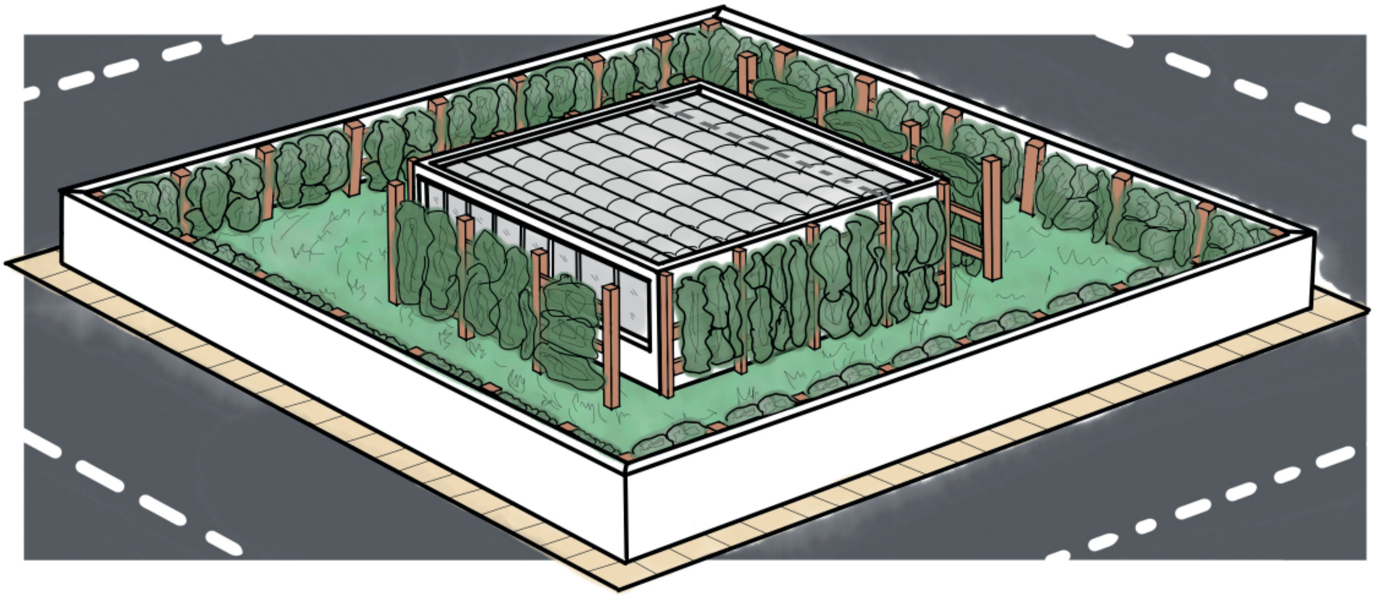

Figure Figure 6.6.12 - Sketch of Scenario 03

4. NS04 and EW04 - Grass + Hedges.

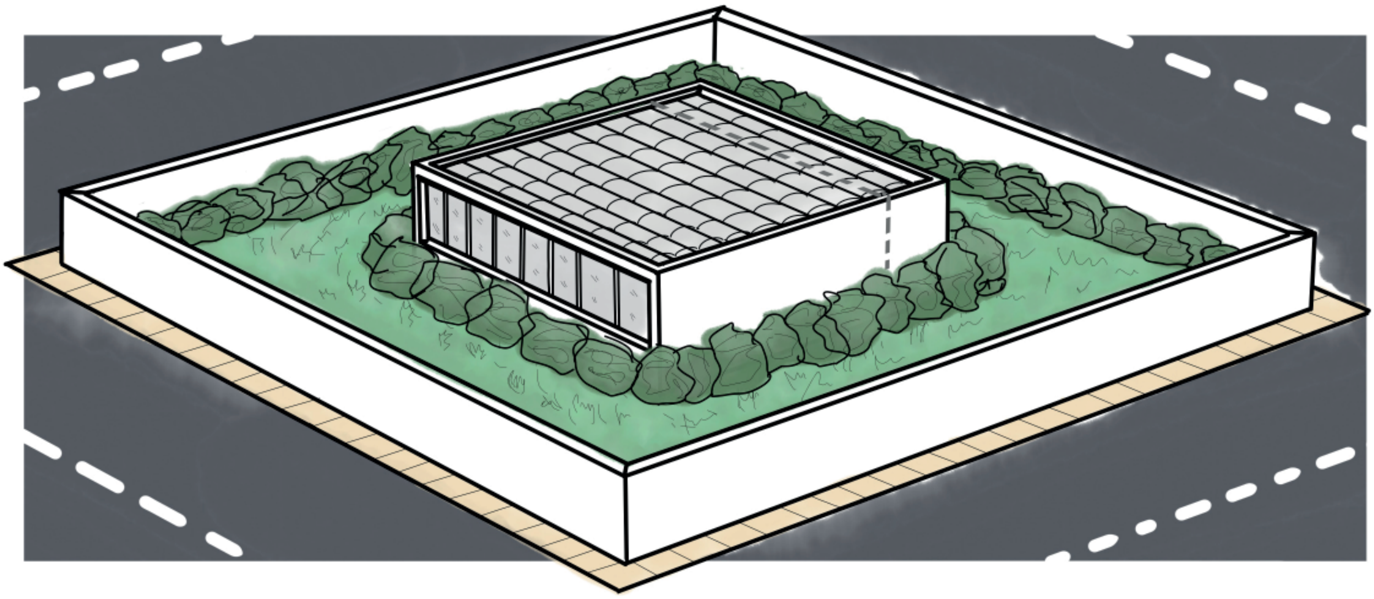

Figure 6.6.14 - Sketch of Scenario 02

5. NS05 and EW05 - Grass + Trees.

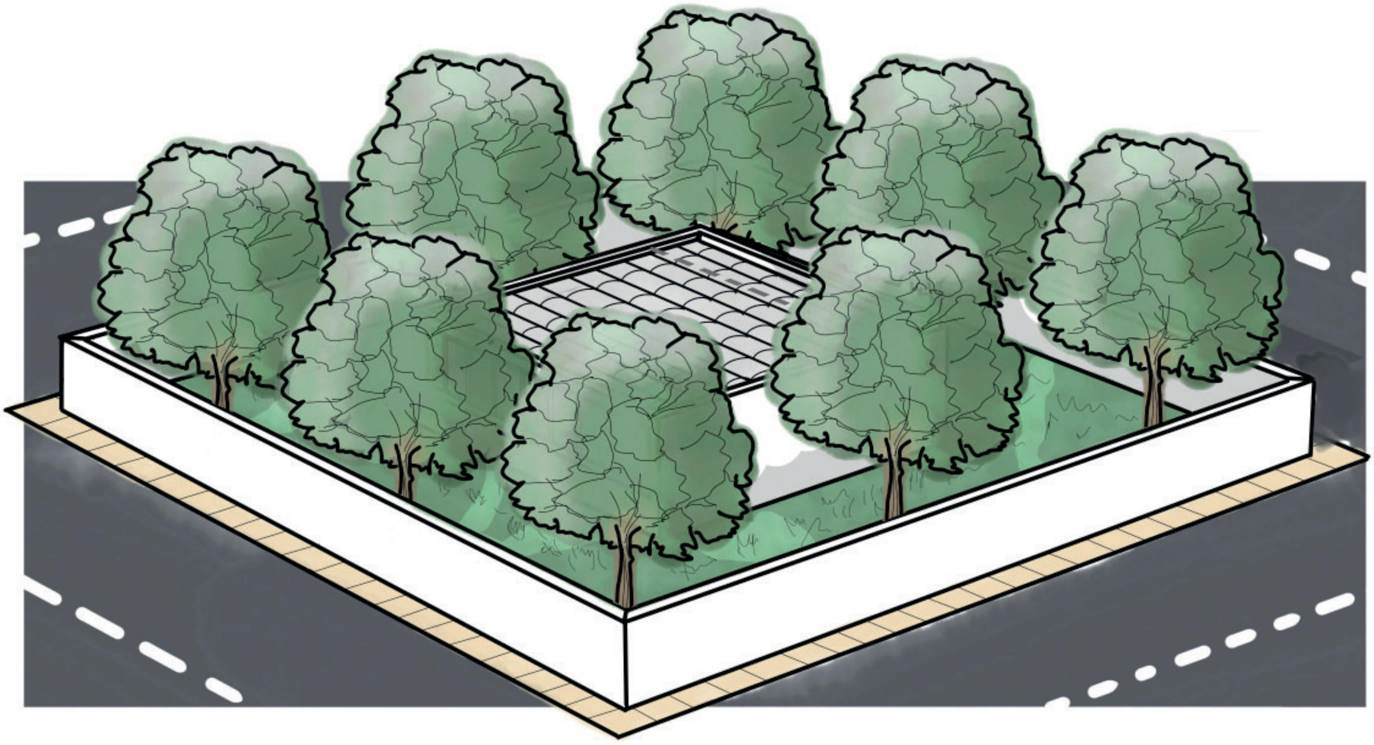

Figure 6.6.15 - Sketch of Scenario 04

6.7. ENVIRONMENTAL CONDITIONS' INPUTS

6.7.1. WEATHER CONDITIONS (DRY BULB TEMPERATURE, HUMIDITY, WIND SPEED AND SKY COVERAGE)

The weather data used for the simulations was obtained from Meteonorm®, a complex calculation and data source tool that provides access to historical weather data and future weather prediction data. Many studies established their experiments by considering weather conditions and other projections for future scenarios, specifically in 2050. Some examples are settled in the UK and Europe (Emmanuel and Loconsole, 2015; Kwon and Østergaard, 2012), having also focused on the impacts on agriculture (Hristov et al., 2020). There are also examples in Saudi (Hassan et al., 2024) and Japan focusing on CO2 emissions (Otsuki et al., 2022). In Brazil, there is also research concerning climate projections in Sao Paulo (Armani et al., 2022) and even a study of the population migration from the Northeast to the city until 2050 (Barbieri et al., 2010). Overall, using the 2050 weather file is justified by the expectation of a warmer climate and higher occurrence of thermal human distress (Armani et al., 2022).

The 2050 data is analysed so that patterns of climatic conditions can be identified and further examined. The weather data investigation spots that the day with the highest temperatures of the entire 2050 is the 11th of October. Moreover, the cited day showcases an average temperature of 26.3°C with the lowest temperature at 5 am (17.4°C) and the highest at 3 pm (34.5°C). Hence, this day is the one selected as the first to be simulated, representing the hottest conditions within 2050. Instead of studying the whole day, the method focuses on three different one-hour periods to reduce simulation time and the number of scenarios. For the selection of the mentioned periods, the main functioning hours of the schools are considered: from 7 am to 7 pm. The hours with the highest, lowest, and average temperatures are selected within the functioning period. Therefore, the first hour is 3 pm, with a dry bulb temperature of 34.5°C, clear sky with no obstructions, 6.5m/s wind speeds prevailing from the east and 53% relative humidity. The second studied period is 7 am, the coldest one, with 19.4°C air temperature, clear sky with no obstructions, 2.4 m/s wind velocities primarily from the south and 84% relative humidity. Finally, the last selected hour of the 11th of October of 2050 is 9 am, the day's average dry bulb temperature. The average hour has a 25.2°C air temperature, clear and unobstructed sky, and the prevailing direction of winds is from the east, with 2.6m/s speed and relative humidity of 83% (see figure 6.7.01).

The second select day simulated is the one with the coldest air temperatures of the year (2050). The chosen date is the 15th of July, with the higher dry bulb temperature being 17.1°C and the lowest 8°C. Moreover, the same method is used for the hour selection for the hottest day. As a result, the hottest spotted hour within the functioning hours of the day is 3 pm, with a dry bulb temperature of 17.1°C, a partially covered sky, 2.1 wind speeds primarily from the west and 57% relative humidity. On the other hand, the coldest period of the studied day is at 7 am, with an air temperature of 8°C, partially obstructed sky, 0.1 wind speeds east prevalent and 100% relative humidity of the air. Finally, at 9 am, the closest value to the average air temperature of the day is spotted: 10.5°C. The mentioned hour showcases a partially covered sky, 0.6m/s wind velocities primarily from east/southeast and relative humidity of 88%. Consequently, the six mentioned periods of one hour divided between the hottest and coldest day of the year show a large range of climatic conditions. Therefore, the above-mentioned hours are selected to represent the extreme and average conditions of the year 2050.

DAY 11 of October								
MONTH	Day of the month	Day of the year	Hours	Dry bulb temperature	Cloud cover	Wind velocity	Wind direction	Relative Humidity
OCT	11	284	1	19.5	3	5.1	268	82
			2	18.6	3	4.4	273	81
			3	18.1	2	5.3	230	83
			4	17.7	2	3.8	249	81
			5	17.4	1	2.1	175	77
			6	17.5	1	2.7	134	83
			7	19.4	0	2.4	176	84
			8	22.2	0	2.6	82	81
			9	25.2	0	2.6	106	83
			10	27.7	0	2.6	34	75
			11	30	0	3.8	61	69
			12	31.9	0	4.8	32	66
			13	33.5	0	6.2	102	59
			14	34.2	0	5.6	70	53
			15	34.5	0	6.5	107	53
			16	34.1	0	7.5	106	53
			17	33	0	7.3	48	52
			18	31.3	1	5.9	99	54
			19	29.6	1	5.6	89	57
			20	28.8	2	4.9	36	63
			21	28	2	4.6	169	66
			22	27.2	3	4.8	132	73
			23	26.3	3	4.6	134	77
			24	25.5	4	3.6	171	82

*Av. temp = 26.3C
*Av. temp from 7 am to 7 pm = 29.7C

Figure 6.7.01 - Table with the climatic condition values of the 11th of October of 2050 (hottest day)

DAY 15 of July								
MONTH	Day of the month	Day of the year	Hours	Dry bulb temperature	Cloud cover	Wind velocity	Wind direction	Relative Humidity
JULY	15	196	1	9.3	6	1	117	88
			2	9	6	0.8	124	91
			3	8.7	6	0.5	99	96
			4	8.5	5	0.4	78	97
			5	8.3	5	0.2	125	97
			6	8.1	5	0.2	81	99
			7	8	5	0.1	109	100
			8	8.9	4	0.3	114	94
			9	10.5	4	0.6	125	88
			10	11.9	7	1.1	107	76
			11	13.1	7	1	96	63
			12	14.3	6	1	154	60
			13	15.8	3	1.5	224	57
			14	16.7	0	1.1	241	57
			15	17.1	0	2.1	279	57
			16	17	0	2.1	209	61
			17	16.1	5	1.7	205	64
			18	14.7	5	1.6	202	67
			19	14.1	5	1.5	261	73
			20	13.4	5	1.3	211	77
			21	12.7	5	1.1	212	77
			22	12.1	6	1	303	79
			23	11.4	6	1	217	79
			24	10.7	6	1.5	178	85

*Av. temp = 11C
*Av. temp from 7 am to 7 pm = 13.7C

Figure 6.7.02 - Table with the climatic condition values of the 15th of July of 2050 (coldest day).

6.7.2. AIR POLLUTION (PM2.5 AND PM10)

This research places significant emphasis on air quality, particularly the dispersion of PM2.5 and PM10. Chapter 03 (The Public Schools) provides a literature review that underscores the importance of these pollutants. The chapter delves into the air quality conditions in the city, their implications, and their correlation with children's health. For the analytical research, ENVI-met® requires hourly PM2.5 and PM10 concentration input to simulate and indicate the concentration levels within the studied scheme. Unlike the dry bulb temperature inputs, the pollutant values remain constant between the hottest and coldest days and their analysed hours. Specifically, for the pollutant concentration, only one value for PM2.5 and another for PM10 will be inputs for all the scenarios examined. Establishing a single representative pollutant figure is crucial to understanding the effects of different microclimatic conditions combined with small-scale green infrastructure (SG) without the influence of too many variables.

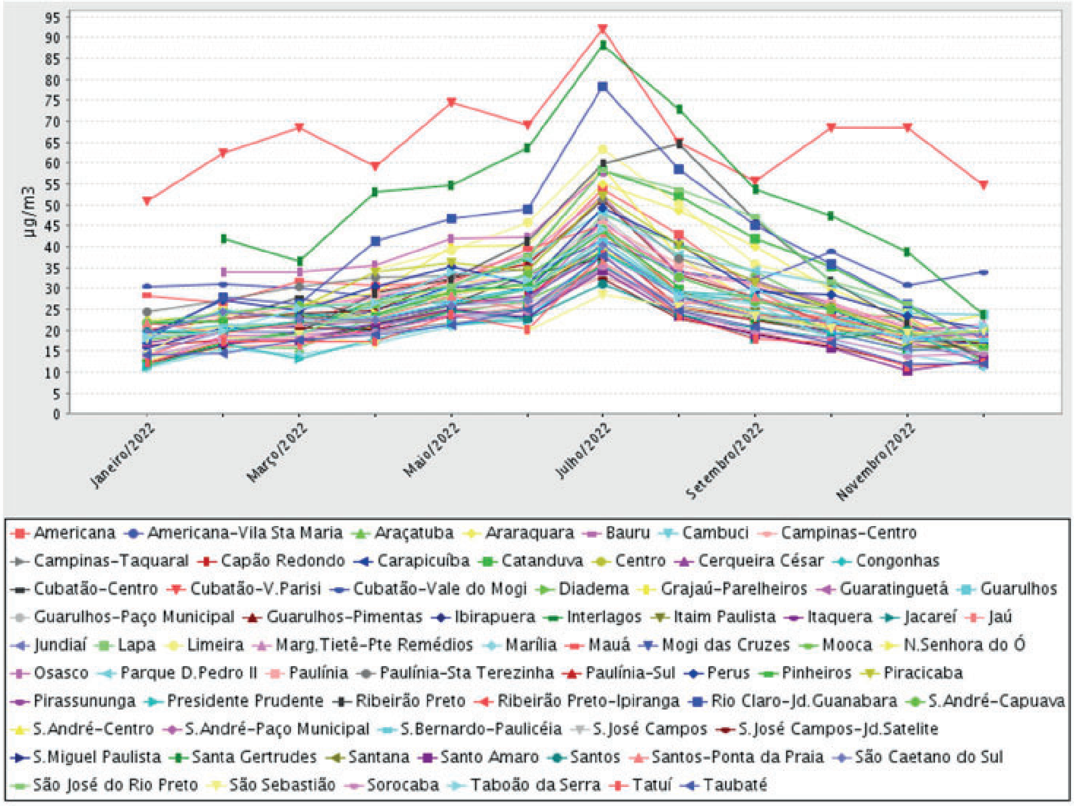

Figure 6.7.03 -Chart showing PM10 monthly average concentrations for all the stations within the State of Sao Paulo in 2022.

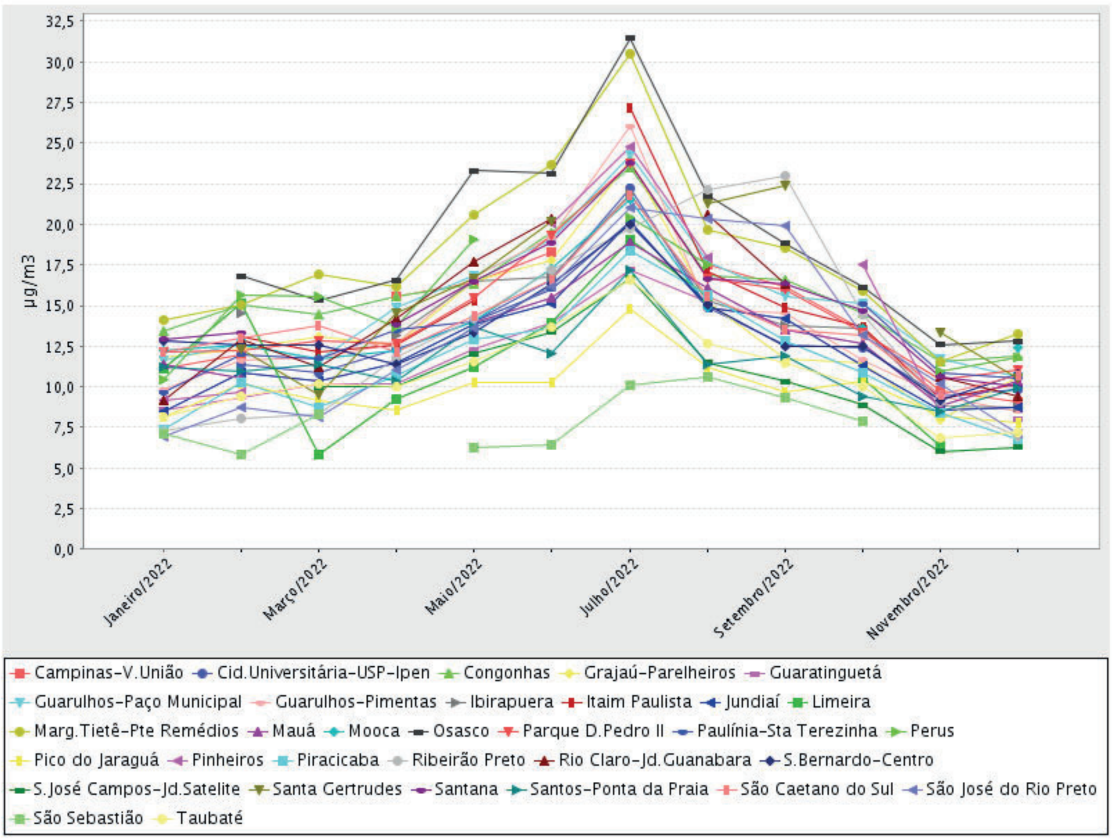

Figure 6.7.04 - Chart showing PM2.5 monthly average concentrations for all the State of Sao Paulo stations in 2022.

The concentration values inputs are determined based on the pollutant patterns within the state of Sao Paulo and the city, which were thoroughly analysed. These characteristics were studied using data extracted from the Environmental Sanitation Technology Company (CETESB). CETESB provides automatic air quality from 62 stations, with 33 stations located in the interior and coastal cities of the state (QUALAR, 2023). The other 29 stations are dedicated only to the area known as the Greater Metropolitan Area of Sao Paulo or "big Sao Paulo (Godoy and Silva, 2022). This territory includes the city of Sao Paulo and other smaller cities with shared boundaries. Furthermore, the material collected by CETESB for the year 2022, with a focus on the 62 stations previously mentioned, was analysed. Mirroring the weather inputs, the pollution intended to focus on 2050 projections. However, it is substantially difficult to define the trends considering the mutable aspect of urban environments. Also, this study aims to comprise schools all over the state of

Figure 6.7.05 - Google Earth top view identifies the air quality monitoring station "Congonhas" (Google, 2023, accessed 20 March 2023).

Figure 6.7.06 - Google Earth 3D view identifying the air quality monitoring station "Congonhas". (Google, 2023, accessed: 20 March 2023).

Sao Paulo with diverse morphological situations. Thus, the year 2022 is utilised for research inputs as it is the latest one with all the twelve months of collected data at the time this exercise was conducted. It is also important to note that in 2022, the state of Sao Paulo didn't see any vehicular transit reduction due to the COVID-19 pandemic. Finally, the focus is on the mean average data for months and hours of the year. Average values are being considered so that all the material collected by CETESB can be easily processed, allowing for a pragmatic but representative definition of only two values (PM10 and PM2.5).

The figures 6.7.03 and 6.7.04 demonstrate the monthly average concentrations of PM10 and PM2.5 in all the air quality monitoring stations in the state. The PM10 data indicates that most stations had overall similar monthly values, from 10 µg/m3 in January and December to 60 µg/m3 in July. Three other stations also showed higher levels in July, with around 80 µg/m3 to 95 µg/m3. All the mentioned stations are in cities outside the greater Sao Paulo. Regarding

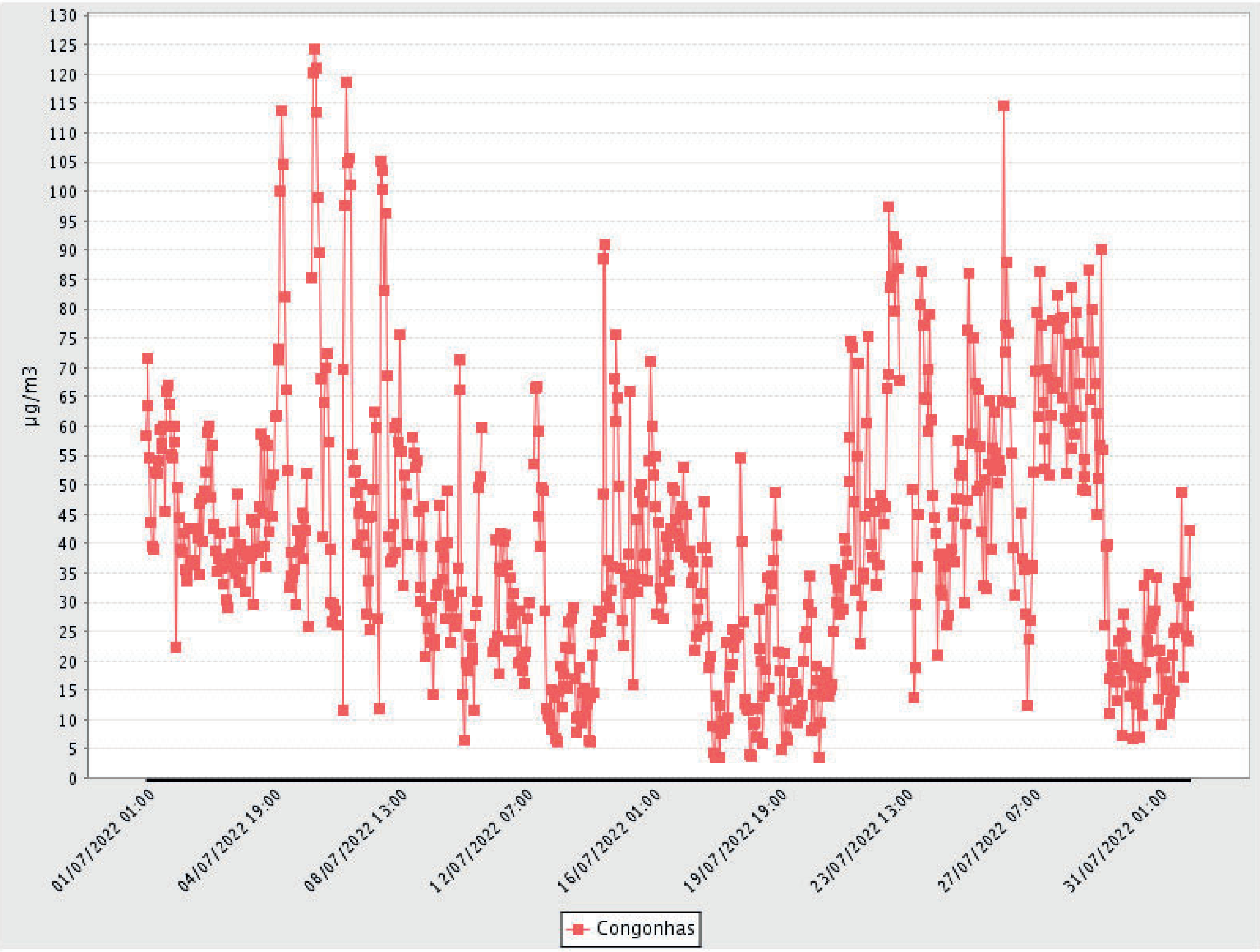

Figure 6.7.07 - Chart – PM10 hourly average concentrations for Congonhas station during July 2022.

PM2.5, the same pattern within locations can be seen, with the month of July showing once more the worst scenarios. However, the higher monthly average concentrations are from 25 µg/m3 to 31 µg/m3 and the lower values from 8 µg/ m3 to 14 µg/m3 in January and December.

In addition to the yearly analysis, the air quality monitoring station Congonhas (figures 6.7.05 and 6.7.06) is used for a monthly study of one location. The station is in the neighbourhood of Vila Congonhas, in the Campo Belo and Jabaquara districts, approximately 10.6km from the city centre. It is situated within a dynamic urban landscape, characterised by numerous structures built around local and collector streets and the prominent presence of two major arterial roads, namely the "Corredor Norte-Sul" and Bandeirantes Avenue. The latest is a high-traffic highway that runs bordering the station. Notably, the northern section of this area boasts a concentration of high-rise buildings. Conversely, the Congonhas airport is in the southeastern corner of this urban landscape and features a substantial open expanse, measuring approximately 2.2 km in length and 440m in width. This airport-induced spatial configuration cre-

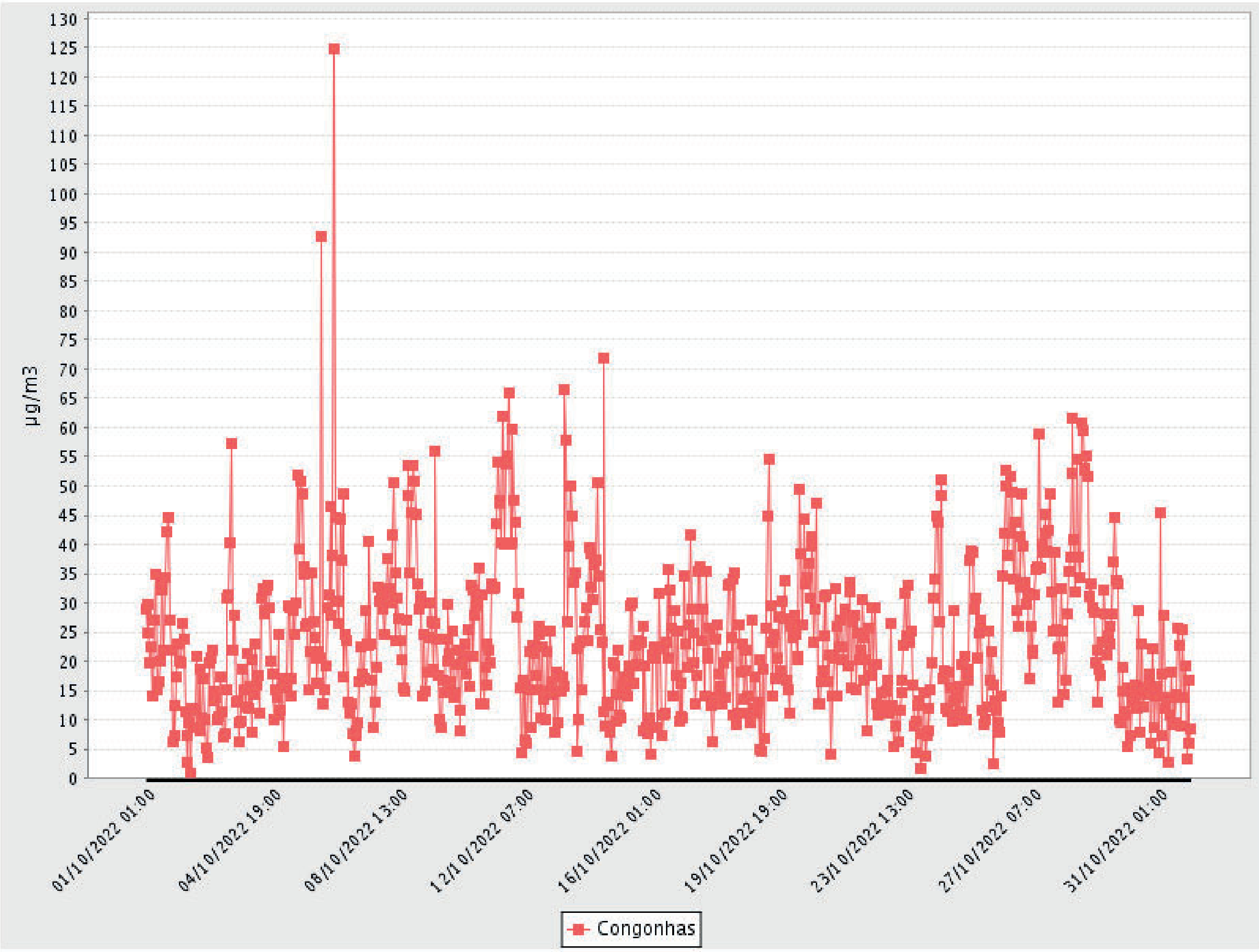

Figure 6.7.08 - Chart – P0 hourly average concentrations for Congonhas Station within the State of Sao Paulo during October 2022.

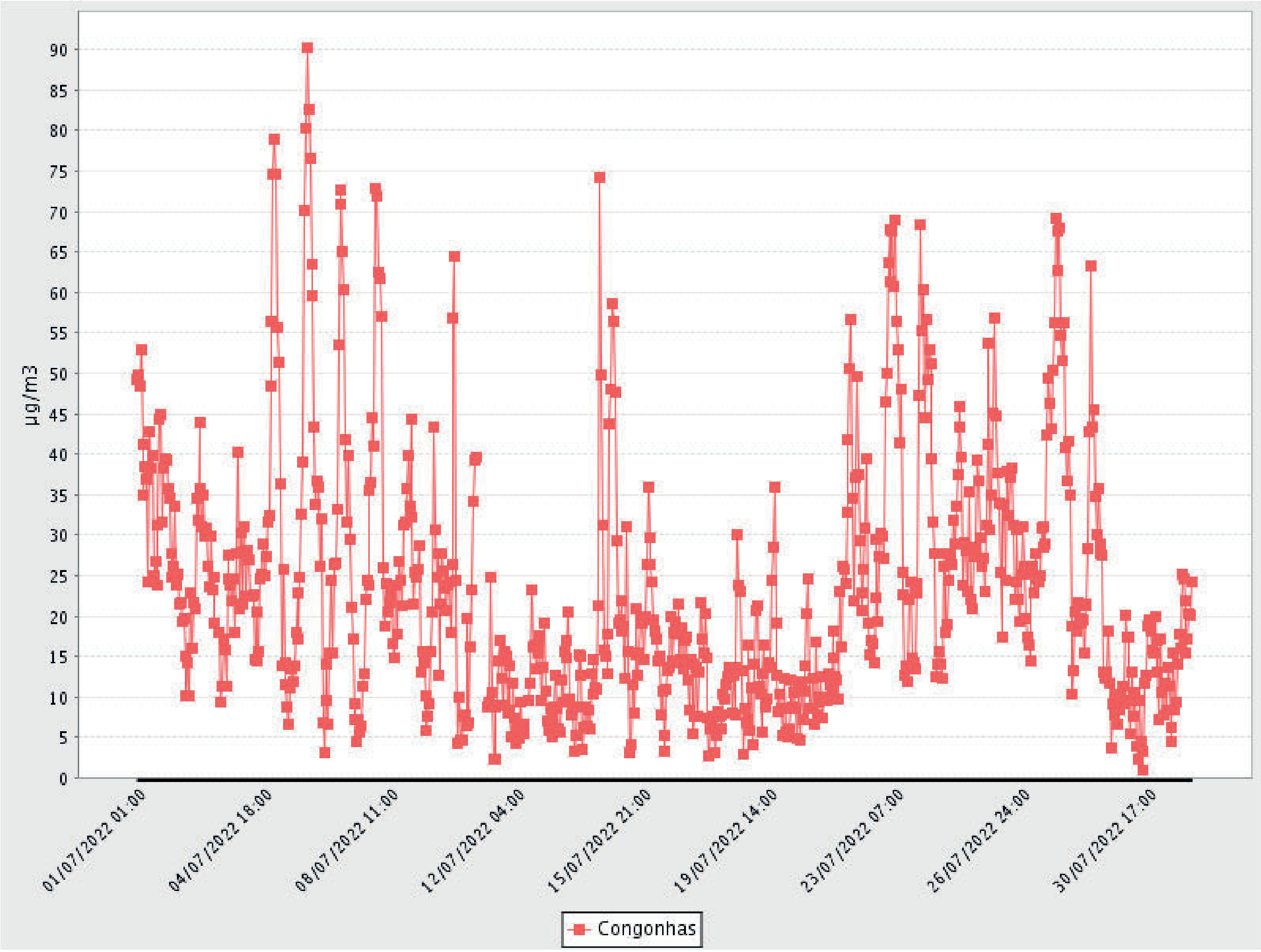

Figure 6.7.09 - Chart – PM2.5 hourly average concentrations for Congonhas station during July 2022.

ates an urban area characterised by low-rise structures. This region comprises a unique fusion of urban density, replete with vehicular activity and more spacious, tranquil segments. This intermediary urban position is used in this research to represent both the centre of Sao Paulo and smaller towns throughout the state.

As previously explained in this chapter, one day in July and another in October were selected for study. Consequently, both cited months are analysed using hourly average data extracted from Congonhas station (CETESB). In the month of July, 5% of the hours registered the highest PM10 concentrations from 85µg/m3 to 125µg/m3. Furthermore, in October 2022, the percentage dropped to 0.3%. Regarding PM2.5, in July, 14% of the hours showcased average values higher than 30µg/m3, with one hour around 93µg/m3 and one with 125µg/m3.During October, the percentage drops to 5%, with only four hours above 45µg/m3 and only one above 55µg/m3. The gathered data illustrates the overall representative particulate matter concentration within the state and city of Sao Paulo. So that the impacts of green elements on the concentration of pollution within the site are clear, higher pollution levels are input. Thus, for PM10 and PM2.5, the value considered is 100µg/m3, representing the higher values found within the studied data. However, as previously exposed, the higher values represent the slightest percentage of time concerning hourly and even monthly concentrations. Therefore, it is necessary to undergo a new batch of simulations with values that would better represent the overall air quality conditions of the state of Sao Paulo, still focusing on higher concentrations. Finally, for the mentioned second assortment of digital analysis, the value considered for PM10 is 60 µg/m3 and 30 µg/m3 for PM2.5.

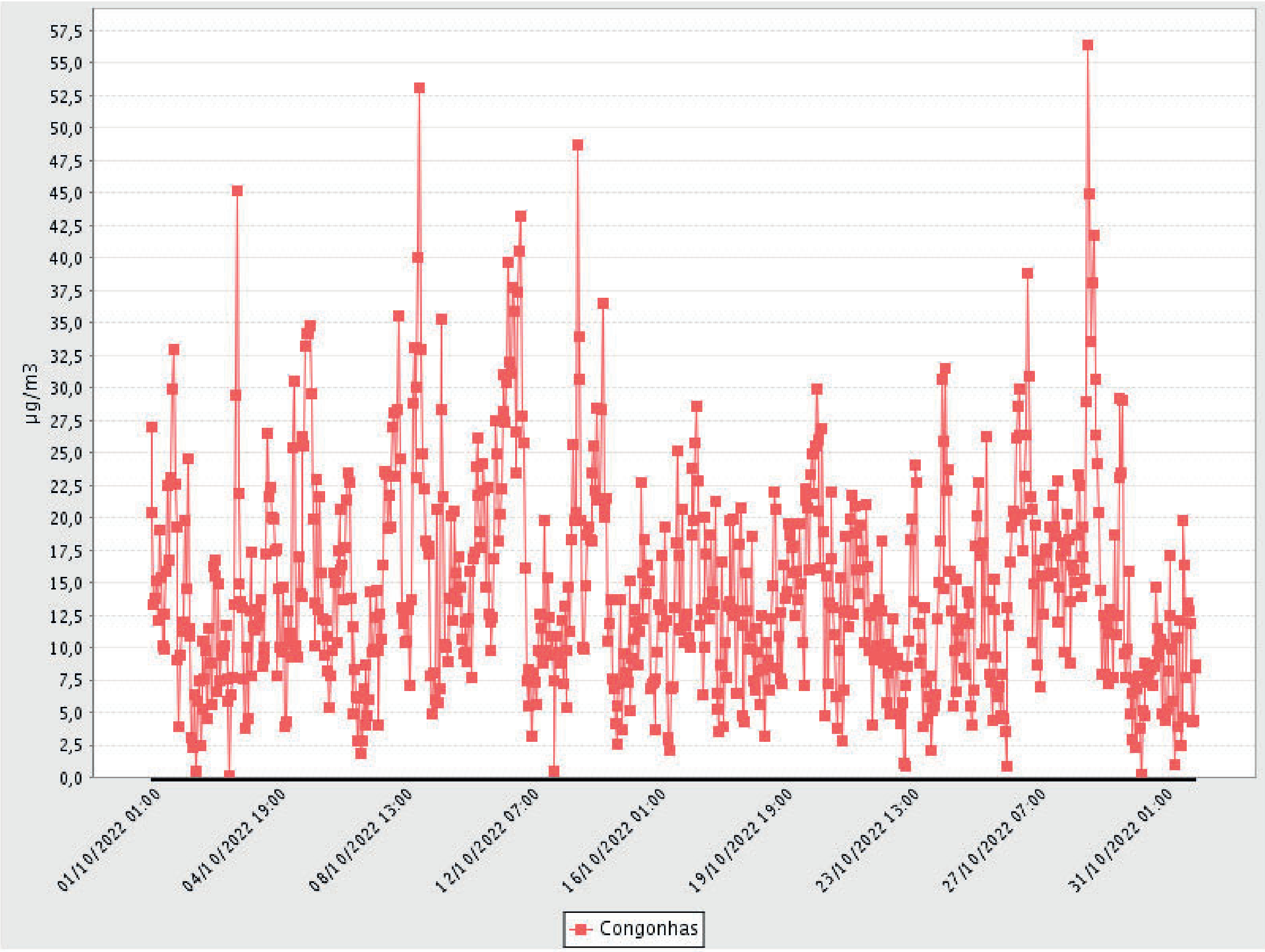

Figure 6.7.10 - Chart – PM2.5 hourly average concentrations for Congonhas station during October 2022.

For the spatial distribution of the pollutants input, the PM10 and PM2.5 values discussed above were placed in a space of four meters (four grids) symmetrically placed around the site. The cited placement allows for a similar dispersion of the particulates independent of the wind direction during the studied period. Moreover, the pollutants started with one meter offset from the site boundary, representing the area of walkways usually preset around a site. The pollutants stand in the area where the asphalt material was applied, representing the vehicular roads. Finally, the 4m size was also defined as simplifying two-way streets, which are common around Sao Paulo schools.

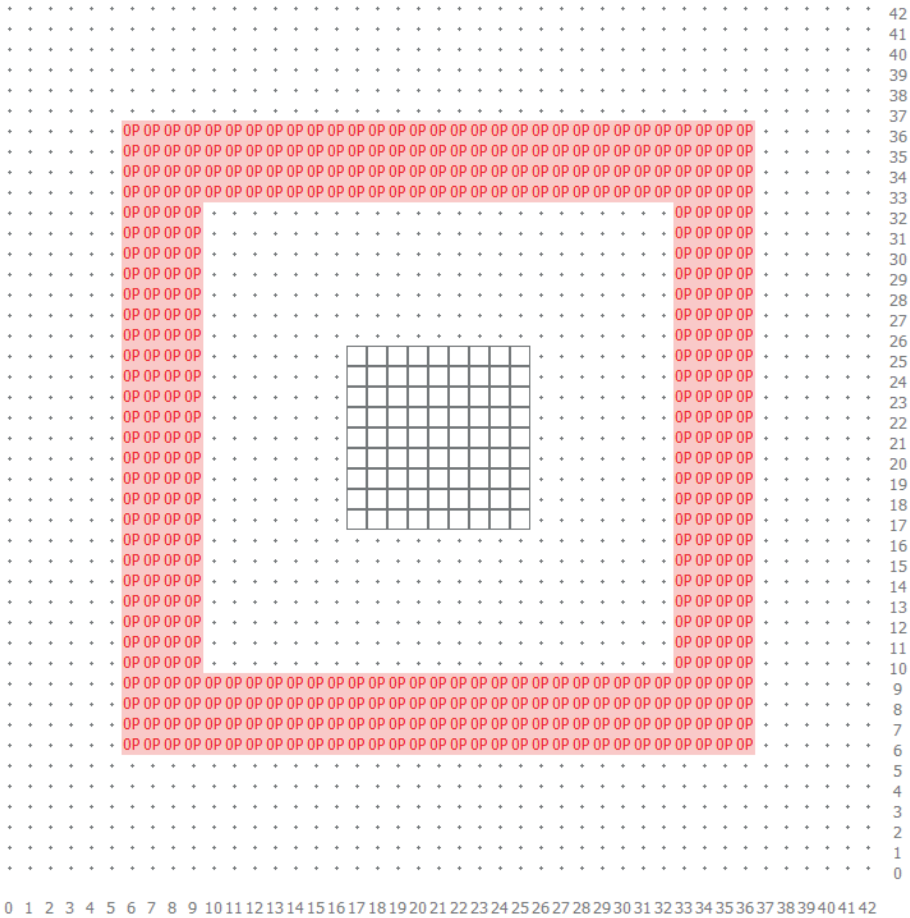

Figure 6.7.11 - ENVI-met model with the pollutant sources' location.

6.8. PSYCHOLOGICAL EQUIVALENT TEMPERATURE (PET)

In 1987, Mayer and Hoppe proposed the MEMI, which is the Munich Energy Model for Individuals. The mentioned model presented new forms of calculating the regulatory sweat rates and heat fluxes, considering separately the parts of the body that are covered and those not covered by clothes. In 1999, Hoppe defined the psychological equivalent temperature (PET) as the equivalent of the air temperature perceived by the body. PET is formed through the calculations of the thermal conditions of the body, skin temperatures and the body's core temperature through the equation models of the Munich Energy Model (MEMI) for the combination of personal and meteorological parameters (Monteiro, L., 2008). Psychological equivalent temperature is also defined as a human-biometeorological index, one of the oldest and most used to define thermal comfort in diverse climatic conditions (Matzarakes, Mayer and Iziomon,1999; Lucchese and Andreasi, 2017; Santos Nouri and Costa, 2017; Hirashima, Assis and Nikolopoulou, 2016). According to Lucchese and Andreasi (2017), "It is calculated based on four climatic variables (mean radiant temperature, air temperature, air velocity and relative humidity) and two personal variables (clothing insulation and metabolic rate)". Furthermore, a study by Liang et al. (2019), as mentioned by Mavkandi et al., 2021), stated that "the PET index gives an enhanced range of sensation temperatures and can predict thermal comfort for the outdoor environment including important thermal benchmarks such as NT and ATR". Finally, the thermal index is widely used in the relevant literature, for example, Matzarakis and Endler 2010; Cohen et al., 2013; Bleta et al., 2014; da Silveira Hirashima et al., 2016; Salata et al., 2016; Krüger et al., 2017a (Pantavou et al., 2018), instilling confidence in its applicability.

Other than the Psychological Equivalent Temperature (PET), the Universal Thermal Climate Index (UTCI) is also used to estimate the perceived or felt temperature based on meteorological variables. As shown in the Case Study Analytical Work chapter, UTCI is used as a parameter to establish the outdoor comfort of EMEF Amorim Lima. However, PET is generally considered more complex and robust than UTCI for several reasons. According to Cheung and Jim (2019, as cited by Makvandi et al., 2021):

> The PET index is one of the most popular thermal indices designed for the investigation of thermal parameters outdoors. It integrates the impacts of all physiologically related climate parameters (relative humidity, air temperature, mean radiant temperature, and wind speed) and personal parameters (metabolic rate and clothing insulation level) to give a single temperature index.

PET is based on personal characteristics like age, gender, clothing, and specific human activities. Meanwhile, UTCI doesn't consider all the previously mentioned aspects (Pantavou et al., 2018). Also, PET is used to express thermal comfort in different weather conditions and has been used in research for several cities around the world, for example, Munich (Mayer and Hoppe, 1987), Taiwan (Lin, 2009), Tian (Lai et al., 2014), Rome (Salata et al., 2016) and Port Said in Egypt (Elraouf et al., 2022). Areas within Brazil have also been studied using the parameter, including Campo Grande (Lucchese and Andreasi, 2017), Belo Horizonte (Hirashima et al., 2018) and Sao Paulo (Spangenberg et al., 2007; Carfan, Galvani and Nery, 2012; Shinzato et al., 2019). Moreover, the PET results are expressed in degrees Celsius (°C), and the human thermal sensation is represented by a comfort index table that ranges from "very cold" to "very hot". Each level of comfort from the mentioned table is defined by a range of temperatures (°C). Considering the range of climatic conditions and cultural contexts that PET can be studied in, it is possible to assume that the comfort index can vary for different locations. Thus, the comfort index table must be adjusted for each climatic condition and cultural context. According to Hirashima et al. (2018):

> The PET neutral comfort value range in Belo Horizonte is from 16 °C to 30 °C PET and the hot range starts at 32 °C, while in Kassel/

Freiburg neutral range is from 18 °C to 28 °C PET and hot range starts with 35 °C PET. A comparison of thermal perception in tropical and temperate climates shows differences in the comfort zone of almost 4 °C PET. This means that a standard calibration of PET is not possible but has to be matched to the respective climate region. Therefore, the results of this study have local validity and may not be applicable in different climates and cultural areas without adaptations.

Some of the reviewed studies that used PET to indicate comfort levels in Brazil calibrated the PET assessment ranges with the use of questionnaires (Lucchese and Andreasi, 2017; Hirashima et al., 2018; Hirashima, Assis and Nikolopoulou, 2016). Hirashima, Assis and Nikolopoulou (2016) conducted 1693 interviews in the summer and winter of 2013. The mentioned study defined a range of: “Cold” for PET values below 19°C, “Neutral” for PET values between 19°C and 27°C, and “Hot” for PET values greater than 27°C. Neutral temperatures were 27.7°C in summer and 15.9°C in winter, while preferred temperatures were 14.9°C in summer and 20.9°C in winter for Belo Horizonte, Minas Gerais state capital. However, the calibration used to interpret the findings of this analytical research is based on research done with Sao Paulo’s population and can be seen in the table below. The values used are proposed by Monteiro and Alucci (2010a, as mentioned by Monteiro 2018) through the correlation of Sao Paulo city meteorological data and a survey applied to 1591 people in winter and summer conditions. Monteiro’s thesis (2018) was conducted at the University of Architecture of Sao Paulo (FAUSP). The research is dedicated to studying thermal perception in outdoor spaces and demonstrates its calibration concerning PET values, specifically for different cities in Brazil, focusing on Sao Paulo.

PET (°C)	Thermal Perception
> 43.0	Very Hot
34.1 - 43.0	Hot
26.1 - 34.1	Slightly Hot
18.0 - 26.0	Comfortable/Neutral
12.0- 17.9	Slightly Cold
6.0 - 11.9	Cold
< 6.0	Very Cold

Figure 6.8.01 - Table with calibration for PET according to Sao Paulo conditions.

6.9. RESULTS

This section starts with individual analyses of the six studied hours to illustrate the microclimatic conditions within the ten scenarios' sites. Afterwards, the section focuses only on thermal comfort and air quality through the Physiological Equivalent Temperature (PET) and PM2.5 parameters for each studied hour, comparing the weighted average value for each scenario. The weighted average sums the value of each m2 and divides it by the entire area to find a figure representing the site. After the first set of results is analysed, a few questions are raised. Thus, a second batch of simulations is carried out, and their results are equally discussed in this section. Finally, a second version of the Environmental Performance Matrix displaying the main results is developed, displaying this chapter's main results and completing this section.

6.9.1. STUDIED HOURS

HOT DAY AT THE HOTTEST HOUR (HH)

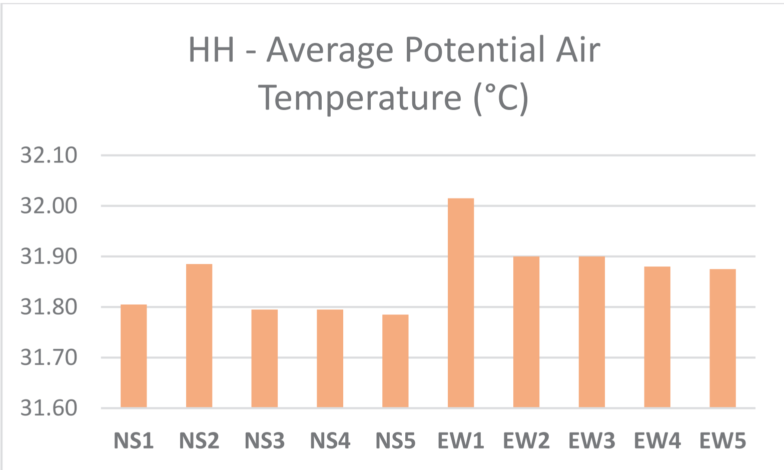

Figure 6.9.01 - Graph comparing the potential air temperature average (°C) within the studied site between cases.

The highest air temperature predicted in the 2050 weather file is 34.5°C at 3 pm on October 11th. The simulation shows that dry bulb temperatures in the site vary from 31.8°C to 32°C. The closest value to the one inputted for this hour (34.5°C) is spotted in the east-west scenario with no vegetation (EW01): 33.41°C. All other cases show average air temperatures equal to or lower than 31.9°C. EW02 and EW03 (grass and grass with living walls) present higher temperatures (31.9°C), followed by NS02 (grass) at 31.8°C. The lowest weighted average temperature is spotted in the NS05 case (grass and trees). For example, NS1(no vegetation), NS2 (grass), and NS3 (grass and living walls) all showcased a maximum velocity of 3.12 m/s. Yet, in the NS4 and EW4 cases, with hedges and grass, the maximum value drops to 2.62 m/s. Even though it could be believed that the results suggest that hedges can be more effective in reducing it, this is not true. The air movement results shown are at the height of 1.50m, which is closer to the hedge vegetation when considering the tree crown starts at 4m. However, the trees have a higher overall mass than hedges. Thus, trees

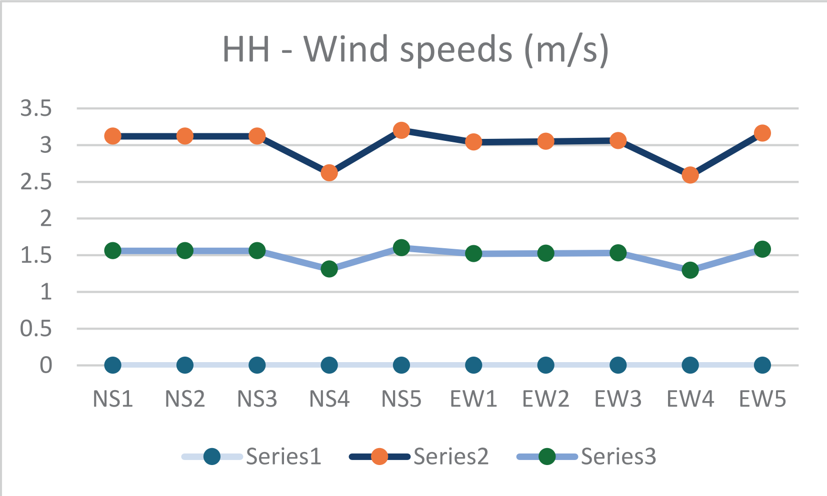

Figure 6.9.02 - Graph comparing the wind speeds (m/s) within the studied site between cases.

have a higher impact on wind speeds and air movement. The mentioned affirmation is confirmed when analysing the wind velocity pattern at different heights. For example, even at 8.5m height, where air movement is enhanced (figure x1 - approximately the middle of the trees' crowns), the wind velocity is lower compared to areas outside the terrain. Moreover, as expected, the mean radiant temperature (MRT) highlights the impact of shading and coverage of hard-scape by green elements, which is a clear indication of human thermal comfort. In all cases, the shaded areas caused by the building and boundary walls show a 1°C MRT decrease. SSome terrain spots also present a further one-degree decrease when the grass is added. When adding living walls, the areas within the site are shaded and covered with

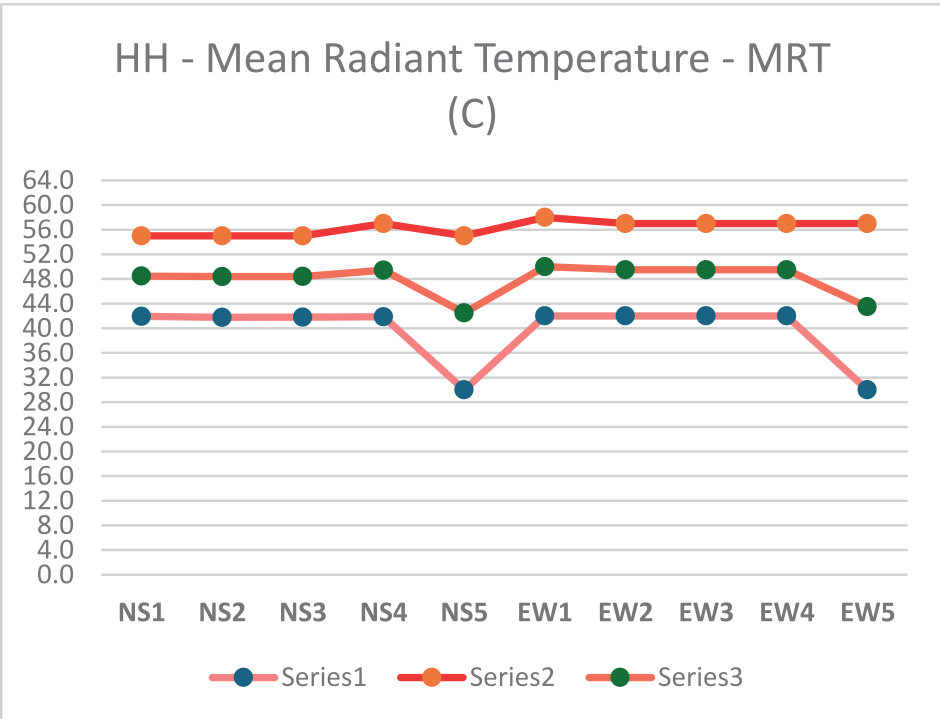

Figure 6.9.03 - Graph comparing the MRT (°C) within the studied site between cases.

grass, and the MRT enhances even further than hedges. However, the more significant impact happens on cases NS5 and EW5 when trees are added, generating shading areas up to 15°C less than the exposed ones (image 03). Overall, it is possible to observe how the maximum, minimum and average MRT values are always lower in the scenarios with trees (image 03). The mentioned results showcase the positive shading impact of the trees on a hot day.

The indoor dry bulb temperatures illustrate a minimal difference between scenarios (image 04). Concerning the north-south cases, the scenarios without vegetation, with grass, and grass + living walls (NS1, NS2 and NS3), the air temperature is 26°C in the classroom and 24°C inside the circulation area, which has the north façade with cobogos. On the NS4 (with hedges), air temperatures in the corridor remain the same as in the cases mentioned (24°C). Yet, the classroom reaches almost 27°C in the case with hedges (NS04), the highest within NS cases. Until now, all the

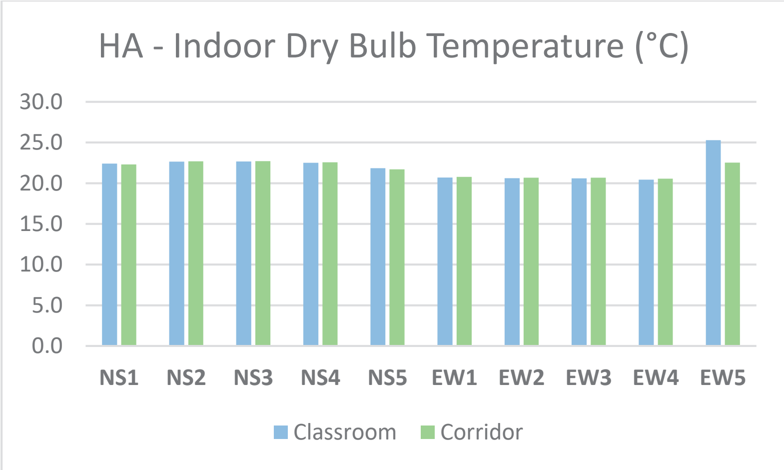

Figure 6.9.04 - Graph comparing the potential air temperature indoors within studied cases.

classroom temperatures are higher than in the corridors. Finally, the lower values are spotted in the NS5 (trees and grass), and for the first time, both the classroom and circulation have the same dry bulb temperature: 22°C. The NS05 results indicate the positive impact of trees as shading elements, reducing the indoor temperature to the same level as the area with a shaded façade (cobogos in the circulation). In east-west iterations, the dry bulb temperatures are also higher in the classroom than in the passage hall in most scenarios. The case with trees (EW5) has a different result once again. Yet, concerning EW cases, EW05 shows a higher dry bulb temperature in the corridor, the highest recorded: 29°C. The mentioned result can be understood when remembering that these measurements are recorded at 3 pm when the sun angles are lower and almost parallel to the western façade, causing negative indoor impact.

HOT DAY AT THE MILD HOUR (HM)

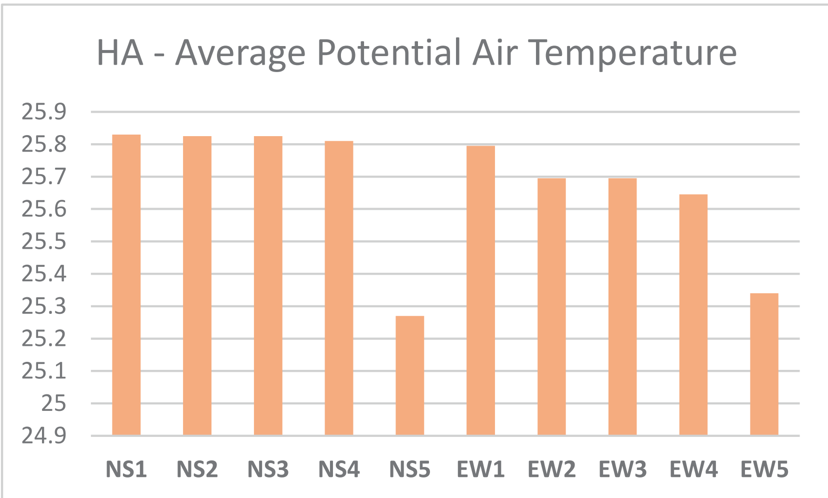

Figure 6.9.04 - Graph comparing the potential air temperature average (°C) between cases within the studied site.

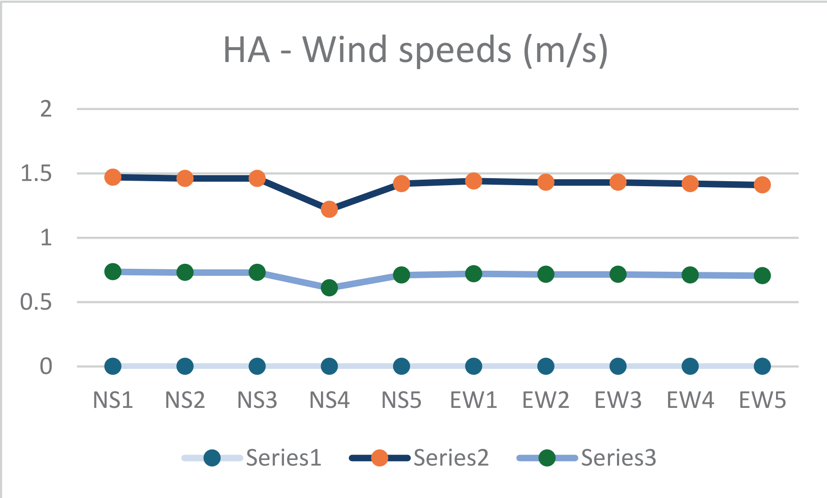

Figure 6.9.05 - Graph wind velocities (m/s) within the studied site between cases.

On the hottest day of 2050, the average temperature is at 09 am, being 25.2°C. The results demonstrate an almost constant air temperature between cases NS1 and NS4 (complete exposure, grass, grass plus living walls and grass plus hedges). However, there is a 0.5°C reduction with the addition of trees. There is a slight air temperature decrease amongst the east-west cases when greenery is added. Once again, the iteration with trees (EW05) shows a more significant difference (0.5°C) when compared to no vegetation (EW01). At this specific period of the day, the wind velocities are substantially lower than at the hottest hour, with the maximum average within the site reaching 0.74m/s. The previous image shows the only case with a more considerable velocity reduction is the NS4 (northeastern building with grass and hedges). Moreover, the mentioned pattern can also be observed in the hottest hour. However, it is essential to state that the EW4 is also built with hedges and grass, but there is no reduction in wind speed. The previous result is an example that the environment can be changed or altered when the same element is placed in different locations.

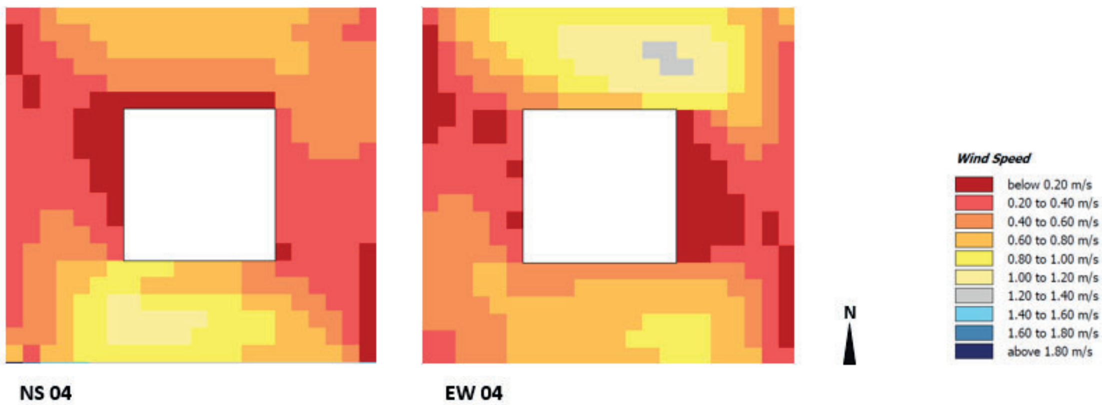

Figure 6.9.06 - Diagrams comparing the wind speeds within the site on case NS04 and EW04.

On the studied hour, the wind prevails from the south, and the hedge is also placed in this direction, generating an area with less air movement (figure 6.9.06).

As expected, the values of MRT (mean radiant temperature) are lower than in the hottest hour. The weighted averages on this hour vary from 39°C to 47°C, reaching a maximum of 54°C. In contrast, the HH (hottest hour) ranges from 48°C to 55°C, with a maximum of 58°C. Once again, there is a reduction in the mean radiant temperature in the scenarios with trees (NS5 and EW5). Moreover, the areas underneath the trees reach 27°C on the NS case and 30°C on the EW. Another example of different performances of the same element when positioned differently. Concerning the indoor

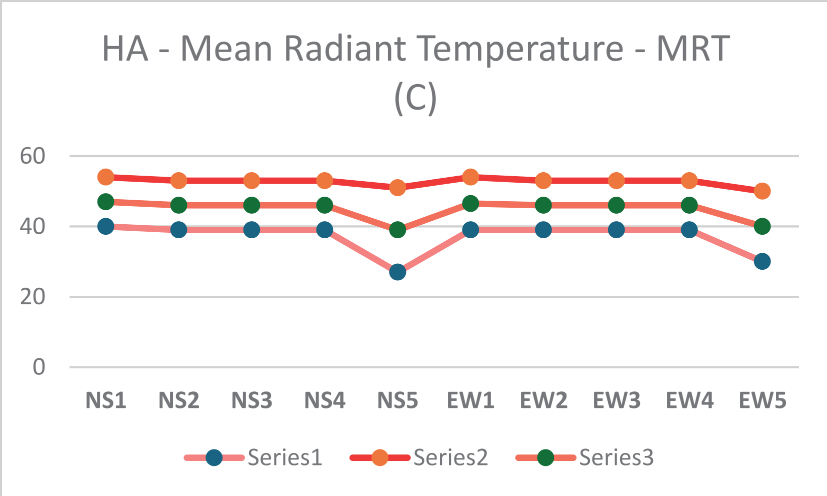

Figure 6.9.07 -Graph comparing the MRT (°C) between cases within the studied site.

dry bulb temperatures, there was a minimal difference between scenarios (figure 6.9.08). However, air temperatures in both indoor spaces within north-south cases (NS) are slightly lower in the scenario without vegetation: 22.4°C and 22.34°C. Moreover, the iteration with trees has the lowest value: 21.9°C. Between the east-west cases, the EW5 (with trees) showcases the higher temperatures for the indoor areas. The mentioned case has an air temperature of 25.3°C in the classroom and 22.5°C in the corridor (almost three degrees difference). The EW5 corridor temperature is the closest indoor value to the outdoors. Contrary to the hottest period of the hot day (HH), the combination of the tree and cobogo is positive for the indoor environment. The result confirms the natural best performance of a room when there is no direct sun, considering the results are recorded here at 9 am. While also confirming the positive impact of architecture (cobogo) and natural shading (trees).

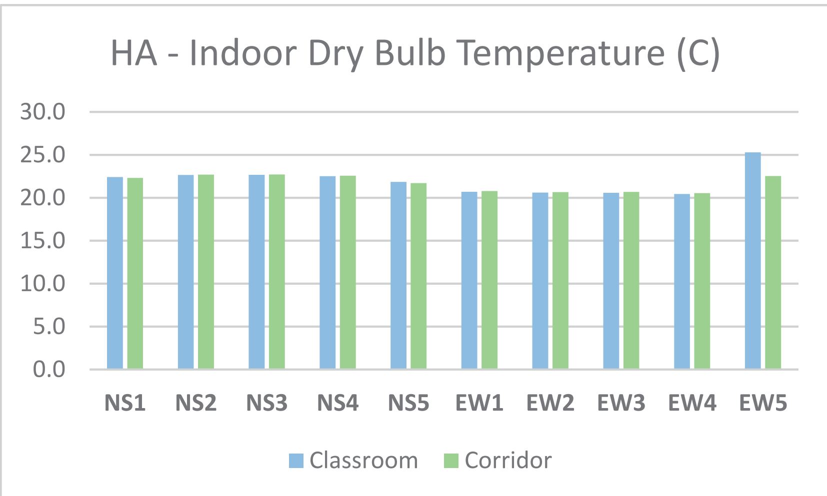

Figure 6.9.08 - Graph comparing the potential air temperature indoors within studied cases.

HOT DAY AT THE COLDEST HOUR (HC)

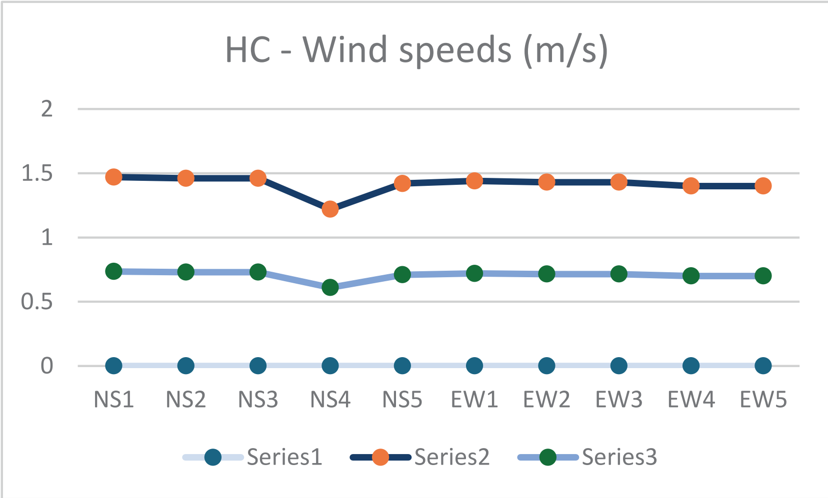

Figure 6.9.09 - Graph comparing the wind speed(m/s) within the studied site between cases

The lowest air temperature on the hottest day is at 07 am, 19.4°C. The simulation captured dry bulb temperatures from 20°C to 20.2°C in all scenarios. The wind speed results are almost identical to the average hour (image 13). The result is expected considering that the wind velocities input for both hours have only a 0.2 m/s difference. With lower air temperatures, the MRTs within the studied site are not higher than 39°C. Even though the coldest hour also presents a clear, unobstructed sky, at 07 am, there is not enough time for solar irradiation to accumulate on the surfaces. Unlike the other analysed periods, the mean radiant temperatures remain constant without expressive changes, even in the

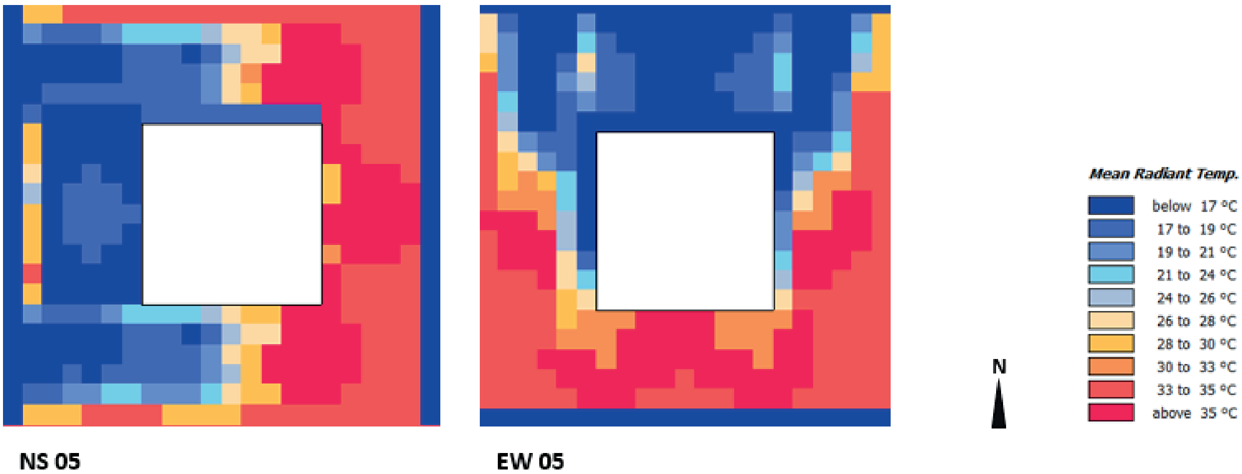

Figure 6.9.10 - Diagrams comparing the MRTs within the site on cases NS05 and EW05.

scenarios with trees. The mentioned result can be the first indication of direct shade-creating spaces where heat is being belatedly released. The phenomenon happens as the shaded area reduces the exchanges with the night sky. With less exchange, the heat is released slower than on exposed surfaces (Hollick, 2012). The indoor temperatures in the

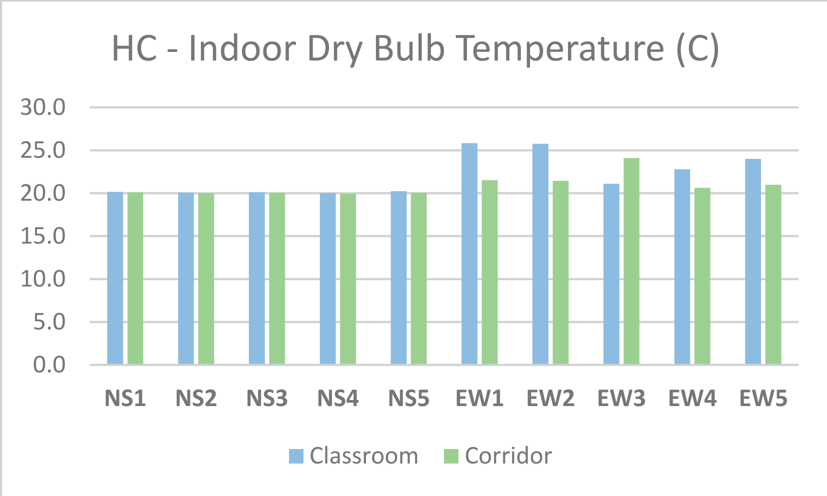

Figure 6.9.10 - Graph comparing the potential air temperature indoors within studied cases.

north-south scenarios are closer to the outdoor ones. Yet, the east-west iterations showcased higher temperatures in the rooms than outside areas. For example, the classrooms in EW1 (no vegetation) and EW2 (with grass) have around 5.0°C higher dry bulb temperatures than the north-south ones. The classrooms face east, which faces the morning sun, so solar irradiance may be enhancing the temperature inside.

COLD DAY AT THE HOTTEST HOUR (CH)

On the coldest day of 2050, the hottest temperature is 17.1°C at 3 p.m., which is the input for the simulation. At this hour, amongst cases, the registered dry bulb temperatures in some areas reach 20.05°C to 20.15°C, which is higher than the last studied hour. Naturally, the mean radiant temperature values registered are higher than previously found.

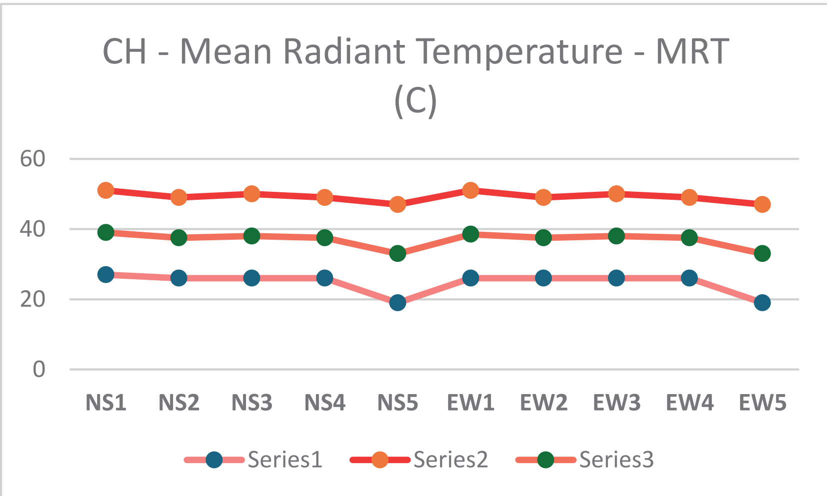

Figure 6.9.11 - Graph comparing the potential air temperature average (°C) within the studied site between cases.

Even though the input temperature is lower, the CH period happens at 3 p.m., the latest one (hottest day, coldest hour) is at 7 a.m., and both periods present a clear sky. Hence, the dry bulb and mean radiant temperature in both cases suggest the effect of the solar radiance on diminishing thermal comfort. Moreover, the scenarios NS05 and EW05 showcase lower MRTs, specifically under the trees. The previous result once more demonstrates how blocking direct sun can make some spaces cooler during periods of higher radiation exposure. The indoor spaces have temperatures of approximately 20°C in almost all cases (figure 6.9.12). The only exceptions are the cases with trees (NS5 and EW5). In the NS5, the corridor's temperature is over 25.3°C, and 24.2°C in the EW5. The corridors' facades face south and west and are treated with cobogos. Thus, the heat loss to the outdoors is reduced. Additionally, shading provided by trees

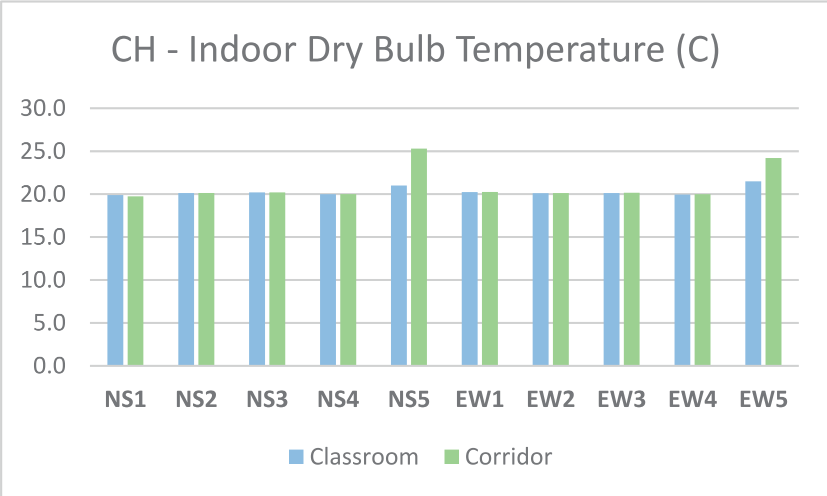

Figure 6.9.12 - Graph comparing the potential air temperature indoors within studied cases.

on the facades decreases even further the mentioned loss. The result is a hotter environment, even in a cooler hour. In previous cases, lower dry bulb temperatures were shown to be connected to higher pollution concentration levels. However, the overall PM2.5 concentration is lower during this period than on the hottest day, at a colder hour (HC). This result probably happens because the dry bulb temperature recorded on-site through simulations is higher than the HC. Also, even though the wind velocities are similar between hours, the prevailing direction is different.

COLD DAY AT THE MILD HOUR (CM)

On the coldest day of 2050, the average temperature is 11.9°C at 10 am, with the sky almost entirely clouded. The dry bulb temperatures within the site range from 13.06°C to 13.15°C. Additionally, wind velocities are the same

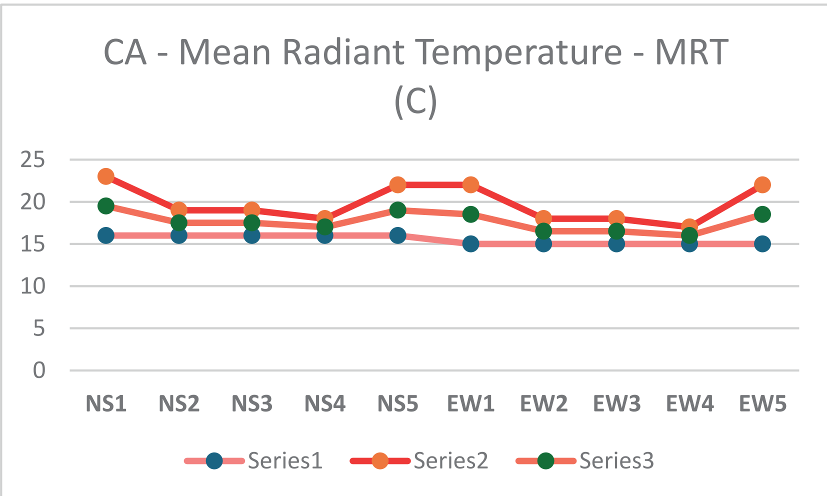

Figure 6.9.13 - Graph comparing the MRT (°C) within the studied site between cases.

amongst cases except for the iterations with trees, where most areas displayed a slightly lower speed. As seen on the CH (the coldest day and hottest hour), the dry bulb temperatures registered at this hour are higher indoors than out-

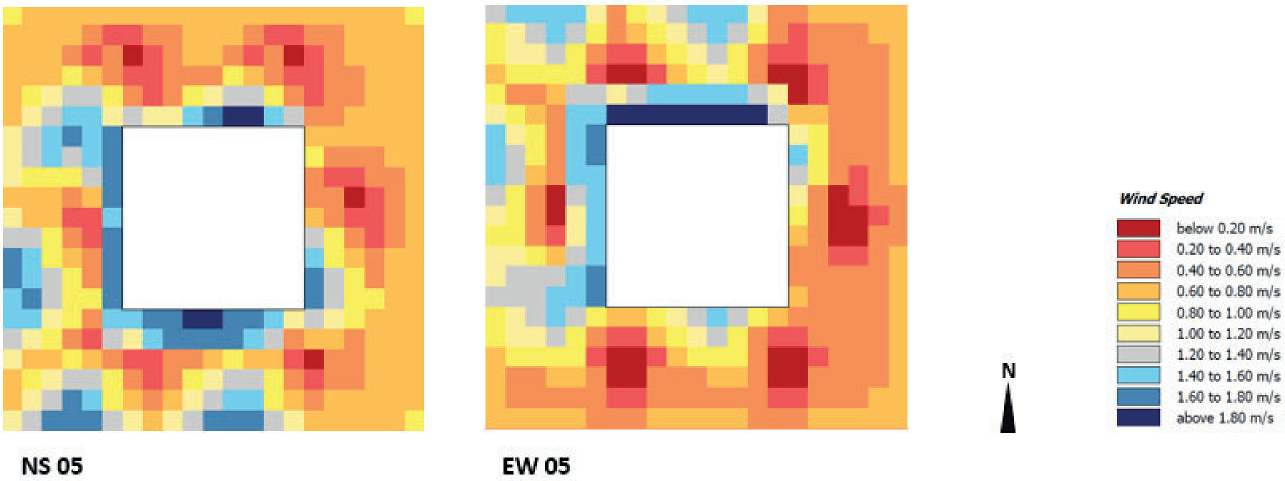

Figure 6.9.15 - Diagrams comparing the wind speeds within the site on cases NS05 and EW05

doors in all scenarios, roughly four degrees (figure 6.9.16). In most cases, the classroom shows higher temperatures than the corridor. Finally, the NS5 and EW5 show higher temperatures again, with the NS5 being the highest: 21.2°C. The result is followed by 20.6°C in the classroom and 20.3°C in the corridor within the EW5. With the lower dry bulb temperature and cloudy sky, this hour shows PM2.5 levels significantly higher than previously studied hours. This day's high sky coverage, 76% humidity, and low wind speed of 0m/s to 0.7m/s are probably responsible for the result.

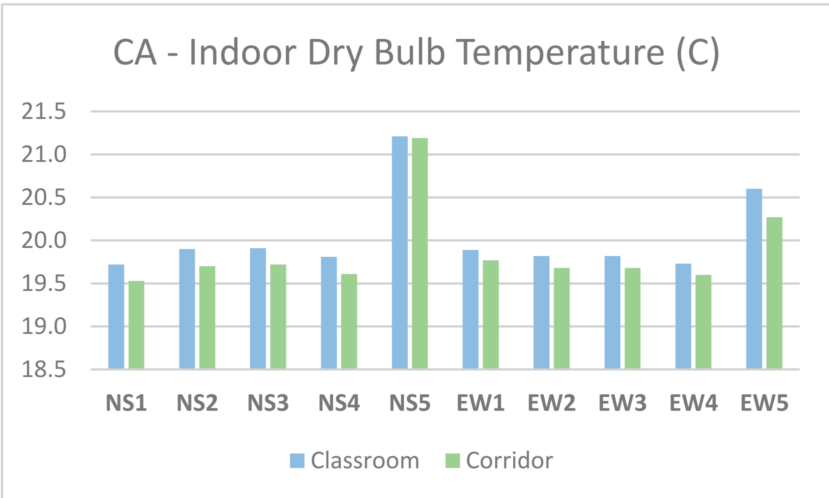

Figure 6.9.16 - Graph comparing the potential air temperature indoors within studied cases

COLD DAY AT THE COLDEST HOUR (CC)

The colder temperature is 8.0°C at 7 a.m. on the coldest day of 2050. Therefore, the simulation's air temperature ranges from 10.75°C to 11.77°C. Furthermore, the MRT average within the site is 3.5°C, except for the cases with hedges and trees (NS04, NS05, EW04 and EW05). Once more, areas under trees showed 7.0°C MRT, being even higher than what was found in the exposed scenarios (NS01 and EW01). The results show how denser vegetation typologies, such as trees and hedges, can benefit the environment even in the coldest conditions. Even though the air temperature out-

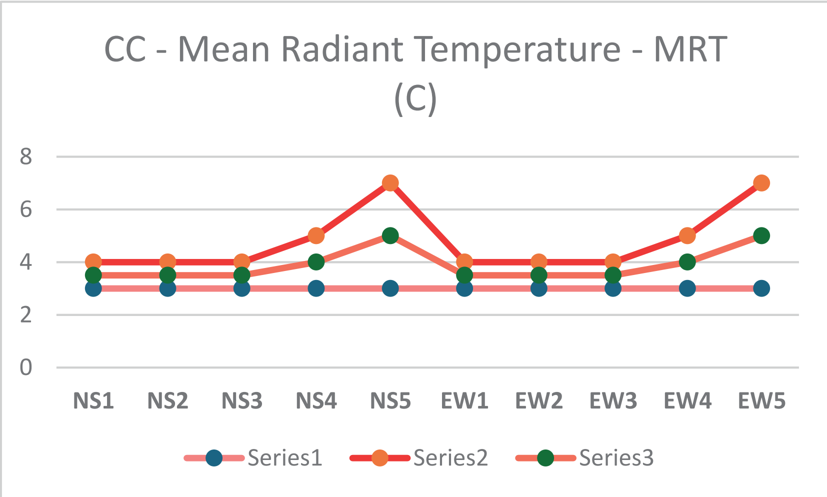

Figure 6.9.17 - Graph comparing the MRT (°C) within the studied site between cases.

doors ranges around 11°C, the registered indoor temperatures vary around 19°C (image 25). Therefore, the mentioned result showcases, once more, the importance of enclosed spaces during critical climatic conditions. Additionally, the classroom has higher temperatures than the corridors in all scenarios.

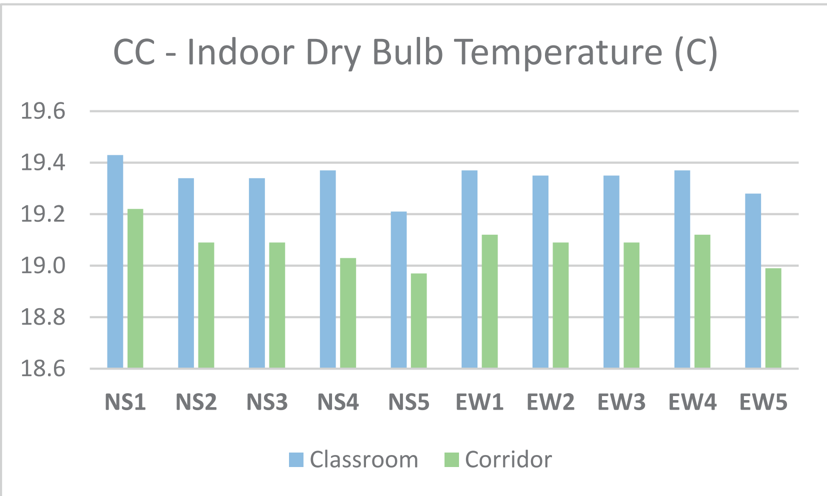

Figure 6.9.18- Graph comparing the potential air temperature indoors within studied cases.

6.9.2. PHYSIOLOGICAL EQUIVALENT TEMPERATURE (PET) STUDY

This section's results analysis is mainly based on the comfort band for each PET value presented in section 6.8 of this chapter. The table mentioned above is presented once more below with the addition of a colour pattern that will be repeated in the following diagrams. However, it is essential to state that there are better and worse conditions within each band of thermal perception.

PET (°C)	Thermal Perception
> 43.0	Very Hot
34.1 - 43.0	Hot
26.1 - 34.1	Slightly Hot
18.0 - 26.0	Comfortable/Neutral
12.0- 17.9	Slightly Cold
6.0 - 11.9	Cold
< 6.0	Very Cold

Figure 6.9.19 - Table of PET values and thermal perception with color legend.

HOT DAY AT THE HOTTEST HOUR (HH)

At this hour, the air temperature is 34.5°C with a clear sky and 6.5m/s wind speed from the east-southeast. The results reveal a mean average PET between 36.5°C to 40.9°C within sites of the EW cases, which is perceived as hot. Moreover, the NS scenarios show PET between 35.5°C and 41.7°C, also hot (or strong heat stress). The NS case has a solid 2m boundary wall around the site, which EW doesn't. The boundaries reduce the wind velocities, consequently increasing the PET. Moreover, NS05 (with grass and trees) is the only NS case with lower PET than EW. The relationship between the tree's location and wind direction could explain the result. As expected, the scenarios with trees have the overall best performance in both situations (NS and EW) due to this green element shading ability. As also expected, the hard pavement cases (NS01 and EW01) have the worst performance, showing a weighted average value within the site of 41.7°C (hot thermal perception).

The cases with hedges (NS04 and EW04) and living walls (NS03 and EW03) perform better than the cases with only grass (NS02 and EW02), which is also expected. However, the NS04 (with hedges) performs poorly in comparison with NS03 (with living walls), which has a superior result than the EW03 and EW04 (living wall and hedges). The results also show the importance of higher vegetation, such as living walls (2m in height). The element generates a more enhanced shaded area than hedges (1m in height). However, in the cases with higher wind velocities (EW), the hedges and living walls have a similar impact due to the lack of boundary walls. The result suggests better vegetation performance in environments protected by solid barriers.

Figure 6.9.20 - Diagrams showcasing the PET levels in the site on the north-south cases.

HOT DAY AT THE MILD HOUR (HM)

Even though the mild hour has an air temperature 10.3°C lower than the hottest hour, 25.2°C, the PET mean average varies about 1°C in the same cases between the two hours. The PET within the site on the East/West cases range from 34.8°C to 40.5°C and from 34.9°C to 41.3°C on the North/South ones. Regarding the environmental conditions input for the mild hour, the wind speed is 2.6m/s instead of 6.5m/s (hottest hour), the relative humidity is 83% instead of 53%, and the sky isn't obstructed. Lastly, the mentioned correlations between the mild and hottest hours input and outputs indicate how lower wind speed, higher humidity, and solar exposure can create a perception of greater heat stress. For the 25.2°C air temperature, the site is under moderate heat stress in all the cases. NS05 and EW05 (with trees) display PET of 34.9°C and 34.8°C, closer to 34°C, which is the limit for slight heat stress perception. Moreover, in both NS and EW, the hedges performed worse than the living walls.

Figure 6.9.21 - Sketch diagram showcasing the PET values on NS and EW cases within the hot day mild hour (°C).

HOT DAY AT THE COLDEST HOUR (HC)

At 7:00 a.m., with an air temperature of 19.4°C, the cases with trees (NS05 and EW05) are the only ones within the slight heat stress band, displaying 26.9°C and 27°C mean average PET. All other scenarios are within moderate heat stress (above 34.1°C). Moreover, the EW cases with no solid boundaries perform better than the NS. Additionally, once more, the living walls display lower PET than the cases with hedges, with NS03 and EW03 having the same mean average value (30.9°C). Lastly, it is essential to state that the relative humidity, cloud cover, and wind speed conditions are approximately equal to those of the mild hour. However, this hour is at 7 am, with less solar radiation accumulation and has a dry bulb temperature reduction of 5.8°C compared to the average hour. The mentioned changes are the main variables that produce a PET decline of around 8°C from the average to the coldest hour in all cases.

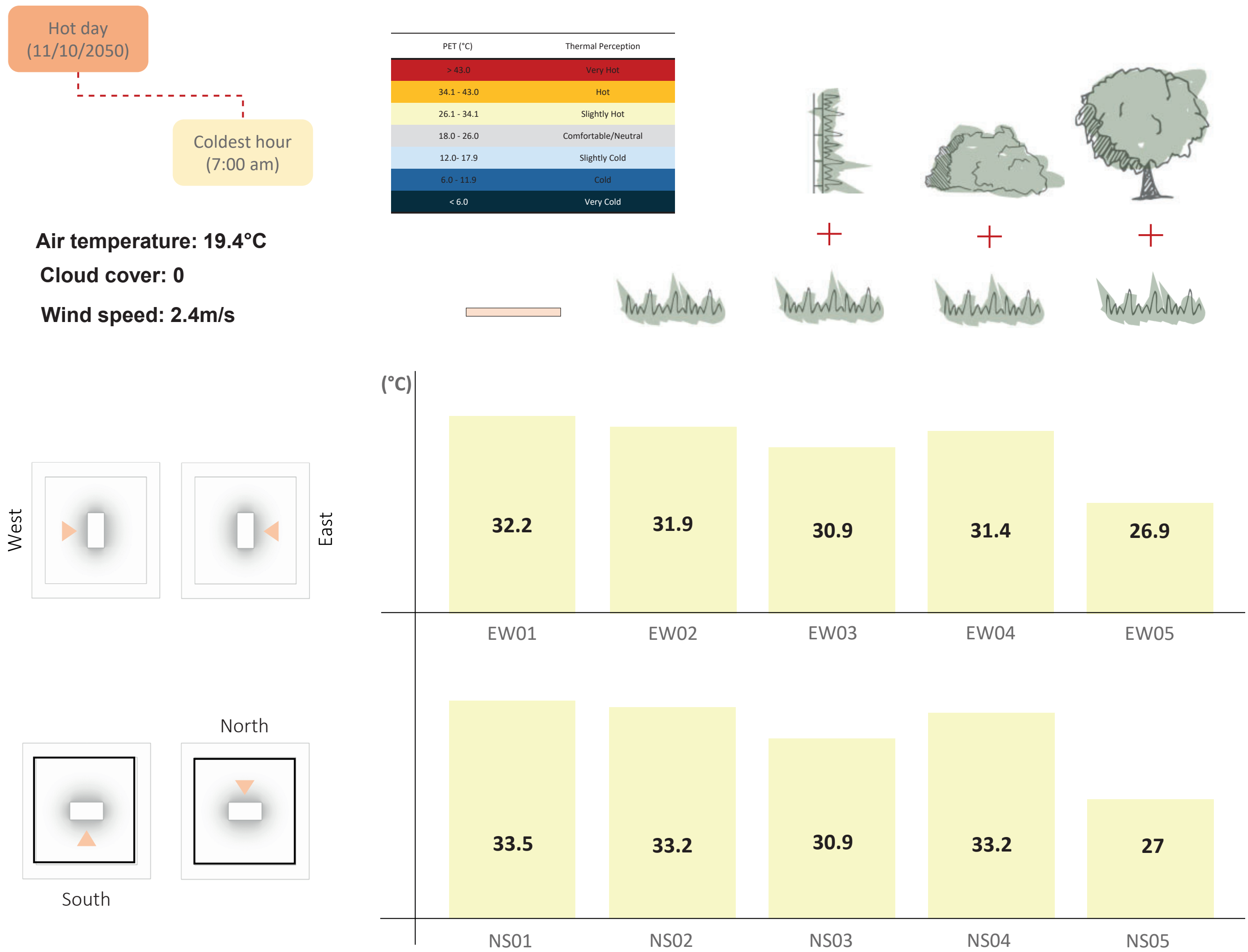

Figure 6.9.22 - Sketch diagram showcasing the PET values on NS and EW cases within the hot day and coldest hour (°C).

COLD DAY AT THE HOTTEST HOUR (CH)

This is the hour with a 17.1°C air temperature, the hottest hour of the coldest day in 2050. In this hour, almost all cases present PET values considered comfortable (18°C to 26°C). The only scenario considered slightly hot is the NS01 (with no vegetation). Overall, the lowest PET is 21°C, and the highest is 26.7°C. That is the first of the given hours with scenarios considered comfortable. The cases with the best performance are, once more, NS05, EW05 (with trees) and EW03 (living walls), which is a case with no solid boundary walls. The results exhibit the impact of solar radiation on clear sky days anew, as the PET levels are still high when considering the 17.1°C dry bulb temperature. Results also maintain the same performance relation of green elements in compassion with the other studied hours.

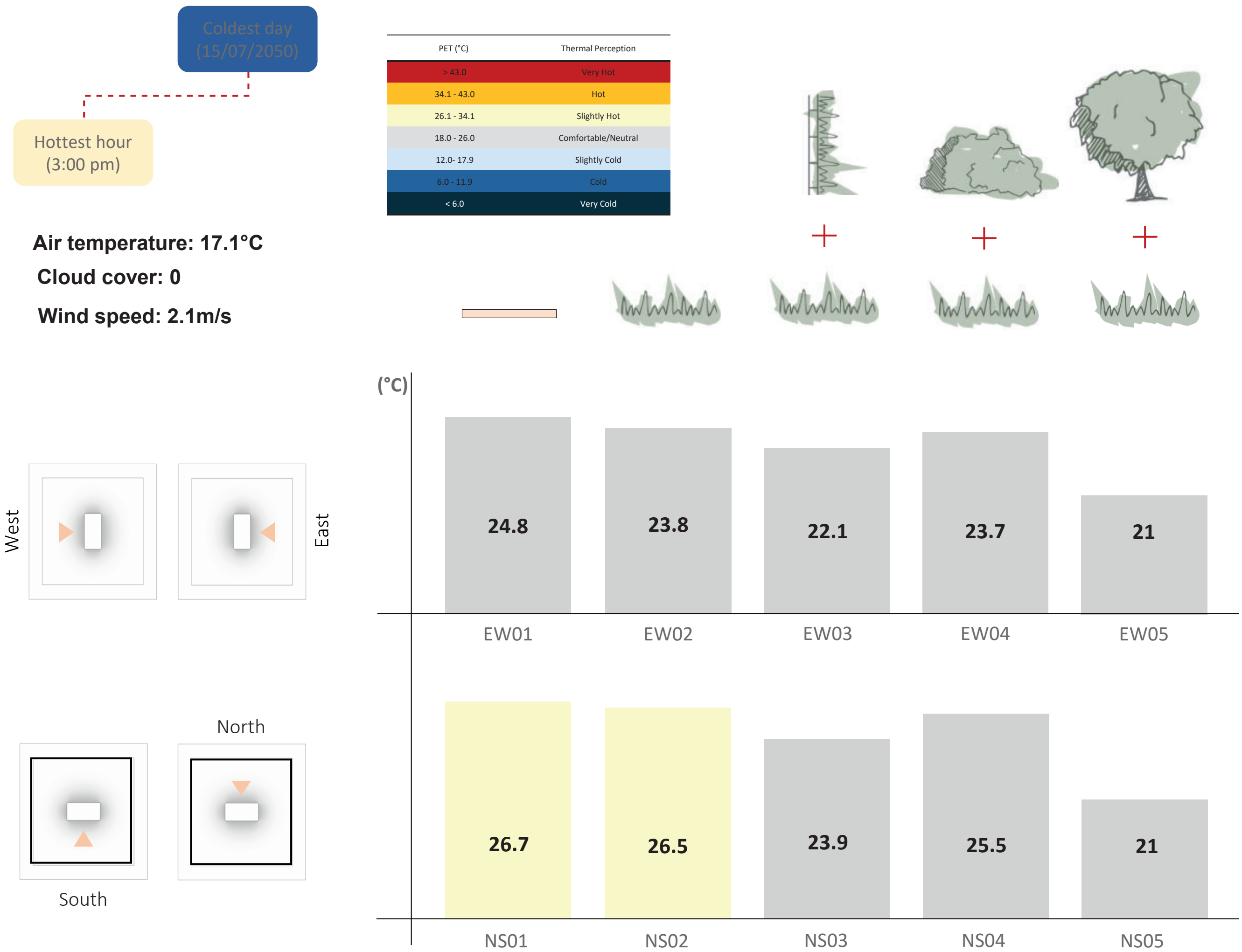

Figure 6.9.23 - Sketch diagram showcasing the PET values on NS and EW cases within the cold day and hottest hour (°C).

COLD DAY AT THE MILD HOUR (CM)

The hour has an 11.5°C dry bulb temperature, a 0.6m/s wind speed, 88% relative humidity and a partially clouded sky for the first time within studied hours. Nonetheless, all East/West cases have higher PET values than the cold day mild hour (CM). Additionally, apart from NS05 (with trees), the North/South cases are lower than CM but with very similar PET: 22°C to 26.3°C in this hour against 21°C to 26.7°C in the previous one. Also, even with an air temperature of 23°C lower than the hottest studied hour of this analytical exercise, the NS01 (no vegetation and with boundary walls) is still considered slightly hot. Once more, NS05 and EW05 (with trees) display the lower values: 22.2°C and 22°C. Additionally, living walls (NS03 and EW03) follow with 23.5°C and 23.4°C. Finally, the results indicate how the lack of air movement and mainly solar irradiation (even when reduced) can increase the perception of warmness despite cold air conditions.

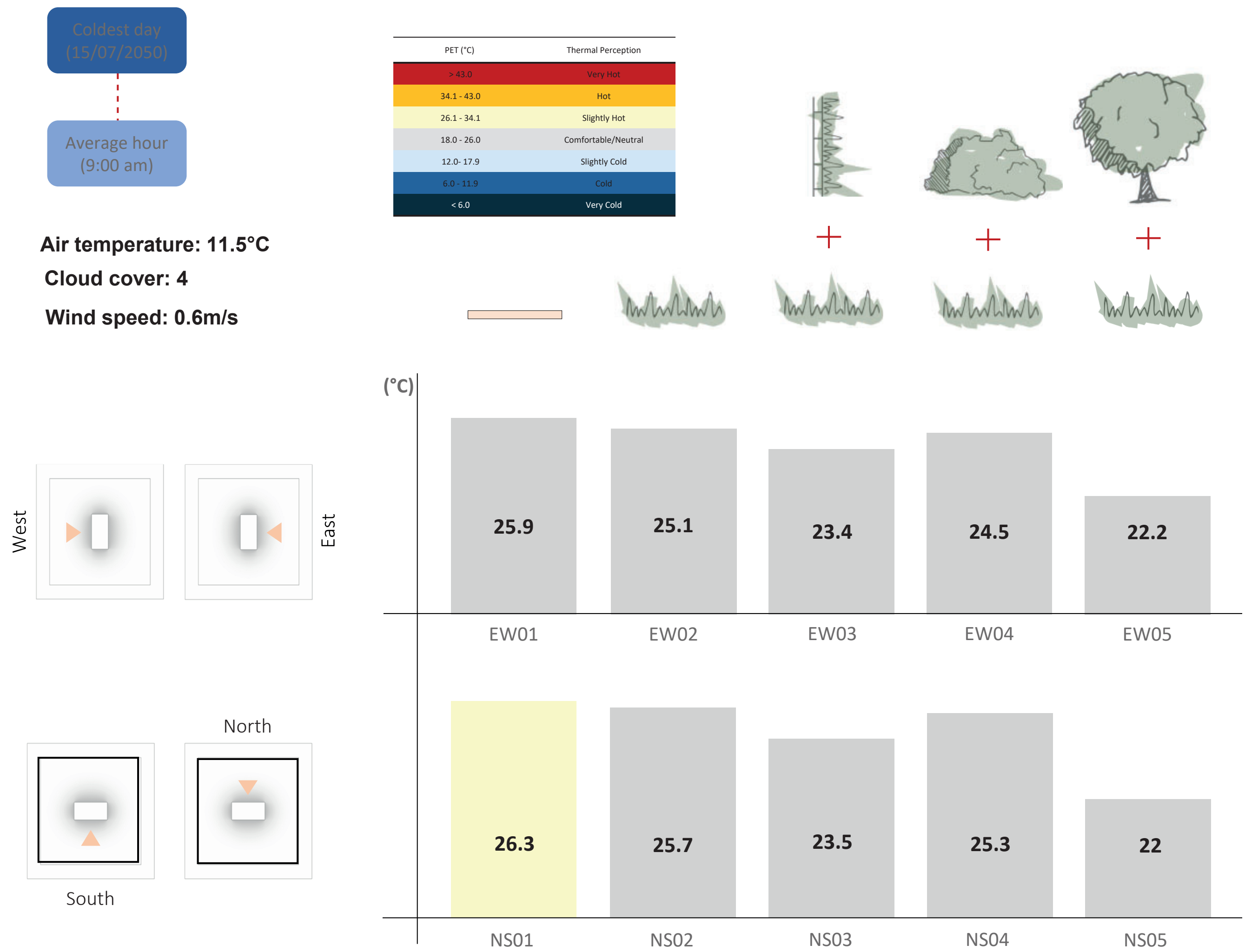

Figure 6.9.24 - Sketch diagram showcasing the PET values on NS and EW cases within the cold day and mild hour (°C).

COLD DAY AT THE COLDER HOUR

At 7:00 am, the air temperature is 8.5°C with partial cloud coverage and wind speed of 01.m/s and 100% humidity. At this hour, all the cases are within the band of no thermal stress apart from the living walls. The weighted average PET figures are 17.6°C (EW03) and 17.7°C (NS03), indicating slight cold stress (below 18°C). The EW01 (no vegetation and no boundary walls) has the highest PET: 18.7°C. The finding may again showcase the potential of exposed materials to instore and transfer heat, even within partially clouded conditions. The sites with trees (NS05 and EW05) register the second-highest mean average PET values: 18.4°C.

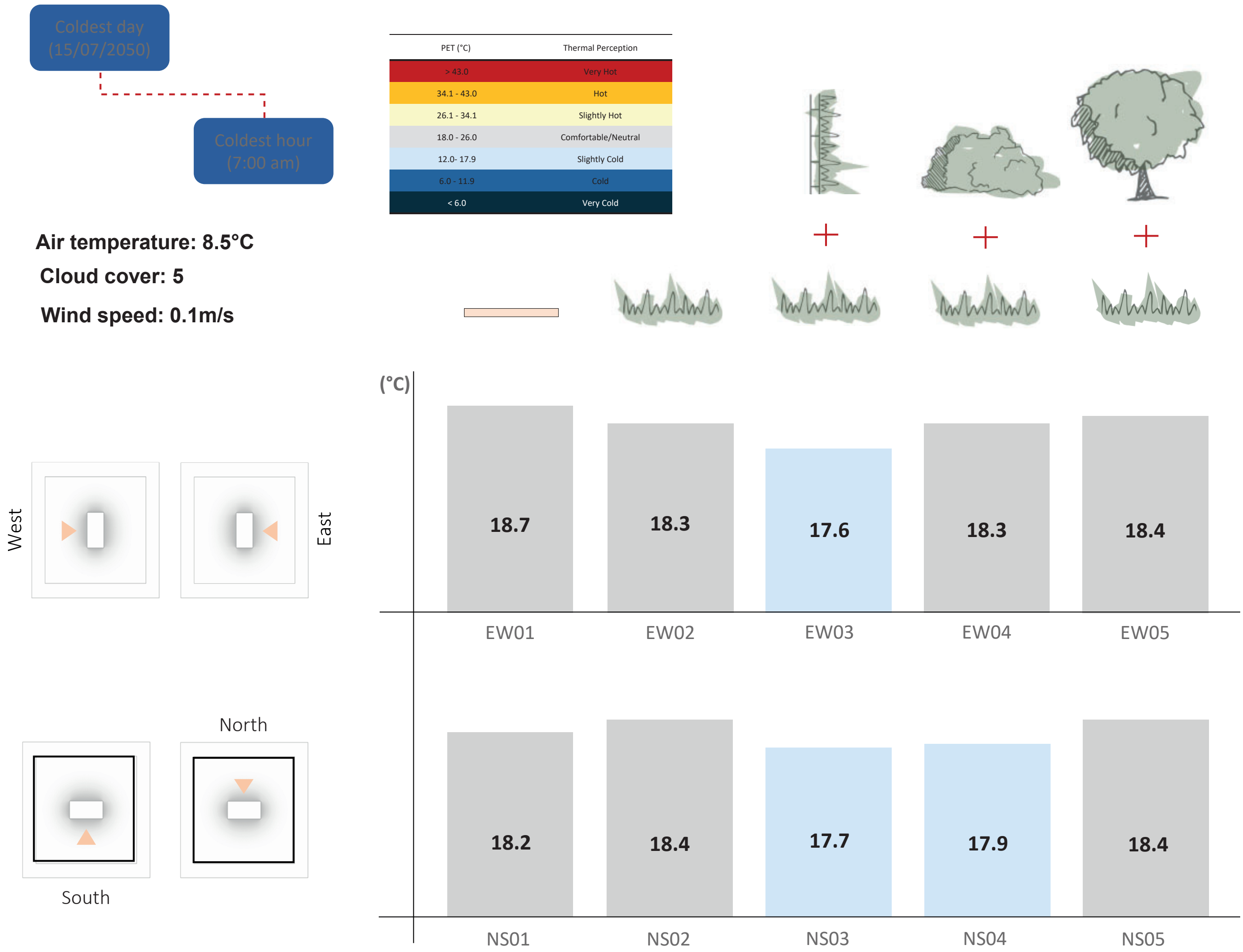

Figure 6.9.25 - Sketch diagram showcasing the PET values on NS and EW cases within the cold day and colder hour (°C).

COMPARISON BETWEEN DAYS

All sixty scenarios studied in this analytical work show the cluster of trees with grass performing well in each studied hour. The results confirm trees as the best overall SGI component for a more constant thermal perception in different weather conditions. In more detail, the cases with trees and grass (NS05 and EW05) during the hours with higher air temperatures always showcased lower PETs than others. On the coldest hour of the coldest day, the NS05 and EW05 have an average PET value equivalent to the other case, with values still within the no thermal stress band. In conclusion, trees reduce the thermal amplitude during the day, bringing temperatures mostly inside the comfortable thermal band: 18°C to 26°C. Furthermore, when considering the average thermal comfort band (22°C), NS05 and EW05 weighted average values remained constantly closer to it.

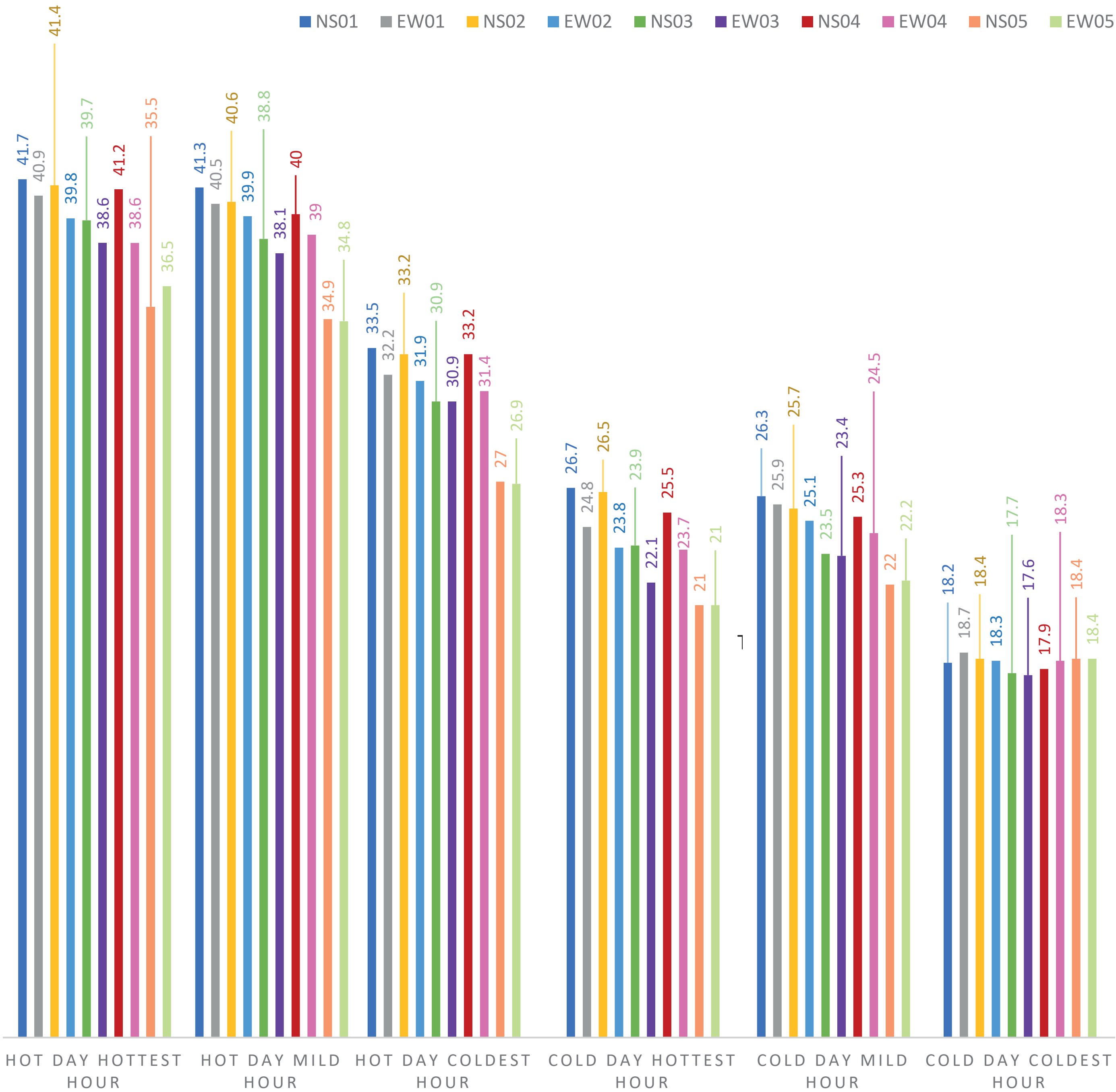

Figure 6.9.26 -Graph showcasing the PET values on NS and EW during the six studied hours (°C).

MAIN OUTCOMES

- The cluster of trees is shown to be the best small-scale green infrastructure to enhance thermal comfort.
- Overall, the 2 m-high living walls perform better than the 1m hedges.
- Hard pavement and only grass have similar performance. However, hard surfaces exposed to solar radiation on extremely cold periods could perform better than grass.
- Higher wind movement is an important variable in increasing psychological thermal comfort during most hours of the year. However, it is not as essential as providing shaded areas.

6.9.3. INHALABLE PARTICULATE MATTER

This section focuses on the weighted average concentration found on each case inside the site. The air quality benchmark is extracted from CETESB, the environmental company of the State of Sao Paulo, which evaluates the pollution levels within the cities in the state. CETESB data was discussed in Chapter 05 to indicate the pollutant input for EMEF Amorim Lima Analytical research. The 6.7.2 section of this chapter also thoroughly discusses the data collected by the mentioned environmental company. Besides recording data, CETESB evaluates air quality conditions and produces annual air quality reports. The last report on the Company's website is from 2022 (CETESB 2022), with different benchmark tables. Most of the public students in the state (as discussed in Chapter 3) are under a half-day learning system. Thus, the concentration of Pm2.5 pollutants will be assessed based on the short-time exposure parameters (below 24 hours) shown below.

Air Quality	PM2.5 concentration	What it means
N1 - GOOD	0 - 40	
N2 - MODERATE	41 - 80	People from sensitive groups (children, the elderly and people with respiratory and heart diseases) may experience symptoms such as dry cough and tiredness. The population, in general, is not affected.
N3 - BAD	81 - 120	The entire population may experience symptoms such as dry cough, tiredness, burning eyes, nose and throat. People from sensitive groups (children, the elderly and people with respiratory and heart diseases) may experience more serious health effects.
N4 - VERY BAD	121 - 200	The entire population may experience worsening of symptoms such as dry cough, tiredness, burning in the eyes, nose and throat, as well as shortness of breath and wheezing. Even more serious effects on the health of sensitive groups (children, the elderly and people with respiratory and heart diseases).
N5 - TERRIBLE	>200	The entire population may be at serious risk of respiratory and cardiovascular diseases. Increase in premature deaths in people from sensitive groups.

Figure 6.9.27 - Diagram showcasing the PM2.5 values on NS and EW cases within the hot day hottest hour (ug/m3).

HOT DAY AT THE HOTTEST HOUR (HH)

This hour showcases lower levels of PM2.5 in the cases with boundary walls (NS) compared to the open sites (EW). The North/South cases have a slight difference of 4.8 µg/m3 from the least to most polluted ones. The cases without vegetation also show lower pollutant concentrations: 22.8 µg/m3 (NS01) and 39.8 µg/m3 (EW01). EW01, without vegetation, is the only within EW cases (without boundary walls) to present the mean average PM2.5 concentration below 40 µg/m3, considered "good" by CETESB (2022). All NS cases (with boundary wall) demonstrate weighted average results inside the good air quality band. Also, within the mentioned cases (NS), the scenario with trees (NS05) has the worst result, with 27.6 µg/m3. The mentioned result is expected due to the potential of trees (higher density) to trap pollutant particles, as shown in the literature review in Chapter 01, in addition to EMEF Amorim Lima's fieldwork and analytical works (chapters 04 and 05). Conversely, the East/West studied situations (with no boundary walls) reveal a different pattern. The grass with hedges case (EW04) has the worst mean average PM2.5 concentration. The poorest results after EW04 are EW03 (with living walls) and EW02 (only grass). However, within the EW cases with vegetation, the trees` scenario performs best: 41.6 µg/m3. These results suggest that trees could function as a barrier to prevent more pollutant particles from entering the site without a boundary wall. The obstruction effect previously mentioned could also be observed in the living wall scenario (EW03), which is 2m in height and performs better than the EW04 (hedges with 1m in height). It is important to note that the East/West cases with greenery are inside the moderate air quality condition band, according to CETESB (2022). This indicates that sensitive groups could present symptoms due to short exposure to this pollutant concentration.

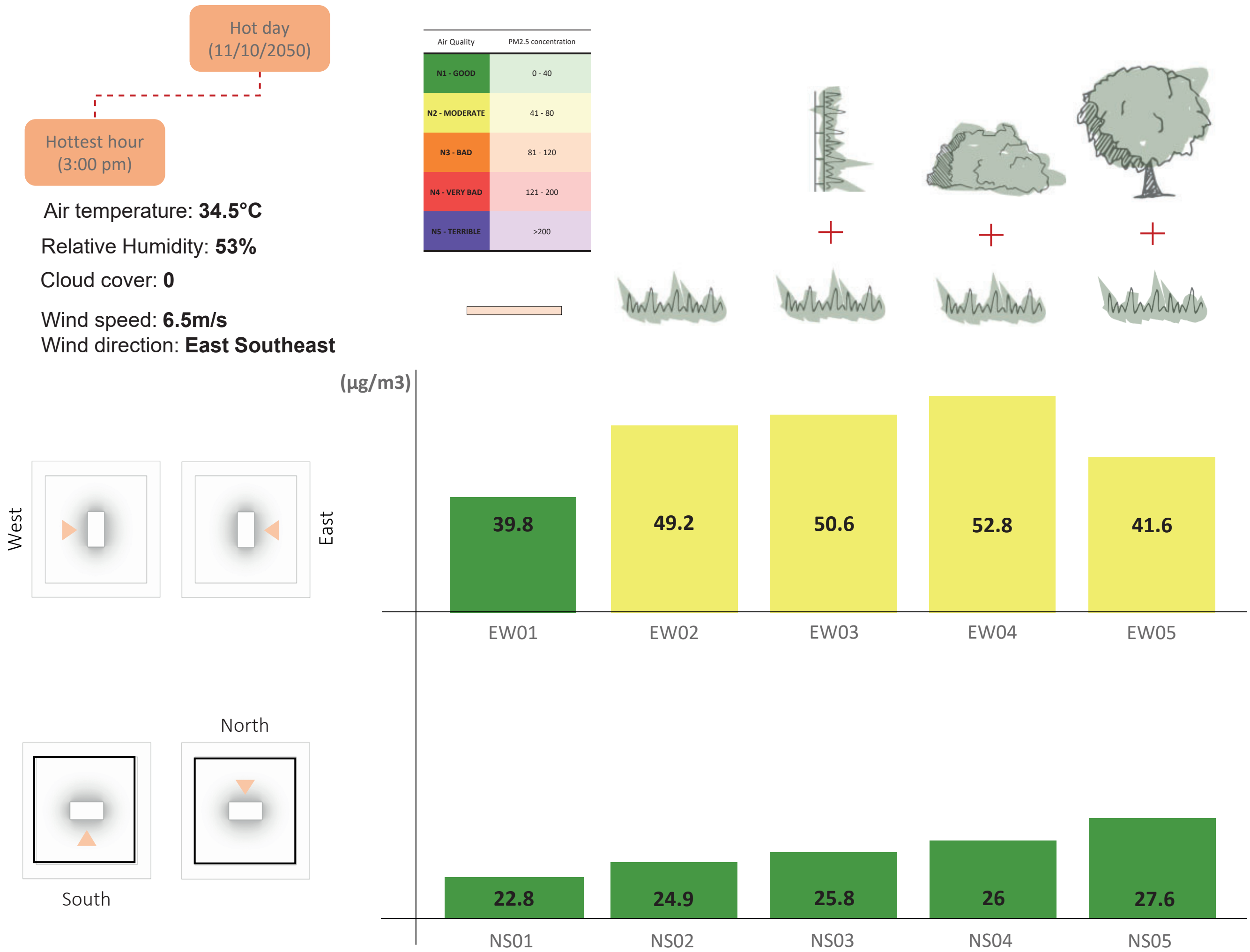

Figure 6.9.28 - Diagram showcasing the PM2.5 values on NS and EW cases within the hot day hottest hour (ug/m3).

HOT DAY AT THE AVERAGE HOUR (HA)

The average hour (HA) is characterised by a lower air temperature of 9.3°C, a 30% higher relative humidity, and a 3.9m/s lower wind speed than the hottest hour (HH). These climatic differences result in mean average PM2.5 concentrations twice as high in each scenario. The simulated weighted average values are considered moderate (41 µg/m3 to 80 µg/m3) for the boundary wall cases (NS). For the EW scenarios (without the wall), the results indicate bad air quality (81 µg/m3 to 120 µg/m3). The correlations between the results shown below and the ones in the hottest hour (previous page) are largely consistent during this period, except for NS04 (with solid barriers and hedges), which records lower PM2.5 concentrations than the living wall case (NS03). The result could be exemplifying the protective impact of boundary walls.

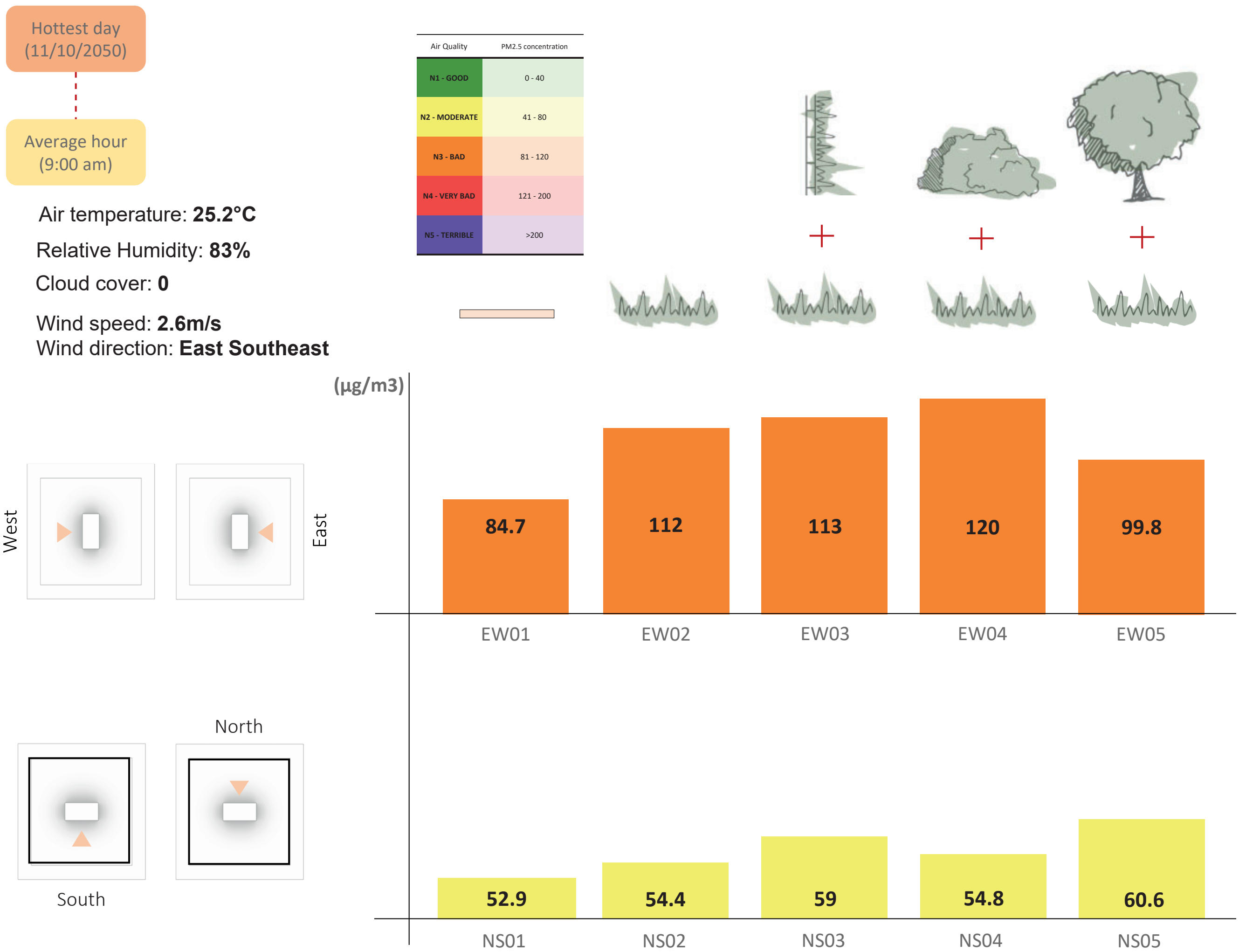

Figure 6.9.29 - Sketch diagram showcasing the PM2.5 values on NS and EW cases within the hot day mild hour (ug/m3).

HOT DAY AT THE COLDEST HOUR (HC)

The dry bulb temperature drops 5.8°C at this hour compared with the average one (HA). However, the results are similar to those of the last studied period, being within the same range of bad to very bad air quality (CETESB, 2022). Once again, the EW cases present much higher PM2.5 concentration levels than the NS. However, the North/South cases, besides those with trees, have similar pollutant concentrations within most cases: NS01 to NS04. However, once more, NS04 performs better, even if slightly. Finally, once more, the NS05 (with trees) has the worst air quality: 74.2 µg/m3 mean average concentration. Another repeated result from the previous studied hours is that the trees are not the worst-performing SGI component within EW scenarios. Yet, hedges perform better than living walls for the first time, even if slightly (1µg/m3).

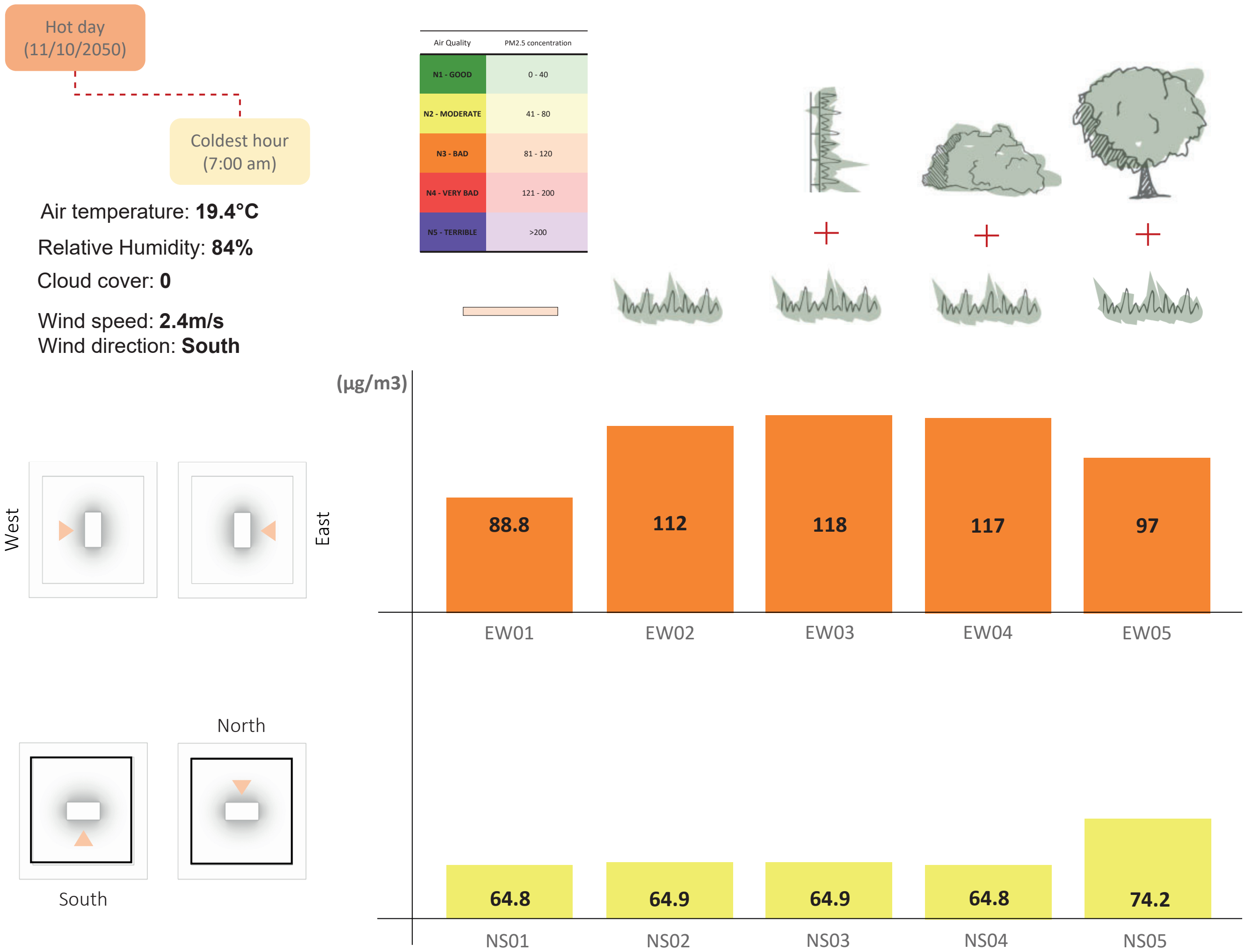

Figure 6.9.30- Sketch diagram showcasing the PM2.5 values on NS and EW cases within the hot day coldest hour (ug/m3).

COLD DAY AT THE HOTTEST HOUR (CH)

At this hour, with an air temperature of 17.1 °C, the air quality is equivalent to the coldest hour of the hot day (HC) (19.4°C air temperature). PM2.5 average values still range from bad to very bad air quality parameters (CETESB, 2022). However, EW01 and EW05 show lives below 80 µg/m3, having moderate performance. The East/West cases are again higher than the North/South cases, and the concentration difference between elements is similar. For the second time, the EW03 (living walls) performs worse than hedges, now with a 3.7µg/m3 difference. Unexpectedly, the hedge scenario (EW05) performs even better than only grass (EW02). Furthermore, the NS04 has the lowest mean average concentration within situations with vegetation, which was also exhibited during the intermediate and coldest hours of the hottest day. This studied period is colder (2.3°C lower), 27% less humid and has a 0.3m/s lower wind speed compared to the coldest hour of the hot day, having the same unobstructed sky conditions. The mentioned climatic differences between studied hours result in a minimal 15µg/m3 mean average PM2.5 concentration difference within cases with the same orientation and vegetation elements. Finally, for the third time, NS04 (grass, hedges and boundary walls) performs better than NS03 (grass, living walls and boundary walls).

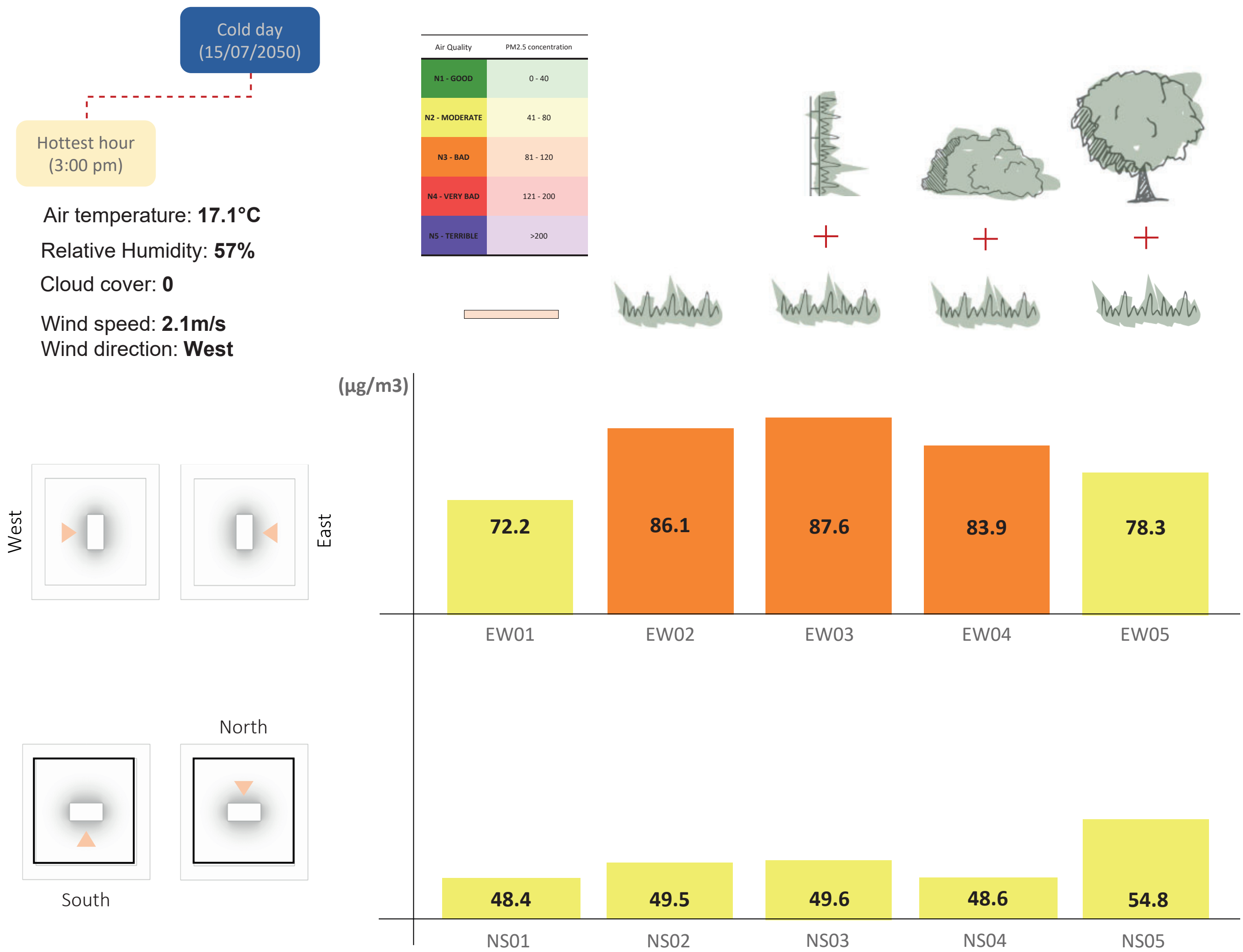

Figure 6.9.31 - Sketch diagram showcasing the PM2.5 values on NS and EW cases within the cold day hottest hour (ug/m3).

COLD DAY AT THE AVERAGE HOUR (CA)

The climatic conditions at this studied hour contrast most significantly to the previously discussed periods: 11.5°C air temperature, 88% relative humidity, cloud coverage of 04 oktas (partially clouded sky) and a 0.6m/s wind speed. It is the first period where very bad (121 μg/m3 to 200 μg/m3) and terrible (>200 μg/m3) air conditions are registered. Naturally, the cases without walls are within the terrible band, while the ones with walls are within the very bad band. Additionally, it is also the first period within the East/West scenarios, where the one with grass (EW03) has a higher PM2.5 concentration than the living walls (EW03) and the hedges (EW04). This hour also registers the worst air pollution concentration in EW05 (trees without boundary walls). Similar to the HH and HA (hot day hottest and average hours), the EW04 (hedges) have a higher mean average PM2.5 concentration than living walls (EW03). Within the North/South scenarios, the one with trees (NS05) also performs worst, as in all previously studied hours. However, NS05, the case with solid barriers, has a mean average PM2.5 concentration of 191 μg/m3 against 241μg/m3 in EW05 (without walls). There is a correlation between the coldest hour of the hot day and this studied period: both have the same resultant value in the cases NS02 and NS03, in addition to NS01 and NS04. NS01 (hard pavement) and NS04 (grass and hedges) have a mean average pollutant concentration of 64.8μg/m3 on the coldest hour of the hot day.

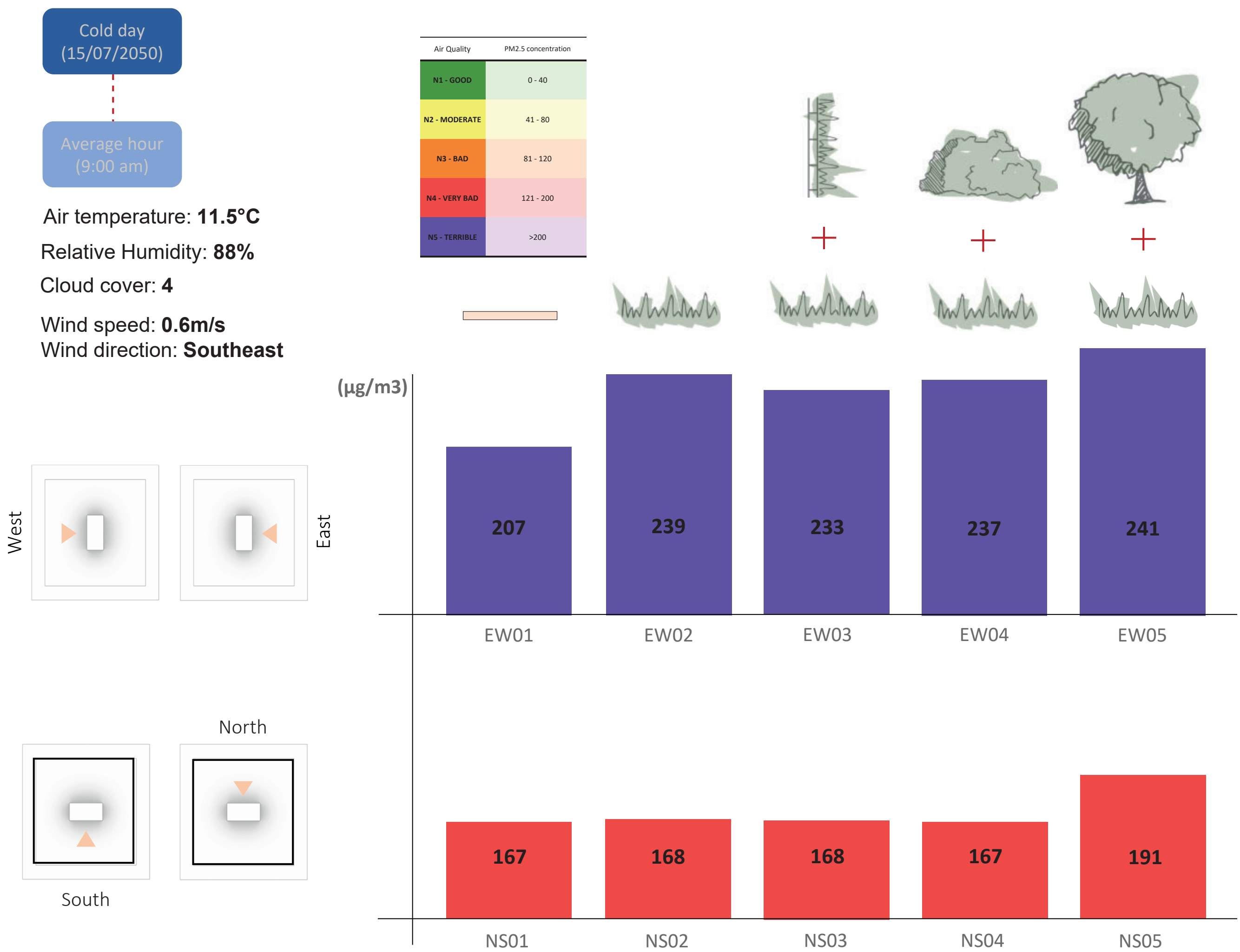

Figure 6.9.32 - Sketch diagram showcasing the PM2.5 values on NS and EW cases within the cold day mild hour (ug/m3).

COLD DAY AT THE COLDEST HOUR (CH)

This period has PM2.5 results higher than the value considered by CETESB as terrible: 200µg/m3 in all scenarios. Higher values than 200 µg/m3 are only exhibited on the East/West cases (without boundary walls) in the previously discussed hour. However, the cited scenarios within this hour are two times higher than the average period. Concerning the climatic conditions, this coldest period has an air temperature of 8.5°C, 0.1 m/s wind speed, 100% humidity and a cloud coverage of 05 oktas. Moreover, within EW, the worst-performing scenarios are the EW03 (living walls) and EW04 (hedges) with a pollutant mean average concentration of 473µg/m3, followed by the case with trees (EW05): 458µg/m3. Finally, within NS, the scenario with hedges (NS04) is the worst, with 414µg/m3 and, subsequently, the NS03 (living walls) and NS05 (trees): 408µg/m3. It is the first period where trees are not the worst-performing SGI component in cases with boundary walls (NS).

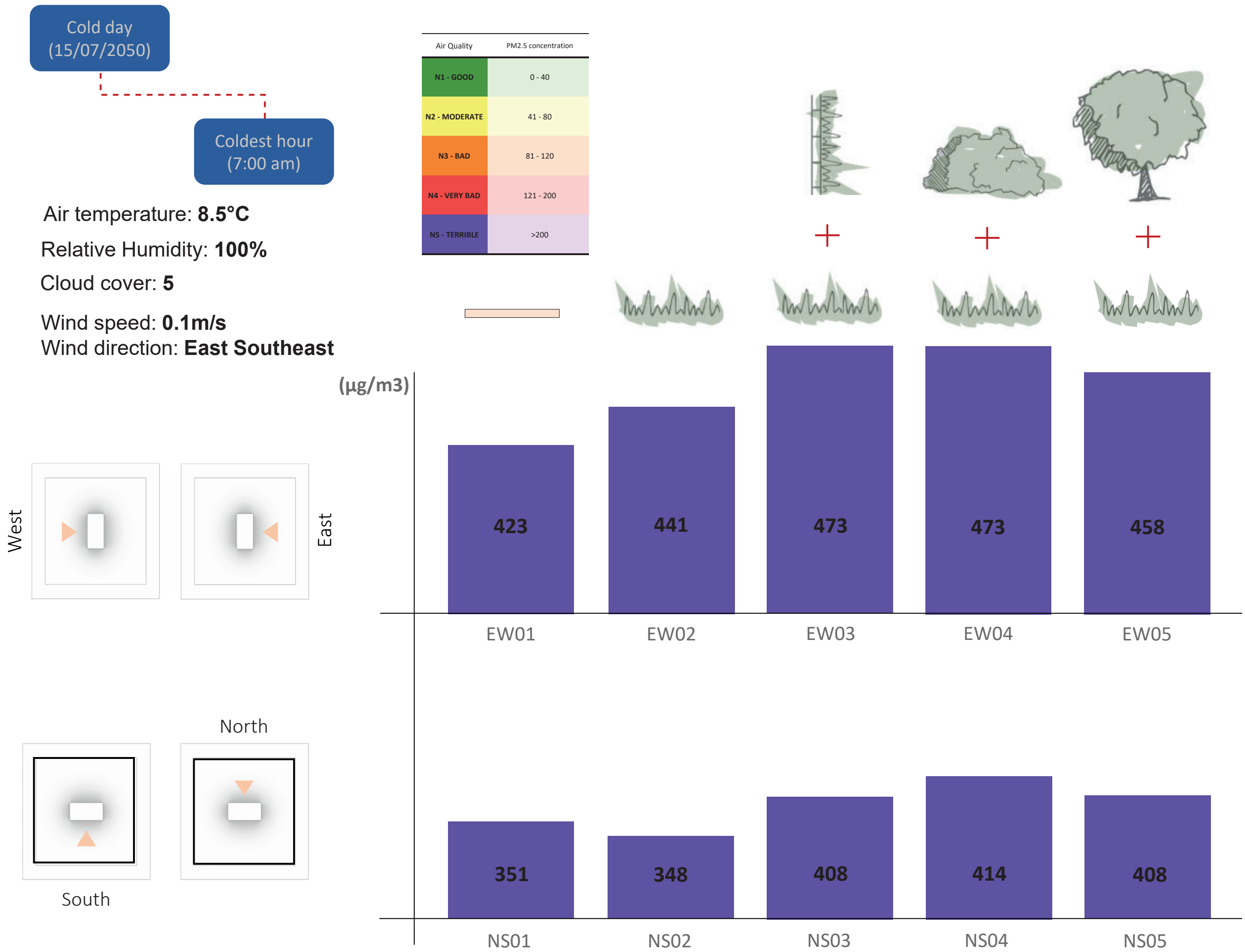

Figure 6.9.33 - Sketch diagram showcasing the PM2.5 values on NS and EW cases within the cold day mild hour (ug/m3).

COMPARISON BETWEEN DAYS AND DISCUSSION

The input PM2.5 value into the source points around the site (as explained in the methodology) is 60µg/m3. Moreover, the mean average pollutant concentration varies from 22.8µg/m3 to 473µg/m3 within all the scenarios and six studied hours. The mentioned range of results combined with the analysis of climatic and morphological variables proves the extreme impact of air movement on the dispersion and detention of pollutant particles. To conclude, the higher the wind speed, the lower the pollution concentration. However, as the colder hours also displayed exceptionally low wind velocities, the analytical work cannot establish the accurate impact of air temperatures on the PM2.5 concentrations. The difficulty in establishing the pattern between different temperatures is also spotted when analysing the days with similar wind speeds. In more detail, there are three studied hours with similar wind velocities: 2.6m/s, 2.4m/s and 2.1m/s, with similar PM2.5 results.

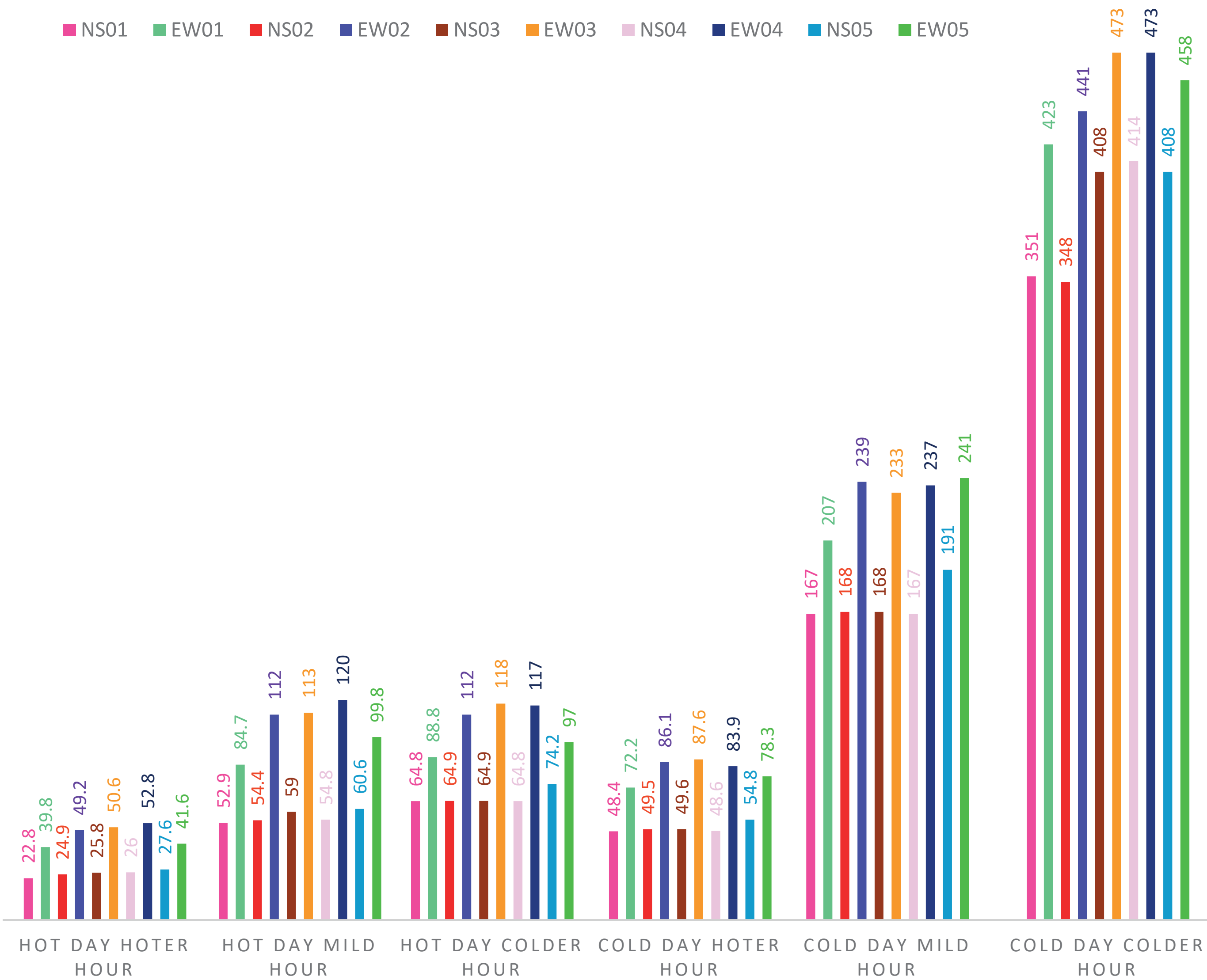

Figure 6.9.34 - Graph showcasing the PM2.5 values on NS and EW during the six studied hours (ug/m3).

The studies also proved the effectiveness of the 2m solid barriers near pollution sources in reducing their concentrations within scenarios at 1.5m height from the ground (studied level). For example, the East/West scenarios (with solid boundary walls) display a higher variance between cases than the NW ones (with borders composed of vegetation). The boundary wall is removed from the East/West scenarios and maintained in the North/South ones (as discussed in the methodology) to record the impacts caused by this built element. This adds a morphological variable to the EW cases, making it impractical to affirm whether different aperture orientations (NS and EW) impact pollutant distribution. Furthermore, within the cases without boundary walls (EW), the hedges and grass (EW04) scenarios had the worst results in four out of the six studied hours. The poor performance of hedges may be due to their density and height. In this study, this element is only one meter in height and has a high LAD (leaf area density), as explained in section 6.4.2. Thus, the component probably traps pollutants particles while not acting as an efficient barrier to pollutant sources. The worst performance is followed by EW03, with living walls and grass without solid walls. In this study, the living wall is an element of the same density as the hedges with a 2m height (also explained in section 6.4.2.). The height difference could be trapping more pollutants around the terrain's border and avoiding higher concentrations within the site. Finally, scenarios with trees, grass, and no boundary walls (EW05) have the worst air quality performance in one of the studied hours. The results above indicate that vegetation at the users' height will further reduce air quality when no built protection exists.

The findings illustrate the potential of different small-scale green infrastructures to reduce the air quality of a space. The potential is enhanced when there aren't boundary walls, a physical barrier against pollutant sources. The importance of a built barrier to achieve better air quality results in NS cases raises the question of how EW scenarios would perform with its addition. This question is answered in the next section (6.10). However, even when there is a solid barrier between pollution sources and green elements, the SGI will still increase pollutant concentrations. This thesis's results have been connected to their capacity to reduce wind speeds. Air movement is proven to be the main variable increasing pollution concentration. Yet studies also suggest that lower dry bulb temperatures are also responsible for reducing air quality. Shin et al. (2021) have already associated lower temperatures with higher pollution risk. Other studies have explored the effect of temperatures on pollution and aggraved mortality (Wine et al., 2022). For example, Vaishali, Verma, and Das (2023) established a strong negative impact on pollution with temperature during high humidity conditions. Furthermore, as the methodology section explains, high pollutant concentration episodes occur only during a reduced portion of the year. Consequently, the question of whether the small-scale green infrastructure would perform the same during hours with lower pollution levels is established. This will be answered in the next section of this chapter (6.10).

MAIN OUTCOMES

- Without boundary walls, the air quality is always worse inside the studied site.
- Low air movement is extremely negative to air quality.
- Low dry bulb temperatures, high humidity and sky coverage are other variables probably connected to higher particulate matter concentration.

Cases with boundary walls (NS):

- The cluster of trees is the SGI component with the best performance on days with higher wind movement.
- On days with minimised air movement, only grass scenarios perform better.

- Overall, living walls and hedges had similar performances. However, the hedges are the worst performance case for four of the six studied hours.

Cases without boundary walls (EW):

- The cases with trees were the worst within five studied hours, with hedges being the worst at the coldest hour.

- Hedges, living walls and grass had similar outcomes. The living walls were the worst case after the trees for three of the six hours.

6.10. FURTHER ANALYSIS

6.10.1. THE EXERCISE

This section of this doctoral research aims to answer the questions raised in the studies of this chapter's analytical exercises. As previously mentioned, the cases where the building openings are oriented to the East and West are studied only without the boundary walls. Thus, this section explores all the EW scenarios by adding the same solid walls used in the NS cases. As shown in the results, the coldest hour has the higher PM2.5 concentrations due to the low wind speed of 0.1m/s. Consequently, the coldest hour of the cold day is chosen to simulate the EW scenarios with boundary walls. Another question concerned the isolated impact of wind speed, air temperature and sky conditions. Hence, the North/South cases are studied once more in the hottest hour of climatic conditions. However, the wind speed is set to be 0.1m/s, the same input in the coldest studied hour, instead of 6.5m/s. Furthermore, the NS scenarios are simulated in the coldest hour, with 6.5m/s wind velocity instead of 0.1m/s. The high levels of pollution input and the knowledge of many public-school contexts having a lower pollution concentration in some periods of the year led to the final question. This is how the same scenarios would perform in a case with less PM2.5 input. The new input value is established based on the data collected by CETESB (2022). The data shows cities within the metropolitan region of Sao Paulo with daily averages of the minimum value of 5µg/m3. The mentioned value is selected as the input for the new batch of simulations to represent low air pollution scenarios.

6.10.2. RESULTS

EW WITH BOUNDARY WALL ADDITION

The results of the EW scenarios with the addition of boundary walls exhibit an expected reduction of the mean average pollution concentrations within the site. Even with the addition of the boundary walls, the PM2.5 concentration levels within EW scenarios were still higher than the NS ones (also with boundary walls). However, the values between NS and EW were much closer than before. The relations between cases were the same between EW with and without boundary walls, except for the living wall case (EW03) and the scenario without greenery (EW01). In more detail, the EW03 with boundaries has a lower PM2.5 concentration (414 µg/m3) than the EW04 (hedges): 420 µg/m3. On the other hand, the living wall (EW03) and hedges (EW04) scenarios without boundary walls registered 473µg/m3. Finally, the case without boundaries and no applied greenery (EW01) has a lower mean average PM2.5 (423µg/m3) than the case with grass (EW02), with 441µg/m3. However, when the boundary wall is added, the EW01 (no greenery) has a higher pollutant concentration (387µg/m3) than EW02 (grass), with 376µg/m3. The results of this new set of simulations confirm the positive impact of having barriers between pollution sources and green elements to enhance air quality. The effect is less expressive in shorter vegetation (hedges and grass) cases. The results also showcase how the arrangement of the built and natural space can change, even in a small percentage, the overall air quality of an environment within identical microclimatic conditions.

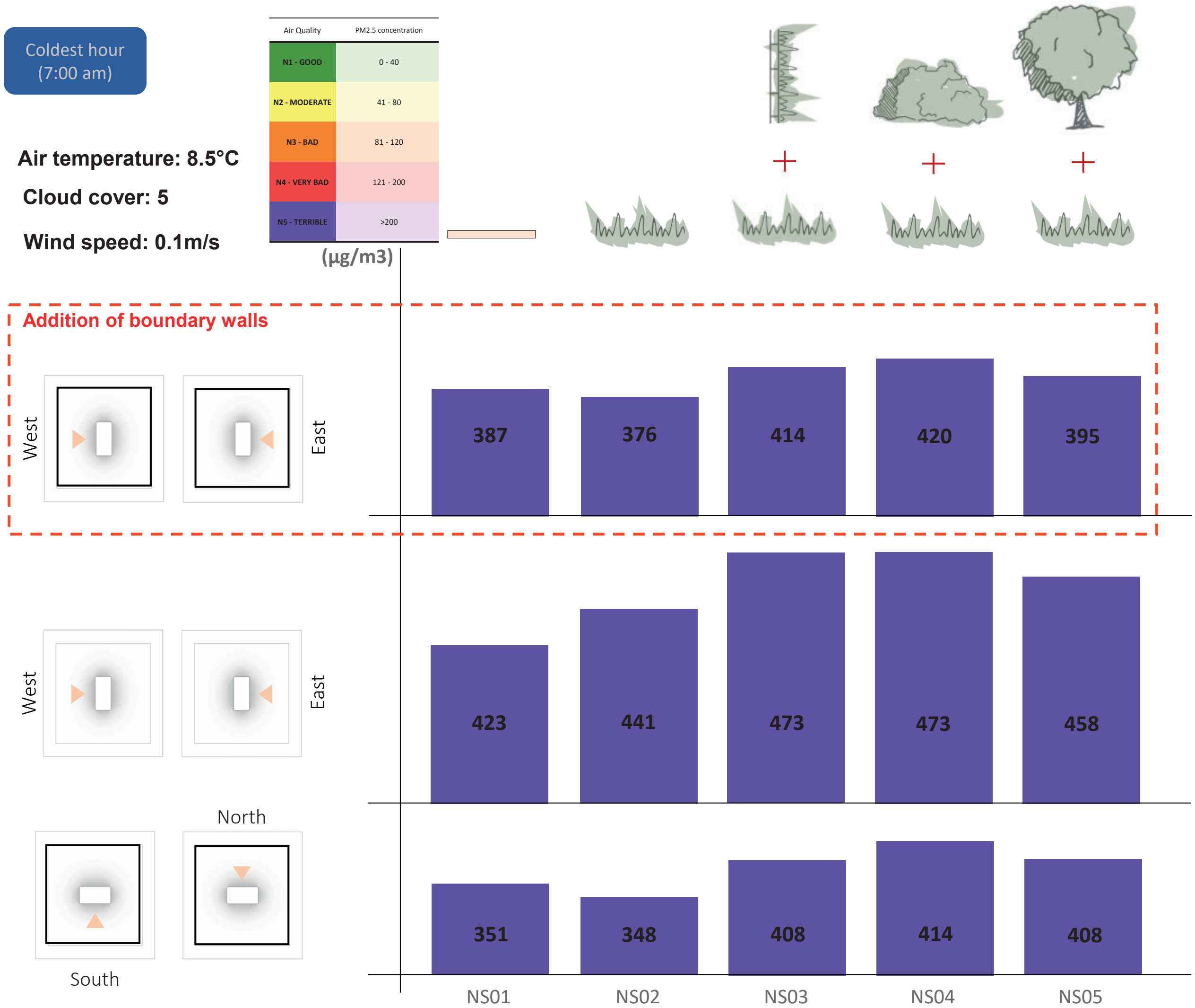

Figure 6.10.01 - Graph showcasing the PM2.5 values on NS and EW with and without boundary walls within the coldest hour (ug/m3).

ALTERING THE WIND SPEEDS

The later set of analytical simulations displays an increase of 69% to 75% of PM2.5 concentration within cases when the air movement is reduced from 6.5m/s to 0.1m/s. The mentioned results occur within the hottest hour of the hot day with an air temperature of 34.5°C. According to the CETESB benchmark (2022), the scenarios that before showed good air quality are now considered bad when diminishing wind speed. Moreover, during the colder period of the cold day, there is a significant decrease in the pollutant concentration when the air movement is increased to 6.5m/s. At the mentioned hour, the decline is 90% to 93% within the scenarios. In this case, all the scenarios had a weighted average value significantly above 200 µg/m3 (terrible air condition). With the air movement enhancement, the value drops below 40 µg/m3 (good air conditions). The results confirm how reduced wind movements decrease PM2.5 concentra-

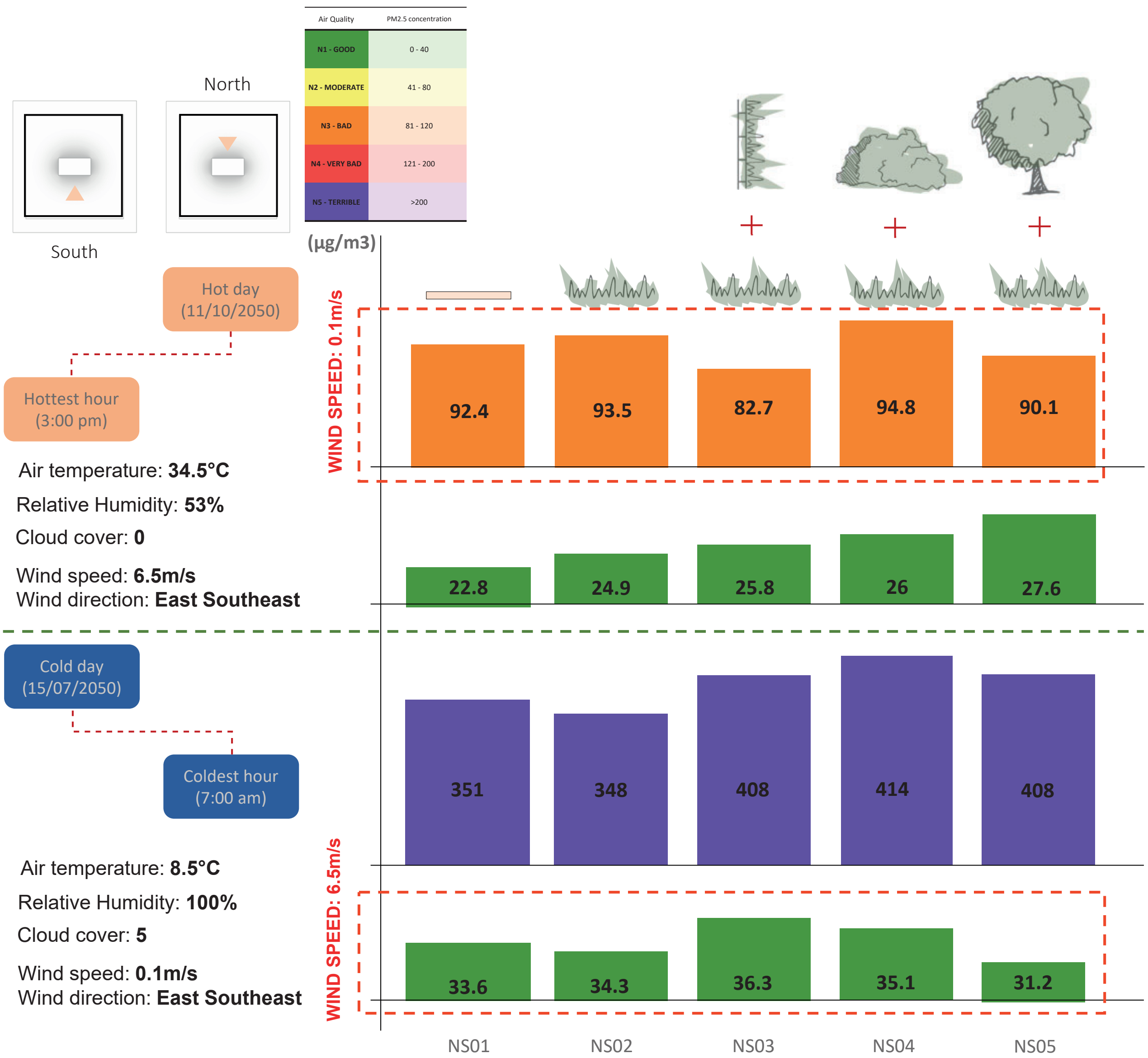

Figure 6.10.02 - Graph showcasing the PM2.5 values on NS within the cold day's coldest hour and hot day's hottest hour with the change of wind speeds (ug/m3).

tions independent of the other climatic conditions. However, the results also show that a decrease in wind speed has a more significant negative impact in the coldest hour than in the hottest. Furthermore, the coldest hour is also 47% more humid with higher cloud coverage. Consequently, the results prove that higher relative humidity and sky coverage will increase particulate matter concentrations even with the same wind speed.

LOWER POLLUTION (PM2.5) INPUT

Compared to the original simulations, the EW cases with a lower input of PM2.5 display 83% to 86% lower pollutant concentrations within scenarios. Regarding the NS scenarios, the difference is 84%. Additionally, the NS has the exact correlation between cases: NS04 has the highest concentration, followed by NS03, NS05, NS01, and finally NS02. However, between EW cases, when the pollution levels are lower, the EW02 (grass) performs better than the hard pavement (EW01). Finally, both NS and EW scenarios move from terrible to moderate air quality conditions according to CETTESB (2022) standards. The results suggest that the performance of each SGI element will be similar independently of the level of source pollution. Additionally, the importance of the solid barrier against sources to enhance air quality within the vegetated areas is maintained.

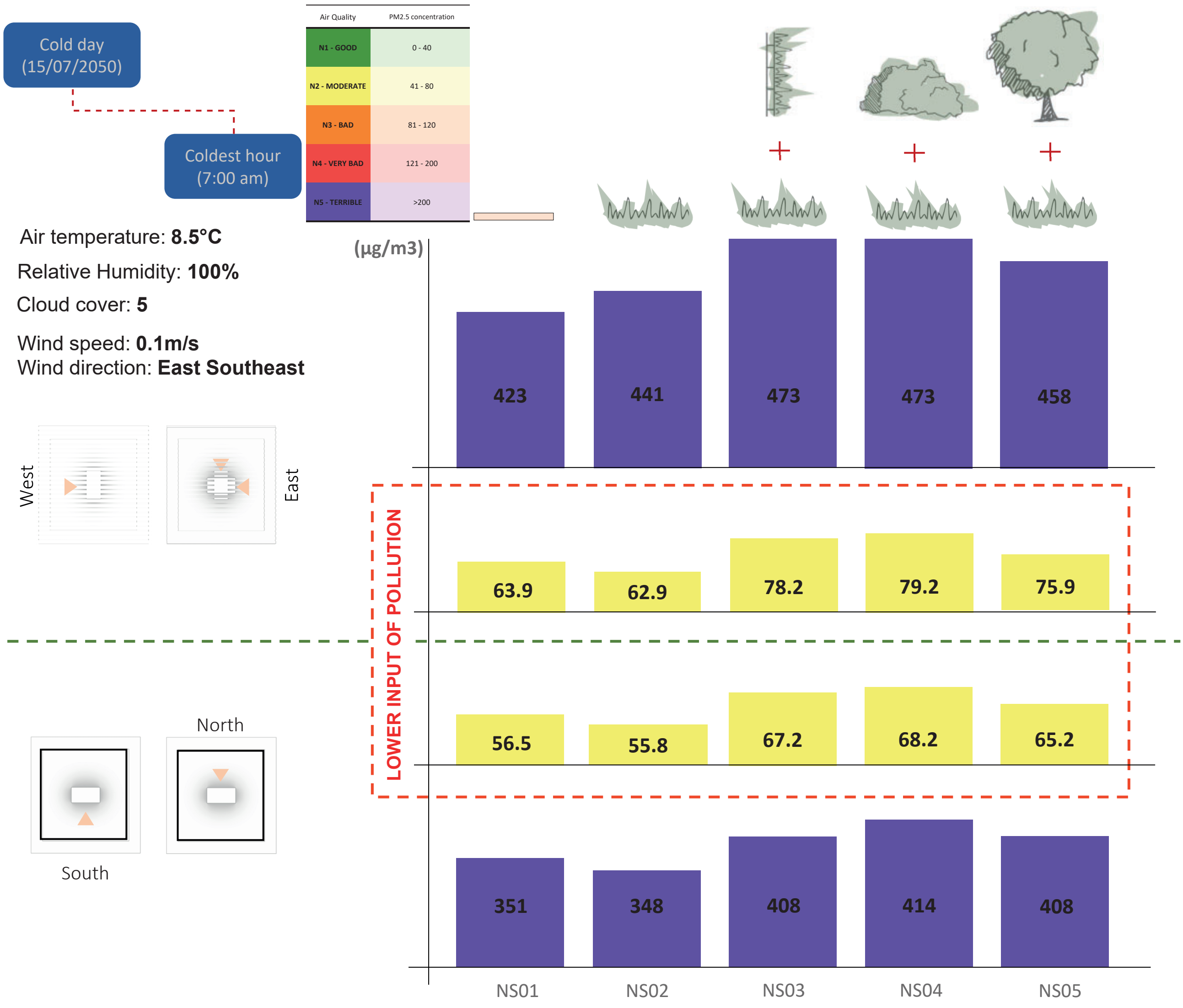

Figure 6.10.03 - Graph showcasing the PM2.5 values within the cold day's coldest hour with a lower pollution input (ug/m3).

MAIN RESULTS

- Boundary walls are confirmed as having the best performance.

- The importance of the location of green elements and other morphological characteristics in defining a space's final air quality.

- Wind movement is the most important variable in defining pollutant concentration.

- Weather conditions such as dry bulb temperature, covered sky, and relative humidity have a greater direct impact on air pollution. Sunny, less humid, and warmer days improve air quality conditions.

- The pollutant particle concentration, regarding different SGIs, will perform similarly within days with higher and lower air pollution sources.

6.11. THE ENVIRONMENTAL PERFORMANCE MATRIX: MAIN OUTCOMES

This version of the matrix has the architectural and SGI components and studied scenarios presented previously in this chapter in the first version. In addition, the main outcomes graphs are added. Hence, this section demonstrates the Environmental Performance Matrix with the results and discusses its main outcomes.

MAIN OUTCOMES

- For most of the studied hours, the best pollution performance is for the scenarios without vegetation, specifically NS01.

- NS01 (no vegetation) has the lowest PM2.5 concentration in the hottest hour of the day: 22.8ug/m3.

- NS01's PET (Physiological Equivalent Temperature) performance during the hottest hour is the worst: 89% above the average thermal comfort.

- The best thermal comfort performance within the hottest hour is in NS05 (with trees and grass), still 61% above the average comfort line.

- EW05 has the best thermal comfort performance for HM, HC, and CM (the mildest and coldest hours of the hot day and the mildest hour of the cold day).

- On the coldest day, the case with no vegetation has the best thermal performance, followed by the case with trees. Living walls have the worst performance.

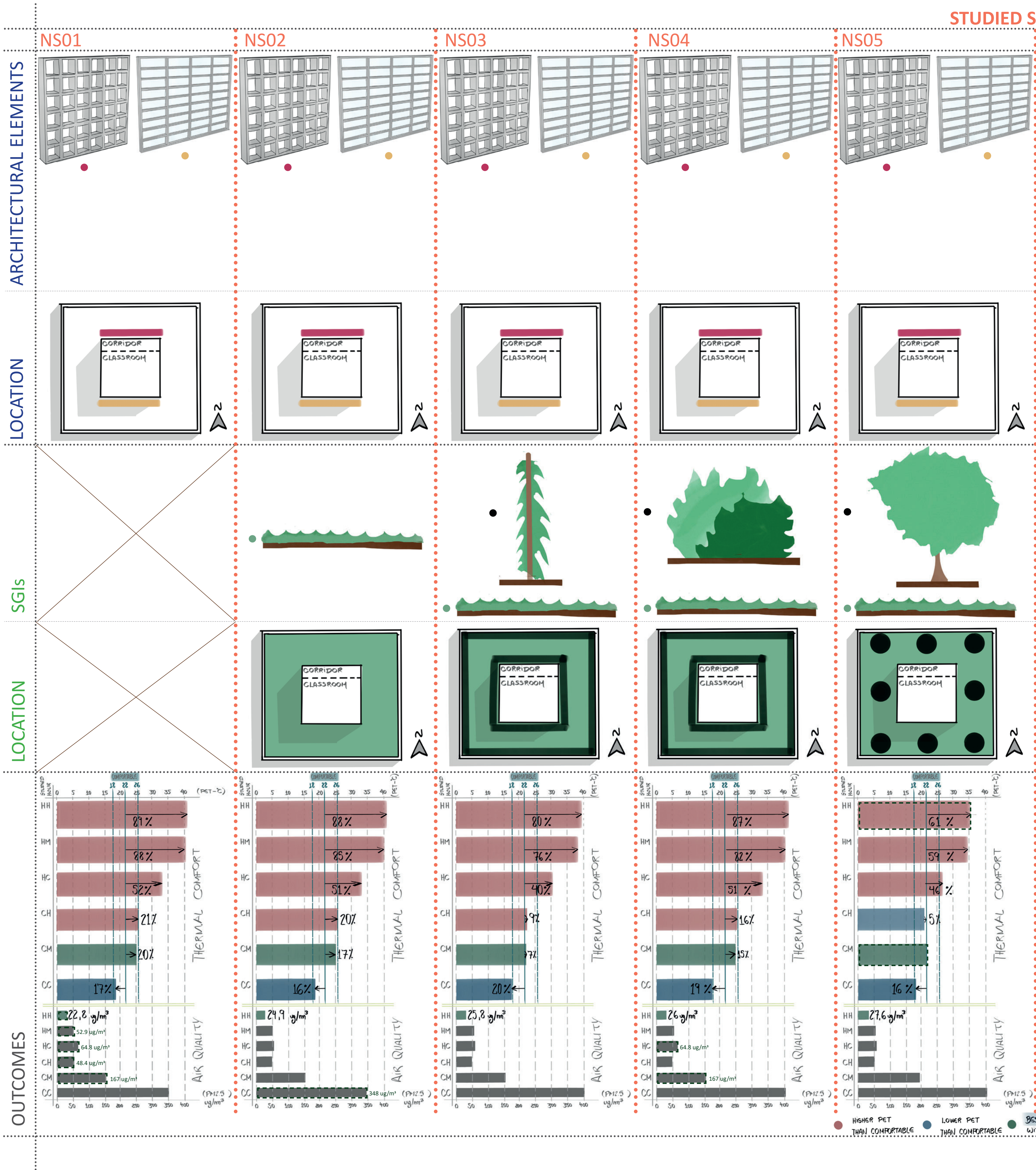

Figure 6.11.01 - Diagram of the 2nd Version of the Environmental Performance Matrix, with the main outcomes addition.

CENARIOS

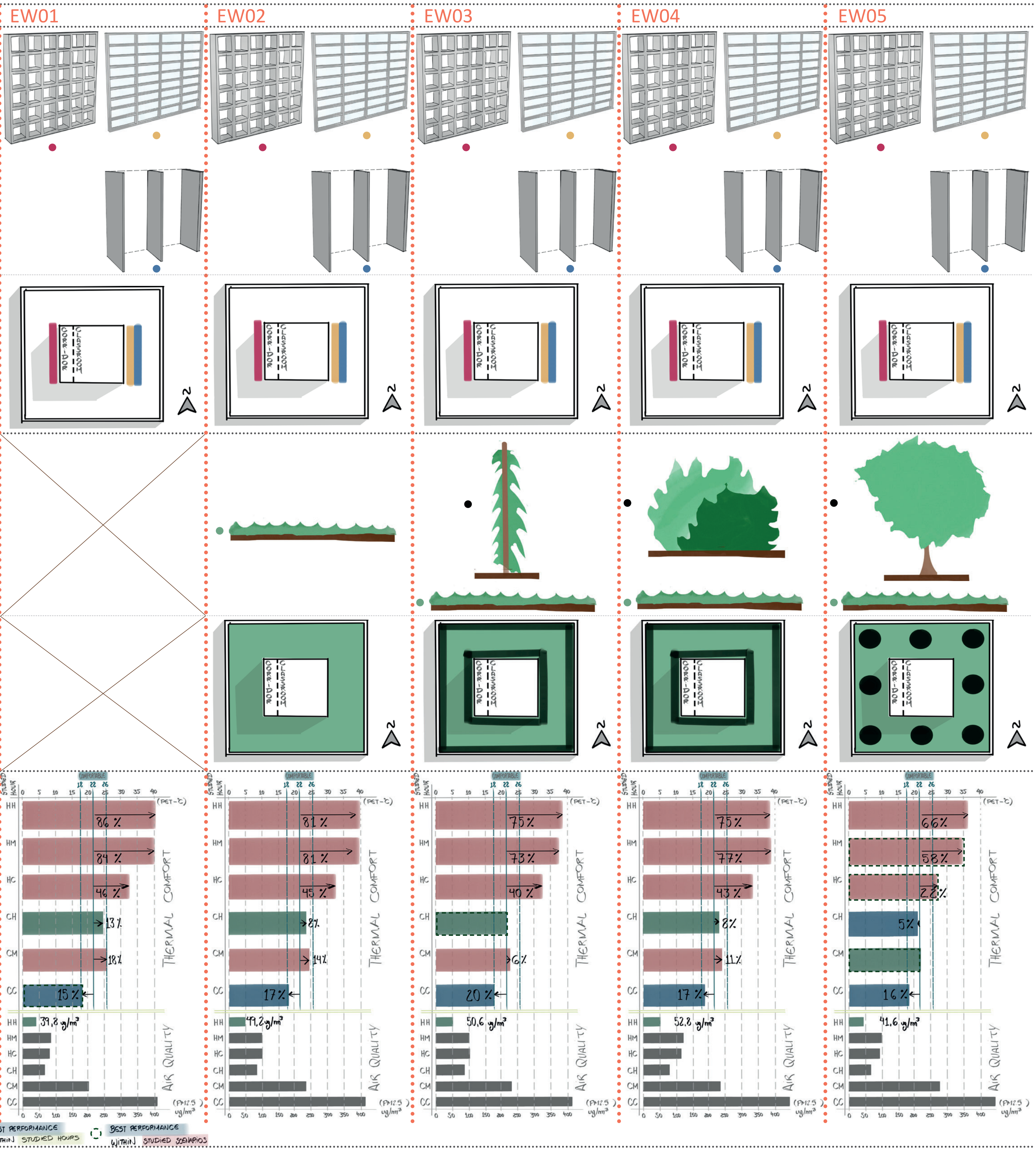

EW01
EW02
EW03
EW04
EW05
THERMAL COMFORT
AIR QUALITY
(PET-°C)
(PM2.5) ug/m³
86 %
84 %
46 %
13%
18%
15 %
39,8 ug/m³
81 %
81 %
45 %
8%
14%
17 %
49,2 ug/m³
75 %
73 %
40 %
6%
20 %
50,6 ug/m³
75 %
77 %
43 %
8%
11%
17 %
52,8 ug/m³
66 %
58 %
22 %
5%
16 %
41,6 ug/m³
BEST PERFORMANCE WITHIN STUDIED SCENARIOS

6.12. CONCLUSION

This chapter establishes the relevant architectural and SGI components of interest to this doctoral research, which are then studied in depth. This chapter meticulously explains the reasons for choosing the mentioned elements through the examples of public schools in Sao Paulo (extensively reviewed in Chapter 3) and the example of School EMEF Amorim Lima (studied in chapters 04 and 05). This chapter then establishes the periods of study based on harsher and milder future conditions. The method section concludes with the Environmental Performance Matrix, presenting the scenarios simulated in this chapter's analytical work. Afterwards, there are four main strategies to analyse the work's extensive results. Each section reveals the main findings, which are discussed below.

6.12.1. STUDIED HOURS

The isolated analyses of each of the six studied periods show that when the dry bulb temperature (DBT) is 34.5°C, the EW01 (no vegetation and no boundary wall) has the worst DBT result, 11% less than the case with boundary wall, trees and grass (NS05). Between both scenarios with trees (EW05 and NS 05), the one with the 2m physical barrier in the terrain's edge has 9% better performance. MRT results are approximately 25% better in areas under trees than in non-vegetated portions of the site. The first hour already shows the extensive impact of trees on reducing overall wind speed. Additionally, the positive impact of vegetation located on window height to enhance thermal comfort in afternoon periods with lower sun is highlighted. Furthermore, when DBT is 25.2°C, the MRT is reduced by 46% in the areas under trees, indicating the enhanced impact in milder conditions. The period with an air temperature of 19.4°C creates areas with MRT 44% lower than areas with only trees. This result underscores the positive impacts of combined building and tree shading. Also, the indoor dry bulb temperatures reached 25°C inside the classrooms in cases without vegetation and with grass (NS01, EW01, NS02 and EW02), demonstrating the importance of vegetation in regulating indoor comfort. In the period with DBT 11.9°C, MRT under trees is the same as the area with no vegetation: approximately 24°C. Indoors, the rooms close to trees in NS05 had a 10% higher DBT when compared to the case with no vegetation (NS01). Finally, at 8°C, MRT is 43% higher in areas under trees (NS05) than NS05. The results highlight the tree's capacity to maintain thermal comfort in warmer and colder periods. Indoors, unprotected areas with glazed facades show the best results, confirming solar radiation's positive impact in increasing thermal comfort.

6.12.2. PET AND PM2.5

Using PET as an indicator, the perceived thermal comfort within different scenarios confirms what was found in the studied hours section. Trees are the best SGI components for maintaining thermal comfort in different weather conditions. It was shown that the cases with trees performed 20% to 28% better in the hottest hour than the scenarios without vegetation. In the coldest hour, the cases with hard pavement perform better than trees. However, trees still perform better than other SGI components. In most studied periods, the living walls performed better than hedges. During colder circumstances (under 10°C DBT), the hard pavement shows better overall thermal comfort when compared with cases with grass (NS02 and EW02). The importance of shading and higher air movement to enhance thermal perception is underscored in the results. The pollutant concentration results also established the wind speed as one of the most important factors in enhancing air quality. On the other hand, trees were shown to be the worst SGI component when considering particulate matter. The PM2.5 results show a 4% to 17% increase from the cases with no vegetation (NS01 and EW01) to the scenario with trees (NS05 and EW05) in the hottest hour. Also, the coldest period has an 11% to 12% increase in the PM 2,5 weight average concentration between the same cases. Even though the increase between cases is comparable, the colder hours with lower air movement and higher humidity have an expressive decrease in air conditions. The built physical barrier at the site boundary is established as essential to enhancing air quality at the site. The mentioned element, when used, showed a 52% reduction between the cases with grass (NS02 and EW02). Afterwards, the further studies section of this chapter answered questions raised in the PET and PM2.5 results. It confirmed the importance of boundary walls but established sun exposure, DBT, and air movement as the most significant variables that define air quality.

6.12.3. FINAL REMARKS

This chapter closes with the second version of the Environmental Performance Matrix. The version is executed to highlight the main impacts of the SGI and architectural components' interactions, which were illustrated in the first version. The matrix overviews the analytical research conducted here, showcasing scenarios and the most important results. The results shown here suggest the best practices to be implemented in public schools in the context of Sao Paulo. The next chapter of this research is dedicated to understanding the current policies in the state and developing guidelines with a focus on architectural and SGI elements and their results, which are discussed in this chapter.

7. APPLICABILITY STUDIES

GUIDELINES FOR THE PUBLIC SCHOOLS OF SAO PAULO

7.1. INTRODUCTION

This chapter culminates the work conducted throughout this doctoral thesis, including EMEF Amorim Lima's field and analytical work and the Environmental Performance Matrix chapter's analytical exercise. It is dedicated to translating the outcomes and acquired knowledge in this thesis into guidelines for the best use of SGIs and architectural features in Sao Paulo's public schools. Additionally, to illustrate the context where this chapter's suggestions could be implemented, examples of existing policies in place in the state are briefly discussed. The design guidelines are presented as the final version of the environmental performance matrix. To simplify and underscore the entire process of this thesis' main analytical exercise. The third version of the Matrix concludes chapters 06 and 07, showing the principal elements, outcomes, and guidelines studied in them. To conclude, the chapter discusses the application of the designed "best practices", identifying how best to inform and apply them.

7.2. OBJECTIVES AND METHODS

Building upon this doctoral research's field and analytical exercises, the findings present a significant opportunity to enhance existing school environments, shape future projects, and establish clear guidelines that can fit into the government's educational department's existing manuals alongside other policies. Implementing these suggestions has the potential to expand the environmental benefits beyond the immediate surroundings of the school site, serving as a model for other tropical megacities with similar urban environments. This underscores the broader applicability and potential impact of the research beyond the immediate context of Sao Paulo.

MAIN OBJECTIVES

- Compose guidelines for the best location of the studied architectural features on public schools` projects concerning environmental performance.
- Produce guidelines on adequately selecting the tree species for different urban contexts in Sao Paulo's public schools.
- Define which areas of school sites are the best for inserting Small Scale Green Infrastructure (SGI) to gain the best environmental performance.

Understanding this thesis's outcomes, discussions, and conclusions is the main method of achieving the abovementioned objectives. The information used in formulating the proposed guidelines is, in essence, the findings from the fieldwork presented in Chapter 04, the outcomes of analytical work for EMEF Amorim lima in Chapter 05, and this research's main analytical exercise in Chapter 06. Additionally, knowledge of the architecture, functioning system, and overall environment of public schools in Sao Paulo (Chapter 03) is valuable for defining the best practices. In the mentioned chapter, another essential piece of information is the existing design manuals with policies to be applied to the mentioned sites on a state level. For example, a specific manual produced by the FDE (Foundation for Educational Development of the State) establishes the vegetation that could and should be used in the schools' terrains. The mentioned manual displays several species of different vegetation typologies and indicates which ones are at risk of extinction. It was extensively used in chapter 06 to define the characteristics of the SGi components to be studied. With the state-provided information and knowledge acquired from the research outcomes, it's possible to indicate how the vegetation should be used. Consequently, a table with best practices for SGI elements is built, which will be seen later in this chapter. Other thesis conclusions are translated into a set of "best practices" represented by sketches and text. It is a simplified set of ideas that could fit into different school environments throughout the state. Another method of this chapter is to present and discuss the main outcomes of this thesis and the best practices draft with an interest group in the context of Sao Paulo's public school architecture. Also, an exercise is conducted to exemplify the use of the guidelines within existing schools in the state.

7.3. INTEREST GROUP DISCUSSION

From the start of the Brazilian colonisation process until the 1930s (the end of the "Old Republic"), the major intention wAs mentioned above, when drafted, the guidelines were tested by two local architects representing the interest group. They have been specialists in the design of public schools for over three decades in Sao Paulo, teaching architectural design at FAUUSP (Faculty of Architecture and Urbanism of the University of Sao Paulo) and revising the adequacy and viability of the applicability or application of the guidelines. Both architects were approached because of their extensive knowledge concerning governmental buildings for educational purposes. These architects are Dr Helena Ayoub Silva and Dr Alexandre Delijaicov. Helena Ayoub has taught architectural design at FAUUSP since 1989 and currently coordinates the Architecture and Urbanism Design studios. In addition to teaching, she acts on governmental projects and school-building developments, working closely with the Foundation for Education Development (FDE-Fundacao pro Desenvolvimento da Educacao). She's also a partner of HASAA, an architectural studio that has designed schools in the state. One of these schools is CEU Parque do Carmo, which is done in association with SIAA studio, another architecture practice in Sao Paulo. She has an extensive understanding of the policies in place and is in direct contact with the FDE professionals who create them. Furthermore, Alexandre Delijaicov is a design tutor at FAUUSP and an architect from EDIF, the city of Sao Paulo's building department. The Building Department of Sao Paulo (EDIF)is connected to the city's public buildings and equipment. Both EDIF and FDE are discussed in "Public Schools in Sao Paulo" (chapter 03), where the CEU Parque do Carmo is also reviewed. Alexandre has worked for the municipal government since 1992 and was involved in building the concept of "CEUs" (Unified Educational Centres) for Sao Paulo city. Their knowledge and knowledge production in this field is of extreme value in validating the guidelines presented in this chapter.

The discussion was held in March 2024 through a video call, during which the guidelines were explained using bullet points and sketches, presented in this chapter in section 7.5.2. Both architects highlighted that discussions are constantly taking place to define how best to implement green components into the schools' environments. Underscoring the relevance and ongoing nature of the topic of SGI components in schools for the design and policy-making community immersed in the context of public buildings. The conversation showed the need for research like this one to keep being produced so those designing those spaces are slightly best informed and equipped with an evidence-based approach. One of the main discussion points was knowing how to inform the guidelines. For example, architects were surprised by the poor performance of highly vegetated areas near vehicular roads in terms of PM2.5 concentrations. Yet, the importance of not establishing the green components as a “bad strategy” was underscored, considering the other known positive impacts that vegetation brings. Additionally, the architects suggested that the vegetation species in the FDE manual should be categorised according to the “best practices”. Thus, this exercise was conducted and is discussed in section 7.5.3. of this research.

Overall, the architects commented on the high informative value of the outcomes and expressed that they have the potential to be transformed into policies. Naturally, for that to happen, the conversation needs to be continued and extended to many other professionals. Mainly the ones creating and revising the policies in the state at the moment. Both Dr Helena Ayoub and Dr Alexandre Delijaicov know most of the mentioned professionals and were keen to share their contacts so that the information can be presented to them in the future. The conversation will only occur after this thesis is finalised; thus, it is not explored in this work. Still, the indication that the findings in the form of guidelines can initiate a conversation to add to governmental policies in the state is exactly what the research aimed to achieve at its conclusion.

7.4. EXISTING POLICIES

7.4.1. BRIEF HISTORY

From the start of the Brazilian colonisation process until the 1930s (the end of the "Old Republic"), the major intention was the occupation and assimilation of territorial riches. Hence, environmental management was more associated with the economic protection of the country's natural resources than with its preservation (CETESB, 2018). However, within the mentioned era, the lack of environmental protection policies was seen worldwide, which only started to change in response to evident environmental issues. For example, the U.S.A. in the 1920s "encouraged the increase in the number of National Parks and Forest Preservation Areas" with a conservationist purpose (Fernandes et al., 2021). The 1930-64 period is acknowledged as having a "rapid rise of governmental-sponsored industrialisation", which consequently drove greater attention to natural resource exploitation. Furthermore, in the 1960s, Brazil's preservation areas started being defined, answering to the Amazonian forest's quick deforestation. (Diegues, 1994, as cited by Abakerli, 2001). Around 1995, the Metropolitan Plan for Greater Sao Paulo was concluded with a focus on sustainable development. Also, the plan states the importance of long-term solutions to the city (Stephens, Akerman, and Maia, 1995). In the year 2000, the National System for Conservation Unites (Sistema Nacional de Unidades de Conservacao – SNUC) was created, embracing the conservation areas. In the Sao Paulo state, there are 141 areas, and only 13.4% have forest cover (Faria, 2004). In recent years, the municipal government of Sao Paulo has encouraged the creation of conservation units and linear parks and the restoration of valley bottoms (Mello-Théry, 2011). Moreover, through Sao Paulo's municipal strategic development for the city's master plan, it was defined in 2002 and 2014 that all the existing green infrastructure should be one of the components of the city's drainage system (Government of Sao Paulo et al., 2023). As a result of this encouragement, projects are created to establish linear parks and leisure areas to establish flood control, such as the Linear Park Perus project in the southern area of the city's metropolitan region (Government of Sao Paulo et al., 2023). Additionally, a program called "100 Parks" launched in 2008 was responsible for the creation of the 113 parks existent in the city (Martins et al., 2024).

7.4.2. FDE MANUALS

As explained in the "The Public Schools" chapter (03), the Education Development Foundation ("Fundacao para o Desenvolvimento da Educacao" – FDE), created in 1987, develops public schools' projects and buildings within the state. It was also mentioned that the FDE produced many catalogues/ manuals dedicated to professionals related to the educational system. The manuals serve as a guide to the ones who design the learning environments and to those who manage them. FDE has a section on its website only containing "technical catalogues", which anyone can access for free (FDE, n.d.). The mentioned catalogues can be found with different subjects related to the school building: rooms, furniture, services, layouts, signs, components, topography, vegetation species, and project BIM material. According to FDE (2012), the catalogues are periodically updated to include any new information due to changes in the technical norms and other policies.

The "rooms" catalogue showcases the entire program of a public school with the dimensions, areas, and suggested layouts of each space. The document displays the characteristics of the rooms and the environmental requirements. For example, it defines that the classrooms require a minimum of 3 meters of floor-to-ceiling height, that 1/5 of the floor area has natural light, and that 1/10 has natural ventilation. As discussed in the "Environmental Performance

Matrix" chapter, the catalogue was used as a reference to build the model studied on the main analytical exercises of this doctoral research.

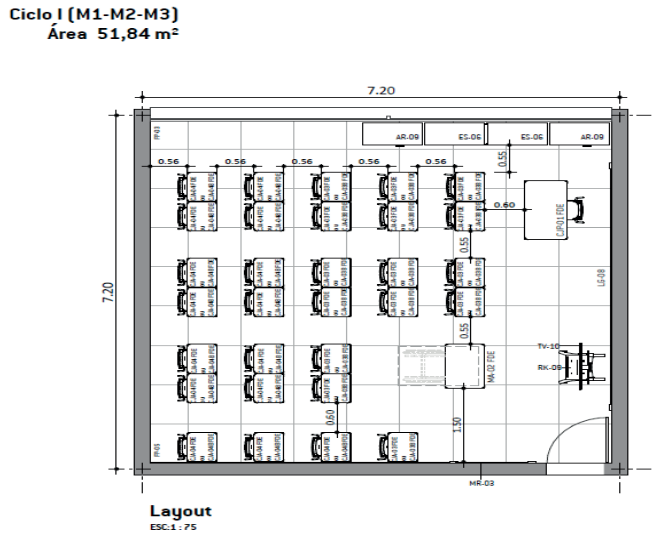

Figure 7.3.01 - Extract of FDE manual showing a classroom layout with dimensions.

Another catalogue that was also used in this thesis analytical research was the vegetation species. The mentioned report exhibits a vast list of different typologies of greenery, including trees, grass, hedges, and climbing plants. The document was published in 2012 and updated in 2015 and declares (FDE, 2012):

> "The landscaping of the external areas of school buildings aims to improve its visual and environmental quality, enhance the characteristics of vegetation in harmony with the construction, provide places that stimulate and promote recreation, social activities, outdoor educational activities, respect for nature, and forming children and young people also concerned with the preservation and appreciation of the environment".

Even if the statement above includes the importance of environmental quality, there is no specific explanation concerning thermal comfort and air quality impacts when utilising the listed vegetation species. Furthermore, the species are chosen according to other published documents produced by other institutions within the state and municipality of Sao Paulo, including FDE. For example, "the list of official species of the Brazilian flora in extinction threat", "ornamental plants in Brazil", and "trees of the Atlantic Forest of Minas Gerais", among others (FDE, 2012).

7.5. GUIDELINES

7.5.1. THE FINAL ENVIRONMENTAL PERFORMANCE MATRIX

This is the final version of the Environmental Performance Matrix, which contains all the parts of this Doctoral Research's main analytical exercise. Here, the ten main studied scenarios are displayed, highlighting the architectural and SGI components and their locations. The main outcomes of each scenario concerning PM2.5 and PET are also contemplated, with the final information being the guidelines. The recommendations in the matrix are basic sketches with bullet points representing overall best practices with a focus on each studied SGI component: grass, hedges, living walls and trees.

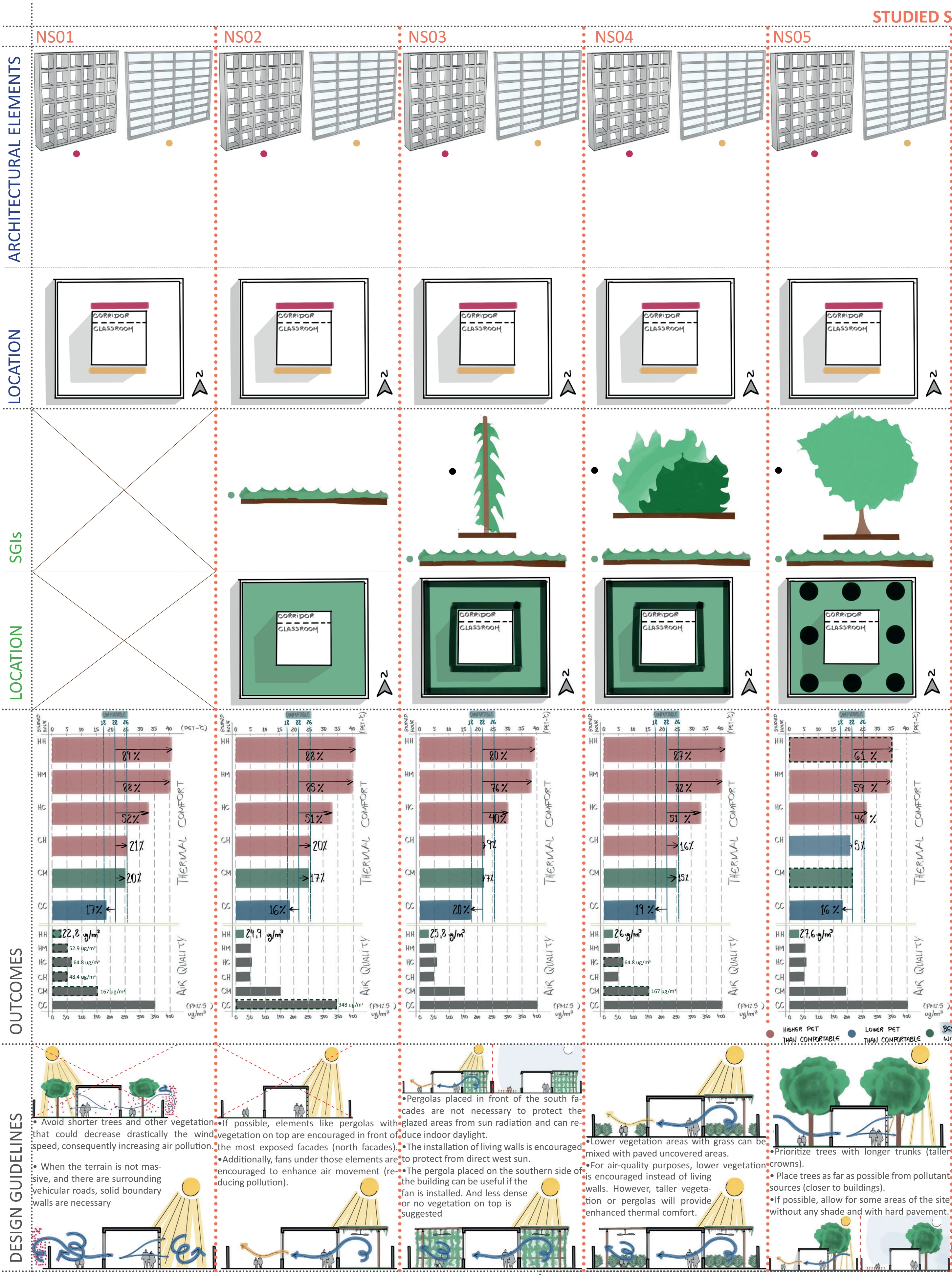

Figure 7.5.01 - Diagram of the Final Version of the Environmental Performance Matrix, with the main guidelines addition.

CENARIOS

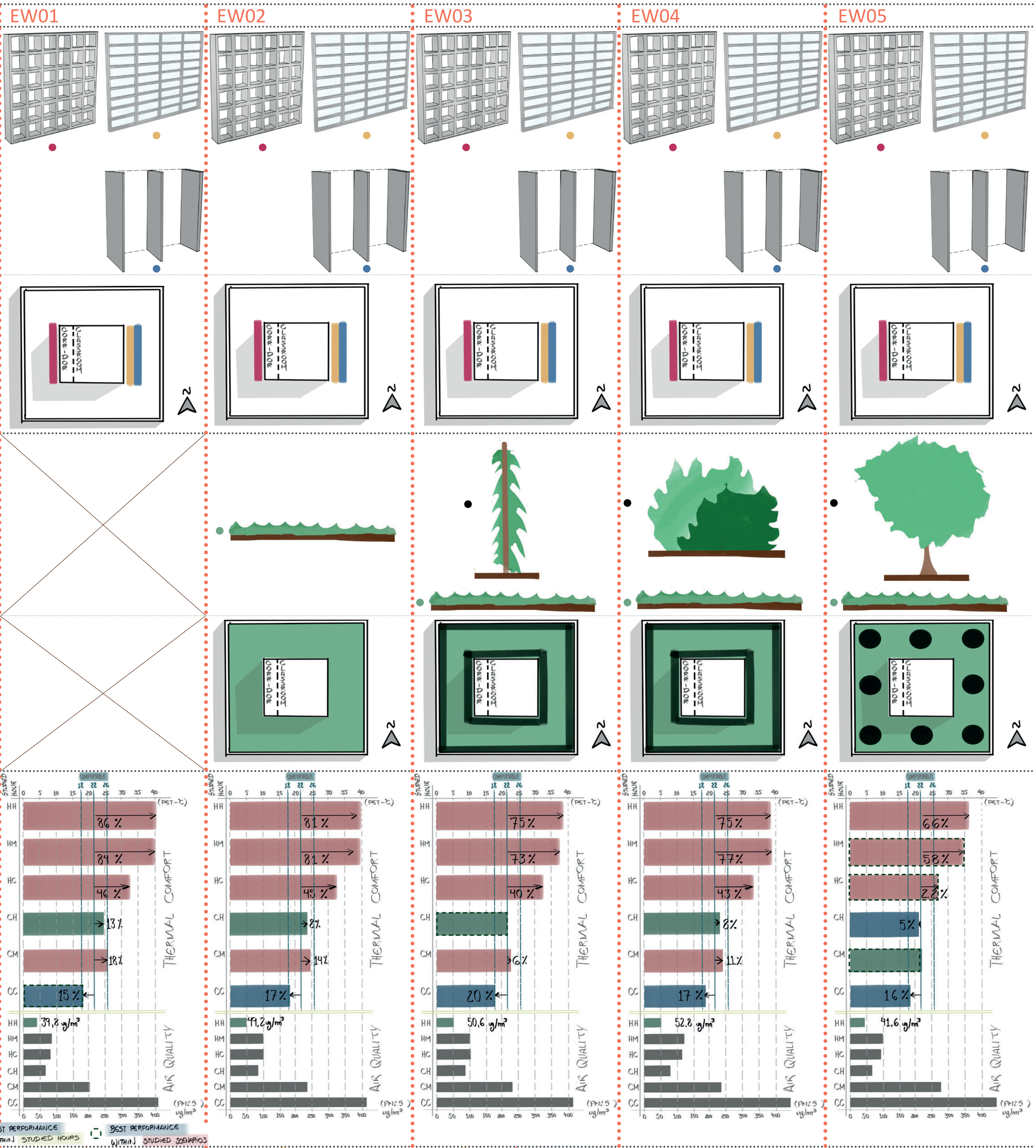

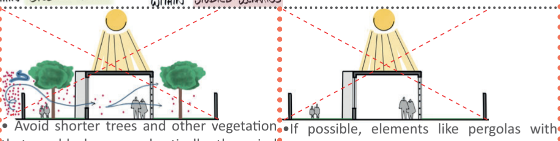

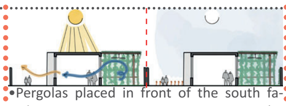

- Avoid shorter trees and other vegetation that could decrease drastically the wind speed, consequently increasing air pollution.
- When the terrain is not massive, and there are surrounding vehicular roads, solid boundary walls are necessary

- If possible, elements like pergolas with vegetation on top are encouraged in front of the most exposed facades (west facades).
- Additionally, fans under those elements are encouraged to enhance air movement (reducing pollution).

- Pergolas placed in front of the south facades are not necessary to protect the glazed areas from sun radiation and can reduce indoor daylight.
- The installation of living walls is encouraged to protect from direct west sun.
- The pergola placed on the southern side of the building can be useful if the fan is installed. And less dense or no vegetation on top is suggested

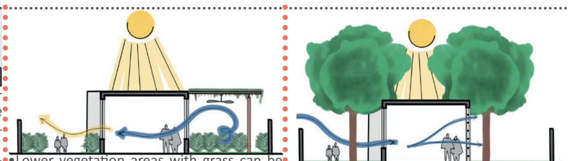

- Lower vegetation areas with grass can be mixed with paved uncovered areas.
- For air-quality purposes, lower vegetation is encouraged instead of living walls. However, taller vegetation or pergolas will provide enhanced thermal comfort.

- Prioritize trees with longer trunks (taller crowns).
- Place trees as far as possible from pollutant sources (closer to building).
- If possible, allow for some areas of the site without any shade and with hard pavement.

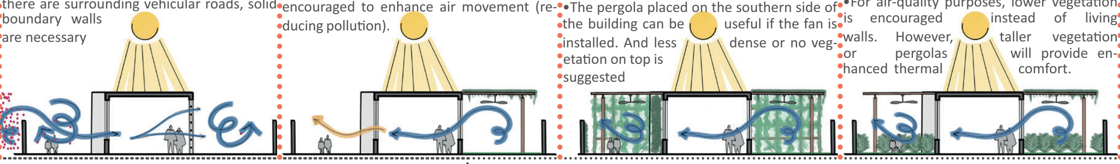

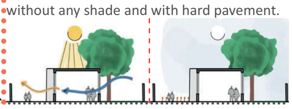

7.5.2. THE BEST PRACTICES

This section explains in more detail the main best practices presented in the Matrix, developed based on the outcomes of this doctoral research. The main information used to establish the guidelines is in the results section of the previous chapter. The mentioned Environmental Performance Matrix chapter evaluates the impacts of each SGI component based on its location. The information produced during the Analytical and Fiewldowrk chapters of the Case Study EMEF Amorim Lima is also essential. Overall, this entire doctoral thesis is fed into the guidelines established below, which will first be explained through sketches and text. Afterwards, the main guidelines are presented as bullet points and explained in detail shortly after.

The combination of trees is an essential SGI component and should be used in open areas of schools, where grass should also be applied. The trees create shaded areas on sunny and hotter days, and grass reduces heat absorbance, enhancing human thermal comfort. However, shorter trees, high hedges, and other tall vegetation are shown to decrease air velocity and enhance pollutant particle concentration. Within this set of procedures, trees considered shorter are those closer to users' height, with 2 to 5 meters. Using trees with crowns above the occupied area increases air quality in these environments. The trees considered in this research analytical exercise have a final 13m height with crowns starting above approximately 4m. The mentioned arrangement already causes wind reduction at the studied height:1.5m. Consequently, lower vegetation with similar density will have an acute impact on air movement and quality. Finally, in areas where the school site is bigger, and the building is far from the vehicular routes, the trees should be implemented on the first meters adjacent to the building, being as far as possible from the roads. This measure will provide shaded areas near the built environment. Trees will also be protected from pollutant particles, and the area underneath, closer to the buildings' openings, will have better air quality.

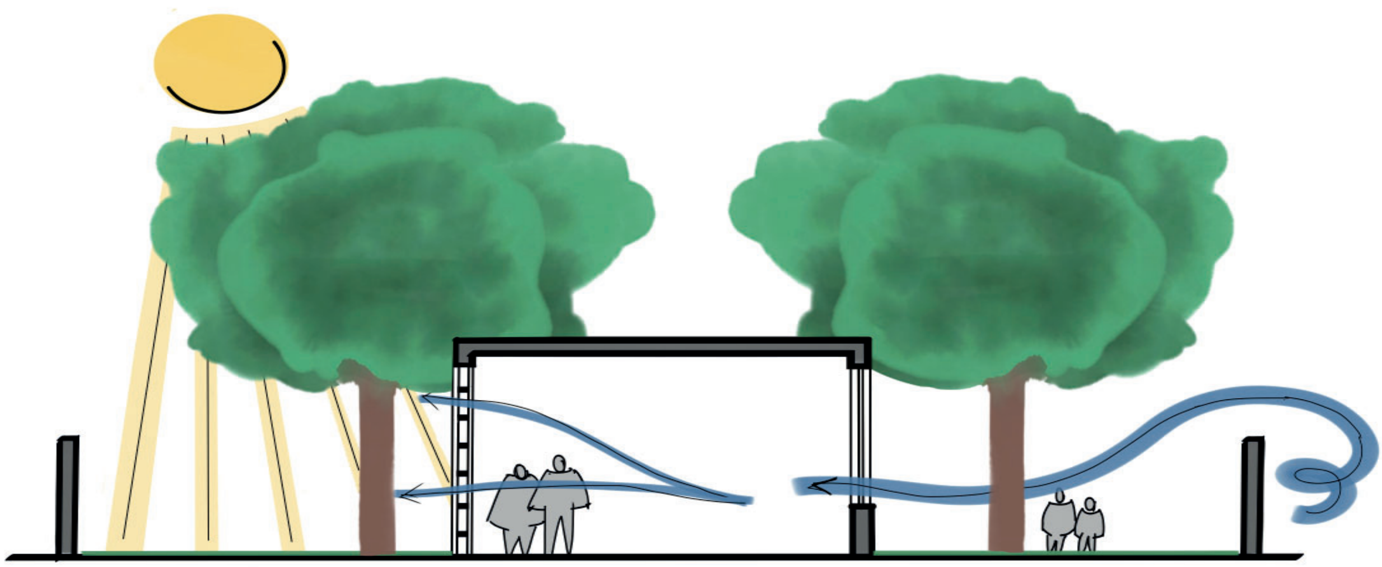

Figure 7.5.02 - Sketch indicating the importance of taller trees.

Pergolas can be a good solution for maintaining vegetation within the sites without prejudicing the air quality in cases close to pollution sources. In those cases, pergolas could be installed at a height that provides shade but is high enough to create less disruption to air movement. The suggestion is an at least 3m high element with vegetation on top. A ceiling fan would also be useful when installing a pergola or any more profound overhang. Even though the fan is not a passive environmental strategy, it can be positive to enhance thermal comfort on hotter days and is essential

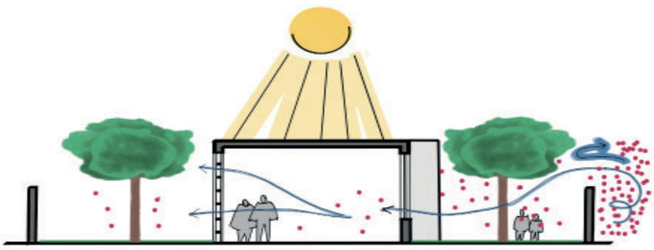

Figure 7.5.03 - Sketch indicating the possible negative impacts of shorter trees on pollutant concentration

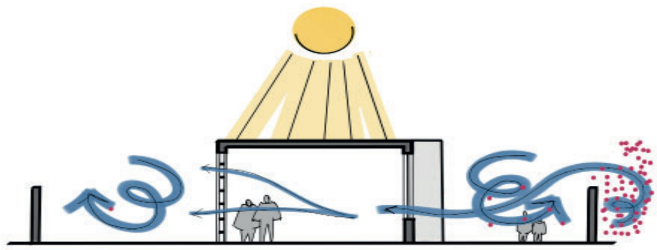

Figure 7.5.04 - Sketch indicating the possible positive impacts of snot having vegetation on pollutant concentration

to enhance air quality. Mainly if it is positioned close to the classroom openings. The mentioned strategy would deliver a similar or even higher shading impact than trees and other SGI components while diminishing pollutant particle concentrations. The fan and shaded area can also help increase cross-ventilation in the indoor space. As this research extensively mentions, the south facades in the southern hemisphere are not exposed to direct sun. Consequently, openings on those facades are encouraged, and no other shading is required. Additionally, living walls on the sides protecting from the west sun could be installed, mainly if a fan is under the pergola, to avoid reducing air movement. The pergola with vegetation in front of the north façade is a good suggestion to reduce direct solar exposure to the glazing, avoiding indoor thermal discomfort and glare. Furthermore, not having a pergola in front of the south façade is an opportunity for a hard pavement space. The outcomes of all analytical exercises in this thesis show that paved areas exposed to the sun during the day can release heat, enhancing thermal comfort on colder nights. Thus, an environment

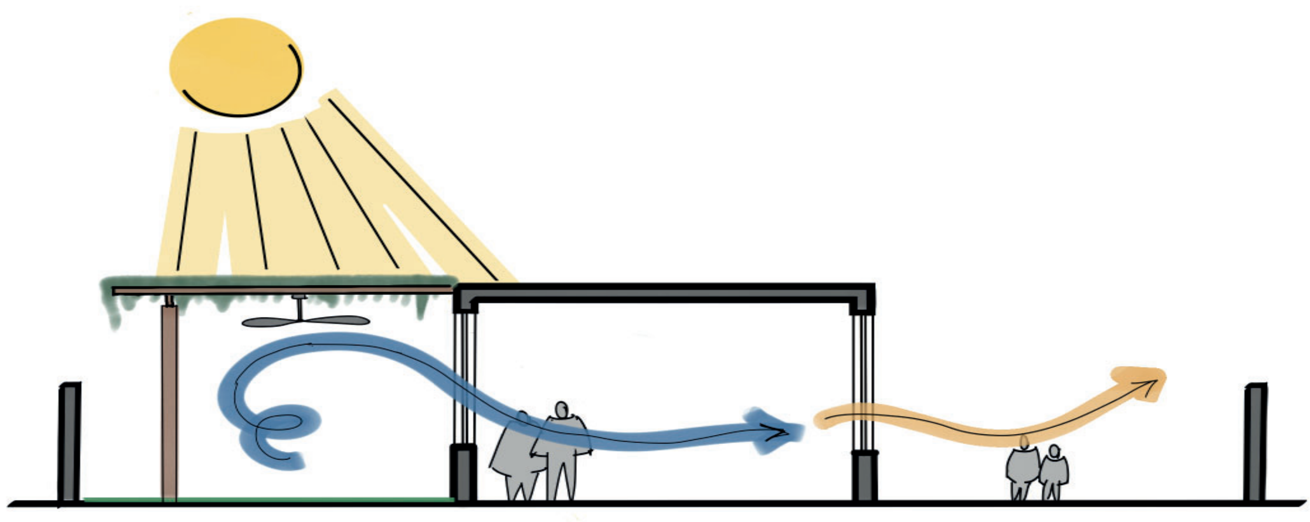

Figure 7.5.05 - Sketch indicating the scenario with pergola in front of the most exposed facade, with a ceiling fan.

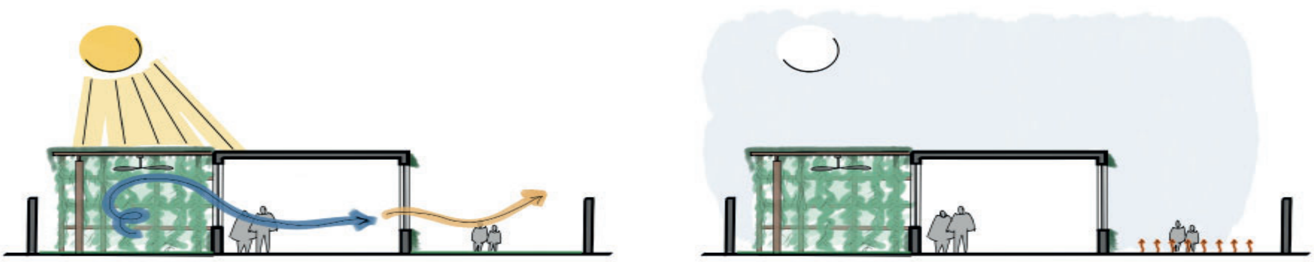

Figure 7.5.06 - Sketches demonstrating the heat exchange effect between day and night within the scenario with pergola on one side of the building.

without SGi and with pavement could enhance thermal comfort and provide higher wind speeds. The lower vegetation tested in this thesis is 1 m high. Consequently, it suggests that SGI typologies lower than this height perform better in terms of air quality and should be prioritised. However, taller SGIs have better thermal comfort impacts due to shading creation. Thus, combining lower vegetation and taller elements, such as pergolas or tall trees, is recommended. As mentioned, it would be suggested that ceiling fans be used to ensure air movement. Finally, as extensively mentioned in this research, the heavy use of SGI components close to pollutant sources can trap particles, decreasing air quality in surrounding areas. Hence, the areas should be avoided. Considering the trapping effect, the areas behind the SGI can present lower pollution levels. Yet, according to the mentioned outcomes, the environment should be unobstructed

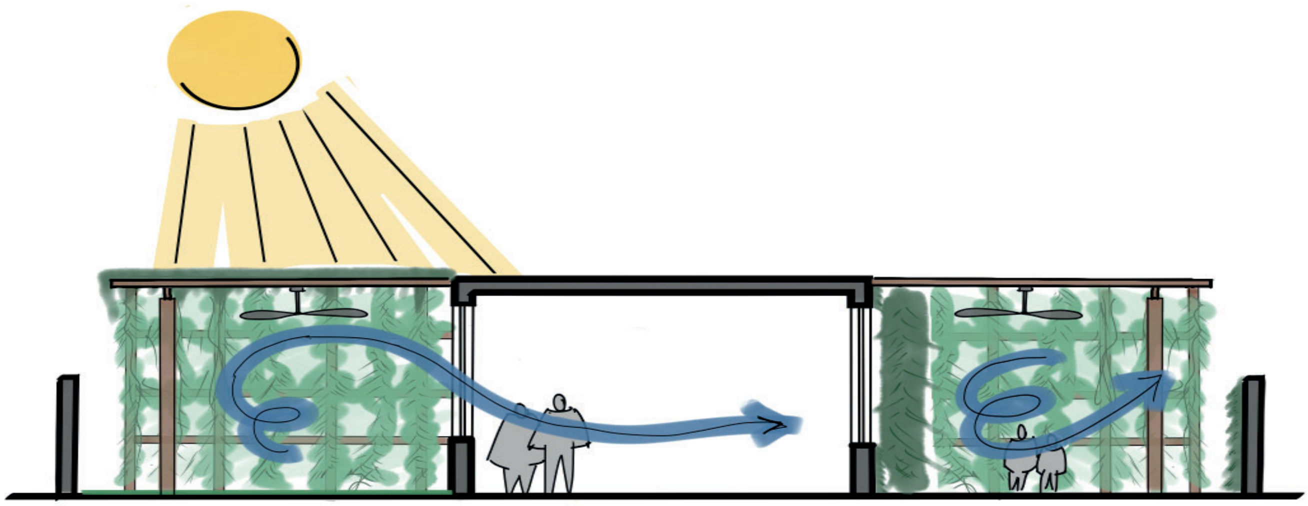

Figure 7.5.07 - Sketch indicating the scenario with pergolas and living walls on both facades, more effective on east/west facades.

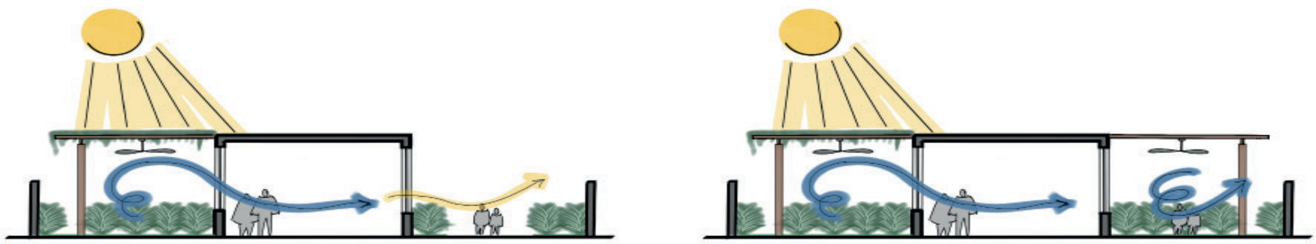

Figure 7.5.08 - Sketches demonstrating the case with hedges and pergolas, which can be on one or both sides of the building.

(non-vegetated) and large enough to have increased ventilation, ensuring air quality.

Figure 7.5.09 - Sketch indicating the possibility of using SGI as a barrier agains pollution, when there is enough space for air movement.

MAIN GUIDELINES:

1) Avoid shorter trees and other vegetation that could drastically decrease wind speed, consequently increasing air pollution. For example, trees with longer trunks (taller crowns) should be prioritised.

2) Place trees as far as possible from pollutant sources (first meter after buildings' facades).

3) If possible, allow for some areas of the site without any shade and with hard pavement.

4) If the site is large (less dense urban areas), allow for areas without obstructions, enhancing air movement.

5) When the terrain is not massive (within dense urban areas), and there are surrounding vehicular roads, solid boundary walls are extremely necessary.

6) If possible, elements like pergolas with vegetation on top are encouraged in front of the most exposed facades (north facades).

7) Additionally, fans under those elements are encouraged to enhance air movement (reducing pollution).

8) If a fan is installed, a pergola placed on the southern side of the building can be useful. Less dense or no vegetation on top is suggested.

9) Pergolas placed in front of the south facades are not necessary to protect the glazed areas from sun radiation and can reduce indoor daylight.

10) Installing living walls is encouraged to protect from direct west sun exposure.

11) Lower vegetation areas with grass can be mixed with paved uncovered areas.

12) Lower vegetation is encouraged instead of living walls for air-quality purposes. However, taller vegetation or pergolas will provide enhanced thermal comfort.

13) If greenery is used as a barrier to particle pollution, guarantee that this area is not constantly used. Also, if possible, allow an open unvegetated area after it.

7.5.3. VEGETATION SPECIES

As cited in the FDE catalogues section in this chapter, the "Vegetation Species" (FDE, 2012) document suggests which species of grass, hedges, trees, and other elements could be used in schools. Thus, it is important to indicate how those species could be applied in this chapter as part of the applicability studies. The mentioned catalogue showcases 70 different species of trees, including ornamental, fruitful, palms and bamboo. Additionally, a group of 03 climbing plants could form living walls, followed by 29 types of hedges. Conclusively, there are 24 species of forage vegetation and 03 of grass. However, the applicability of this catalogue information will be focused on trees.

As explained previously in the guideline section, the overall best practice for elements such as hedges and living walls is to be used as far as possible from pollutant sources in protected environments. Trees constructed for the analysis consider overall height, crown dimensions, and height from the ground (trunk height). This information is discussed in 6.6.1. section of the previous chapter: " Materials and vegetation". Based on the characteristics of the used tree and their environmental impacts shown in the last chapter's outcomes, the species in the FDE catalogue (2021) are classified in this section. The capacity of shading creation of each species is already contemplated in the FDE guidelines (2012), so this grading is focused on air quality impacts. Moreover, the tree LAD is not defined in the catalogue, and the information needs to be measured for each species. Thus, the ranking is defined through the sketches displayed in the catalogue and online information about the tree's density. The best practices exercise forms the table "FDE manual trees organised into groups" (figure 7.5.16).

The table separates the species into three main groups. The first is contemplating trees that represent an extreme probability of enhancing pollution levels within the site if placed adjacent to the pollutant sources (vehicular roads). Those species are, in their majority, smaller than the one studied in the analytical research (13m). The main characteristic of this group of trees is having lower crown-to-floor heights. The criteria used is that the mentioned height is similar to or lower than the human height. The second group has the species that would enhance pollution levels within the site if placed close to the pollutant sources. These species have similar sizes or are more extensive than the one studied in the analytical work, which had a 4m floor-to-crown height. All species in this group have the mentioned characteristics or are taller. The third and last tree arrangement is composed of trees that, if placed on the first meters after the vehicular road, will not enhance pollution levels within the site. Those species are tall, with their crown significantly far from human height. This characteristic makes it safe to assume that the wind movement and air quality will not be disturbed at the human level. Below are the main lessons of this exercise with the final guidelines. However, it is essential to remember that the information displayed here is a set of suggestions. Each species and its context should be analysed individually for the final choice of trees to be implemented.

KEY LESSONS LEARNT:

1) 27 out of 70 should not be planted close to vehicular roads.

2) 38 species should be avoided close to vehicular roads, but if planted, solid boundary walls against the pollutant sources should exist or be built.

3) Only 5 species from the FDE list could be placed close to the roads, even without boundary walls.

	Type	Page No	Name	
1	Ornamental Trees	13	Aldrago	
2		15	Alecrim-de-campina	
3		17	Araçá	
4		19	Aroeira-do-sertão	
5		21	Aroeira-salsa	
6		23	Bico-de-pato	
7		25	Canela-preta	
8		27	Canela-sassafrás	
9		29	Caneleira	
10		31	Caputuna-preta	
11		33	Caroba	
12		35	Caroba-branca	
13		37	Carobão	
14		39	Carvalho brasileiro	
15		41	Cássia-grande	
16		43	Castanha-do-pará	
17		45	Cedro-rosa	
18		47	Chá-de-bugre	
19		49	Chuva-de-ouro	
20		51	Dedaleiro	
21		53	Diadema	
22		55	Embaúba	
23		57	Embiruçu	
24		59	Fedegoso	
25		61	Feijoa	
26		63	Guanandi	
27		65	Imbuia	
28		67	Ipê-amarelo	
29		69	Ipê-amarelo-da-serra	
30		71	Ipê-branco	
31		73	Ipê-roxo-de-bola	
32		75	Ipê-roxo-de-sete-folhas	
33		77	Jaborandi	
34		79	Jacarandá-paulista	
35		81	Jatobá	
36		83	Jequitibá-branco	
37		85	Jequitibá-rosa	
38		87	Manacá-da-serra	
39		89	Mirindiba	
40		91	Mulungu	
41		93	Mulungu-do-litoral	
42		95	Pata-de-vaca-branca	
43		97	Pau-brasil	
44		99	Pau-cigarra	
45		101	Pau-ferro	
46		103	Peroba-rosa	
47		105	Pinheiro-do-paraná	
48		107	Quaresmeira	
49		109	Sibipiruna	
50		111	Tarumã	
51		113	Unha-de-vaca	
52		115	Urucum	

53	Fruitfull Trees	119	Acerola	
54		121	Amoreira	
55		123	Angelim-doce	
56		125	Cerejinha	
57		127	Gabiroba	
58		129	Goiabeira	
59		131	Grumixama	
60		133	Jabuticabeira	
61		135	Jenipapo	
62		137	Pitangueira	
63		139	Uvaia	
64	Palm Trees	143	Açaí	
65		145	Guariroba	
66		147	Indaiá	
67		149	Jerivá	
68		151	Palmito-juçara	
69		153	Pupunha	
70	Bamboo Trees	157	Bambuzinho	

Extreme probability of enhancing pollution levels within site if placed close to the pollutant sources (vehicular roads).

Probability of enhancing pollution levels within site if placed close to the pollutant sources (vehicular roads).

Will not enhance pollution levels within site if placed close to the pollutant sources (vehicular roads).

Figure 7.5.16 - Table - FDE manual trees organized into groups.

7.6. APPLICABILITY STUDIES

7.6.1. EXISTENT SCHOOLS

At this point, there is a need to take a step further and imagine how the schools in Sao Paulo estate would potentially apply the guidelines presented in this research. The mentioned exercise is essential to exemplify to the policymakers, architects and others involved in public school projects in the estate how to use the "best practices". A few of the schools presented in Chapter 03 (The Public Schools) are selected to exemplify. The exercise is developed from an environmental design perspective, which includes increasing vegetation whenever possible.

1. SCHOOL PARQUE DORUADO V

The first example is the School Parque Dourado V, which is an estate school surrounded by open vegetated areas and small-scale buildings. The northeastern outer limit of the site has one heavier traffic road. Another vehicle road is at the site's southeastern perimeter, which apparently has less vehicular activity. Additionally, there is an expressive open paved area on the site's northeastern portion. Some of the previously discussed guidelines could be applied to this environment. For example, the northwestern portion of the site could be heavily vegetated. The northwestern façade is heavily exposed to direct solar radiation most of the day, including the afternoon when temperatures increase. Thus, proposing an SGI for this area with tall elements would diminish direct sun exposure to the mentioned façade. Naturally, the vegetation would also enhance the area's ecosystem while extensively enhancing thermal com-

Figure 7.6.01 - Satellite Image of School Parque Dourado V (Google, 2024).

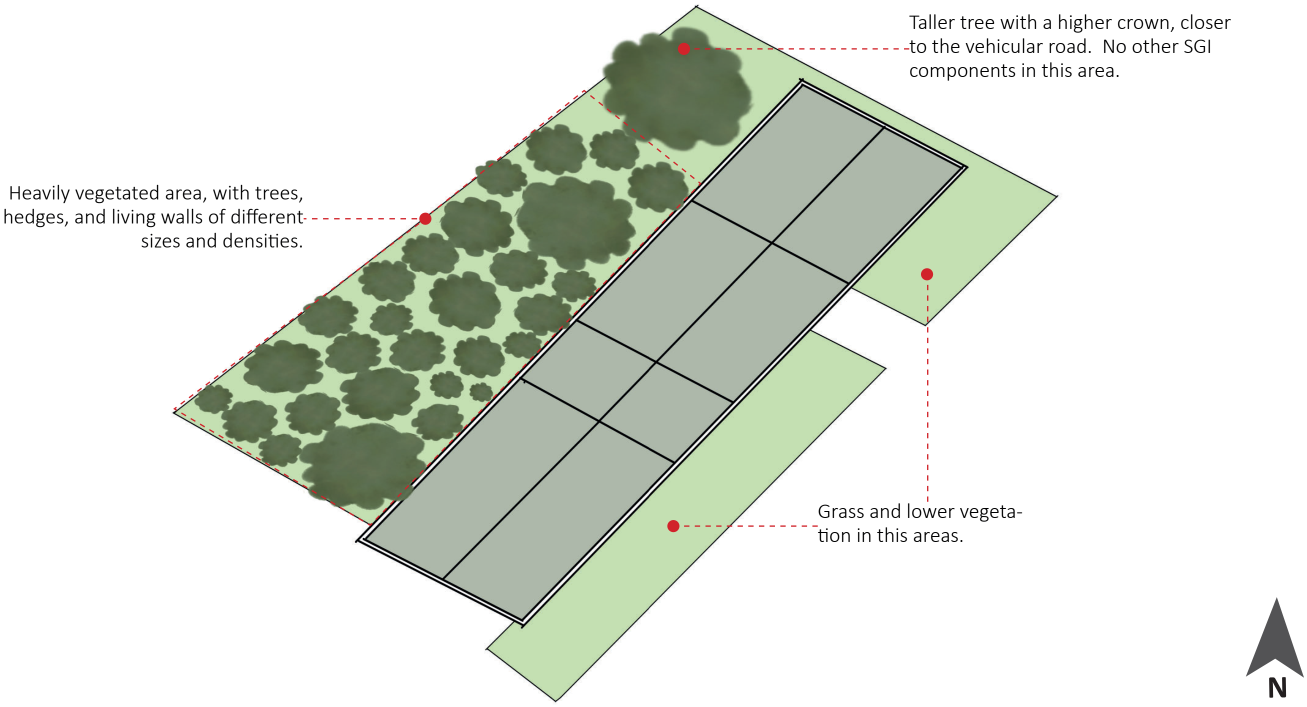

Figure 7.6.02 - Sketch with SGI proposal for School Parque Dourado V.

fort on the site. Most importantly, the air quality wouldn't be reduced due to the lack of pollution sources on the site's northwestern boundary. Additionally, it would be advised that the area closer to the northeastern vehicular road wouldn't be vegetated or have taller trees. Finally, the southeastern portion has less sun radiation exposure on the facades and is attached to a vehicular road. Hence, the suggestion is that the area could have less vegetation and shorter SGI components.

2. SCHOOL SALVADOR ROMANO

The second example is the estate school Salvador Romano, which is a fit model of an environment with a larger built space. The reduced unbuilt land area forces SGI elements to be on its perimeter, adjacent to the surrounding vehicular streets. Also, the school has a courtyard space with a meagre vegetable area. The morphological configuration of this school represents an opportunity for a fully vegetated courtyard. The northeastern portion of the courtyard could have shorter SGI elements to reduce obstruction to the southern façade. A lower coverage of this facade enhances daylight as it is a surface with meagre direct sun radiation. Considering that the mentioned space is not massive and blocked by buildings on all sides, a usual lower wind movement is expected. Thus, if vegetated, the proposition is that the courtyard would have a tall element as a tree that wouldn’t reduce the air speeds even further. Another possibility is having vegetation with a lower height than adjacent buildings. For example, hedges, living walls, and smaller trees wouldn't provide the same shading impact but would be more protected from pollution sources by the buildings. Furthermore, hypothetically, the trees facing the roads could be removed within the southeastern portion of the terrain with smaller blocks. The area would probably have enhanced air movement and better air quality. However, additional shading for the facades would need to be provided. If possible, the space between the two buildings (that act as a barrier) could be heavily vegetated with almost no risk of pollutant concentration.

Figure 7.6.03 - Satellite Image of School Salvador Romano (Google, 2024).

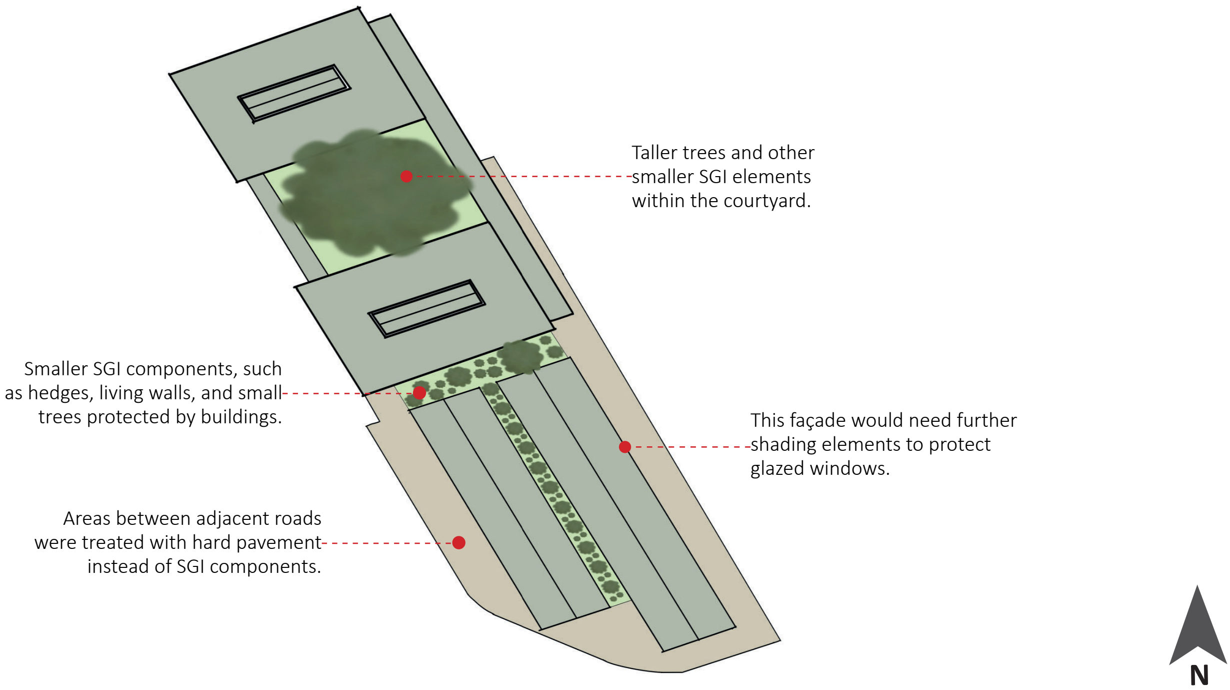

Figure 7.6.04 - Sketch with SGI proposal for School Salvador Romano.

3. SCHOOL PARQUE SAO BENTO

School Parque Sao Bento is also surrounded by vehicular roads. However, this school has a substantial outdoor area. Even though this environment could harbour a dense small-scale green infrastructure, the latter could diminish air quality. This would be a suitable example to suggest vegetation closer to the building, as already seen in the current conditions. The ideal would be to have more elements enhancing thermal comfort around the blocks. The strategy creates a transitional space between the more controlled indoors' and the harsher outdoor conditions. Parque Sao Bento

Figure 7.6.05 - Satellite Image of School Parque Sao Bento (Google, 2024).

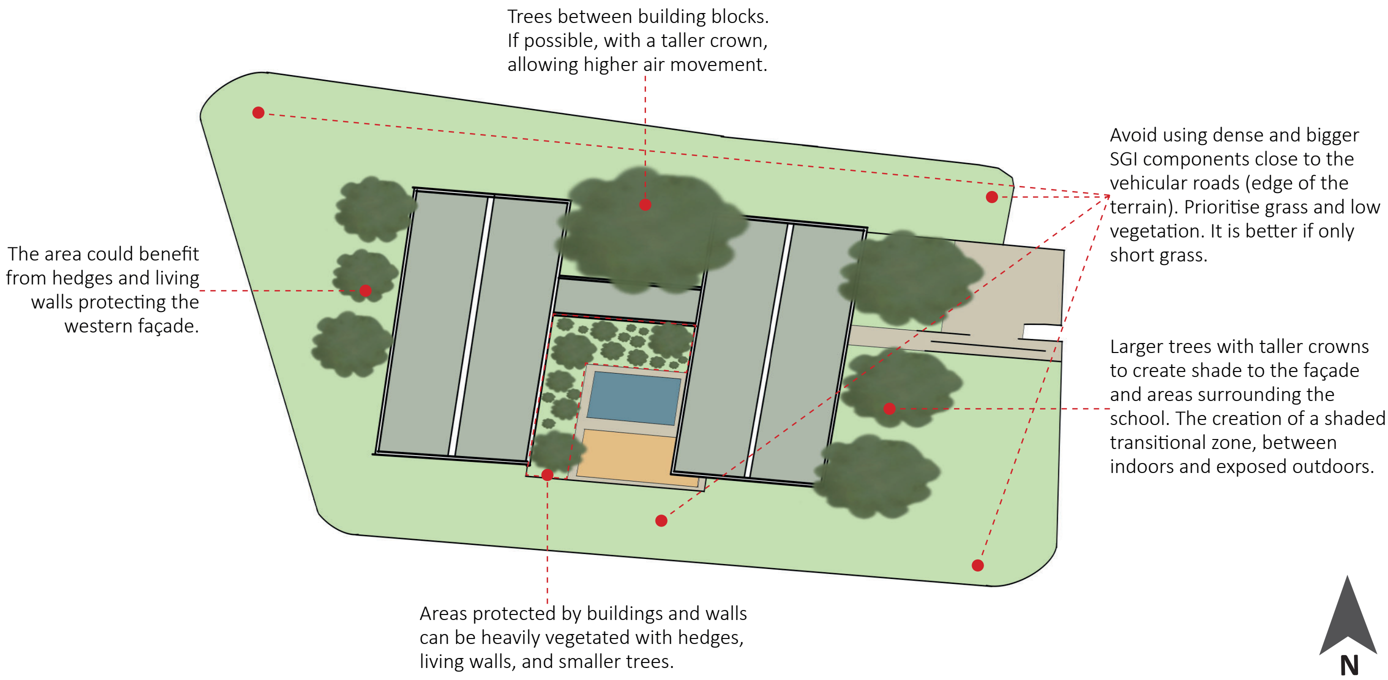

Figure 7.6.08 - Sketch with SGI proposal for School Parque Sao Bento.

also has a courtyard surrounded by a building and a boundary wall. A perfect space to receive dense vegetation.

4. SELMA MARIA STATE SCHOOL

Another example is the Selma Maria State School. Similar to Parque Dourado V, there is a considerable open area in the western portion of the site, and the adjacent area is being opened. The suggestion here is the same as previously explained for Parque Dourado: a dense SGi is encouraged. The main difference between this school and the

Figure 7.6.09 - Satellite Image of School Selma Maria (Google, 2024).

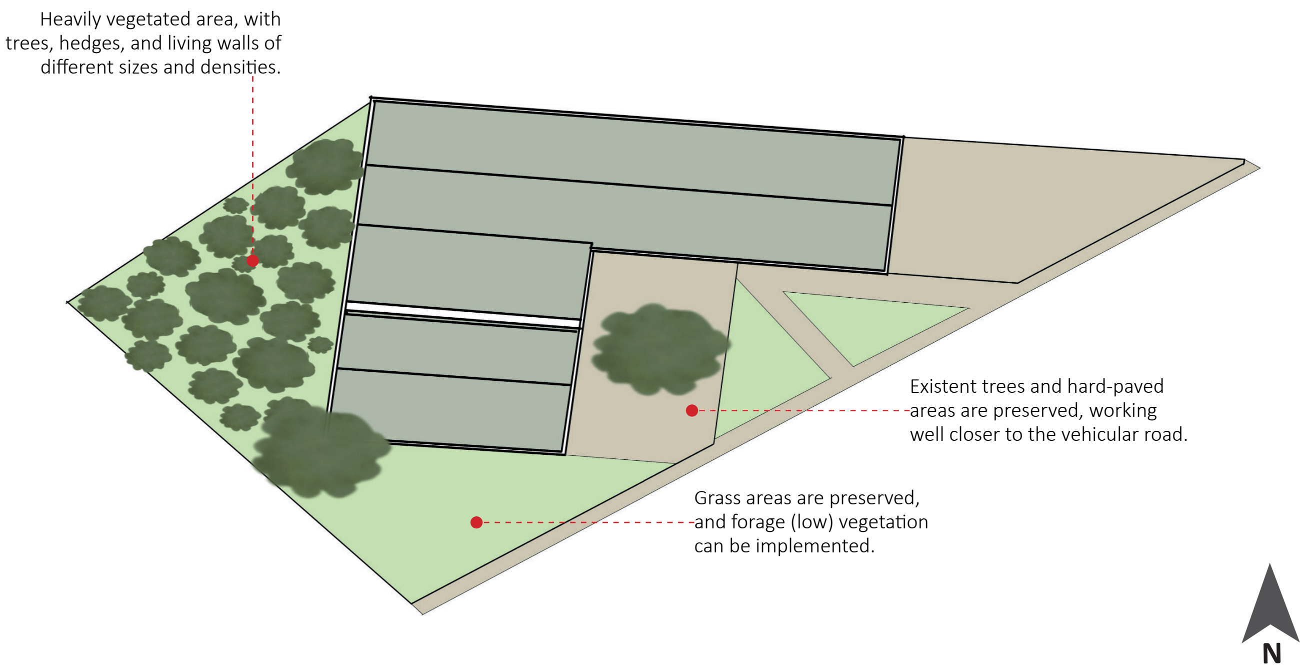

Figure 7.6.10 - Satellite Image of School Selma Maria (Google, 2024).

other cases so far is the northern façade, which is exposed to direct radiation most of the day and has clear-glazed classroom windows. The project is correctly designed with horizontal shading and recessed facades, which is probably enough to avoid direct radiation. Moreover, the mentioned northern façade is close to a vehicular road. Even though it is plausible to assume that the discussed area is performing well in terms of thermal comfort, some level of pollutant particles could reach the classrooms. The small northern portion of this site could represent an opportunity to have a pergola element installed. As mentioned in the guidelines, the element could bring vegetation without diminishing air velocity. In this case, vertical vegetation could be installed to act as a barrier against inhalable particles. A fan would even further enhance the air quality of the protected space. This exemplifies a bolder applicability form of combining architectural and SGI components as an environmental strategy, and all suggestions in this section would need to be further discussed.

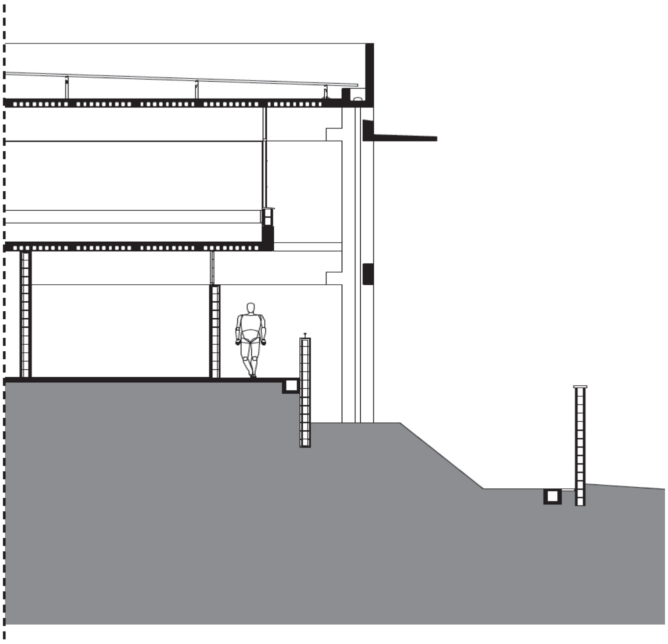

Figure 7.6.11 - Original Section from Architects for School Selma Maria (© GrupoSP).

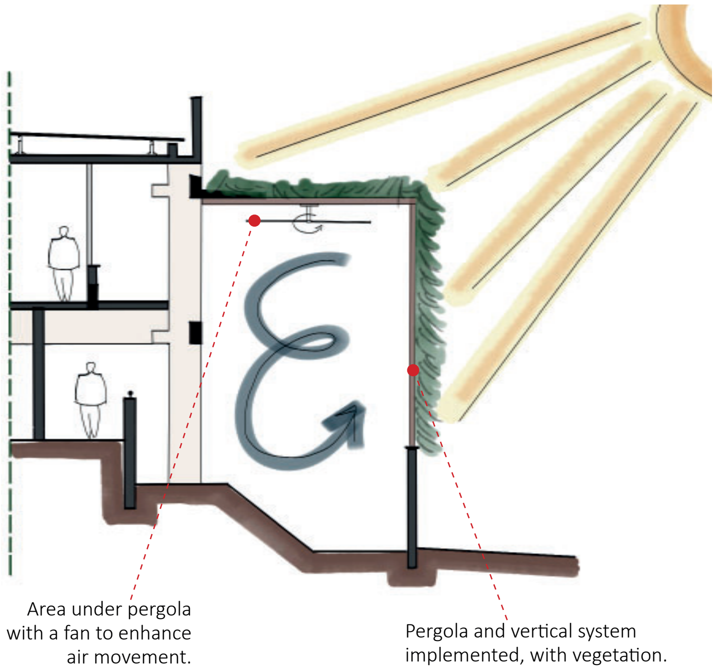

Figure 7.6.12 - Sketch of section with SGI proposal for School Selma Maria.

7.6.2. EMEF DESEMBARGADOR AMORIM LIMA (CASE STUDY)

The EMEF Desembargador Amorim Lima is the case study of this doctoral project, which was essential for establishing the current conditions of a school environment with an expressive SGI. Hence, the applicability study is naturally developed. This is the last example of a set of suggestions for implementing this chapter's guidelines. The façade design and possible improvements are thoroughly discussed in Chapter 04 (Case Study—Fieldwork). The main information to be echoed here is that the northern façade should be more protected, and the southern should be exposed to daylight. Likewise, cobogos could be applied to the northern façade. Yet, another option is the extension of northern overhangs to protect from direct sun. While allowing the sun to enter on colder days due to lower sun angles. Also, living walls could be installed as a vertical shading against the western sun. As shown in the fieldwork and analytical

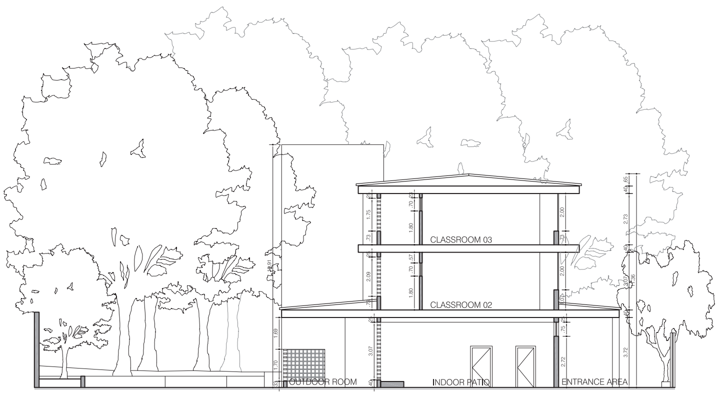

Figure 7.6.13 - EMEF Amorim Lima Section BB (personal archive).

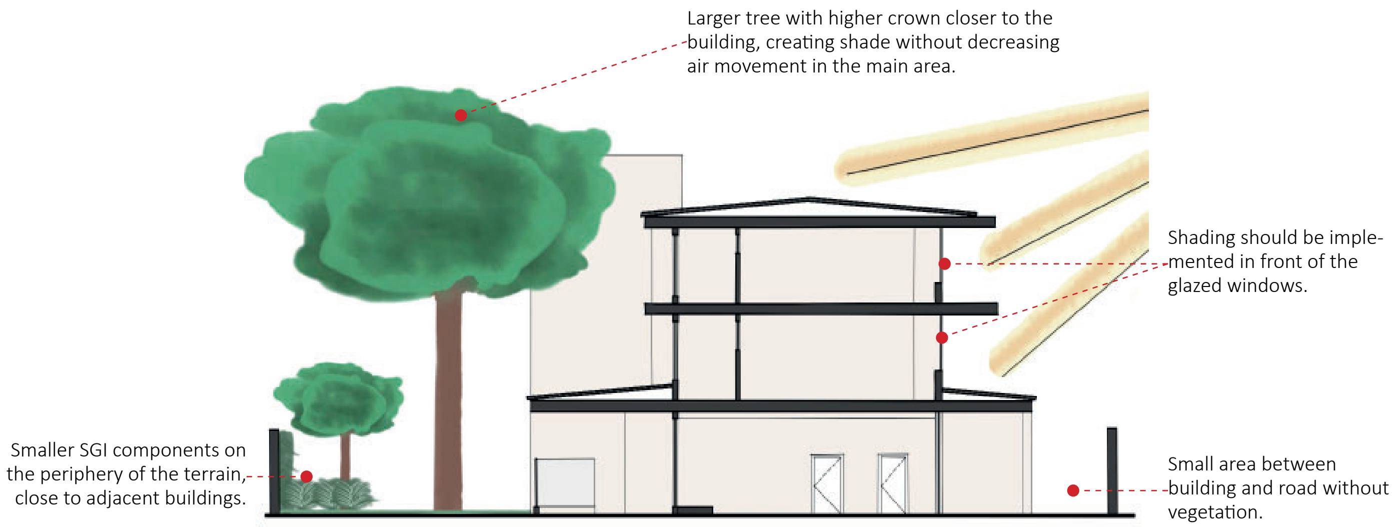

Figure 7.6.14 - Sketch of EMEF Amorim Lima Section BB, with SGI proposal (personal archie).

work of the Case Study, the vegetated area on the northeastern portion of the site shows lower pollution levels. Yet, due to shorter, less dense vegetation, thermal comfort levels are not as high as in the southwestern area (Cora Coralina Park 01). Consequently, SGi components in the mentioned area, protected by adjacent buildings, could be taller and denser, enhancing shade and cooling. The uncovered sports court is limited by living walls, which could be denser on the sides further from the street. The site shows a southern portion in front of the main building, which is treated with hard pavement. (Cora Coralina 03). The mentioned area could be vegetated and enhanced carefully so as not to reduce drastically daylight indoors and airspeed. Thus, taller trees should be planted in the central space. The Cora Coralina

Figure 7.6.15 - Satellite Image of School EMEF Amorim Lima (Google, 2024).

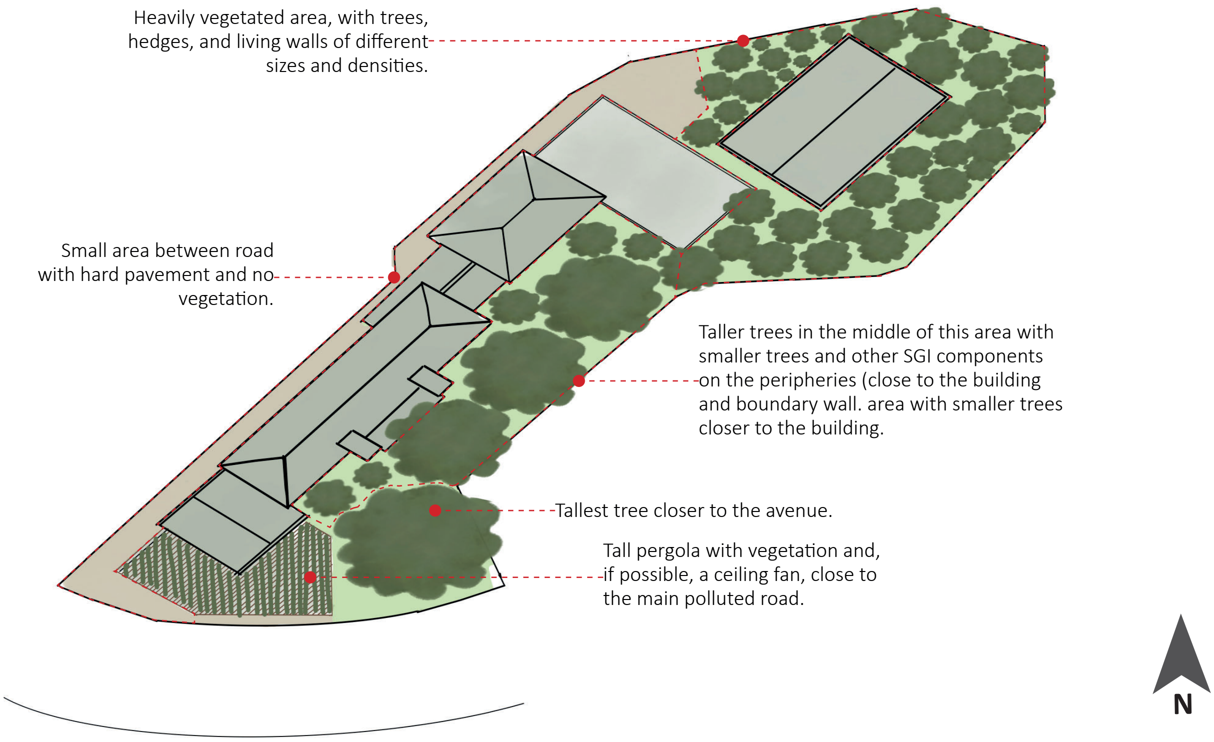

Figure 7.6.16 - Sketch with SGI proposal for School EMEF Amorim Lima.

Park 01 is the southwestern portion of the site and is mostly vegetated. As extensively mentioned in the outcomes of the case study chapters, air pollution is usually higher in this area. The environment represents an opportunity to implement a pergola to create the same or even higher level of shade. The level of greenery would probably be reduced. However, proposing a higher element with a ceiling fan would increase wind speed and enhance air quality. Finally, there are trees between the northwestern façade and the vehicular road. If the vegetation is eliminated, pollution concentration could be reduced.

7.6.3. INTERPRETING THE ENVIRONMENTAL PERFORMANCE MATRIX

The matrix already displays the studied architectural elements, SGI components, cases, central outcomes (focusing on PET and PM2.5) and the main guidelines for each case. However, this section briefly exemplifies how the Environmental Performance Matrix can be interpreted and used within a factual context. Thus, a flow chart (figure xx) was developed to serve as a "step-by-step" mode of reading the Matrix information and even indicating where to find other relevant material present in the thesis (concerning guidelines).

To begin using the matrix, two primary factors need to be considered. The first step is to understand the characteristics of the specific school building's project or built environment to be accessed. The facades' treatments and orientations are the first aspect to understand. Hence, the first question to be answered is: where are the main openings? To

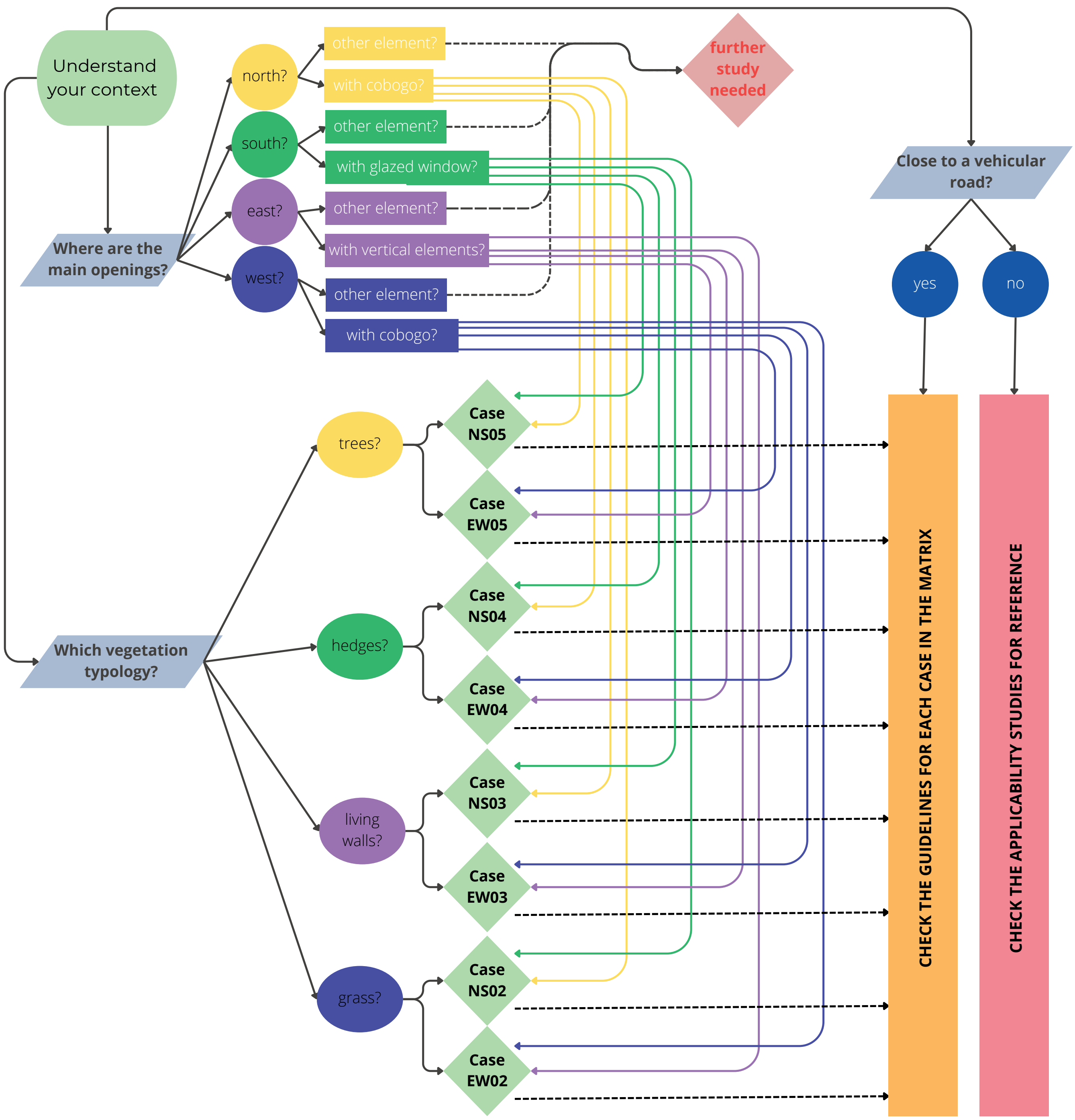

Figure 7.6.17 - Sketch with SGI proposal for School EMEF Amorim Lima.

determine the orientation. Afterwards, the façade treatments should be paired with one of the architectural elements of the matrix. If the façade design is entirely different from one of the mentioned components or is not on the indicated orientation, further study is necessary to understand its environmental impacts, as that is out of the matrix's scope. Moreover, the question of which vegetation typology will be applied or is available in the school's terrain needs to be answered. The choice of the SGI and architectural components and their located façade orientations leads to the specific scenarios' outcomes and guidelines. However, the matrix comprises cases with pollutant sources approximately two to five meters close to the vegetation elements. Thus, a last question is asked: Is the area where the vegetation is located, or where it will be planted, adjacent to a vehicular road? If the answer is yes, the guidelines on the matrix are accurate and can be followed. Nonetheless, if the answer to the question above is no, other examples shown through the applicability studies (sections 7.6.1 and 7.6.2) would illustrate how to proceed.

7.6.4. IMPLEMENTING THE ENVIRONMENTAL PERFORMANCE MATRIX

The matrix and guidelines presented in this thesis are intended to be given and converted into official governmental policies for public schools in the state. A few routes could be considered for the mentioned implementation and overall use of the matrix. The first route is through the policymakers and consists of preparing a presentation in Portuguese illustrating the matrix, guidelines, applicability studies, and other main findings of this thesis. This presentation would then be shown to the focus group, including the two architects mentioned in section 7.3 of this chapter. In addition to Helena Ayoub and Alexandre Delijaicov, the matrix will be discussed with the architects who work at the Educational Development Foundation (FDE) and are responsible for drafting the policies implemented in the state. The outcomes will also be presented and discussed with Sao Paulo's building department (EDIF) team, which consists of architects that design the schools in the city. The mentioned conversations will be vital to the auxiliary in defining the final format for the Environmental matrix and its guidelines to become official policies. To have the matrix within the official state's policies, the people responsible for managing the state's money and allowing it to be injected into the schools must also be convinced of its positive impacts. Thus, a discussion will also need to be held with government members who can allow such a policy to be implemented.

The second path for using the Environmental Performance Matrix is to present it to the schools. The concepts and outcomes of this thesis should also be shown to the school heads, teachers, and students to familiarise them with the necessity of implementing it within their built environment. The matrix and main guidelines could be printed and handed out to students to add their drawings and/or written comments, which could be discussed in a group workshop. These workshops would also allow for understanding at a community level the positive effects that the matrix could have, making it easier to implement later. The school management has a significant role in its success as the team is responsible for ensuring that the changes proposed by the guidelines can be implemented throughout the year within the schools' environments.

7.7. DISCUSSION AND CONCLUSION

As discussed throughout this chapter, the guidelines and applicability studies presented here are derived from this thesis's extensive study of over 60 scenarios and the field and analytical work conducted for EMEF Amorim Lima. Still, the analysis considers one type of each SGI component (grass, hedges, living walls and trees). Also, as explained in the previous chapter, the analytical exercise is conducted in a simplified modelled environment that mirrors the main characteristics of a school in Sao Paulo. Thus, further analysis is encouraged for every SGI component in each context. The best practices and applicability suggestions in this chapter represent global information that is useful for any school in the state and beyond if the weather conditions are similar. The presented recommendations alone have the potential to create positive impacts on users' health and comfort. However, a specific analysis should be conducted to ensure accurate knowledge of an environment's performance. Moreover, the applicability study section focuses solely on what is best for enhanced environmental performance. It does not consider the specificities of each school's program and the best outdoor organisation to match those necessities. Thus, the applicability study is a set of suggestions that require a more in-depth understanding of the complexity of each case to be adequately proposed.

It is essential to note that an assessment considering the biodiversity and ecology impacts of adding or subtracting SGI components has not been conducted in this research as it is out of its scope. For example, in the Amorim Lima applicability study, the mentioned impacts are not considered when suggesting substituting trees for a pergola with vegetation. Despite the positive environmental impacts that a modification of this magnitude would achieve, a proper ecological and biological study should be established. The research would probably establish if it's worth performing such a change. Ideally, this chapter's guidelines and application suggestions should be connected to complex ecological and well-being research. Finally, the discussion with the interest group validates the importance of this research's guidelines to the architectural community connected to public school buildings in Sao Paulo. For example, the discussion raised the necessity of identifying how the species in the FDE catalogue could be used in schools. The conversation also indicates the possibility of discussing the guidelines with other professionals directly connected to EDIF (building department) and FDE (foundation for educational development). Presenting the guidelines to the mentioned group is a channel to refine them so that they can possibly be officially applied to government manuals.

This chapter concludes this thesis work and starts by discussing the group of interest composed of two architects from Sao Paulo who were invited to validate this work. Validation is achieved by affirming how interesting the outcomes and guidelines are while establishing the possibility of further conversation with other related professionals to transform them into policies. The chapter continues by showcasing a brief history of the country's policies and a few of their impacts, focusing on the city of Sao Paulo. The mentioned section illustrated how, late in the 19th century, concerns about environmental issues and the need for policies were raised. Furthermore, the FDE guidelines review demonstrates the level of detail concerning building guidelines to be followed and the importance of having nature within school environments. However, the study also shows the lack of specific procedures concerning SGI components. Afterwards, the final version of the Environmental Performance Matrix illustrates a simplified rendition of this thesis's main analytical exercise, including studied components, outcomes and guidelines. The best practices discussion then elaborates on where and how to use each SI component, focusing on cases with north/south and east/west building openings, accomplishing a list with the most relevant guidelines. The Guideline subchapter also organised 70 tree species catalogued in the FDE manual into three main groups, indicating their potential to enhance pollution levels. Only five species are indicated to be placed close to vehicular roads. The applicability studies close the chapter by extending the basic guidelines into broader suggestions using built schools. The school examples show the vast possibility of the application of the SGI component. As previously mentioned in the discussion, this chapter contains the final product of this thesis, which is material that could be developed into official Sao Paulo state policies.

8. CONCLUSION

8.1. RESEARCH ANSWERS

This doctoral project answers the research's initial questions by concluding that small-scale green infrastructure (SGI) inside a school in the tropical megacity of Sao Paulo can increase users' thermal comfort. The thesis states that children, adolescents, and school staff with access to outdoor spaces can experience an enhancement of 20% to 28% in thermal comfort in the hottest hour of 2050. The improvement occurs when comparing environments with no vegetation to an area with a cluster of 13m high trees with high Leaf Area Density (LAD). When comparing a non-green space with an area with grass coverage, the enhancement in comfort is 1% to 5%. In contrast to living walls, the increase is between 9% to 11%. In the case of hedges, the increase varies from 2% to 11%. Furthermore, considering the exact same comparisons, in the coldest hour of 2050, there is a thermal comfort reduction of 1% when a cluster of trees is added to the environment. The space with grass also shows a 1% decrease compared to the hard-paved area. The alteration in comfort due to the addition or subtraction of each SGI component clearly indicates that when combined, forming a full small-scale green infrastructure significantly impacts perceived thermal conditions at any time of the year. The positive impacts are clearer in warmer periods of the year. In the coldest times, trees are the components with the best performance; however, all vegetation elements slightly decrease thermal comfort. Regarding the health aspect of the research question, a literature review indicates that vegetation is essential in improving mental health and well-being, including in school environments. With the thesis' focus on pollutant particles and a health indicator for children and teenagers' health, the outcomes indicate otherwise. In the hottest studied hour, when comparing the case with no vegetation with the tree cluster, the latter showed a 21% increase in pollutant concentration when there were no boundary walls. With boundary walls, the air quality decreases by only 5%. The other cases with individual SGIs also show increased pollutant concentrations, mainly when no walls are on the site's edge. The outcomes answer that when focusing on PM10 and PM2.5, SGI can help to decrease physiological health. However, each SGI component's specific characteristics and morphological configuration define the final impact on physical health. In addition to other conditions of the environment, such as solid boundary walls.

The second research question concerns which design guidelines could be proposed for schools in Sao Paulo to improve their environmental performance. Also, the third and final question raises how design guidelines for one studied school could be replicated in other contexts with similar climatic and morphological conditions. The doctoral research answered these questions in the previous chapter (07). As previously discussed, Chapter 07 is this work's culmination, where the outcomes are adapted into policies and practical approach studies. The guidelines are informative, with architects, other professionals, and policymakers related to public school design and management in Sao Paulo state as the interest group, which provided feedback through a focus group. The best practices mainly advise on the SGI components' location in outdoor school environments, focusing on pollutant sources. The size and density of the green elements are also commented on as important variables in identifying suitable placements. There are also suggestions concerning when not having vegetation or reducing their density. Beyond the vegetation, the guidelines also delve into shading architectural elements such as pergolas and non-passive solutions such as ceiling fans. The mentioned proposition is an example of combining architecture and SGI to concurrently improve thermal comfort and air quality. To have a direct link to the policies in place, the chapter identifies how the tree species from the foundation for the educational development (FDE) manual can be best placed. Finally, a study is conducted applying the outcomes of chapters

04, 05, and 06 and the best practices into possible approaches utilising schools that were reviewed in chapter 03. Chapters 04 and 05 are oriented to EMEF Amorim Lima, yet Chapter 06 is designed so that the studied generic environment is relatable to any other school site within similar environmental conditions. The mentioned approach validates the exercise outcomes for different contexts. Thus, this research identifies solutions to improve the environmental performance of schools in Sao Paulo while also providing a set of procedures that can be applied in any situation with similar morphological and climatic conditions.

8.2. SUMMARY AND DISCUSSION

Through a comprehensive multicriteria evaluation, this dissertation uncovers the intricate relationship between Small-Scale Green Infrastructure (SGI) and school outdoor environments. This exploration is crucial within urban planning and human well-being and health. Two quantitative-oriented studies delve into this topic. The first employs the concept of a "case study" to analyse, through field and analytical exercises, the current characteristics of an existing school within the denser urban environment of Sao Paulo city. It highlights the overall potential of SGI components to enhance children's human thermal comfort. While also proving a more complex and possibly negative relationship between vegetation and pollutant particle concentrations. The second study focuses on the individual environmental potential of each SGI element spotted in schools' outdoor areas. It is conducted through a comparison-based approach to analytical work. The exercise discloses the capacity of denser vegetation to trap pollutant particles and concurrently significantly enhance human thermal comfort. It also showcases the opposite outcomes when analysing the green elements of less size and density. Furthermore, in addition to the quantitative studies, qualitative research is present in the form of the literature review of concepts discussed in this thesis. The thesis also presents an architectural review of schools in Sao Paulo based on the knowledge of environmental design and sustainability principles, which feeds into the cited quantitative work. Together, these studies clarify vegetation's role in possibly augmenting the concentration of airborne particulate matter pollutants while confirming the positive thermal outcomes. However, it also provides a valuable translation between outcomes and discussions into guidelines within the context of Sao Paulo's existing public school policies, offering practical additional insights into it and overall urban planning.

8.2.1. SMALL SCALE GREEN INFRASTRUCTURE

Chapter 02 establishes that **megacities comprise 10% of the global population, with only 2% of the earth's surface coverage. Four are in Latin America**, thirteen are in Asia, and two are in Africa. This indicates the dense character of these essential urban environments and their presence in tropical climate areas. The chapter also indicates that if changes concerning the current pollutant emissions are not made over the next 100 years, **megacities will be responsible for 25% of global warming**. The urban heat island (UHI) term, created in 1958, and its existence within the dense urban settlements until today are also discussed, with 48% of the world population living in areas exposed to heating-related environmental issues. The research on Sao Paulo also demonstrates the problems that this thesis' city of interest, with 21 million inhabitants, currently administers regarding thermal comfort and air quality. **Representing 11% of Brazil's population, the city displays pollution levels usually above national and international guidelines**. Additionally, an increase in hospitalisation has been connected to PM2.5 and PM10 levels, causing a total cost of 111 million USD. Environmental issues, specifically in the city because of UHI, have also been identified. For example, there is an increase in flood risks and the development of A. aegypti mosquito larvae, which causes Dengue disease.

The environmental impacts of the SGI components already registered in the literature are exposed in the chapter. The discussion shows that the areas surrounding living walls within an urban context had a dry bulb temperature of 1.5°C lower than the uncovered wall in some periods of the day. It has also established a 15°C terrestrial surface temperature difference between vegetated and non-vegetated areas in a Brazilian city. Also, my own master's thesis is referenced as showing a 25% mean radiation reduction in a park caused by implementing trees. Some of the previous outcomes exemplify the positive thermal impact of SGI. **Research also suggests that vegetation, when in school environments, can reduce the symptoms of attention deficit and hyperactivity disorder in children**. The chapter also discusses vegetation's positive and negative impacts on air quality. The discussion is exemplified by cases where **trees in street canyons reduced air quality due to reduced tree crown porosity**. On the contrary, other research confirms the capacity of vegetation to remove gases (O3, NO2, SO2 CO) and PM10.

8.2.2. SAO PAULO AND PUBLIC SCHOOLS

Chapter 03 illustrates the **higher negative impact of environmental issues, mainly air pollution, on children's health compared to adults.** It is established that **93% of the world's children live in environments with air pollution levels higher than the WHO guidelines, with one in five of them dying due to environmental-related risks.** It was mentioned that **children are more sensitive to extreme thermal conditions due to psychological, behavioural, and metabolic characteristics**. Research shows an increase in NO2 pollution concentration in London schools' paths. Also, research conducted during the COVID-19 pandemic exemplified **the positive physical and mental health impacts of physical learning environments on children and adolescents.** The examples mentioned and the complete literature review in Chapter 03 validate the relevance of studying the environmental conditions of school environments and children's health. This research section also explained the development of public schools in Sao Paulo and the overall governmental structure around them. State and city departments responsible for the school's design, program definitions, and administration are also discussed. The chapter establishes the importance of modernist architecture in school buildings and the similarities between state and city projects. The review conducted in twelve schools in the state reveals the extensive use of prefabricated concrete structures, aluminium roofs above concrete slabs, glazed windows with metallic frames, and concrete cobogos. **The architecture review shows schools where the shading elements, such as cobogos, perforated roof tiles and wood panels, are placed correctly on northern and western facades**. The examples also show the corridors in front of the classrooms acting as horizontal overhangs. **The mentioned horizontal shading is seen to be correctly placed in front of other facades, protecting from sun radiation during summer and allowing incidence during winter.** However, other examples, such as **EMEF Amorim Lima, illustrate the incorrect use of shading elements, with the cobogos placed on the southeastern façade (less exposed façade). Clear glazing windows face the most exposed façade (northwest).**

8.2.3. CASE STUDY - FIELDWORK

Chapter 04 is dedicated to the fieldwork done over 14 days, divided into two main exercises, over a span of two years at the EMEF Amorim Lima school, located in a moderately dense area of Sao Paulo city. The school's outdoor space with more dense vegetation (trees, hedges, living walls, and grass) indicates the best thermal comfort within other open areas through dry-bulb and surface temperature outcomes. Within the summer days of exercise, in the sunnier and warmer studied periods, air temperatures were consistently lower in areas of the school's terrain, with trees tall and dense enough to provide shading. The 08 am study hour with less solar exposure and colder overall dry-bulb temperatures demonstrate the opposite outcomes. Air temperatures are lower in the areas with taller trees than the rest of the school's site. The results suggest a **more constant temperature in the areas with trees which provide shade.** Outcomes establish **the importance of enhanced air movement in possibly increasing thermal comfort** through lower air temperature measurements in areas with higher wind speeds.

The study in the indoor environment shows higher dry-bulb temperatures and glare in the classroom with glazed windows exposed to direct sun radiation. This **confirms the negative impacts of inadequate façade design and the importance of crossed ventilation.** The chapter also illustrates the **negative impact of dense vegetation when placed close to ground-floor windows through the available daylight outcomes**. Concerning air quality, the fieldwork using PM10 and PM2.5 measurements as indicators shows that **lower pollution concentrations are spotted in sunnier, warmer periods, while they increase in colder hours.** The research also establishes the higher concentration of pollutant particles (PM10 and PM2.5) in the spot below a higher number of tall trees. However, there is a substantial reduction in the spot inside the school terrain compared to the pollutant concentration spotted in the area outside the terrain boundary wall. **Areas of the school with higher wind movement were the spaces with the best air quality.**

8.2.4. CASE STUDY – ANALYTICAL WORK

Chapter 05 focuses on the analytical study of the EMEF Amorim Lima's outdoor environment through a year, focusing on the colder and warmer seasons and using MRT (mean radiant temperature) and UTCI (universal thermal climate index) as main thermal comfort indicators. PM2.5 and PM10 concentrations also demonstrate air quality conditions in this chapter. **The outcomes corroborate the fieldwork results concerning the tree's capacity to reduce the thermal amplitude during the day and night**. It illustrated vegetated areas of the school with higher MRTs and UTCI levels during the winter day. Meanwhile, the UTCI index and MRTs were lower during the summer hours in the same area. **The inadequate façade design of the school's main building is confirmed in this chapter. The accumulative annual irradiation on the northwestern façade, which is glazed without shading elements, was 40% higher than the southeastern façade treated with cobogos**. Concerning thermal comfort, the outcomes also confirm the field exercise by defining that the thermal amplitude is reduced when vegetation obstructs the view of the sky. The new findings in this section establish the **lack of human-perceived thermal comfort in the entire outdoor environment of the school during winter days at 04 pm. The areas under dense trees are 13% less comfortable at the mentioned period than on a summer day.** It is pointed out that at this period, lower sun angles are responsible for higher ground exposure. On other periods of the summer and winter days **with lower temperatures and higher sun angles, the vegetation's potential to provide comfortable areas is augmented. For example, at 04 pm on the winter day, areas under trees were perceived as 28% less comfortable compared to 11 am on the summer day**. The PM2.5 and PM10 concentrations also corroborated the fieldwork results. **The air quality is lower in the vegetated areas of EMEF Amorim Lima, which are close to pollution sources. At 8 am on the summer day, the park close to the avenue had 60% more pollutant concentration than the vegetated area protected by adjacent buildings. Additionally, the periods with higher dry bulb temperatures again have lower pollution. The peak PM2.5 concentration in the adjacent avenue at 08 am was 49% higher than at 04 pm. Finally, the areas with lower wind speeds are more polluted.**

8.2.5. ENVIRONMENTAL PERFORMANCE MATRIX

Chapter 06, the main analytical exercise of this thesis, focuses on individual SGI components' performance on warmer and colder days in 2050, confirming all the outcomes discussed in chapters 04 and 05. Concerning the indexes used to represent the air quality and thermal comfort, the change was in using PET (Physiological Equivalent

Temperature) instead of UTCI. The chapter illustrates that within 10 different studied scenarios, the ones without any vegetation addition have the lowest airborne pollutant particle concentration. **The lowest amount of PM2.5 registered within the site was in the case with no vegetation in the hottest studied period, which also showcased the worst thermal comfort performance: 89% above the average comfort band.** The mentioned period indicated a lack of human thermal comfort in any studied scenario (SGI typologies). **Boundary walls between pollutant sources and school terrain were confirmed as the best strategy to enhance air quality, even when implementing vegetation.** However, **air movement was also confirmed as the most significant microclimatic condition to impact particle distribution**. It was also established that independent of the number of pollutants being released, the performance of the SGI components remains constant. Moreover, **the tree was proven to be the overall SGI element with the best thermal performance and lower air quality efficiency.** Still, the boundary walls can enhance the result even with the use of trees when wind velocities are higher. **Hedges and living walls had similar performances concerning pollutants, with the living wall performing slightly better when analysing thermal comfort**. In cases with boundary walls, hedges have an overall performance; the opposite happens in cases without walls. It suggested how **denser bodies of vegetation can still act as barriers against pollution but are not as effective as the combination of architecture and vegetation (hedges and walls).**

8.2.6. APPLICABILITY STUDIES

As previously mentioned, the combination of chapters 04, 05 and 06 outcomes bring this thesis to a conclusion through chapter 07's guidelines and applicability studies. **The Applicability Studies chapter contains a set of suggestions that focus on the arrangement and selection of SGI components within the context of Sao Paulo's public school environment**. The chapter also highlights that the presented "best practices" require a deep study of each school so that there is scientific certainty in the proposal for each case. An ecological study of the propositions is also required to add to the environmental impact aspect discussed in this thesis. Chapter 07 shows that **the suggestions derived from this work's field and analytical works are tested with a focus group of Brazilian architects** who work with state school projects in the city. **The conversation underscored the importance of the SGI inside school environments** for the ones in charge of designing it. Both architects explained that **discussions were being held on the best way to integrate greenery into public school sites**. The **focus group expressed how informative and useful the presented guidelines were** and showed interest in continuing the conversation by involving other professionals **so that it could possibly be implemented in the future**.

8.3. LIMITATIONS AND FURTHER RESEARCH

The parameters of interest in this research to represent air quality conditions are the airborne particulate matter. The decision is made based on the risk that the mentioned pollutants represent, mainly to children. Hence, as previously underscored, the recommendations established in the thesis are a response to their portrayal of the field and analytical exercises. This research is then limited to partially understanding SGI performance regarding air pollution. The literature review indicated how vegetation reduces pollutants such as NO2, CO2 and O2. Thus, a future research avenue could be to investigate the potential of small green infrastructure components to impact the cited pollutants. This knowledge level within this work's morphological and climatic conditions would reinforce decision-making concerning SGI location and other policies presented here.

One of the most significant limitations of this research, as discussed in Chapter 06, is its restricted resources, which mainly concern time. To deliver comprehensive and straightforward outcomes, the thesis focuses on reducing the number of variables. The editing mentioned establishes a unique scenario within the analytical framework. The scenario is composed of a ground-floor building, even though most schools in the state usually have ground plus two floors. The decision reduces the number of variables and different outcomes. It is, as the EMEF Amorim Lima fieldwork (chapter 04) indicated that the outcomes in the area closer to the pollutant sources will always perform worse than in the other heights. Furthermore, a unique representative of each studied component is set. For example, their matching simplified renditions represent vertical shading, horizontal hangs, cobogo panels, and glazed windows. The same happens with the SGI, where there is only one type of tree with a specific height and LAD. The concept is repeated with living walls, grass, and hedges. The simplification is an understandable approach that permits the focus to be set on comparing cases. However, it limits this research from fully understanding the performance of elements with other characteristics. It opens the path to future research to delve into the complexity of vegetation species and define their true environmental impacts. The guidelines produced in this research can be used as overall guidance. However, specific studies could be conducted to determine the best practices for each scenario. Thus, ideally, each school environment and its design proposals should be analysed individually.

Chapter 04, which contains this thesis fieldwork, sets another limitation. The work was developed in a scenario of the COVID-19 pandemic (2020) and post-pandemic (2021) in Brazil, which is not this author's country of residence. The mentioned context limited access to the school and its users. Consequently, the first idea of a methodology also based on interviews as an indicator of health and well-being was discarded, with the main indication being achieved through a literature review. Further work could focus on the qualitative perception of vegetation within school environments, focusing on questionnaires and workshops with students, tutors, and other staff. Moreover, the limitations of access to the school due to the necessity of travel within the context of the COVID-19 pandemic resulted in a 14-day study with point-int-time measurement collected data. It strongly indicated the site-related environmental patterns. However, it represents an opportunity for future research within the context of a school in Sao Paulo. Research can be conducted through nonstop data collection over a longer period.

In Chapter 05, more specifically for the annual solar radiation studies, the trees are modelled as solid elements. The mentioned method illustrates a limitation of this body of work. When the mentioned study was undertaken, the software did not allow for applying some level of translucency for vegetation modelling. The modelling method mentioned would best represent the natural characteristics of the trees in EMEF Amorim Lima. Even though the simulation results indicate the level of shading the trees cause, they don't accurately express the amount of radiation that falls into the facades beyond the trees. Thus, further studies could be conducted with other software to mimic the trees' characteristics better. Concerning the same chapter (05 – EMEF Amorim Lima Analytical work), another limitation was calibrating the ENVI-met software by comparing it with the fieldwork. The grid was considered as one meter to acquire a high resolution of the simulations' outcomes. The software is significantly robust, and with a small grid, each simulated case took over fourteen hours to run. Thus, the number of iterations should be reduced as much as possible. Additionally, this section focused on the annual performance represented by summer and winter days. Consequently, the exact days and conditions of the fieldwork were not mimicked in the software. However, the trends observed in the fieldwork study could also be seen in the ENVI-met analysis, validating the fieldwork outcomes.

Once again, in chapter 06, the thesis indicates the indoor environment; still, it doesn't explore its performance in more detail. Due to the ENVI-met's constraints, only dry bulb temperatures are calculated for each indoor modelled space, which is analysed in the chapter outcomes. Even though there is a lack of a specific definition of thermal comfort and air quality indoors, the outdoor conditions are a reliable indication of the situation inside the building. The public school buildings in the city and state provide indoor air movement through passive strategies, establishing the necessity of crossing ventilation for enhanced performance during warmer periods. Further research could delve into the indoor environment by conducting outdoor wind pattern analyses to ensure wind movement within the interior. This thesis does not take the abovementioned approach, as its main interest is the outside areas of schools.

8.4. CONTRIBUTION TO KNOWLEDGE

This thesis contributes significantly to knowledge in the complex context of the design and development of school environments within environmental challenges. It is singular in the fact it quantifies, using a few parameters, the impacts of different vegetation typologies. The findings confirm characteristics of vegetation that have been tested and proved for the past years. It is one of the examples of works that focus on the local (immediate) results of having trees and other vegetation. For example, some SGI elements' capacity to trap and increase an environmental pollutant concentration. In addition to positive human well-being and thermal comfort outcomes when they are implemented. Still, it is expressed in the literature review that further research is needed to identify the patterns of airborne particle dispersion, which is accomplished by this work. Additionally, the multicriteria evaluation through quantitative and qualitative research focusing on SGI components and their impact on the indoors is a novelty of this thesis. It achieves an understanding of the qualitative impacts through a literature review discussion. The quantitative section is expressed through field and analytical exercises in a context where fieldwork is a less common method to produce scientific evidence (as explained in Chapter 01). This thesis's unique achievement is the profound demonstration and discussion of wind patterns and barriers composed of brick as school boundary walls impact particulate matter dispersion and concentration patterns. Ranking by quantification of thermal comfort and air quality indicators, the performance of grass, hedges, living walls and trees (using a sample of each) is also a new approach in itself. Additionally, the mentioned evaluation, combined with the architectural components characteristic of the public schools of a state in Brazil, is an even more unique approach.

8.5. FINAL REMARKS

This doctoral research identifies the individual impacts of grass, hedges, living walls and trees on airborne pollutants and perceived thermal comfort in percentages. The thesis group of interest is composed of the future of the world's society, relating directly to the sustainability sciences and work fields that aim to preserve and enhance future human life by doing the same for this planet's environment. Using field analyses combined with the robust and pioneer modelling software ENVI-met, this research delves into the complex task of advising on choosing and locating vegetation focusing on dense urban settlements, where 10% of our global population resides. This level of quantitative research on the impacts of vegetation on design guidance in the context of public schools in Sao Paulo has never been previously achieved. Also, this work applies to the entire state due to the mentioned background and the school guidelines already in place. The existence of a system built through manuals developed and administered by architects and policymakers facilitates the use of the evidence-based suggestions produced in this thesis. Regarding findings, the most predictable one was the excellent performance of trees in enhancing thermal comfort and, in contrast, confirming the capability of trees to trap pollutant particles and decrease air quality. Additionally, the overall best performance of living walls, not only in terms of thermal comfort but specifically for the air quality compared to hedges, was unexpected. Finally, the thesis also displays remarkable findings, such as the 35% increase in air pollution within cases with the same wind velocities. Additionally, when air movement drastically drops, air quality further decreases by 40%. Furthermore, this doctoral work highlights the challenges of comprehending the characteristics and defining the best uses of living structures, such as greenery as a tool for urban development and having schools as a starting point. Still, it also underscores the potential of technological advancements and data analysis to develop urban spaces with a responsible and mindful approach toward green infrastructure. The infrastructure must be carefully planned to provide the best possible outcomes within cities in rushed and constant growth.

BIBLIOGRAPHY

Abakerli, S. (2001). A critique of development and conservation policies in environmentally sensitive regions in Brazil. Geoforum, 32(4), pp.551–565. doi:https://doi.org/10.1016/s0016-7185(01)00015-x.

Abdulateef, M.F. and A. S. Al-Alwan, H. (2021). The effectiveness of urban green infrastructure in reducing surface urban heat island. Ain Shams Engineering Journal. doi:https://doi.org/10.1016/j.asej.2021.06.012.

Abhijith, K.V., Kumar, P., Gallagher, J., McNabola, A., Baldauf, R., Pilla, F., Broderick, B., Di Sabatino, S. and Pulvirenti, B. (2017). Air pollution abatement performances of green infrastructure in open road and built-up street canyon environments – A review. Atmospheric Environment, 162, pp.71–86. doi:https://doi.org/10.1016/j.atmosenv.2017.05.014.

Akbari, H., Bretz, S., Kurn, D.M. and Hanford, J. (1997). Peak power and cooling energy savings of high-albedo roofs. Energy and Buildings, 25(2), pp.117–126. doi:https://doi.org/10.1016/s0378-7788(96)01001-8.

Akpinar, A. (2016). How is high school greenness related to students' restoration and health? Urban Forestry & Urban Greening, 16, pp.1–8. doi:https://doi.org/10.1016/j.ufug.2016.01.007.

Akpinar, A., Barbosa-Leiker, C. and Brooks, K.R. (2016). Does green space matter? Exploring relationships between green space type and health indicators. Urban Forestry & Urban Greening, 20, pp.407–418. doi:https://doi.org/10.1016/j.ufug.2016.10.013.

Al-Dabbous, A.N. and Kumar, P. (2014). The influence of roadside vegetation barriers on airborne nanoparticles and pedestrians exposure under varying wind conditions. Atmospheric Environment, [online] 90, pp.113–124. doi:https://doi.org/10.1016/j.atmosenv.2014.03.040.

Alammar, A., Jabi, W. and Lannon, S. (2021). Predicting incident solar radiation on building's envelope using machine learning.

Ambrosini, D., Galli, G., Mancini, B., Nardi, I. and Sfarra, S. (2014). Evaluating Mitigation Effects of Urban Heat Islands in a Historical Small Center with the ENVI-Met® Climate Model. Sustainability, 6(10), pp.7013–7029. doi:https://doi.org/10.3390/su6107013.

Andrade, M. de F., Kumar, P., de Freitas, E.D., Ynoue, R.Y., Martins, J., Martins, L.D., Nogueira, T., Perez-Martinez, P., de Miranda, R.M., Albuquerque, T., Gonçalves, F.L.T., Oyama, B. and Zhang, Y. (2017). Air quality in the megacity of São Paulo: Evolution over the last 30 years and future perspectives. Atmospheric Environment, [online] 159, pp.66–82. doi:https://doi.org/10.1016/j.atmosenv.2017.03.051.

Aquino, J.G. and Sayão, R. (2004). Da construção de uma escola democrática: a experiência da Emef Amorim Lima. Eccos (Sao Paulo, Brazil), 6(2), pp.15–38. doi:https://doi.org/10.5585/eccos.v6i2.378.

Araujo, R.V., Albertini, M.R., Costa-da-Silva, A.L., Suesdek, L., Franceschi, N.C.S., Bastos, N.M., Katz, G., Cardoso, V.A., Castro, B.C., Capurro, M.L. and Allegro, V.L.A.C. (2015). São Paulo urban heat islands have a higher incidence of dengue than other urban areas. The Brazilian Journal of Infectious Diseases, 19(2), pp.146–155. doi:https://doi.org/10.1016/j.bjid.2014.10.004.

ArchDaily Brasil. (2015). Escola Estadual Nova Cumbica / H+F Arquitetos. [online] Available at: https://www.archdaily.com.br/br/767036/escola-estadual-nova-cumbica-herenu-plus-ferroni-arquitetos [Accessed 12 Oct. 2023].

ArchDaily Brasil. (2020). Escola Estadual Jardim Romano / H+F Arquitetos. [online] Available at: https://www.archdaily.com.br/br/953033/escola-estadual-jardim-romano-h-plus-f-arquitetos?ad_medium=mobile-widget&ad_name=more-from-office-article-show [Accessed 12 Oct. 2010].

ArchDaily. (2022). Parque do Carmo Unified Education Center / SIAA + HASAA. [online] Available at: https://www.archdaily.com/987972/parque-do-carmo-unified-education-center-siaa-plus-hasaa?ad_medium=gallery [Accessed 12 Oct. 2023].

Armani, G., Beserra de Lima, N.G., Pelizzon Garcia, M.F. and de Lima Carvalho, J. (2022). Regional climate projections for the State of São Paulo, Brazil, in the 2020 - 2050 period. Derbyana, 43. doi:https://doi.org/10.14295/derb.v43.773.

Arquitetos, F. (2012). FDE - Escola Várzea Paulista / FGMF. arch daily. Available at: https://www.archdaily.com.br/br/01-19508/fde-escola-varzea-paulista-fgmf?ad_source=search&ad_medium=projects_tab.

Baek, S.-O., Kim, Y.-S. and Perry, R. (1997). Indoor air quality in homes, offices and restaurants in Korean urban areas—indoor/outdoor relationships. Atmospheric Environment, 31(4), pp.529–544. doi:https://doi.org/10.1016/s1352-2310(96)00215-4.

Baklanov, A., Molina, L.T. and Gauss, M. (2016). Megacities, air quality and climate. Atmospheric Environment, 126, pp.235–249. doi:https://doi.org/10.1016/j.atmosenv.2015.11.059.

Bakos, N. and Schiano-Phan, R. (2021). Bioclimatic and Regenerative Design Guidelines for a Circular University Campus in India. Sustainability, 13(15), p.8238. doi:https://doi.org/10.3390/su13158238.

Barbieri, A.F., Domingues, E., Queiroz, B.L., Ruiz, R.M., Rigotti, J.I., Carvalho, J.A.M. and Resende, M.F. (2010). Climate change and population migration in Brazil's Northeast: scenarios for 2025–2050. Population and Environment, 31(5), pp.344–370. doi:https://doi.org/10.1007/s11111-010-0105-1.

Baró, F., Camacho, D.A., Pérez, C., Triguero-Mas, M. and Anguelovski, I. (2021). School greening: Right or privilege? Examining urban nature within and around primary schools through an equity lens. Landscape and Urban Planning, [online] 208, p.104019. doi:https://doi.org/10.1016/j.landurbplan.2020.104019.

Barwise, Y. and Kumar, P. (2020). Designing vegetation barriers for urban air pollution abatement: a practical review for appropriate plant species selection. npj Climate and Atmospheric Science, 3(1). doi:https://doi.org/10.1038/s41612-020-0115-3.

Bazafkan, E., Pont, U. and Mahdavi, A. (2019). Usability and Usefulness of Non-Conventional Building Performance Simulation Tools in Architectural Design Processes. Applied Mechanics and Materials, 887, pp.219–226. doi:https://doi.org/10.4028/www.scientific.net/amm.887.219.

Behrens, T., Taeger, D., Maziak, W., Duhme, H., Rzehak, P., Weiland, S.K. and Keil, U. (2004). Self-reported traffic density and atopic disease in children. Results of the ISAAC Phase III survey in Muenster, Germany. Pediatric Allergy and Immunology, 15(4), pp.331–339. doi:https://doi.org/10.1111/j.1399-3038.2004.00157.x.

Benton-Short, L., Keeley, M. and Rowland, J. (2017). Green infrastructure, green space, and sustainable urbanism: geography's important role. Urban Geography, 40(3), pp.330–351. doi:https://doi.org/10.1080/02723638.2017.1360105.

Berglund, B., Lindvall, T. and Schwela, D.H. (1999). New Who Guidelines for Community Noise. Noise & Vibration Worldwide, [online] 31(4), pp.24–29. doi:https://doi.org/10.1260/0957456001497535.

Betti, G., Tartarini, F., Nguyen, C, Schiavon, S. CBE Clima Tool: A free and open-source web application for climate analysis tailored to sustainable building design. Build. Simul. (2023). https://doi.org/10.1007/s12273-023-1090-5. Version: 0.8.17

Blazejczyk, K., Epstein, Y., Jendritzky, G., Staiger, H. and Tinz, B. (2011). Comparison of UTCI to selected thermal indices. International Journal of Biometeorology, 56(3), pp.515–535. doi:https://doi.org/10.1007/s00484-011-0453-2.

Blazejczyk, K., Jendritzky, G., Bröde, P., Baranowski, J., Fiala, D., bullet, G., Havenith, G., bullet, Y., Epstein, Y., Psikuta, bullet and Kampmann, B. (2013). An introduction to the universal thermal climate index (UTCI). Geographia Polonica, 86, pp.5–10. doi:https://doi.org/10.7163/GPol.2013.1.

Borna, M. and Schiano-Phan, R. (2020). PLEA 2020 A CORUÑA Planning Post Carbon Cities Improving Hyperlocal Air Quality in Cities Impact of vegetation on pollutants concentration at pedestrian level https://doi.org/10.17979/spudc.9788497497947.

Bornstein, R. and Lin, Q. (2000). Urban heat islands and summertime convective thunderstorms in Atlanta: three case studies. Atmospheric Environment, 34(3), pp.507–516. doi:https://doi.org/10.1016/s1352-2310(99)00374-x.

Brantley, H.L., Hagler, G.S.W., J. Deshmukh, P. and Baldauf, R.W. (2014). Field assessment of the effects of roadside vegetation on near-road black carbon and particulate matter. Science of The Total Environment, 468-469, pp.120–129. doi:https://doi.org/10.1016/j.scitotenv.2013.08.001.

Brimblecombe, P. (2011). The big smoke: A history of air pollution in london since medieval times. [online] Routledge. Available at: https://books.google.co.uk/books?id=bx4wAFE8xGUC.

British Lung Foundation and National Education Union (2019). Air pollution guidance for school staff. [online] Leicester City Council. Available at: chrome-extension://efaidnbmnnnibpcajpcglclefindmkaj/https://schools.leicester.gov.uk/media/5334/air-pollution-guidance-for-school-staff-neu.pdf [Accessed 21 May 2024].

Bröde, P., Krüger, E.L., Rossi, F.A. and Fiala, D. (2011). Predicting urban outdoor thermal comfort by the Universal Thermal Climate Index UTCI—a case study in Southern Brazil. International Journal of Biometeorology, 56(3), pp.471–480. doi:https://doi.org/10.1007/s00484-011-0452-3.

Brumberg, H.L. and Karr, C.J. (2021). Ambient Air Pollution: Health Hazards to Children. Pediatrics, [online] 147(6). doi:https://doi.org/10.1542/peds.2021-051484.

Bruse, D. (2023). Now Available: ENVI-met V5.6 - Faster, User-Friendly, and Optimized for PrecisionRelease ENVI-met V5.6. [online] ENVI-met. Available at: https://www.envi-met.com/introducing-envi-met-v5-6-advanced-environmental-simulation-enhancements-and-new-features/#:~:-text=We%20are%20thrilled%20to%20announce [Accessed 15 Apr. 2024].

Bruse, M. (1999). Die Auswirkungen Kleinskaliger Umweltgestaltung Auf Das Mikroklima. PhD Thesis.

Bruse, M. (2004a). ENVI-met 3.0: Updated Model Overview. [online] Available at: https://www.researchgate.net/publication/238622880_ENVI-met_30_Updated_Model_Overview [Accessed 12 Mar. 2024].

Bruse, M. (2004b). ENVI-met implementation of the Jacobs A − gs Model to calculate the stomata conductance. [online] Available at: chrome-extension://efaidnbmnnnibpcajpcglclefindmkaj/https://envi-met.info/documents/new_a_gs.pdf [Accessed 8 Apr. 2022].

Bruse, M. (2007). Particle filtering capacity of urban vegetation: A microscale numerical approach. Berliner Geographische Arbeiten., [online] 109. Available at: https://www.researchgate.net/publication/265449484_Particle_filtering_capacity_of_urban_vegetation_A_microscale_numerical_approach [Accessed 12 Mar. 2024].

Bruse, M. and Fleer, H. (1998). Simulating surface–plant–air interactions inside urban environments with a three dimensional numerical model. Environmental Modelling & Software, 13(3-4), pp.373–384. doi:https://doi.org/10.1016/s1364-8152(98)00042-5.

Buccolieri, R., Gromke, C., Di Sabatino, S. and Ruck, B. (2009). Aerodynamic effects of trees on pollutant concentration in street canyons. Science of The Total Environment, 407(19), pp.5247–5256. doi:https://doi.org/10.1016/j.scitotenv.2009.06.016.

Buchanan, D., Hargreaves, E. and Quick, L. (2022). Schools closed during the pandemic: Revelations about the well-being of 'lower-attaining' primary-school Children. Education 3-13, [online] 3(13), pp.1–14. doi:https://doi.org/10.1080/03004279.2022.2043405.

Calderón-Garcidueñas, L., Reed, W., Maronpot, R.R., Henríquez-Roldán, C., Delgado-Chavez, R., Calderón-Garcidueñas, A., Dragustinovis, I., Franco-Lira, M., Aragón-Flores, M., Solt, A.C., Altenburg, M., Torres-Jardón, R. and Swenberg, J.A. (2004). Brain inflammation and Alzheimer's-like pathology in individuals exposed to severe air pollution. Toxicologic Pathology, [online] 32(6), pp.650–658. doi:https://doi.org/10.1080/01926230490520232.

Cameron, R.W.F., Blanuša, T., Taylor, J.E., Salisbury, A., Halstead, A.J., Henricot, B. and Thompson, K. (2012). The domestic garden – Its contribution to urban green infrastructure. Urban Forestry & Urban Greening, [online] 11(2), pp.129–137. doi:https://doi.org/10.1016/j.ufug.2012.01.002.

Carfan, A., Galvani, E. and Nery, J.T.Nery. (2012). Study of thermal comfort in the City of São Paulo using ENVI-met model. Investigaciones Geograficas, 78.

CETESB (2019). Boletim Diário» Qualidade do Ar. [online] Available at: https://cetesb.sp.gov.br/ar/boletim-diario/ [Accessed 15 Apr. 2024].

CETESB (2021). Qualidade do ar no estado de Sao Paulo 2020. [online] Av. Prof. Frederico Hermann Jr., 345 - Alto de Pinheiros Tel. 3133.3000 - CEP 05459-900 - São Paulo/SP - Brasil: CETESB, Companhia Ambiental Do Estado De São Paulo. Available at: https://cetesb.sp.gov.br/ar/wp-content/uploads/sites/28/2021/05/Relatorio-de-Qualidade-do-Ar-no-Estado-de-Sao-Paulo-2020.pdf [Accessed 15 Apr. 2024].

CETESB (2022). Relatorio de Qualidade do Ar no Estado de Sao Paulo. [online] CETESB. Sao Paulo. Governo do Estado. Sao Paulo: CETESB. Available at: https://cetesb.sp.gov.br/ar/publicacoes-relatorios/ [Accessed 5 May 2023].

CETESB, C.A. do E. de S.P. (2018). Politicas Publicas Ambientais . [online] Apostila Politicas Publicas Ambientais Volume I - Online PDF. CETESB. Available at: chrome-extension://efaidnbmnnnibpcajpcglclefindmkaj/https://cetesb.sp.gov.br/aguasinteriores/wp-content/uploads/sites/33/2018/08/Apostila-Politicas-Publicas-Ambientais-Volume-I.pdf.

Challoner, A. and Gill, L. (2014). Indoor/outdoor air pollution relationships in ten commercial buildings: PM2.5 and NO2. Building and Environment, 80, pp.159–173. doi:https://doi.org/10.1016/j.buildenv.2014.05.032.

Chan, E., Lam, H., So, S., Goggins, W., Ho, J., Liu, S. and Chung, P. (2018). Association between Ambient Temperatures and Mental Disorder Hospitalizations in a Subtropical City: A Time-Series Study of Hong Kong Special Administrative Region. International Journal of Environmental Research and Public Health, 15(4), p.754. doi:https://doi.org/10.3390/ijerph15040754.

Chatzimentor, A., Apostolopoulou, E. and Mazaris, A.D. (2020). A review of green infrastructure research in Europe: Challenges and opportunities. Landscape and Urban Planning, 198, p.103775. doi:https://doi.org/10.1016/j.landurbplan.2020.103775.

Chiesa, G. and Li, Y. (2021). Including Urban Heat Island in Bioclimatic Early-Design Phases: A Simplified Methodology and Sample Applications. Sustainability, 13(11), p.5918. doi:https://doi.org/10.3390/su13115918.

Crnosija, N., Levy Zamora, M., Rule, A.M. and Payne-Sturges, D. (2022). Laboratory Chamber Evaluation of Flow Air Quality Sensor PM2.5 and PM10 Measurements. International Journal of Environmental Research and Public Health, 19(12), p.7340. doi:https://doi.org/10.3390/ijerph19127340.

Department for Education UK (2016). Guidelines on ventilation, thermal comfort and indoor air quality in schools Building Bulletin 101 Draft for public consultation. [online] Department for Education UK. Department for Education UK. Available at: chrome-extension://efaidnbmnnnibpcajpcglclefindmkaj/https://consult.education.gov.uk/capital/bb101-school-design-iaq-comfort-and-ventilation/supporting_documents/DfE%20Ventilation%20guide%20consultation%20draft%2029%2006%202016.pdf [Accessed 21 May 2024].

Di Giulio, G.M., Bedran-Martins, A.M.B., Vasconcellos, M. da P., Ribeiro, W.C. and Lemos, M.C. (2018). Mainstreaming climate adaptation in the megacity of São Paulo, Brazil. Cities, 72, pp.237–244. doi:https://doi.org/10.1016/j.cities.2017.09.001.

Douglas, I. (2019). 50 years change in urban land use and ecological planning globally in the era of design with nature. Ecosystem Health and Sustainability, 5(1), pp.185–198. doi:https://doi.org/10.1080/20964129.2019.1656111.

Duarte, D. and Goncalves, J. (2006). Environment and Urbanization: Microclimatic Variations in a Brownfield Site in Sao Paulo, Brazil. [online] Available at: https://www.researchgate.net/publication/240640821_Environment_and_Urbanization_Microclimatic_Variations_in_a_Brownfield_Site_in_Sao_Paulo_Brazil [Accessed 28 May 2024].

Elraouf, R.A., ELMokadem, A., Megahed, N., Eleinen, O.A. and Eltarabily, S. (2022). Evaluating urban outdoor thermal comfort: a validation of ENVI-met simulation through field measurement. Journal of Building Performance Simulation, 15(2), pp.268–286. doi:https://doi.org/10.1080/19401493.2022.2046165.

EMEF Des. Amorim Lima (n.d.). A Escola – EMEF Desembargador Amorim Lima. [online] EMEF Desembargador Amorim Lima. Available at: https://amorimlima.org.br/institucional/ [Accessed 5 Mar. 2024].

Emmanuel, R. and Loconsole, A. (2015). Green infrastructure as an adaptation approach to tackling urban overheating in the Glasgow Clyde Valley Region, UK. Landscape and Urban Planning, 138, pp.71–86. doi:https://doi.org/10.1016/j.landurbplan.2015.02.012.

ENVI-met GmbH (2021). UTCI [A holistic microclimate model]. [online] envi-met.info. Available at: https://envi-met.info/doku.php?id=apps:biomet_utci [Accessed 20 Dec. 2022].

ENVI-met GmbH (2024). Microclimate Simulation Software | ENVI-met | Analyze Climate Change & Air PollutionSoftware. [online] ENVI-met. Available at: https://www.envi-met.com/microclimate-simulation-software/ [Accessed 15 Apr. 2024].

ENVI-met. (2019). ENVI-met - Decode urban nature with ENVI-met software. [online] Available at: https://www.envi-met.com/ [Accessed 11 Apr. 2024].

Escola Superior da CETESB (2018). Conformidade Ambiental com Requisitos Tecnicos e Legais. [online] Available at: chrome-extension://efaidnbmnnnibpcajpcglclefindmkaj/https://cetesb.sp.gov.br/aguasinteriores/wp-content/uploads/sites/33/2018/08/Apostila-Politicas-Publicas-Ambientais-Volume-I.pdf.

Evola, G., Nocera, F., Costanzo, V., Detommaso, M., Bonaccorso, S. and Marletta, L. (2021). Greenery Systems for the Mitigation of the Urban Heat Island: A Simulation Experience for Southern Italy. Lecture notes in civil engineering, pp.427–438. doi:https://doi.org/10.1007/978-3-030-68824-0_46.

Fachinello Krebs, L. and Johansson, E. (2021). Influence of microclimate on the effect of green roofs in Southern Brazil – A study coupling outdoor and indoor thermal simulations. Energy and Buildings, 241, p.110963. doi:https://doi.org/10.1016/j.enbuild.2021.110963.

Fantozzi, F., Monaci, F., Blanusa, T. and Bargagli, R. (2015). Spatio-temporal variations of ozone and nitrogen dioxide concentrations under urban trees and in a nearby open area. Urban Climate, 12, pp.119–127. doi:https://doi.org/10.1016/j.uclim.2015.02.001.

Faria, H.H. de (2004). Eficacia De Gestao De Unidades De Conservacao Gerenciadas Pelo Instituto Florestal De Sao Paulo, Brasil. [Masters Thesis] Available at: https://repositorio.unesp.br/items/0e7cf8cd-8acd-434e-927e-67e683d0b810.

Fasi, M.A. and Budaiwi, I.M. (2015). Energy performance of windows in office buildings considering daylight integration and visual comfort in hot climates. Energy and Buildings, 108, pp.307–316. doi:https://doi.org/10.1016/j.enbuild.2015.09.024.

FDE (2012). Catalogo De Especies Vegetais - Especificacoes Da Edificacao Escolar. [online] FDE, Produtos Tecnicos. Available at: https://produtostecnicos.fde.sp.gov.br/Pages/CatalogosTecnicos/Default.aspx.

FDE (n.d.). Fundação para o Desenvolvimento da Educação - CATÁLOGOS TÉCNICOS. [online] www.fde.sp.gov.br. Available at: https://www.fde.sp.gov.br/PagePublic/Interna.aspx?codigoMenu=158 [Accessed 14 Nov. 2023].

Fegert, J.M., Vitiello, B., Plener, P.L. and Clemens, V. (2020). Challenges and burden of the Coronavirus 2019 (COVID-19) pandemic for child and adolescent mental health: a narrative review to highlight clinical and research needs in the acute phase and the long return to normality. Child and Adolescent Psychiatry and Mental Health, 14(1), pp.1–11.

Fernandes, G. (2011a). FDE - Escola Parque Dourado V / Apiacás Arquitetos. [online] ArchDaily Brasil. Available at: https://www.archdaily.com.br/br/01-3326/fde-escola-parque-dourado-v-apiacas-arquitetos [Accessed 12 Oct. 2023].

Fernandes, G. (2011b). FDE - Jardim Maria Helena / + K Arquitetos. [online] ArchDaily Brasil. Available at: https://www.archdaily.com.br/br/01-254/fde-jardim-maria-helena-mais-k-arquitetos [Accessed 12 Oct. 2010].

Fernandes, G. (2011c). FDE Campinas - Escola Estadual Parque São Bento / bvy arquitetos. [online] ArchDaily Brasil. Available at: https://www.archdaily.com.br/br/01-9727/fde-campinas-escola-estadual-parque-sao-bento-bvy-arquitetos [Accessed 12 Oct. 2023].

Fernandes, G. (2012). FDE - Escola Várzea Paulista / FGMF. [online] ArchDaily Brasil. Available at: https://www.archdaily.com.br/br/01-19508/fde-escola-varzea-paulista-fgmf?ad_source=search&ad_medium=projects_tab [Accessed 12 Oct. 2023].

Fernandes, V., Andreoli, C.V., Bruna, G.C. and Philippi Jr, A. (2021). History and Evolution of the Environmental Management System in Brazil. Historia Ambiental Latinoamericana y Caribeña (HALAC) revista de la Solcha, 11(2), pp.275–310. doi:https://doi.org/10.32991/2237-2717.2021v11i2.p275-310.

Feyisa, G.L., Dons, K. and Meilby, H. (2014). Efficiency of parks in mitigating urban heat island effect: An example from Addis Ababa. Landscape and Urban Planning, 123, pp.87–95. doi:https://doi.org/10.1016/j.landurbplan.2013.12.008.

Fluhrer, T., Chapa, F. and Hack, J. (2021). A methodology for assessing the implementation potential for retrofitted and multifunctional urban green infrastructure in public areas of the global south. Sustainability, [online] 13. doi:https://doi.org/10.3390/su13010384.

Folberth, G.A., Butler, T.M., Collins, W.J. and Rumbold, S.T. (2015). Megacities and climate change – A brief overview. Environmental Pollution, [online] 203, pp.235–242. doi:https://doi.org/10.1016/j.envpol.2014.09.004.

Font, A., Guiseppin, L., Blangiardo, M., Ghersi, V. and Fuller, G.W. (2019). A tale of two cities: is air pollution improving in Paris and London? Environmental Pollution, 249, pp.1–12. doi:https://doi.org/10.1016/j.envpol.2019.01.040.

Fracalossi, I. (2011). Escola Estadual Telêmaco Melges / UNA Arquitetos. [online] ArchDaily Brasil. Available at: https://www.archdaily.com.br/br/01-13116/escola-estadual-telemaco-melges-una-arquitetos [Accessed 12 Oct. 2023].

Fracalossi, I. (2012). CEU Pimentas / Biselli + Katchborian arquitetos. [online] ArchDaily Brasil. Available at: https://www.archdaily.com.br/br/01-26029/ceu-pimentas-biselli-mais-katchborian-arquitetos [Accessed 12 Oct. 2023].

Fricker, M. and Willmer, C. (2012). Stomata. Springer Science & Business Media.

FUNDAÇÃO PARA O DESENVOLVIMENTO DA EDUCAÇÃO (2023). Fundação para o Desenvolvimento da Educação - HISTÓRIA DA CONSTRUÇÃO ESCOLAR PAULISTA. [online] www.fde.sp.gov.br. Available at: https://www.fde.sp.gov.br/PagePublic/Interna.aspx?codigoMenu=261 [Accessed 15 Nov. 2023].

Fundacao para o desenvolvimento da Educacao (2022). Fundação para o Desenvolvimento da Educação - ANO LETIVO DE 2023 COMEÇA EM 3 DE FEVEREIRO NA REDE ESTADUAL DE SÃO PAULO. [online] www.fde.sp.gov.br. Available at: https://www.fde.sp.gov.br/PagePublic/InternaNoticias.aspx?codNoticia=7443&codigoMenu=49 [Accessed 12 Oct. 2023].

Gallagher, J., Baldauf, R., Fuller, C.H., Kumar, P., Gill, L.W. and McNabola, A. (2015). Passive methods for improving air quality in the built environment: A review of porous and solid barriers. Atmospheric Environment, 120, pp.61–70. doi:https://doi.org/10.1016/j.atmosenv.2015.08.075.

García, M., Vera, S., Fabien Rouault, Gironás, J. and Bustamante, W. (2022). Cooling potential of greenery systems for a stand-alone retail building under semiarid and humid subtropical climates. Energy and Buildings, [online] 259, p.111897. doi:https://doi.org/10.1016/j.enbuild.2022.111897.

Gasparrini, A., Guo, Y., Hashizume, M., Lavigne, E., Zanobetti, A., Schwartz, J., Tobias, A., Tong, S., Rocklöv, J., Forsberg, B., Leone, M., De Sario, M., Bell, M.L., Guo, Y.-L.L., Wu, C., Kan, H., Yi, S.-M., de Sousa Zanotti Stagliorio Coelho, M., Saldiva, P.H.N. and Honda, Y. (2015). Mortality risk attributable to high and low ambient temperature: a multicountry observational study. The Lancet, 386(9991), pp.369–375. doi:https://doi.org/10.1016/s0140-6736(14)62114-0.

Government of Sao Paulo, Urban Projects Division, Environmental Planning Coordination and Secretariat for Green and Environment (2023). Parque Linear Perus - Estrategias de Projeto. [online] Parque Linear Perus - Estrategias de Projeto. Available at: chrome-extension://efaidnbmnnnibpcajpcglclefindmkaj/https://www.prefeitura.sp.gov.br/cidade/secretarias/upload/meio_ambiente/arquivos/projetos_dpu/Caderno%20Perus%20FINAL.pdf [Accessed 2 Apr. 2024].

Grasshopper Docs (2021). Honeybee - Addon for Grasshopper. [online] Grasshopper Docs. Available at: http://grasshopperdocs.com/addons/honeybee.html [Accessed 10 May 2021].

Greater London Authority (2002). Connecting with London’s nature The Mayor’s Biodiversity Strategy. [online] Mayor of London. Greater London Authority. Available at: https://www.london.gov.uk/programmes-and-strategies/environment-and-climate-change/environment-publications/connecting-london%E2%80%99s-nature-mayor%E2%80%99s-biodiversity [Accessed 20 Aug. 2020].

Greater London Authority (2019). London Atmospheric Emissions Inventory (LAEI) 2019 – London Datastore. [online] Greater London Authority. Available at: https://data.london.gov.uk/dataset/london-atmospheric-emissions-inventory--laei--2019 [Accessed 26 Aug. 2020].

Greater London Authority (2018). Mayor’s Transport Strategy. [online] Mayor of London. City Hall The Queen’s Walk More London London SE1 2AA: Greater London Authority . Available at: https://www.london.gov.uk/programmes-strategies/transport/our-vision-transport/mayors-transport-strategy-2018.

Grigorieva, E. and Lukyanets, A. (2021). Combined Effect of Hot Weather and Outdoor Air Pollution on Respiratory Health: Literature Review. Atmosphere, 12(6), p.790. doi:https://doi.org/10.3390/atmos12060790.

Gromke, C., Jamarkattel, N. and Ruck, B. (2016). Influence of roadside hedgerows on air quality in urban street canyons. Atmospheric Environment, 139, pp.75–86. doi:https://doi.org/10.1016/j.atmosenv.2016.05.014.

Gromke, C. and Ruck, B. (2007). Influence of trees on the dispersion of pollutants in an urban street canyon—Experimental investigation of the flow and concentration field. Atmospheric Environment, 41(16), pp.3287–3302. doi:https://doi.org/10.1016/j.atmosenv.2006.12.043.

Gromke, C. and Ruck, B. (2008). On the Impact of Trees on Dispersion Processes of Traffic Emissions in Street Canyons. Boundary-Layer Meteorology, 131(1), pp.19–34. doi:https://doi.org/10.1007/s10546-008-9301-2.

Hagan, S. (2014). Ecological Urbanism: The Nature of the City. [online] Taylor and Francis. Available at: https://www-taylorfrancis-com.uow.idm.oclc.org/books/mono/10.4324/9781315761480/ecological-urbanism-nature-city-susannah-hagan.

Hagler, G.S.W., Lin, M.-Y., Khlystov, A., Baldauf, R.W., Isakov, V., Faircloth, J. and Jackson, L.E. (2012). Field investigation of roadside vegetative and structural barrier impact on near-road ultrafine particle concentrations under a variety of wind conditions. Science of The Total Environment, 419, pp.7–15. doi:https://doi.org/10.1016/j.scitotenv.2011.12.002.

Hassan, Q., Sameer Algburi, Marek Jaszczur, Patrik Viktor, Iqbal, A., Ali Khudhair Al-Jiboory, Talib Munshid Hanoon, Barakat, M. and Aws Zuhair Sameen (2024). Implement and evaluate resilient energy infrastructures capable of withstanding spatial, temporal, and annual weather fluctuations in Saudi Arabia by 2050. Sustainable futures, 7, pp.100182–100182. doi:https://doi.org/10.1016/j.sftr.2024.100182.

Hassanvand, M.S., Naddafi, K., Faridi, S., Arhami, M., Nabizadeh, R., Sowlat, M.H., Pourpak, Z., Rastkari, N., Momeniha, F., Kashani, H., Gholampour, A., Nazmara, S., Alimohammadi, M., Goudarzi, G. and Yunesian, M. (2014). Indoor/outdoor relationships of PM10, PM2.5, and PM1 mass concentrations and their water-soluble ions in a retirement home and a school dormitory. Atmospheric Environment, 82, pp.375–382. doi:https://doi.org/10.1016/j.atmosenv.2013.10.048.

Higgins, S., Hall, E., Wall, K., Woolner, P. and McCaughey, C. (2005). The Impact of School Environments: A literature review. The Centre for Learning and Teaching-School Education, Communication and Language Science. University of Newcastle, 1(1).

Hirashima, S., Katzschner, A., Ferreira, D., Assis, E. and Katzschner, L. (2018). Thermal comfort comparison and evaluation in different climates. Urban Climate, 23, pp.219–230. doi:https://doi.org/10.1016/j.uclim.2016.08.007.

Hirashima, S.Q. da S., Assis, E.S. de and Nikolopoulou, M. (2016). Daytime thermal comfort in urban spaces: A field study in Brazil. Building and Environment, 107, pp.245–253. doi:https://doi.org/10.1016/j.buildenv.2016.08.006.

Hodson, C.B. and Sander, H.A. (2019). Relationships between vegetation in student environments and academic achievement across the continental U.S. Landscape and Urban Planning, 189, pp.212–224. doi:https://doi.org/10.1016/j.landurbplan.2019.04.027.

Hollick, J. (2012). Nocturnal Radiation Cooling Tests. Energy Procedia, 30, pp.930–936. doi:https://doi.org/10.1016/j.egypro.2012.11.105.

Höppe, P. (1999). The physiological equivalent temperature - a universal index for the biometeorological assessment of the thermal environment. International Journal of Biometeorology, 43(2), pp.71–75. doi:https://doi.org/10.1007/s004840050118.

Howard, E. (2010). Garden cities of tomorrow. Illustrated ed. ed. Gloucester: Dodo Press.

Hristov, J., Toreti, A., Pérez Domínguez, I., Dentener, F., Fellmann, T., Elleby, C., Ceglar, A., Fumagalli, D., Niemeyer, S., Cerrani, I., Panarello, L. and Bratu, M. (2020). Analysis of climate change impacts on EU agriculture by 2050: JRC PESETA IV project : Task 3. [online] Publications Office of the European Union. LU: Publications Office of the European Union. Available at: https://op.europa.eu/en/publication-detail/-/publication/c1e0914c-99bd-11ea-aac4-01aa75ed71a1/language-en.

Huttner, S. (2012). Further development and application of the 3D microclimate simulation ENVI-met. [Dissertation] Available at: https://openscience.ub.uni-mainz.de/handle/20.500.12030/2024 [Accessed 20 Feb. 2024].

Huys, N., De Cocker, K., De Craemer, M., Roesbeke, M., Cardon, G. and De Lepeleere, S. (2017). School Gardens: A Qualitative Study on Implementation Practices. International Journal of Environmental Research and Public Health, 14(12), p.1454. doi:https://doi.org/10.3390/ijerph14121454.

IBGE (2016). IBGE divulga as estimativas populacionais dos municípios em 2016 | Agência de Notícias. [online] Agência de Notícias - IBGE. Available at: https://agenciadenoticias.ibge.gov.br/agencia-sala-de-imprensa/2013-agencia-de-noticias/releases/9497-ibge-divulga-as-estimativas-populacionais-dos-municipios-em-2016 [Accessed 1 Mar. 2024].

Iñiguez, C., Schifano, P., Asta, F., Michelozzi, P., Vicedo-Cabrera, A. and Ballester, F. (2016). Temperature in summer and children's hospitalizations in two Mediterranean cities. Environmental Research, 150, pp.236–244. doi:https://doi.org/10.1016/j.envres.2016.06.007.

INMET (2016). Instituto Nacional de Meteorologia - INMET. [online] Instituto Nacional de Meteorologia. Available at: https://portal.inmet.gov.br/normais.

Iojă, C.I., Grădinaru, S.R., Onose, D.A., Vânău, G.O. and Tudor, A.C. (2014). The potential of school green areas to improve urban green connectivity and multifunctionality. Urban Forestry & Urban Greening, 13(4), pp.704–713. doi:https://doi.org/10.1016/j.ufug.2014.07.002.

Jacobi, P. (1997). Environmental Problems in Sao Paulo: The Challenge for Co-Responsibility and Innovative Crisis Management. Journal of Contingencies and Crisis Management, 5(3), pp.131–139. doi:https://doi.org/10.1111/1468-5973.00049.

Jang, H.S., Kim, H.J. and Jeon, J.Y. (2015). Scale-model method for measuring noise reduction in residential buildings by vegetation. Building and Environment, 86, pp.81–88. doi:https://doi.org/10.1016/j.buildenv.2014.12.020.

Jerome, G. (2016). Defining community-scale green infrastructure. Landscape Research, 42(2), pp.223–229. doi:https://doi.org/10.1080/01426397.2016.1229463.

Jia, Z., Tang, S., Luo, W., Li, S. and Zhou, M. (2016). Small scale green infrastructure design to meet different urban hydrological criteria. Journal of Environmental Management, 171, pp.92–100. doi:https://doi.org/10.1016/j.jenvman.2016.01.016.

Jin, H., Liu, Z., Jin, Y., Kang, J. and Liu, J. (2017). The Effects of Residential Area Building Layout on Outdoor Wind Environment at the Pedestrian Level in Severe Cold Regions of China. Sustainability, 9(12), p.2310. doi:https://doi.org/10.3390/su9122310.

Joshi, S.V. and Ghosh, Sat. (2014). On the air cleansing efficiency of an extended green wall: A CFD analysis of mechanistic details of transport processes. Journal of Theoretical Biology, 361, pp.101–110. doi:https://doi.org/10.1016/j.jtbi.2014.07.018.

Kambites, C. and Owen, S. (2006). Renewed prospects for green infrastructure planning in the UK 1. Planning Practice and Research, 21(4), pp.483–496. doi:https://doi.org/10.1080/02697450601173413.

Kiker, G.A., Bridges, T.S., Varghese, A., Seager, T.P. and Linkov, I. (2005). Application of Multicriteria Decision Analysis in Environmental Decision Making. Integrated Environmental Assessment and Management, 1(2), p.95. doi:https://doi.org/10.1897/ieam_2004a-015.1.

King's College London (2020a). Children exposed to five times more air pollution on school run. [online] King's College London . Available at: https://www.kcl.ac.uk/news/children-exposed-to-five-times-more-air-pollution-on-school-run [Accessed 29 Aug. 2020].

King's College London (2020b). World's largest study to monitor air quality exposure of 250 children. [online] King's College London. Available at: https://www.kcl.ac.uk/news/worlds-largest-study-to-monitor-air-quality-exposure-of-250-children [Accessed 29 Aug. 2020].

Kon, N. (2018). Escola FDE – Jardim Umuarama, Estúdio 6 - São Paulo/SP, 2005. [online] Nelson Kon. Available at: https://www.nelsonkon.com.br/escola-fde-jardim-umuarama/ [Accessed 12 Oct. 2023].

Kwon, P.S. and Østergaard, P.A. (2012). Comparison of future energy scenarios for Denmark: IDA 2050, CEESA (Coherent Energy and Environmental System Analysis), and Climate Commission 2050. Energy, 46(1), pp.275–282. doi:https://doi.org/10.1016/j.energy.2012.08.022.

Lai, D., Guo, D., Hou, Y., Lin, C. and Chen, Q. (2014). Studies of outdoor thermal comfort in northern china. Building and Environment, 77. doi:https://doi.org/10.1016/j.buildenv.2014.03.026.

Landscape Institute (2013). Green Infrastructure An integrated approach to land use Landscape Institute Position Statement Landscape Institute Inspiring great places. [online] https://www.landscapeinstitute.org/policy/green-infrastructure/. Available at: https://landscapewpstorage01.blob.core.windows.net/www-landscapeinstitute-org/2016/03/Green-Infrastructure_an-integrated-approach-to-land-use.pdf.

Larson, R.W. and Verma, S. (1999). How children and adolescents spend time across the world: Work, play, and developmental opportunities. Psychological Bulletin, 125(6), pp.701–736. doi:https://doi.org/10.1037/0033-2909.125.6.701.

Lee, S.C. and Chang, M. (2000). Indoor and outdoor air quality investigation at schools in Hong Kong. Chemosphere, 41(1-2), pp.109–113. doi:https://doi.org/10.1016/s0045-6535(99)00396-3.

Li, J., Zheng, B., Chen, X., Qi, Z., Bedra, K., Zheng, J., Li, Z. and Liu, L. (2020). Study on a full-year improvement of indoor thermal comfort by different vertical greening patterns. Journal of Building Engineering, 35, p.101969. doi:https://doi.org/10.1016/j.jobe.2020.101969.

Lima, G.N. de and Magaña Rueda, V.O. (2018). The urban growth of the metropolitan area of Sao Paulo and its impact on the climate. Weather and Climate Extremes, 21, pp.17–26. doi:https://doi.org/10.1016/j.wace.2018.05.002.

Lin, P., Gou, Z., Lau, S. and Qin, H. (2017). The Impact of Urban Design Descriptors on Outdoor Thermal Environment: A Literature Review. Energies, 10(12), p.2151. doi:https://doi.org/10.3390/en10122151.

Lin, T.P. (2009). Thermal perception, adaptation and attendance in a public square in hot and humid regions. Building and Environment, 44, pp.2017–2026. doi:https://doi.org/10.1016/j.buildenv.2009.02.004.

Lombardo, M.A. (1985). Ilha de calor nas metropoles o exemplo de sao paulo. [online] Hucitec. Available at: https://repositorio.usp.br/item/000755316.

Lopes, A., Alves, E., Alcoforado, M.J. and Machete, R. (2013). Lisbon Urban Heat Island Updated: New Highlights about the Relationships between Thermal Patterns and Wind Regimes. Advances in Meteorology, [online] 2013, pp.1–11. doi:https://doi.org/10.1155/2013/487695.

López-Bueno, R., López-Sánchez, G.F., Casajús, J.A., Calatayud, J., Tully, M.A. and Smith, L. (2021). Potential health-related behaviors for pre-school and school-aged children during COVID-19 lockdown: A narrative review. Preventive Medicine, 143, p.106349. doi:https://doi.org/10.1016/j.ypmed.2020.106349.

Lucchese, J. and Andreasi, W. (2017). Designing thermally pleasant open areas: The influence of microclimatic conditions on comfort and adaptation in midwest brazil. Journal of Sustainable Development, 10, p.11. doi:https://doi.org/10.5539/jsd.v10n4p11.

Magklara, K., Lazaratou, H., Barbouni, A., Poulas, K. and Farsalinos, K. (2022). The impact of COVID-19 lockdown on children's and adolescents' mental health in Greece. Children & Society, 37(2). doi:https://doi.org/10.1111/chso.12605.

Makvandi, M., Zhou, X., Li, C. and Deng, Q. (2021). A Field Investigation on Adaptive Thermal Comfort in an Urban Environment Considering Individuals' Psychological and Physiological Behaviors in a Cold-Winter of Wuhan. Sustainability, 13(2), pp.678–678. doi:https://doi.org/10.3390/su13020678.

Martins, L., Junior, C., Silva, D. and Melo, A. (2024). Urban Parks: Protection and recovery of fragile areas in the landscape - Case Study in the city of Sao Paulo, Brazil. Revista Políticas Públicas & Cidades, 13(1), pp.e743–e743. doi:https://doi.org/10.23900/2359-1552v13n1-15-2024.

Matsler, A.M., Meerow, S., Mell, I.C. and Pavao-Zuckerman, M.A. (2021). A 'green' chameleon: Exploring the many disciplinary definitions, goals, and forms of 'green infrastructure'. Landscape and Urban Planning, 214, p.104145. doi:https://doi.org/10.1016/j.landurbplan.2021.104145.

Matzarakis, A., Mayer, H. and Iziomon, M. (1999). Applications of a universal thermal index: Physiological equivalent temperature. International journal of biometeorology, 43, pp.76–84. doi:https://doi.org/10.1007/s004840050119.

Mayer, H. and Hoppe, P. (1987). Thermal comfort of man in different urban environments. Theoretical and Applied Climatology, 38(1), pp.43–49. doi:https://doi.org/10.1007/bf00866252.

McKay, G. and Parker, M. (2005). Epidemics. In: Humanitarianism. Routledge.

Meerow, S., Natarajan, M. and Krantz, D. (2021). Green infrastructure performance in arid and semi-arid urban environments. Urban Water Journal, pp.1–11. doi:https://doi.org/10.1080/1573062x.2021.1877741.

Mello-Théry, N.A. de (2011). Conservation of natural areas in São Paulo. Estudos Avançados, [online] 25(71), pp.175–188. doi:https://doi.org/10.1590/S0103-40142011000100012.

Ministry of Housing, Communities & Local Government (2019). Natural environment. [online] GOV.UK. Available at: https://www.gov.uk/guidance/natural-environment#green-infrastructure [Accessed 21 May 2020].

Molina, L.T., Zhu, T., Wan, W. and Gurjar, B.R. (2020). Impacts of Megacities on Air Quality: Challenges and Opportunities. Oxford Research Encyclopedia of Environmental Science. doi:https://doi.org/10.1093/acrefore/9780199389414.013.5.

Monn, Ch., Fuchs, A., Högger, D., Junker, M., Kogelschatz, D., Roth, N. and Wanner, H.-U. . (1997). Particulate matter less than 10 µm (PM10) and fine particles less than 2.5 µm (PM2.5): relationships between indoor, outdoor and personal concentrations. Science of The Total Environment, 208(1-2), pp.15–21. doi:https://doi.org/10.1016/s0048-9697(97)00271-4.

Montávez, J., Rodríguez, A. and Jimenez, J. (2000). A study of the urban heat island of granada. International Journal of Climatology, 20, pp.899–911. doi:https://doi.org/10.1002/1097-0088(20000630)20:8%3C899::AID-JOC433%3E3.0.CO;2-I.

Monteiro, L.M. (2015). Modelos preditivos de conforto térmico: quantificação de relações entre variáveis microclimáticas e de sensação térmica para avaliação e projeto de espaços abertos. doi:https://doi.org/10.11606/t.16.2008.tde-25032010-142206.

Montgomery, M.R. (2008). The Urban Transformation of the Developing World. Science, [online] 319(5864), pp.761–764. doi:https://doi.org/10.1126/science.1153012.

Nasrollahi, N. and Shokri, E. (2016). Daylight illuminance in urban environments for visual comfort and energy performance. Renewable and Sustainable Energy Reviews, 66, pp.861–874. doi:https://doi.org/10.1016/j.rser.2016.08.052.

Natanian, J. and Aleksandrowicz, O. (2018). ENVIRONMENTAL EDUCATION OF AN ARCHITECT: THE CASE OF FINAL-YEAR DESIGN STUDIO AT THE TECHNION, ISRAEL. International Journal of Architectural Research: ArchNet-IJAR, 12(1), p.356. doi:https://doi.org/10.26687/archnet-ijar.v12i1.1305.

Netto, S.V., Sobral, M.F.F., Ribeiro, A.R.B. and Soares, G.R. da L. (2020). Concepts and Forms of greenwashing: a Systematic Review. Environmental Sciences Europe, [online] 32(1), pp.1–12. doi:https://doi.org/10.1186/s12302-020-0300-3.

Nieuwenhuijsen, M.J. (2021). Green infrastructure and health. Annual Review of Public Health, [online] 42, pp.317–328. doi:https://doi.org/10.1146/annurev-publhealth-090419-102511.

Norton, B.A., Coutts, A.M., Livesley, S.J., Harris, R.J., Hunter, A.M. and Williams, N.S.G. (2015). Planning for cooler cities: A framework to prioritise green infrastructure to mitigate high temperatures in urban landscapes. Landscape and Urban Planning, [online] 134, pp.127–138. doi:https://doi.org/10.1016/j.landurbplan.2014.10.018.

Nouri, A.S. and Costa, J.P. (2017). Addressing thermophysiological thresholds and psychological aspects during hot and dry mediterranean summers through public space design: The case of Rossio. Building and Environment, 118, pp.67–90. doi:https://doi.org/10.1016/j.buildenv.2017.03.027.

Nowak, D.J., Hirabayashi, S., Bodine, A. and Hoehn, R. (2013). Modeled PM2.5 removal by trees in ten U.S. cities and associated health effects. Environmental Pollution, 178, pp.395–402. doi:https://doi.org/10.1016/j.envpol.2013.03.050.

Oke, T.R. (2006). Initial guidance to obtain representative meteorological observations at urban sites. [online] Available at: https://www.researchgate.net/publication/265347633_Initial_guidance_to_obtain_representative_meteorological_observations_at_urban_sites [Accessed 28 May 2024].

Oliveira, F.V. (2010). Educacional architecture in São Paulo in the 30´s. [Master's Dissertation] Available at: https://www.teses.usp.br/teses/disponiveis/16/16133/tde-20052010-152808/en.php.

Olivieri, F., Olivieri, L. and Neila, J. (2014). Experimental study of the thermal-energy performance of an insulated vegetal façade under summer conditions in a continental mediterranean climate. Building and Environment, 77, pp.61–76. doi:https://doi.org/10.1016/j.buildenv.2014.03.019.

Otsuki, T., Obane, H., Kawakami, Y., Shimogori, K., Mizuno, Y., Morimoto, S. and Matsuo, Y. (2022). Energy mix for net zero CO2 emissions by 2050 in Japan. Electrical Engineering in Japan, 215(4). doi:https://doi.org/10.1002/eej.23396.

Padilha, P.R. and Silva, R. da (2004). Educação com qualidade social - A experiência dos CEUs de São Paulo. [online] Instituto Paulo Freire. Available at: https://acervo.paulofreire.org/items/6ec1f63a-af3e-49fd-8d1b-687247115693.

Pantavou, K., Lykoudis, S., Nikolopoulou, M. and Tsiros, I.X. (2018). Thermal sensation and climate: a comparison of UTCI and PET thresholds in different climates. International Journal of Biometeorology, 62(9), pp.1695–1708. doi:https://doi.org/10.1007/s00484-018-1569-4.

Park, S., Tuller, S.E. and Jo, M. (2014). Application of Universal Thermal Climate Index (UTCI) for microclimatic analysis in urban thermal environments. Landscape and Urban Planning, 125, pp.146–155. doi:https://doi.org/10.1016/j.landurbplan.2014.02.014.

Parry, M. and Chandler, T.J. (1966). The Climate of London. The Geographical Journal, 132(1), p.84. doi:https://doi.org/10.2307/1793062.

Pekey, B., Bozkurt, Z.B., Pekey, H., Doğan, G., Zararsız, A., Efe, N. and Tuncel, G. (2010). Indoor/outdoor concentrations and elemental composition of PM10/PM2.5 in urban/industrial areas of Kocaeli City, Turkey. Indoor Air, 20(2), pp.112–125. doi:https://doi.org/10.1111/j.1600-0668.2009.00628.x.

Peters, B. and Peters, T. (2018). Computing the environment : digital design tools for simulation and visualisation of sustainable architecture. Chichester, West Sussex, Uk: Wiley.

Plume Labs (2018). A Handheld Revolution Against Air Pollution. [online] Plume Labs Blog. Available at: https://blog.plumelabs.com/2018/08/29/a-handheld-revolution-against-air-pollution/?_gl=1 [Accessed 4 Mar. 2024].

Plume Labs (2024). Flow, by Plume Labs | The First Smart Air Quality Tracker. [online] Plumelabs.com. Available at: https://plumelabs.com/en/flow/ [Accessed 29 May 2024].

Poupard, O., Blondeau, P., Iordache, V. and Allard, F. (2005). Statistical analysis of parameters influencing the relationship between outdoor and indoor air quality in schools. Atmospheric Environment, 39(11), pp.2071–2080. doi:https://doi.org/10.1016/j.atmosenv.2004.12.016.

Prakash, S., Goswami, M., Khan, Y.D.I. and Nautiyal, S. (2021). Environmental impact of COVID-19 led lockdown: A satellite data-based assessment of air quality in Indian megacities. Urban Climate, 38, p.100900. doi:https://doi.org/10.1016/j.uclim.2021.100900.

Prata-Shimomura, A. and Da, A. (2020). Remotely Piloted Aircraft as support for the study of urban parameters.

Pugh, T.A.M., MacKenzie, A.R., Whyatt, J.D. and Hewitt, C.N. (2012). Effectiveness of Green Infrastructure for Improvement of Air Quality in Urban Street Canyons. Environmental Science & Technology, 46(14), pp.7692–7699. doi:https://doi.org/10.1021/es300826w.

Puglisi, G., Kang, J., Smyrnova, Y. and Astolfi, A. (2013). Effect of vegetation on sound fields in idealised urban open spaces.

Purelogic Labs India Pvt Ltd (2020). World AQI Air Quality Map | Real-time Air Quality Index. [online] www.aqi.in. Available at: https://www.aqi.in/air-quality-map [Accessed 4 Autumn 2024].

Qingsong, M. and Fukuda, H. (2016). Parametric Office Building for Daylight and Energy Analysis in the Early Design Stages. Procedia - Social and Behavioral Sciences, 216, pp.818–828. doi:https://doi.org/10.1016/j.sbspro.2015.12.079.

Rakesh, D., Zalesky, A. and Whittle, S. (2023). The Role of School Environment in Brain Structure, Connectivity, and Mental Health in Children: A Multimodal Investigation. Biological Psychiatry: Cognitive Neuroscience and Neuroimaging, [online] 8(1), pp.32–41. doi:https://doi.org/10.1016/j.bpsc.2022.01.006.

Rana, A. and Daniel, R. (2023). Insights into the Education System in India and the Current Impact of COVID-19 on Child Rights. Inclusion, Equity, Diversity, and Social Justice in Education, pp.77–90. doi:https://doi.org/10.1007/978-981-19-5008-7_6.

Road Safety GB (2020). Guidance provides steps for schools to reduce pollution. [online] Road Safety GB. Available at: https://roadsafetygb.org.uk/news/guidance-provides-steps-for-schools-to-reduce-pollution/ [Accessed 23 Feb. 2024].

Romero, R.A.S. (2023). Origem da Rede Municipal de Ensino de Sao Paulo. [online] XXVIII National Symposium of History. Available at: chrome-extension://efaidnbmnnnibpcajpcglclefindmkaj/https://anpuh.org.br/uploads/anais-simposios/pdf/2019-01/1548945016_015accbda516f8aaf81bc1aa10add467.pdf [Accessed 19 Nov. 2023].

Roy, S., Byrne, J. and Pickering, C. (2012). A systematic quantitative review of urban tree benefits, costs, and assessment methods across cities in different climatic zones. Urban Forestry & Urban Greening, [online] 11(4), pp.351–363. doi:https://doi.org/10.1016/j.ufug.2012.06.006.

Rui, L., Buccolieri, R., Gao, Z., Gatto, E. and Ding, W. (2018a). Study of the effect of green quantity and structure on thermal comfort and air quality in an urban-like residential district by ENVI-met modelling. Building Simulation, 12, pp.1–12. doi:https://doi.org/10.1007/s12273-018-0498-9.

Rui, L., Buccolieri, R., Gao, Z., Gatto, E. and Ding, W. (2018b). Study of the effect of green quantity and structure on thermal comfort and air quality in an urban-like residential district by ENVI-met modelling. Building Simulation, 12, pp.1–12. doi:https://doi.org/10.1007/s12273-018-0498-9.

Salata, K.D. and Yiannakou, A. (2016). Green Infrastructure and climate change adaptation. TeMA - Journal of Land Use, Mobility and Environment, [online] 9(1), pp.7–24. doi:https://doi.org/10.6092/1970-9870/3723.

Salmond, J.A., Tadaki, M., Vardoulakis, S., Arbuthnott, K., Coutts, A., Demuzere, M., Dirks, K.N., Heaviside, C., Lim, S., Macintyre, H., McInnes, R.N. and Wheeler, B.W. (2016). Health and climate related ecosystem services provided by street trees in the urban environment. Environmental Health, [online] 15(S1). doi:https://doi.org/10.1186/s12940-016-0103-6.

Salvi, S. (2007). Health effects of ambient air pollution in children. Paediatric Respiratory Reviews, 8(4), pp.275–280. doi:https://doi.org/10.1016/j.prrv.2007.08.008.

Sanesi, G., Lafortezza, R., Bonnes, M. and Carrus, G. (2006). Comparison of two different approaches for assessing the psychological and social dimensions of green spaces. Urban Forestry & Urban Greening, 5(3), pp.121–129. doi:https://doi.org/10.1016/j.ufug.2006.06.001.

Santana, J.C.C., Miranda, A.C., Yamamura, C.L.K., Silva Filho, S.C. da, Tambourgi, E.B., Lee Ho, L. and Berssaneti, F.T. (2020). Effects of Air Pollution on Human Health and Costs: Current Situation in São Paulo, Brazil. Sustainability, [online] 12(12), p.4875. doi:https://doi.org/10.3390/su12124875.

Santos, R., Andrade, T., Branco, N., Borja, P., Pedrassoli, J. and Vale, T. (2017). Vegetation cover and surface temperature in urban areas: An analysis using remote sensing in the city of salvador, bahia, brazil.

Schneider, R.M. and Leite, A. (2018). São Paulo - Climate. In: Encyclopedia Britannica, ed., Encyclopedia Britannica. [online] Available at: https://www.britannica.com/place/Sao-Paulo-Brazil/Climate [Accessed 29 May 2024].

Schneider, R.M., Leite, A. and Minkel, C.W. (2024). São Paulo - South of the centre | Britannica. [online] www.britannica.com. Available at: https://www.britannica.com/place/Sao-Paulo-Brazil/South-of-the-centre [Accessed 5 Jun. 2024].

Schuurman, T.M., Henrichs, L.F., Schuurman, N.K., Polderdijk, S. and Hornstra, L. (2021). Learning Loss in Vulnerable Student Populations After the First Covid-19 School Closure in the Netherlands. Scandinavian Journal of Educational Research, 67(2), pp.1–18. doi:https://doi.org/10.1080/00313831.2021.2006307.

Schwartz, J. (2004). Air Pollution and Children's Health. Pediatrics, [online] 113(Supplement_3), pp.1037–1043. doi:https://doi.org/10.1542/peds.113.S3.1037.

Ścibor, M., Balcerzak, B., Galbarczyk, A., Targosz, N. and Jasienska, G. (2019). Are we safe inside? Indoor air quality in relation to outdoor concentration of PM10 and PM2.5 and to characteristics of homes. Sustainable Cities and Society, [online] 48, p.101537. doi:https://doi.org/10.1016/j.scs.2019.101537.

Seaton, A., Godden, D., MacNee, W. and Donaldson, K. (1995). Particulate air pollution and acute health effects. The Lancet, 345(8943), pp.176–178. doi:https://doi.org/10.1016/s0140-6736(95)90173-6.

Secretaria Municipal de Educacao de Sao Paulo (2019). Tipos de Unidades Educacionais e alimentação. [online] SME Portal Institucional. Available at: https://educacao.sme.prefeitura.sp.gov.br/programa-de-alimentacao-escolar/tipos-de-unidades-educacionais-e-alimentacao/ [Accessed 12 Oct. 2023].

Seigneur, C. (2019). Gaseous Pollutants. Cambridge University Press eBooks, [online] pp.146–189. doi:https://doi.org/10.1017/9781108674614.008.

Shackleton, C.M., Blair, A., De Lacy, P., Kaoma, H., Mugwagwa, N., Dalu, M.T. and Walton, W. (2018). How important is green infrastructure in small and medium-sized towns? Lessons from South Africa. Landscape and Urban Planning, 180, pp.273–281. doi:https://doi.org/10.1016/j.landurbplan.2016.12.007.

Shan, Y., Cai Jingping, Chen Liping, Shen Zhemin, Zou Xiaodong, Dan, W. and Wang Wenhua (2007). Effects of vegetation status in urban green spaces on particle removal in a street canyon atmosphere. Acta Ecologica Sinica, [online] 27, pp.4590–4595. doi:https://doi.org/10.1016/S1872-2032(08)60007-4.

Shin, J., Oh, J., Kang, I.-S., Ha, E. and Pyun, W.-B. (2021). Effect of Short-Term Exposure to Fine Particulate Matter and Temperature on Acute Myocardial Infarction in Korea. International Journal of Environmental Research and Public Health, 18(9), p.4822. doi:https://doi.org/10.3390/ijerph18094822.

Shinzato, P. (2014). Impacto da vegetação nos microclimas urbanos em função das interações solo-vegetação-atmosfera. [Thesis Dissertation]

Available at: https://www.teses.usp.br/teses/disponiveis/16/16132/tde-12092014-115829/pt-br.php [Accessed 21 Apr. 2020].

Shinzato, P., Simon, H., Silva Duarte, D.H. and Bruse, M. (2019). Calibration process and parametrization of tropical plants using ENVI-met V4 – Sao Paulo case study. Architectural Science Review, 62(2), pp.112–125. doi:https://doi.org/10.1080/00038628.2018.1563522.

Shishegar, N. and Boubekri, M. (2017). Quantifying electrical energy savings in offices through installing daylight responsive control systems in hot climates. Energy and Buildings, 153, pp.87–98. doi:https://doi.org/10.1016/j.enbuild.2017.07.078.

Silva Dias, M.A.F., Dias, J., Carvalho, L.M.V., Freitas, E.D. and Silva Dias, P.L. (2012). Changes in extreme daily rainfall for São Paulo, Brazil. Climatic Change, 116(3-4), pp.705–722. doi:https://doi.org/10.1007/s10584-012-0504-7.

Silva, C., Santos, T. and Tenedório, J. (2017). Urban vegetation as a strategy to reduce heat island effects in the Mediterranean climate context, Lisbon-Portugal.

Silva, J. (2019). Urban and Building Integrated Vegetation. [Masters Dissertation] Available at: https://issuu.com/msc.exhibition2019 [Accessed 9 Mar. 2020].

Simon, H. (2016). Modeling urban microclimate : development, implementation and evaluation of new and improved calculation methods for the urban microclimate model ENVI-met. [Dissertation] Available at: https://openscience.ub.uni-mainz.de/handle/20.500.12030/4044 [Accessed 20 Feb. 2024].

Simon, H., Sinsel, T. and Bruse, M. (2021). Advances in Simulating Radiative Transfer in Complex Environments. Applied Sciences, 11(12), p.5449. doi:https://doi.org/10.3390/app11125449.

Simpson, J.R. (2002). Improved estimates of tree-shade effects on residential energy use. Energy and Buildings, 34(10), pp.1067–1076. doi:https://doi.org/10.1016/s0378-7788(02)00028-2.

Singh, S., Roy, D., Sinha, K., Parveen, S., Sharma, G. and Joshi, G. (2020). Impact of COVID-19 and Lockdown on Mental Health of Children and Adolescents: A Narrative Review with Recommendations. Psychiatry Research, [online] 293(113429). doi:https://doi.org/10.1016/j.psychres.2020.113429.

Sinsel, T., Simon, H., Ouyang, W., dos Santos Gusson, C., Shinzato, P. and Bruse, M. (2022). Implementation and evaluation of mean radiant temperature schemes in the microclimate model ENVI-met. Urban climate, 45(1010279), pp.101279–101279. doi:https://doi.org/10.1016/j.uclim.2022.101279.

Siu, L.W. and Hart, M.A. (2012). Quantifying urban heat island intensity in Hong Kong SAR, China. Environmental Monitoring and Assessment, 185(5), pp.4383–4398. doi:https://doi.org/10.1007/s10661-012-2876-6.

Soflaei, F., Shokouhian, M., Tabadkani, A., Moslehi, H. and Berardi, U. (2020). A simulation-based model for courtyard housing design based on adaptive thermal comfort. Journal of Building Engineering, 31, p.101335. doi:https://doi.org/10.1016/j.jobe.2020.101335.

Solmaz, A.S. (2019). A CRITICAL REVIEW ON BUILDING PERFORMANCE SIMULATION TOOLS. Alam Cipta, [online] 12(2). Available at: chrome-extension://efaidnbmnnnibpcajpcglclefindmkaj/https://frsb.upm.edu.my/upload/dokumen/20200102112912paper_2_dis_2019.pdf [Accessed 21 May 2020].

Spangenberg, J., Shinzato, P., Johansson, E. and Duarte, D. (2007). The impact of urban vegetation on microclimate in hot humid sao paulo.

Spangenberg, J., Shinzato, P., Johansson, E. and Duarte, D. (2008). Simulation of the influence of vegetation on microclimate and thermal comfort in the city of Sao Paulo. Revista da Sociedade Brasileira de Arborização Urbana, 3, pp.1–19. doi:https://doi.org/10.5380/revsbau.v3i2.66265.

Spira, V.A.G. (2015). Chalenges of embracing and spatial practices: the Unified Educational Centers (CEUs) of São Paulo. [Master's Dissertation] Available at: https://www.teses.usp.br/teses/disponiveis/8/8134/tde-09062015-121048/pt-br.php.

Stephens, C., Akerman, M. and Maia, P.B. (1995). Health and environment in Sao Paulo, Brazil: methods of data linkage and questions of policy. World Health Statistics Quarterly, [online] 48(2), pp.95–107. Available at: https://www.semanticscholar.org/paper/Health-and-environment-in-S%C3%A3o-Paulo%2C-Brazil%3A-of-and-Stephensa-Akermanb/17bae32893a51304d0befef56a7a1ea7d35e1f7c.

Susca, T., Gaffin, S.R. and Dell'Osso, G.R. (2011). Positive effects of vegetation: Urban heat island and green roofs. Environmental Pollution, 159(8-9), pp.2119–2126. doi:https://doi.org/10.1016/j.envpol.2011.03.007.

Szabo, S. and Webster, J. (2021). Perceived Greenwashing: The Effects of Green Marketing on Environmental and Product Perceptions. Journal of Business Ethics, [online] 171(4), pp.719–739. doi:https://doi.org/10.1007/s10551-020-04461-0.

Takiya, A. (2010). Public architecture in São Paulo city public building project departament since 1948. [Master's Dissertation] Available at: https://www.teses.usp.br/teses/disponiveis/16/16138/tde-10052010-141328/pt-br.php.

Tan, S.H.A. and Smith, T.E.L. (2020). An optimal environment for our optimal selves? An autoethnographic account of self-tracking personal exposure to air pollution. Area, 53(2), pp.353–361. doi:https://doi.org/10.1111/area.12671.

Tan, Z., Lau, K.K.-L. and Ng, E. (2016). Urban tree design approaches for mitigating daytime urban heat island effects in a high-density urban environment. Energy and Buildings, 114, pp.265–274. doi:https://doi.org/10.1016/j.enbuild.2015.06.031.

Taylor, J., Wilkinson, P., Davies, M., Armstrong, B., Chalabi, Z., Mavrogianni, A., Symonds, P., Oikonomou, E. and Bohnenstengel, S.I. (2015). Mapping the effects of urban heat island, housing, and age on excess heat-related mortality in London. Urban Climate, 14, pp.517–528. doi:https://doi.org/10.1016/j.uclim.2015.08.001.

The World Air Quality Index Project (2020). Air Pollution in Sao Paulo: Real-time Air Quality Index Visual Map. [online] aqicn.org. Available at: https://aqicn.org/map/saopaulo/ [Accessed 15 Apr. 2024].

Tong, Z., Baldauf, R.W., Isakov, V., Deshmukh, P. and Max Zhang, K. (2016). Roadside vegetation barrier designs to mitigate near-road air pollution impacts. Science of The Total Environment, [online] 541, pp.920–927. doi:https://doi.org/10.1016/j.scitotenv.2015.09.067.

Torres , P.H.C. and Jacobi, P.R. (2020). SPECIAL ISSUE SÃO PAULO MACROMETROPOLIS ENVIRONMENTAL GOVERNANCE FORUM. Ambiente & Sociedade, 23(2). doi:https://doi.org/10.1590/1809-4422asoceditorialvu2020l2ed.

Touloupaki, E. and Theodosiou, T. (2017). Performance Simulation Integrated in Parametric 3D Modeling as a Method for Early Stage Design Optimization—A Review. Energies, 10(5), p.637. doi:https://doi.org/10.3390/en10050637.

Tran, H.M., Tsai, F.-J., Lee, Y.-L., Chang, J.-H., Chang, L.-T., Chang, T.-Y., Chung, K.F., Kuo, H.-P., Lee, K.-Y., Chuang, K.-J. and Chuang, H.-C. (2023). The impact of air pollution on respiratory diseases in an era of climate change: A review of the current evidence. Science of The Total Environment, [online] 898, p.166340. doi:https://doi.org/10.1016/j.scitotenv.2023.166340.

Trees for Cities (2018). Home | Trees for Cities. [online] Trees for Cities. Available at: https://www.treesforcities.org/ [Accessed 1 Jul. 2020].

Tsoka, S., Tsikaloudaki, A. and Theodosiou, T. (2018). Analyzing the ENVI-met microclimate model's performance and assessing cool materials and urban vegetation applications–A review. Sustainable Cities and Society, 43, pp.55–76. doi:https://doi.org/10.1016/j.scs.2018.08.009.

Twum-Antwi, A., Jefferies, P. and Ungar, M. (2019). Promoting child and youth resilience by strengthening home and school environments: A literature review. International Journal of School & Educational Psychology, [online] 8(2), pp.78–89. doi:https://doi.org/10.1080/21683603.2019.1660284.

Umezaki, A.S., Ribeiro, F.N.D., Oliveira, A.P. de, Soares, J. and Miranda, R.M. de (2020). Numerical characterization of spatial and temporal evolution of summer urban heat island intensity in São Paulo, Brazil. Urban Climate, 32, p.100615. doi:https://doi.org/10.1016/j.uclim.2020.100615.

UN-Habitat (2022). Envisaging the Future of Cities. [online] UN-Habitat, World Cities Report 2022 . United Nations Human Settlements Programme (UN-Habitat). Available at: https://unhabitat.org/sites/default/files/2022/06/wcr_2022.pdf [Accessed 28 May 2024].

United Nations (2014). World Urbanization Prospects. [online] Available at: chrome-extension://efaidnbmnnnibpcajpcglclefindmkaj/https://population.un.org/wup/Publications/Files/WUP2014-Highlights.pdf [Accessed 28 Aug. 2020].

Vaishali, N., Verma, G. and Das, R.M. (2023). Influence of Temperature and Relative Humidity on PM2.5 Concentration over Delhi. MA PAN-Journal of Meteorology Society of India. doi:https://doi.org/10.1007/s12647-023-00656-8.

Van Dijk-Wesselius, J.E., Maas, J., Hovinga, D., van Vugt, M. and van den Berg, A.E. (2018). The impact of greening schoolyards on the appreciation, and physical, cognitive and social-emotional well-being of schoolchildren: A prospective intervention study. Landscape and Urban Planning, 180, pp.15–26. doi:https://doi.org/10.1016/j.landurbplan.2018.08.003.

Van Renterghem, T., Botteldooren, D. and Verheyen, K. (2012). Road traffic noise shielding by vegetation belts of limited depth. Journal of Sound and Vibration, [online] 331(10), pp.2404–2425. doi:https://doi.org/10.1016/j.jsv.2012.01.006.

Vasigh, B. and Shiri, T. (2021). Climatic Adaptation of the Dome Body Based on Solar Radiation Received Climatic Adaptation of the Dome Body Based on Solar Radiation Received; Case Study: The Domes of Shah Mosque, Sheikh Lotfollah Mosque, Al-Nabi Mosque of Qazvin and Jameh Mosque of Urmia. doi:https://doi.org/10.22034/AAUD.2019.174964.1831.

Vos, P.E.J., Maiheu, B., Vankerkom, J. and Janssen, S. (2013). Improving local air quality in cities: To tree or not to tree? Environmental Pollution, 183, pp.113–122. doi:https://doi.org/10.1016/j.envpol.2012.10.021.

Wania, A., Bruse, M., Blond, N. and Weber, C. (2012). Analysing the influence of different street vegetation on traffic-induced particle dispersion using microscale simulations. Journal of Environmental Management, 94(1), pp.91–101. doi:https://doi.org/10.1016/j.jenvman.2011.06.036.

Watanabe, T. and Yamada, S. (1996). Sound attenuation through absorption by vegetation. Journal of the Acoustical Society of Japan../Journal of the Acoustical Society of Japan. E, 17(4), pp.175–182. doi:https://doi.org/10.1250/ast.17.175.

Watkins, J. (2020). Air Quality Monitoring Along the 14th Street Busway: Public Health Impacts in an Urban Planning Context. [Masters Dissertation] Available at: https://academiccommons.columbia.edu/doi/10.7916/d8-jgky-x575 [Accessed 29 May 2024].

Watson, A.Y., Bates, R.R. and Kennedy, D. (1988). Atmospheric Transport and Dispersion of Air Pollutants Associated with Vehicular Emissions. [online] www.ncbi.nlm.nih.gov. National Academies Press (US). Available at: https://www.ncbi.nlm.nih.gov/books/NBK218142/ [Accessed 4 Nov. 2023].

Weather Spark (2021). Average Weather in São Paulo, Brazil, Year Round - Weather Spark. [online] weatherspark.com. Available at: https://weatherspark.com/y/30268/Average-Weather-in-S%C3%A3o-Paulo-Brazil-Year-Round [Accessed 2 Jul. 2021].

Wilby, R.L. (2003). Past and projected trends in London's urban heat island. Weather, 58(7), pp.251–260. doi:https://doi.org/10.1256/wea.183.02.

Wilby, R.L. and Perry, G.L.W. (2006). Climate change, biodiversity and the urban environment: a critical review based on London, UK. Progress in Physical Geography: Earth and Environment, 30(1), pp.73–98. doi:https://doi.org/10.1191/0309133306pp470ra.

Wine, O., Osornio Vargas, A., Campbell, S.M., Hosseini, V., Koch, C.R. and Shahbakhti, M. (2022). Cold Climate Impact on Air-Pollution-Related Health Outcomes: A Scoping Review. International Journal of Environmental Research and Public Health, [online] 19(3), p.1473. doi:https://doi.org/10.3390/ijerph19031473.

Wong, N.H. and Yu, C. (2005). Study of green areas and urban heat island in a tropical city. Habitat International, 29(3), pp.547–558. doi:https://doi.org/10.1016/j.habitatint.2004.04.008.

World Health Organisation - WHO (2018). AIR POLLUTION AND CHILD HEALTH. [online] World Health Organisation - WHO. Available at: https://www.who.int/publications/i/item/WHO-CED-PHE-18-01.

World Health Organization (2024). How air pollution is destroying our health. [online] https://www.who.int/. Available at: https://www.who.int/news-room/spotlight/how-air-pollution-is-destroying-our-health#:~:text=Every%20year%2C%20442%20000%20children [Accessed 29 May 2024].

World Population Review (2024). Sao Paulo Population 2020 (Demographics, Maps, Graphs). [online] worldpopulationreview.com. Available at: https://worldpopulationreview.com/world-cities/sao-paulo-population [Accessed 29 May 2024].

Xu, R., Zhao, Q., Coelho, M.S.Z.S., Saldiva, P.H.N., Abramson, M.J., Li, S. and Guo, Y. (2020). Socioeconomic level and associations between heat exposure and all-cause and cause-specific hospitalization in 1,814 Brazilian cities: A nationwide case-crossover study. PLOS Medicine, 17(10), p.e1003369. doi:https://doi.org/10.1371/journal.pmed.1003369.

Xu, Z., Etzel, R.A., Su, H., Huang, C., Guo, Y. and Tong, S. (2012). Impact of ambient temperature on children's health: A systematic review. Environmental Research, [online] 117, pp.120–131. doi:https://doi.org/10.1016/j.envres.2012.07.002.

Zani, A., Mainini, A., Cadena, B. and Arens, E. (2018). A new modeling approach for the assessment of the effect of solar radiation on indoor thermal comfort.

Zhang, J.-S., Gui, Z.-H., Zou, Z.-Y., Yang, B.-Y., Ma, J., Jing, J., Wang, H.-J., Luo, J.-Y., Zhang, X., Luo, C.-Y., Wang, H., Zhao, H.-P., Pan, D.-H., Bao, W.-W., Guo, Y.-M., Ma, Y.-H., Dong, G.-H. and Chen, Y.-J. (2021). Long-term exposure to ambient air pollution and metabolic syndrome in children and adolescents: A national cross-sectional study in China. Environment International, [online] 148, p.106383. doi:https://doi.org/10.1016/j.envint.2021.106383.

Zhang, X.X., Wu, P.F. and Chen, B. (2010). Relationship between vegetation greenness and urban heat island effect in Beijing City of China. Procedia Environmental Sciences, 2, pp.1438–1450. doi:https://doi.org/10.1016/j.proenv.2010.10.157.

Zheng, G.J., Duan, F.K., Su, H., Ma, Y.L., Cheng, Y., Zheng, B., Zhang, Q., Huang, T., Kimoto, T., Chang, D., Pöschl, U., Cheng, Y.F. and He, K.B. (2015). Exploring the severe winter haze in Beijing: the impact of synoptic weather, regional transport and heterogeneous reactions. Atmospheric Chemistry and Physics, 15(6), pp.2969–2983. doi:https://doi.org/10.5194/acp-15-2969-2015.

APPENDIX

APPENDIX A- SUPPORTING INFORMATION FOR CHAPTERS 04 AND 05

		Sao Paulo	Internal points				
			Ground floor			First floor	
			I1 Big room	**I2** 1st year	**I3** Entrance	**I4** Classrom 01	**I5** Laboratory
	Day 01_25/03_(11:00am)	27	26.9	28.8	28.4	27.4	27.8
	Day 02_26/03_ (11:00am)	31	27.2	28	32	29.7	28.6
	Day 03_27/03_ (04:00pm)	29	28.6	28.3	28.5	29.6	29.2
	Day 04_29/03_ (08:00 am)	23	24.2	24.8	24.1	25.2	25.5
	Day 05_30/03_(06:00 pm)	21	22.5	22.2	22.7	24.3	24.2
	Day 06_31/03_(06:00 pm)		21.6	23.3	21.7	22.7	21.1
	Day 07_01/04_(04:00 pm)		23.8	23.4	24.6	24.5	23.9
	Day 08_02/04_(08:00 am)		20.4	20.9	28.3	21	21.3
	Day 09_04/04_(11:00 am)	23	23.2	22.8	23.3	23	23.3
Temperature (C)	Day 10_05/04_(04:00 pm)	23	23.7	23.5	24.5	23.8	24
	Day 01 (11:00am)		55.4	54.8	54.1	55.5	54.5
	Day 02 (11:00am)		55.9	58	47	51	57.8
	Day 03 (04:00pm)		46.4	52.1	47.1	50.2	51.2
	Day 04 (08:00 am)		67.7	69.7	68.5	65.6	64.3
	Day 05		72	70	69.9	65.8	64.4
	Day 06		65.1	65.6	64.2	63.7	69.5
	Day 07		59.6	60.9	56.1	58	60
	Day 08		69.4	69.5	68.1	61	66.4
	Day 09		60.7	63.1	59.8	59.9	59.6
Humidity (%)	Day 10		63.4	63.6	60	62.2	62.3
	Day 01 (11:00am)		0 /1.6m/s (between doors)	0	0.3	0	0
	Day 02 (11:00am)		0	0	0.1	0	0
	Day 03 (04:00pm)		1	0 (1.7 with door open)	1.1	1	1.2
	Day 04 (08:00 am)		0	0	0	0	0
	Day 05		0.3	0	0	0	0
	Day 06		0	0	1	0.2	0.8
	Day 07		0.2	0 (0.5 with open door)	0	0.4	1.1
	Day 08		0.3	0	0.6	0.2	0
	Day 09		1.2	0 (0.6 with door open)	1.2	1	1.2
Wind Speed (m/s)	Day 10		0.6	0 (0.4 with door open)	1.1	0.9	1.8
	Day 01_25/03_(11:00am)		49.9	47.6 (56.2 with open door)	233	514	1211
	Day 02_26/03_ (11:00am)		62.1	46.6 (68.5 with open door)	196.6	311	787
	Day 03_27/03_ (04:00pm)		100.9	17.3 (28.9 with door open)	471	75.6	212
	Day 04_29/03_ (08:00 am)		62.5	35.5 (52 with door open)	158.1	166.6	328
	Day 05_30/03_(06:00 pm)						
	Day 06_31/03_(06:00 pm)						
	Day 07_01/04_(04:00 pm)		215	40.9 (51.8 with door open)	806	377	2040
	Day 08_02/04_(08:00 am)		74.4	33.6 (47.7 with door open)	121.9	255	657
	Day 09_04/04_(11:00 am)		70.6	52.8 (66.5 with door open)	252	517	1275
Illuminance (lux)	Day 10_05/04_(04:00 pm)		41.7	92.2 (111.1 with door open)	886	1876	1367
	Day 01 (11:00am)		25.1	27.7	25.3	27.3	26.5
	Day 02 (11:00am)		24.8	24.4	25.1	27	26.5
	Day 03 (04:00pm)		25.4	24.7	26.5	27.9	27.6
	Day 04 (08:00 am)		24.4	24.7	24.9	26	26.6
	Day 05		24.6	24.8	24.8	26.6	27
	Day 06		23.6	24.1	24.2	24.9	24.9
	Day 07		23.4	23.5	24	25.2	24.5
	Day 08		21.9	22.9	21.7	22.6	22.3
	Day 09		22.5	22.9	22.8	23.9	23.2
Surface temperature	Day 10		22.8	22.8	23.6	24.3	23.8
	Day 01_25/03_(11:00am)		49.6	46.8 (97.7 with open door)	47.7	37.5	47
	Day 02_26/03_ (11:00am)		49	42.6 (52 with open door)	38.6	38.7	58.2
	Day 03_27/03_ (04:00pm)		45.4	35.8 (46.9 with open door)	35.5	36.8	37.2
	Day 04_29/03_ (08:00 am)		44.9	39.4 (51.8 with open door)	42.4	43.1	37
	Day 05_30/03_(06:00 pm)		66.7	41.2 (48.4 with open door)	48.1	38.3	43.1
	Day 06_31/03_(06:00 pm)		47.3	39.6 (52.8 with open door)	51.4	43.1	53.3
	Day 07_01/04_(04:00 pm)		51.9	45.4 (67.3 with open door)	46.1	61.4	45.9
	Day 08_02/04_(08:00 am)		43.5	41.2 (60.2 with open door)	51.6	36.7	59.4
	Day 09_04/04_(11:00 am)		42.2	37.8 (45.7 with door open)	49.9	57.8	39.4
Sound levels (dB)	Day 10_05/04_(04:00 pm)		51.3	41.8 (58 with door open)	49.3	52.8	41.8

Table A.01 - Table with the collected data in the fieldwork of EMEF Amorim Lima

			External points							
Second floor										
I6 Classrom 02 (SS)	**I7** Classrom 03 (DS)		**E1** Entrance	**E2** Cora 01	**E3** Cora 02	**E4** Cora 03	**E5** Open classrom	**E6** Covered football court	**E7** Garden	**E8** Football court
28.5	28.2		27.9	30.1	28.6	31.4	32.1	29.3	28.7	31.3
29.2	28.7		28.5	29.7	28.8	37.3	28.8	33.7	32.3	34.2
30.2	29.9		29.7	34.7	31.2	31.7	31.6	30.8	32.3	32.8
25.4	25.4		24.3	23.6	23.6	23.7	24.3	23.9	24.6	24.5
24.3	24.1		21.1	20.7	21	21.5	21.9	23.8	20.8	20.9
23	22.5		21.1	20	19.9	19.7	20.1	19.4	19.1	19.2
26	25.4		25.1	24	23.4	23.9	23.4	22.6	22.7	23.6
21	21.8		21	20.5	21.1	23	25.2	22.3	24.3	24.7
23.4	23.5		23.5	25	24.1	25	24.6	24.5	25.4	28.2
25.1	24.7		24.1	24.2	23.9	23.7	23.6	23.6	24.5	24.8
51.9	53.7		54.1	48.1	52.2	46.9	43.3	50.5	52.6	47.5
57.8	53.7		56.3	53.1	54.1	36.8	58	43	44	43
50.2	47		43	36.3	39.5	35.5	35.4	37.1	37.2	36.6
63.4	63.8		67.4	71.2	71.1	69.5	68.3	69.9	68	67.6
64.1	64.2		72	78.1	77	75.5	73.2	65.9	76.2	81.2
61.7	69.1		69.5	73.8	74.9	76	67.2	76.7	77.5	77.3
53.7	55.7		59.6	59.1	61.6	70.4	65.9	65.7	64.6	61.8
64.4	61.1		66.1	66	65.6	61.2	56.6	60.8	57.7	53.7
59.9	60.5		63.3	58.8	61.3	59.3	60.3	59.6	57.2	48.3
58.3	61.6		62.3	60.7	62.2	63.1	63.3	63	62.2	58.8
0	0		0	0	0.4	1.2	0	0	0.6	0
0	0		1.1	0.3	0.6	0	0	0.2	0.7	0.8
0.7	1.7		1	0.5	1.3	2.4	0	0	0.4	0.7
0	0		0	0.9	0.4	0.5	0	0	0.8	0.3
0	1		1	0.4	0.3	1	0.3	0.7	0.2	1.1
0	1.2		0.6	1.1	0.5	1.3	0.2	1	0.3	0.7
0.1	1		0.5	2.1	2.7	1.1	0.4	1	2	1.6
0	1.3		0.8	1.3	1.2	1.1	0	1.1	1.8	1.7
1	2.8		1.1	1	1.2	1.8	0.6	2.2	1.1	1.6
1.2	1.6		0.7	1.8	1.9	1.7	0.5	1	0.9	1.5
1152	953		20,300	6,900	4,050	115,500	3,210	52	942,000	124,000
772	605		95,500	25,000	2,580	16,810	2,530	156.7	111,700	120,600
117.8	180.6		6,030	5,990	3,500	13,890	2,240	52.3	14,550	14,690
268	490		3,500	4,410	4,880	22,700	5,110	117.6	16,860	19,200
22700	13750		5040	3090	2030	5830	593	61.9	5830	12090
665	462		1999	7270	2380	60600	3960	146.5	78400	70900
735	1135		5610	9340	4000	21500	1342	77.7	28100	69300
2450	1201		5140	6760	3920	11300	1937	103.4	7200	13850
27.8	27.5		36.2	27.7	25.5	47.4	27	29.2	36.7	47.2
26.9	27.4		35.8	26	25.6	46.4	26.3	29.5	37.3	46.3
29.3	30.1		28.3	32.6	26.5	40.3	27.1	27.1	27.4	39.5
25.5	26.1		23.2	22.3	22.3	26.6	25.3	24.8	25.2	26.4
27.5	27.7		23.5	20.5	20.7	24.5	25.1	25.1	21	26
26.2	23.6		22.3	20.9	19.2	24.8	23.2	22.8	18	23.8
31.3	27		27.4	24	21.7	31.5	24	25.3	21.5	32.8
23	22.5		20.6	21.7	20.6	25.9	21.5	23.4	25.5	26.7
23.7	23		25.2	24	24.2	34.7	25.3	24.6	27.3	37.8
30.8	27.7		27.2	26.8	23.3	32.4	24	25.8	23	34.6
55.1	47		54.1	62.5	55.5	55.2	52.8	47.1	45.9	48.2
37.4	52.5		62.9	59.7	54.3	52.1	49.5	42.3	36.2	40.6
41.6	53.9		46.1	52.5	58.3	49.3	44.7	39	39	42.3
55	47.9		47.8	53.9	60.7	52	56.2	45.4	42.2	39.8
55.1	50.6		52.8	55.7	60.5	48.5	49.3	45.5	44.3	48.3
43.5	59.7		50	67.6	62.9	49.5	46.6	47.2	70.5	46.4
50.7	53.7		59.4	56.9	56.1	52.2	54.4	47.5	51.5	48.9
37.8	43.2		54.3	56.1	56.5	48.5	53.5	52.3	42.4	43.9
44.8	47.2		49.7	55.4	52.3	48.8	44.4	48.3	42.3	45.7
50.8	52.7		64.9	52.3	54	49.6	48.7	54.7	50.6	50.9

		Internal points								External points										
		Ground floor			First floor		Second floor													
		I1 Big roon	**I2** 1st year	**I3** Entrance	**I4** Classrom	**I5** Laborato	**I6** Classrom	**I7** Classrom 03 (DS)		**E1** Entrance	**E2** Cora 01	**E3** Cora 02	**E4** Cora 03	**E5** Open cl	**E6** Covered fo	**E7** Garden	**E8** Football court		AVENUE	STREET
DAY 01 (20/01/22) 12am	PM10	11µg/m3	10µg/m3	11µg/m3	11µg/m3	11µg/m3	10µg/m3	10µg/m3		11µg/m3	12µg/m3	12µg/m3	12µg/m3	12µg/m3	12µg/m3	12µg/m3	12µg/m3		10µg/m3	
	PM2.5	4µg/m3	4µg/m3	4µg/m3	4µg/m3	4µg/m3	4µg/m3	4µg/m3		5µg/m3	4µg/m3	4µg/m3	4µg/m3	4µg/m3	4µg/m3	4µg/m3	4µg/m3		4µg/m3	
	NO2	1µg/m3	2µg/m3	1µg/m3	2µg/m3	2µg/m3	2µg/m3	2µg/m3		0µg/m3	0µg/m3	0µg/m3	0µg/m3	1µg/m3	1µg/m3	1µg/m3	1µg/m3		1µg/m3	
	VOC	11µg/m3	10µg/m3	11µg/m3	10µg/m3	11µg/m3	11µg/m3	11µg/m3		12µg/m3	12µg/m3	12µg/m3	11µg/m3	11µg/m3	11µg/m3	11µg/m3	11µg/m3		13µg/m3	
DAY 02 (21/01/22) 8am	PM10	75µg/m3	75µg/m3	79µg/m3	66µg/m3	65µg/m3	64µg/m3	62µg/m3		78µg/m3	78µg/m3	64µg/m3	89µg/m3	89µg/m3	87µg/m3	84µg/m3	75µg/m3		73µg/m3	67µg/m3
	PM2.5	42µg/m3	42µg/m3	42µg/m3	41µg/m3	41µg/m3	41µg/m3	41µg/m3		47µg/m3	47µg/m3	50µg/m3	43µg/m3	43µg/m3	43µg/m3	43µg/m3	42µg/m3		49µg/m3	51µg/m3
	NO2	0µg/m3	0µg/m3	0µg/m3	0µg/m3	0µg/m3	0µg/m3	0µg/m3		0µg/m3	0µg/m3	0µg/m3	0µg/m3	0µg/m3	0µg/m3	0µg/m3	0µg/m3		0µg/m3	0µg/m3
	VOC	30µg/m3	30g/m3	25µg/m3	40µg/m3	40µg/m3	36µg/m3	33µg/m3		13µg/m3	13µg/m3	14µg/m3	15µg/m3	15µg/m3	15µg/m3	15µg/m3	30µg/m3		13µg/m3	12µg/m3
DAY 03 (22/01/22) 12am	PM10	04µg/m3	03µg/m3	05µg/m3	06µg/m3	05µg/m3	05µg/m3	04µg/m3		11µg/m3	15µg/m3	15µg/m3	15µg/m3	15µg/m3	13µg/m3	10µg/m3	08µg/m3			
	PM2.5	02µg/m3	02µg/m3	02µg/m3	02µg/m3	02µg/m3	02µg/m3	02µg/m3		04µg/m3	07µg/m3	05µg/m3	05µg/m3	05µg/m3	06µg/m3	04µg/m3	03µg/m3			
	NO2	0µg/m3	0µg/m3	0µg/m3	0µg/m3	0µg/m3	0µg/m3	0µg/m3		0µg/m3	0µg/m3	0µg/m3	0µg/m3	0µg/m3	0µg/m3	0µg/m3	0µg/m3			
	VOC	09µg/m3	212µg/m3	09µg/m3	10µg/m3	09µg/m3	10µg/m3	10µg/m3		10µg/m3	08µg/m3	07µg/m3	07µg/m3	07µg/m3	07µg/m3	08µg/m3	08µg/m3			
DAY 04 (27/01/22) 04pm	PM10	03µg/m3	03µg/m3	04µg/m3	05µg/m3	04µg/m3	04µg/m3	02µg/m3		03µg/m3	03µg/m3	04µg/m3	05µg/m3	04µg/m3	04µg/m3	02µg/m3	02µg/m3			
	PM2.5	08µg/m3	08µg/m3	02µg/m3	02µg/m3	02µg/m3	03µg/m3	02µg/m3		08µg/m3	08µg/m3	02µg/m3	02µg/m3	02µg/m3	03µg/m3	02µg/m3	02µg/m3			
	NO2							99µg/m3		92µg/m3		106µg/m3								
	VOC							26µg/m3		27µg/m3		18µg/m3								

Table A.02 - Table with the collected data in the fieldwork of EMEF AMORIM LIMA with focus on pollutants.

EMEF DESEMBARGADOR AMORIM LIMA

Nº	Nome comum	Nome científico	DAP ≥ 3(cm)	Σ DAP (cm)	altura (m)	origem	estado fitossanitário	Observações
1	aglaia	*Aglaia odorata*		19	10	exótica	bom	próxima da cerca; inclinada para rua
2	aglaia	*Aglaia odorata*		21	9	exótica	bom	lesão no tronco
3	morta	-			-	-	-	junto ao muro
4	amoreira	*Morus nigra*	15+6	21	7	exótica	bom	contato com grade; galhos com podridão; próximo a muro
5	amoreira	*Morus nigra*	10+8+9	27	6	exótica	regular	troncos cruzados; contato com grade; lesões no tronco; galhos cruzados
6	pau-de-viola	*Cytharexyllum myrianthum*		49	12	nativa	regular	poda inadequada com brotações; contato com grade
7	goiabeira	*Psidium guajava*		11	5	nativa	regular	contato com muro; lesão no tronco
8	alfeneiro	*Ligustrum lucidum*	34+37	71	13	exótica	regular	brotações laterais; lesão no tronco com fenda; ramos epicórmicos; lesão por poda
9	toco	--			-	-	-	dac=50cm
10	areca-bambu	*Dypsis lutescens*	4+4	7.5	2.5	exótica	bom	junto ao muro
11	jerivá	*Syagrus romanzoffiana*		28	8	nativa	bom	contato com grade
12	jerivá	*Syagrus romanzoffiana*		8	2.8	nativa	bom	contato com muro
13	sabiá	*Mimosa caesalpiniifolia*		15	5	nativa	regular	poda drástica com brotação; próximo a muro
14	sabiá	*Mimosa caesalpiniifolia*	8+27	35	10	nativa	regular	poda inadequada com brotação; lesões no tronco; próximo a muro
15	podocarpus	*Podocarpus sp.*	8+4+3+4	19	4	exótica	bom	contato com grade e muro
16	podocarpus	*Podocarpus sp.*	4+3	7	3	exótica	bom	contato com muro; bifurcado da base
17	podocarpus	*Podocarpus sp.*		10	4	exótica	bom	contato com muro e grade
18	podocarpus	*Podocarpus sp.*		5	4	exótica	bom	contato com muro e grade; fenda no tronco
19	toco	--			-	-	-	dac=20cm
20	jerivá	*Syagrus romanzoffiana*		31	8	nativa	bom	lesões no estipe
21	toco	--			-	-	-	dac=59cm
22	ipê-amarelo-cascudo	*Tabebuia chrysotricha*	7+5	12	3.5	nativa	bom	painel de lesão no galho
23	acerola	*Malpighia glabra*	3+4+4+4+3	18	2.5	nativa	regular	contato com muro; lesões no tronco e galhos
24	acerola	*Malpighia glabra*	6+3+3+4	16	3.8	nativa	regular	contato com muro; lesões no tronco e galhos
25	toco	--			-	-	-	dac=83cm
26	chapéu-de-sol	*Terminalia catappa*	3+4	7	2	exótica	regular	poda inadequada com brotações; lesões no tronco
26A	toco	--			-	-	-	-
27	acerola	*Malpighia glabra*	3+5	8	2.5	nativa	regular	lesões no tronco; galhos cruzados; paineis de lesão no galho; fenda
28	tuia	*Thuja sp.*		9	4.5	exótica	bom	-
29	carambola	*Averrhoa carambola*	7+8+8+10+9+9+4	55	5	exótica	regular	podas inadequadas; lesões no tronco; painel de lesão no galho
30	romã	*Punica granatum*		3	2.8	exótica	regular	polifurcada da base; lesões no tronco
31	gonçaleiro	*Astronium sp.*	7+4+5	16	3	nativa	regular	trifurcada da base; lesões no tronco; tronco cruzado
32	pitangueira	*Eugenia uniflora*		6	4	nativa	bom	-
33	freixo	*Fraxinus americana*		69	14	exótica	bom	podas inadequadas; lesão no tronco; fenda no tronco
34	mexiriqueira	*Citrus reticulata*	4+8+6+7+3+7+6	41	3	exótica	bom	contato com telhado; painel de lesão no galho; folhas atacadas por lagarta; tronco com casca inclusa; trifurcado na base
35	toco	--			-	-	-	dac=61cm
36	jaboticaba	*Myrciaria trunciflora*	3+3+3	9	2	nativa	bom	polifurcada da base; tronco cruzado
37	toco	--			-	-	-	dac=48cm
38	alfeneiro	*Ligustrum lucidum*		68	12	exótica	regular	erva de passarinho; podas inadequadas; painel de lesão no tronco; galho cruzado; ramos epicórmicos por poda de galho
39	alfeneiro	*Ligustrum lucidum*		50	12	exótica	regular	lesões no tronco; podas inadequadas; ramos epicórmicos por poda de galho
40	alfeneiro	*Ligustrum lucidum*		31	12	exótica	bom	inclinada para construção; erva de passarinho; lesões no tronco
41	alfeneiro	*Ligustrum lucidum*		31	12	exótica	bom	inclinada para construção; erva de passarinho; lesões no tronco
42	alfeneiro	*Ligustrum lucidum*		51	13	exótica	regular	lesões no tronco; podas inadequadas; ramos epicórmicos por poda de galho; lesão no colo
43	amoreira	*Morus nigra*	7+13+9+6	35	5	exótica	regular	painel de lesão no tronco; troncos cruzados; lesões no tronco; trifurcado na base; fenda no galho
44	pessegueiro	*Prunus persica*	13+14	20	4.5	exótica	regular	contato com poste; painel de lesão no galho
45	goiabeira	*Psidium guajava*		14	3.5	nativa	regular	junto ao muro; inclinada; lesões no tronco; painel de lesão no tronco
46	alfeneiro	*Ligustrum lucidum*	18+24	42	8	exótica	bom	bifurcada da base; lesões no tronco; contato com telhado; ramos epicórmicos por poda de galho
47	amoreira	*Morus nigra*	4+9	12.6	5	exótica	regular	lesões no tronco; próximo a muro; bifurcado na base
48	morta	-			-	-	-	-
49	mangueira	*Mangifera indica*		13	7	exótica	bom	lesão no tronco; broca
50	alfeneiro	*Ligustrum lucidum*		54	14	exótica	bom	lesões no tronco e galhos
51	resedá	*Lagerstroemia indica*		13	5	exótica	ruim	lesões no tronco com podridão; oco no tronco
52	alfeneiro	*Ligustrum lucidum*		44	8	exótica	regular	lesões no tronco; erva de passarinho; contato com grade
53	alfeneiro	*Ligustrum lucidum*		26	9	exótica	regular	lesões no tronco; levemente inclinada; ramos epicórmicos por poda de galho; lesão no colo
54	tipuana	*Tipuana tipu*		46	13	exótica	bom	levemente inclinada
55	alfeneiro	*Ligustrum lucidum*		18	8	exótica	regular	lesões no tronco; inclinada
55A	toco	-			-	-	-	-
56	tipuana	*Tipuana tipu*		42	12	exótica	regular	lesões no tronco; inclinada
57	alfeneiro	*Ligustrum lucidum*	15+25+18	58	8	exótica	regular	erva de passarinho; lesões no tronco; tronco com casca inclusa; lesões no colo
58	alfeneiro	*Ligustrum lucidum*	17+12+19+14	62	7	exótica	ruim	galhos secos; lesões no tronco; tronco com casca inclusa; trifurcado na base; lesão no colo; painel de lesão no tronco
59	alfeneiro	*Ligustrum lucidum*		20	8	exótica	regular	galho seco; lesão no tronco; ramos epicórmicos
60	alfeneiro	*Ligustrum lucidum*		40	10	exótica	bom	poda inadequada; tronco com casca inclusa; broca
61	amoreira	*Morus nigra*		6	4	exótica	bom	contato com grade
62	alfeneiro	*Ligustrum lucidum*	13+16	29	6	exótica	regular	lesões no tronco e colo; erva-de-passarinho
63	goiabeira	*Psidium guajava*		16	6	nativa	regular	inclinada; lesões no tronco e colo
63A	toco	-			-	-	-	-
64	goiabeira	*Psidium guajava*		15	5	nativa	regular	contato com grade e fiação; painel de lesão no tronco; lesão no tronco
65	freixo	*Fraxinus americana*		44	13	exótica	bom	levemente inclinada
66	ameixeira	*Eriobotrya japonica*	8+11	19	5	exótica	regular	bifurcada da base; contato com grade e lesões no tronco
67	alfeneiro	*Ligustrum lucidum*	12+11+14	37	5	exótica	regular	trifurcada da base; contato com grade; lesões no tronco
68	resedá	*Lagerstroemia indica*	11+13+11	35	6	exótica	bom	trifurcada da base; contato com construção
69	alfeneiro	*Ligustrum lucidum*	16+19	35	6	exótica	regular	lesões no tronco; bifurcado na base; lesão nos galhos
70	freixo	*Fraxinus americana*		48	13	exótica	bom	galho cruzado
71	morta	-			-	-	-	-
72	alfeneiro	*Ligustrum lucidum*		20	8	exótica	regular	contato com fiação e poste; lesões no tronco; junto ao muro
73	pitangueira	*Eugenia uniflora*	7+7	14	6	nativa	bom	lesões no tronco; próximo a muro; contato com cerca
74	pitangueira	*Eugenia uniflora*	5+4+3	12	4	nativa	bom	
75	goiabeira	*Psidium guajava*		23	8	nativa	regular	lesões no tronco; painel de lesão no tronco; podada
76	toco	--			-	-	-	
77	freixo	*Fraxinus americana*		36	13	exótica	bom	-
78	alfeneiro	*Ligustrum lucidum*	25+42	67	12	exótica	regular	contato com fiação; grade e iluminação; ramos epicormicos; lesão no tronco; tronco com casca inclusa; lesão nos galhos
79	alfeneiro	*Ligustrum lucidum*	17+21	38	9	exótica	regular	bifurcada da base; erva-de-passarinho; painel de lesão no tronco
80	freixo	*Fraxinus americana*		22	12	exótica	bom	lesões no tronco
81	alfeneiro	*Ligustrum lucidum*	18+24	42	9	exótica	ruim	galhos secos; túneis de cupim; contato com grade e fiação; painéis de lesão no colo e tronco; painel de lesão do colo ao galho secundário
82	freixo	*Fraxinus americana*		48	14	exótica	bom	lesão no tronco; contato com fiação
82A	toco	-			-	-	-	-
83	amoreira	*Morus nigra*		23	9	exótica	regular	lesões no tronco; ramos epicórmicos
84	alfeneiro	*Ligustrum lucidum*		69	10	exótica	regular	bifurcada da base; lesões no tronco e colo; painel de lesão no tronco; galho cruzado; lesão no colo; bifurcado na base; erva-de-passarinho
85	alfeneiro	*Ligustrum lucidum*		26	9	exótica	bom	contato com fiação e grade; próxima ao muro; lesão no tronco
86	alfeneiro	*Ligustrum lucidum*			6	exótica	bom	próximo ao muro
87	abacateiro	*Persea americana*		19	7	nativa	bom	painel de lesão no tronco; lesão no tronco; inclinada
88	nespereira	*Eriobotrya japonica*		14	5	exótica	regular	painel de lesão no tronco; lesões no tronco
89	ingá	*Inga sp*		23	6	nativa	bom	lesões no tronco; fenda; inclinada
90	alfeneiro	*Ligustrum lucidum*		52	12	exótica	regular	painel de lesão no tronco; próximo ao muro; lesões no tronco e galhos
91	alfeneiro	*Ligustrum lucidum*	23+25	34	10	exótica	regular	painéis de lesões nos galhos; lesões no tronco; junto ao muro
92	alfeneiro	*Ligustrum lucidum*		32	10	exótica	bom	painel de lesão no tronco; próximo ao muro
93	alfeneiro	*Ligustrum lucidum*		24	10	exótica	bom	lesões no tronco;junto ao muro
94	citrus	*Citrus sp.*		7	8	exótica	bom	próximo ao muro
95	alfeneiro	*Ligustrum lucidum*		36	17	exótica	regular	lesões no tronco; painel de lesão no colo; erva-de-passarinho; junto ao muro

Table A.03 - Table with the information of the treea and other vegetation species in EMEF Amorim Lima, used to build the ENVI-met model (given by the school).

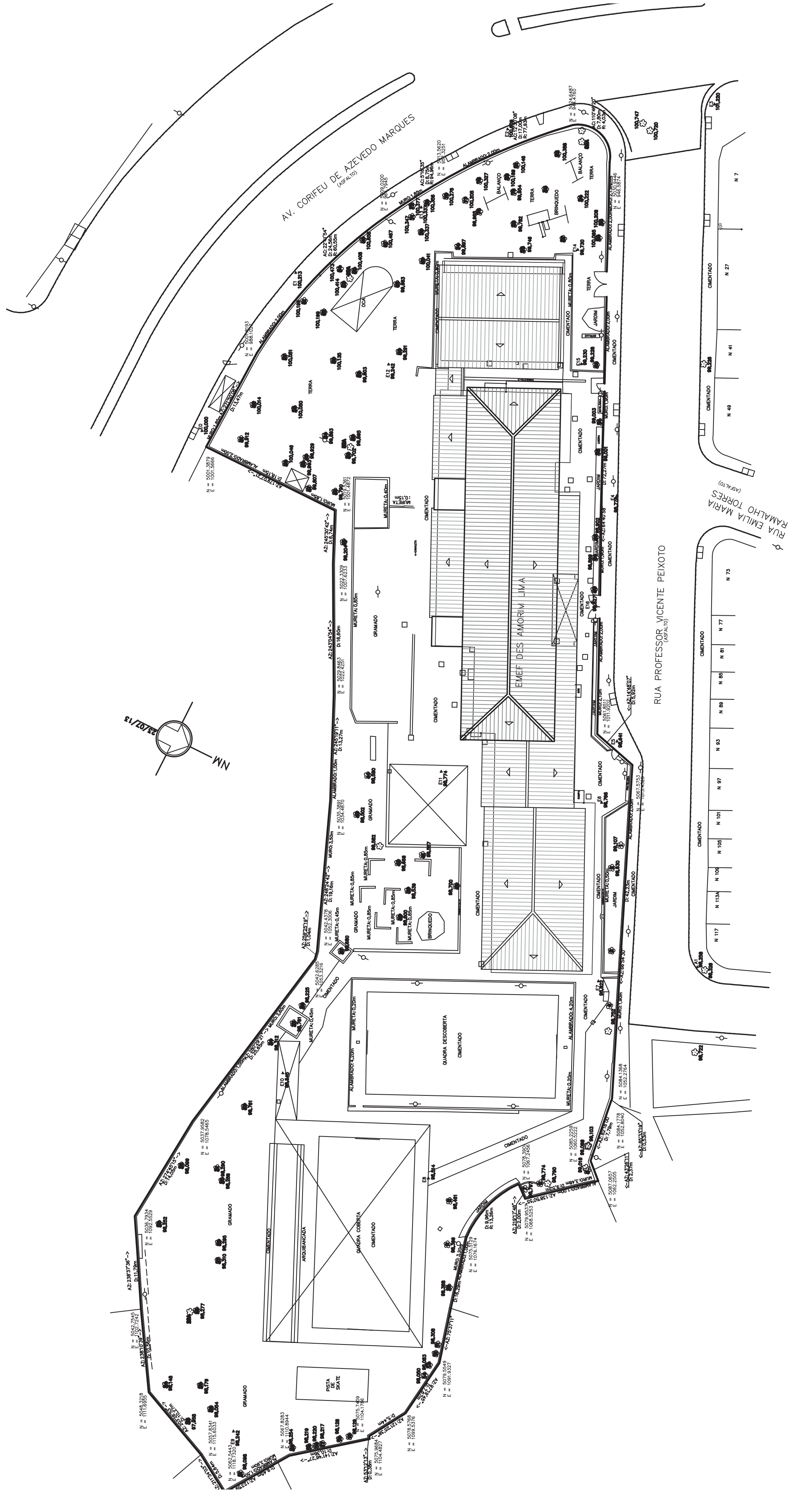

Figure A.04 - Roof plan of EMEF Amorim Lima containing the location of each existing tree (given by the school).

APPENDIX B- SUPPORTING INFORMATION FOR CHAPTER 06

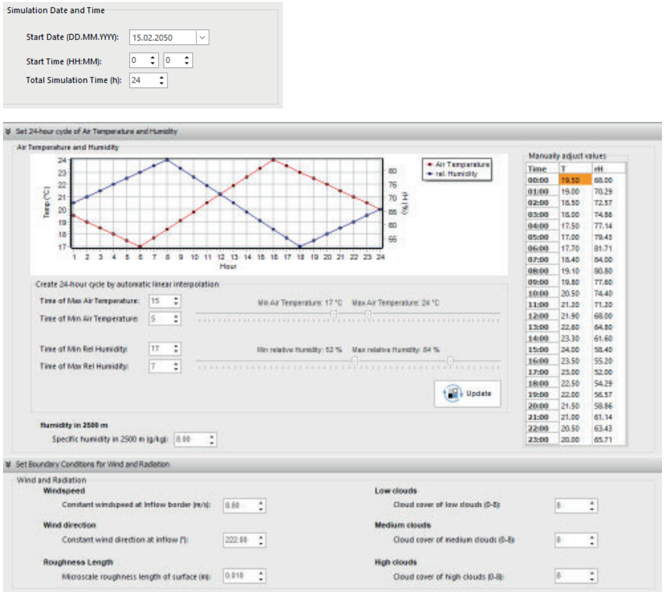

Figure B.01 - Microclimatic conditions inputed in ENVI-met® for the hot studied day.

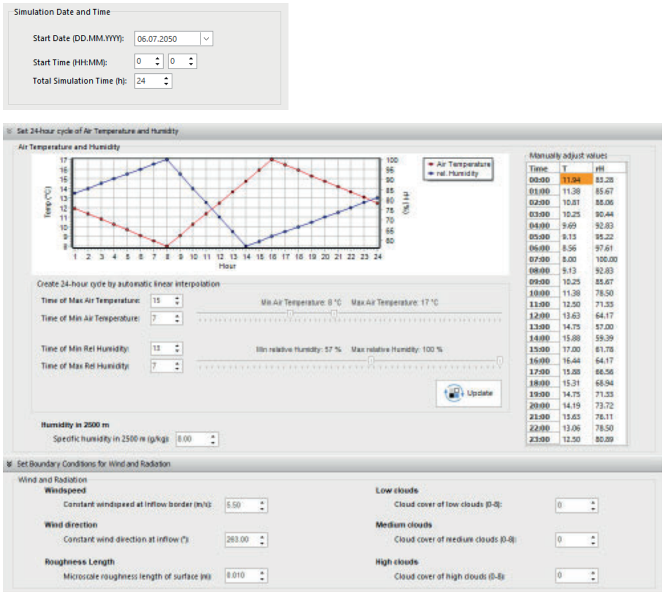

Figure B.02 - Microclimatic conditions inputed in ENVI-met® for the cold studied day.

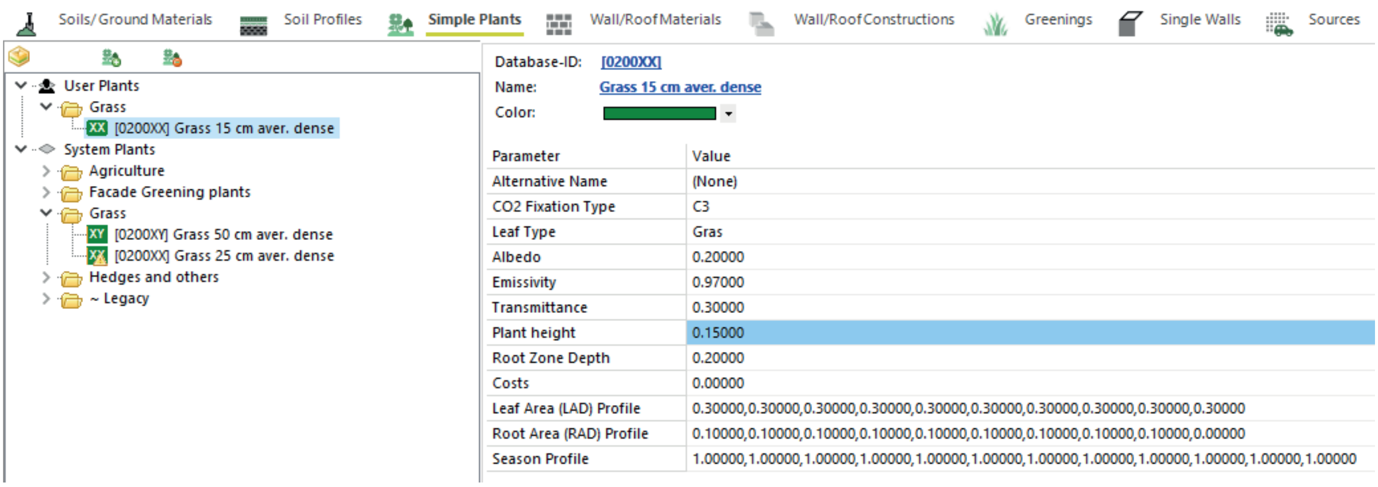

Figure B.03 - Image of an extract of the ENVI-met®s DBManager® with constructed grass.

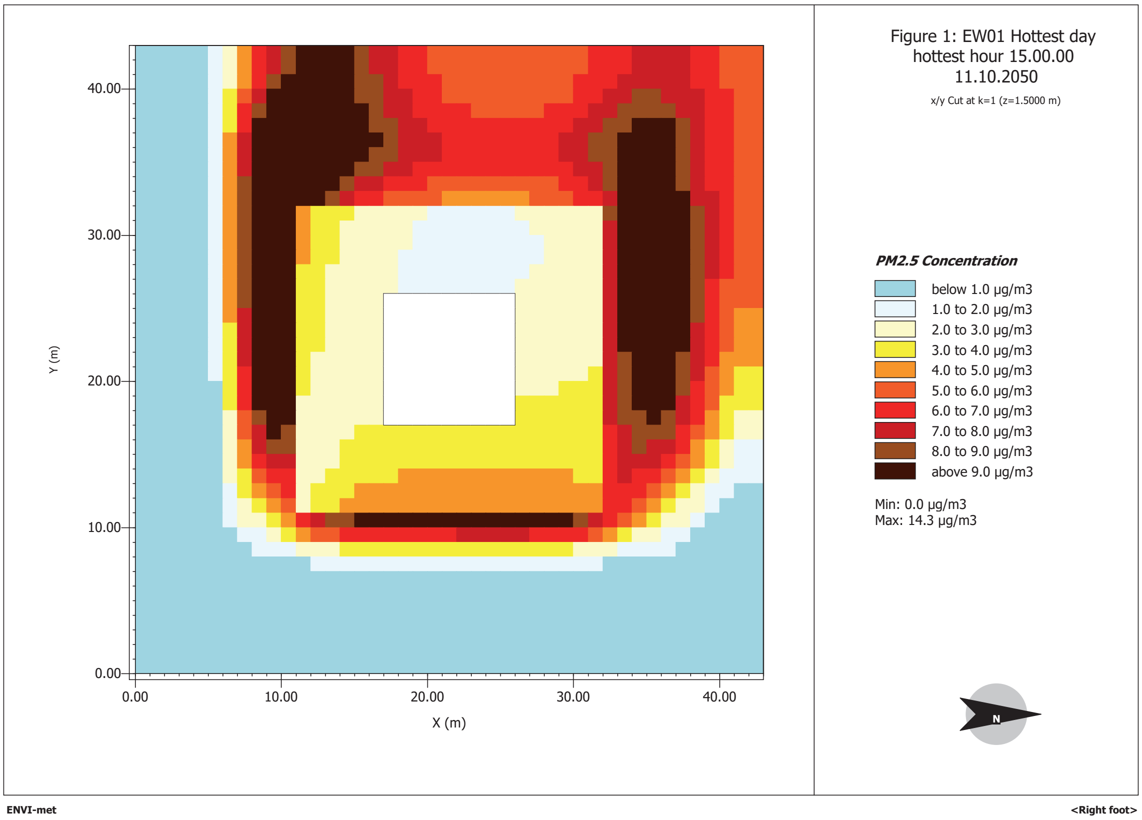

Figure B.04 - Outcome EW01, Hot day Hot Hour, PM2.5.

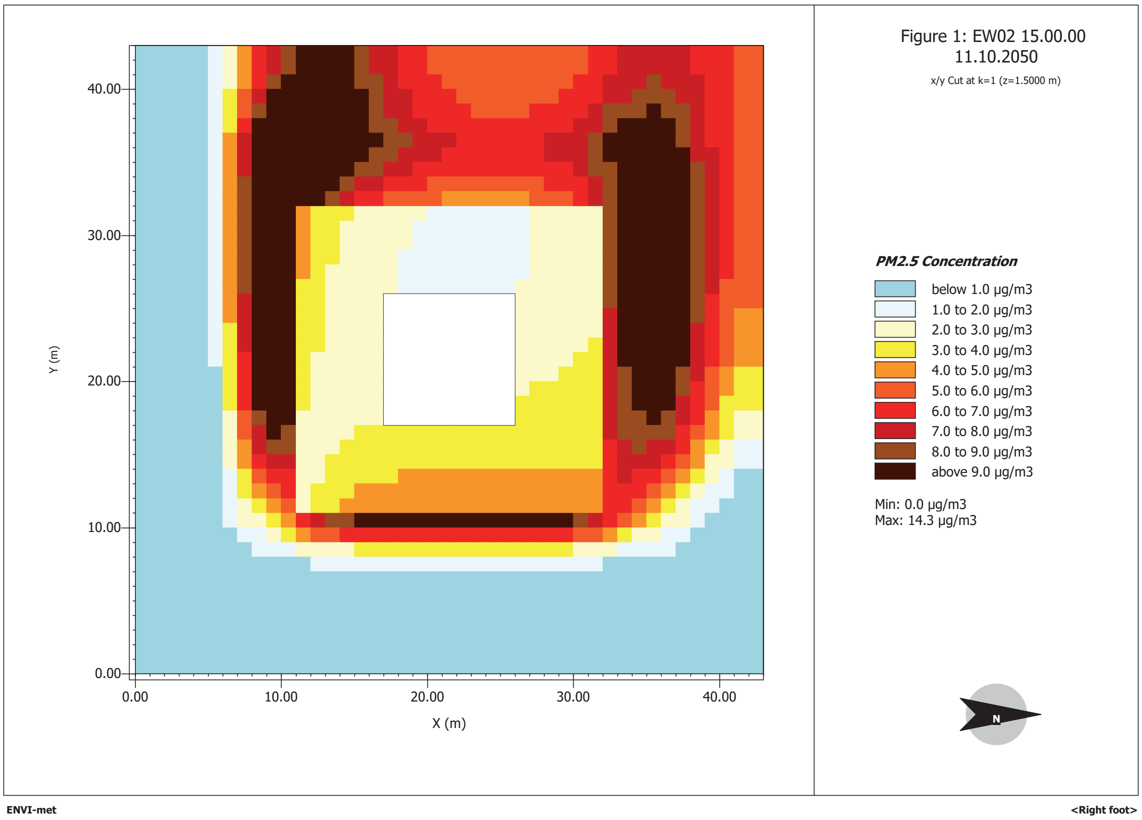

Figure B.05 - Outcome EW02, Hot day Hot Hour, PM2.5.

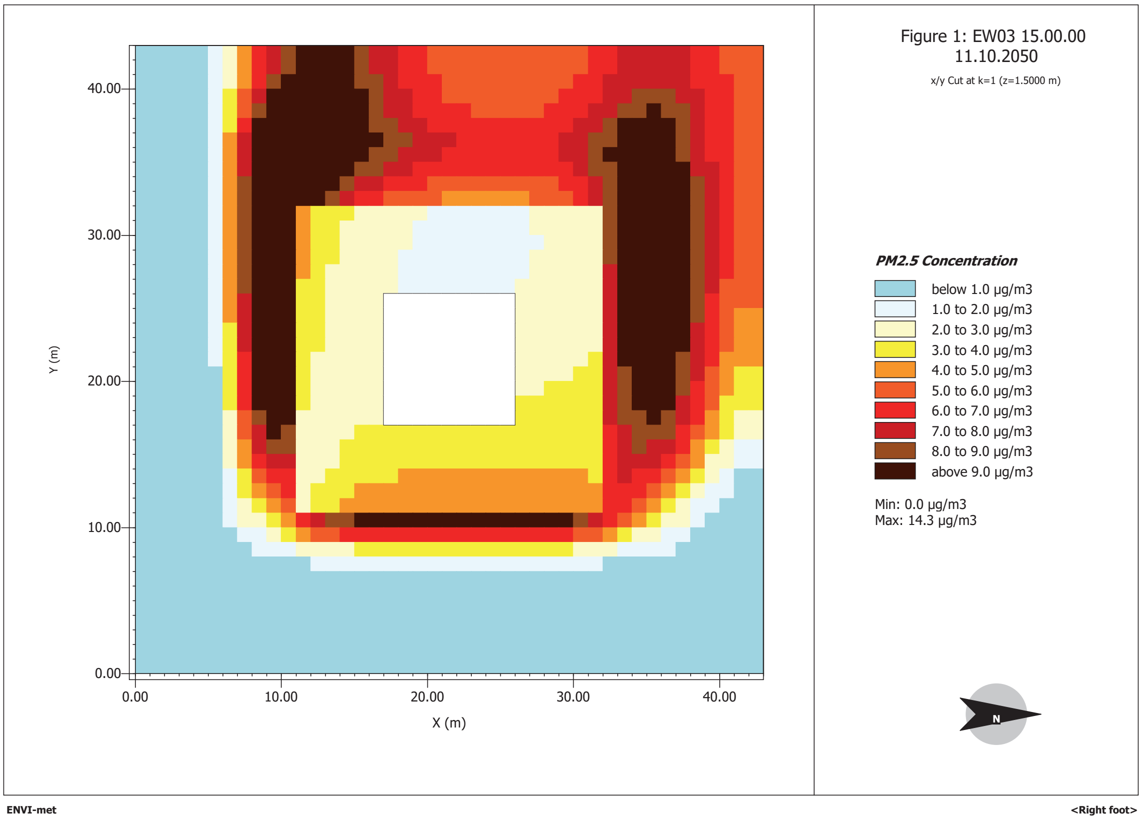

Figure B.06 - Outcome EW03, Hot day Hot Hour, PM2.5.

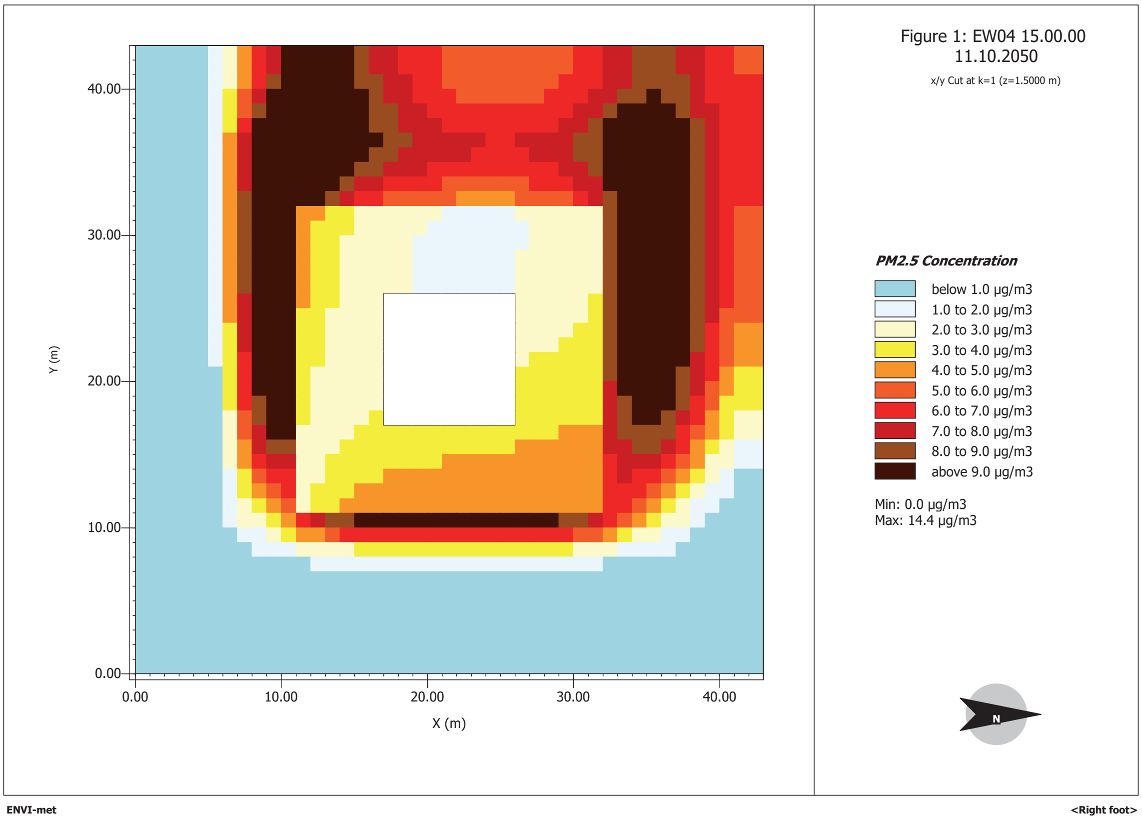

Figure B.07 - Outcome EW04, Hot day Hot Hour, PM2.5.

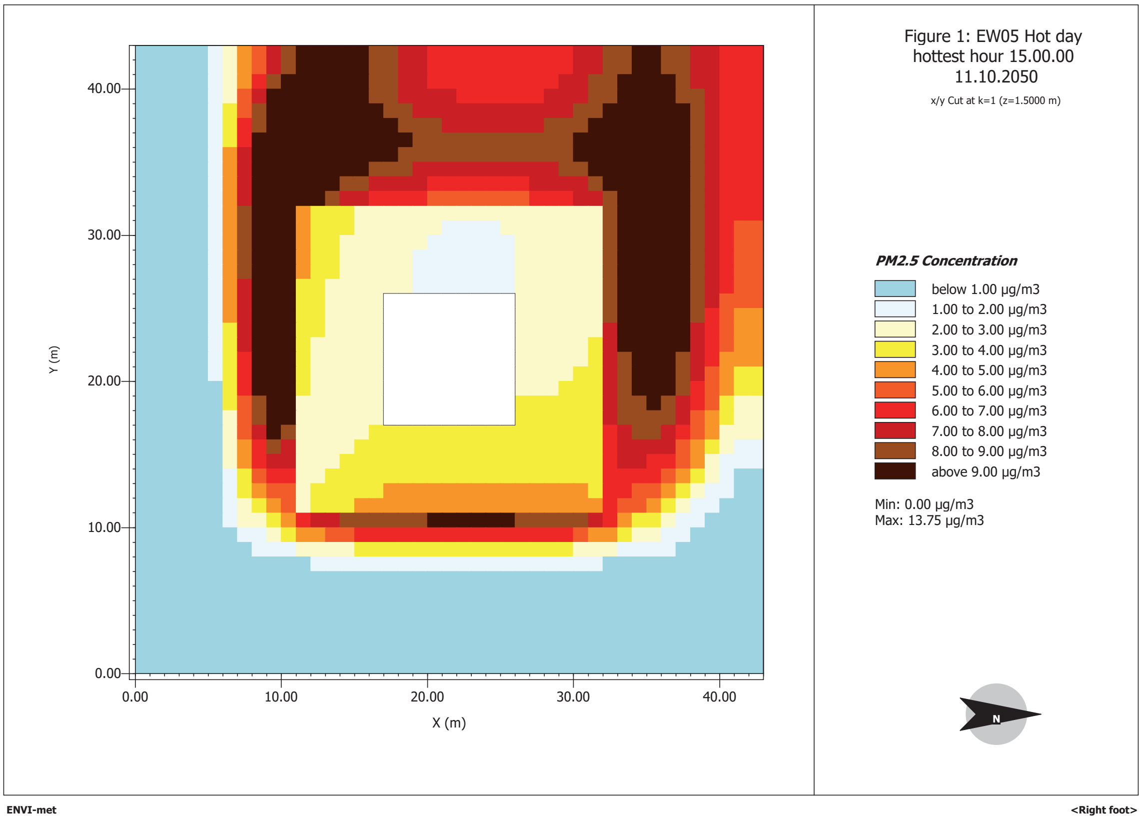

Figure B.08 - Outcome EW05, Hot day Hot Hour, PM2.5.

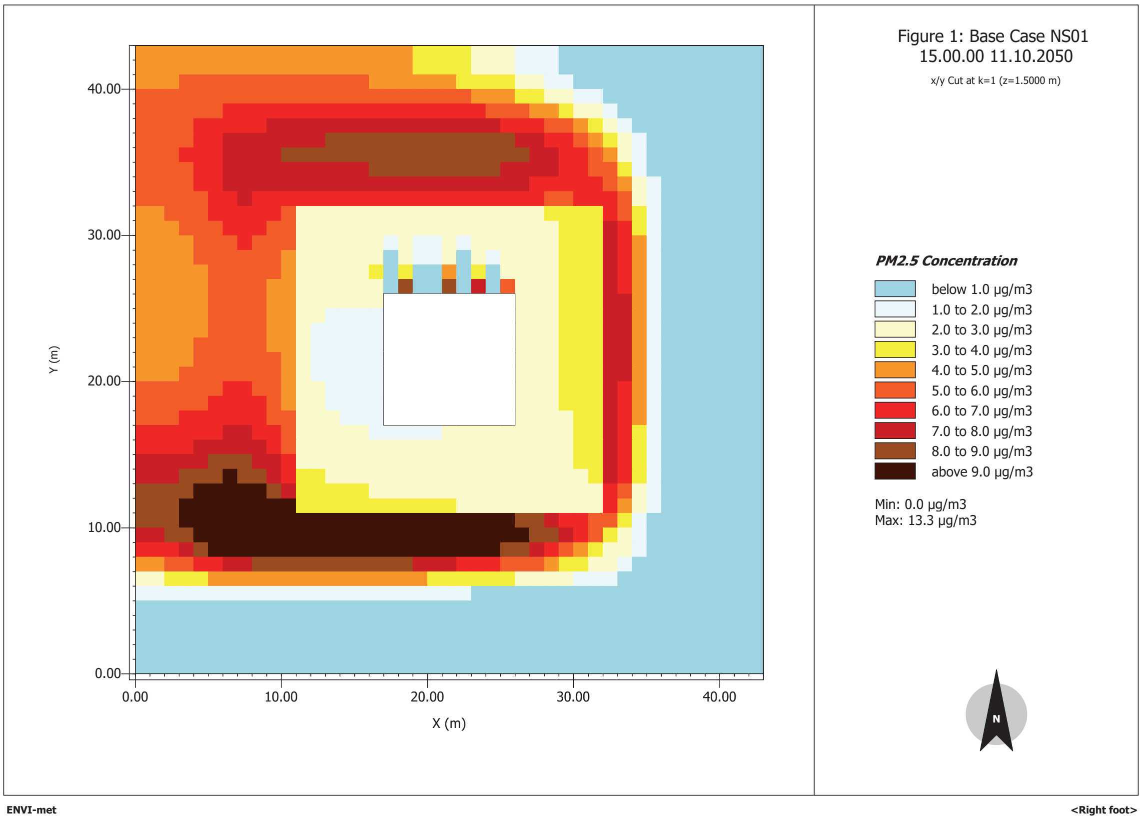

Figure B.09 - Outcome NS01, Hot day Hot Hour, PM2.5.

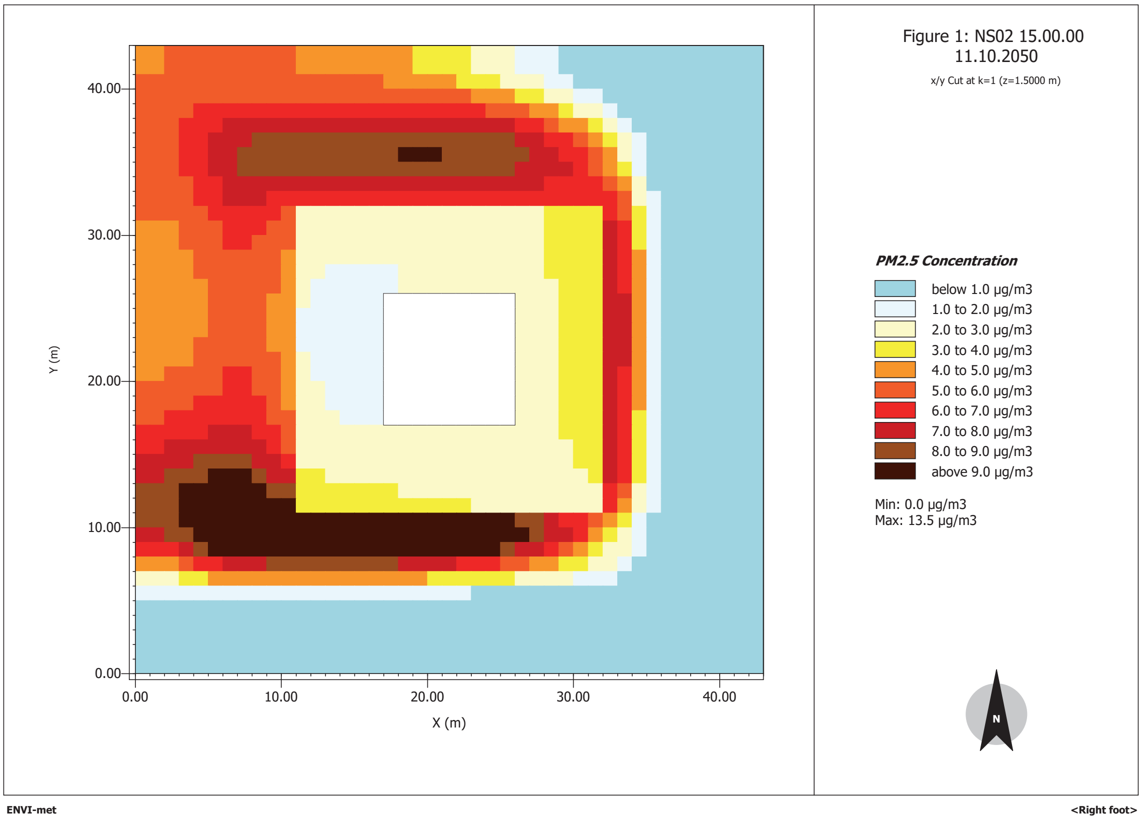

Figure B.10 - Outcome NS02, Hot day Hot Hour, PM2.5.

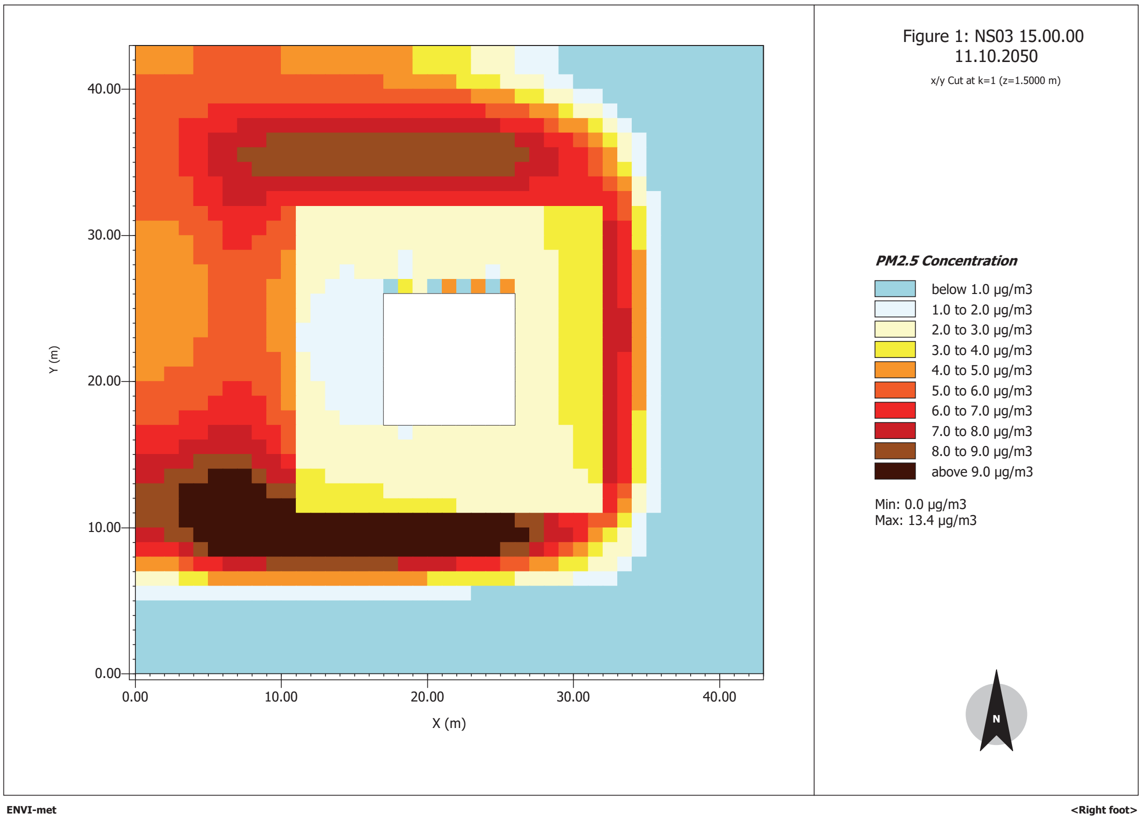

Figure B.11 - Outcome NS03 , Hot day Hot Hour, PM2.5.

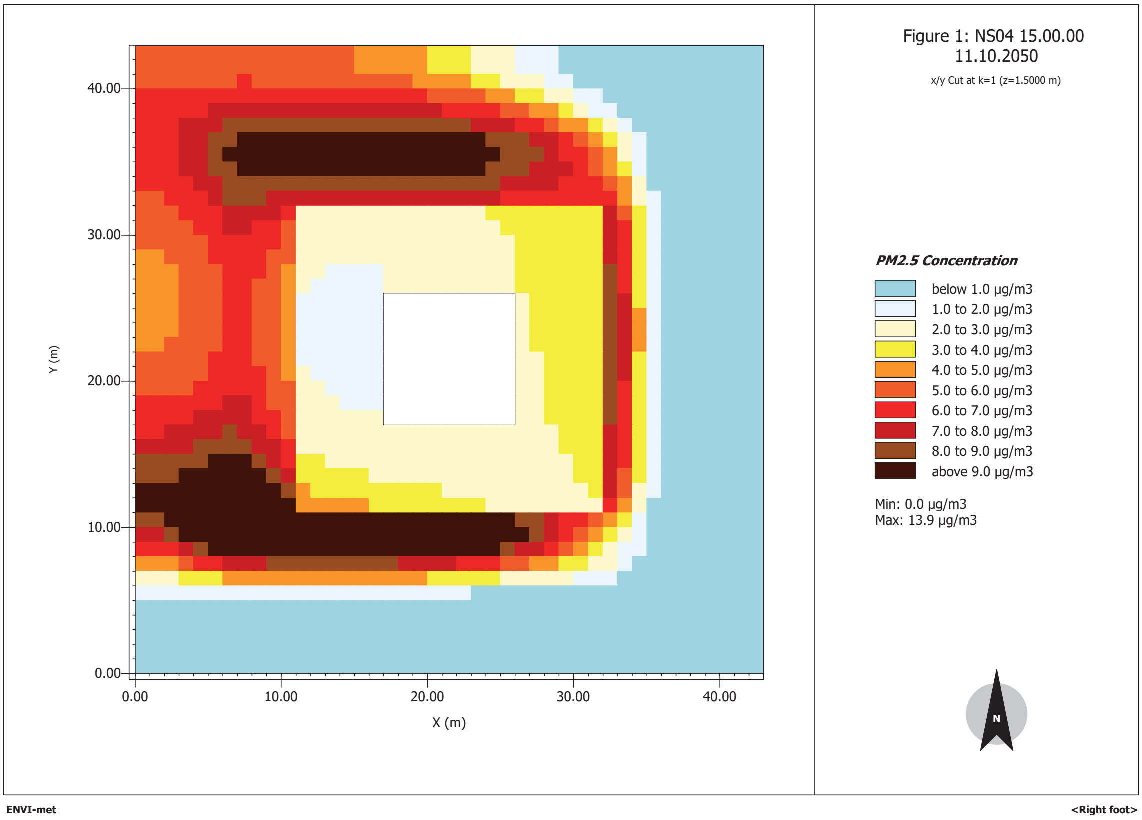

Figure B.12 - Outcome NS04, Hot day Hot Hour, PM2.5.

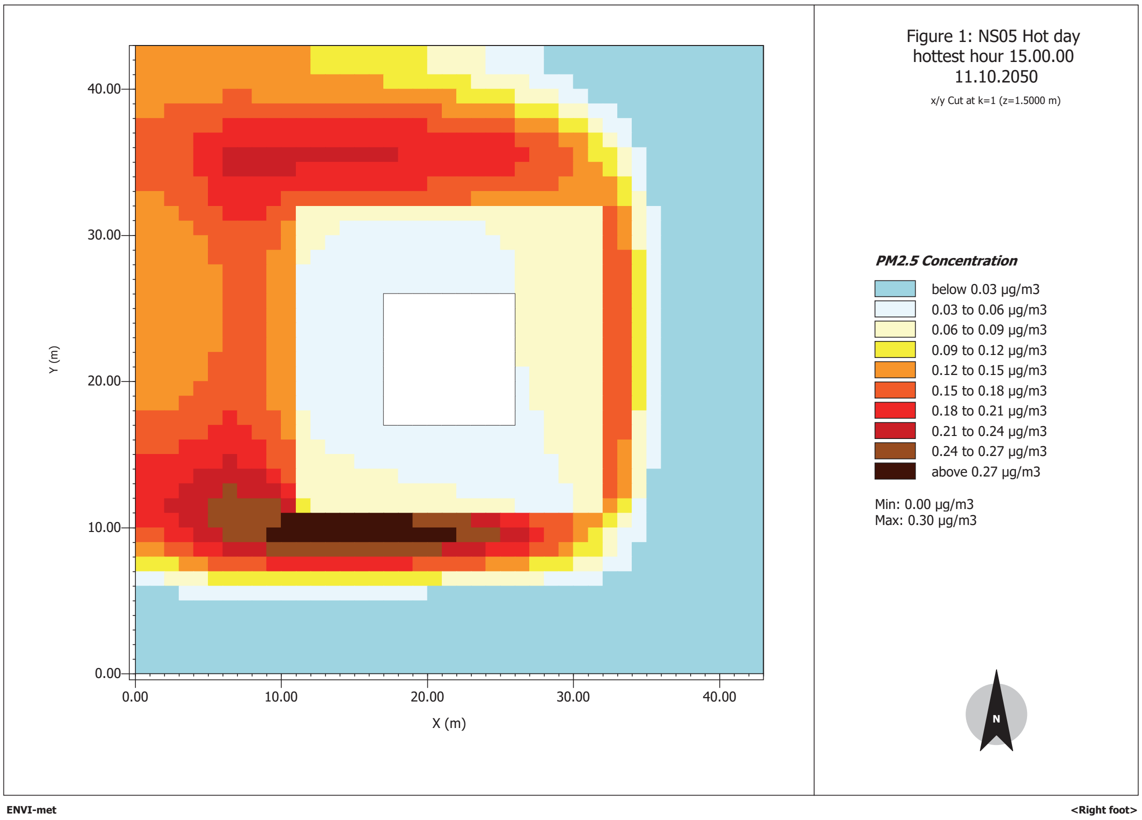

Figure B.13 - Outcome NS05, Hot day Hot Hour, PM2.5.

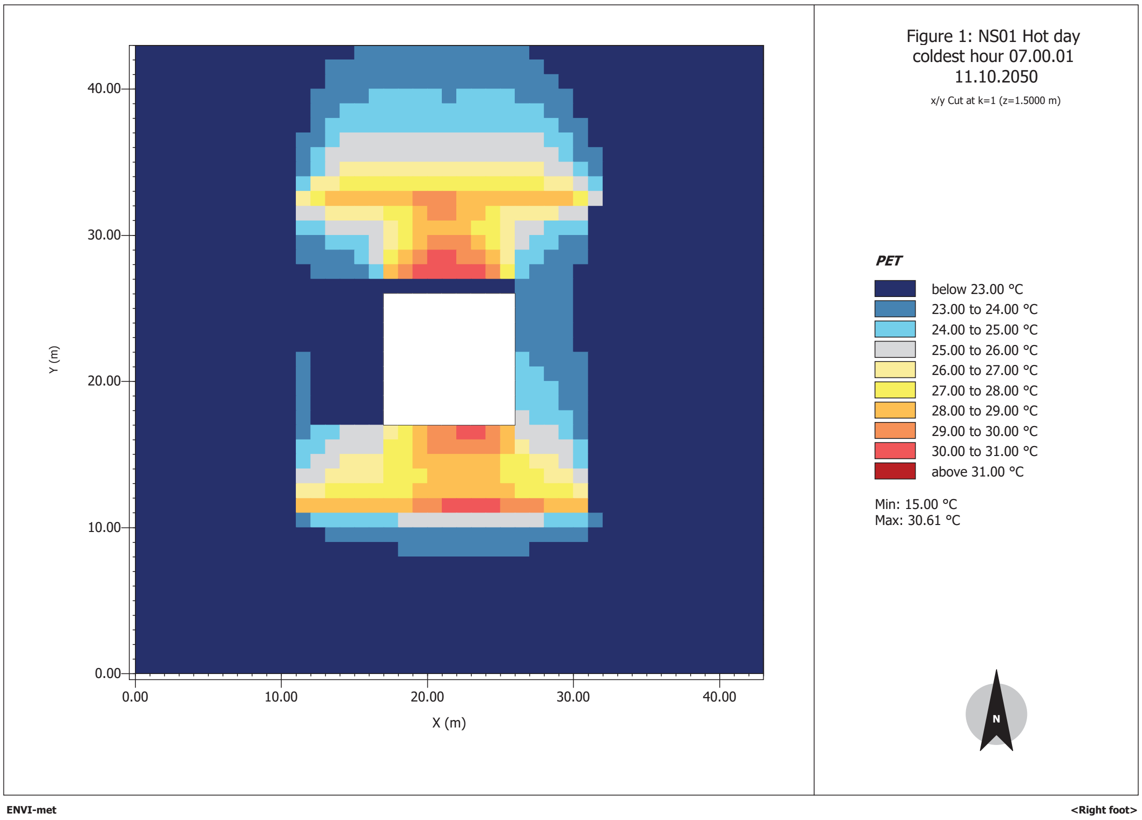

Figure B.27 - Outcome NS01, Hot day Coldest Hour, PET.

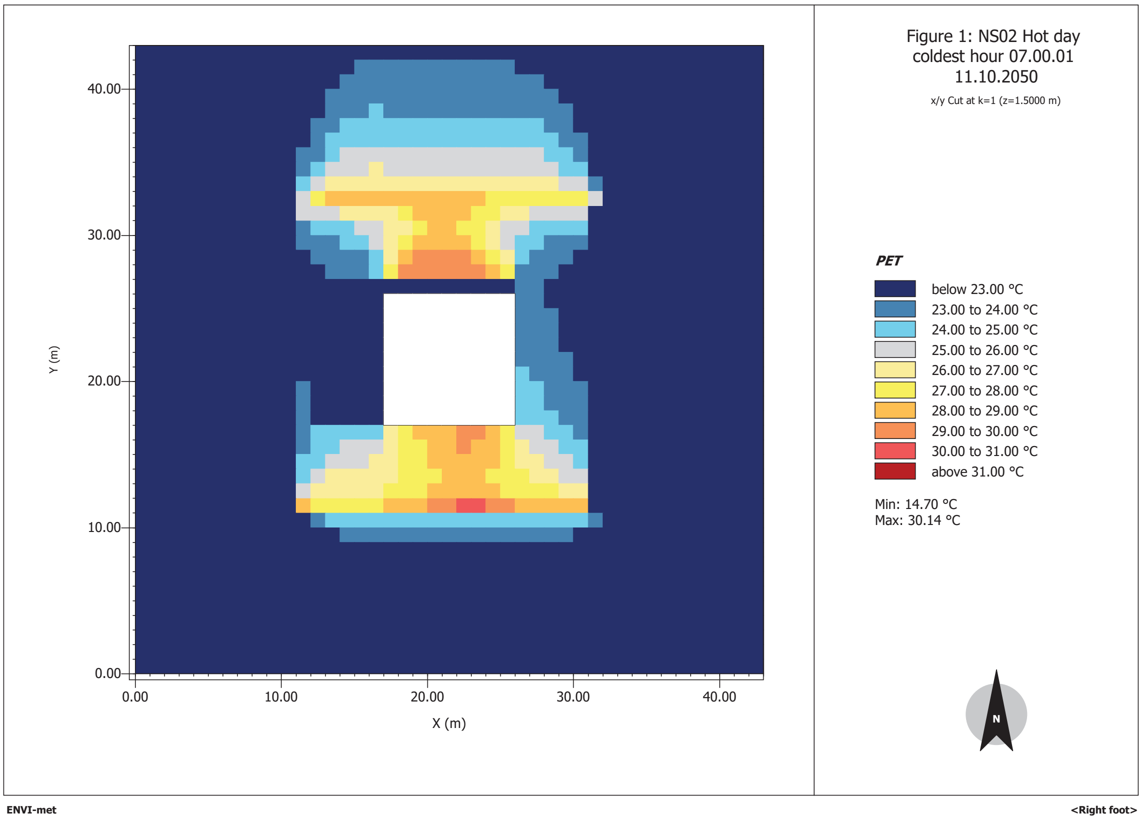

Figure B.28 - Outcome NS02, Hot day Coldest Hour, PET.

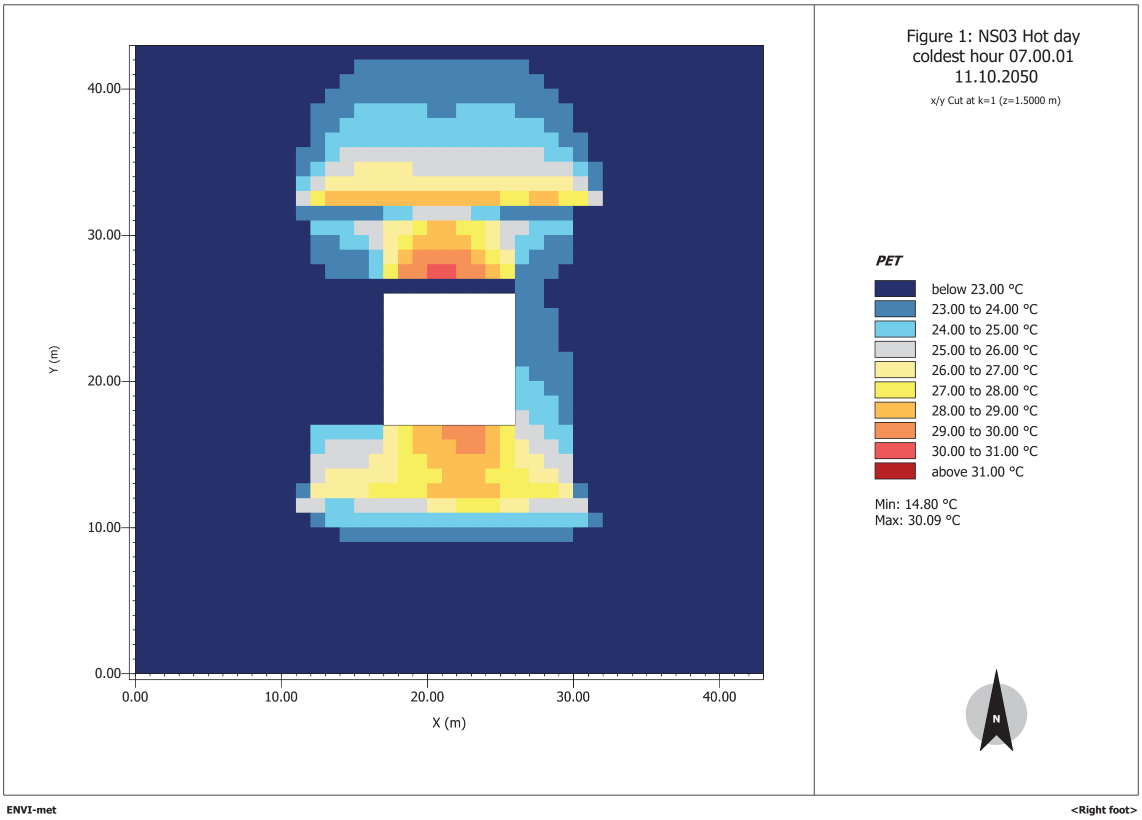

Figure B.29 - Outcome NS03, Hot day Coldest Hour, PET.

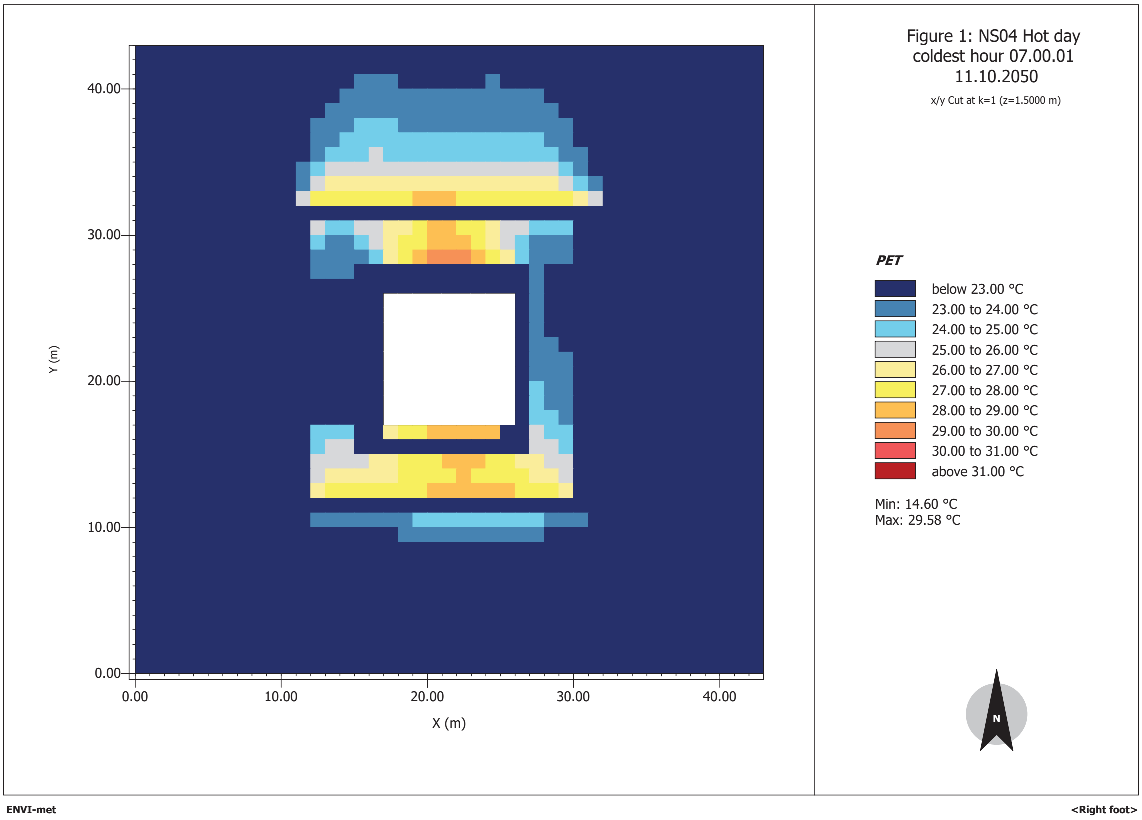

Figure B.30 - Outcome NS04, Hot day Coldest Hour, PET.

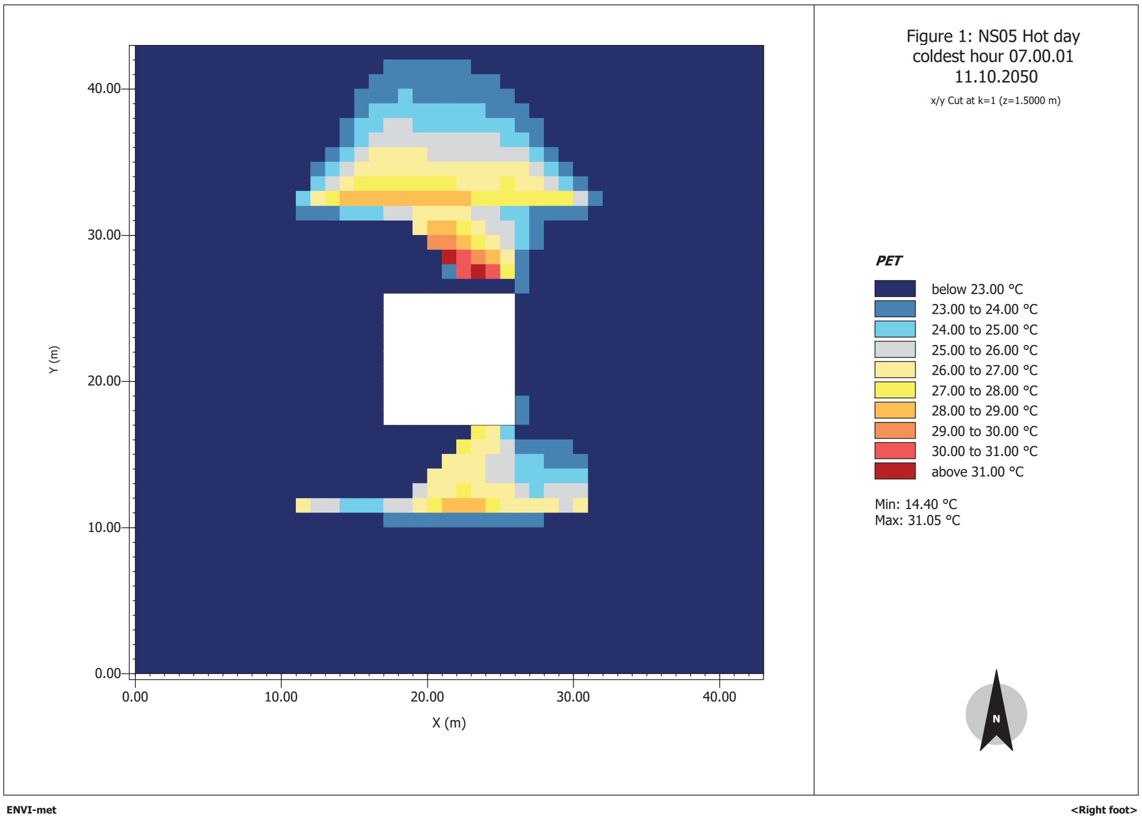

Figure B.29 - Outcome NS05, Hot day Coldest Hour, PET.

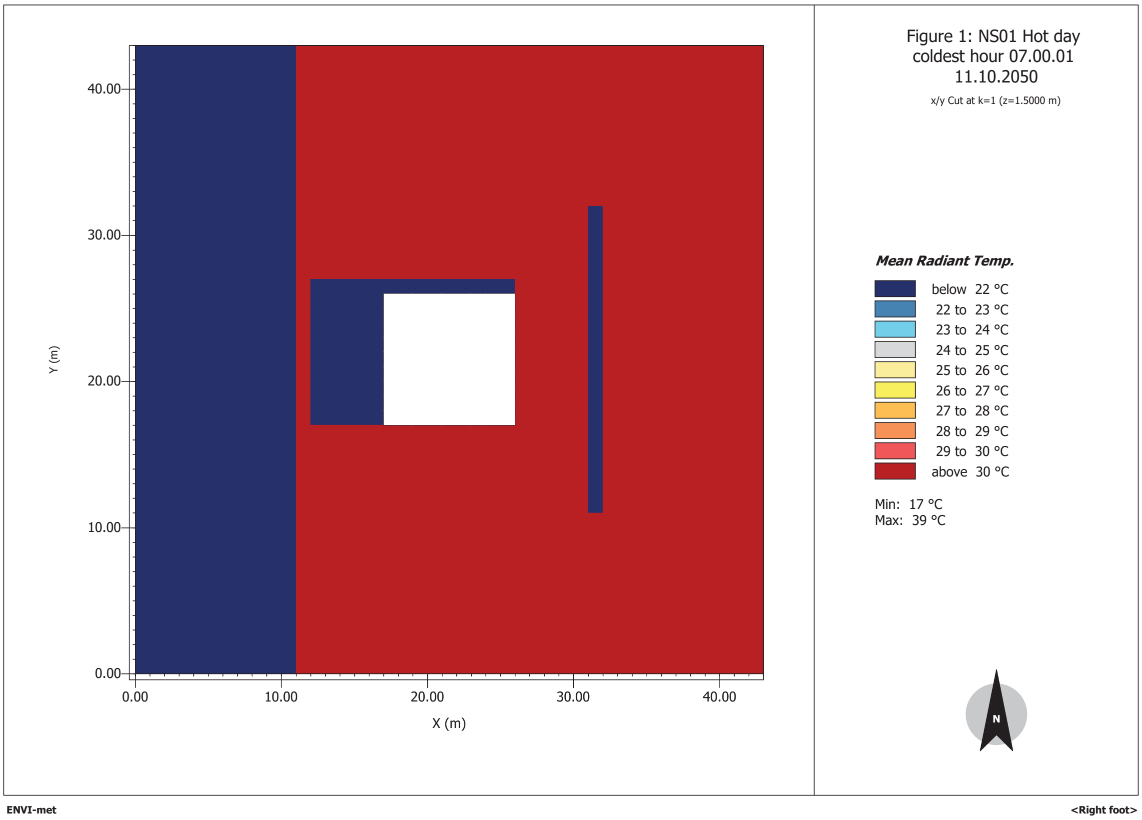

Figure B.30 - Outcome NS01, Hot day Coldest Hour, MRT.

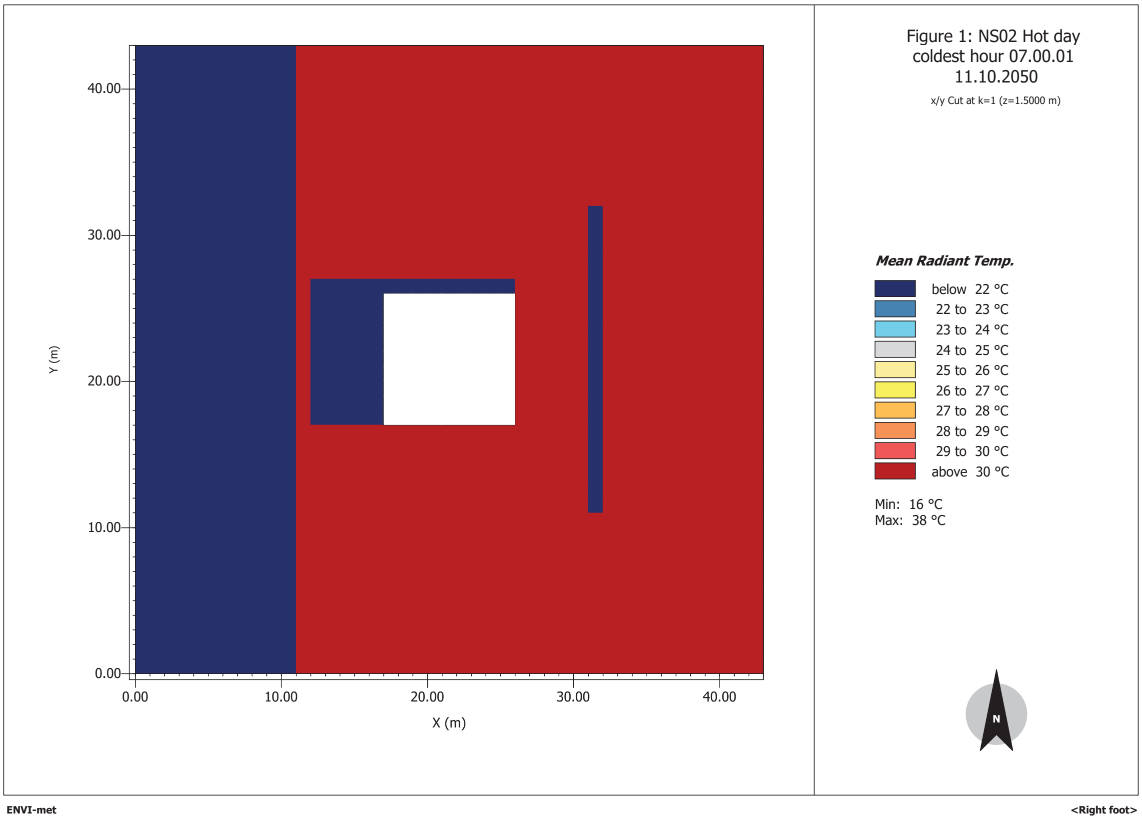

Figure B.27 - Outcome NS02, Hot day Coldest Hour, MRT.

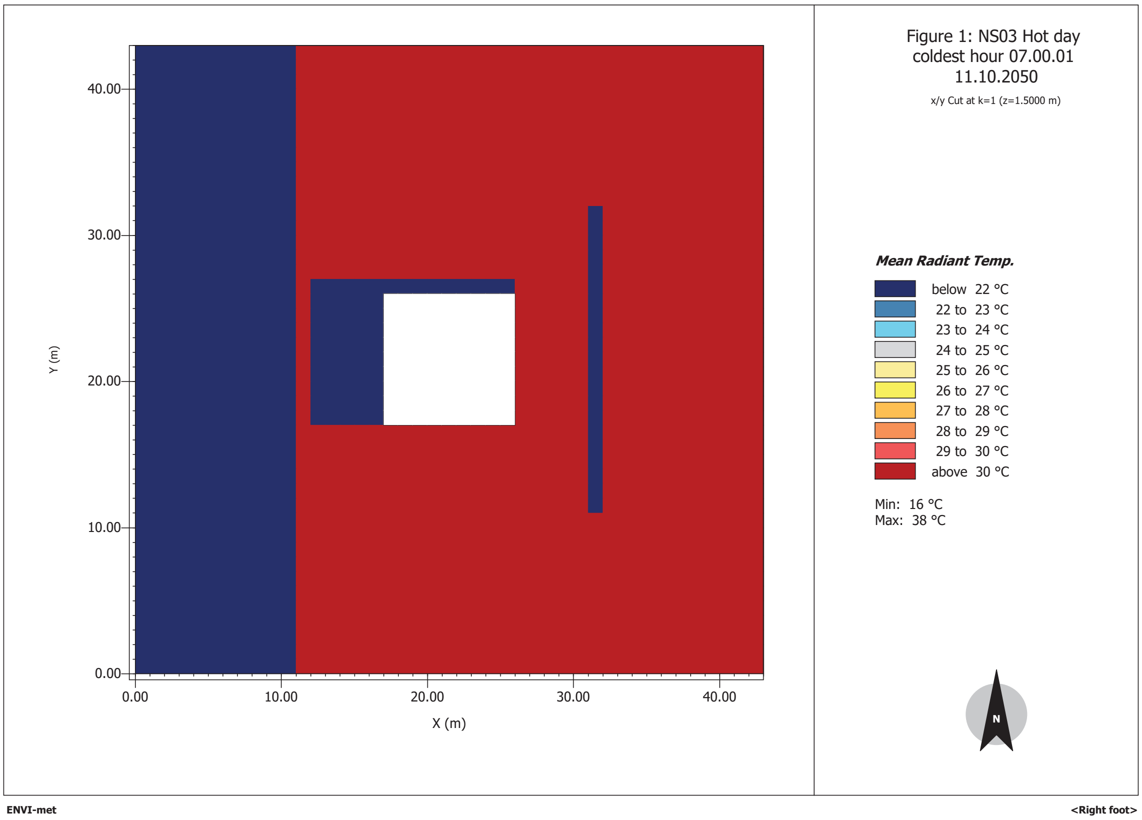

Figure B.28 - Outcome NS03, Hot day Coldest Hour, MRT.

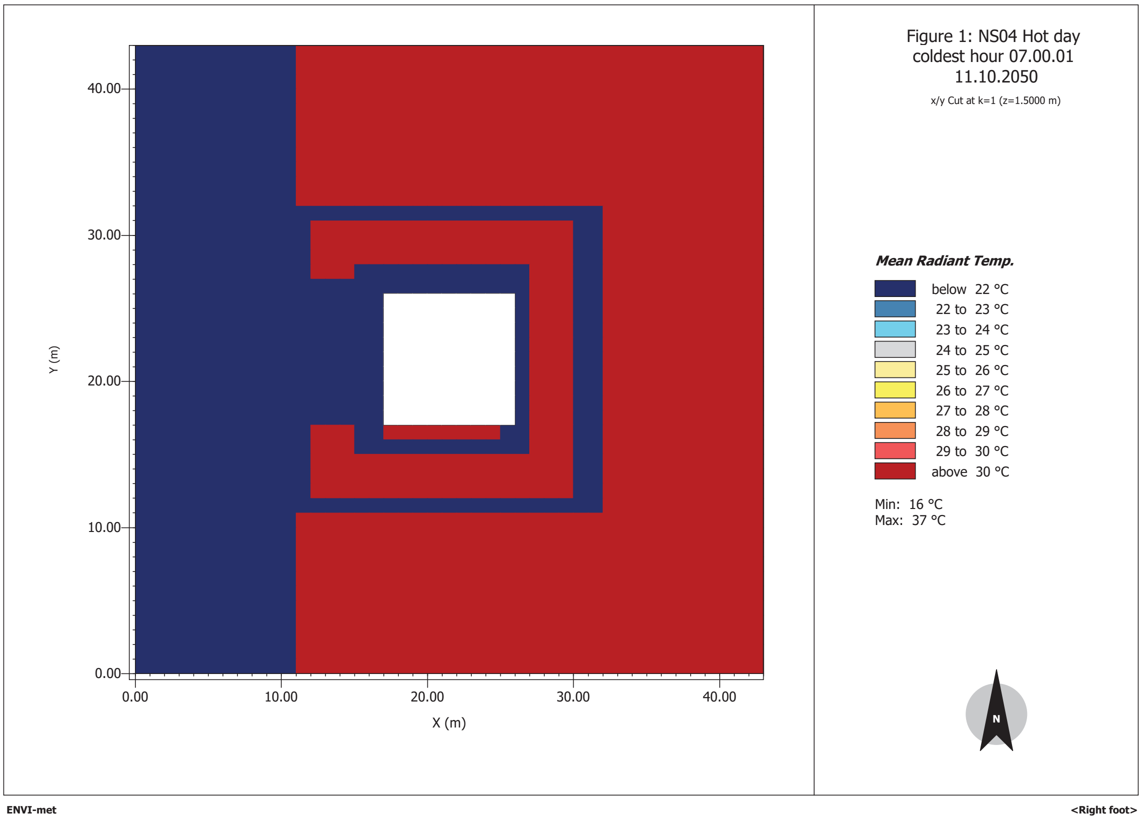

Figure B.29 - Outcome NS04, Hot day Coldest Hour, MRT.

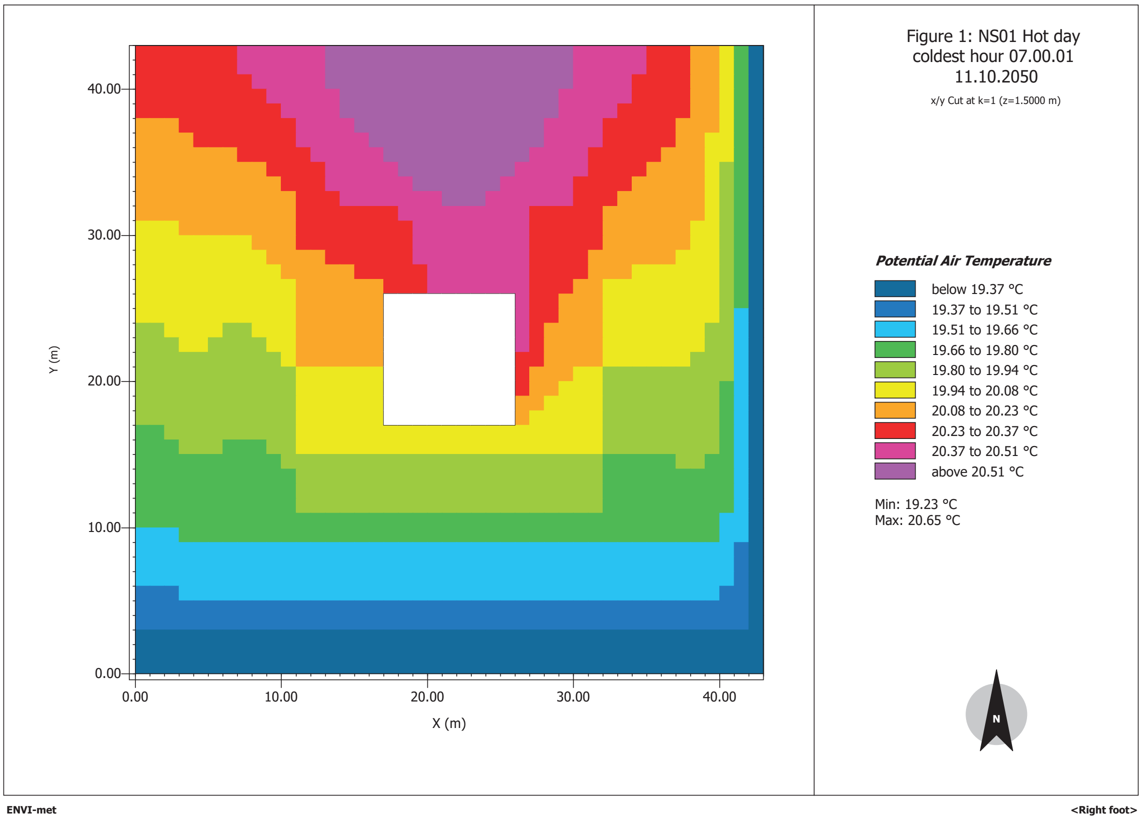

Figure B.30 - Outcome NS01, Hot day Coldest Hour, Potential Air Temperature.

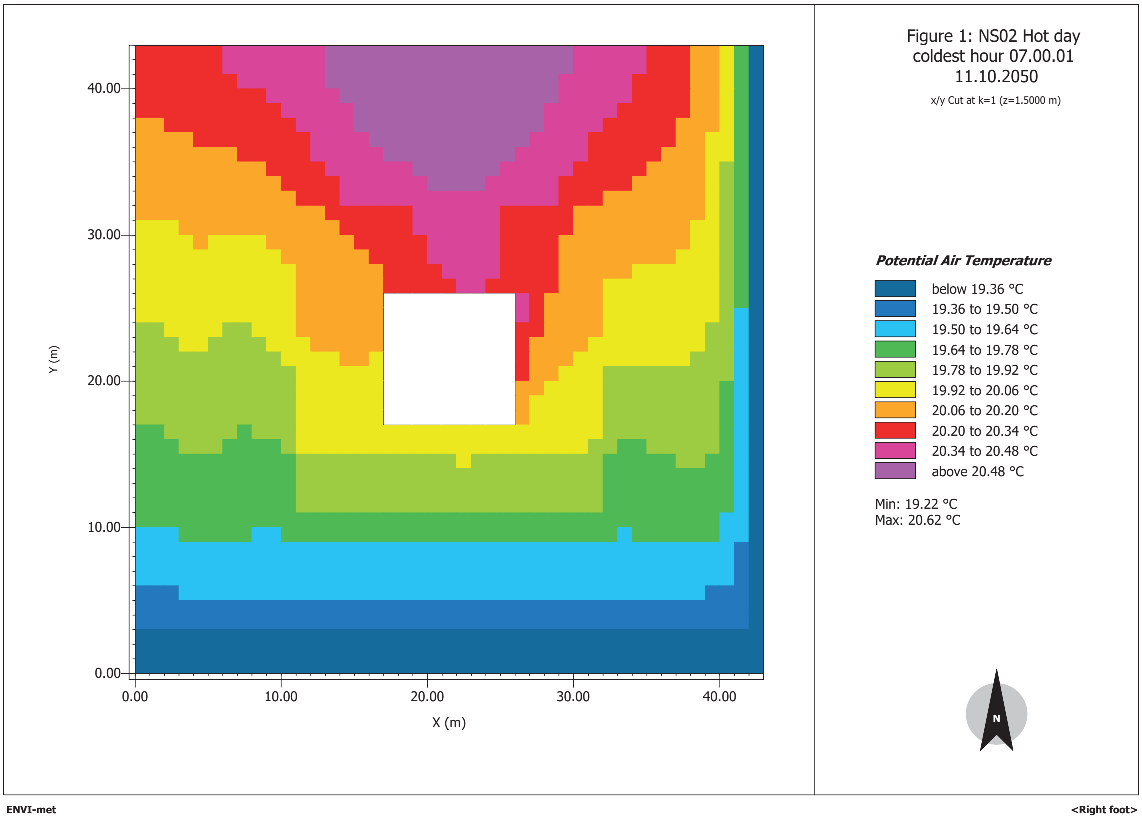

Figure B.29 - Outcome NS02, Hot day Coldest Hour, Potential Air Temperature.

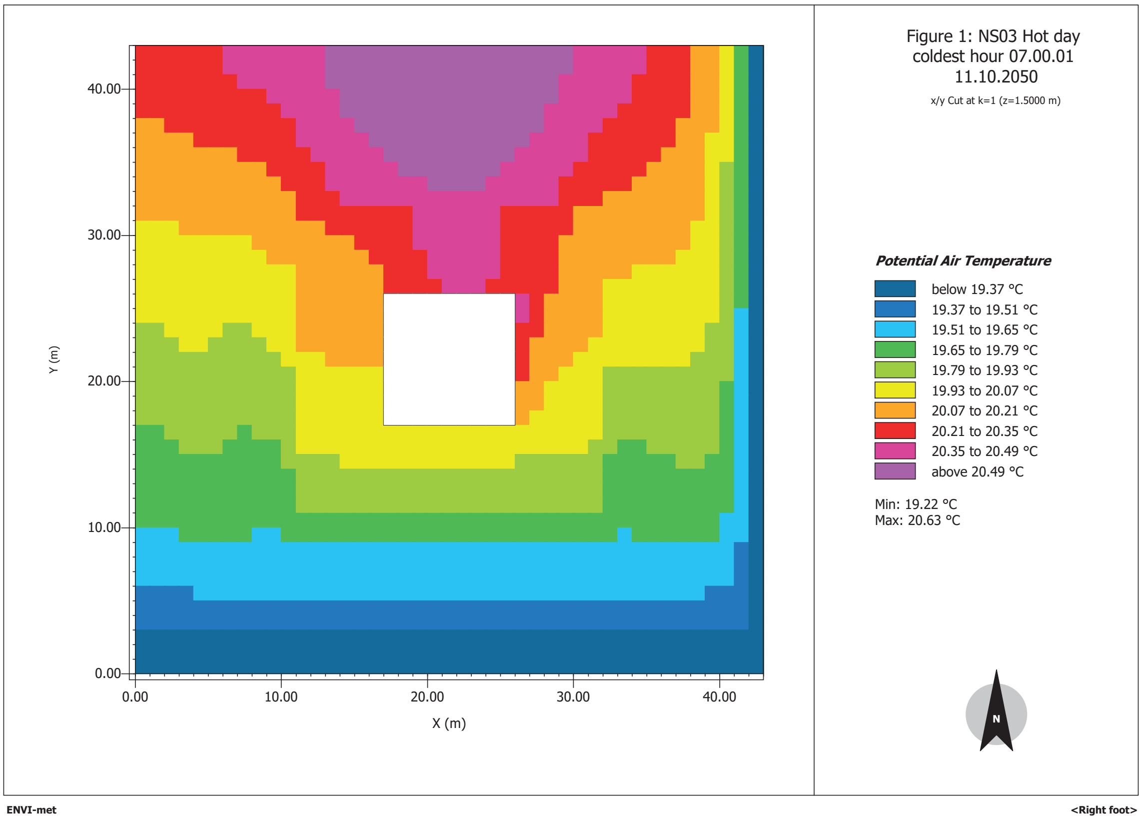

Figure B.30 - Outcome NS03, Hot day Coldest Hour, Potential Air Temperature.

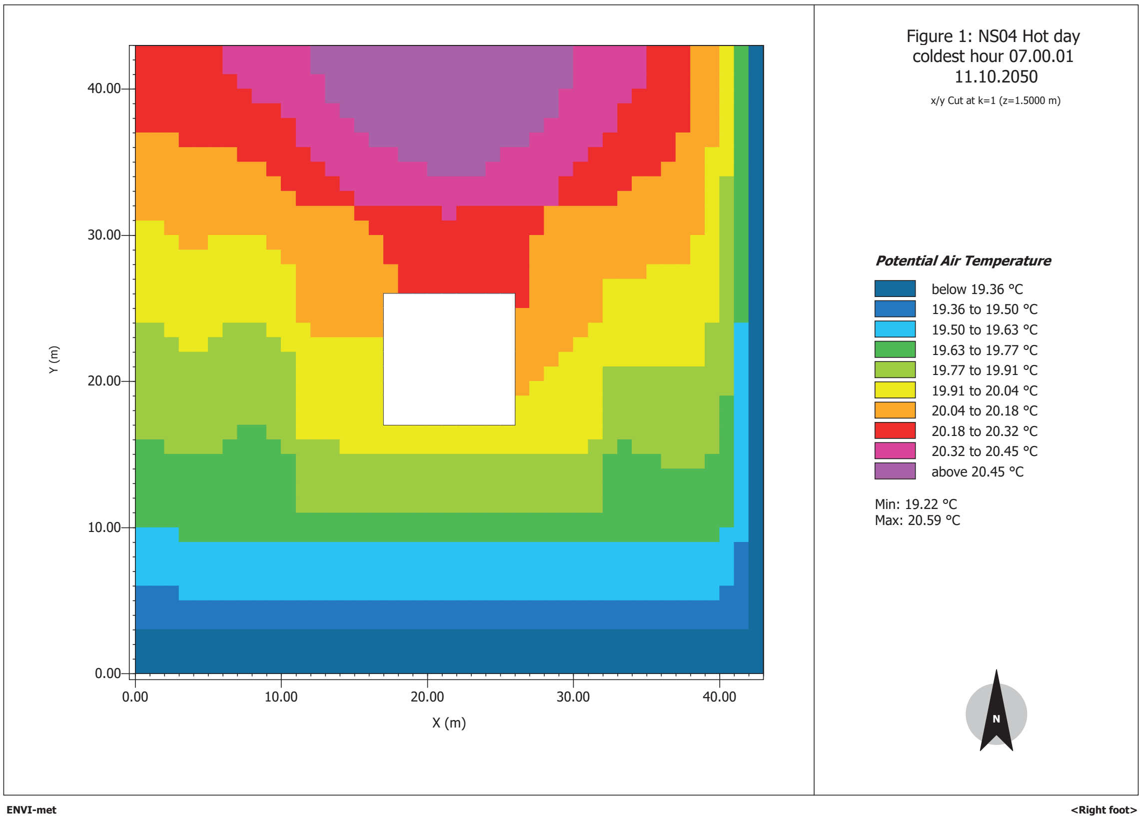

Figure B.29 - Outcome NS04, Hot day Coldest Hour, Potential Air Temperature.